

Georgia State University

ScholarWorks @ Georgia State University

Chemistry Dissertations

Department of Chemistry

Spring 5-9-2016

Novel Anticancer Agents That Upregulate p53 and A New Type of Neighbouring Group Assisted Click Reactions

Alexander B. Draganov

Follow this and additional works at: https://scholarworks.gsu.edu/chemistry_diss

Recommended Citation

Draganov, Alexander B., "Novel Anticancer Agents That Upregulate p53 and A New Type of Neighbouring Group Assisted Click Reactions." Dissertation, Georgia State University, 2016.
doi: <https://doi.org/10.57709/8476886>

This Dissertation is brought to you for free and open access by the Department of Chemistry at ScholarWorks @ Georgia State University. It has been accepted for inclusion in Chemistry Dissertations by an authorized administrator of ScholarWorks @ Georgia State University. For more information, please contact scholarworks@gsu.edu.

NOVEL ANTICANCER AGENTS THAT UPREGULATE P53 AND A NEW TYPE OF
NEIGHBOURING GROUP ASSISTED CLICK REACTIONS

by

ALEXANDER DRAGANOV

Under the Direction of Binghe Wang, PhD

ABSTRACT

In the everlasting battle against cancer the development of drugs targeting new therapeutic pathways is of crucial importance. In the attempt to develop new anticancer agents we have synthesized a library of anthraquinone compounds that show selectivity against leukemia. Mechanistic evaluation of the lead compound reveal that this class of compounds achieve their effects through inhibition of MDM2-MDM4 heterodimer and upregulation of the tumor suppressor p53. Computer aided rational design resulted in the development of a number of compounds with activities in the nanomolar range against various cancer cells. Analysis of the physicochemical properties of selected compounds allowed for their evaluation as potential drug candidates. The successful development of non-toxic formulations permits for the further *in vivo* investigation of the compounds.

Click reactions have found wide spread applications in sensing, materials chemistry, bioconjugation, and biolabeling. A number of very useful click reactions have been discovered, which allow for various applications. In bioconjugation applications, the ability to conduct a secondary conjugation will be very useful in, e.g., protein pull down and binding site identification. Along this line, we describe a neighboring group-assisted facile condensation between an aldehyde and a vicinal aminothiols moiety, leading to the formation of benzothiazoles. The conversion is completed within 5 minutes at low micromolar concentrations at ambient temperature. The facile reaction was attributed to the presence of a neighboring boronic acid, which functions as an intramolecular Lewis Acid in catalyzing the reaction. The boronic acid group is compatible with most functional groups in biomolecules and yet can also be used for further functionalization via a large number of well-known coupling reactions.

INDEX WORDS: Rhein, MDM2, MDM4, p53, anticancer, Click chemistry, Boronic acids,
Biorthogonal conjugation

NOVEL ANTICANCER AGENTS THAT UPREGULATE P53 AND A NEW TYPE OF
NEIGHBOURING GROUP ASSISTED CLICK REACTIONS

by

ALEXANDER DRAGANOV

A Dissertation Submitted in Partial Fulfillment of the Requirements for the Degree of

Doctor of Philosophy

in the College of Arts and Sciences

Georgia State University

2016

Copyright by
Alexander Boryanov Draganov
2016

NOVEL ANTICANCER AGENTS THAT UPREGULATE P53 AND A NEW TYPE OF
NEIGHBOURING GROUP ASSISTED CLICK REACTIONS

by

ALEXANDER DRAGANOV

Committee Chair: Binghe Wang

Committee: David Wilson

Suri Iyer

Electronic Version Approved:

Office of Graduate Studies

College of Arts and Sciences

Georgia State University

May 2016

DEDICATION

I would like to dedicate this work to my grandmother Dr. Danka Pavlova who has been an inspiration and a role model for me my whole life. I only wish you could share this moment with us; may you rest in peace.

I would also like to dedicate this dissertation to my parents Boryan Draganov and Temenuzhka Draganova. Without their encouragement and endless support this would have never been possible. I love you both and I thank you with all my heart!

My wife, Elizabeth Bennett Draganova, has been right next to me in this intellectual journey. I would like to dedicate my work to her as well. You have been my rock, you brought peace to my soul, your love, care and support made this possible. I love you!

ACKNOWLEDGEMENTS

I would like to express my gratitude to my advisor Dr. Binghe Wang. His guidance and support throughout the years shaped me as a scientist and the professional that I am today. I would like to thank Dr. David Wilson and Dr. Suri Iyer for their help, support and advice throughout this journey. I would like to especially thank Dr. Chaofeng Dai who answered every question that I had and was a significant contribution to my training in the skill of organic synthesis. I would like to thank Dr. Nanting Ni, Dr. Yunfeng (Jerry) Cheng, Dr. Weixuan Chen, Dr. Hanjing Peng, Dr. Ke Wang, Dr. Danzhu Wang, Dr. Sarah Zingales, Dr. Krishna Damera, Dr. Lifang Wang, Dr. Bowen Ke and Dr. Siming Wang for the educational and inspiring discussions and collaborations throughout the years. I would like to thank Jalisa Holmes, Zeus De Los Santos, Yueqin Zheng, Sarah Laughlin-Toth, Mengyuan Zhu, Dr. Arpana Sagwal, and Dr. Mei Cui for being such a great and supportive group of people that made the days in graduate school seem to pass so quickly. Last, but not least I would like to thank all other, present and past group members. Every single one of you have left a trace in my life and I have learned a lot from you.

TABLE OF CONTENTS

ACKNOWLEDGEMENTS	v
LIST OF TABLES	x
LIST OF FIGURES	xi
List of Schemes	xiii
1 Novel anticancer agents that upregulate p53	1
<i>1.1 Background and introduction</i>	<i>1</i>
<i>1.1.1 p53.....</i>	<i>1</i>
<i>1.1.2 MDM2/MDM4</i>	<i>3</i>
<i>1.1.3 Compounds targeting MDM2-p53 interactions as anticancer therapeutic strategy</i>	<i>6</i>
<i>1.1.4 Anthraquinone compounds used as anticancer agents</i>	<i>14</i>
<i>1.1.5 References</i>	<i>16</i>
<i>1.2 Mechanistic studies of the lead compound BW-AQ-101</i>	<i>23</i>
<i>1.2.1 Experimental section.....</i>	<i>30</i>
<i>1.2.2 References</i>	<i>34</i>
<i>1.3 Design and synthesis of novel potent anthraquinone compounds as anticancer agents</i>	<i>34</i>
<i>1.3.2 Synthesis of 1,8-diethoxyanthracene-9,10-dione compounds</i>	<i>40</i>
<i>1.3.3 Synthesis of 1,8-dipropoxyanthracene-9,10-dione compounds.....</i>	<i>45</i>

1.3.4	<i>Synthesis of 1,8-bis(benzyloxy)anthracene-9,10-dione compounds</i>	52
1.3.5	<i>Synthesis of 1,8-bis(2-azidoethoxy)anthracene-9,10-dione compounds.....</i>	55
1.3.6	<i>Synthesis of 1,8-bis(vinyloxy)anthracene-9,10-dione compounds.....</i>	58
1.3.7	<i>Synthesis of 1,8-diisobutoxyanthracene-9,10-dione compounds</i>	61
1.3.8	<i>Synthesis of 1,8-bis(isopentyloxy)anthracene-9,10-dione compounds</i>	65
1.3.9	<i>Synthesis of additional anthracene-9,10-dione analogs.....</i>	70
1.3.10	<i>Computational evaluation of the designed compounds.....</i>	73
1.3.11	<i>References</i>	80
1.4	<i>Biological evaluation of novel potent anthraquinone compounds as anticancer agents</i>	81
1.4.1	<i>Evaluation of the 1,8-dimethoxyanthracene-9,10-dione compounds</i>	81
1.4.2	<i>Evaluation of the 1,8-diethoxyanthracene-9,10-dione compounds</i>	82
1.4.3	<i>Evaluation of 1,8-dipropoxyanthracene-9,10-dione compounds.....</i>	83
1.4.4	<i>Evaluation of 1,8-bis(benzyloxy)anthracene-9,10-dione compounds.....</i>	84
1.4.5	<i>Evaluation of 1,8-bis(2-azidoethoxy)anthracene-9,10-dione compounds ..</i>	85
1.4.6	<i>Evaluation of 1,8-bis(allyloxy)anthracene-9,10-dione compounds</i>	86
1.4.7	<i>Evaluation of 1,8-diisobutoxyanthracene-9,10-dione compounds</i>	87
1.4.8	<i>Evaluation of 1,8-bis(isopentyloxy)anthracene-9,10-dione compounds.....</i>	88
1.4.9	<i>Evaluation of additional anthracene-9,10-dione analogs</i>	88
1.4.10	<i>Summary/Discussions</i>	89

1.4.11	<i>Experimental section</i>	90
1.5	<i>Solubility, formulation, and stability studies of selected anthraquinone analogs</i>	
	91	
1.5.1	<i>Solubility evaluation of potent anthraquinone analogs</i>	92
1.5.2	<i>Formulation of selected anthraquinone analogs</i>	97
1.5.3	<i>Stability studies of selected anthraquinone analogs</i>	104
1.5.4	<i>References</i>	107
1.6	<i>Conclusions</i>	107
2	<i>A new type of neighboring group assisted click reactions</i>	108
2.1	<i>Introduction</i>	108
2.1.1	<i>Click and click: biorthogonal reactions allowing for secondary functionalization</i>	109
2.1.2	<i>Dual orthogonal conjugations</i>	112
2.1.3	<i>Multiple orthogonal conjugations</i>	113
2.2	<i>Neighbouring boronic acid promoted click reaction</i>	115
2.3	<i>Conclusion</i>	121
2.4	<i>Experimental section</i>	122
2.5	<i>References</i>	128
	APPENDICES	137
	Appendix A NMR data for the compounds described in Chapter 1	137

Appendix B HPLC data for the stability studies described in Chapter 1	239
Appendix C NMR data for the compounds described in Chapter 2	301

LIST OF TABLES

Table 1.1 IC ₅₀ values of synthesized 1,8-dimethoxyanthracene-9,10-dione analogs	82
Table 1.2 IC ₅₀ values of synthesized 1,8-diethoxyanthracene-9,10-dione analogs	83
Table 1.3 IC ₅₀ values of synthesized 1,8-dipropoxyanthracene-9,10-dione analogs	84
Table 1.4 IC ₅₀ values of synthesized 1,8-bis(benzyloxy)anthracene-9,10-dione analogs	85
Table 1.5 IC ₅₀ values of synthesized 1,8-bis(2-azidoethoxy)anthracene-9,10-dione analogs	86
Table 1.6 IC ₅₀ values of synthesized 1,8-bis(allyloxy)anthracene-9,10-dione analogs	87
Table 1.7 IC ₅₀ values of synthesized 1,8-diisobutoxyanthracene-9,10-dione analogs.....	87
Table 1.8 IC ₅₀ values of synthesized 1,8-bis(isopentyloxy)anthracene-9,10-dione analogs	88
Table 1.9 IC ₅₀ values of synthesized anthracene-9,10-dione analogs.....	89
Table 1.10 Physicochemical characteristics of selected rhein analogs.....	95
Table 1.11 Formulation of BW-AQ-101	98
Table 1.12 Formulation of BW-AQ-112	99
Table 1.13 Formulation of BW-AQ-113	100
Table 1.14 Formulation of BW-AQ-124	101
Table 1.15 Formulation of BW-AQ-126	102
Table 1.16 Formulation of BW-AQ-131	103
Table 1.17 Stability studies in solution at 37 °C.....	105
Table 2.1 Biorthogonal reactants used in single molecule for sequential “click” reactions/ conjugations.	111
Table 2.2 Design of boronic acid facilitated “click” reaction.....	116
Table 2.3 Scope of the developed cyclization reaction.....	119

LIST OF FIGURES

Figure 1.1.1 A cartoon representation of the p53's response to cellular stress.	3
Figure 1.1.2 A cartoon representation of the MDM2 and MDM4 primary structures.	5
Figure 1.1.3 A cartoon representation of the MDM2-p53 regulatory loop.	6
Figure 1.1.4 Selected examples of potent MDM2-p53 PPI inhibitors.....	11
Figure 1.1.5 Selected MDM2 ligase inhibitors.	14
Figure 1.1.6 Rhein and selected clinically used anthraquinone anticancer agents.	16
Figure 1.2.1 Structure and activity (based on MTT assay) of BW-AQ-101.....	24
Figure 1.2.2 Effects of BW-AQ-101 on p53, MDM2 and MDM4;.....	26
Figure 1.2.3 The binding pocket of MDM2:.....	27
Figure 1.2.4 ITC binding assay of BW-AQ-101 against: A) MDM2 and B) MDM4	29
Figure 1.2.5 Comet assay of EU-1 cells	30
Figure 1.3.1 1,8-dimethoxyanthracene-9,10-dione analogs.....	38
Figure 1.3.2 Synthesis of 1,8-diethoxyanthracene-9,10-dione analogs	42
Figure 1.3.3 Synthesis of 1,8-dipropoxyanthracene-9,10-dione analogs.....	47
Figure 1.3.4 Synthesized of 1,8-bis(benzyloxy)anthracene-9,10-dione analogs	53
Figure 1.3.5 Synthesized of 1,8-bis(2-azidoethoxy)anthracene-9,10-dione analogs.....	57
Figure 1.3.6 Synthesized of 1,8-bis(vinyloxy)anthracene-9,10-dione analogs.	60
Figure 1.3.7 Synthesized of 1,8-diisobutoxyanthracene-9,10-dione analogs	62
Figure 1.3.8 Synthesized of 1,8-bis(isopentyloxy)anthracene-9,10-dione analogs	66
Figure 1.3.9 Synthesized of various anthracene-9,10-dione analogs.....	71

Figure 1.3.10 Structures of the MDM2 RING homodimer and the MDM2-MDM4 RING heterodimer	74
Figure 1.3.11: The Residues forming the binding cavity of the MDM2 RING homodimer	75
Figure 1.3.12 Superimposed MDM2 RING domain extracted from the heterodimer and the homodimer	76
Figure 1.3.13 View of successfully bound anthraquinone analogues.....	77
Figure 1.3.14: Relative docking score of selected compounds.....	77
Figure 1.3.15 Various athraquinone analogs docked in the binding pocket.....	78
Figure 1.3.16 The binding hypothesis.....	79

LIST OF SCHEMES

Scheme 1.1 General synthetic route to various active anthraquinones.....	36
Scheme 1.2: General synthetic route to compounds 8a-8d	37
Scheme 1.3 Synthesis of compound 11 through Sonogashira coupling	37
Scheme 1.4 General synthetic route to compounds 14a-14g	41
Scheme 1.5 Synthesis of compound 14h	41
Scheme 1.6 General synthetic route to compounds 16a-16i	46
Scheme 1.7 Synthesis of compound 16j	46
Scheme 1.8 General synthetic routes to compounds 18a-18d	52
Scheme 1.9 Synthesis of compound 18e	52
Scheme 1.10 Synthesis of compound 21a and 21b	56
Scheme 1.11 General synthetic route to compounds 23a and 23b	59
Scheme 1.12 Synthesis of compound 23c	59
Scheme 1.13 General synthetic route to compounds 25a-25e	62
Scheme 1.14 General synthetic route to compounds 27a-27f	65
Scheme 1.15 Synthesis of compound 27g	66
Scheme 1.16 Synthesis of compound 29, 31, 33	71
Scheme 2.1 Proposed mechanism (R1 = H, Me, OMe, OBn, OCF ₃ , F; R2 = H, Cl, CF ₃).....	120
Scheme 2.2 The use of the boronic acid as a handle for further modifications	121

1 NOVEL ANTICANCER AGENTS THAT UPREGULATE P53

1.1 Background and introduction

Cancer is one of the leading causes of death in modern society and the medical and scientific communities throughout the world have been engaged in an ongoing battle with this deadly disease for decades. Although, incremental progress in controlling this modern-day “plague” has been achieved and the grand statistics for 2015 have shown a decrease in mortality, the number of global cancer incidence steadily keeps rising.¹ Furthermore, the incidence in adolescent acute solid tumor and leukemia have been increasing by approximately 0.6 % per year since 1975.¹ Thus, new and more efficient therapeutic strategies against cancer are of immediate need. Herein, we disclose the development of series of anthraquinone-based compounds that show potency against a number of cancer cell lines. These compounds show preferential inhibition against leukemia cell lines as well as efficacy against drug resistant cancer cells. The developed lead compound induces cellular death through the inhibition of MDM2/MDM4 interactions, consequently elevating p53 levels in the cell, leading to apoptosis.

1.1.1 p53

One of the key factors in the mammalian system responsible for the cellular viability in a “stress” situations is the transcription factor p53. This so-called “genome guardian” is a tumor suppressor protein that is 43.7 kDa in size and its levels in normal cells are tightly regulated.² In addition to protein suppression through transcription, p53 possesses regulatory cytoplasmic activity.^{3,4} p53 has been shown to interact with proteins from the Bcl-2 family, thus activating, in a non-transcriptional manner, the pro-apoptotic BH3 proteins.⁵ There are also reports indicating the importance of p53 in double-stranded RNA degradation, autophagy inhibition, and improved mitochondrial permeability of the Bcl-2 proteins.⁶ Thus, regulation of this protein in the

mammalian cell is of extreme importance. There is a number of ways to regulate p53 activity; through translocation and degradation via ubiquitin ligases, post-translational modifications, transcriptional co-activator, etc.⁷ However, the key player in the p53 regulatory process is MDM2; an active E3 ubiquitin ligase. The importance of this ligase has been exemplified in a number of studies where deletion of *Mdm2* gene resulted in early embryonic death due to p53-induced apoptosis.⁸ Although tightly regulated under physiological cellular environment, in stress conditions p53 regulation is swiftly abolished and activated p53 establishes a stress response (Figure 1). Activation of p53 has been shown in response to DNA damage, genotoxic disturbances, abnormal cell proliferation, hypoxia, and nutrient deprivation.^{4,9-12} There is a number of ways that p53 suppresses tumor development: apoptosis, autophagy, senescence, and promotion of growth arrest.^{13,14} In the case of DNA damage, for example due to radiation, two major kinases ATM (ataxia telangiectasia mutated) and Chk2 activate p53 through subsequent phosphorylation events.¹⁵⁻¹⁷ Overexpression of p53 in this case will directly signal for either programmed cell death through transcription of the Bax gene or stimulation of other pro-apoptotic proteins from the Bcl-2 family.¹³ Abnormal cell proliferation and growth activate p53 through the p14^{ARF} protein.¹⁸ This protein inhibits the negative regulation of p53 and is a product of increased mitotic signaling, normally due to the production of the Ras and Myc oncogenes during the process of cellular division.¹⁸ These events result in cell cycle arrest through p53 dependent expression of p21, a cyclin-dependent kinase (CDK) inhibitor. Unfortunately, about 50% of the cancer cells have developed p53 mutations, thus keeping it dormant.^{2,19} Despite that, the majority of cancers control p53 levels by overexpressing its lead negative regulator; MDM2.^{2,20} Overexpression of the MDM2 ubiquitin ligase and its homolog MDM4 are benchmark source of inactivation/regulation of the tumor suppressor p53.¹⁰ The p53 protein in normal cells is present at low concentration and has a

short half-life (10 – 15 min).² There is a constant cycle of proteosomal-dependent degradation and production of p53.² There are numbers of E3 ubiquitin ligases that play part in this process, however, the major contributor to the p53 degradation is MDM2.²¹⁻²³ The inhibition of MDM2 allows the buildup of p53 to be quickly achieved under stress conditions in normal cells. Furthermore, this process is clearly observed under stress conditions such as, hypoxia, pH shock, heat stress, genotoxic stress, and ribosomal stress.^{24,25} Cancer cells that possess wild-type p53 have developed a mechanism where MDM2 levels are kept high, resulting in down regulation of p53 and inhibition of pro-apoptotic response. This makes MDM2 an attractive therapeutic target.

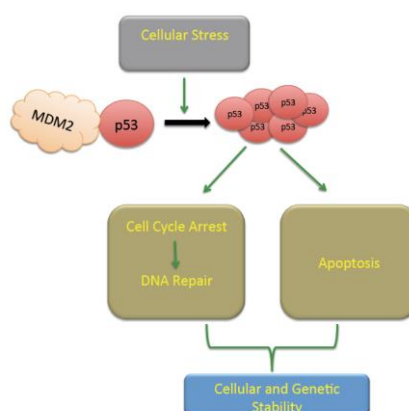


Figure 1.1.1 A cartoon representation of the p53's response to cellular stress.

1.1.2 MDM2/MDM4

The MDM2 (murine double minute 2) protein was first isolated from 3T3DM mouse cell lines in the 1980s.² Shortly after the protein was isolated it was found that it can bind and inhibit p53 tumor suppressor.²⁶ MDM2 is an E3-ubiquitin ligase from the RING (Really Interesting New Gene) family that exists as a homodimer under physiological conditions. MDM2 consists of 491 amino acids and has three major domains: the C-terminal RING domain (the E3 ligase domain), a Zinc finger domain, and the p53-binding N-terminal domain (Figure 2). As a p53

inhibitor, the regulation of MDM2 is very strictly controlled. MDM2 undergoes post-translational modifications under cellular stress, so the p53 protein concentrations can be stabilized or increased.² On the other hand when cells are under physiological conditions and there is lack of external cellular stress, MDM2 inactivates p53 in two major ways. The first and most obvious way of p53 regulation by the MDM2 is through the E3 ubiquitin ligase activity; meaning that p53 is being ubiquitinated and proteosomally degraded.^{27,28} The second method of p53 inactivation by MDM2 is shown to be through binding to the transactivation domain of p53 and blocking its transcriptional activity.^{26,29} Studies have shown that MDM2 itself is oncogenic and can cause tumor formations in nude mice when overexpressed.³⁰ MDM2 has been found to be overexpressed in a number of cancer cells containing wild-type p53 including, but not limited to, leukemia cells, osteosarcomas and sarcomas.^{31,32} Direct regulation of MDM2 can be achieved via post-translational modifications such as inactivation through phosphorylation by ATM or Chk2 kinases.¹⁷ Another major regulatory way of this ligase is through a negative feedback loop that uses overexpressed p53 to abolish the MDM2 gene transcription (Figure 3).³³ An interesting fact is that MDM2 can regulate itself through self-ubiquitination as well.²⁴ This can be achieved via post-translational modifications (phosphorylation, SUMOlation, etc.) independent from MDM2's activity against p53.^{34,35} Weissman and co-workers showed that the self-ubiquitination activity of MDM2 is RING independent.³⁵ The RING domain is a common structural feature of the RING E3 ubiquitin ligase family. In an experiment where the RING region of MDM2 was replaced with PRAJA1 domain, the p53 ubiquitination was abolished but the self-ubiquitination activity was retained.³⁵ This clearly shows the complexity of the p53-MDM2 network.

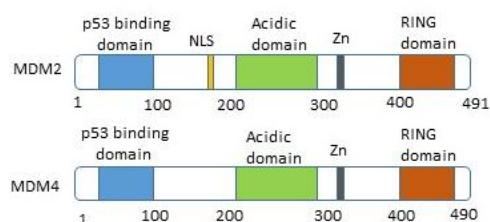


Figure 1.1.2 A cartoon representation of the MDM2 and MDM4 primary structures.

A number of p53 and MDM2 knockout studies has given proof that MDM2 is in fact a direct negative regulator of p53.³⁶⁻³⁸ As previously mentioned, a crucial structural feature of MDM2 is the RING domain.³⁹ The transfer of ubiquity from E2 ligases to a target protein is not the only essential function of this domain, it is also utilized as a handle for protein-protein interactions; MDM2 uses the RING region to form stable heterodimeric structures with its homolog MDM4.² Although MDM4 is a structural homolog of MDM2, it does not carry E3 ligase activity. However, it has been proposed that through the heterodimer of the two homologs, MDM2 and MDM4, has enhanced E3 ubiquitin ligase activity compared to the MDM2 homodimer.^{40,41} In fact, evidence has shown that the MDM2-MDM4 complex is responsible for polyubiquitination of p53 compared to monoubiquitination by sole MDM2 homodimer.^{2,42} In addition, MDM2 serves as negative regulator of MDM4 through direct ubiquitination.^{42,43} MDM4 is a 90% homolog of MDM2 and has been found to be overexpressed in a number of cancer cells that contain the p53 wild-type protein.^{2,44,45} This fact suggests that MDM4 plays an important role in the regulation of p53. In fact MDM4 binds to p53 and directly regulates its activity.^{24,46} There are two major theories that place MDM4 in the regulation pathway of p53.² The first theory deals with the idea that MDM2 and MDM4 play distinct roles in the regulation of p53 and the second theory is that the MDM2-MDM4 complex is the main p53 regulatory machine.² Both theories are supported by

experimental results and the question of what is the exact mechanism of p53 regulation regarding MDM2 and MDM4 stays open. Various *in vivo* tests show that MDM2 inhibits the apoptotic activity of p53 and MDM4 inhibits the cell arrest activity of p53.⁴⁷⁻⁴⁹ On the other hand a number of structural studies have shown that MDM2 and MDM4 depend on each other not only for improvement of the E3 ligase activity, but also the fact that they must function as a unit and control p53 during embryotic development.^{19,50-52} It has also been reported that MDM2 and MDM4 form energetically much more stable heterodimer as compared to the MDM2 homodimer.⁵³ As the question for the exact regulation of p53 stays open, it is clear that the disruption of the p53-MDM2-MDM4 regulatory cycle is an attractive therapeutic strategy.

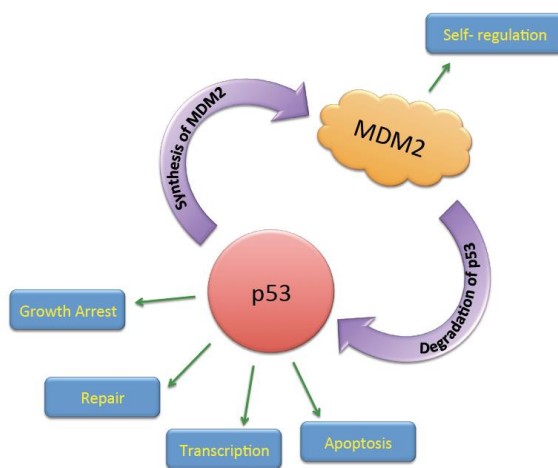


Figure 1.1.3 A cartoon representation of the MDM2-p53 regulatory loop.

1.1.3 Compounds targeting MDM2-p53 interactions as anticancer therapeutic strategy

In addition to the fact that MDM2 and MDM4 are overexpressed in over 50% of cancers, their importance in the negative regulation of the vital tumor suppressor p53 makes these two proteins very critical anticancer targets. In fact there is a number of academic and industrial groups that have been actively pursuing this idea and as of 2015 there are seven compounds that reached

clinical trials.⁵⁴ The development of small molecules to successfully block protein-protein interactions (PPIs) is one of the biggest challenges in medicinal chemistry. Generally speaking protein-protein interactions are dynamic processes and occur on a relatively large and hydrophobic surface area of the proteins. Thus, it is understandable that in order to be efficient, a small molecule inhibitor of PPIs must be an extremely specific and potent binder. This section of the chapter briefly describes some of the most potent MDM2-p53 inhibitors.

1.1.3.1 Nutlin and nutlin-based analogs as MDM2 binders

The breakthrough discovery in the field of MDM2-p53 inhibition was done by Hoffman La Roche with the development of nutlin.⁵⁴ This compound has an $IC_{50} = 90$ nM (enzymatic inhibition) and was the first small molecule to be co-crystalized with MDM2. The crystal structure of this binding truly opened the door for the development of a number of active compounds targeting this binding pocket. Nutlin and its analogs target the *N*-terminal residues of MDM2 that form a hydrophobic pocket (Phe19, Trp23, Leu26), which has been shown to be the key interface in the MDM2-p53 interactions. Although, nutlin showed cellular growth inhibition in the range of 1-2 μ M IC_{50} and lack of obvious toxicity at 200 mg/kg twice a day for 20 days in mouse models, it needed improvement in its pharmacokinetic properties.^{54,55} An optimized version of nutlin (RO5045337) with a lower molecular weight reached phase I clinical trials after showing improvement in MDM2 binding affinity ($IC_{50} = 18$ nM), pharmacokinetic properties, improved metabolic profile, and improved redox stability (Figure 4).^{55,56} Despite the fact that the compound showed potency, the phase I results indicated that the drug candidate showed some hematological toxicity, making it unsuitable for further development.

1.1.3.2 Pyrrolidine-containing MDM2 inhibitors

La Roche developed a second compound (RO5503781) that reached phase I clinical trials (Figure 4).^{57,58} This compound was developed based on the crystal structure of nutlin bound to MDM2; however, the compound is structurally very different. RO5503781 retains the general three aromatic rings peripheral groups responsible for pi-pi interactions in the binding pocket. However, the five membered core is pyrrolidine rather than being an imidazole ring. This of course is a basis for a completely new class of compounds targeting the inhibition of MDM2-p53 interactions. RO5503781 has an $IC_{50} = 6$ nM, 80 % oral bioavailability, and good tolerance in mice. The reported maximum tolerated dose is 500 mg, in a 5 day schedule, twice daily.⁵⁸ The compound did exhibit side effects, such as neutropenia, and diarrhea at the maximum tolerated dose. The disclosed side effects were well within the acceptable limits, and as of 2015, the compound was scheduled to progress to phase II clinical trials.

1.1.3.3 Spirooxindole-containing MDM2 inhibitors

An MDM2 inhibitor (SAR405838) developed by Shaomeng Wang's group at University of Michigan was advanced to clinical trials by Sanofi S.A. in 2012 (Figure 4).^{54,59} This compound contains a central pyrrolidine ring; however, a spirooxindole structural feature significantly distinguishes this compound from the previously discussed MDM2 inhibitors. The compound was developed through computational design and docking studies, in an attempt to obtain a strong fit in the Phe19, Trp23, Leu26 binding pocket of MDM2. Co-crystal structure of compound SAR405838 and MDM2 showed that in addition to the mimicked interactions of the p53 binding residues to Phe19, Trp23, Leu26 the compound is stabilized in the pocket through additional interactions.⁵⁹ For example, the 2-fluoro-3-chlorophenyl is actively involved in a pi-pi stacking with a histidine group of MDM2, the Cl attached to the oxindole ring participates in hydrophobic

interactions. These structural features allow for the compound to have MDM2 binding constant of about 0.88 nM with cellular IC_{50} range of 100-200 nM in various cancer cell lines.⁵⁹ The phase I clinical trial results have not been disclosed at this point, however, the compound has shown significant tumor regression at 100 mg/kg daily dose through oral administration in animal models.⁶⁰ SAR405838 is the most successful example among a number of spirooxindole MDM2 inhibitors that have been developed thus far.

1.1.3.4 Piperidinone-containing MDM2 inhibitors

Virtual exploration of the Phe19, Trp23, Leu26 binding pocket of MDM2 led to the discovery of another class of active p53-MDM2 interaction inhibitors. This class of compounds and in particular AMG 232 developed by Amgen is structurally different not only by the central core ring, but also with the branched chains (Figure 4).⁶¹ The only resemblance of this compound with the active analogs from the spirooxindole, pyrrolidine, and nutlin based MDM2 inhibitors is the two aromatic side chains containing Cl on positions 2 and 3 respectively. AMG 232 and inhibitors from its class contain a piperidinone core ring, a six membered cyclic amide. This structural feature introduces a hydrogen bond acceptor in the core structure. In addition, a free carboxylic acid and a sulfonyl group were introduced as side chains. These structural features not only allow for additional hydrogen bond and salt bridge formations in the MDM2 binding pocket, but also contribute to the bioavailability and pharmacokinetic properties of the compound. AMG 232 has enzymatic IC_{50} of 0.6 nM and cellular growth inhibition of 9.1 nM in the p53 wild-type SJSA-1 cell line.⁶¹ The compound has shown complete tumor regression in *in vivo* models through oral administration of 60 mg/kg daily and 16 mg/kg twice daily dose in SJSA-1 and HCT-116 xenograft mice models.^{61,62} To our best knowledge, as of 2015 no significant side toxicity or side

effects of this compound have been reported, and its pharmacokinetic and pharmacodynamics properties are being further investigated.

1.1.3.5 Dihydroisoquinolinone-based MDM2 inhibitors

Another very potent class of MDM2 inhibitors developed from virtual screening and computational design based on the Phe19, Trp23, Leu26 binding pocket came from Novartis with their discovery of CGM097 (Figure 4).⁶³ This is a compound that has a dihydroisoquinolinone core structure. The cyclic amide fragment resembles the piperidinone cores of the class of compounds described in section 1.3.4; however, CGM097 and the analogs from its class are much more constrained as per the presence of a fused aromatic system. The presence of 4-chlorophenyl ring is another reoccurring structural feature that is of importance in making the hydrophobic contact in the MDM2 binding pocket. These functionalities resulted in excellent binding with an affinity of CGM097 to MDM2 of about 1.7 nM. These results were supported by promising proliferation inhibition values in the range of 200-300 nM for various p53 wild-type cancer cell lines.⁶⁴ The developed compound did not show significant toxicity. However, a minor fraction in animals (mouse and monkey) studies indicated perturbations in the organs with high cellular turnover (i.e. bone marrow, the lymphoid organs, the GI tract, etc.).⁶⁴ The results were considered sufficiently promising that the compound was advanced to phase I clinical trials.

1.1.3.6 Additional potent MDM2 inhibitors and compounds in clinical trial

Two additional inhibitors with undisclosed chemical structures SCH 900242 and MK-8242 have been reported in clinical trials by Daiichi Sankyo Inc. and Merck respectively.⁵⁴ These compounds are being tested in advanced leukemia and solid-state tumor patients in combination with cytarabine. There is a large number of other potent agents that are designed to mimic the p53 helical region that binds to the Phe19, Trp23, Leu26 binding pocket, but have not really reached the

potential to be considered drug candidates. The importance of this therapeutic target is clear and there is a number of outstanding reviews that go into details describing each class of compounds.^{54,65,66} Some of the most noteworthy classes that may lead to compounds entering clinical trials are chalcones, benzodiazepine, isoindolinone, chromenotriazolopyrimidine, and dihydroimidazothiazol-containing compounds. In addition, a number of the reported compounds with the following structures have shown dual inhibition of MDM2 and MDM4 binding to p53: *cis*-imidazolines, indolyl-hydantoins, pyrrolopyrimidines, and oxalopiperidinone lactams.⁵⁴ Although highly potent, none of the compounds that belong to the listed classes have yet reached clinical trials.

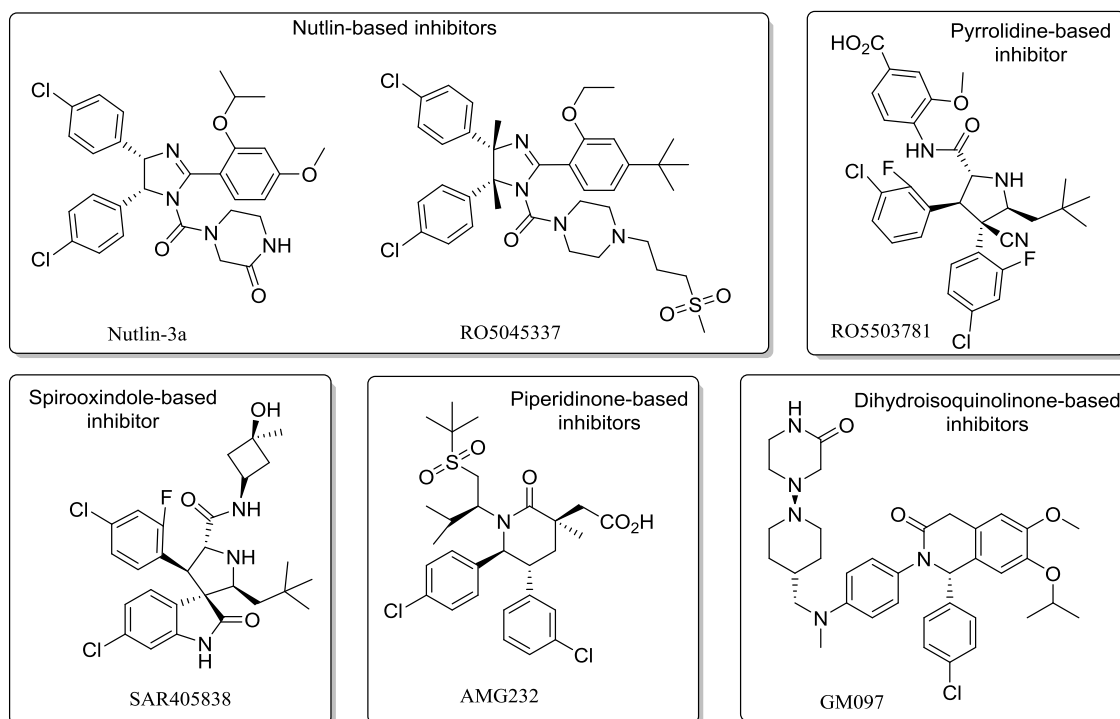


Figure 1.1.4 Selected examples of potent MDM2-p53 PPI inhibitors.

1.1.3.7 Peptides as MDM2 inhibitors.

As it was discussed earlier in this chapter, generally speaking disruption of PPI by small molecules is very difficult. In the case of MDM2 inhibitor development, a vast majority of small molecules have been designed based on the structure of the Phe19, Trp23, Leu26 binding pocket. It has been shown that this pocket binds an α -helical region of p53, thus substantial effort has been applied towards the development of successful molecular mimics of this helical interaction with MDM2. Since the natural substrate of this binding pocket is a helical peptide, the development of synthetic peptides as MDM2 binders has been attempted as well. Thus, employing the strategy of synthetically binding or “stapling” peptides, so that they retain specific structure (i.e. α -helix), as MDM2 binders has shown promise. The downside of this strategy is that synthetic linear peptides can exist in various conformations under physiological conditions. The idea of structurally constraining small peptides as active agents has been extensively explored in the field of antibiotics development.⁶⁷⁻⁶⁹ Two examples of stapled peptides targeting MDM2-p53 interactions stand out in the literature: SAH-p53-8 and ATSP-7041. After a number of modifications in an attempt to develop stabilized α -helix (SHA) of p53 as a potent PPI inhibitor Walensky and co-workers developed SAH-p53-8.⁷⁰ The developed peptides used olefin metathesis to staple strategically incorporated hydrocarbons together and stabilize the helical structure. SAH-p53-8 is a compound that actively permeates cellular membrane and has proliferation inhibition of 8.5 μ M against SJSA-1 cell line. The *in vitro* data clearly shows p53 dependent apoptosis of the cancer cells after treatment with the designed peptide.⁷⁰ In addition, the peptide was reported to be more potent MDM4 binder ($K_D = 2.3$ nM) than MDM2 ($K_D = 55$ nM).⁷¹ *In vivo* experiments showed the significant inhibition of tumor growth in a JEG-3 xenograft mouse model and lack of significant toxicity to normal cells.⁷¹ The lack of detailed pharmacokinetic (PK) and pharmacodynamics (PD)

data for SAH-p53-8 does not allow for this compound to be advanced to clinical trials at this point. Another very potent stapled peptide as dual MDM2, MDMX inhibitor was developed by Aileron Therapeutics, Inc.⁷² The peptide successfully induces apoptosis through the p53 signaling network. ATSP-7041 was developed through a similar olefin metathesis as utilized by Walensky's lab. *In vitro* and *in vivo* studies showed the efficacy of this peptide in reducing tumor growth.⁷² The compound was tested in 3 animal models, mouse, rat, and monkey and exhibited promising PK and PD profiles.⁷² These peptides serve as examples that the dual inhibition of MDM2 and MDM4 interactions with p53 might be an alternative in the development of new anticancer strategy.

1.1.3.8 Inhibitors of the MDM2 E3 Ligase

In addition to MDM2-p53 PPI inhibition and the dual MDM2/MDM4-p53 PPI inhibition, a third strategy to activate the p53 pathway has emerged in the recent years; selective inhibition of the MDM2 activity. This strategy aims to develop selective binders to the E3 active center (the RING domain) of MDM2, thus inactivating its ligase activity towards p53 upon binding. To our best knowledge, there have only been two reports of MDM2 inhibitors that activate the p53 apoptotic pathway upon binding to the E3 ligase RING domain.^{42,73,74} Both groups came across these two classes of compound after high-throughput screening of libraries of compounds against RING E3 ligases. In 2005 Weissman and co-worker reported the first pyrimido-dione-quinoline as MDM2 RING domain binder.⁷⁴ This compound opened a new class of inhibitors, which possess a flat aromatic core structure. The first generation of compounds (HLI98) described by Weissman generally suffered from poor water solubility, hindering the ability to develop the compounds as potent therapeutic agents (Figure 5). In terms of proof of principle, these compounds showed selective inhibition of MDM2 in the 20-50 μM (PRE cells) range and mechanistic studies clearly indicated the activation of the p53 pathway.⁷⁴ The same group reported the water soluble HLI373,

possessing pyrimido-dione-quinoline and improved IC_{50} value of 3 μM against PRE cells.⁷³ The compound, however, showed off-target effects that did not allow for their further development as therapeutic agent.

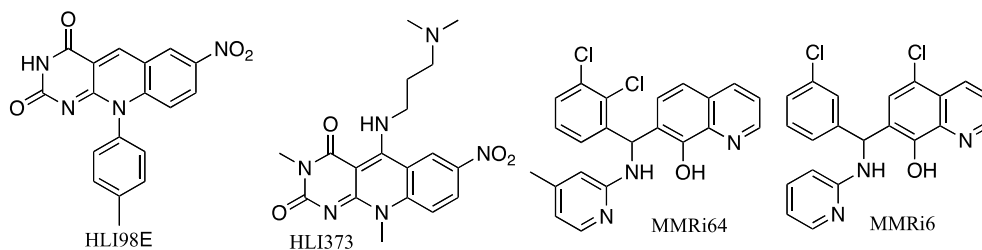


Figure 1.1.5 Selected MDM2 ligase inhibitors.

Utilizing Foster resonance energy transfer (FRET)-based high-throughput assay, a quinoline-based MDM2-MDM4 RING-RING PPI inhibitors were reported by Wang and co-workers in 2015 (Figure 5).⁴² These inhibitors showed significant upregulation of p53 and downregulation of MDM2 in leukemia cell lines. In addition to the reported $IC_{50} = 0.5 \mu M$ against lymphoma cell lines (wt-p53); interestingly the self-ubiquitination activity of MDM2 was retained. The retention of self-ubiquitination activity is evidence for the specific blockage of MDM2-MDM4 RING-RING interactions, but not MDM2-MDM2 interactions. The inhibition of MDM2-MDM4 PPIs with the purpose of activation of p53 is truly a novel anticancer therapeutic strategy. The therapeutic evaluation of the reported compounds, MMri6 and MMri64, needs to be further investigated; however, the mechanistic evidence of their action truly opens a new therapeutic ground for exploration.

1.1.4 Anthraquinone compounds used as anticancer agents

The development of novel (in terms of mechanism of action and structural scaffold) nontoxic, target-specific anticancer agents is of great need. In attempt to solve this issue, a number of scientists across the world have turned to nature for a solution. Though evolutionary

development, nature has found a way to control abnormalities in earth's eco-system. One of the ways that nature does that is through the enzymatic/evolutionary development of natural products, which have served as active agents against a number health-threatening conditions. With this in mind and in the search of new anticancer therapies we looked to nature and into the anthraquinone-based natural product rhein.

Rhein is a natural product isolated from the ground plant Rhubarb, which belongs to the Rheum family. Compounds that have structural similarities to rhein, such as doxorubicin, daunorubicin and mitoxanthrone, have been successfully marketed as anticancer drugs (Figure 5).⁷⁵⁻⁷⁷ These compounds belong to the anthracycline family and have been extensively used in clinical settings for the treatment of various cancers. Despite the excellent anticancer activity, however, they have shown serious side effects such as cardiotoxicity.^{75,77} Generally speaking the compounds from the anthracycline family have been reported to follow one or more of the following mechanisms of action: a) DNA intercalation and inhibition of its synthesis, b) DNA damage through free radical generation, c) binding of DNA, d) DNA alkylation/cross-linking, e) DNA damage through topoisomerase II inhibition, and f) direct topoisomerase II inhibition.⁷⁸ A common belief is that the cardiotoxicity of doxorubicin and daunorubicin derives from their redox chemistry leading to free radical formation and the subsequent lipid peroxidation.⁷⁸ It is well known that single electron addition to the dienone ring of the anthracycline core generates reactive oxygen species (ROS), which lead to cellular damage. The generation of ROS and oxidative DNA damage has been observed at supraclinical concentrations of doxorubicin; however, at low micromolar concentration the effects of DNA damage through topoisomerase inhibition is predominant. The generation of ROS at high treatment concentrations is of major concern and potentially the cause of the potentially lethal side effects developed by patients treated with this

family of drugs. Recent findings that carbon monoxide can ameliorate doxorubicin's cardiotoxicity through mitochondrial biogenesis also lends insight into the mechanism of the cardiotoxic actions of doxorubicin.^{79,80} Clinical studies have shown that 36% of patients treated with multiple doses of 500 mg/m² doxorubicin develop cardiomyopathy.⁸¹

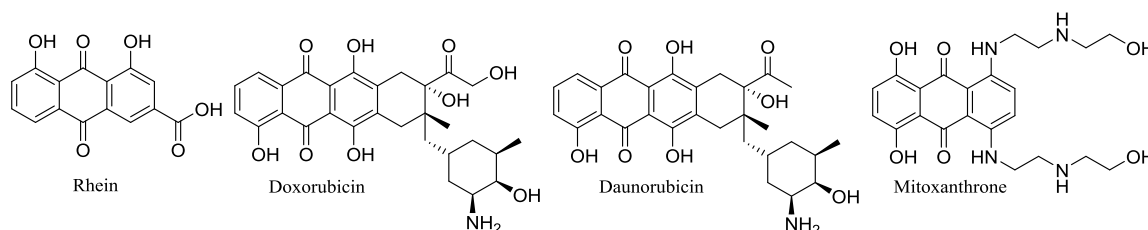


Figure 1.1.6 Rhein and selected clinically used anthraquinone anticancer agents.

There is no question of the efficiency of this class of drugs against various cancers; however, the observed lethal side effects are a serious issue that needs to be addressed. Studies have shown that rhein is well tolerated by the human body when used as a laxative, but it has relatively low anticancer activity with IC₅₀ in the range of 12~120 μ M.⁸²⁻⁸⁶ The low, but promising anticancer activity of rhein and its lack of toxicity make this molecule an excellent starting point for the development of chemical analogs, which can potentially become drug candidates. The development of a new anticancer agent based on the clinically used anthraquinone scaffold, yet lacking intrinsic toxicity to normal cells, is a plausible strategy. The following sections of this chapter describe the utilization of this strategy to develop novel, active anticancer compounds based on rhein.

1.1.5 References

- (1) <http://www.cancer.org/research/cancerfactsstatistics/cancerfactsfigures2015/> 2015.
- (2) Miriam Shadfan, V. L.-P., Zhi-Min Yuan *Transl Cancer Res.* **2012**, *1*, 88.

- (3) Chipuk, J. E.; Bouchier-Hayes, L.; Kuwana, T.; Newmeyer, D. D.; Green, D. R. *Science* **2005**, *309*, 1732.
- (4) Vousden, K. H.; Lane, D. P. *Nature Rev. Mol. Cell Biol.* **2007**, *8*, 275.
- (5) Yee, K. S.; Vousden, K. H. *Carcinogenesis* **2005**, *26*, 1317.
- (6) Green, D. R.; Kroemer, G. *Nature* **2009**, *458*, 1127.
- (7) Laptenko, O.; Prives, C. *Cell Death Differ.* **2006**, *13*, 951.
- (8) Marine, J. C.; Francoz, S.; Maetens, M.; Wahl, G.; Toledo, F.; Lozano, G. *Cell Death Differ.* **2006**, *13*, 927.
- (9) Levine, A. J.; Hu, W.; Feng, Z. *Cell Death Differ.* **2006**, *13*, 1027.
- (10) Levine, A. J.; Oren, M. *Nat. Rev. Cancer* **2009**, *9*, 749.
- (11) Nordstrom, W.; Abrams, J. M. *Cell Death Differ.* **2000**, *7*, 1035.
- (12) Derry, W. B.; Putzke, A. P.; Rothman, J. H. *Science* **2001**, *294*, 591.
- (13) Vousden, K. H.; Prives, C. *Cell* **2009**, *137*, 413.
- (14) Donehower, L. A.; Lozano, G. *Nat. Rev. Cancer* **2009**, *9*, 830.
- (15) Vogelstein, B.; Lane, D.; Levine, A. J. *Nature* **2000**, *408*, 307.
- (16) Carr, A. M. *Science* **2000**, *287*, 1765.
- (17) Cheng, Q.; Chen, J. *Cell Cycle* **2010**, *9*, 472.
- (18) Sherr, C. J.; Weber, J. D. *Curr. Opin. Genet. Dev.* **2000**, *10*, 94.
- (19) Huang, L.; Yan, Z.; Liao, X.; Li, Y.; Yang, J.; Wang, Z.-G.; Zuo, Y.; Kawai, H.; Shadfan, M.; Ganapathy, S.; Yuan, Z.-M. *P. Natl. Acad. Sci.* **2011**, *108*, 12001.
- (20) Hollstein, M.; Sidransky, D.; Vogelstein, B.; Harris, C. C. *Science* **1991**, *253*, 49.
- (21) Wang, X.; Jiang, X. *Febs Lett.* **2012**, *586*, 1390.
- (22) Scheffner, M. *J. Pharm. Thera.* **1998**, *78*, 129.

- (23) Brooks, C. L.; Gu, W. *Mol. Cell* **2006**, *21*, 307.
- (24) Wade, M.; Wang, Y. V.; Wahl, G. M. *Trends Cell Biol.* **2010**, *20*, 299.
- (25) Zhang, Y.; Lu, H. *Cancer Cell* **2009**, *16*, 369.
- (26) Momand, J.; Zambetti, G. P.; Olson, D. C.; George, D.; Levine, A. J. *Cell* **1992**, *69*, 1237.
- (27) Haupt, Y.; Maya, R.; Kazaz, A.; Oren, M. *Nature* **1997**, *387*, 296.
- (28) Honda, R.; Tanaka, H.; Yasuda, H. *Febs Lett.* **1997**, *420*, 25.
- (29) Oliner, J. D.; Pietsenpol, J. A.; Thiagalingam, S.; Gvuris, J.; Kinzler, K. W.; Vogelstein, B. *Nature* **1993**, *362*, 857.
- (30) Fakharzadeh, S. S.; Trusko, S. P.; George, D. L. *EMBO* **1991**, *10*, 1565.
- (31) Cordoncardo, C.; Latres, E.; Drobnjak, M.; Oliva, M. R.; Pollack, D.; Woodruff, J. M.; Marechal, V.; Chen, J. D.; Brennan, M. F.; Levine, A. J. *Cancer Res.* **1994**, *54*, 794.
- (32) Leach, F. S.; Tokino, T.; Meltzer, P.; Burrell, M.; Oliner, J. D.; Smith, S.; Hill, D. E.; Sidransky, D.; Kinzler, K. W.; Vogelstein, B. *Cancer Res.* **1993**, *53*, 2231.
- (33) Piette, J.; Neel, H.; Marechal, V. *Oncogene* **1997**, *15*, 1001.
- (34) de Bie, P.; Ciechanover, A. *Cell Death Differ.* **2011**, *18*, 1393.
- (35) Fang, S. Y.; Jensen, J. P.; Ludwig, R. L.; Vousden, K. H.; Weissman, A. M. *J. Biol. Chem.* **2000**, *275*, 8945.
- (36) Montes De Oca Luna, R.; Wagner, D. S.; Lozano, G. *Nature* **1995**, *378*, 203.
- (37) Jones, S. N.; Roe, A. E.; Donehower, L. A.; Bradley, A. *Nature* **1995**, *378*, 206.
- (38) Ringshausen, I.; O'Shea, C. C.; Finch, A. J.; Swigart, L. B.; Evan, G. I. *Cancer Cell* **2006**, *10*, 501.
- (39) Geyer, R. K.; Yu, Z. K.; Maki, C. G. *Nat. Cell Biol.* **2000**, *2*, 569.

- (40) Stad, R.; Ramos, Y. F. M.; Little, N.; Grivell, S.; Attema, J.; van der Eb, A. J.; Jochemsen, A. G. *J. Biol. Chem.* **2000**, *275*, 28039.
- (41) Sharp, D. A.; Kratowicz, S. A.; Sank, M. J.; George, D. L. *J. Biol. Chem.* **1999**, *274*, 38189.
- (42) Wu, W.; Xu, C.; Ling, X.; Fan, C.; Buckley, B. P.; Chernov, M. V.; Ellis, L.; Li, F.; Munoz, I. G.; Wang, X. *Cell Death Dis* **2015**, *6*, e2035.
- (43) Pan, Y.; Chen, J. D. *Mol. Cell. Biol.* **2003**, *23*, 5113.
- (44) Danovi, D.; Meulmeester, E.; Pasini, D.; Migliorini, D.; Capra, M.; Frenk, R.; de Graaf, P.; Francoz, S.; Gasparini, P.; Gobbi, A.; Helin, K.; Pelicci, P. G.; Jochemsen, A. G.; Marine, J. C. *Mol. Cell. Biol.* **2004**, *24*, 5835.
- (45) Riemenschneider, M. J.; Buschges, R.; Wolter, M.; Reifemberger, J.; Bostrom, J.; Kraus, J. A.; Schlegel, U.; Reifemberger, G. *Cancer Res.* **1999**, *59*, 6091.
- (46) Toledo, F.; Wahl, G. M. *Int. J. Bio. Cell Biol.* **2007**, *39*, 1476.
- (47) Parant, J.; Chavez-Reyes, A.; Little, N. A.; Yan, W.; Reinke, V.; Jochemsen, A. G.; Lozano, G. *Nature Gen.* **2001**, *29*, 92.
- (48) Grier, J. D.; Xiong, S. B.; Elizondo-Fraire, A. C.; Parant, J. M.; Lozano, G. *Mol. Cell. Biol.* **2006**, *26*, 192.
- (49) Chavez-Reyes, A.; Parant, J. M.; Amelse, L. L.; Luna, R. M. D.; Korsmeyer, S. J.; Lozano, G. *Cancer Res.* **2003**, *63*, 8664.
- (50) Priest, C.; Prives, C.; Poyurovsky, M. V. *Nucleic Acids Res.* **2010**, *38*, 7587.
- (51) Gu, J. J.; Kawai, H.; Nie, L. G.; Kitao, H.; Wiederschain, D.; Jochemsen, A. G.; Parant, J.; Lozano, G.; Yuan, Z. M. *J. Biol. Chem.* **2002**, *277*, 19251.

- (52) Pant, V.; Xiong, S.; Iwakuma, T.; Quintas-Cardama, A.; Lozano, G. *PNAS* **2011**, *108*, 11995.
- (53) Liu, T.; Zhang, H. L.; Xiong, J.; Yi, S.; Gu, L. B.; Zhou, M. X. *Mol. Cancer* **2015**, *14*, 12.
- (54) Zhao, Y.; Aguilar, A.; Bernard, D.; Wang, S. *J. Med. Chem.* **2015**, *58*, 1038.
- (55) Vu, B.; Wovkulich, P.; Pizzolato, G.; Lovey, A.; Ding, Q.; Jiang, N.; Liu, J.-J.; Zhao, C.; Glenn, K.; Wen, Y.; Tovar, C.; Packman, K.; Vassilev, L.; Graves, B. *Med. Chem. Lett.* **2013**, *4*, 466.
- (56) *ClinicalTrials.gov identifiers for RG7112: NCT00559533, NCT00623870, NCT01677780, NCT01164033, NCT01605526, NCT01143740, and NCT01635296.*
- (57) Ding, Q.; Zhang, Z.; Liu, J.-J.; Jiang, N.; Zhang, J.; Ross, T. M.; Chu, X.-J.; Bartkovitz, D.; Podlaski, F.; Janson, C.; Tovar, C.; Filipovic, Z. M.; Higgins, B.; Glenn, K.; Packman, K.; Vassilev, L. T.; Graves, B. *J. Med. Chem.* **2013**, *56*, 5979.
- (58) Siu, L. L.; Italiano, A.; Miller, W. H.; Blay, J.-Y.; Gietema, J. A.; Bang, Y.-J.; Mileschkin, L. R.; Hirte, H. W.; Reckner, M.; Higgins, B.; Jukofsky, L.; Blotner, S.; Zhi, J.; Middleton, S.; Nichols, G. L.; Chen, L. C. *J. Clin. Oncol.* **2014**, *32*.
- (59) Wang, S.; Sun, W.; Zhao, Y.; McEachern, D.; Meaux, I.; Barriere, C.; Stuckey, J. A.; Meagher, J. L.; Bai, L.; Liu, L.; Hoffman-Luca, C. G.; Lu, J.; Shangary, S.; Yu, S.; Bernard, D.; Aguilar, A.; Dos-Santos, O.; Besret, L.; Guerif, S.; Pannier, P.; Gorge-Bernat, D.; Debussche, L. *Cancer Res.* **2014**, *74*, 5855.
- (60) *ClinicalTrials.gov identifiers for MI-77301/SAR405838: NCT01636479 and NCT01985191.*

(61) Sun, D.; Li, Z.; Rew, Y.; Gribble, M.; Bartberger, M. D.; Beck, H. P.; Canon, J.; Chen, A.; Chen, X.; Chow, D.; Deignan, J.; Duquette, J.; Eksterowicz, J.; Fisher, B.; Fox, B. M.; Fu, J.; Gonzalez, A. Z.; De Turiso, F. G.-L.; Houze, J. B.; Huang, X.; Jiang, M.; Jin, L.; Kayser, F.; Liu, J.; Lo, M.-C.; Long, A. M.; Lucas, B.; McGee, L. R.; McIntosh, J.; Mihalic, J.; Oliner, J. D.; Osgood, T.; Peterson, M. L.; Roveto, P.; Saiki, A. Y.; Shaffer, P.; Toteva, M.; Wang, Y.; Wang, Y. C.; Wortman, S.; Yakowec, P.; Yan, X.; Ye, Q.; Yu, D.; Yu, M.; Zhao, X.; Zhou, J.; Zhu, J.; Olson, S. H.; Medina, J. C. *J. Med. Chem.* **2014**, *57*, 1454.

(62) *ClinicalTrials.gov identifiers for AMG 232: NCT01723020 and NCT02016729.*

(63) Holzer, P.; Masuya, K.; Furet, P.; Kallen, J.; Valat-Stachyra, T.; Ferretti, S.; Berghausen, J.; Bouisset-Leonard, M.; Buschmann, N.; Pissot-Soldermann, C.; Rynn, C.; Ruetz, S.; Stutz, S.; Chene, P.; Jeay, S.; Gessier, F. *J. Med. Chem.* **2015**, *58*, 6348.

(64) Holzer, P.; Masuya, K.; Furet, P.; Kallen, J.; Valat-Stachyra, T.; Ferretti, S.; Berghausen, J.; Bouisset-Leonard, M.; Buschmann, N.; Pissot-Soldermann, C.; Rynn, C.; Ruetz, S.; Stutz, S.; Chene, P.; Jeay, S.; Gessier, F. *J. Med. Chem.* **2015**, *58*, 6348.

(65) Wang, W.; Hu, Y. *Med. Res. Rev.* **2012**, *32*, 1159.

(66) Vassilev, L. T. *Trends Mol. Med.* **2007**, *13*, 23.

(67) Boman, H. G. *Annu. Rev. Immunol.* **1995**, *13*, 61.

(68) Fischbach, M. A.; Walsh, C. T. *Chem. Rev.* **2006**, *106*, 3468.

(69) Hancock, R. E. W.; Chapple, D. S. *Antimicrob. Agents Ch.* **1999**, *43*, 1317.

(70) Bernal, F.; Tyler, A. F.; Korsmeyer, S. J.; Walensky, L. D.; Verdine, G. L. *J. Am. Chem. Soc.* **2007**, *129*, 5298.

(71) Bernal, F.; Wade, M.; Godes, M.; Davis, T. N.; Whitehead, D. G.; Kung, A. L.; Wahl, G. M.; Walensky, L. D. *Cancer Cell* **2010**, *18*, 411.

- (72) Chang, Y. S.; Graves, B.; Guerlavais, V.; Tovar, C.; Packman, K.; To, K.-H.; Olson, K. A.; Kesavan, K.; Gangurde, P.; Mukherjee, A.; Baker, T.; Darlak, K.; Elkin, C.; Filipovic, Z.; Qureshi, F. Z.; Cai, H.; Berry, P.; Feyfant, E.; Shi, X. E.; Horstick, J.; Annis, D. A.; Manning, A. M.; Fotouhi, N.; Nash, H.; Vassilev, L. T.; Sawyer, T. K. *P. Natl. Acad. Sci.* **2013**, *110*, E3445.
- (73) Kitagaki, J.; Agama, K. K.; Pommier, Y.; Yang, Y.; Weissman, A. M. *Mol. Cancer Ther.* **2008**, *7*, 2445.
- (74) Yang, Y. L.; Ludwig, R. L.; Jensen, J. P.; Pierre, S. A.; Medaglia, M. V.; Davydov, I. V.; Safiran, Y. J.; Oberoi, P.; Kenten, J. H.; Phillips, A. C.; Weissman, A. M.; Vousden, K. H. *Cancer Cell* **2005**, *7*, 547.
- (75) Tan, J. H.; Zhang, Q. X.; Huang, Z. S.; Chen, Y.; Wang, X. D.; Gu, L. Q.; Wu, J. *Y. Eur. J. Med. Chem.* **2006**, *41*, 1041.
- (76) Katzhendler, J.; Gean, K.-F.; Bar-ad, G.; Tashma, Z.; Ben-shoshan, R.; Ringel, I.; Bachrach, U.; Ramu, A. *Eur. J. Med. Chem.* **1989**, *24*, 23.
- (77) Huang, H. S.; Chin, H. F.; Yeh, P. F.; Yuan, C. L. *Helv Chim Acta* **2004**, *87*, 999.
- (78) Minotti, G.; Menna, P.; Salvatorelli, E.; Cairo, G.; Gianni, L. *Pharmacol. Rev.* **2004**, *56*, 185.
- (79) Bartz, R. R.; Suliman, H. B.; Piantadosi, C. A. *Front. Physiol.* **2015**, *6*, 8.
- (80) Ji, X.; Damera, K.; Zheng, Y.; Yu, B.; Otterbein, L. E.; Wang, B. *J. Pharm. Sci.*, *105*, 406.
- (81) Lefrak, E. A.; Pitha, J.; Rosenheim, S.; Gottlieb, J. A. *Cancer* **1973**, *32*, 302.
- (82) Ip, S. W.; Weng, Y. S.; Lin, S. Y.; Mei-Dueyang; Tang, N. Y.; Su, C. C.; Chung, J. G. *Anticancer Res* **2007**, *27*, 379.

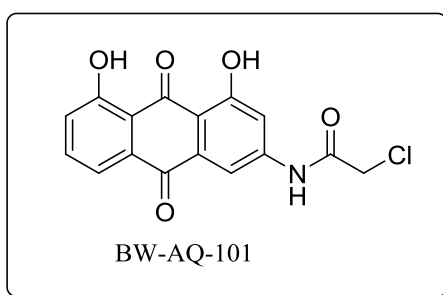
- (83) Cui, X. R.; Tsukada, M.; Suzuki, N.; Shimamura, T.; Gao, L.; Koyanagi, J.; Komada, F.; Saito, S. *Eur. J. Med. Chem.* **2008**, *43*, 1206.
- (84) van Gorkom, B. A. P.; Timmer-Bosscha, H.; de Jong, S.; van der Kolk, D. M.; Kleibeuker, J. H.; de Vries, E. G. E. *Brit J Cancer* **2002**, *86*, 1494.
- (85) Cichewicz, R. H.; Zhang, Y. J.; Seeram, N. P.; Nair, M. G. *Life Sci* **2004**, *74*, 1791.
- (86) Shi, P.; Huang, Z. W.; Chen, G. C. *Am J Chinese Med* **2008**, *36*, 805.

1.2 Mechanistic studies of the lead compound BW-AQ-101

**All biological and mechanistic work described in this section was performed exclusively by Dr. Muxiang Zhou's lab at Emory University. The author of the chapter contributed with synthetic route optimization, preliminary MTT screening against six cell lines, and computational analysis.*

In the pursuit of novel active agents from the anthraquinone family our initial efforts resulted in the development of a few active compounds.¹ One in particular (BW-AQ-101) stood out as a potent agent against leukemia cell lines; $IC_{50} = 0.69 \mu M$ against Molt4 cells. These preliminary findings gave us the stimulus to develop a more efficient synthetic route to BW-AQ-101 and further examine its biological activity and mechanism of action. The synthetic development of a more efficient route was previously disclosed by the author and will not be covered in this section.² Extensive examination against number solid and leukemia cell lines showed that compound BW-AQ-101 has selectivity over leukemia cell lines (Figure 1.2.1). The compound showed low micromolar IC_{50} values against solid tumor cell lines (Hela, KB, Cos 7, and drug resistant T98G) and mid nanomolar activity against selected leukemia cell lines (Molt4,

K562, EU-1). Understanding the mechanism of action of a given compound is of extreme importance in the drug development process. Although there is a number of examples of active agents that have reached clinical trials and even market, the targeted therapeutics strategy has been proven to be the key to the development of safe and efficient drug candidates.^{3,4} Therefore, in collaboration with Dr. Zhou (Emory University) we explored the possible mechanism of action of this compound. As previously described p53 is the key player in cellular response upon cellular stress. Our effort was focused on the examination of the p53 signaling network upon cellular treatment with BW-AQ-101.



Compound	Hela (μ M)	KB (μ M)	Cos7 (μ M)	T98G (μ M)	Molt4 (μ M)	K562 (μ M)	EU1 (μ M)
BW-AQ-101	2.2	16	3.0	>13	0.69	0.93	0.83

Figure 1.2.1 Structure and activity (based on MTT assay) of BW-AQ-101.

Because BW-AQ-101 showed potency against leukemia cell lines, the investigation of its mechanism of action was done by utilizing a number of leukemia cell lines. Five previously-characterized acute lymphoblastic leukemia (ALL) cell lines were selected; Sup-B13, EU-1 and EU-3 cells that have the wt-p53; EU-6 that has a p53 mutation; and EU-8 that has a p53-null phenotype. All cell lines except EU-8 express MDM2 and MDM4. Interestingly BW-AQ-101 showed strong cytotoxic effect in all cell lines expressing wt-p53 and MDM2 and considerably less effect on the other two cell lines (data not shown). This was the first indication that the active compound induces apoptosis in p53-dependent manner. In this line of thought, it was hypothesized

that BW-AQ-101 interrupts the p53-MDM2-MDM4 regulatory cycle, causing apoptosis. Western blot assays indicated significant downregulation of MDM2 in the p53 wild type cell lines treated with the compound, which supported the established hypothesis (Figure 1.2.2 A). In addition, BW-AQ-101 did not show significant effect on the expression of MDM4. As previously discussed, p53 and MDM2 exist in a “love-hate” regulatory cycle, where p53 expresses MDM2 when needed and on the other hand MDM2 downregulates p53 through ubiquitination. Thus, the evaluation of the transcriptional effect of BW-AQ-101 on MDM2 was curtail. RT-PCR experiments demonstrated that the MDM2 mRNA level was significantly elevated by BW-AQ-101. Furthermore, BW-AQ-101 showed no direct inhibitory effect on MDM2 mRNA expression (Figure 1.2.2 B). These results lead to the conclusion that the transcriptional activity of p53 was not abolished. On the contrary, the enhanced MDM2 mRNA expression upon BW-AQ-101 treatment was a result of p53 activation.

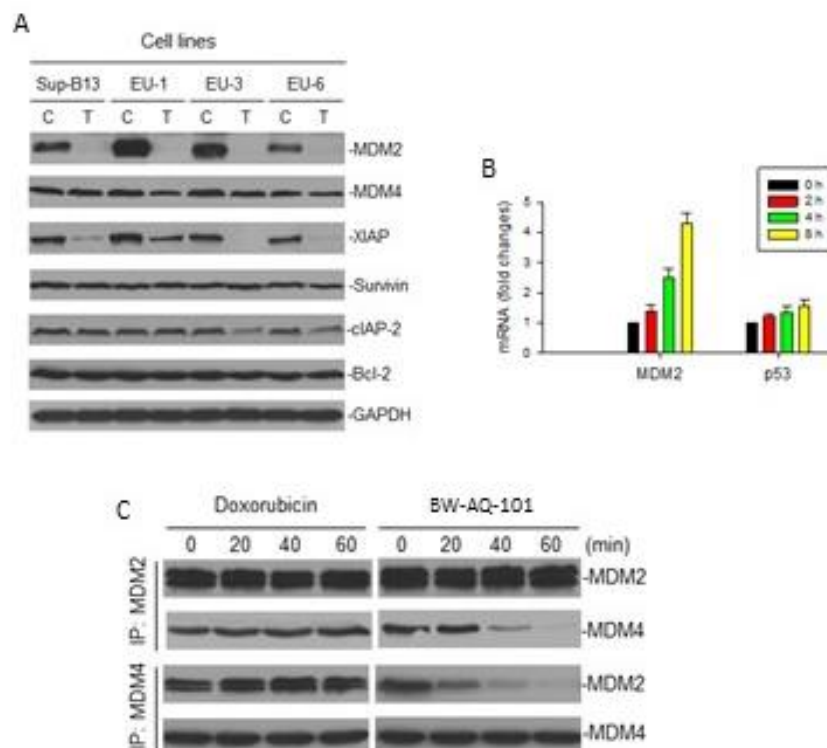


Figure 1.2.2 Effects of BW-AQ-101 on p53, MDM2 and MDM4;

A) Western blot assays for expression of proteins, as indicated in four MDM2-positive ALL cell lines, treated with 1 μ M BW-AQ-101 for 24 h. C, control; T, treatment. B) The mRNA levels of MDM2 and p53 at different time intervals upon treatment with 1 μ M BW-AQ-101. C) IP-western blot assays of EU-1 cells upon treatment with 1 μ M BW-AQ-101

Since it was indicated that BW-AQ-101 appears to induce MDM2 protein degradation, and as discussed in the introductory chapter, the regulation of MDM2 protein stabilization is mainly controlled by its own C-terminal RING domain. Computational tools were utilized to exploit potential interactions between the developed compound and the RING domain of MDM2. One of the key aspects that should be kept in mind is that MDM2 forms a homodimer or a heterodimer with MDM4 through direct RING-RING domain interactions. The purpose of the molecular modeling analysis was to see whether there was a potential binding pocket for BW-AQ-101 in the MDM2 RING domain. The molecular docking was examined using a simulated aqueous environment. After a careful analysis of the homodimer of MDM2, two identical and symmetric

binding pockets formed by the two MDM2 RING domains' interactions were revealed (Figure 1.2.3A). However, the heterodimeric structure of MDM2-MDM4 showed absence of any cavities (Figure 1.2.3B). It has been reported that the MDM2 RING domains are very unstable in solution and that they easily form dimeric or other types of aggregate structures; therefore, it is safe to assume that the binding pockets seen in the homodimer exist under physiological conditions. The BW-AQ-101 docking study was in good agreement with the observed activity, and did not show any sites for possible covalent modifications. The computational results gave insight into the possible mechanism of action of BW-AQ-101. The docking studies revealed clear binding pocket and potential for stable interactions of the compound with the MDM2 RING domain. However, the residues involved in these interactions do not play part in the MDM2-MDM4 heterodimer formation (Figure 1.2.3 C, D). The fact that the MDM2 RING domains predominantly exist in dimeric or more complex aggregate forms entails for constant, dynamic conformational changes that allow for the formation of complexes and their stabilizations. The conformational changes open large surface areas that can serve as interfaces for the formation of stable MDM2-MDM4 heterodimer. We hypothesize that upon binding of BW-AQ-101 to the MDM2 RING homodimer, the MDM2 RING structure “locks” into a folded conformation, which prevents unfolding and thus inhibits MDM2-MDM4 heterodimer formation.

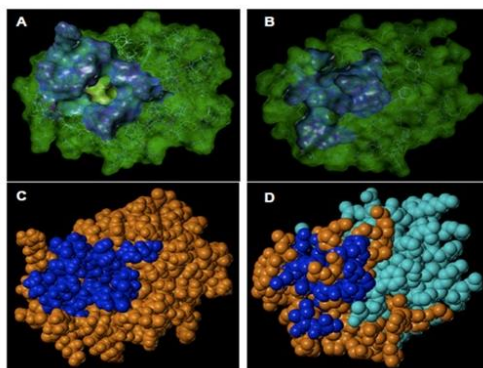


Figure 1.2.3 The binding pocket of MDM2:

A) MDM2 homodimer showing the relative cavity depth of the binding pocket (blue: no cavity; yellow: cavity). B) MDM2-MDM4 heterodimer, showing the lack of a cavity by coloring the surface of the MDM2 RING residues involved in cavity formation in the homodimeric form. C) MDM2 homodimer (orange) and the binding pocket forming amino acid residues (blue). D) MDM2 (orange)-MDM4 (cyan) heterodimer and the MDM2 amino acid residues (blue) participating in pocket formation in the homodimeric form. The image shows the absence of a binding cavity as well as lack of direct interactions between the pocket-forming amino acid residues of MDM2 (blue) with the MDM4 monomer (cyan).

In order to validate the computational results, two types of binding assays were performed; fluorescent titration and ITC assays. After titration of BW-AQ-101 to the GST-MDM2 RING protein a $K_d = 0.31 \mu\text{M}$ was obtained from the fluorescence assay (data not shown). The control titration of BW-AQ-101 to the GST protein itself, did not result in any binding. The ITC assays, showed similar binding affinity of $K_d = 0.29 \mu\text{M}$ and confirmed that BW-AQ-101 binds to the MDM2 RING domain. ITC experiment with MDM4 did not detect binding of BW-AQ-101 (Figure 1.2.4). Furthermore, both the fluorescent titration and ITC assays for detection of possible binding between BW-AQ-101 and an MDM2 fragment (residues 1 - 424) with deletion of the RING domain, were performed and no binding activity was detected (data not shown). In order to validate the theory that BW-AQ-101 binds to the MDM2 homodimer and blocks MDM4 interaction, co-immunoprecipitation (Co-IP) experiments were performed. Previous studies had demonstrated that the MDM2 protein becomes stabilized in the heterodimer form (MDM2-MDM4).⁵ Binding of BW-AQ-101 to MDM2 may disrupt the formation of the MDM2-MDM4 heterodimer, resulting in MDM2 destabilization. Co-IP and Western blot assays, showed that BW-AQ-101 dissociated MDM2 from the MDM2-MDM4 complex (Figure 1.2.2C). Because BW-AQ-101 has an anthraquinone core, these experiments were performed against doxorubicin. MDM2 and MDM4 were unaffected in a co-ip experiment with doxorubicin (Figure 1.2.2C). Thus, the result suggest that BW-AQ-101, but not doxorubicin, was able to dissociate these two proteins.

Naturally another comparison between the two compounds has to be made to verify that the mechanism of action of BW-AQ-101 is truly as proposed above. Flat aromatic, polycyclic compounds are known DNA binders and it is well known that doxorubicin induces apoptosis through DNA damage. In order to verify that BW-AQ-101 does not interact with DNA in the utilized concentrations, a comet assay was performed. The assay indicated that at 1 μM concentration, doxorubicin induced clear DNA damage after 4 hours, while BW-AQ-101 exhibited only DNA fragmentation after 8 hour treatment (Figure 1.2.5).

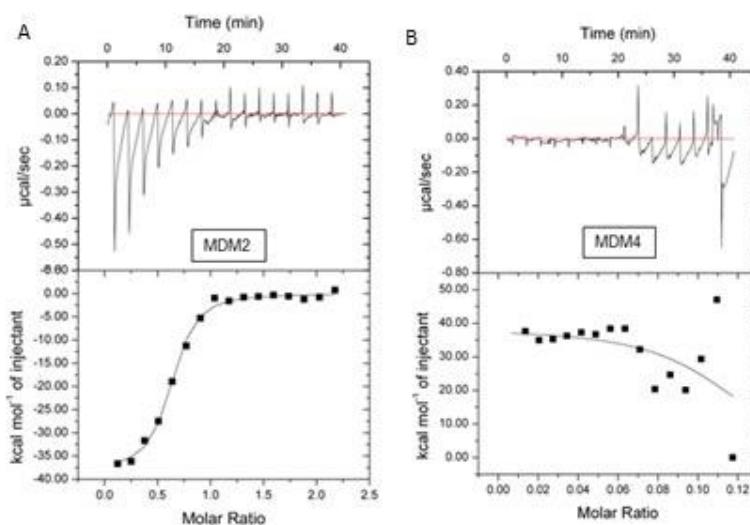


Figure 1.2.4 ITC binding assay of BW-AQ-101 against: A) MDM2 and B) MDM4

The computational results as well as the mechanistic experiments described above show strong evidence that the lead compound BW-AQ-101 is indeed a MDM2 RING binder. The compound does not show significant DNA damage and correlation between molecular modeling and binding assays agree with the hypothesis that the compound induces apoptosis through disruption of the p53-MDM2 regulatory mechanism. These observations give an indication that a new class of compounds inhibiting the p53-MDM2 regulation may be developed based on the lead

compound BW-AQ-101. The correlation between *in vitro* and *in silico* binding studies allows us to develop a computational model and design other active rhein-based anticancer agents.

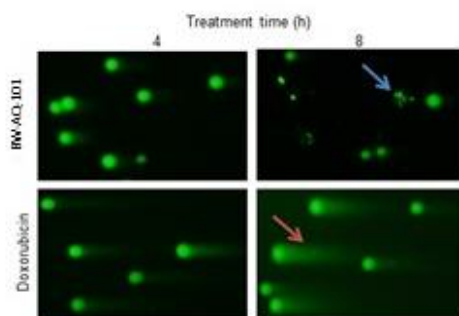


Figure 1.2.5 Comet assay of EU-1 cells

Cells were treated with 1 μ M of either AQ-101 or doxorubicin, for 4 h and 8 h. Red arrow indicates DNA damage, blue arrow indicates nuclear fragmentation/apoptosis.

1.2.1 Experimental section

Compound-protein binding assay

The binding properties between AQ-101 and the MDM2/MDM4 RING domains were examined by both fluorescent titration (data not shown) and isothermal titration calorimetry (ITC) assays. The expression and purification of the MDM2 and MDM4 RING domain proteins was performed as described previously.⁶

ITC assay

The MDM2 RING protein in a Hepes buffer (10 mM Hepes, pH 7.2 and 150 mM NaCl) solution was placed in a loading 96 DeepWell PP plate (Nunc, Thermo Fisher Scientific). The test compound (120 μ L of 24 μ M stock solution) was automatically transferred by the auto-iTC200 instrument (MicroCal, GE) into the sample cell. The compound solution (2 μ L) was titrated stepwise into the protein sample cell using a syringe, for a total of 16 injections (excepting the first

injection, which was 0.4 μL). The equilibrium time between two adjacent injections was 210 s. The binding stoichiometry (n), dissociation constant (K_d) and thermodynamic parameters (ΔH and ΔS) were determined by fitting the titration curve to a one-site binding mode, using the Origin software provided by the manufacturer.

Cells

This study used five established cell lines derived from children with acute lymphoblastic leukemia. Four of these cell lines (EU-1, EU-3, EU-6 and EU-8) were established at Emory University (Atlanta, GA, USA), and one (SUP-B13) was obtained from Stephen D. Smith (University of Kansas Medical Center, Kansas City, KS, USA). All ALL cell lines were authenticated and their p53 phenotypes were as follows: Sup-B13, EU-1 and EU-3 cells (wt-p53); EU-6 (mutant p53); and EU-8 (p53-null). Four of the p53-positive cell lines, including the p53-mutant EU-6, express MDM2; whereas MDM2 is not expressed in the EU-8 cells (Zhou et al., 1995). The 293T cell line, purchased from the American Type Tissue Collection (ATCC) was used for gene transfection assays.

Fresh leukemia samples were selected from 16 pediatric patients treated for ALL (either at diagnosis or first relapse), with peripheral total white blood cell (WBC) counts higher than $100 \times 10^6/\text{mL}$ (Table s1). Normal human bone marrow mononuclear (NBMM) cells were obtained from 5 donors following informed consent. Of the 16 ALL patients, 13 had B-cell precursor (BCP) ALL and 3 had T-ALL, as diagnosed by standard immunologic, morphologic and cytochemical criteria. Mononuclear cells were separated by centrifugation in Ficoll-Hypaque (1.077g/mL). Leukemic blasts from patient samples were further isolated by removing adherent monocytes. Specimens collected for these studies contained more than 90% blasts, following purification. Cells and cell

lines were grown in standard culture medium (RPMI 1640 containing 10% fetal bovine serum (FBS), 2 mmol/L L-glutamine, 50 U/mL penicillin, and 50 µg/mL streptomycin), at 37⁰ C in 5% CO₂.

Comet assay

To test whether AQ-101 induces DNA damage, we used a single-cell gel-electrophoresis Comet assay (Trevigen), a method as previously described.⁷ Briefly, cells with or without AQ-101 treatments were gently harvested, embedded in an agarose layer on a microscope slide, and lysed to remove cellular proteins. DNA was uncoiled under alkaline conditions, electrophoresed for 20 min and then stained with fluorescent dye. In contrast to undamaged nuclear DNA, damaged DNA demonstrates a characteristic ‘comet tail’ in this assay which is directly proportional to the amount of damaged DNA.

Quantitative RT-PCR

Total RNA was extracted from cells using the RNeasy Mini Kit (Qiagen). First-strand cDNA synthesis was performed with a mixture of random monomers and oligo-dT as primers. Amplification was performed with a 7500 Real-Time PCR System (Applied Biosystems), using the QuantiFast SYBR Green RT-PCR kit (Qiagen), according to the manufacturer’s instructions. All gene-specific primers were purchased from Qiagen.

Molecular modeling

The NMR structure of the MDM2 RING homodimer is available through the Protein Data Bank (PDB) under the ID 2HDP.⁸ The X-ray RING structure of the MDM2-MDM4 heterodimer

is also available through the PDB (ID 2VJE), with a resolution of 2.2 Å.⁹ We performed molecular docking to see whether there was a potential binding pocket for AQ-101 in the MDM2 RING protein. The target protein and AQ-101 were prepared by removing of all zinc ions, water residues, and other ligands. All hydrogen atoms were added and the protein termini were fixed. Minimization was performed by using Sybyl X 2.0 and applying standard parameters: Powell method, Tripos force field, and Pullman charges. Simulated water environment was used by assigning the dielectric constant to 80. Docking was performed by Surflex-Dock module in Sybyl X 2.0. Virtual preparation of the heterodimeric structure was performed following the above-described protocol.

MTT assay

HeLa and Cos7 cell lines were cultured in DMEM medium and T98G and KB cell lines in MEM medium. All other the cell lines (EU1, Molt4, K562) were cultured in RPMI-1640 medium. The medium was supplemented with 10% fetal bovine serum and 1% penicillin/streptomycin. For the cytotoxicity assays, cells were seeded into 96- well plate (3.0×10^4 for all solid state cell lines and 3×10^5 for all leukemia cell lines in 100 µL per well). The compounds were dissolved or suspended in DMSO to make 10 mM stock solutions. The stock solution was diluted using DMSO to various concentrations. 1µL of each concentration was diluted 100 fold with medium into the well plate keeping the DMSO < 1% throughout the experiment. Addition of compounds was performed after adherent cells reached 40-50 % confluence. After incubation for 24 h. at 37 ° C in humidified atmosphere with 5 % CO₂, 10 µL of MTT (5 mg/mL in PBS) was added. After addition of MTT the cells were incubated for another 4 h. The culture medium was then aspirated and 100 µL of DMSO was added to each well. The 96-well plate was read by microarray reader for optical

density at 490 nm. All tests were performed in triplicates and IC₅₀ values were estimated from the averaged response curves.

1.2.2 References

- (1) Yang, X.; Sun, G.; Yang, C.; Wang, B. *ChemMedChem* **2011**, 6, 2294.
- (2) Draganov, A. B. *Thesis, Georgia State University* **2011**.
- (3) Drews, J. *Science* **2000**, 287, 1960.
- (4) Gregori-Puigjane, E.; Setola, V.; Hert, J.; Crews, B. A.; Irwin, J. J.; Lounkine, E.; Marnett, L.; Roth, B. L.; Shoichet, B. K. *PNAS* **2012**, 109, 11178.
- (5) Sharp, D. A.; Kratowicz, S. A.; Sank, M. J.; George, D. L. *J. Biol. Chem.* **1999**, 274, 38189.
- (6) Gu, L.; Zhu, N.; Zhang, H.; Durden, D. L.; Feng, Y.; Zhou, M. *Cancer cell* **2009**, 15, 363.
- (7) Olive, P. L.; Banath, J. P. *Nat. Protoc.* **2006**, 1, 23.
- (8) Kostic, M.; Matt, T.; Martinez-Yamout, M. A.; Dyson, H. J.; Wright, P. E. *J. Mol. Biol.* **2006**, 363, 433.
- (9) Linke, K.; Mace, P. D.; Smith, C. A.; Vaux, D. L.; Silke, J.; Day, C. L. *Cell Death Differ.* **2008**, 15, 841.

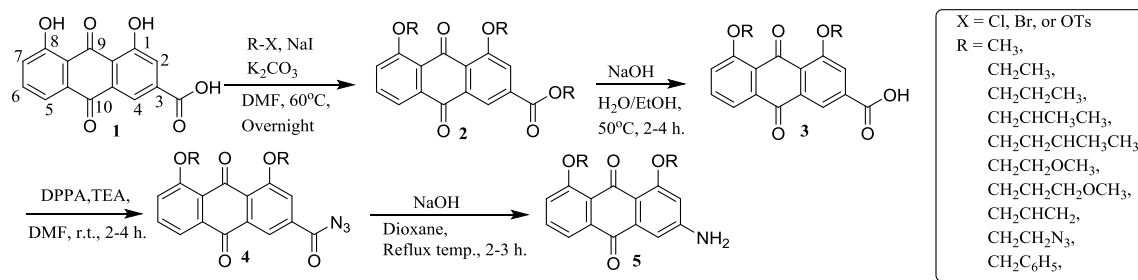
1.3 Design and synthesis of novel potent anthraquinone compounds as anticancer agents

Compound BW-AQ-101 showed potent activity against leukemia cell lines and evidence that it disrupts the p53-MDM2 regulatory cycle. Unfortunately, this compound shows poor solubility under physiological conditions (3 μ M in phosphate buffer (PBS)). Compounds'

solubility is one of the key aspects in the drug development process. The structure of BW-AQ-101 consists of a flat, polycyclic, aromatic system with two free phenolic groups. This type of structures are prone to pi-pi stacking, which decreases the compound's solubility. In addition to the pi-pi stacking, the two phenolic groups located in an α -position to a hydrogen bond acceptor (the carbonyl groups of the anthraquinone core) are capable of inter and/or intramolecular hydrogen bond formation. These interactions can further stabilize the packing and significantly contribute to the poor solubility of the compound. With this in mind and the idea that potential derivatives of BW-AQ-101 will be successful MDM2 RING binders, a series of compounds with various substituents at the 1 and 8 positions of the anthraquinone core were designed and synthesized. We aimed to alkylate the two phenolic groups with various substituents in order to break the hydrogen bonding. In addition the alkylation of the 1 and 8 positions of the anthraquinone moiety will introduce flexible functional groups, thus interrupting stacking and improving general water solubility. The herein disclosed compounds were carefully evaluated *in silico* against the structure of the MDM2 RING domain. All chemical modifications sought improvement of solubility and binding to the pocket of MDM2 RING domain.

The designed compounds are separated into nine groups based on the substituents on the 1 and 8 positions of the anthraquinone core (see sections 1.1.31-1.1.39). All of the synthesized compounds follow a common four step synthetic route with slight variations (Scheme 1.3.1). The synthesis of the BW-AQ-101 analogs starts with the alkylation of commercially available rhein (**1**) with various alkylating agents (Scheme 1.3.1). All alkylating agents used for this step are commercially available except for 2-azidoethyl 4-methylbenzenesulfonate used for the synthesis of 1,8-bis(2-azidoethoxy)anthracene-9,10-diones (**21a** and **21b**) (Figure 1.3.5). The detailed synthetic route towards compounds **21a** and **21b** is described in section 1.3.5 below. All

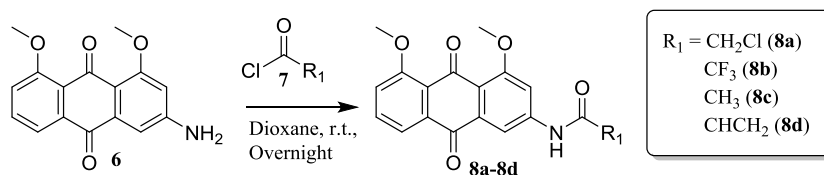
compounds described in sections 1.2.1-1.3.4 and 1.3.6-1.3.7 follow the four step synthetic route to the aniline type of intermediate (**5**) (Scheme 1.3.1). The commercially available rhein (**1**) is reacted with a commercially available alkylating agent, consisting of either Br or Cl as a leaving group, under basic conditions (K_2CO_3) in the presence of catalytic amount of NaI. The reaction is stirred overnight at 60 °C – 70 °C in dimethylformamide (DMF) and in all cases results in quantitative yields of intermediates **2**. The second step of the synthetic route involves a hydrolysis in 0.5 N/1 N NaOH in ethanol/water (1:1, v/v) solution to form the free carboxylic acid (**3**) in quantitative yield. Carboxylic acid (**3**) is then reacted with diphenylphosphoryl azide (DPPA) in the presence of triethyl amine (TEA) to form the acyl azide (**4**). Due to the lack of stability, intermediate **4** was not purified and directly used as a crude starting material for the next step. The conversion of compound **4** to **5** occurs through a Curtius rearrangement. In all of the below-described classes of compounds, intermediate **5** was used without purification. The slight variations in reaction time between the different classes of compounds is mostly based on poor solubility of the starting materials.



Scheme 1.1 General synthetic route to various active anthraquinones

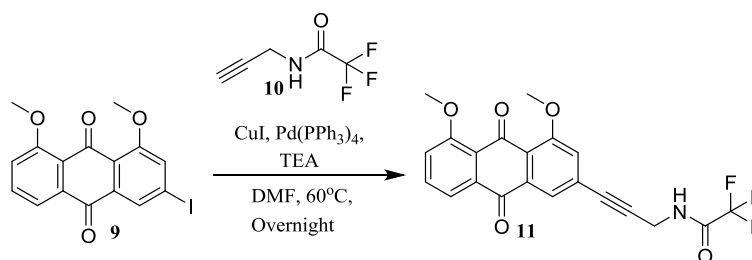
The first class of compounds described in this section are the 1,8-dimethoxyanthracene-9,10-dione-based analogs of BW-AQ-101. Four of the five compounds that belong to this group were synthesized following the general synthetic route described in Scheme 1.3.1. Compounds **8a-8d** were synthesized through an acylation reaction from aniline (**6**). Compounds **8a-8d** were

obtained through acylation of compound **6** with chloroacetyl chloride, 2,2,2-trifluoroacetyl chloride, acetyl chloride, or acryloyl chloride respectively (Scheme 1.3.2 and Figure 1.3.1).



Scheme 1.2: General synthetic route to compounds 8a-8d

Compound **11** was prepared via classic Sonogashira reaction and following previously reported procedures.¹ Starting material (**9**) was synthesized by Dr. Chaofeng Dai from Prof. Binghe Wang's lab, thus details procedure and characterization of the compound is not included in this work. Compound (**9**) was reacted with alkyne (**10**) using tetrakis(triphenylphosphine)palladium and copper (I) iodide under basic conditions. The reaction was stirred overnight at 60°C giving product (**11**).



Scheme 1.3 Synthesis of compound 11 through Sonogashira coupling

** Compound 11 was synthesized following published procedure.¹*

All synthesized compounds that belong to the 1,8-dimethoxyanthracene-9,10-dione class are summarized in figure 1.3.1. The biological activity of these compounds is described in Section 1.4. of this chapter.

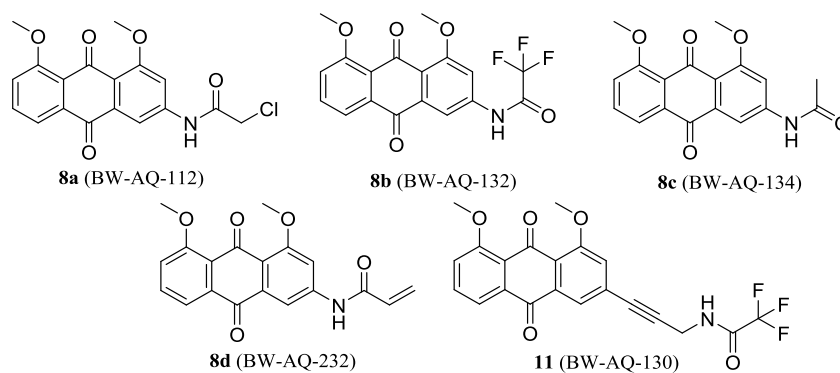


Figure 1.3.11,8-dimethoxyanthracene-9,10-dione analogs

1.3.1.1 Experimental section

Rhein (**1**) was purchased from Nanjing Zelang Medical Technology Co and directly used without further purification. Other starting materials were purchased from Sigma-Aldrich, VWR, or Acros. Analytical-grade solvents were used for all reactions except for moisture-sensitive reactions in which anhydrous solvents were used. TLC analysis was conducted on silica gel plates (Silica G UV254); and column chromatography was carried out on flash silica gel (230–400 mesh). NMR spectra were recorded at 400 MHz for ¹H and 100 MHz for ¹³C on Bruker Avance NMR spectrometers with TMS (δ = 0.00 ppm) or residual solvent as the internal reference. Data are reported as follows: chemical shift, multiplicity (s = singlet, d = doublet, t = triplet, m = multiplet), coupling constant, and integration. High-resolution mass spectrometry (HRMS) was performed using electrospray ionization (ESI).

General experimental procedure for the synthesis of compounds **8a-8d**:

Compound **6** (1.0 eq.) was dissolved and stirred in 1, 4-dioxane at room temperature followed by addition of the corresponding acyl halide (**7**, 1.5 eq.). After reaction completion, the reaction mixture was diluted with distilled water/ice. Yellow to orange solids precipitated out and were isolated either by centrifugation at 5000 rpm for 10 min followed by decantation and

complete removal of water by putting the crude product in high vacuum pump system, or by vacuum filtration. The crude product was purified by silica gel column chromatography using a dichloromethane (DCM)/ethyl acetate (EtAc) gradient mixture to afford the pure product **8a-8d**.

8a (BW-AQ-112), 2-chloro-N-(4,5-dimethoxy-9,10-dioxo-9,10-dihydroanthracen-2-yl)acetamide:

Isolated yield over two steps 45 %. ^1H NMR ($\text{DMSO-}d_6$): δ 10.80 (s, 1H), 7.85 (d, J = 1.6 Hz, 1H), 7.759 (d, J = 1.6 Hz 1H), 7.72-7.50 (m, 2H), 7.49 (d, J = 8.4 Hz, 1H), 4.32 (s, 2H), 3.89 (s, 3H) 3.86 (s, 3H); ^{13}C NMR ($\text{DMSO-}d_6$): δ 183.50, 180.54, 165.98, 160.35, 159.26, 143.89, 135.31, 134.46, 134.43, 123.78, 119.59, 119.52, 118.64, 108.64, 108.34, 56.74, 56.54, 44.08. HRMS (ESI-TOF) m/z $[\text{M}+1]^+$ calcd. for $\text{C}_{18}\text{H}_{14}\text{ClNO}_5$ 360.0633, found 360.0619.

8b (BW-AQ-132), N-(4,5-dimethoxy-9,10-dioxo-9,10-dihydroanthracen-2-yl)-2,2,2-trifluoroacetamide:

Isolated yield over two steps 50 %. ^1H NMR ($\text{DMSO-}d_6$): δ 8.09 (d, J = 1.6 Hz, 1H), 7.80 (d, J = 2 Hz, 1H), 7.74 (t, J = 8.0 Hz, 1H), 7.68 (d, J = 7.2 Hz, 1H), 7.53 (d, J = 8 Hz, 1H), 3.90 (s, 3H), 3.89 (s, 3H); ^{13}C NMR ($\text{DMSO-}d_6$): δ 183.30, 180.66, 160.08, 159.30, 141.83, 135.36, 134.70, 134.41, 123.72, 121.04, 119.61, 118.72, 110.23, 110.13, 56.79, 56.72. HRMS (ESI-TOF) m/z $[\text{M}+1]^+$ calcd. for $\text{C}_{18}\text{H}_{12}\text{F}_3\text{NO}_5$ 380.0740, found 380.0724.

8c (BW-AQ-134), N-(4,5-dimethoxy-9,10-dioxo-9,10-dihydroanthracen-2-yl)acetamide:

Isolated yield over two steps 47 %. ^1H NMR ($\text{DMSO-}d_6$): δ 10.46 (s, 1H), 7.84 (d, J = 1.6 Hz, 1H), 7.78 (d, J = 1.6 Hz, 1H), 7.72-7.63 (m, 2H), 7.49 (d, J = 7.6 Hz, 1H), 3.89 (s, 3H), 3.85 (s, 3H), 2.10 (s, 3H); ^{13}C NMR ($\text{DMSO-}d_6$): δ 183.68, 180.57, 169.78, 160.38, 159.25, 144.75, 135.24, 134.49, 134.39, 123.85, 119.49, 118.98, 118.62, 108.37, 107.91, 66.81, 56.73, 56.46, 24.73. HRMS (ESI-TOF) m/z $[\text{M}+1]^+$ calcd. for $\text{C}_{18}\text{H}_{15}\text{NO}_5$ 326.1023, found 326.1007.

8d (BW-AQ-232), *N*-(4,5-dimethoxy-9,10-dioxo-9,10-dihydroanthracen-2-yl)acrylamide:

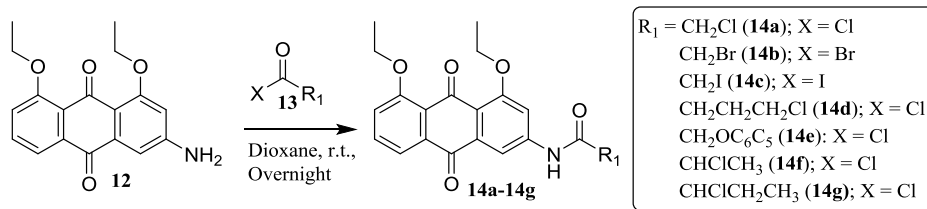
Isolated yield over two steps 52 %. ^1H NMR (DMSO- d_6): δ 10.69 (s, 1H), 7.95 (d, $J = 2$ Hz, 2H), 7.93 7.66 (m, 2H), 7.53-7.50 (m, 1H), 6.49-6.42 (m, 1H), 6.36-6.31 (m, 1H), 5.87-5.84 (m, 1H), 3.90 (s, 3H), 3.88 (m, 2H); ^{13}C NMR (DMSO- d_6): δ 183.65, 180.61, 164.35, 160.38, 159.28, 144.52, 135.30, 134.50, 134.48, 131.78, 128.85, 123.89, 119.58, 119.38, 118.67, 108.84, 108.43, 66.82, 56.77, 56.54. HRMS (ESI-TOF) m/z $[\text{M}+\text{Na}]^+$ calcd. for $\text{C}_{19}\text{H}_{15}\text{NO}_5$ 360.0848, found 360.0856.

8e (BW-AQ-130), *N*-(3-(4,5-dimethoxy-9,10-dioxo-9,10-dihydroanthracen-2-yl)prop-2-yn-1-yl)-2,2,2-trifluoroacetamide:

Isolated yield over two steps 60 %. ^1H NMR (DMSO- d_6): δ 10.13 (s, 1H), 7.73 (t, $J = 8.0$ Hz, 1H), 7.65-7.59 (m, 2H), 7.52 (d, $J = 8.4$ Hz, 1H), 7.46 (d, $J = 1.2$ Hz, 1H), 4.35 (d, $J = 5.6$ Hz, 2H), 3.92 (s, 3H), 3.90 (s, 3H); ^{13}C NMR (DMSO- d_6): δ 182.97, 180.96, 159.25, 159.22, 134.82, 134.74, 134.28, 131.99, 131.90, 129.27, 129.16, 127.66, 123.78, 121.20, 120.97, 119.55, 89.11, 81.71, 57.02, 56.77, 29.94. HRMS (ESI-TOF) m/z $[\text{M}+1]^+$ calcd. for $\text{C}_{21}\text{H}_{14}\text{F}_3\text{NO}_5$ 418.0897, found 418.0881.

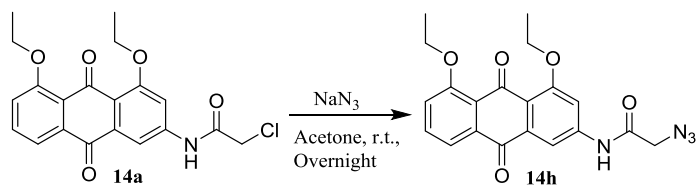
1.3.2 Synthesis of 1,8-diethoxyanthracene-9,10-dione compounds

The 1,8-diethoxyanthracene-9,10-dione class of compounds consist of eight analogs (**14a-14h**) synthesized from aniline **12**. Compound **12** was synthesized following synthetic scheme 1.3.1. The aniline (**12**) was then reacted with the corresponding acyl chloride (Scheme 1.3.4) in 1,4-dioxane at room temperature to give compounds **14a-14g** at various yields (Figure 1.3.2, see the experimental section for yields).



*Scheme 1.4 General synthetic route to compounds **14a-14g***

Compound **14a** was used as a starting material in the synthesis of azide **14h** (Scheme 1.3.5). A substitution reaction between **14a** and excess of sodium azide in acetone resulted in compound **14h**. The reaction was stirred at room temperature overnight to give **14h** in quantitative yields.



*Scheme 1.5 Synthesis of compound **14h***

All synthesized compounds that belong to the 1,8-diethoxyanthracene-9,10-dione class are summarized in figure 1.3.2. The biological activity of these compounds is described in section 1.4. of this chapter.

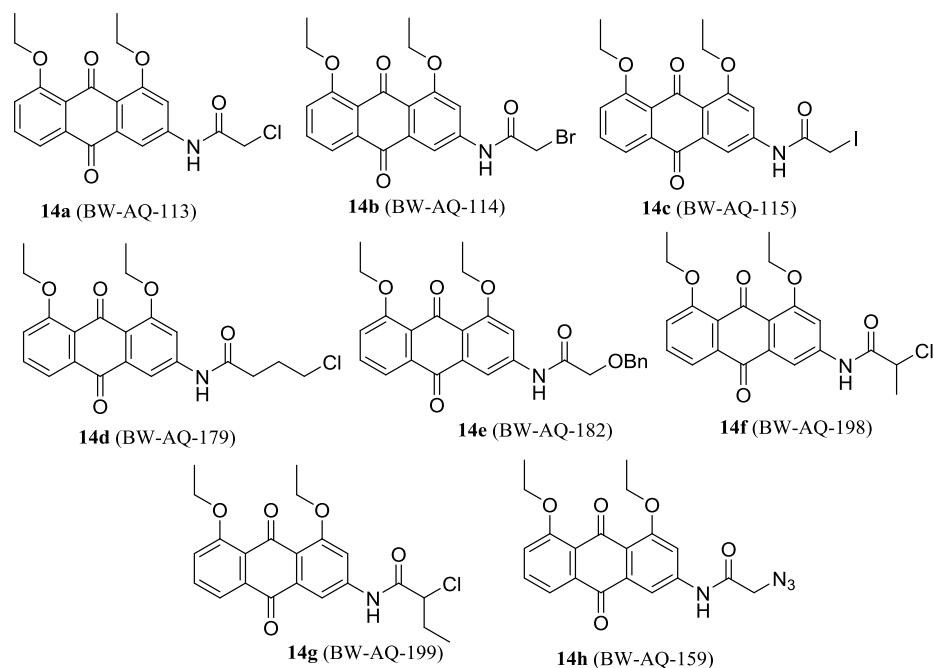


Figure 1.3.2 Synthesis of 1,8-diethoxyanthracene-9,10-dione analogs

1.3.2.1 Experimental section

General experimental procedure for the synthesis of compounds (14a-14g):

Compound **12** (1.0 eq.) was dissolved and stirred in 1, 4-dioxane at room temperature followed by addition of the corresponding acyl halide (**13**, 1.5 eq.). After reaction completion, the reaction mixture was diluted with distilled water/ice. Yellow to orange solids precipitated out and were isolated either by centrifugation at 5000 rpm for 10 min followed by decantation and complete removal of water by putting the crude product in high vacuum pump system, or by vacuum filtration. The crude product was purified by silica gel column chromatography using a dichloromethane (DCM)/ethyl acetate (EtAc) gradient mixture to afford the pure product **14a-14g**.

Experimental procedure for the synthesis of compound 14h:

Compound **14a** (1.0 eq.) was dissolved and stirred in acetone at room temperature followed by addition of sodium azide (2.0 eq.). After overnight stirring, the acetone was partially

evaporated and the remaining residue was diluted with water/ice. Yellow to orange solid precipitated out and was isolated either by centrifugation at 5000 rpm for 10 min followed by decantation and complete removal of water by putting the crude product in high vacuum pump system, or by vacuum filtration.

14a (BW-AQ-113), 2-chloro-N-(4,5-diethoxy-9,10-dioxo-9,10-dihydroanthracen-2-yl)acetamide:

Isolated yield over two steps 50 %. ^1H NMR (DMSO- d_6): δ 10.78 (s, 1H), 7.85 (s, 1H), 7.77 (s, 1H), 7.67-7.65 (m, 2H), 7.48 (d, J = 6.8 Hz, 1H), 4.31 (s, 2H), 4.18-4.13 (m, 4H), 1.44-1.38 (m, 6H); ^{13}C NMR (DMSO- d_6): δ 183.61, 180.29, 165.98, 159.69, 158.63, 143.75, 135.38, 134.52, 134.35, 123.90, 120.66, 119.70, 118.64, 109.42, 108.69, 65.12, 65.06, 44.08, 15.07, 14.98. HRMS (ESI-TOF) m/z $[\text{M}+1]^+$ calcd. for $\text{C}_{20}\text{H}_{18}\text{ClNO}_5$ 388.0946, found 388.0934.

14b (BW-AQ-114), 2-bromo-N-(4,5-diethoxy-9,10-dioxo-9,10-dihydroanthracen-2-yl)acetamide:

Isolated yield over two steps 48 %. ^1H NMR (DMSO- d_6): δ 10.89 (s, 1H), 7.88 (s, 1H), 7.78 (s, 1H), 7.71-7.67 (m, 2H), 7.51 (d, J = 6.8 Hz, 1H), 4.23-4.14 (m, 4H), 4.09 (s, 2H), 1.44-1.38 (m, 6H); ^{13}C NMR (DMSO- d_6): δ 183.33, 179.98, 171.98, 159.06, 158.12, 143.49, 134.87, 134.17, 133.86, 123.52, 120.21, 119.07, 118.17, 109.57, 108.63, 64.67, 64.56, 62.00, 14.58, 14.50. HRMS (ESI-TOF) m/z $[\text{M}+1]^+$ calcd. for $\text{C}_{20}\text{H}_{18}\text{BrNO}_5$ 432.0441, found 432.0434.

14c (BW-AQ-115), N-(4,5-diethoxy-9,10-dioxo-9,10-dihydroanthracen-2-yl)-2-iodoacetamide:

Isolated yield over two steps 54 %. ^1H NMR (DMSO- d_6): δ 10.80 (s, 1H), 7.83 (d, J = 1.6 Hz, 1H), 7.74 (d, J = 1.6 Hz, 1H), 7.68-7.64 (m, 2H), 7.48 (dd, J = 2, 7.2 Hz, 1H), 4.32-4.12 (m, 4H), 3.89 (s, 2H), 1.42-1.38 (m, 6H); ^{13}C NMR (DMSO- d_6): δ 183.62, 180.26, 168.04, 159.74,

158.63, 144.13, 135.36, 134.52, 134.32, 123.90, 120.65, 119.53, 118.63, 109.10, 108.47, 65.12, 65.06, 15.07, 15.0. HRMS (ESI-TOF) m/z $[M+1]^+$ calcd. for $C_{20}H_{18}INO_5$ 480.0302, found 480.0291.

14d (BW-AQ-179), 4-chloro-N-(4,5-diethoxy-9,10-dioxo-9,10-dihydroanthracen-2-yl)butanamide:

Isolated yield over two steps 30 %. 1H NMR ($CDCl_3$): δ 8.26 (s, 1H), 8.06 (s, 1H), 7.82 (d, $J = 7.6$ Hz, 1H), 7.60 (t, $J = 7.6$ Hz, 1H), 7.52 (d, $J = 1.6$ Hz, 1H), 7.31 (d, $J = 8.4$ Hz, 1H), 4.29-4.22 (m, 4H), 3.68 (t, $J = 6$ Hz, 2H), 2.67 (t, $J = 7.2$ Hz, 2H), 2.23 (t, $J = 6.4$ Hz, 2H), 1.55 (t, $J = 6.8$ Hz, 6H); ^{13}C NMR ($DMSO-d_6$): δ 184.68, 179.63, 161.12, 158.51, 154.29, 135.94, 134.65, 133.55, 124.53, 120.84, 118.50, 113.28, 103.95, 102.95, 65.12, 64.44, 55.38, 15.12. HRMS (ESI-TOF) m/z $[M+Na]^+$ calcd. for $C_{22}H_{22}ClNO_5$ 438.1084, found 438.1103.

14e (BW-AQ-182), 2-(benzyloxy)-N-(4,5-diethoxy-9,10-dioxo-9,10-dihydroanthracen-2-yl)acetamide:

Isolated yield over two steps 51 %. 1H NMR ($CDCl_3$): δ 8.65 (s, 1H), 8.17 (s, 1H), 7.78 (d, $J = 7.6$ Hz, 1H), 7.55 (t, $J = 8$ Hz, 1H), 7.47 (s, 1H), 7.36 (s, 5H), 7.26 (d, $J = 8$ Hz, 1H), 4.65 (s, 2H), 4.26-4.18 (m, 4H), 4.09 (s, 2H), 1.53-1.49 (m, 6H); ^{13}C NMR ($CDCl_3$): δ 183.85, 181.23, 168.27, 160.52, 159.00, 142.00, 136.23, 135.43, 134.71, 133.47, 128.84, 128.60, 128.18, 124.26, 120.19, 119.94, 118.99, 109.65, 108.75, 73.91, 69.42, 65.44, 14.72, 14.57. HRMS (ESI-TOF) m/z $[M+Na]^+$ calcd. for $C_{27}H_{25}NO_6$ 482.1580, found 482.1566.

14f (BW-AQ-198), 2-chloro-N-(4,5-diethoxy-9,10-dioxo-9,10-dihydroanthracen-2-yl)propanamide:

Isolated yield over two steps 43 %. 1H NMR ($CDCl_3$): δ 8.60 (s, 1H), 8.16 (d, $J = 1.6$ Hz, 1H), 7.82 (d, $J = 7.6$ Hz, 1H), 7.59 (t, $J = 8$ Hz, 1H), 7.53 (d, $J = 1.6$ Hz, 1H), 7.30-7.26 (m, 1H),

4.59-4.57 (m, 1H), 4.29-4.21 (m, 4H), 1.84 (d, $J = 7.2$ Hz, 3H), 1.56-1.52 (m, 6H); ^{13}C NMR (DMSO- d_6): δ 183.62, 180.32, 168.62, 159.70, 158.64, 143.81, 135.38, 134.52, 134.37, 123.92, 120.68, 119.75, 118.65, 109.54, 108.85, 65.12, 65.08, 55.15, 21.27, 15.06, 14.99. HRMS (ESI-TOF) m/z $[\text{M}+\text{Na}]^+$ calcd. for $\text{C}_{21}\text{H}_{20}\text{ClNO}_5$ 424.0928, found 424.0940.

14g (BW-AQ-199), 2-chloro-*N*-(4,5-diethoxy-9,10-dioxo-9,10-dihydroanthracen-2-yl)butanamide:

Isolated yield over two steps 53 %. ^1H NMR (CDCl_3): δ 8.62 (s, 1H), 8.16 (d, $J = 1.6$ Hz, 1H), 7.82 (d, $J = 7.6$ Hz, 1H), 7.59 (t, $J = 8$ Hz, 1H), 7.54 (d, $J = 1.6$ Hz, 1H), 7.29 (d, $J = 8$ Hz, 1H), 4.49-4.46 (m, 1H), 4.29-4.21 (m, 4H), 2.25-2.20 (m, 1H), 2.13-2.08 (m, 1H), 1.57-1.52 (m, 6H), 1.12 (t, $J = 7.2$ Hz, 3H); ^{13}C NMR (DMSO- d_6): δ 183.64, 180.35, 168.18, 159.72, 158.65, 143.72, 135.41, 134.54, 134.42, 120.72, 119.85, 118.67, 109.62, 108.88, 65.12, 61.20, 28.01, 15.06, 15.00, 11.06. HRMS (ESI-TOF) m/z $[\text{M}+\text{Na}]^+$ calcd. for $\text{C}_{22}\text{H}_{22}\text{ClNO}_5$ 438.1084, found 438.1096.

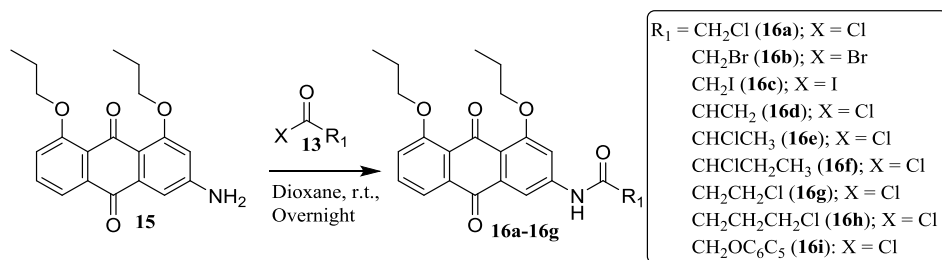
14h (BW-AQ-159), 2-azido-*N*-(4,5-diethoxy-9,10-dioxo-9,10-dihydroanthracen-2-yl)acetamide:

Isolated yield 100 %. ^1H NMR (CDCl_3): δ 8.35 (s, 1H), 8.16 (s, 1H), 7.84 (d, $J = 7.6$ Hz, 1H), 7.63-7.55 (m, 2H), 7.31 (d, $J = 8.0$ Hz, 1H), 4.29-4.22 (m, 6H), 1.58 (m, 6H); ^{13}C NMR (CDCl_3): δ 183.74, 165.26, 160.50, 159.02, 141.73, 135.53, 134.69, 133.57, 119.96, 119.02, 109.73, 108.85, 65.50, 65.43, 52.95, 42.92, 14.72, 14.56. HRMS (ESI-TOF) m/z $[\text{M}+1]^+$ calcd. for $\text{C}_{20}\text{H}_{18}\text{N}_4\text{O}_5$ 395.1350, found 395.1336.

1.3.3 Synthesis of 1,8-dipropoxyanthracene-9,10-dione compounds

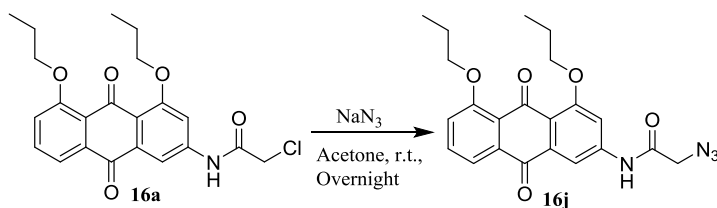
The 1,8-dipropoxyanthracene-9,10-dione class of compounds consist of ten analogs (**16a-16j**) synthesized from aniline **15**. Compound **15** was synthesized following synthetic scheme

1.3.1. The aniline (**15**) was reacted with the corresponding acyl chloride (Scheme 1.3.6) in 1,4-dioxane at room temperature to give compounds **16a-16i** at various yields (Figure 1.3.3, see the experimental section for yields).



*Scheme 1.6 General synthetic route to compounds **16a-16i***

Compound **16a** was used as a starting material in the synthesis of azide **16j** (Scheme 1.3.7). A substitution reaction between **16a** and excess of sodium azide in acetone resulted in compound **16j**. The reaction was stirred at room temperature overnight to give **16j** in quantitative yields.



*Scheme 1.7 Synthesis of compound **16j***

All synthesized compounds that belong to the 1,8-dipropoxyanthracene-9,10-dione class are summarized in figure 1.3.3. The biological activity of these compounds is described in section 1.4. of this chapter.

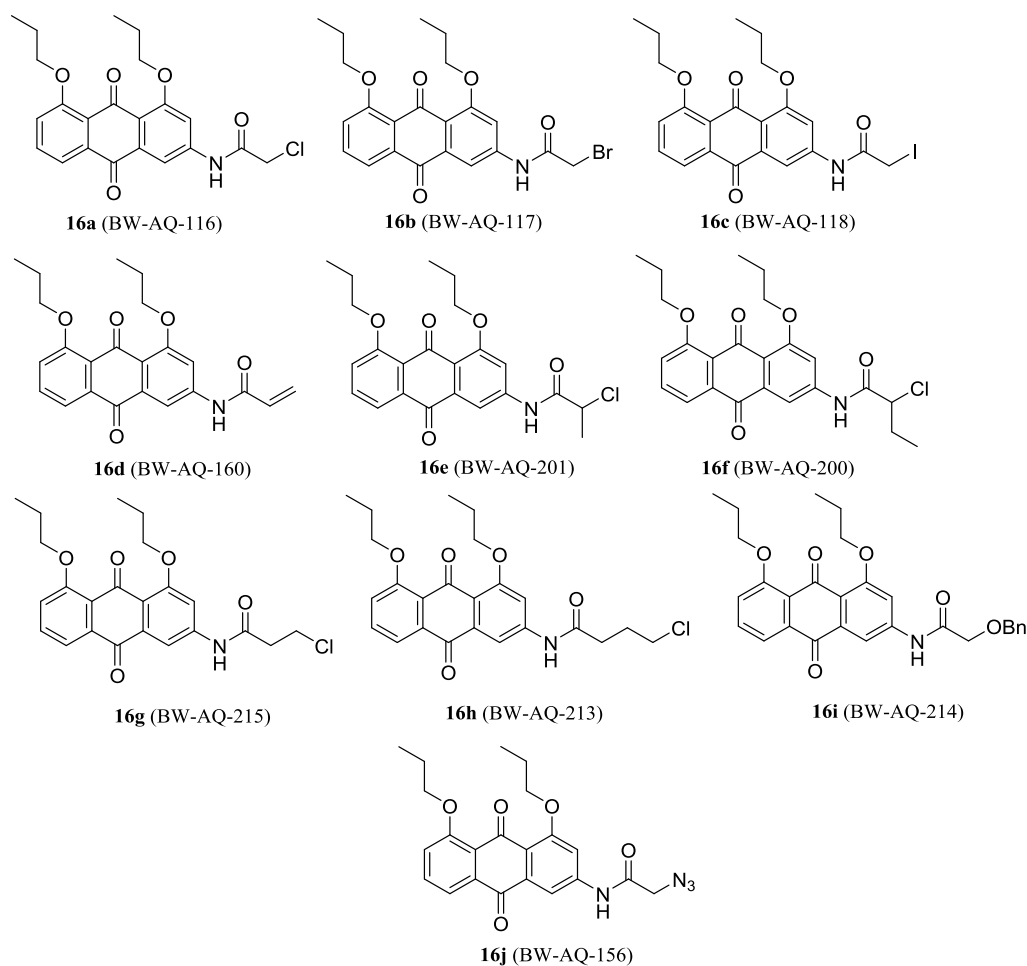


Figure 1.3.3 Synthesis of 1,8-dipropoxyanthracene-9,10-dione analogs

1.3.3.1 Experimental section

General experimental procedure for the synthesis of compounds (16a-16i):

Compound **15** (1.0 eq.) was dissolved and stirred in 1, 4-dioxane at room temperature followed by addition of the corresponding acyl halide (**13**, 1.5 eq.). After reaction completion, the reaction mixture was diluted with distilled water/ice. Yellow to orange solids precipitated out and were isolated either by centrifugation at 5000 rpm for 10 min followed by decantation and complete removal of water by putting the crude product in high vacuum pump system, or by

vacuum filtration. The crude product was purified by silica gel column chromatography using a dichloromethane (DCM)/ethyl acetate (EtAc) gradient mixture to afford the pure product **16a-16i**.

Experimental procedure for the synthesis of compound **16j**:

Compound **16a** (1.0 eq.) was dissolved and stirred in acetone at room temperature followed by addition of sodium azide (2.0 eq.). After overnight stirring, acetone was partially evaporated and the remaining residue was diluted with water/ice. Yellow to orange solid precipitated out and was isolated either by centrifugation at 5000 rpm for 10 min followed by decantation and complete removal of water by putting the crude product in high vacuum pump system, or by vacuum filtration.

16a (BW-AQ-116), *2-Chloro-N-(9,10-dioxo-4,5-dipropoxy-9,10-dihydroanthracen-2-yl)acetamide*:

Isolated yield over two steps: 40%. ¹H NMR (DMSO-d₆): δ 10.77 (s, 1H), 7.85 (s, 1H), 7.76 (s, 1H), 7.66-7.64 (m, 2H), 7.48 (d, *J* = 6.4 Hz, 1H), 4.31 (s, 2H), 4.07-4.00 (m, 4H), 1.83-1.75 (m, 4H), 1.06 (d, 6H); ¹³C NMR (DMSO-d₆): δ 183.63, 180.26, 165.95, 159.83, 158.77, 143.72, 135.34, 134.50, 134.27, 124.02, 120.63, 119.85, 118.58, 109.43, 108.64, 70.81, 70.75, 55.37, 22.53, 22.45, 10.81, 10.76. HRMS (ESI-TOF) *m/z* [M+1]⁺ calcd. for C₂₂H₂₂ClNO₅ 416.1259, found 416.1240.

16b (BW-AQ-117), *2-Bromo-N-(9,10-dioxo-4,5-dipropoxy-9,10-dihydroanthracen-2-yl)acetamide*:

Isolated yield over two steps: 30%. ¹H NMR (DMSO-d₆): δ 10.88 (s, 1H), 7.86 (d, *J* = 2 Hz, 1H), 7.76 (d, *J* = 2 Hz, 1H), 7.68-7.66 (m, 2H), 7.48 (dd, *J* = 1.6, 6 Hz, 1H), 4.09 (s, 2H), 4.07-4.01 (m, 4H), 1.84-1.76 (m, 4H), 1.08-1.03 (m, 6H); ¹³C NMR (DMSO-d₆): δ 183.66, 180.29, 166.15, 159.85, 158.78, 143.84, 135.38, 134.52, 134.32, 124.05, 120.68, 119.89, 118.61,

109.33, 108.58, 70.83, 70.77, 30.73, 22.53, 22.45, 10.82, 10.77. HRMS (ESI-TOF) m/z $[M+1]^+$ calcd. for $C_{22}H_{22}BrNO_5$ 460.0754, found 460.0749.

16c (BW-AQ-118), *N*-(9,10-dioxo-4,5-dipropoxy-9,10-dihydroanthracen-2-yl)-2-iodoacetamide:

Isolated yield over two steps: 35%. 1H NMR ($CDCl_3$): δ 8.39 (s, 1H), 8.15 (s, 1H), 7.79 (d, $J = 7.2$ Hz, 1H), 7.58 (t, $J = 8.4$ Hz, 1H), 7.50 (s, 1H), 7.29 (d, $J = 8.4$ Hz, 1H), 4.13-4.08 (m, 4H), 3.91 (s, 2H), 1.84-1.76 (m, 4H), 1.96-1.90 (m, 4H), 1.10 (s, 6H); ^{13}C NMR ($CDCl_3$): δ 184.27, 181.22, 166.08, 160.60, 159.15, 142.53, 135.32, 134.67, 133.51, 124.45, 120.54, 120.05, 118.89, 109.75, 108.70, 71.35, 71.33, 22.51, 22.40, 10.47. HRMS (ESI-TOF) m/z $[M+1]^+$ calcd. for $C_{22}H_{22}INO_5$ 508.0615, found 508.0596.

16d (BW-AQ-118), *N*-(9,10-dioxo-4,5-dipropoxy-9,10-dihydroanthracen-2-yl)-2-iodoacetamide:

Isolated yield over two steps: 35%. 1H NMR ($CDCl_3$): δ 8.39 (s, 1H), 8.15 (s, 1H), 7.79 (d, $J = 7.2$ Hz, 1H), 7.58 (t, $J = 8.4$ Hz, 1H), 7.50 (s, 1H), 7.29 (d, $J = 8.4$ Hz, 1H), 4.13-4.08 (m, 4H), 3.91 (s, 2H), 1.84-1.76 (m, 4H), 1.96-1.90 (m, 4H), 1.10 (s, 6H); ^{13}C NMR ($CDCl_3$): δ 184.27, 181.22, 166.08, 160.60, 159.15, 142.53, 135.32, 134.67, 133.51, 124.45, 120.54, 120.05, 118.89, 109.75, 108.70, 71.35, 71.33, 22.51, 22.40, 10.47. HRMS (ESI-TOF) m/z $[M+1]^+$ calcd. for $C_{22}H_{22}INO_5$ 508.0615, found 508.0596.

16e (BW-AQ-201), *2-Chloro-N*-(9,10-dioxo-4,5-dipropoxy-9,10-dihydroanthracen-2-yl)butanamide:

Isolated yield over two steps: 52%. 1H NMR ($CDCl_3$): δ 8.77 (s, 1H), 8.15 (d, $J = 1.6$ Hz, 1H), 7.79 (d, $J = 7.6$ Hz, 1H), 7.60-7.56 (m, 2H), 7.29 (d, $J = 8.4$ Hz, 1H), 4.49-4.46 (m, 1H), 4.14-4.08 (m, 4H), 2.23-2.11 (m, 1H), 2.09-2.05 (m, 1H), 1.96-1.90 (m, 4H), 1.12-1.09 (m, 9H); ^{13}C

NMR (CDCl₃): δ 183.91, 181.18, 167.62, 160.59, 159.12, 141.87, 135.41, 134.65, 133.48, 124.44, 120.76, 119.97, 118.92, 109.76, 108.96, 71.33, 62.55, 28.85, 22.50, 22.40, 10.47, 10.40. HRMS (ESI-TOF) m/z [M+Na]⁺ calcd. for C₂₄H₂₆ClNO₅ 466.1397, found 466.1390.

16f (BW-AQ-200), 2-Chloro-N-(9,10-dioxo-4,5-dipropoxy-9,10-dihydroanthracen-2-yl)propanamide:

Isolated yield over two steps: 37%. ¹H NMR (CDCl₃): δ 8.87 (s, 1H), 8.14 (d, J = 1.6 Hz, 1H), 7.78 (d, J = 7.6 Hz, 1H), 7.57 (t, J = 8 Hz, 2H), 7.29-7.26 (m, 1H), 4.64-4.58 (m, 1H), 4.14-4.07 (m, 4H), 1.95-1.89 (m, 4H), 1.82 (d, J = 7.2 Hz, 3H), 1.11-1.08 (m, 6H); ¹³C NMR (CDCl₃): δ 183.88, 181.28, 168.22, 160.54, 159.10, 142.05, 135.38, 134.64, 133.50, 124.40, 120.68, 119.94, 118.92, 109.77, 109.03, 71.31, 55.68, 22.49, 22.38, 22.20, 10.46. HRMS (ESI-TOF) m/z [M+Na]⁺ calcd. for C₂₃H₂₄ClNO₅ 452.1241, found 452.1262.

16g (BW-AQ-215), 3-Chloro-N-(9,10-dioxo-4,5-dipropoxy-9,10-dihydroanthracen-2-yl)propanamide:

Isolated yield over two steps: 45%. ¹H NMR (DMSO-*d*₆): δ 10.59 (s, 1H), 7.88-7.84 (m, 2H), 7.69-7.65 (m, 2H), 7.50 (d, J = 7.4 Hz, 1H), 4.09-4.02 (m, 4H), 3.90 (t, J = 6.0 Hz, 2H), 2.89 (t, J = 6.4 Hz, 2H), 1.84-1.76 (m, 4H), 1.08-1.04 (m, 6H); ¹³C NMR (DMSO-*d*₆): δ 183.8, 180.3, 169.5, 159.9, 158.8, 144.2, 135.4, 134.6, 134.3, 124.1, 120.7, 119.5, 118.6, 109.2, 108.5, 70.8, 70.7, 22.5, 22.5, 10.8, 10.8. HRMS (ESI-TOF) m/z [M+H]⁺ calcd. for C₂₃H₂₄ClNO₅ 430.1416, found 430.1402.

16h (BW-AQ-213), 4-Chloro-N-(9,10-dioxo-4,5-dipropoxy-9,10-dihydroanthracen-2-yl)butanamide:

Isolated yield over two steps: 45%. ¹H NMR (DMSO-*d*₆): δ 10.50 (s, 1H), 7.88-7.84 (m, 2H), 7.71-7.65 (m, 2H), 7.50 (d, J = 7.6 Hz, 1H), 4.09-4.01 (m, 4H), 3.72 (t, J = 6.4 Hz, 2H), 2.55-

2.53 (m, 2H), 2.07-2.05 (m, 2H), 1.82-1.78 (m, 4H), 1.08-1.03 (m, 6H); ^{13}C NMR (DMSO- d_6): δ 183.8, 180.3, 171.7, 159.9, 158.8, 144.5, 135.3, 134.6, 134.3, 124.1, 120.7, 118.6, 109.2, 108.5, 70.8, 70.7, 34.0, 28.1, 22.5, 22.5, 10.8. HRMS (ESI-TOF) m/z $[\text{M}+\text{H}]^+$ calcd. for $\text{C}_{24}\text{H}_{26}\text{ClNO}_5$ 444.1572, found 444.1555.

16i (BW-AQ-215), 3-Chloro-N-(9,10-dioxo-4,5-dipropoxy-9,10-dihydroanthracen-2-yl)propanamide:

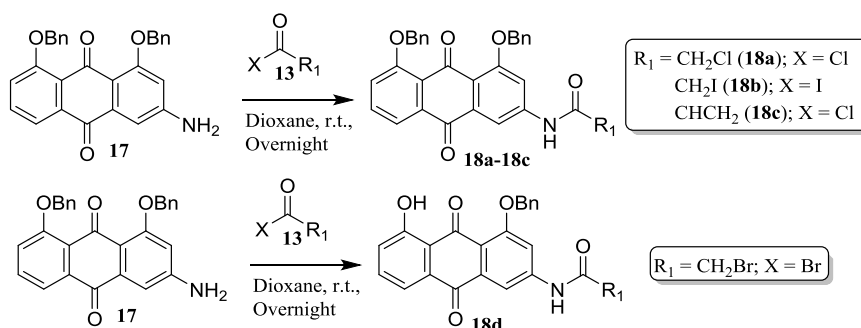
Isolated yield over two steps: 45%. ^1H NMR (DMSO- d_6): δ 10.59 (s, 1H), 7.88-7.84 (m, 2H), 7.69-7.65 (m, 2H), 7.50 (d, $J = 7.4$ Hz, 1H), 4.09-4.02 (m, 4H), 3.90 (t, $J = 6.0$ Hz, 2H), 2.89 (t, $J = 6.4$ Hz, 2H), 1.84-1.76 (m, 4H), 1.08-1.04 (m, 6H); ^{13}C NMR (DMSO- d_6): δ 183.8, 180.3, 169.5, 159.9, 158.8, 144.2, 135.4, 134.6, 134.3, 124.1, 120.7, 119.5, 118.6, 109.2, 108.5, 70.8, 70.7, 22.5, 22.5, 10.8, 10.8. HRMS (ESI-TOF) m/z $[\text{M}+\text{H}]^+$ calcd. for $\text{C}_{23}\text{H}_{24}\text{ClNO}_5$ 430.1416, found 430.1402.

16j (BW-AQ-156), 2-Azido-N-(9,10-dioxo-4,5-dipropoxy-9,10-dihydroanthracen-2-yl)acetamide:

Isolated yield: 99%. ^1H NMR (DMSO- d_6): δ 8.62 (s, 1H), 8.11 (s, 1H), 7.79 (d, $J = 7.6$ Hz, 1H), 7.60-7.56 (m, 2H), 7.29 (d, $J = 8.8$ Hz, 1H), 4.21 (s, 2H), 7.29 (d, $J = 4.4$ Hz, 4H), 1.95-1.89 (m, 4H), 1.12-1.09 (m, 6H); ^{13}C NMR (DMSO- d_6): δ 183.73, 180.34, 167.84, 159.88, 158.79, 143.72, 135.41, 134.55, 134.36, 124.10, 120.74, 119.80, 118.63, 109.44, 108.63, 70.85, 70.80, 51.87, 22.53, 22.46, 10.83, 10.79. HRMS (ESI-TOF) m/z $[\text{M}+1]^+$ calcd. for $\text{C}_{22}\text{H}_{22}\text{N}_4\text{O}_5$ 423.1663, found 423.1643.

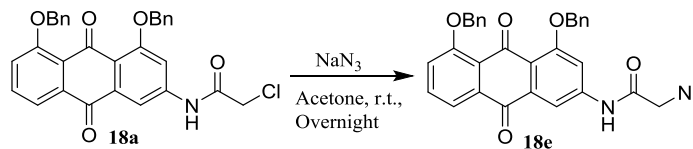
1.3.4 Synthesis of 1,8-bis(benzyloxy)anthracene-9,10-dione compounds

The 1,8-bis(benzyloxy)anthracene-9,10-dione class of compounds consists of five analogs (**18a-18e**) synthesized from aniline **17**. Compound **17** was synthesized following synthetic Scheme 1.3.1. The aniline (**17**) was reacted with the corresponding acyl chloride (Scheme 1.3.8) in 1,4-dioxane at room temperature to give compounds **18a-18d** at various yields (Figure 1.3.4, see the Experimental Section for yields). During the synthesis of **18d**, the byproduct (HBr) of the reaction between aniline **17** and bromoacetyl bromide resulted in the deprotection of one of the benzyl groups attached to either position 1 or 8 of the anthraquinone core.



Scheme 1.8 General synthetic routes to compounds **18a-18d**

Compound **18a** was used as a starting material in the synthesis of azide **18e** (Scheme 1.3.9). A substitution reaction between **18a** and excess of sodium azide in acetone resulted in compound **18e**. The reaction was stirred at room temperature overnight to give **18e** in quantitative yields.



Scheme 1.9 Synthesis of compound **18e**

All synthesized compounds that belong to the 1,8-bis(benzyloxy)anthracene-9,10-dione class are summarized in Figure 1.3.4. The biological activity of these compounds is described in Section 1.4. of this chapter.

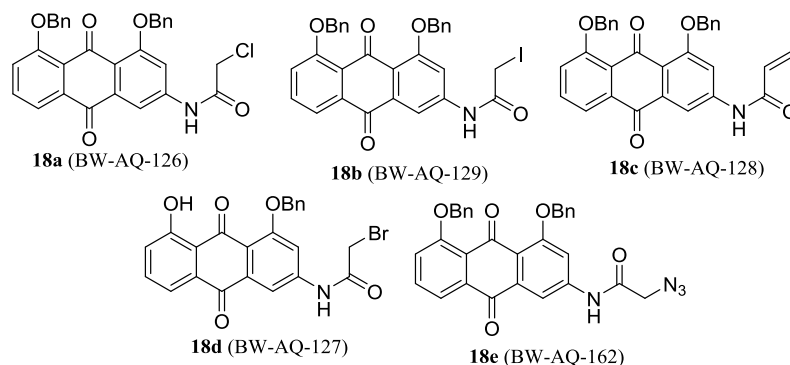


Figure 1.3.4 Synthesized of 1,8-bis(benzyloxy)anthracene-9,10-dione analogs

1.3.4.1 Experimental Section

General experimental procedures for the synthesis of compounds (18a-18d):

Compound **17** (1.0 eq.) was dissolved and stirred in 1, 4-dioxane at room temperature followed by addition of the corresponding acyl halide (**13**, 1.5 eq.). After reaction completion, the reaction mixture was diluted with distilled water/ice. Yellow to orange solids precipitated out and were isolated either by centrifugation at 5000 rpm for 10 min followed by decantation and complete removal of water by putting the crude product in high vacuum pump system, or by vacuum filtration. The crude product was purified by silica gel column chromatography using a dichloromethane (DCM)/ethyl acetate (EtAc) gradient mixture to afford the pure product **18a-18d**.

Experimental procedure for the synthesis of compound 18e:

Compound **18a** (1.0 eq.) was dissolved and stirred in acetone at room temperature followed by addition of sodium azide (2.0 eq.). After overnight stirring, the acetone was partially evaporated

and the remaining residue was diluted with water/ice. Yellow to orange solid precipitated out and was isolated either by centrifugation at 5000 rpm for 10 min followed by decantation and complete removal of water by putting the crude product in high vacuum pump system, or by vacuum filtration.

18a (BW-AQ-126), *N-(4,5-bis(benzyloxy)-9,10-dioxo-9,10-dihydroanthracen-2-yl)-2-chloroacetamide:*

Isolated yield over two steps: 68%. ¹H NMR (DMSO-*d*₆): δ 10.82 (s, 1H), 7.89 (s, 2H), 7.69-7.63 (m, 7H), 7.40-7.36 (m, 6H), 5.29 (s, 2H), 5.24 (s, 2H), 4.32 (s, 2H); ¹³C NMR (DMSO-*d*₆): δ 183.41, 180.55, 165.99, 159.34, 158.23, 143.88, 137.38, 137.09, 135.41, 134.58, 134.44, 128.89, 128.76, 128.09, 128.02, 127.43, 127.29, 124.22, 121.09, 119.98, 119.13, 109.85, 109.13, 70.60, 70.49, 44.08. HRMS (ESI-TOF) *m/z* [M+1]⁺ calcd. for C₃₀H₂₂ClNO₅ 512.1259, found 512.1234.

18b (BW-AQ-129), *N-(4,5-bis(benzyloxy)-9,10-dioxo-9,10-dihydroanthracen-2-yl)-2-iodoacetamide:*

Isolated yield over two steps: 85%. ¹H NMR (DMSO-*d*₆): δ 10.87 (s, 1H), 7.89-7.66 (m, 2H), 7.73-7.60 (m, 6H), 7.43-7.35 (m, 7H), 5.30 (s, 2H), 5.26 (s, 2H), 3.87 (s, 2H); ¹³C NMR (DMSO-*d*₆): δ 183.48, 180.59, 168.11, 159.38, 158.23, 144.28, 137.38, 137.10, 135.44, 134.61, 134.47, 128.77, 128.10, 128.04, 127.33, 127.30, 124.27, 121.13, 119.85, 119.14, 109.55, 108.92, 70.61, 70.49. HRMS (ESI-TOF) *m/z* [M+1]⁺ calcd. for C₃₀H₂₂INO₅ 604.0615, found 604.0588.

18c (BW-AQ-128), *N-(4,5-bis(benzyloxy)-9,10-dioxo-9,10-dihydroanthracen-2-yl)acrylamide:*

Isolated yield over two steps: 77%. ¹H NMR (DMSO-*d*₆): δ 10.76 (s, 1H), 8.06 (s, 1H), 7.97 (d, *J* = 1.2 Hz, 1H), 7.73-7.59 (m, 7H), 7.44-7.35 (m, 7H), 6.49-6.33 (m, 2H), 5.87 (d, *J* = 1.6

Hz, 1H), 5.85 (s, 2H), 5.84 (s, 2H); ^{13}C NMR (DMSO- d_6): δ 183.55, 180.64, 164.36, 159.36, 158.24, 144.50, 137.39, 137.13, 135.39, 134.64, 134.46, 131.76, 128.89, 128.77, 128.11, 128.04, 127.33, 127.31, 124.33, 121.15, 119.77, 119.15, 109.91, 109.32, 70.62, 70.50, 66.82. HRMS (ESI-TOF) m/z $[\text{M}+1]^+$ calcd. for $\text{C}_{31}\text{H}_{23}\text{NO}_5$ 490.1649, found 490.1625.

18d (BW-AQ-127), *N*-(4-(benzyloxy)-4-hydroxy-9,10-dioxo-9,10-dihydroanthracen-2-yl)-2-bromoacetamide:

Isolated yield over two steps: 30%. ^1H NMR (DMSO- d_6): δ 13.11(s, 1H), 11.02 (s, 1H), 7.95 (d, J = 2 Hz, 2H), 7.91 (t, J = 2 Hz, 1H), 7.68-7.58 (m, 3H), 7.44 (t, J = 7.6 Hz, 2H), 7.36-7.29 (m, 4H), 5.28 (s, 2H), 4.10 (s, 2H); ^{13}C NMR (DMSO- d_6): δ 187.25, 182.21, 166.42, 162.03, 161.22, 145.77, 136.66, 136.43, 136.33, 132.74, 128.92, 128.24, 127.48, 124.90, 118.77, 117.07, 116.31, 110.33, 108.96, 70.67, 30.70. HRMS (ESI-TOF) m/z $[\text{M}+1]^+$ calcd. for $\text{C}_{23}\text{H}_{16}\text{BrNO}_5$ 466.0285, found 466.0263.

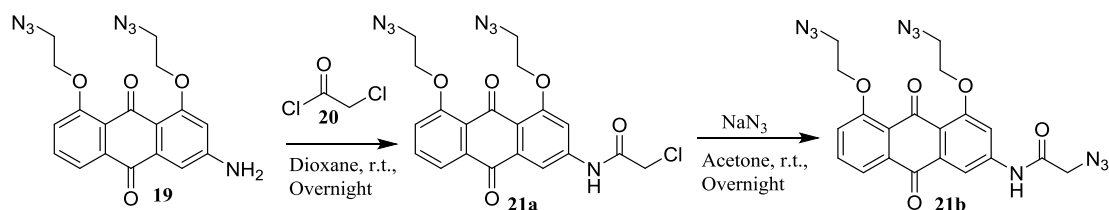
18e (BW-AQ-162), 2-Azido-*N*-(4,5-bis(benzyloxy)-9,10-dioxo-9,10-dihydroanthracen-2-yl)acetamid:

Isolated yield: 98%. ^1H NMR (DMSO- d_6): δ 10.70 (s, 1H), 7.92 (s, 2H), 7.74-7.61 (m, 7H) 7.44-7.35 (m, 6H), 5.32 (s, 2H), 5.28 (s, 2H), 4.13 (s, 2H); ^{13}C NMR (DMSO- d_6): δ 183.51, 180.65, 167.86, 159.39, 158.24, 143.88, 137.39, 137.09, 135.49, 134.63, 134.51, 128.78, 128.12, 128.06, 127.33, 127.31, 124.32, 121.18, 119.94, 119.16, 109.84, 109.11, 70.63, 70.53, 51.89. HRMS (ESI-TOF) m/z $[\text{M}+1]^+$ calcd. for $\text{C}_{30}\text{H}_{22}\text{N}_4\text{O}_5$ 519.1663, found 519.1640.

1.3.5 Synthesis of 1,8-bis(2-azidoethoxy)anthracene-9,10-dione compounds

Two compounds that belong to the 1,8-bis(2-azidoethoxy)anthracene-9,10-dione class (**21a**, **21b**) were synthesized from aniline **19**. Compound **19** was synthesized following synthetic Scheme 1.3.1. Rhein (**1**) was reacted with iodomethane (1 eq.) in the presence of sodium

bicarbonate (2 eq.), in DMF. The reaction was stirred at room temperature overnight and yielded intermediate **2**; where R at 1 and 8 positions are “H” and at position 3 is “CH₃”. The described intermediate (**2**) was then reacted with 2-azidoethyl-4-methylbenzenesulfonate (reagent synthesized following reported protocols²) under basic conditions (K₂CO₃, NaI, DMF, 60°C, overnight) to give intermediate **2** (quantitative yield); where R at the 1 and 8 positions are “CH₂CH₂N₃” and at position 3 is “CH₃.” Aniline **19** was then synthesized as described in Scheme 1.3.1. Compounds **21a** was obtained upon reaction of **19** with chloroacetyl chloride in 1,4 –dioxane at room temperature (Scheme 1.3.10).



*Scheme 1.10 Synthesis of compound **21a** and **21b***

Compound **21a** was used as a starting material in the synthesis of azide **21b** (Scheme 1.3.10). A substitution reaction between **21a** and excess of sodium azide in acetone resulted in compound **21b**. The reaction was stirred at room temperature overnight to give **21b** in 98 % yield.

The synthesized compounds that belong to the 1,8-bis(2-azidoethoxy)anthracene-9,10-dione class are summarized in Figure 1.3.5. These compounds contain free azido groups allowing for further functionalization through copper catalyzed or copper free “click” reactions. The biological activity of these compounds is described in Section 1.4. of this chapter.

1.3.5.1 *Experimental Section*

Compound **19** (1.0 eq.) was dissolved and stirred in 1, 4-dioxane at room temperature followed by addition of the corresponding acyl halide (**20**, 1.5 eq.). After reaction completion, the reaction mixture was diluted with distilled water/ice. Yellow to orange solid precipitated out and was isolated either by centrifugation at 5000 rpm for 10 min followed by decantation and complete removal of water by putting the crude product in high vacuum pump system, or by vacuum filtration. The crude product was purified by silica gel column chromatography using a dichloromethane (DCM)/ethyl acetate (EtAc) gradient mixture to afford the pure product

Compound **21a** (1.0 eq.) was dissolved and stirred in acetone at room temperature followed by addition of sodium azide (2.0 eq.). After overnight stirring, the acetone was partially evaporated and the remaining residue was diluted with water/ice. Yellow to orange solid precipitated out and was isolated either by centrifugation at 5000 rpm for 10 min followed by decantation and complete removal of water by putting the crude product in high vacuum pump system, or by vacuum filtration.

21a (BW-AQ-124), *N*-(4,5-bis(2-azidoethoxy)-9,10-dioxo-9,10-dihydroanthracen-2-yl)-2-chloroacetamide:

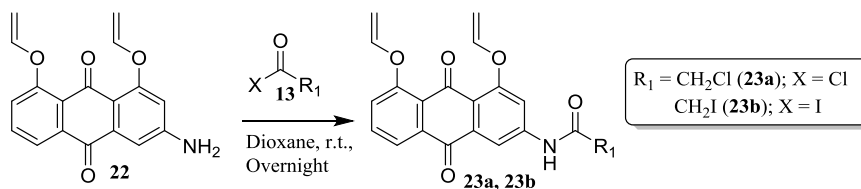
Isolated yield over two steps: 55%. ^1H NMR (DMSO- d_6): δ 10.81 (s, 1H), 7.92 (d, $J = 1.6$ Hz, 1H), 7.84 (d, $J = 1.2$ Hz, 1H), 7.72-7.71 (m, 2H), 7.54-7.51 (m, 1H), 4.33 (s, 2H), 4.28-4.21 (m, 4H), 3.72-3.68 (m, 4H); ^{13}C NMR (DMSO- d_6): δ 183.33, 179.86, 166.02, 159.27, 158.20, 143.78, 135.37, 134.53, 134.43, 124.34, 121.50, 120.13, 119.51, 110.37, 109.52, 68.90, 68.86, 50.22, 50.14, 44.06. HRMS (ESI-TOF) m/z $[\text{M}+1]^+$ calcd. for $\text{C}_{20}\text{H}_{16}\text{ClN}_7\text{O}_5$ 470.0974, found 470.0954.

21b (BW-AQ-140), 2-Azido-N-(4,5-bis(2-azidoethoxy)-9,10-dioxo-9,10-dihydroanthracen-2-yl)acetamide:

Isolated yield: 98%. ^1H NMR (DMSO- d_6): δ 10.67 (s, 1H), 7.89 (s, 1H), 7.80 (s, 1H), 7.71 (d, $J = 4.0$ Hz, 2H), 7.52 (t, $J = 4.0$ Hz, 1H), 4.28-4.21 (m, 4H), 4.11 (s, 2H), 3.72-3.68 (m, 4H); ^{13}C NMR (DMSO- d_6): δ 183.35, 179.85, 167.84, 159.30, 158.19, 143.74, 135.36, 134.53, 134.40, 124.35, 121.51, 119.96, 119.50, 110.23, 109.43, 68.91, 68.85, 51.86, 50.22, 50.14. HRMS (ESI-TOF) m/z $[\text{M}+1]^+$ calcd. for $\text{C}_{20}\text{H}_{16}\text{N}_{10}\text{O}_5$ 477.1351, found 477.1358.

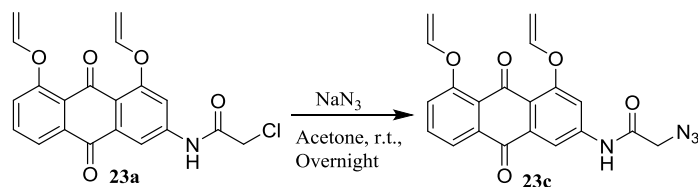
1.3.6 Synthesis of 1,8-bis(vinyloxy)anthracene-9,10-dione compounds

The 1,8-bis(vinyloxy)anthracene-9,10-dione class of compounds consists of three analogs (**23a-23c**) synthesized from aniline **22**. Compound **22** was synthesized following synthetic Scheme 1.3.1. The aniline (**22**) was then reacted with the corresponding acyl chloride (Scheme 1.3.6) in 1,4-dioxane at room temperature to give compounds **23a** and **23b** (Figure 1.3.11, see the experimental section for yields).



*Scheme 1.11 General synthetic route to compounds **23a** and **23b***

Compound **23a** was used as a starting material in the synthesis of azide **23c** (Scheme 1.3.12). A substitution reaction between **23a** and excess of sodium azide in acetone resulted in compound **23c**. The reaction was stirred at room temperature overnight to give **23c** (80% yield).



*Scheme 1.12 Synthesis of compound **23c***

Unfortunately, this class of compounds was limited to only three analogs due to their lack of solubility. The attachment of allyl groups to positions 1 and 8 of the anthraquinone core resulted in the development of compounds with poor solubility, thus making them unsuitable drug candidates; so additional modifications at position 3 were not explored. All synthesized compounds that belong to the 1,8-bis(vinylloxy)anthracene-9,10-dione class are summarized in Figure 1.3.6. The biological activity of these compounds is described in Section 1.4. of this chapter.

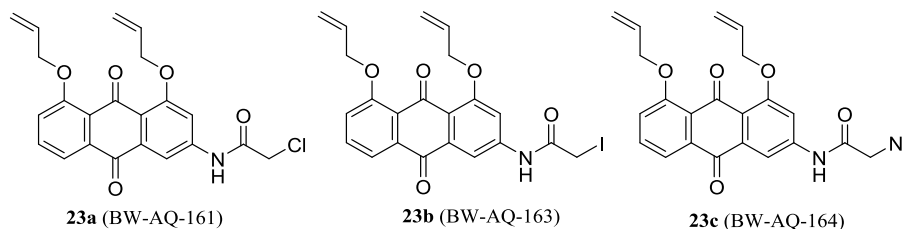


Figure 1.3.6 Synthesized of 1,8-bis(vinyloxy)anthracene-9,10-dione analogs.

1.3.6.1 Experimental section

General experimental procedure for the synthesis of compounds **23a** and **23b**:

Compound **22** (1.0 eq.) was dissolved and stirred in 1, 4-dioxane at room temperature followed by addition of the corresponding acyl halide (**13**, 1.5 eq.). After reaction completion, the reaction mixture was diluted with distilled water/ice. Yellow to orange solids precipitated out and were isolated either by centrifugation at 5000 rpm for 10 min followed by decantation and complete removal of water by putting the crude product in high vacuum pump system, or by vacuum filtration. The crude product was purified by silica gel column chromatography using a dichloromethane (DCM)/ethyl acetate (EtAc) gradient mixture to afford the pure product **23a** and **23b**.

Experimental procedure for the synthesis of compound **23c**:

Compound **23a** (1.0 eq.) was dissolved and stirred in acetone at room temperature followed by addition of sodium azide (2.0 eq.). After overnight stirring, acetone was partially evaporated and the remaining residue was diluted with water/ice. Yellow to orange solid precipitated out and was isolated either by centrifugation at 5000 rpm for 10 min followed by decantation and complete removal of water by putting the crude product in high vacuum pump system, or by vacuum filtration.

23a (BW-AQ-161), *N*-(4,5-bis(allyloxy)-9,10-dioxo-9,10-dihydroanthracen-2-yl)-2-chloroacetamide:

Isolated yield over two steps: 73%. ^1H NMR ($\text{DMSO-}d_6$): δ 9.56 (s, 1H), 7.81 (s, 1H), 7.81-7.68 (m, 3H) 7.53-7.50 (m, 1H), 6.14-6.05 (m, 2H), 5.72-5.63 (m, 2H), 5.36-5.30 (m, 2H), 4.73 (t, $J = 4$ Hz, 4H), 3.56 (s, 2H); ^{13}C NMR ($\text{DMSO-}d_6$): δ 183.74, 180.41, 159.51, 158.21, 152.33, 144.91, 135.41, 134.61, 134.31, 133.59, 133.38, 124.07, 120.90, 118.91, 118.62, 117.67, 117.53, 108.75, 108.20, 69.59, 66.82. HRMS (ESI-TOF) m/z $[\text{M}+1]^+$ calcd. for $\text{C}_{22}\text{H}_{18}\text{ClINO}_5$ 412.0946, found 412.0927.

23b (BW-AQ-163), *N,N*-(4,5-bis(allyloxy)-9,10-dioxo-9,10-dihydroanthracen-2-yl)-2-iodoacetamide:

Isolated yield over two steps: 80%. ^1H NMR ($\text{DMSO-}d_6$): δ 9.51 (s, 1H), 7.77 (s, 1H), 7.68 (d, $J = 4.4$ Hz, 3H) 7.49 (d, $J = 4.4$ Hz, 1H), 6.12-6.08 (m, 2H), 5.72-5.63 (m, 2H), 5.33 (t, $J = 4$ Hz, 2H), 4.72 (s, 4H); ^{13}C NMR ($\text{DMSO-}d_6$): δ 183.75, 180.42, 159.51, 158.21, 144.93, 135.42, 134.63, 134.33, 133.59, 133.38, 124.09, 120.93, 118.92, 118.64, 117.68, 117.54, 108.80, 108.23, 69.60. HRMS (ESI-TOF) m/z $[\text{M}+1]^+$ calcd. for $\text{C}_{22}\text{H}_{18}\text{INO}_5$ 504.0302, found 504.0278.

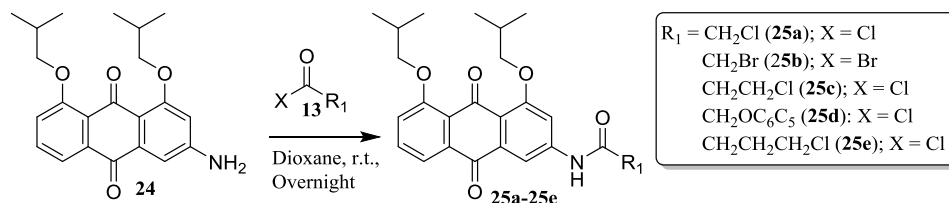
23c (BW-AQ-164), 2-Azido-*N*-(4,5-bis(allyloxy)-9,10-dioxo-9,10-dihydroanthracen-2-yl)acetamide:

Isolated yield: 80%. ^1H NMR ($\text{DMSO-}d_6$): δ 9.55 (s, 1H), 7.78 (s, 1H), 7.69 (s, 3H) 7.50 (s, 1H), 6.16-6.06 (m, 2H), 5.72-5.63 (m, 2H), 5.33 (t, $J = 4$ Hz, 2H), 4.73 (s, 4H); ^{13}C NMR ($\text{DMSO-}d_6$): δ 183.76, 180.41, 159.50, 158.20, 135.41, 134.62, 134.31, 133.59, 133.38, 124.08, 120.91, 118.91, 118.59, 117.68, 117.53, 108.76, 108.23, 69.60, 69.56.

1.3.7 Synthesis of 1,8-diisobutoxyanthracene-9,10-dione compounds

The 1,8-diisobutoxyanthracene-9,10-dione class of compounds consists of five analogs (**25a-25e**) synthesized from aniline **24**. Compound **24** was synthesized following synthetic Scheme 1.3.1. The aniline (**24**) was then reacted with the corresponding acyl chloride (Scheme

1.3.13) in 1,4-dioxane at room temperature to give compounds **25a- 25e** (Figure 1.3.7, see the experimental section for yields).



Scheme 1.13 General synthetic route to compounds 25a-25e

All synthesized compounds that belong to the 1,8-diisobutoxyanthracene-9,10-dione class are summarized in Figure 1.3.7. The biological activity of these compounds is described in Section 1.4. of this chapter.

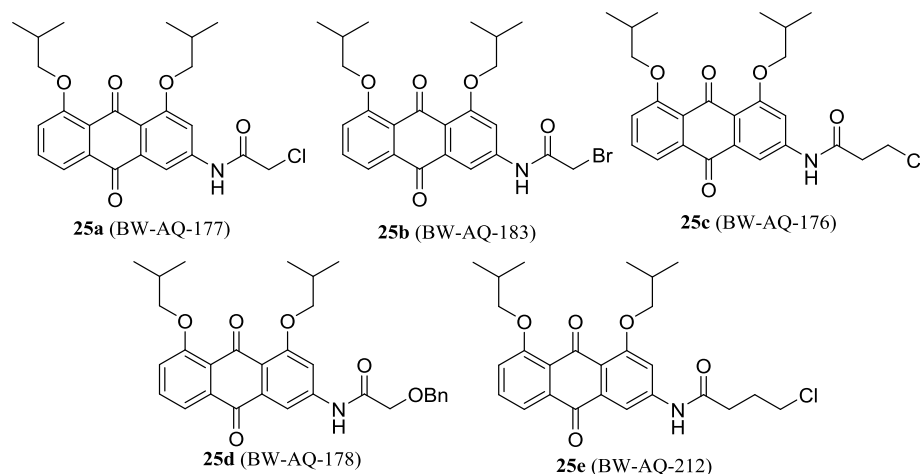


Figure 1.3.7 Synthesized of 1,8-diisobutoxyanthracene-9,10-dione analogs

1.3.7.1 Experimental section

General experimental procedure for the synthesis of compounds 25a-25e:

Compound **24** (1.0 eq.) was dissolved and stirred in 1, 4-dioxane at room temperature followed by addition of the corresponding acyl halide (**13**, 1.5 eq.). After reaction completion, the

reaction mixture was diluted with distilled water/ice. Yellow to orange solids precipitated out and were isolated either by centrifugation at 5000 rpm for 10 min followed by decantation and complete removal of water by putting the crude product in high vacuum pump system, or by vacuum filtration. The crude product was purified by silica gel column chromatography using a dichloromethane (DCM)/ethyl acetate (EtAc) gradient mixture to afford the pure products **25a-25e**.

25a (BW-AQ-177), *2-Chloro-N-(4,5-diisobutoxy-9,10-dioxo-9,10-dihydroanthracen-2-yl)acetamide*:

Isolated yield over two steps: 30%. ¹H NMR (CDCl₃): δ 8.54 (s, 1H), 8.06 (s, 1H), 7.78 (d, *J* = 7.6 Hz, 1H), 7.57 (t, *J* = 8 Hz, 1H), 7.52 (s, 1H), 7.28-7.26 (m, 1H), 4.23 (s, 2H), 3.91-3.87 (m, 4H), 2.98-2.95 (m, 2H), 1.12-1.10 (m, 12H); ¹³C NMR (CDCl₃): δ 183.88, 180.96, 164.39, 160.47, 159.06, 141.39, 135.44, 134.61, 133.38, 124.67, 121.26, 119.75, 118.77, 109.61, 108.68, 75.97, 42.91, 28.46, 28.40, 19.15. HRMS (ESI-TOF) *m/z* [M+Na]⁺ calcd. for C₂₄H₂₆ClNO₅ 466.1397, found 466.1389.

25b (BW-AQ-183), *2-Bromo-N-(4,5-diisobutoxy-9,10-dioxo-9,10-dihydroanthracen-2-yl)acetamide*:

Isolated yield over two steps: 25%. ¹H NMR (CDCl₃): δ 8.68 (s, 1H), 8.08 (d, *J* = 2 Hz, 1H), 7.77 (d, *J* = 7.6 Hz, 1H), 7.57 (t, *J* = 8 Hz, 1H), 7.52 (d, *J* = 1.6 Hz, 1H), 7.28-7.26 (m, 1H), 4.07 (s, 2H), 3.91-3.87 (m, 4H), 2.27-2.19 (m, 2H), 1.16-1.10 (m, 12H); ¹³C NMR (CDCl₃): δ 184.00, 181.04, 164.25, 160.46, 159.05, 141.84, 135.34, 134.59, 133.40, 124.62, 121.06, 119.78, 118.76, 109.59, 108.67, 76.72, 76.03, 75.96, 29.37, 28.44, 28.38, 19.15. HRMS (ESI-TOF) *m/z* [M+Na]⁺ calcd. for C₂₄H₂₆BrNO₅ 510.0892, found 510.0887.

25c (BW-AQ-176), 3-Chloro-N-(4,5-diisobutoxy-9,10-dioxo-9,10-dihydroanthracen-2-yl)propanamide:

Isolated yield over two steps: 27 %. ^1H NMR (CDCl_3): δ 8.42 (s, 1H), 8.24 (s, 1H), 7.77 (d, $J = 7.6$ Hz, 1H), 7.58 (t, $J = 8$ Hz, 1H), 7.52 (s, 1H), 7.29-7.27 (m, 1H), 3.92-3.88 (m, 6H), 2.98-2.95 (m, 2H), 2.27-2.20 (m, 2H), 1.13-1.10 (m, 12H); ^{13}C NMR (CDCl_3): δ 184.63, 181.07, 168.67, 160.55, 159.08, 142.66, 135.17, 134.64, 133.35, 124.69, 120.51, 119.89, 118.67, 109.90, 108.60, 40.45, 39.38, 28.44, 28.40, 19.17, 19.15. HRMS (ESI-TOF) m/z $[\text{M}+\text{Na}]^+$ calcd. for $\text{C}_{25}\text{H}_{28}\text{ClNO}_5$ 480.1554, found 480.1565.

25d (BW-AQ-178), 2-(Benzyloxy)-N-(4,5-diisobutoxy-9,10-dioxo-9,10-dihydroanthracen-2-yl)acetamide:

Isolated yield over two steps: 35%. ^1H NMR (CDCl_3): δ 8.61 (s, 1H), 8.16 (d, $J = 1.6$ Hz, 1H), 7.79 (d, $J = 7.2$ Hz, 1H), 7.58 (t, $J = 7.6$ Hz, 1H), 7.45-7.39 (m, 6H), 7.28-7.26 (m, 1H), 4.70 (s, 2H), 4.13 (s, 2H), 3.93-3.88 (m, 4H), 2.28-2.06 (m, 2H), 1.14-1.10 (m, 12H); ^{13}C NMR (CDCl_3): δ 184.04, 180.97, 168.17, 160.51, 159.03, 141.76, 136.22, 135.39, 134.68, 133.24, 128.86, 128.62, 128.19, 124.79, 120.77, 119.74, 118.74, 109.53, 108.48, 76.04, 75.90, 73.94, 69.43, 28.47, 28.41, 19.16. HRMS (ESI-TOF) m/z $[\text{M}+\text{Na}]^+$ calcd. for $\text{C}_{31}\text{H}_{33}\text{NO}_6$ 538.2206, found 538.2222.

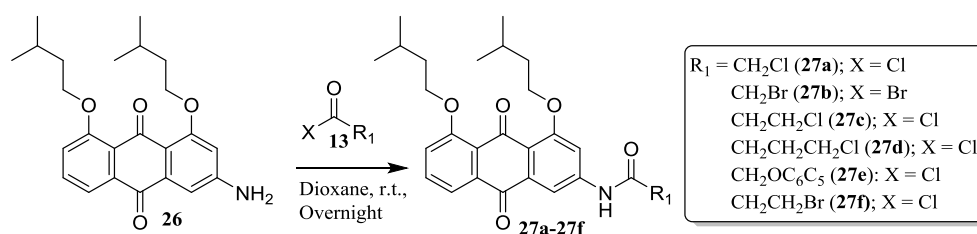
25e (BW-AQ-212), 4-Chloro-N-(4,5-diisobutoxy-9,10-dioxo-9,10-dihydroanthracen-2-yl)butanamide

Isolated yield over two steps: 20%. ^1H NMR (CDCl_3): δ 8.22 (s, 1H), 8.08 (s, 1H), 7.78 (d, $J = 7.2$ Hz, 1H), 7.58 (t, $J = 7.6$ Hz, 1H), 7.49 (d, $J = 2$ Hz, 1H), 7.29-7.26 (m, 1H), 3.92- 3.88 (m, 4H), 3.67 (t, $J = 7.2$ Hz, 2H), 2.69-2.65 (m, 2H), 2.26-2.21 (m, 4H), 1.13-1.10 (m, 12H); ^{13}C NMR (CDCl_3): δ 184.46, 180.97, 170.77, 160.58, 159.08, 142.70, 135.27, 134.67, 133.27, 124.77,

120.45, 119.85, 118.67, 109.67, 108.30, 76.05, 75.88, 44.27, 34.23, 29.71, 28.46, 28.42, 27.57, 19.16. HRMS (ESI-TOF) m/z $[M+Na]^+$ calcd. for $C_{26}H_{30}ClNO_5$ 494.1710, found 494.1698.

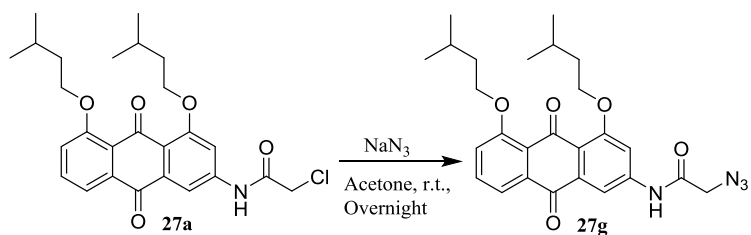
1.3.8 Synthesis of 1,8-bis(isopentyloxy)anthracene-9,10-dione compounds

The 1,8-bis(isopentyloxy)anthracene-9,10-dione class of compounds consists of seven analogs (**27a-27f**) synthesized from aniline **26**. Compound **26** was synthesized following synthetic Scheme 1.3.1. The aniline (**26**) was then reacted with the corresponding acyl chloride (Scheme 1.3.14) in 1,4-dioxane at room temperature to give compounds **27a-27f** (Figure 1.3.8, see the experimental section for yields).



Scheme 1.14 General synthetic route to compounds **27a-27f**

Compound **27a** was used as a starting material in the synthesis of azide **27g** (Scheme 1.3.15). A substitution reaction between **27a** and excess of sodium azide in acetone resulted in compound **27g**. The reaction was stirred at room temperature overnight to give **27g** in quantitative yields.



Scheme 1.15 Synthesis of compound 27g

All synthesized compounds that belong to the 1,8-diisobutoxyanthracene-9,10-dione class are summarized in Figure 1.3.8. The biological activity of these compounds is described in Section 1.4. of this chapter.

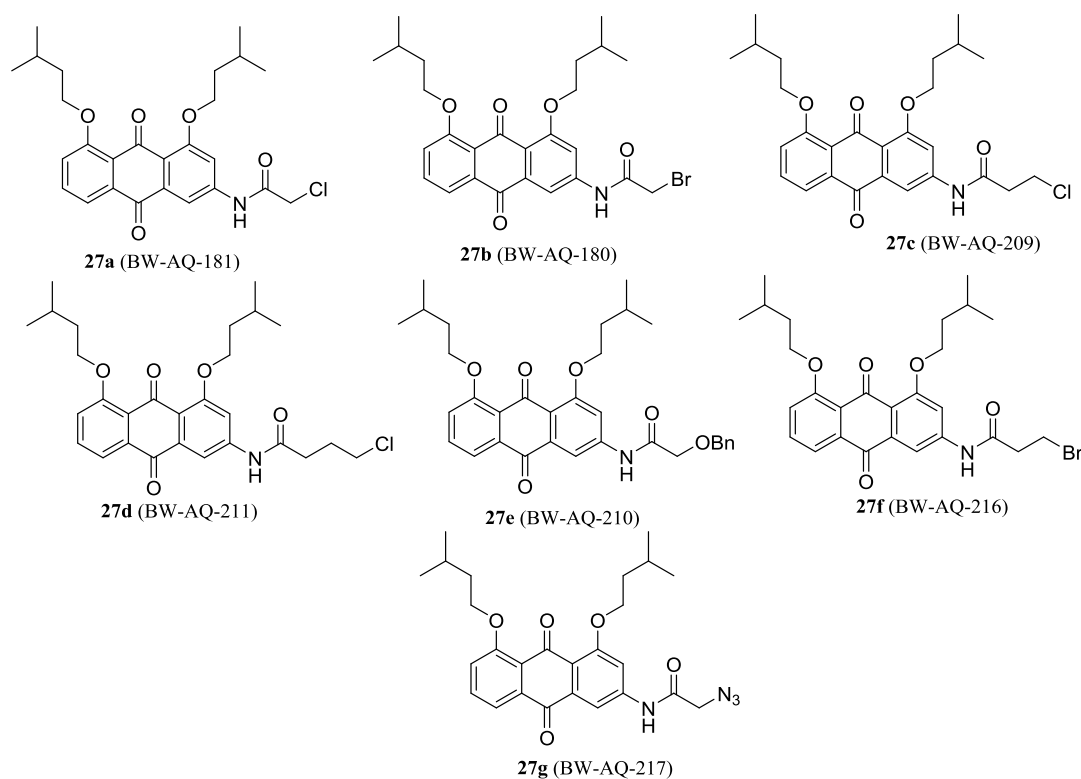


Figure 1.3.8 Synthesized of 1,8-bis(isopentyloxy)anthracene-9,10-dione analogs

1.3.8.1 Experimental section

General experimental procedure for the synthesis of compounds 27a-27f:

Compound **26** (1.0 eq.) was dissolved and stirred in 1, 4-dioxane at room temperature followed by addition of the corresponding acyl halide (**13**, 1.5 eq.). After reaction completion, the reaction mixture was diluted with distilled water/ice. Yellow to orange solids precipitated out and were isolated either by centrifugation at 5000 rpm for 10 min followed by decantation and complete removal of water by putting the crude product in high vacuum pump system, or by vacuum filtration. The crude product was purified by silica gel column chromatography using a dichloromethane (DCM)/ethyl acetate (EtAc) gradient mixture to afford the pure product **27a-27f**.

Experimental procedure for the synthesis of compound **27g**:

Compound **27a** (1.0 eq.) was dissolved and stirred in acetone at room temperature followed by addition of sodium azide (2.0 eq.). After overnight stirring, the acetone was partially evaporated and the remaining residue was diluted with water/ice. Yellow to orange solid precipitated out and was isolated either by centrifugation at 5000 rpm for 10 min followed by decantation and complete removal of water by putting the crude product in high vacuum pump system, or by vacuum filtration.

27a (BW-AQ-181), *N*-(4,5-bis(isopentyloxy)-9,10-dioxo-9,10-dihydroanthracen-2-yl)-2-chloroacetamide:

Isolated yield over two steps: 47%. ¹H NMR (CDCl₃): δ = 8.64 (s, 1H), 8.14 (s, 1H), 7.81 (d, *J* = 7.8 Hz, 1H), 7.60 (t, *J* = 8 Hz, 1H), 7.56 (s, 1H), 7.31 (d, *J* = 7.6 Hz, 1H), 4.25 (s, 2H), 4.21-4.15 (m, *J* = 4.6 Hz, 4H), 2.04-1.98 (m, *J* = 8 Hz, 2H), 1.85-1.79 (m, 4H), 1.02 (s, 6H), 1.00 (s, 6H); ¹³C NMR (CDCl₃): δ = 183.8, 181.0, 164.4, 160.5, 159.0, 141.5, 135.5, 134.6, 133.5, 124.5, 121.0, 119.9, 118.9, 109.6, 108.8, 68.3, 68.2, 42.9, 37.8, 37.6, 25.0, 25.0, 22.6. HRMS (ESI-TOF): *m/z* [M+Na]⁺ calcd for C₂₆H₃₀ClNO₅: 494.1710, found: 494.1694.

27b (BW-AQ-180), *N-(4,5-bis(isopentyloxy)-9,10-dioxo-9,10-dihydroanthracen-2-yl)-2-bromoacetamide:*

Isolated yield over two steps: 25%. ¹H NMR (CDCl₃): δ 8.74 (s, 1H), 8.15 (s, 1H), 7.80 (d, *J* = 7.6 Hz, 1H), 7.59 (t, *J* = 8 Hz, 1H), 7.55 (s, 1H), 7.30 (d, *J* = 8.4 Hz, 1H), 4.20-4.14 (m, 4H), 4.08 (s, 2H), 2.06-1.96 (m, 2H), 1.83-1.75 (m, 4H), 1.00-0.98 (m, 12H); ¹³C NMR (CDCl₃): δ 183.92, 181.29, 164.90, 160.47, 159.04, 142.49, 135.22, 134.58, 133.52, 124.32, 120.46, 119.83, 118.83, 109.67, 108.92, 68.28, 37.74, 37.60, 29.56, 24.98. HRMS (ESI-TOF) *m/z* [M+Na]⁺ calcd. for C₂₆H₃₀BrNO₅ 538.1205, found 538.1196.

27c (BW-AQ-209), *N-(4,5-bis(isopentyloxy)-9,10-dioxo-9,10-dihydroanthracen-2-yl)-3-chloropropanamide:*

Isolated yield over two steps: 55%. ¹H NMR (DMSO-*d*₆): δ 10.59 (s, 1H), 8.14 (s, 1H), 7.85 (s, 1H), 7.70-7.67 (m, 2H), 7.53-7.51 (m, 1H), 4.14-4.07 (m, 4H), 3.90 (t, *J* = 6.0 Hz, 2H), 2.89 (t, *J* = 6 Hz, 2H), 1.97 (m, 2H), 1.70-1.66 (m, 4H), 0.97-0.94 (m, 12H); ¹³C NMR (DMSO-*d*₆): δ 183.8, 180.3, 169.5, 159.8, 158.7, 144.2, 135.4, 134.6, 134.3, 124.2, 120.8, 119.7, 118.6, 109.3, 108.5, 67.9, 67.8, 55.4, 37.9, 37.8, 24.8, 22.9, 22.9. HRMS (ESI-TOF) *m/z* [M+H]⁺ calcd. for C₂₇H₃₂ClNO₅ 486.2042, found 486.2023.

27d (BW-AQ-211), *N-(4,5-bis(isopentyloxy)-9,10-dioxo-9,10-dihydroanthracen-2-yl)-4-chlorobutanamide:*

Isolated yield over two steps: 43%. ¹H NMR (DMSO-*d*₆): δ 10.50 (s, 1H), 7.87 (s, 1H), 7.85 (s, 1H), 7.69-7.67 (m, 2H), 7.53 (s, 1H), 4.14-4.06 (m, 4H), 3.72 (t, *J* = 6.4 Hz, 2H), 2.55 (t, *J* = 7.2 Hz, 2H), 2.07-1.97 (m, 4H), 1.69-1.65 (m, 4H), 0.96-0.94 (m, 12H); ¹³C NMR (DMSO-*d*₆): δ 183.8, 180.3, 171.7, 159.8, 158.7, 144.5, 135.3, 134.6, 134.2, 124.3, 120.7, 119.5, 118.6,

109.3, 108.5, 67.9, 67.7, 55.4, 45.4, 37.9, 37.8, 34.0, 28.1, 24.8, 22.9, 22.9. HRMS (ESI-TOF) m/z $[M+H]^+$ calcd. for $C_{28}H_{34}ClNO_5$ 500.2198, found 500.2176.

27e (BW-AQ-210), 2-(Benzyloxy)-N-(4,5-bis(isopentyloxy)-9,10-dioxo-9,10-dihydroanthracen-2-yl)acetamide:

Isolated yield over two steps: 58%. 1H NMR ($CDCl_3$): δ 8.48 (s, 1H), 7.82 (s, 1H), 7.80 (s, 1H), 7.59 (t, $J = 8.4$ Hz, 1H), 7.47-7.46 (m, 1H), 7.44-7.39 (m, 4H), 7.31-7.28 (m, 1H); ^{13}C NMR ($CDCl_3$): δ 184.0, 180.9, 168.2, 160.6, 159.1, 141.8, 136.2, 135.4, 134.7, 133.3, 128.9, 128.6, 128.2, 124.6, 120.6, 119.9, 118.9, 109.6, 108.5, 69.4, 68.3, 37.8, 37.7, 25.0, 22.6. HRMS (ESI-TOF) m/z $[M+Na]^+$ calcd. for $C_{33}H_{37}NO_6$ 566.2519, found 566.2498.

27f (BW-AQ-216), N-(4,5-bis(isopentyloxy)-9,10-dioxo-9,10-dihydroanthracen-2-yl)-3-bromopropanamide:

Isolated yield over two steps: 53%. 1H NMR ($DMSO-d_6$): δ 10.56 (s, 1H), 7.86 (s, 1H), 7.82 (s, 1H), 7.68-7.64 (m, 2H), 7.51-7.49 (m, 1H), 4.12-4.05 (m, 4H), 3.73 (t, $J = 6.4$ Hz, 2H), 3.00 (t, $J = 6.4$ Hz, 2H), 1.98-1.92 (m, 2H), 1.69-1.64 (m, 4H), 0.95-0.92 (m, 12H); ^{13}C NMR ($DMSO-d_6$): δ 183.8, 180.3, 169.7, 159.8, 158.7, 144.2, 134.3, 124.3, 120.8, 119.7, 118.6, 109.3, 108.5, 67.9, 67.8, 37.9, 37.8, 29.2, 24.8, 22.9, 22.9. HRMS (ESI-TOF) m/z $[M+H]^+$ calcd. for $C_{27}H_{32}BrNO_5$ 530.1537, found 530.1515.

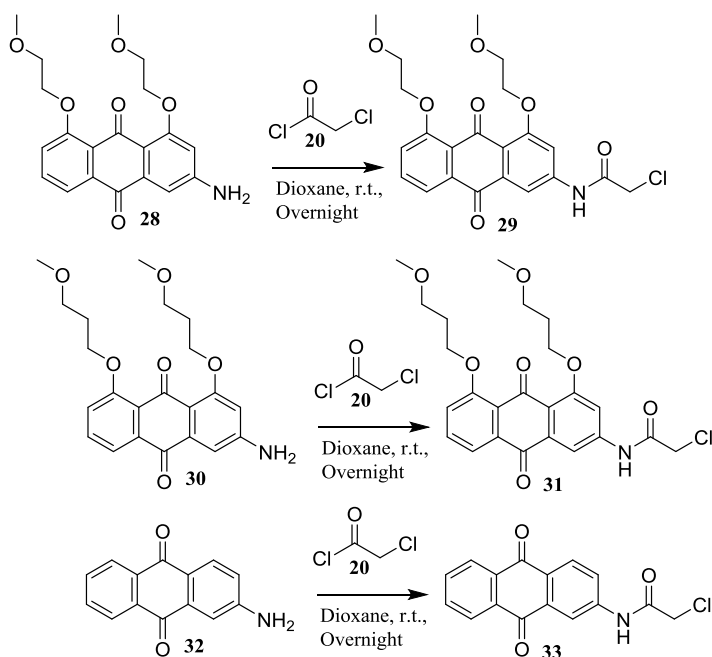
27g (BW-AQ-217), 2-Azido-N-(4,5-bis(isopentyloxy)-9,10-dioxo-9,10-dihydroanthracen-2-yl)acetamide:

Isolated yield: 97%. 1H NMR ($CDCl_3$): δ 8.64 (s, 1H), 8.14 (s, 1H), 7.81 (d, $J = 7.8$ Hz, 1H), 7.60 (t, $J = 8.0$ Hz, 1H), 7.56 (s, 1H), 7.31 (d, $J = 7.6$ Hz, 1H), 4.25 (s, 2H), 4.21-4.15 (m, $J = 4.6$ Hz, 4H), 2.04-1.98 (m, $J = 8$ Hz, 2H), 1.85-1.79 (m, 4H), 1.02 (s, 6H), 1.00 (s, 6H); ^{13}C NMR ($CDCl_3$): δ 183.8, 181.0, 164.4, 160.5, 159.0, 141.5, 135.5, 134.6, 133.5, 124.5, 121.0, 119.9,

118.9, 109.6, 108.8, 68.3, 68.2, 42.9, 37.8, 37.6, 25.0, 25.0, 22.6. HRMS (ESI-TOF) m/z $[M+H]^+$ calcd. for $C_{26}H_{30}N_4O_5$ 494.1710, found 494.1694.

1.3.9 *Synthesis of additional anthracene-9,10-dione analogs*

This section of the chapter describes three compounds that cannot be placed in a specific structural class at this point, but exhibit potent activity. Compounds **29** and **31** were synthesized following the general synthetic rout described in Scheme 1.3.1 with slight variations in intermediate **2**. Rhein (**1**) was reacted with iodomethane (1 eq.) in the presence of sodium bicarbonate (2 eq.), in DMF. The reaction was stirred at room temperature overnight and yielded intermediate **2**; where R at the 1 and 8 positions are “H” and at position 3 is “CH₃.” The described intermediate (**2**) was then reacted with 1-chloro-2-methoxyethane or 1-chloro-3-methoxypropane under basic conditions (K₂CO₃, NaI, Acetone, 90°C, overnight) to give intermediate **2** (quantitative yield) where R at the 1 and 8 positions are “CH₂CH₂OCH₃” or “CH₂CH₂CH₂OCH₃” respectively and at position 3 is “CH₃.” Anilines **28** and **30** were synthesized as described in Scheme 1.3.1 from the two respective intermediates (**2**). Compounds **29** and **31** were obtained upon reaction of **28** and **30** with chloroacetyl chloride in 1,4 –dioxane at room temperature (Scheme 1.3.16).



Scheme 1.16 Synthesis of compound 29, 31, 33

Compound **33** was synthesized by reacting the commercially available aniline **32** with chloroacetyl chloride at room temperature in 1,4-dioxane (Scheme 1.3.16). All of the compounds were purified via silica gel column chromatography. The biological activity of the compounds shown in Figure 1.3.9 is described in Section 1.4. of this chapter.

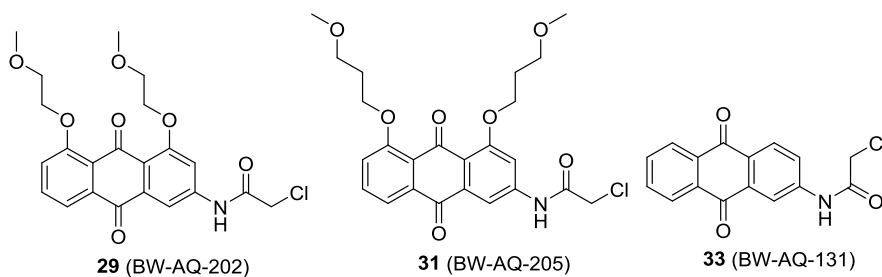


Figure 1.3.9 Synthesized of various anthracene-9,10-dione analogs

1.3.9.1 Experimental section

General experimental procedure for the synthesis of compounds **29**, **31**, and **33**:

Compound **29**, **31**, or **33** (1.0 eq.) was dissolved and stirred in 1, 4-dioxane at room temperature followed by addition of the corresponding acyl halide (**20**, 1.5 eq.). After reaction completion, the reaction mixture was diluted with distilled water/ice. Yellow to orange solids precipitated out and were isolated either by centrifugation at 5000 rpm for 10 min followed by decantation and complete removal of water by putting the crude product in high vacuum pump system, or by vacuum filtration. The crude product was purified by silica gel column chromatography using a dichloromethane (DCM)/ethyl acetate (EtAc) gradient mixture to afford the pure product **29**, **31**, and **33**.

29 (BW-AQ-202), *N*-(4,5-bis(2-methoxyethoxy)-9,10-dioxo-9,10-dihydroanthracen-2-yl)-2-chloroacetamide:

Isolated yield over two steps: 34%. ¹H NMR (CDCl₃): δ 8.68 (s, 1H), 8.09 (s, 1H), 7.82 (d, *J* = 7.6 Hz, 1H), 7.61-7.57 (m, 2H), 7.33 (d, *J* = 8.4 Hz, 1H), 4.28 (s, 4H), 4.23 (s, 2H), 4.11 (s, 2H), 3.88 (s, 4H), 3.53-3.52 (m, 6H); ¹³C NMR (CDCl₃): δ 183.39, 181.15, 164.61, 160.23, 158.84, 141.83, 135.40, 134.55, 133.71, 120.85, 120.77, 119.71, 110.12, 109.47, 70.93, 70.71, 69.68, 69.54, 59.48, 42.97, 29.70. HRMS (ESI-TOF) *m/z* [M+Na]⁺ calcd. for C₂₂H₂₂ClNO₇ 470.0982, found 470.0960.

31 (BW-AQ-205), *N*-(4,5-bis(3-methoxypropoxy)-9,10-dioxo-9,10-dihydroanthracen-2-yl)-2-chloroacetamide:

Isolated yield over two steps: 41%. ¹H NMR (CDCl₃): δ 8.60 (s, 1H), 8.08 (s, 1H), 7.80 (d, *J* = 7.6 Hz, 1H), 7.60-7.57 (m, 2H), 7.32 (d, *J* = 8.4 Hz, 1H), 4.25-4.21 (m, 6H), 3.72-3.69 (m, 4H), 3.37 (s, 6H), 2.17-2.16 (m, 4H); ¹³C NMR (CDCl₃): δ 183.66, 180.97, 164.43, 160.38, 158.97,

141.63, 135.45, 134.60, 133.58, 124.30, 120.82, 119.88, 119.07, 109.69, 108.99, 69.06, 66.60, 66.53, 58.72, 58.68, 42.92, 29.48, 29.29. HRMS (ESI-TOF) m/z $[M+Na]^+$ calcd. for $C_{24}H_{26}ClNO_7$ 498.1295, found 498.1312.

33 (BW-AQ-131), 2-chloro-N-(9,10-dioxo-9,10-dihydroanthracen-2-yl)acetamide:

Isolated yield: 70%. 1H NMR (DMSO- d_6): δ 10.91 (s, 1H), 8.38 (s, 1H), 8.14 (s, 3H), 8.02 (d, J = 7.6 Hz, 1H), 7.88 (d, J = 2.8 Hz, 2H), 4.35 (s, 2H); ^{13}C NMR (DMSO- d_6): δ 182.72, 181.74, 166.01, 144.35, 135.02, 134.70, 134.57, 133.51, 128.99, 128.80, 127.17, 127.10, 124.41, 116.50, 44.06. HRMS (ESI-TOF) m/z $[M+1]^+$ calcd. for $C_{16}H_{10}ClNO_3$ 300.0409, found 300.0422.

1.3.10 Computational evaluation of the designed compounds

In the pursuit of developing new active MDM2-MDM4 inhibitors, we turned to molecular modeling to examine the binding potential of the newly designed compounds. In a previous section of this chapter, the hypothesis that BW-AQ-101 binds to the MDM2 RING homodimer to inhibit MDM2-MDM4 formation was discussed. Biological and *in silico* studies of BW-AQ-101 with the proposed target supported this hypothesis. We herein discuss molecular docking studies aimed at evaluating the potential of the above-described BW-AQ-101 analogs as MDM2 RING binders.

Docking studies are based on two major protein structures; the MDM2-MDM4 heterodimer RING domain and the MDM2 homodimer RING domain. The RING structure of the heterodimer is available through the protein data bank (PDB) with a structure ID 2VJE (Figure 1.3.10, right).³ The heterodimer's (2VJE) crystal structure was derived through X-ray crystallography with a resolution of 2.2 Å.³ The structure of the RING MDM2 homodimer is also available through the PDB under the ID 2HDP; this structure however, was derived from solution NMR (Figure 1.3.10, left).⁴

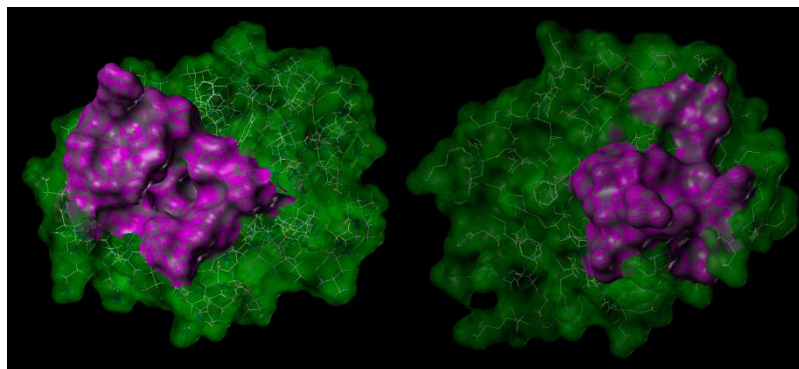


Figure 1.3.10 Structures of the MDM2 RING homodimer and the MDM2-MDM4 RING heterodimer

Left: The RING domain structure of MDM2 homodimer

Right: The RING domain structure of MDM2-MDMX heterodimer

**Highlighted in magenta are the key residues that form a binding pocket in the homodimer and the same residues in the heterodimer that fail to form a binding pocket.*

The study begins with careful analysis and preparation of the obtained structures. The docking studies were done with constricted dielectric constant value of 80 (water), attempting to simulate the physiological environment, which is aqueous. The homodimer was carefully examined and its symmetric structure revealed two identical and symmetric binding pockets formed by the two RING domains (Figure 1.3.11, left). It has been reported that the RING domains are very unstable in solution and they easily form dimeric or other types of aggregate structures; therefore it is safe to assume that the binding pockets that the homodimer forms exist under physiological conditions. The critical amino acids that form a binding pocket in the MDM2 RING homodimeric structures are: A/Val439, A/Ile 440, A/Leu468, A/Lys 473, A/Pro474, A/His452, A/Gln480, A/Cys 478, A/Val 477, A/Pro 476, A/His457, A/Cys 475, B/Pro491, B/Leu432; residues forming the deep inner surface of the pocket: A/His 457, A/Leu 458, A/Ala 460, A/Ile 450, A/ile482, A/Lys 469, A/Ala465. The surface that these residues form can be seen in Figure 1.3.10 (left, colored in magenta). The depth of the pocket formed by these residues can be seen in Figure 1.3.11 (left, colored in blue and yellow). The identified critical residues do not form a binding pocket when translated in the MDM2-MDM4 heterodimeric structure (Figure 1.3.11,

right). The heterodimeric model reveals that the residues of the MDM2 RING responsible for the pocket formation in the homodimeric structure have undergone structural perturbations and simply form the outer surface of the MDM2-MDM4 heterodimer (Figure 1.3.11, right). Interestingly, these residues do not have direct participation in the MDM2-MDM4 RING surface interactions (Figure 1.3.11, bottom). Thus it is safe to assume that binding pocket collapse is due to major conformational changes upon heterodimer formation. These observations support the hypothesis established earlier that the anthraquinone compound described above bind to the homodimeric binding pocket and stabilize the structure, thus locking it in place.

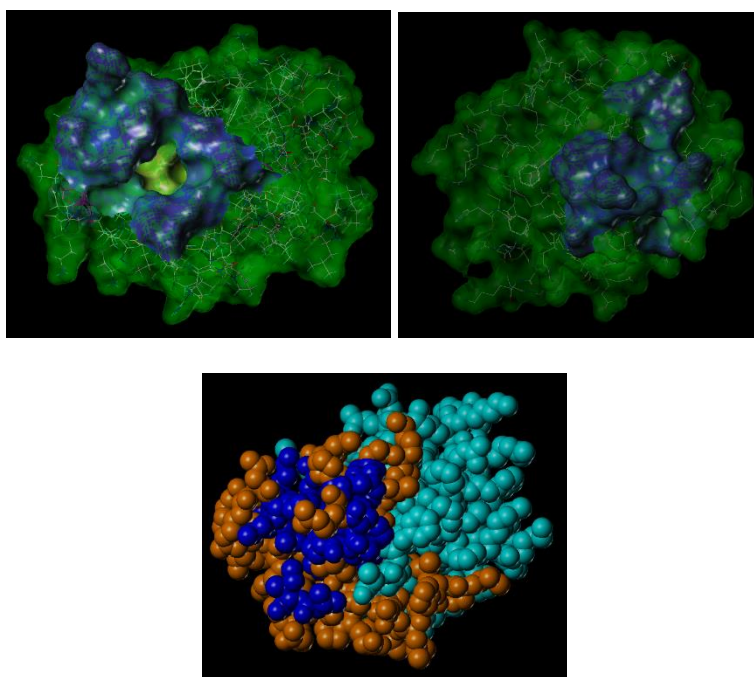


Figure 1.3.11: The Residues forming the binding cavity of the MDM2 RING homodimer

Left: The RING domain structure of MDM2's homodimer showing the relative cavity depth of the binding pocket.

Right: The RING domain structure of MDM2-MDM4's heterodimer showing the lack of cavity by coloring the MDM2 RING residues that form cavity in the homodimeric form.

**Coloring scheme showing the depth of the cavity: blue (no cavity), yellow (cavity)*

Bottom: Space filling model of MDM2 (orange)-MDM4 (cyan) heterodimer and the MDM2 amino acid residues (blue) participating in pocket formation in the homodimeric form.

Comparative analysis of the MDM2 RING monomer extracted from the 2HDP and 2VJE structures gave further insights into the significant structural differences of its heterodimeric vs homodimeric form. Although the MDM2 RING sequences from the homodimer and the heterodimer are identical, structural alignment revealed a major difference (Figure 1.3.12). As seen in Figure 1.3.12, the RING domain of MDM2 from the homodimeric form clearly forms a cavity (surface highlighted in purple) and the same domain from the heterodimer does not (surface highlighted in red). These observations further indicate that the cavity of the MDM2 RING homodimer can serve as a binding target for the development of therapeutics. The function of the binding pocket is not yet known; however, it can be deduced that the conformational changes that the MDM2 RING undergo in this region are important for the binding to the MDM4 RING. Therefore, if a compound binds tightly to the pocket it will not allow for the RING motif to undergo conformational changes therefore inhibiting the MDM2-MDM4 interactions.

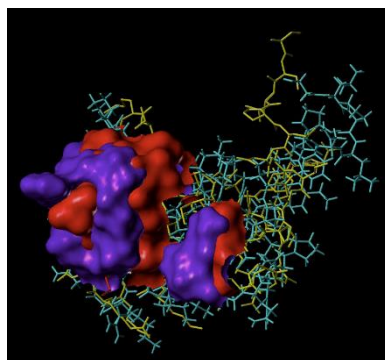


Figure 1.3.12 Superimposed MDM2 RING domain extracted from the heterodimer and the homodimer

**Surface areas derived by the residues participating in the binding pocket formation: in the homodimer highlighted in purple and in the heterodimer highlighted in red.*

The majority of the synthesized compounds were successfully docked into the MDM2 RING binding pocket. Example of some of the tighter binders can be seen in Figure 1.3.13. One

can clearly see that the pocket accommodates the anthraquinone skeleton very well. In addition, hydrogen bond interactions in the region just outside of the binding pocket can further stabilize and anchor the compounds in the pocket.

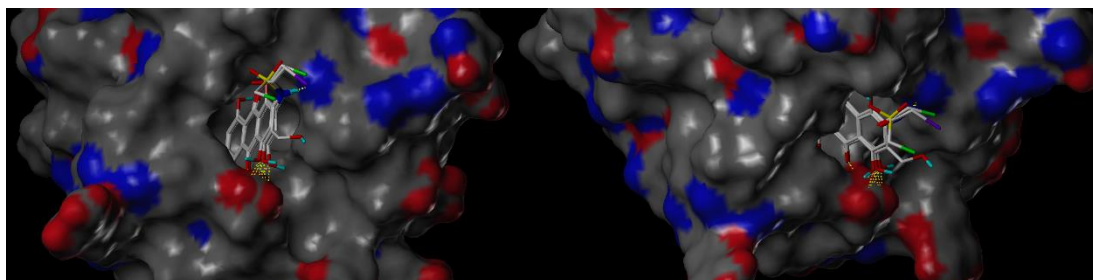


Figure 1.3.13 View of successfully bound anthraquinone analogues
**Protein surface area is colored based on hydrogen bonding: H-bond acceptors (blue), H-bond donors (red).*

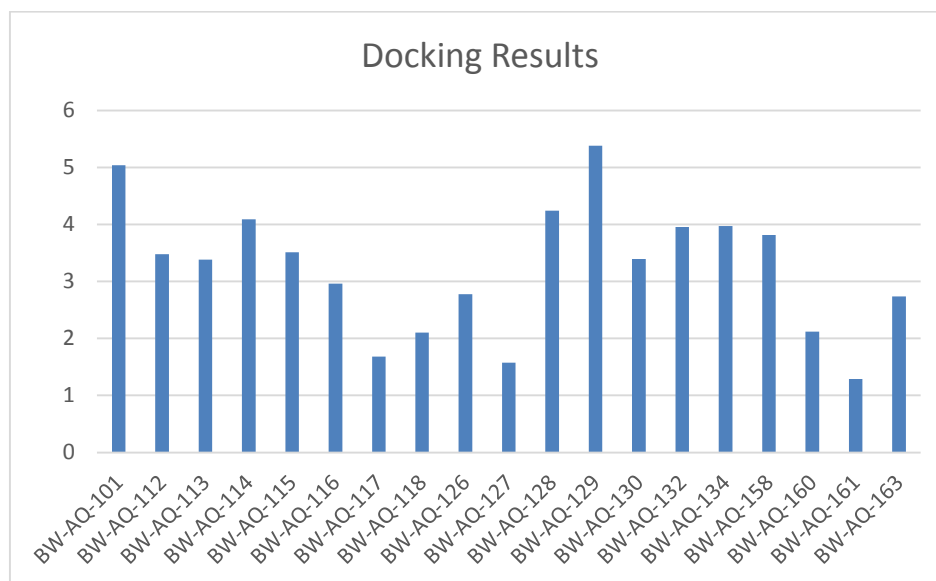


Figure 1.3.14: Relative docking score of selected compounds

The internal surface of the pocket is mostly lipophilic as it can be seen from the images in Figure 1.3.15. The pocket is large enough to accommodate aliphatic functional groups such as ethyl and propyl substituents. The relative binding score slightly drops with the introduction of

propyl moieties at the 1,8 positions of the anthraquinone core (Figure 1.3.14). However, the pocket accommodates bulky substituents like a benzyl group. In fact the relative docking results indicate that the presence of aromatic substituents improves binding (Figure 1.3.14). The slight drop of docking score for BW-AQ-127, with a single benzyl group, indicates the stabilizing interactions that these groups carry. As these large substituents are being anchored in the pocket through Van der Waals interactions the hydrogen bond donors and acceptors at the cavity opening can further increase the binding interactions (Figure 1.3.15). All of the above discussed aspects have been taken in consideration in the process of designing new anthraquinone analogues targeting MDM2-MDM4 interactions. Of course another priority is the improvement of water solubility and the introduction of aromatic substituents will not allow us to achieve that. Molecular modeling can be a very beneficial tool in the drug discovery and development process. However, at this stage of the project we can only use it as a guiding tool to build a library of successful inhibitors.

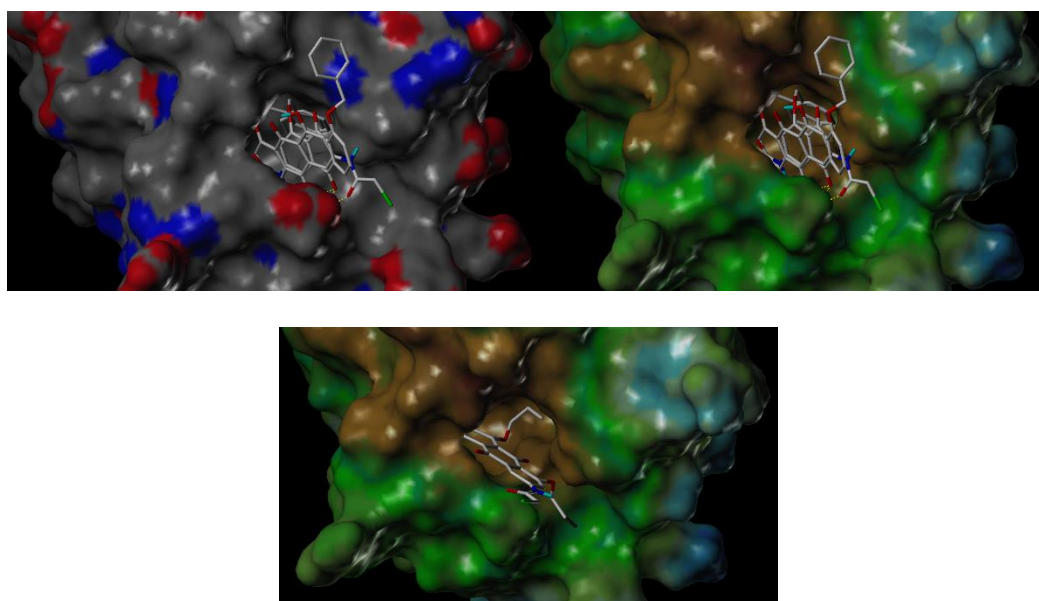


Figure 1.3.15 Various anthraquinone analogs docked in the binding pocket

Top left: View of successfully bound anthraquinone analogues containing bulky substituents at 1,8- positions (H-bonding surface map).
Top right: View of successfully bound anthraquinone analogues containing bulky substituents at 1,8- positions (lipophilicity surface map).
Bottom: View of successfully bound anthraquinone analogues containing propyl substituents at 1,8- positions (lipophilicity surface map).
** Lipophilicity surface coloring: strong lipophilic character (brown), weak lipophilic character (blue)*

In summary, we have identified a clear binding cavity in the MDM2 RING homodimer. This cavity can serve as a potential binding pocket for the developed anthraquinone analogs described in the previous sections. A careful examination of the available MDM2 RING homodimer and MDM2-MDM4 RING heterodimeric structures and docking studies support the hypothesis that BW-AQ-101 and its analogs can bind to the MDM2 RING homodimer (Figure 1.3.16). This binding can potentially stabilize the homodimer and prevent the formation of MDM2-MDM4 heterodimer formation.

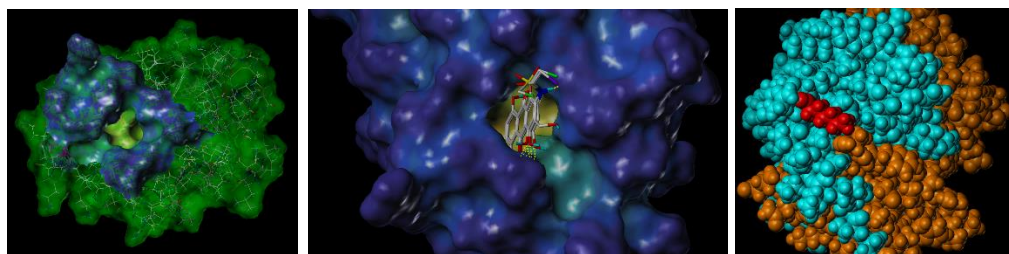


Figure 1.3.16 The binding hypothesis
Left: MDM2 RING homodimer and its cavity
Middle: MDM2 RING and anthraquinone analogues bound to it
Left: Space filling model of the MDM2 RING heterodimer (cyan and orange) and BW-AQ-101 (red) bound to it.

1.3.10.1 Experimental Section

The NMR structure of the MDM2 RING homodimer is available through the Protein Data Bank (PDB) under the ID 2HDP.⁴ The X-ray RING structure of the MDM2-MDM4 heterodimer is also available through the PDB (ID 2VJE), with a resolution of 2.2 Å.³ We performed molecular docking to see whether there was a potential binding pocket for AQ-101 in the MDM2 RING protein. The target protein and AQ-101 were prepared by removing of all zinc ions, water residues, and other ligands. All hydrogen atoms were added and the protein termini were fixed. Minimization was performed by using Sybyl X 2.0 and applying standard parameters: Powell method, Tripos force field, and Pullman charges. Simulated water environment were used by assigning the dielectric constant to 80. Docking was performed by Surflex-Dock module in Sybyl X 2.0. Virtual preparation of the heterodimeric structure was performed following the above-described protocol.

1.3.11 *References*

- (1) Lin, N.; Yan, J.; Huang, Z.; Altier, C.; Li, M.; Carrasco, N.; Suyemoto, M.; Johnston, L.; Wang, S.; Wang, Q.; Fang, H.; Caton-Williams, J.; Wang, B. *Nucleic Acids Res.* **2007**, *35*, 1222.
- (2) Jiao, L.; Qiu, Q.; Liu, B.; Zhao, T.; Huang, W.; Qian, H. *Bioorg. Med. Chem.* **2014**, *22*, 6857.
- (3) Linke, K.; Mace, P. D.; Smith, C. A.; Vaux, D. L.; Silke, J.; Day, C. L. *Cell Death Differ.* **2008**, *15*, 841.
- (4) Kostic, M.; Matt, T.; Martinez-Yamout, M. A.; Dyson, H. J.; Wright, P. E. *J. Mol. Biol.* **2006**, *363*, 433.

1.4 Biological evaluation of novel potent anthraquinone compounds as anticancer agents

All compounds disclosed in the previous section (1.3) of this chapter were tested for anticancer activity against seven cell lines. Three of the cell lines were leukemia cell lines (Molt4, EU1, and K562). The additional four cell lines are solid tumor cells: Hela (cervical cancer), KB (cervical cancer derived from Hela), Cos7 (derived from monkey kidney tissue), and T98G (glioblastoma). All experiments were done in triplicates and using a well-established protocol for the 3-(4,5-dimethylthiazol-2-yl)-2,5-diphenyltetrazolium bromide (MTT) assay. The exact protocol can be found in the experimental section (1.4.11). The initial testing of each compound begins with high concentration (50 μ M, 25 μ M, 12.5 μ M, 6.25 μ M) screening against one/two leukemia cell lines and one/two solid state cells to establish relative activity of the compound. The IC₅₀ (the concentration at which 50% of the cells are dead) values were then established with a secondary screening of the active compounds at the appropriate concentration ranges. All potent compounds (IC₅₀ < 1 μ M) were then tested against additional cell lines to determine the cellular selectivity of the specific compounds. Data analysis of the various groups of compounds tested can be found in the subsections below.

1.4.1 Evaluation of the 1,8-dimethoxyanthracene-9,10-dione compounds

Compound **8a** was tested against all seven cell lines available while compounds **8b-8d** and **11** were tested only against selected cell lines due to their general lack of activity. After initial screening, compound **8a** showed potency against solid and leukemia cells (Table 1.4.1). The compound appears to be selectively more potent against leukemia cells where its IC₅₀ values range from 0.79 μ M to 0.14 μ M. The compound shows relatively good activity against Cos7 cells, but the activity significantly decreased when tested against Hela and KB cells. Interestingly, compound **8a** shows activity against the drug resistant T98G cell line as well. When compared to

the marketed doxorubicin **8a** exhibits comparable activity against Cos7 and Hela cells, and superiority against K562 and T98G cells.

IC₅₀ values of synthesized 1,8-dimethoxyanthracene-9,10-dione analogs.* All values reported are in μ M concentration and determined via MTT assay.

Table 1.1 IC₅₀ values of synthesized 1,8-dimethoxyanthracene-9,10-dione analogs
** All values reported are in μ M concentration and determined via MTT assay.*

Compound	BW-AQ ID	Hela	KB	Cos7	T98G	Molt4	K562	EU1
8a	112	3.3	4.3	1.2	2-12	0.14	0.79	0.74
8b	132	>50	>50	>50	>12.5	>1.6	>6.3	ND
8c	134	>50	>50	>50	>50	>1.6	>6.3	ND
8d	232	24	ND	ND	ND	>25	ND	ND
11	130	>50	42	29	>12	>1.6	>6.3	ND
	Doxorubicin	2.5	1.6	2.1	>50	0.015	2.0	0.032

Unfortunately none of the other compounds from the 1,8-dimethoxyanthracene-9,10-dione class showed potency against any of the cell lines. Comparison between the activity of compound **8a** and BW-AQ-101 (Figure1.2.1) reveals that the alkylation at positions 1 and 8 of the anthraquinone core is very important in terms of retaining or even improving activity. However, the conclusion drawn from the data obtained for the 1,8-dimethoxyanthracene-9,10-dione compounds is that the α -chloro acetamide substituent at position 3 is crucial for the activity of this class of compounds.

1.4.2 Evaluation of the 1,8-diethoxyanthracene-9,10-dione compounds

Three (**14a-14c**) of the eight compounds that belong to the 1,8-diethoxyanthracene-9,10-dione class showed potency against leukemia cell lines and some solid state cells (Table 1.4.2). Compound **14a** showed activity in the mid nano molar range (120 nM - 480 nM) against Molt4 and EU1. Compounds **14b** and **14c** also showed low IC₅₀ values of 280 nM and 180 nM

against Mol4 cells. In addition, these three compounds showed promise against the solid state Cos7 cell line with IC₅₀ values in the low single digit micro molar concentrations (Table 1.4.2). Unfortunately none of the other five (**14d-14h**) compounds that were synthesized showed high potency in any of the cell lines.

Table 1.2 IC₅₀ values of synthesized 1,8-diethoxyanthracene-9,10-dione analogs

** All values reported are in μ M concentration and determined via MTT assay*

Compound	BW-AQ ID	Hela	KB	Cos7	T98G	Molt4	K562	EU1
14a	113	2.1	5.5	1.1	5.2	0.12	0.74	0.48
14b	114	3.9	10	2.1	>13	0.28	0.84	ND
14c	115	3.9	6.6	1.6	10	0.18	0.83	0.89
14d	179	>50	>50	>50	~50	20	11	18
14e	182	47	>50	>50	>50	17	>25	17
14f	198	58	ND	>6.3	ND	>25	ND	>6.3
14g	199	70	ND	>6.3	ND	18	ND	>6.3
14h	159	>6.3	>6.3	23	36	>13	12	16

It appears that the addition of a two carbon aliphatic chains to the 1 and 8 positions of the anthraquinone core retains and even slightly improves activity against leukemia cells when position 3 is a α -halo acetamide. It is very interesting that the three active compounds also exhibit activity against drug resistant T98G. It is important to note that compounds **14g** and **14h** contain a halogen at the α -carbon of the amide substituent. However, the halogen present in compounds **14g** and **14h** is secondary carbon rather than primary as in the case of **14a-14c**, which appears to decrease their potency. These result lead to the conclusion of possible alkylation as mechanism of action of the active compounds.

1.4.3 Evaluation of 1,8-dipropoxyanthracene-9,10-dione compounds

Because three of the 1,8-diethoxyanthracene-9,10-dione analogs showed potency against leukemia cell lines, it was decided to develop a group of compounds with longer aliphatic chains at the 1 and 8 positions of the anthraquinone core. Ten 1,8-dipropoxyanthracene-9,10-dione analogs

were synthesized and tested (Table 1.4.3). To our disappointment only three of these compounds (**16a-16c**) showed potency against Molt4 (Table 1.4.3). Compound **16j** has promising activity against Molt4 (0.49 μ M) and EU1 (1.09 μ M) as well. However, none of the other six compounds exhibited potency in the primary screening, thus they were not tested against all cell lines. Compounds **16a-16c** show IC_{50} values below or about 2 μ M against Cos7, making this the only solid tumor cell line susceptible to these compounds.

Table 1.3 IC_{50} values of synthesized 1,8-dipropoxyanthracene-9,10-dione analogs
** All values reported are in μ M concentration and determined via MTT assay*

Compound	BW-AQ ID	Hela	KB	Cos7	T98G	Molt4	K562	EU1
16a	116	2.5	6.6	1.2	8.0	0.12	1.1	3.5
16b	117	2.5	8.5	2.1	13	0.16	1.6	ND
16c	118	3.4	12	1.8	15	0.14	1.3	0.36
16d	160	15	16	8.1	25	4.0	6.9	4.8
16e	201	>13	ND	>13	ND	6.0	ND	>13
16f	200	>13	ND	>13	ND	13	ND	>13
16g	215	21	ND	ND	ND	>25	ND	>13
16h	213	25	ND	ND	ND	18	ND	>13
16i	214	>25	ND	ND	ND	>25	ND	>13
16j	156	1.5	3.0	3.0	18	0.49	2.8	1.09

One clear conclusion can be made from the obtained data; the presence of α -halo acetamide at position 3 of the core anthraquinone is absolutely crucial for the activity of the compounds. The potency of compound **16j** against Molt4 and EU1 suggests that the α -aza acetamide can be another alternative for a substituent at position 3 that may lead to an active anticancer agent.

1.4.4 Evaluation of 1,8-bis(benzyloxy)anthracene-9,10-dione compounds

The compounds that belong to the 1,8-bis(benzyloxy)anthracene-9,10-dione class are significantly different from the three classes of compounds described in sections 1.4.1-1.4.3 above. Compounds **18a-18e** have aromatic (benzyl) substituents at the 1 and 8 positions of the anthraquinone core. The presence of these aromatic functionalities resulted in compound **18b**,

which exhibited low nanomolar IC₅₀ values against Molt4 (28 nM) and EU1 (84 nM). Interestingly, compound **18b** has α -iodo acetamide as a substituent at position 3. In addition, compound **18a** shows potency against Molt4 (0.24 μ M), but not against EU1 or K562 (Table 1.4.4).

Table 1.4 IC₅₀ values of synthesized 1,8-bis(benzyloxy)anthracene-9,10-dione analogs

** All values reported are in μ M concentration and determined via MTT assay*

Compound	BW-AQ ID	Hela	KB	Cos7	T98G	Molt4	K562	EU1
18a	126	6.1	9	2.5	>13	0.24	3.3	1.1
18b	129	5.6	5.4	1.7	14	0.028	2.0	0.084
18c	128	8.6	5.7	5.5	9.8	0.98	>6.3	>1.6
18d	127	>50	>50	>50	>13	1.6	>6.3	ND
18e	162	1.6	0.594	11	25	>25	>20	18

The compounds with a Michael acceptor (**18c**) and α -aza acetamide (**18e**) at position 3 do not show significant activity except in Molt4 and KB. This class of compounds serves as evidence that the combination of α -halo acetamide at position 3 and the presence of lipophilic/ conjugated system at positions 1 and 8 leads to active anticancer compounds. The presence of aromatic systems at position 1 and 8, however, leads to more lipophilic character of the analogs, which are expected have decreased water solubility.

1.4.5 Evaluation of 1,8-bis(2-azidoethoxy)anthracene-9,10-dione compounds

In an attempt to explore the biological effects of various unsaturated substituents at the 1 and 8 positions of the anthraquinone core, the 1,8-bis(2-azidoethoxy)anthracene-9,10-dione class of compounds was developed. This class of compounds introduces an azidoethyl group, which can be helpful in a number of ways. For example, the azidoethyl groups are linear, yet they carry an electron rich unsaturated system that can potentially participate in pi-pi interactions with the binding pocket of the targeted protein. In addition, the azido group can be involved in ionic interactions, thus improving solubility and/or protein binding. The two compounds (**21a** and **21b**) that were tested showed consistent potency against Molt4 and EU1 at sub-micro molar values

(Table 1.4.5). Compound **21a** even showed low nano molar activity against Mot4 (77 nM). What is interesting about this pair of compounds is that they have selectivity towards leukemia cell, yet retain IC₅₀ values in the 2-3 μ M range against solid tumor cells.

Table 1.5 IC₅₀ values of synthesized 1,8-bis(2-azidoethoxy)anthracene-9,10-dione analogs

** All values reported are in μ M concentration and determined via MTT assay*

Compound	BW-AQ ID	Hela	KB	Cos7	T98G	Molt4	K562	EU1
21a	124	2.4	3.6	0.85	4.8	0.077	1.1	0.28
21b	140	3.1	3.4	2.2	14	0.21	3.2	0.69

In addition, **21a** has α -halo acetamide at position 3 and **21b** has α -aza acetamide functionality. Although very different in chemical characters it appears that these groups do not significantly alter the biological activity of the 1,8-bis(2-azidoethoxy)anthracene-9,10-dione compounds. Compound **21b** is the first compound, thus far, that shows nano molar activity against leukemia and low micro molar activity against solid tumor cells and yet lacks an α -halo moiety in its structure. Thus the azidoethoxy groups at the 1 and 8 positions are important for the cytotoxic effects of this pair.

1.4.6 Evaluation of 1,8-bis(allyloxy)anthracene-9,10-dione compounds

The attachment of allyl groups at the 1 and 8 positions were done in order to further explore the effects of a unsaturated functional groupson the anthraquinone analogs. None of the three developed compounds showed significant activity against either solid or leukemia cancer cells that were tested (Table 1.4.6). In fact all compounds showed poor solubility; thus it is clear that this class of compounds will not lead to a pharmaceutically relevant agent.

Table 1.6 IC₅₀ values of synthesized 1,8-bis(allyloxy)anthracene-9,10-dione analogs

** All values reported are in μ M concentration and determined via MTT assay*

Compound	BW-AQ ID	Hela	KB	Cos7	T98G	Molt4	K562	EU1
23a	161	>20	>20	>20	>50	>10	>10	>10
23b	163	>50	14.7	>50	>50	>25	>25	>25
23c	164	>50	>50	>50	>50	>25	>25	>25

1.4.7 Evaluation of 1,8-diisobutoxyanthracene-9,10-dione compounds

Based on the positive data obtained from the classes of compounds containing ethyloxy and propyloxy substituents at the 1 and 8 positions of the anthraquinone core, the biological activity of compounds containing branched aliphatic chains was evaluated. Compounds **25a** and **25b** show potency against Molt4 and EU1; however they do not show significant activity against all other cell lines (Table 1.4.7). The observed activity of compounds **25a** and **25b** can be related to the fact that both of these compounds have an α -halo acetamide as substituent at position 3.

Table 1.7 IC₅₀ values of synthesized 1,8-diisobutoxyanthracene-9,10-dione analogs

** All values reported are in μ M concentration and determined via MTT assay*

Compound	BW-AQ ID	Hela	KB	Cos7	T98G	Molt4	K562	EU1
25a	177	4.3	5.2	1.7	11	0.2-1.1	2.8	0.52
25b	183	4.0	6.3	3.6	17	0.93	3.8	1.3
25c	176	7.2	5.6	17	>50	>25	15	18
25d	178	>50	>50	>50	>50	>25	>25	>25
25e	212	>13	ND	>13	ND	>13	ND	>13

None of the other three compounds (**25c-25e**) exhibit potency against either leukemia or solid tumor cells. This again suggests that in the case of aliphatic substitutions at the 1 and 8 positions, the presence of an α -halo acetamide at position 3 is important for the activity of these compounds.

1.4.8 Evaluation of 1,8-bis(isopentyloxy)anthracene-9,10-dione compounds

Another seven compounds containing branched chain aliphatic substituents at the 1 and 8 positions were tested against various cell lines. Only two (**27a** and **27b**) of the compounds that belong to the 1,8-bis(isopentyloxy)anthracene-9,10-dione analogs showed some activity against Molt4 and EU1 cells (Table 1.4.8). None of the other compounds showed significant activity against any of the seven cell lines tested. Compounds **27a** and **27b** were ineffective against solid tumor cells.

Table 1.8 IC₅₀ values of synthesized 1,8-bis(isopentyloxy)anthracene-9,10-dione analogs
** All values reported are in μ M concentration and determined via MTT assay*

Compound	BW-AQ ID	Hela	KB	Cos7	T98G	Molt4	K562	EU1
27a	181	>50	>50	1.9	>50	0.2-1.0	ND	0.70
27b	180	17	13	2.0	>50	0.63	7.3	0.68
27c	209	23	ND	ND	ND	11	ND	>13
27d	211	>25	ND	ND	ND	19	ND	>13
27e	210	>25	ND	ND	ND	>25	ND	>13
27f	216	10	ND	ND	ND	3.0	ND	8.8
27g	217	>12.3	ND	>13	ND	ND	ND	>13

The obtained data suggests that extension and branching of the side chains at the 1 and 8 positions of the anthraquinone core do not improve activity. The presence of α -halo acetamide at position 3 appears to be important for activity against some leukemia cell lines, but has no effect against solid cancer cells.

1.4.9 Evaluation of additional anthracene-9,10-dione analogs

The final group of compounds described in this work was developed with the idea of testing the effects of methoxyethyl (**29**) and methoxypropanyl (**31**) functional groups at positions 1 and 8. In addition the lack of functional groups (compound **33**) at the 1 and 8 positions was also studied. All of the tested compounds showed effects against Mol4 and EU1 cells (Table

1.4.9). The developed compounds showed activity in the low micro molar range against Cos7 cell line.

Table 1.9 IC₅₀ values of synthesized anthracene-9,10-dione analogs

** All values reported are in μ M concentration and determined via MTT assay*

Compound	BW-AQ ID	Hela	KB	Cos7	T98G	Molt4	K562	EU1
29	202	>13	ND	1.5	ND	<3.3	ND	2.1
31	205	>13	ND	1.9	ND	<3.3	ND	<0.78
33	131	2.6	5.6	1.4	ND	0.26	1.42	0.68

The three compounds (**29**, **31**, **33**) have one similar structural feature in addition to the anthraquinone core: the α -halo acetamide substituent at position 3. Although further investigation of the activity of potential analogs of compounds **29**, **31**, and **33** is needed to draw specific conclusions, it is fairly clear that the α -halo acetamide is the key moiety responsible for the selective activity against leukemia cells.

1.4.10 Summary/Discussions

All tested compounds were separated into nine classes based on structural features of the core and the substituents present at the 1 and 8 positions of the core anthraquinone structure. The compounds were tested against seven cell lines; three leukemia and four solid tumor cells. The majority of the active analogs have the α -halo acetamide moiety at position 3 of the core. It is safe to conclude that this structural feature is of great importance for the activity of these anthraquinones. In addition these compounds appear to have preferential cytotoxic effect over leukemia cells. Among all the compounds disclosed, nine compounds stand out in terms of activity against more than two cell lines; **14a**, **14b**, **14c**, **16c**, **16j**, **18b**, **21a**, **21b**, and **33**. Only two (**16j** and **21b**) out of these nine compounds do not contain the α -halo acetamide functionality at position 3. The importance of this lies beneath the reactivity of the α -halo acetamide group. A halide in an

alpha position to a carbonyl group is an excellent alkylating agent and highly susceptible to nucleophilic attacks. Thus, the presence of this functional group in a drug candidate is not desirable as it can easily undergo substitution reaction under physiological conditions with some of the naturally occurring nucleophiles (thiols, free amines, etc). The reactivity of these α -halo acetamides is also affected by the halogen itself. A “Cl” substituent will be much less likely to undergo alkylation reaction at physiological conditions compared to “Br” or “I”. Therefore, the presence of a reactive functional groups from this type (“Br” or “I”) may lead to non-specific bindings and undesired side reactions *in vivo*. This can lead to serious side effects of the drug candidates as well. Nevertheless, marketed compounds like Nasonex and Asmanex contain highly reactive functionalities such as α -chloro ketones or/and Michael acceptors, yet they lack significant side effects and have been approved for clinical use. All these issues need to be considered seriously and the compounds should be carefully evaluated before further development. With this in mind the two compounds (**16j** and **21b**) are good candidates for further evaluation.

In conclusion, the attachment of aliphatic side chains at position 1 and 8 of the core compound appeared as a successful strategy in the development of active anticancer agents. The attachment of benzyl and azido ethyl groups at the 1 and 8 positions resulted in some of the most potent compounds described in this work. All of the developed anthraquinone analogs that showed activity have a common structural feature; the α -halo acetamide functionality at position 3.

1.4.11 Experimental section

HeLa and Cos7 cell lines were cultured in DMEM medium and T98G and KB cell lines in MEM medium. All other cell lines (Molt4, K562, EU1) were cultured in RPMI-1640 medium. The medium was supplemented with 10% fetal bovine serum and 1% penicillin/streptomycin. For the

cytotoxicity assays, cells were seeded into 96-well plate (3.0×10^4 for all solid state cell lines and 3×10^5 for all leukemia cell lines in 100 μ L per well). The compounds were dissolved in DMSO to make 10 mM stock solutions. The stock solution was diluted using DMSO to various concentrations. 1 μ L of each concentration was diluted 100 fold with medium into the well plate keeping the DMSO < 1% throughout the experiment. Addition of compounds was performed after adherent cells reached 40-50% confluence. After incubation for 24 h. at 37 ° C in humidified atmosphere with 5 % CO₂, 10 μ L of MTT (5 mg/mL in PBS) was added. After addition of MTT the cells were incubated for another 4 h. The culture medium was then aspirated and 100 μ L of DMSO was added to each well. The 96-well plate was read by microarray reader for optical density at 490 nm. All tests were performed in triplicates and IC₅₀ values were estimated from the averaged response curves.

1.5 Solubility, formulation, and stability studies of selected anthraquinone analogs

After careful evaluation of the synthesized anthraquinone compounds (section 1.3 and 1.4), a group of potent analogs was selected and their physicochemical properties were further evaluated. As previously mentioned, this class of anthraquinone analogs exhibits poor water solubility. In order to identify the most water-soluble compounds and evaluate their potential to become drug candidates, water solubility studies were performed (section 1.5.1). To address the solubility issues with the active compounds, various non-toxic formulations were developed. (section 1.5.2). Another potential issues with this class of compounds is the fact that the majority of the active rhein analogs contain an α -halo acetamide, which i) is a reactive functional group that may undergo substitution reactions and ii) may affect the compounds' stability under physiological conditions. Thus the stability of selected group of active rhein analogs was evaluated under various conditions (section 1.5.3).

1.5.1 Solubility evaluation of potent anthraquinone analogs

The identification of active and non-toxic agents is merely the beginning of the drug discovery and development process. In order to become a drug candidate, every active compound should possess favorable physicochemical properties; i.e. good water solubility, blood brain barrier permeability, and of course favorable absorption, distribution, metabolism, and excretion (ADME). One of the major hurdles in the drug development process is the ability to develop water-soluble compounds. Poorly water-soluble compounds carry issues with drug delivery, targeting, bioavailability etc. In the herein described study we aimed to identify potential anthraquinone drug candidates through the evaluation of their physicochemical properties.

Two major solubility determination techniques stand out in the literature; the saturation shake-flask method and turbidimetric method.^{1,2} Before the introduction of these two methods, the commonly perceived definition of solubility should be introduced. When discussing solubility two important terms need to be considered: kinetic solubility and thermodynamic/ equilibrium solubility. The term kinetic solubility deals with the concentration of a compound at which precipitation appears in solution after predetermined amount of time. Thermodynamic/ equilibrium solubility refers to the concentration of a compound under saturation conditions in the presence of excess solid, where the solid and solution are at equilibrium. These two terms are very important as the turbidimetric method measures kinetic solubility and the shake flask method measures thermodynamic solubility. While the turbidimetric method can be done on a high throughput scale and requires minimum amount of compound, it cannot give exact solubility values, but an approximation. Nevertheless this method is widely used in pharmaceutical settings and is very suitable for early stage drug development studies. The shake-flask method can give a

precise solubility reading, however, it is time-consuming and requires large amounts of compound samples.

The basic idea behind the turbidimetric solubility assay is to dissolve a given compound in organic solvent such as DMSO. The stock solution is then aliquoted into a buffer and the turbidity at different concentrations is read typically by a UV instrument at 620 nm. The solubility can be estimated by a plot of turbidity vs concentration. Although a very rapid method, it lacks precision of the estimation and can give large solubility variations. The shake-flask method on the other hand can give relatively quantitative value of the thermodynamic solubility of a given compound as the data is obtained normally by HPLC. The general principle behind this method is that excess amount of a compound is saturated in a buffer and shaken in a closed vessel for 24 hours. Then the suspension is filtered off and the solution is analyzed via HPLC. Additional downside of this methodology is that basic or acidic compounds, which in excess can alter the pH of the buffer, cannot be tested. Of course there are more compound specific solubility determination methods such as potentiometric titrations, pH-solubility profiling, and salt solubility studies.²⁻⁴ In addition there are computational methods that can predict the solubility of given class of compounds, however, these methods will not be discussed in detail in this work.⁵

In an attempt to determine the solubility of the developed anthraquinone compounds, dynamic light scattering (DLS) instrumentation was used. Since, precise solubility data cannot be obtained from the UV turbidometric assay, we attempted to pair this method with a particle size analyzer instead. Dynamic light scattering can give precise information of particles size and homogeneity in solution. The improved precision in the solubility determination when using DLS technique comes from the fact that DLS uses laser with a beam size of approximately 60 nm (He-Ne laser). As the laser beam goes through the sample it “hits” the particles thus scattering the light.

The scattered light is detected and analyzed. Because particles are not static in solution, DLS detects the Brownian motion of the particles and translates it to size; larger particles have slower Brownian motion than smaller particles. A correlation software compares the detected particle sizes, as a function of time, and establishes a dispersity curve. The function gives information of the dispersity of the various particles in solution. This allows us to track the specific concentration at which the compounds start precipitating out of solution.

The ability of the instrument to read the particle dispersity in solution and the particle size allows for improved estimation of the compounds' solubility. The selected compounds were dissolved in an array of concentrations from 0 μM to 150 μM in phosphate buffer (PBS), pH 7.4 at room temperature from 10 mM stock solutions in DMSO. The final concentration of DMSO in the aliquoted solutions is 1%. The solutions are then allowed to sit at room temperature overnight to obtain thermodynamic equilibrium and then tested for precipitations. The solubility of the compounds is then determined to be the point of an exponential curve that monodisperse particles were observed. The curve indicates the uniform particle formation at the tested concentration. The obtained data can be seen in Table 1.5.1. The utilized protocol requires overnight equilibration of the solutions and allows for the measurement of thermodynamic solubility without the use of large quantities of the active compounds. Precipitations are visually observed for some compounds at high concentrations and these samples are not analyzed, as the precipitation is obvious.

Table 1.10 Physicochemical characteristics of selected rhein analogs

Compounds	MW [g/mol]	Solubility [μ M]	Log P	Log S	H-bond donors	H-bond acceptors
BW-AQ-101	331.70	3	2.28	-3.65	3	6
BW-AQ-112	369.76	20	2.79	-4.42	1	6
BW-AQ-113	387.81	30	3.69	-4.74	1	6
BW-AQ-114	432.27	100	3.81	-5.08	1	6
BW-AQ-115	479.27	30	4.05	-4.81	1	6
BW-AQ-116	415.87	20	4.38	-5.26	1	6
BW-AQ-117	460.32	100	4.57	-5.49	1	6
BW-AQ-118	507.32	5	4.81	-5.3	1	6
BW-AQ-124	469.84	10	3.2	-3.98	1	12
BW-AQ-126	511.96	1	5.77	-6.7	1	6
BW-AQ-128	489.15	1	5.66	-6.34	1	6
BW-AQ-129	603.41	1	6.21	-6.51	1	6
BW-AQ-131	299.71	30	2.92	-4.5	1	4
BW-AQ-140	476.41	10	3.15	-3.49	1	15

Some of the most active compounds show extremely poor solubility; full solubilization achieved in the ranges from 1 μ M to 3 μ M (Table 1.5.1). However, poor solubility can be overcome by the development of proper formulation. In order to fully evaluate the potential of a compound to become a drug candidate, other physicochemical properties need to be considered. In the process of selecting potent compounds at early drug development stage, the evaluation of the basic physicochemical parameter is of extreme importance. Thus, the selected anthraquinone analogs were evaluated against the Lipinski's "rule of five". The partition coefficient (log P) and the solubility coefficient (log S) were calculated using VCCLAB online software.⁶ These coefficients predict the absorption properties of the drug candidates. Additional factor that affects the permeability properties of the drugs is the number of hydrogen bond donors and acceptors in the molecule. Too many hydrogen bond donors/acceptors negatively affects membrane permeability of the compound. Thus the Lipinski's rule of five states that "poor absorption or permeation are more likely when: i) there are more than five hydrogen bond donors, ii) log P is over 5, iii)

molecular weight of the compound is over 500, iv) there are more than 10 hydrogen bond acceptors.”⁵ In addition a favorable log S value below zero and greater than -4 entails good permeability.

The derived parameters disclosed in Table 1.5.1 show that the majority of compounds fall within the Lipinski's rule of five, and solely based on this analysis can be considered as drug candidates. However, as previously discussed the presence of reactive functionalities like α -iodo acetamide or α -bromo acetamide is undesirable in a potential drug candidate. Therefore, compounds BW-AQ-115, BW-AQ-118, BW-AQ-129 should not be considered for further evaluation. Although BW-AQ-101 has poor solubility all its predicted physicochemical parameters fit within the Lipinski's rule of five. Development of proper drug delivery system/ formulation can solve the solubility issue for this compound, so it can be considered for further evaluations. Compounds BW-AQ-113 and BW-AQ-131 also appear as good drug candidates based on the examined physicochemical properties. Compound BW-AQ-124 has 12 hydrogen bond acceptors thus falling out of the Lipinski's rule. However, this calculation is based on the number of Ns and Os present in the molecule. The compound has two azido groups and it will be unreasonable to consider them as six hydrogen acceptors. Therefore, compound BW-AQ-124 can be considered an exception and a potential drug candidate. Formulations for all compounds that exhibit reasonable physicochemical parameters were developed and discussed in section 1.5.2 below.

1.5.1.1 Experimental Section

All solvents used in this experiment were purchased from Sigma-Aldrich; and the nylon filters were purchased from Fisher Scientific. The solubility was determined using BIC 90 Plus Particle Size Analyzer. The DMSO and PBS used in the experiments were filtered through 0.22 μ m nylon filters. All compounds were dissolved in pre-filtered DMSO giving a 10 mM stock

solution. All tubes, vials and cuvettes were rinsed with nano-pure filtered water and dried under reduced pressure to ensure that no dust particles are present in them. Various concentrations from 0 μM to 150 μM were prepared through dilution of the stock solution into the filtered buffer. The total DMSO amount per sample was kept at 1%. The prepared samples were allowed to sit at room temperature overnight then the solubility was determined via a particle size analyzer instrument.

1.5.2 Formulation of selected anthraquinone analogs

One of the more direct ways to overcome the issues related to compounds with poor solubility is to develop a formulation that will allow for the compounds to stay in solution. In various *in vitro* studies and evaluation techniques, compounds are often dissolved in DMSO and introduced to the media. This method cannot be utilized *in vivo* due to intrinsic toxicity issues and the fact that DMSO is an irritant and should not be allowed to come in contact with live tissue. In addition, DMSO carries *in vitro* cytotoxicity, which is the reason why this chemical should be kept at levels no more than 5% (v/v) during any given set of experiments. An alternative compound delivery method would be through the use of non-toxic solvents such as isopropanol and ethanol. However, lipophilic/ nonpolar compounds will not be dissolved in these solvents, thus limiting their utility. The development of water-soluble pro-drugs and colloidal systems (micelles, liposomes, nanoparticle, etc.) are other feasible alternatives for compound delivery. However, these methods require time and sufficient effort in their development and are not useful at the early drug discovery stage. An efficient method to overcome poor compound solubility and the related issues is through the development of pharmaceutical formulation. A commonly used solubilization method in the cancer drug discovery process is the development of formulation using surfactants, i.e. Tween 80, Solutol, and Cremophor.⁷ The utilization of various formulations aims to prepare the compounds for i.v. (intravenous) or i.p. (intraperitoneal) administration. With the use of

isopropanol and ethanol as co-solvents and the three surfactants (Tween 80, Solutol, and Cremophor), various formulations were developed in an attempt to overcome the issues related with the poorly soluble compounds disclosed in this work.

The formulation studies were designed so that the developed solvent/surfactant combinations allow for the delivery of the highest possible dose at the lowest possible volume. This experimental design allows for the development of a delivery system without knowing the therapeutic or the maximum tolerated doses of the tested compounds. The use of clinically approved formulation components stands for the safety of the developed methodology. Formulation for six of the active compounds was developed (Tables 1.1.52-1.57).

Table 1.11 Formulation of BW-AQ-101

Entry	Amount of compound (mg)	Solvent Combination (1/4) (v/v)	Total Volume (μL)	Final Concentration (mM)	Results	
					48 h. at Room Temp	6 x PBS dilution
1	1.075	Solutol/ Ethanol	700	4.6	Solubilized	Minor Precipitated after 1.5 h.
2	1.02	Cremophor/ Ethanol	700	4.4	Solubilized	Solubilized
3	1.035	Tween 80/ Ethanol	700	4.5	Solubilized	Minor Precipitated after 1.5 h.
4	0.966	Cremophor/ Isopropanol	400	7.3	Solubilized	Precipitated after 40 min.
5	1.079	Solutol/ Isopropanol	400	8.1	Solubilized	Precipitated after 20 min.
6	1.2	Tween 80/ Isopropanol	400	9.1	Solubilized	Precipitated after 10 min.
7	1.118	Isopropanol	800	4.2	Solubilized	Precipitated

Compound BW-AQ-101 showed to be completely soluble below 3 μM in PBS. In order to improve its solubility, seven formulation conditions were examined (Table 1.5.2). The compound was solubilized completely at various surfactant/solvent combinations. However, after six fold

dilution with PBS buffer the compound either precipitated immediately or within one and a half hours in six out of the seven tested conditions (Table 1.5.2). The combination of cremophor and ethanol in one to four ratio (v/v) was the only one that did not result precipitation after dilution with buffer.

Table 1.12 Formulation of BW-AQ-112

Entry	Amount of compound (mg)	Solvent Combination (1/4) (v/v)	Total Volume (μL)	Final Concentration (mM)	Results	
					24 h. at Room Temp	6 x PBS dilution
1	1.092	Solutol/ Ethanol	1100	2.8	Precipitated	-
2	1.067	Cremophor/ Ethanol	1300	2.3	Precipitated	-
3	1.13	Tween 80/ Ethanol	1100	2.9	Precipitated	-
4	1.141	Cremophor/ Isopropanol	1000	3.2	Solubilized	Solubilized
5	1.094	Solutol /Isopropanol	1000	3	Solubilized	Solubilized
6	1.028	Tween 80/ Isopropanol	1000	2.9	Solubilized	Solubilized
7	1.083	Isopropanol	1200	2.5	Solubilized	Precipitated after 20 min.

Compound BW-AQ-112 showed significantly better solubility (20 μM) compared to BW-AQ-101 (Table 1.5.1). Three out of the seven formulation combinations showed to be successful in keeping BW-AQ-112 in solution (Table 1.5.3). Combination of all tested surfactants with isopropanol appeared to be a successful formulation for compound BW-AQ-112. On the other hand, the use of ethanol did not show any positive effects on BW-AQ-112.

Table 1.13 Formulation of BW-AQ-113

Entry	Amount of compound (mg)	Solvent Combination (1/4) (v/v)	Total Volume (μL)	Final Concentration (mM)	Results	
					48 h. at Room Temp	6 x PBS dilution
1	0.885	Solutol/Ethanol	600	3.8	Solubilized	Solubilized
2	1.296	Cremophor/Ethanol	600	5.6	Solubilized	Solubilized
3	1.242	Tween 80/Ethanol	600	5.3	Solubilized	Solubilized
4	1.425	Solutol/Isopropanol	400	9.2	Solubilized	Precipitated after 2 h.
5	1.195	Cremophor/Isopropanol	400	7.7	Solubilized	Precipitated after 2 h.
6	1.124	Tween 80/Isopropanol	400	7.2	Solubilized	Precipitated after 2 h.
7	1.162	Isopropanol	600	5	Solubilized	Precipitated

Interestingly compound BW-AQ-113, which is structurally very similar to BW-AQ-112, was more favorable towards surfactant combinations with ethanol and not isopropanol. Although BW-AQ-113 stayed in solution for two hours after the six fold dilution in PBS, the combinations of ethanol with cremophor, tween 80, and solutol respectively allowed it to stay in solution for a longer period of time. Based on the absorption, distribution, metabolism and excretion profile of a given compound, formulation that allows for the compound to stay in solution between two and three hours can be useful for drug delivery. The ADME profiles of the developed compounds remain to be determined.

Table 1.14 Formulation of BW-AQ-124

Entry	Amount of compound (mg)	Solvent Combination (1/4) (v/v)	Total Volume (μL)	Final Concentration (mM)	Results	
					24 h. at Room Temp	6 x PBS dilution
1	1.115	Solutol/ Ethanol	500	4.7	Solubilized	Precipitated after 3 h.
2	0.94	Cremophor/ Ethanol	500	4	Solubilized	Solubilized
3	1.343	Tween 80/ Ethanol	600	4.8	Solubilized	Precipitated after 3 h.
4	1.064	Cremophor/ Isopropanol	400	5.7	Solubilized	Precipitated after 3 h.
5	0.975	Solutol/ Isopropanol	400	5.2	Solubilized	Solubilized
6	1.205	Tween 80/ Isopropanol	400	6.4	Solubilized	Precipitated after 3 h.
7	1.04	Isopropanol	600	3.7	Solubilized	Precipitated after 0 min.

A successful formulation of compound BW-AQ-124 was achieved through the combination of solutol and isopropanol in 1/4 (v/v) ratio. The combination did not result in any precipitation after dilution with PBS (Table 1.5.5). All other tested combinations resulted at initial solubilization. However, upon dilution, the compound precipitated out after three hours, or in the case of the sole use of isopropanol immediately. These combinations can prove to be therapeutically useful as precipitation after three hours occurred only at fairly high concentrations: 1.2 mM for Entry 6 (Table 1.5.5).

Table 1.15 Formulation of BW-AQ-126

Entry	Amount of compound (mg)	Solvent Combination (1/4) (v/v)	Total Volume (μL)	Final Concentration (mM)	Results	
					24 h. at Room Temp	6 x PBS dilution
1	1.194	Solutol/ Ethanol	1100	2.1	Precipitated	-
2	1.085	Cremophor/ Ethanol	1300	1.6	Solubilized	Solubilized
3	1.241	Tween 80/ Ethanol	1100	2.2	Precipitated	-
4	1.232	Cremophor/ Isopropanol	600	4	Precipitated	-
5	1.235	Solutol/ Isopropanol	800	3	Solubilized	Solubilized
6	1.184	Tween 80/ Isopropanol	600	3.8	Precipitated	-
7	1.215	Isopropanol	1000	2.4	Precipitated	-

Although highly potent, compound BW-AQ-126 showed poor solubility (Table 1.5.1). Formulation development for this compound was proven difficult and only the combination of cremophor/ethanol and solutol/isopropanol resulted in complete solubilization at fairly low concentrations (Table 1.5.6). All other tested combinations gave immediate precipitation upon PBS dilution.

Table 1.16 Formulation of BW-AQ-131

Entry	Amount of compound (mg)	Solvent Combination (1/4) (v/v)	Total Volume (μL)	Final Concentration (mM)	Results	
					24 h. at Room Temp	6 x PBS dilution
1	1.137	Solutol/ Ethanol	1000	3.7	Solubilized	Solubilized
2	1.25	Cremophor/ Ethanol	900	4.6	Solubilized	Solubilized
3	1.043	Tween 80/ Ethanol	800	4.4	Solubilized	Solubilized
4	1.15	Cremophor/ Isopropanol	600	6.4	Solubilized	Solubilized
5	1.102	Solutol/ Isopropanol	800	4.6	Solubilized	Solubilized
6	1.054	Tween 80/ Isopropanol	600	5.8	Solubilized	Solubilized
7	1.056	Isopropanol	800	4.4	Precipitated	-

Because BW-AQ-131 showed fairly good solubility in preliminary experiments (Table 1.5.1), it was not a surprise that all of the tested formulation combinations were successful (Table 1.5.7). At some instances solubilization was achieved at fairly high concentrations: entries 4 and 6 (Table 1.5.7). Not surprisingly, the sole use of isopropanol was not successful.

The majority of the rhein analogs exhibit poor water solubility. The development of a successful formulation allows for the active compounds to be further evaluated and potentially considered as drug candidates. After physicochemical and structure-activity evaluation of the synthesized analogs, various formulations for six of the most promising compounds were developed. These formulations can be used for further evaluation of the compounds' stability and *in vivo* studies.

1.5.2.1 Experimental Section

General procedure for the formulation development

All surfactants, Cremophor RH 40, Kholliohor HS 15 (solutol) and Tween 80, were purchased from Sigma Aldrich. All solutions were prepared by suspending the reported amount of compound in a surfactant (Cremophor RH 40, Kholliohor HS 15 (Solutol) and Tween 80)/solvent (ethanol, isopropanol) mixture, heating it for approximately one minute at 40 °C, followed by vortexing for approximately 15 seconds and sonication for one minute. 100 µL increments from the solvent/surfactant mixture were added repeatedly until the compound was fully solubilized. The fully solubilized samples were allowed to sit at room temperature for 24 or 48 hours at room temperature. 200 µL of each sample were then added to 1 mL of PBS buffer at room temperature. The solutions were thoroughly mixed and allowed to sit at room temperature. The solutions were examined for precipitation formation every 10 to 15 minutes.

1.5.3 Stability studies of selected anthraquinone analogs

The stability evaluation of a selected group of compounds was done in three different experiments aiming to answer the following questions: i) are the compounds stable at physiological conditions, ii) are the compounds stable in the formulation solutions and iii) what would be the ideal storage conditions for the compounds. In order to answer these questions, three sets of experiments were designed. The first one consists of dissolving the compounds in the above-described formulations followed by six times dilution in PBS (pH = 7.4) and incubation at 37 °C for 24 hours. Samples were periodically injected into an HPLC instrument and the real-time decomposition of the compound was monitored. Compounds BW-AQ-112, BW-AQ-124, and BW-AQ-131 appeared to be relatively stable (Table 1.5.8). The compounds showed about 5.5 %, 4.9 %, and 0.8 % respective decomposition at simulated physiological conditions. The lead compound BW-AQ-101 showed about 8.3 % decomposition at the same condition after 24 hours,

however, only 1.6 % after two hours incubation. These results are indicative for the general stability of the structures and their therapeutic potential. Unfortunately compound BW-AQ-126 showed significant decomposition of over 38 % (Table 1.5.8) at close to physiological conditions. The lack of stability if this compound eliminates it from further consideration for a drug candidate. Nevertheless, the other four compounds that were tested showed good stability and promise to be taken for further pre-clinical evaluations.

Table 1.17 Stability studies in solution at 37 °C

** 0 min. readings indicate the initial purity of the compounds.*

	BW-AQ-101	BW-AQ-112	BW-AQ-124	BW-AQ-131	BW-AQ-126
0 min.	97.2 %	98.6 %	99.1 %	87.7 %	95.3 %
120 min.	95.6 %	98.4 %	97.6 %	87.2 %	91.2 %
24 h.	88.9 %	93.0 %	94.2 %	86.9 %	56.4 %

The purpose of the second stability study that was performed was to evaluate the storage capability of the active compounds in the established formulation solutions for an extended period of time (up to eight weeks). This long-term stability test was done on BW-AQ-101, BW-AQ-112, BW-AQ-113, and BW-AQ-124 based on their activities and physicochemical properties. These compounds were dissolved in the most appropriate formulations (discussed in section 1.5.2) and stored under three different conditions: room temperature, 4 °C, and -20 °C. None of the compounds exhibited significant decomposition at -20 °C after eight weeks (data shown in the appendix). Compounds BW-AQ-101 and BW-AQ-124 showed about 1 % and 2 % decomposition at 4 °C and the solutions of BW-AQ-112, BW-AQ-113 appeared completely stable at this temperature. Eight-week solution storage at room temperature resulted in minor decomposition of all compounds. While BW-AQ-101 and BW-AQ-112 showed only 3 % and 4 % decomposition, compounds BW-AQ-124 and BW-AQ-113 showed 9 % and 7 % decomposition respectively. The

eight-week study revealed that solution storage may be suitable for some of the rhein analogs at low temperatures (4 °C, and -20 °C), but cannot be utilized at room temperature.

The third storage stability evaluation of these compounds was done at solid state and under the following temperature conditions: room temperature, 4 °C, and -20 °C. The compounds showed no significant decomposition after 17 weeks storage in a solid form at 4 °C, and -20 °C (data presented in the appendix). Compounds BW-AQ-101 and BW-AQ-124 showed about 1 % decomposition when stored in a solid form at room temperature. Furthermore, BW-AQ-112 and BW-AQ-113 showed no significant evidence for decomposition when stored as solids at room temperature.

The above-described stability studies show that the active rhein analogs are relatively stable compounds and can be stored as solids for prolonged periods of time. Ideal storage conditions will require low temperatures (4 °C or -20 °C). Most compounds appear tolerable to storage at room temperature as well. Short-term storage in a solution form at -20 °C are plausible for these compounds, however, long term (over 8 weeks) solution storage at these conditions is not recommended.

1.5.3.1 Experimental section

All solutions for the stability determination of compounds BW-AQ-101 and BW-AQ-124 were prepared using ethanol/cremophor 4/1 (v/v) ration. All solutions for the stability determination of compounds BW-AQ-112 and BW-AQ-113 were prepared using isopropanol/solutol 4/1 (v/v) ration. 1 mM stock solutions of each compound were prepared in the appropriate formulation. 30-fold dilution in PBS was done to achieve 30 µM final concentration samples of the tested compounds. The prepared samples were then injected into the HPLC (Shimadzu UFLC SIL-20AHT) with Waters SinFire C18, 3.5 µm, 4.6 × 100 mm column. The

mobile phase was either acetonitrile/water (0.25 % TFA) (50/50, v/v) for BW-AQ-101 and BW-AQ-124, or acetonitrile/water (0.25 % TFA) (40/60, v/v) for BW-AQ-112 and BW-AQ-113 with flow rate of 1 mL/ min. The data was collected at 250 nm with threshold 50 and minimum detectable are of 7000 (< 1 %).

1.5.4 References

- (1) Baka, E.; Comer, J. E. A.; Takacs-Novak, K. *J.Pharmaceut. Biomed.* **2008**, *46*, 335.
- (2) Volgyi, G.; Baka, E.; Box, K. J.; Comer, J. E. A.; Takacs-Novak, K. *Anal. Chim. Acta* **2010**, *673*, 40.
- (3) Glomme, A.; Marz, J.; Dressman, J. B. *J. Pharm. Sci.* **2005**, *94*, 1.
- (4) Box, K. J.; Volgyi, G.; Baka, E.; Stuart, M.; Takacs-Novak, K.; Comer, J. E. A. *J. Pharm. Sci.* **2006**, *95*, 1298.
- (5) Lipinski, C. A.; Lombardo, F.; Dominy, B. W.; Feeney, P. J. *Adv. Drug Delivery Rev.* **2012**, *64*, 4.
- (6) Tetko, I. V.; Gasteiger, J.; Todeschini, R.; Mauri, A.; Livingstone, D.; Ertl, P.; Palyulin, V.; Radchenko, E.; Zefirov, N. S.; Makarenko, A. S.; Tanchuk, V. Y.; Prokopenko, V. *J. Comput. Aid. Mol. Design* **2005**, *19*, 453.
- (7) Gelderblom, H.; Verweij, J.; Nooter, K.; Sparreboom, A. *Eur. J. Cancer* **2001**, *37*, 1590.

1.6 Conclusions

Nine distinct groups of rhein analogs, were synthesized as potential anticancer agents. *In vitro* and *in silico* mechanistic evaluations of the lead compound BW-AQ-101 suggest that these

classes of anthraquinone compounds could potentially be binding to MDM2, inhibiting its interactions with MDM4, thus upregulating the tumor suppressor p53. Further mechanistic studies of the active compounds are needed to support the consistency of this hypothesis within the different classes of developed anthraquinones. The activity of all compounds were tested against seven different cancer cell lines, including leukemia and solid state tumor cells. A number of active compounds exhibiting mid to low nanomolar activity were identified. Majority of the developed compounds exhibited selectivity towards the leukemia cell lines. The physiochemical properties of selected group of compounds were studied in an attempt to evaluate their potential to become drug candidates. The majority these compounds exhibit poor water solubility, thus various non-toxic formulations were developed to overcome this drawback and to allow for the further evaluation of these active anthraquinones.

2 A NEW TYPE OF NEIGHBORING GROUP ASSISTED CLICK REACTIONS

2.1 Introduction

Click chemistry describes reactions that are fast and versatile, require mild conditions, and achieve high yields after minimum purification effort.¹ A number of reactions in this category has been reported. Some examples are the well-known copper-catalyzed and strain promoted/copper-free azide-alkyne cycloaddition reactions,²⁻⁴ tetrazine and strained alkyne/alkene Diels-Alder type of reactions,⁵⁻⁷ and the Staudinger–Bertozzi ligation.⁸ These types of reactions have found wide-spread utility in a number of applications including bioconjugation, drug delivery, development of libraries of compounds, materials chemistry, and DNA modifications.⁹⁻¹² In many such applications, the ability to undergo a secondary reaction will be very useful.^{13,14} The idea of orthogonal click-click reactions is also reflected in our earlier effort in tuning reaction rates for staged labeling.⁷ A recent and very significant report of protecting strained alkynes with

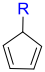
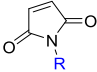
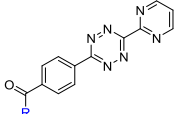
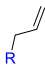
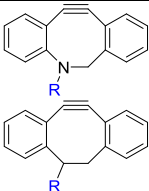
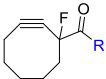
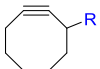
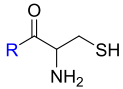
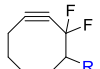
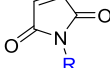
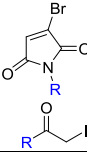
Cu(I) also allows for sequential click reactions.¹⁵ Incorporation of the azido/alkyne chemistry and cyanobenzothiazole/1,2-aminothiol chemistry pairs into a single molecule would also allow for sequential click reactions and thus staged labeling.¹⁶⁻¹⁸ Herein, we report a simple system, which allows for sequential reactions by utilizing a neighboring boronic acid-mediated click cyclization. The boronic acid functional group can then be used for a secondary modification reaction under mild conditions. The initial cyclization is very fast, complete within minutes in excellent yields (up to > 95 %), does not need an external catalyst, and uses mild/inert conditions. The key aspects of the developed methodology are 1) the reaction is promoted through activation of the aldehyde by an ortho-positioned boronic acid; 2) the reaction is tolerant of various substituents on the formyl aromatic ring; and 3) the benzothiazole product carries a boronic acid moiety that can be used as a handle for further modifications using a large number of well-established conditions.¹⁹⁻²⁵

2.1.1 Click and click: biorthogonal reactions allowing for secondary functionalization

There is a wide array of different types of biorthogonal reactions suitable for bioconjugation that have been developed and there is a number of outstanding reviews that thoroughly describe them.^{1,26-30} Thus this chapter will not focus on the in depth analysis of this type of chemistry. Herein we describe a brief overview of the utility of sequential biorthogonal reactions in chemical biology. The combination of the following biorthogonal reactions have been successfully utilized in the development of sequential dual or multi click systems: copper catalyzed alkyne-azide conjugations (CuACC), Diels-Alder reactions (DA), strain promoted alkyne-azide conjugations (SPACC), oxime ligations (OL), thiol promoted Michael additions (TMA), thiol halogen ligations (THL), thiol-ene reactions (TER), inverse electron demand Diels-Alder reactions (IEDA), and native chemical ligations (NCL).^{2,15,31-57} The combinations of these reactions have

been utilized in dual or multi sequential conjugations and have found various applications in polymer chemistry and biocompatible ligations.

Table 2.1 Biorthogonal reactants used in single molecule for sequential “click” reactions/ conjugations.

		$R-OH_2$		$R \equiv$		
$R \equiv$	Ref: 37 DA – CuAAC Surface immobilization	Ref: 38, 41 OL – CuAAC Heteropeptide conjugation	-	Ref: 30, 50, 52 CuAAC – CuAAC Two step synthesis and fluorophore conjugations	Ref: 57 IEDA – CuAAC Fluorophore conjugation	-
$R-N_3$	-	Ref: 38 OL – SPAAC Protein conjugation	-	-	-	Ref: 31, 32, 34 CuAAC – TER Peptide crosslink.
	-	Ref: 38, 51 OL-SPAAC Protein and sugar conjugations	-	-	-	-
	-	-	Ref: 41 TMA – IEDA TMA – SPAAC Protein-drug conjugation	-	-	-
	-	-	Ref: 38 TMA – SPAAC Targeting conjugation	Ref: 15, 40 SPAAC – CUAAC Fluorophore conjugation	-	-
	-	-	-	Ref: 34 NCL – CuAAC Glucose conjugation	-	-
	-	-	-	-	-	Ref: 31, 32, 34 SPAAC – TER Peptide crosslink
	-	Ref: 41 OL – TMA cRGD conjugation	-	-	Ref: 38 IED – TMA Drug conjugation	-
	-	Ref: 41 OL – THL cRGD conjugation	-	-	-	-
$R-C(=O)-S-R'$	-	-	-	Ref: 34 NCL – CuAAC Glucose conjugation	-	-

2.1.2 Dual orthogonal conjugations

Click chemistry carries the huge advantage of reaction selectivity. The reactions occur only between specific click pairs, thus allowing for multi-functionality conjugations to occur in a one pot fashion. This strategy could be utilized for various biologically relevant conjugations such as protein labelling, protein – carbohydrate conjugations, protein – protein conjugations, DNA conjugations etc. Table 2.1 summarizes some biorthogonal functionalities that have been incorporated in a single molecule and recently used for sequential conjugation reactions. There is one major concern that needs to be kept in mind when designing a double click labelled reagents: reactions should not be possible between the two click tags or their corresponding reaction partners. Hosoya's and Koning's groups have developed methodologies where two alkyne functionalities in a single molecule can be sequentially reacted in a copper catalyzed fashion with azides.^{15,50} These methodologies, however, require either alkyne protection-deprotection step. Koning and co-workers utilized triisopropylsilyl ether (TIPS) alkyne protection to achieve two steps sequential biorthogonal ligation.⁵⁰ Hosoya utilized (MeCN)CuBF₄ as a “protecting” ligand for strained cyclooctynes allowing for the functionalization of the terminal alkyne in the same molecule.¹⁵ These two examples show that sequential click labeling can occur in the presence of identical functionalities in a single molecule, however, the methodologies are not suitable for single step bioconjugations.

An excellent example of the proper selection of click pairs that allow for one pot bioconjugation was presented by Kent's group.³³ The one pot conjugation of two peptides followed immediately by ligation with azido-labelled GalNac was achieved in up to 95 % yields.³³ One of the peptides was modified through the installation of a propargyl alkyne, a substrate for a CuAAC reaction, and a thioester, a potential substrate for NCL. The peptide moieties were conjugated via

native chemical ligation between a free cysteine of one peptide and the preinstalled thioester of the other. The alkyne functionalities were then reacted with the azido-labelled GalNac in the presence of CuSO_4 .³³ One down side of this methodology is the use of toxic copper as a catalyst for the secondary functionalization. The ideal bioconjugation methodology would consist of a pair of selective reactants that are safe and do not require addition of potentially toxic catalysts.

The use of strain promoted alkyne-azide conjugation pair or inverse Diels-Alder tetrazene-alkyne ligation allow for facile reactions without the need for any catalysts. These ligations are compatible, and have been utilized in sequential manner with thiol-maleimide Michael addition reactions.^{29,38} In an effort to deliver antibody Fc fragments possessing a C-terminal selenocysteine residue (Fc-Sec), Burke and co-workers developed folate conjugated molecule containing maleimide functionality on one end and strained cyclooctyne on the other.³⁸ The Fc-Sec was linked to the maleimide through Michael type of addition. Consecutive inverse Diels-Alder reaction between the developed cyclooctyne – Fc-Sec – folate conjugate and a tetrazene tagged biotin, resulted in the successful synthesis of this anticancer “warhead”.³⁸ The use of biotin established the feasibility of the methodology, and it can be replaced with an active cytotoxic agent for therapeutic purposes. This type of chemistry can also be used not only as a pair couplings, but also for tri and multi biorthogonal conjugations.

2.1.3 Multiple orthogonal conjugations

As previously exemplified click chemistry has found a number of applications through sequential ligations. This type of conjugation chemistry has been utilized in chemical biology in triple or multiple sequential click reactions manner.²⁹ Click chemistry is an excellent tool for biomolecular modifications in a rapid and safe manner without the need of extensive purification. The fact that the different types of biorthogonal reactions can be combined in

sequential manner truly elevates the utility of this technique. The application of more than two click pairs for bioconjugation purposes can be of significant contribution to the fields of chemical biology. Table 2.1 shows pairs of click reagents that have been utilized in a single molecule, however, combinations of these functionalities can exist in multiples rather than just as a pair. For example Renard and co-workers, incorporated an azide, free thiol, and an oxime in a single molecule.⁴² The application of this “tripod” was exemplified through the development of Forster energy transfer (FRET) cassette and fluorescent renewable immunoassay biochips based on the trifunctional molecules. One major consideration that has to be taken when developing single molecule with multiple click functionalities is not just cross reactivity, but also stability and reactivity sequence of the click pairs. Thiols can be oxidized in the presence of copper, thus the TMA or THL reaction has to happen before the CuAAC conjugation. Although innovative and useful, major down side of the developed methodology is that it cannot be accomplished in one pot manner.

Successful examples of one pot multi-click conjugations were published by Boturyn and co-workers.^{40,41} A modified cyclodecapeptide containing multiple free alkyne functionalities, a free aldehyde, and a maleimide was synthesized. In addition, RGD peptides were modified by installing azido functionalities that react in a CuAAC fashion with the free alkyne groups on the cyclodecapeptide. Glc- β -ONH₂ was reacted with the free aldehyde and a thiol containing nucleic acid was reacted in Michael addition fashion with the maleimide.⁴¹ Number of other cyclodecapeptide analogues containing three different functional groups and three different conjugation methods were successfully synthesized.⁴¹ The key aspect in this work was the correct choice of click reaction sequence. In the presence of a free aldehyde, the CuAAC reaction was utilized last, as aldehydes are not stable in the presence of copper. Another interesting aspect of

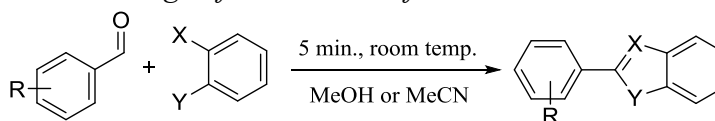
this work is not just the three different types of ligations used, but their utility in the presence of a variety of biomolecular functionalities.⁴¹ The use of three different biomolecules (peptides, nucleic acids, and sugars) in this proof of principle example stands to show how versatile and powerful is the sequential click conjugation methodology.

2.2 Neighbouring boronic acid promoted click reaction

In the process of searching for new bioorthogonal click reactions, we are interested in condensations involving aldehydes. It is well known that aldehydes can undergo facile condensation reactions with compounds that have vicinal nucleophiles. Aldehyde condensations with aryl diamines, aminobenzothiols, aminophenols, and cysteine have been previously reported.⁵⁸⁻⁶⁰ For example, aminobenzothiols and aminophenols have been condensed with an aldehyde in the presence of ZnO nanoparticles⁶⁰ or in toluene at refluxing temperature; and similar reactions using cysteine analogs took 6-15 hours to complete at room temperature.⁵⁸ Recently, Ai and colleagues reported a facile oxidative condensation of aldehydes with *o*-phenylenediamine analogs under acid catalysis.⁶¹ This was used for protein conjugation for various applications. Such reactions are also similar to the cyanobenzothiazole-cysteine condensation reactions.^{16,17,62} We are interested in taking advantage of this class of reactions by developing mild and facile conjugation chemistry that occurs without the use of acid. In doing so, we were interested in exploring the ability of a boronic acid group to function as a Lewis acid. Our lab has had a long-standing interest in boronic acid chemistry, exploring its applications in sensing,⁶³⁻⁶⁸ catalysis,^{69,70} drug design,^{39,71,72} and imaging⁷³⁻⁷⁶ as well as its behavior in mass spectrometry.⁷³ It is well known that a Lewis base/nucleophile in a 1,5-relationship with an arylboronic acid can donate its lone pair electrons to the boron open shell. This has been shown with amino and hydroxyl groups.⁷⁷⁻⁸³ Our lab has also shown that an aldehyde carbonyl oxygen can also engage in such coordination and

intermolecular aldehyde-boronic acid interactions facilitate aldehyde reduction.⁷⁰ In addition, it has been previously reported that *o*-formyl boronic acids can easily form imines with an amine under physiological conditions.⁸⁴ Recently, Gillingham and co-workers reported oxime condensation with *o*-formylphenylboronic acid as a linking tool for various chemical biology applications.⁸⁵ This could very well be due to the ability for boronic acid to catalyze the reaction through coordination. Another piece of evidence seems to suggest that the boron atom in an *o*-formyl arylboronic acid tends to stay in the tetrahedral form, suggesting coordination.³⁹ For all these reasons, we envisioned that a boronic acid group ortho to the aldehyde would be able to interact with the aldehyde oxygen atom and thus promote its acid-mediated cyclization reaction. Thus, we examined whether *o*-formylphenylboronic acid would undergo facile cyclization reactions with compounds containing vicinal nucleophiles at room temperature (Table 2.2).

Table 2.2 Design of boronic acid facilitated “click” reaction



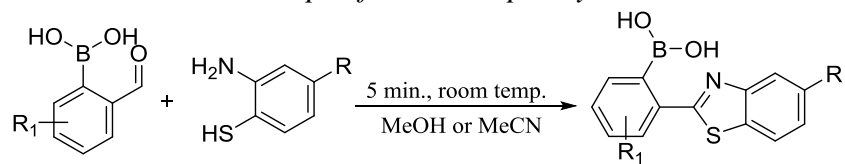
Compound	X	Y	R	Isolated Yield (%)
34	NH ₂	OH	2-B(OH) ₂	-
35	NH ₂	NH ₂	2-B(OH) ₂	-
36	NH ₂	SH	2-B(OH) ₂	85
37	NH ₂	SH	3-B(OH) ₂	-
38	NH ₂	SH	4-B(OH) ₂	-
39	NH ₂	SH	H	10

We first tried the reaction with phenylenediamine. Much to our surprise, the reaction generated a complex mixture. We did not examine the detailed composition of the reaction mixture because it was clear that this was not going to be a successful click reaction. However, all indications are that polymerization and cross-linking are possible side reactions. With this in mind, we were interested in using a structural moiety that has only one of the nucleophiles being “divalent.” In such a case, polymerization becomes not possible. With this consideration, we studied the same reaction with *o*-aminophenol and *o*-aminobenzothiol. With *o*-aminophenol, the cyclization product was not isolated. However, when the reaction was conducted with *o*-aminobenzothiol, it was very fast (Tables 2.2 and 2.3). We hypothesize that the open shell of the boron atom can serve as Lewis acid and coordinate with the oxygen of the adjacent aldehyde group in facilitating the first step of the reaction (Scheme 2.1). Furthermore, we reasoned that the boron atom could also coordinate with the nitrogen of the imine intermediate and thus facilitate the second step of the reaction as well (Scheme 2.1). In order to examine whether the cyclization was indeed facilitated by the O-B interaction that afforded the enhanced reactivity of the aldehyde group, we examined the same reactions using *m*- and *p*-formylphenylboronic acids and benzaldehyde. Not surprisingly, reacting aminobenzothiol and benzaldehyde without the boronic acid moiety gave no more than 10% of the cyclized product **39**. Furthermore, the reaction did not reach completion even after 24 h. Indeed, when the boronic acid is not positioned ortho to the aldehyde functional group, no such cyclization happened (Table 2.2). Thus, the presence of a boronic acid moiety at a position ortho to the aldehyde was crucial to the reaction. The reaction was also examined using cysteine and homocysteine as naturally occurring molecules with two adjacent nucleophiles. However, no new spots or consumption of the starting material was observed by TLC within one hour of stirring at room temperature; consequently, the reaction was

not further examined. Thus, a system with two adjacent nucleophiles is needed for the click-like cyclization with *o*-formylphenylboronic acid to occur.

In order to examine the scope of this reaction, six *o*-formylbenzylboronic acids, with various substitutions on the aromatic ring, were examined for their reactivity against three different *o*-aminobenzothiols (Table 2.3). The substituents did not seem to have much of an effect on the reaction outcome. The difference in the isolated yield of the oxidized final products was largely due to purification issues as TLC indicated full conversion in all reactions. The purification issues arise from the challenge of separating the cyclized intermediate **63** and the oxidized final product **64** (Scheme 2.1).

Table 2.3 Scope of the developed cyclization reaction

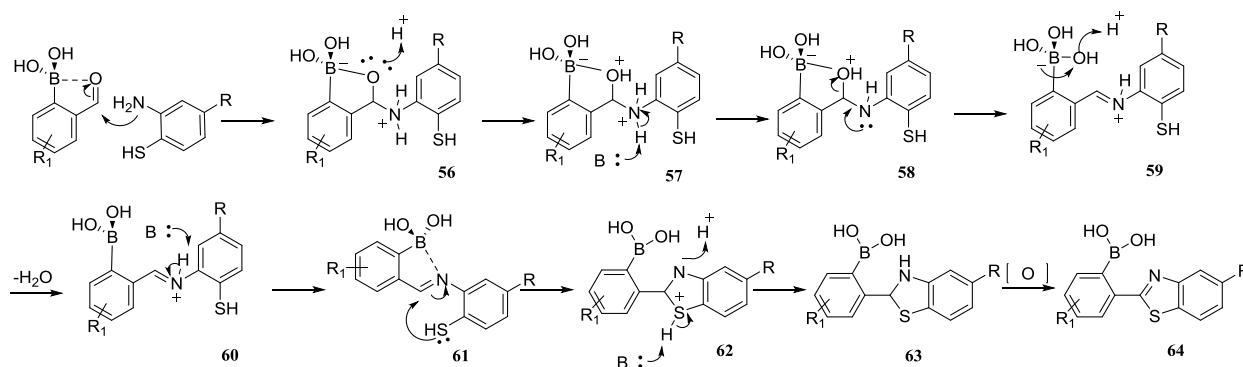


Compound	R ₁	R ₂	Conversion (%)	Isolated Yield (%)
40	4-Me ^a	H ^a	100	95
41	4-OCF ₃ ^a	H ^a	100	97
42	3-OBn ^a	H ^a	100	60
43	4-F ^a	H ^a	100	78
44	3-OMe ^a	H ^a	100	95
45	H ^a	Cl ^b	100	84
46	4-Me ^a	Cl ^b	100	75
47	3-OBn ^a	Cl ^b	100	77
48	4-F ^a	Cl ^b	100	52
49	3-OMe ^a	Cl ^b	100	74
50	H ^a	CF ₃ ^c	100	56
51	4-Me ^a	CF ₃ ^c	100	79
52	4-OCF ₃ ^a	CF ₃ ^c	100	56
53	3-OBn ^a	CF ₃ ^c	100	74
54	4-F ^a	CF ₃ ^c	100	68
55	3-OMe ^a	CF ₃ ^c	100	94

^a 1 equivalence of the reagent used. ^b 2 equivalence of the reagent used. ^c 1.2 equivalence of the reagent used.

It should be noted that the reaction sequence also involves oxidation, which we assume is air-oxidation because no other reagent was added. The oxidation step appears to be much slower compared to the click-like cyclization reaction. Addition of one equivalent of DDQ and stirring for 30 min substantially increased the oxidation rate and isolated yields (data not shown). However, the use of harsh oxidizing reagents is undesirable and simple overnight air oxidation resulted in the desired fully oxidized products (example: compounds **40**, **41**, **44**, **55**, Table 2.3).

This is also consistent with the condensation work by others that air-oxidation would drive the reaction to produce the fully aromatized system.⁸⁶



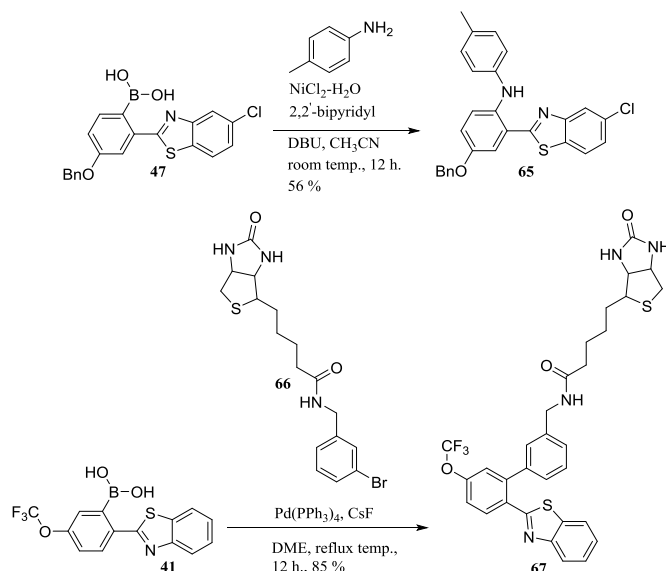
Scheme 2.1 Proposed mechanism ($R_1 = H, Me, OMe, OBn, OCF_3, F$; $R_2 = H, Cl, CF_3$)

To further explore the scope of the reaction, commercially available 2-amino-4-(trifluoromethyl)thiophenol and 2-amino-4-chlorothiophenol were selected. One of these reagents introduces an electron withdrawing group in the nucleophilic system and the other a slightly electron donating group that can potentially be used as a functionalization site (Table 2.3, compounds **45-55**).

Although aminobenzothiol has two nucleophilic groups, we propose that imine formations happens first (**59**, Scheme 2.1), followed by intramolecular cyclization driven by 1) boronic acid activated imine (**61**) and 2) energetically favorable five-membered ring formation (**62**, Scheme 2.1). As previously mentioned, the presence of a boronic acid at a position ortho- to the aldehyde not only is crucial for the cyclization reaction, but also provides a handle for further modifications of the synthesized benzothiazole.

The functionalization of the synthesized boronic acid benzothiazoles can easily be achieved through a number of coupling methods for various applications.^{16,17,62} For example, molecules can be conjugated to the benzothiazole via Suzuki coupling or the Chan – Lam reaction (Scheme 2.2).

In one such test, we conjugated biotin to the cyclization product benzothiazole. This can be extremely useful for the evaluation of biologically active compounds in binding studies such as SPR, QCM, QCM-D, and ELISA studies. Therefore, this new neighboring group assisted benzaldehyde cyclization reaction can be a versatile tool for various applications.



Scheme 2.2 The use of the boronic acid as a handle for further modifications

2.3 Conclusion

In summary, a facile neighboring group assisted cyclization reaction between formylphenylboronic acid and amino thiol has been developed. The reaction achieves full conversion at room temperature without the use of harsh conditions. The benzothiazole products can easily be modified through various boronic acid-based coupling methodologies for different applications such as bioconjugation, biolabeling, and fluorescent tagging, thus giving two sequential facile reactions. In addition, benzothiazole compounds have shown a wide array of biological activities including anticancer,⁸⁷⁻⁹² anti-inflammation,⁹³ antiviral,⁹⁴ antidiabetic,⁹⁵⁻⁹⁷ antimicrobial^{98,99} and anticonvulsant¹⁰⁰⁻¹⁰³ activities. This class of compounds is perhaps most useful in the area of diagnostics where it has been clinically used for amyloid fibrils imaging for

Alzheimer's disease detection.¹⁰⁴⁻¹⁰⁶ More recently, benzothiazole analogs have been utilized in studying the biologically important and naturally occurring gasotransmitter molecules, hydrogen sulfide^{107,108} and carbon monoxide.¹⁰⁹ Consequently, the new chemistry described here has a wealth of synthetic applications as well.

2.4 Experimental section

All reagents and solvents were of reagent grade. All formylphenylboronic acids were provided by Frontier Scientific Inc.; 2-aminobezothiol and 2-amino-4 (trifluoromethyl)thiophenol were purchased from Alpha Aeser; and 2-amino-4-chlorothiophenol was purchased from Sigma-Aldrich. Column chromatography was carried out on flash silica gel (Sorbent 230–400 mesh). TLC analysis was conducted on silica gel plates (Sorbent Silica G UV254). NMR spectra were recorded at 400 MHz for ¹H and 100 MHz for ¹³C on a Bruker instrument. Chemical shifts (δ values) and coupling constants (J values) are given in ppm and hertz, respectively, using the appropriate deuterated solvents as references.

General procedure for the preparation of compounds 36-55:

2-Formylphenylboronic acid (120 mg, 0.8 mmol) was dissolved in 4 ml methanol. 2-Aminobenzothiol (100 mg, 85.5 μ L, 0.8 mmol) was added and the reaction was stirred at room temperature open to air. Full consumption of the starting materials was achieved within 5 min (confirmed by TLC, DCM: EtOAc = 9:1) of stirring. The organic solvent was then evaporated and the yellow oily residue was purified via gradient silica gel flash column chromatography (eluent DCM: EtOAc = 100:1 and DCM: MeOH= 200:1; 100:1; 50:1).

Compound 36, (2-(benzo[d]thiazol-2-yl)phenyl)boronic acid:

Isolated yield 85 %. ¹H NMR (CD₃OD): δ 8.00 (t, J = 6.8 Hz, 2H), 7.82 (d, J = 7.6 Hz, 1H), 7.55–7.42 (m, 6H); ¹³C NMR (CD₃OD): δ 170.6, 149.9, 135.0, 134.6, 131.1, 130.8, 128.6,

126.9, 126.3, 125.8, 125.6, 122.3, 121.2. HRMS (ESI-TOF) m/z $[M+1]^+$ calcd. for $C_{13}H_{10}BNO_2S$ 256.0598, found 256.0600.

Compound 39, 2-phenylbenzo[d]thiazole:

Spectroscopic data matches that of literature report.¹¹⁰

Compound 40, (2-(benzo[d]thiazol-2-yl)-5-methylphenyl)boronic acid:

Isolated yield 95%. 1H NMR (CD_3OD): δ 7.98 (d, J = 8 Hz, 1H), 7.93 (d, J = 8 Hz, 1H), 7.66 (d, J = 7.6 Hz, 1H), 7.52 (t, J = 7.6 Hz, 1H), 7.39 (t, J = 7.6 Hz, 1H), 7.29 (s, 1H), 7.22 (d, J = 7.6 Hz, 1H), 2.38 (s, 1H); ^{13}C NMR (CD_3OD): δ 170.7, 149.8, 141.8, 134.5, 132.5, 131.5, 129.2, 126.8, 125.8, 125.4, 122.3, 121.0, 20.4. HRMS (ESI-TOF) m/z $[M+1]^+$ calcd. for $C_{14}H_{12}BNO_2S$ 270.0755, found 270.0757.

Compound 41, (2-(benzo[d]thiazol-2-yl)-5-(trifluoromethoxy)phenyl)boronic acid:

Isolated yield 97%. 1H NMR (CD_3OD): δ 8.01 (d, J = 8 Hz, 1H), 7.96 (d, J = 8 Hz, 1H), 7.86 (d, J = 8 Hz, 1H), 7.55 (t, J = 7.2 Hz, 1H), 7.43 (t, J = 7.6 Hz, 1H), 7.35 – 7.29 (m, 2H); ^{13}C NMR (CD_3OD): δ 170.5, 152.7, 136.1, 134.9, 130.2, 128.7, 128.5, 127.2, 124.1, 123.8, 123.1, 122.5, 122.0, 120.5. HRMS (ESI-TOF) m/z $[M+1]^+$ calcd. for $C_{14}H_9BF_3NO_3S$ 340.0421, found 340.0423.

Compound 42, (2-(benzo[d]thiazol-2-yl)-4-(benzyloxy)phenyl)boronic acid:

Isolated yield 60%. 1H NMR ($DMSO-d_6$): 8.13 (d, J = 8.0 Hz, 1H), 8.07 (s, 1H), 7.98 (d, J = 8.0 Hz, 1H), 7.57- 7.52 (m, 2H), 7.50-7.46 (m, 3H), 7.45-7.39 (m, 3H), 7.34 (d, J = 8.0 Hz, 1H), 7.18 (d, J = 8.0 Hz, 1H), 5.23 (s, 2H). ^{13}C NMR ($DMSO-d_6$): 169.7, 158.9, 153.3, 137.5, 137.3, 135.4, 135.3, 129.0, 128.4, 128.1, 127.0, 125.9, 123.1, 122.7, 116.8, 115.4, 69.7, 48.4, 48.2, 48.0. HRMS (ESI-TOF) m/z $[M+1]^+$ calcd. for $C_{20}H_{16}BNO_3S$ 362.1017, found 362.1009.

Compound 43, (2-(benzo[d]thiazol-2-yl)-5-fluorophenyl)boronic acid:

Isolated yield 78%. ^1H NMR (CD_3OD): δ 8.03 (d, J = 8.4 Hz, 2H), 7.91-7.87 (m, 1H), 7.59 (t, J = 7.2 Hz, 1H) 7.48 (t, J = 7.6 Hz, 1H), 7.24-7.16 (m, 2H); ^{13}C NMR (CD_3OD): δ 170.2, 163.9, 148.4, 134.5, 131.1, 127.7, 127.3, 125.8, 122.6, 120.7, 117.6, 117.4, 115.5, 115.2. HRMS (ESI-TOF) m/z $[\text{M}+1]^+$ calcd. for $\text{C}_{13}\text{H}_9\text{BFNO}_2\text{S}$ 274.0504, found 274.0507.

Compound 44, (2-(benzo[d]thiazol-2-yl)-4-methoxyphenyl)boronic acid:

Isolated yield 95%. ^1H NMR (CD_3OD): δ 8.00 (t, J = 3.2 Hz, 2H), 7.56 (t, J = 7.6 Hz, 1H), 7.46-7.38 (m, 3H), 7.11 (d, J = 7.6 Hz, 1H), 3.88 (s, 3H); ^{13}C NMR (CD_3OD): δ 169.9, 160.3, 150.7, 136.5, 134.7, 132.1, 126.7, 126.3, 125.5, 122.1, 121.6, 116.4, 111.8, 54.5. HRMS (ESI-TOF) m/z $[\text{M}+1]^+$ calcd. for $\text{C}_{14}\text{H}_{12}\text{BNO}_3\text{S}$ 286.0704, found 286.0706.

Compound 45, (2-(5-chlorobenzo[d]thiazol-2-yl)phenyl)boronic acid:

Isolated yield 84%. ^1H NMR (CD_3OD): δ 7.96-7.94 (m, 2H), 7.84 (d, J = 7.2 Hz, 2H), 7.54-7.39 (m, 4H); ^{13}C NMR (CD_3OD): δ 171.9, 152.3, 134.8, 133.2, 132.6, 131.1, 131.0, 128.7, 126.7, 125.7, 123.2, 121.3. HRMS (ESI-TOF) m/z $[\text{M}+1]^+$ calcd. for $\text{C}_{13}\text{H}_9\text{BClNO}_2\text{S}$ 290.0251, found 290.0215.

Compound 46, (2-(5-chlorobenzo[d]thiazol-2-yl)-5-methylphenyl)boronic acid:

Isolated yield 75%. ^1H NMR (CD_3OD): δ 8.00-7.95 (m, 2H), 7.78 (d, J = 8 Hz, 1H), 7.44 (d, J = 8 Hz, 1H), 7.33-7.30 (m, 2H), 2.43 (s, 3H); ^{13}C NMR (CD_3OD): δ 172.0, 152.3, 142.0, 133.1, 132.6, 132.3, 131.7, 129.4, 127.1, 126.6, 125.5, 123.2, 121.1, 20.3. HRMS (ESI-TOF) m/z $[\text{M}+1]^+$ calcd. for 304.0387, found 304.0370.

Compound 47, (4-(Benzyloxy)-2-(5-chlorobenzo[d]thiazol-2-yl)phenyl)boronic acid:

Isolated yield 77%. ^1H NMR (CD_3OD): δ 8.00 (d, J = 32.0 Hz, 2H), 7.50-7.31 (m, 8H), 7.22 (d, 1H), 5.19 (s, 2H); ^{13}C NMR (CD_3OD): δ 171.5, 159.4, 152.7, 136.9, 136.3, 133.3, 132.5,

132.4, 128.2, 127.6, 127.2, 125.6, 123.1, 121.4, 117.5, 113.4, 69.8; HRMS (ESI-TOF) m/z : $[M + 1]^+$ calcd for $C_{20}H_{15}BClNO_3S$ 396.0622, found: 396.0632.

Compound 48, (2-(5-Chlorobenzof[d]thiazol-2-yl)-4-fluorophenyl)boronic acid:

Isolated yield 52%. 1H NMR (CD_3OD): δ 8.04 (d, $J = 22.0$ Hz, 2H), 7.97 (dd, $J = 13.0, 22.0$ Hz, 1H), 7.49 (dd, $J = 5.0, 22.0$ Hz, 1H), 7.26-7.22 (m, 2H); ^{13}C NMR (CD_3OD): δ 171.1, 151.2, 133.2, 132.9, 131.0, 128.6, 125.8, 123.3, 120.9, 117.9, 117.7, 115.7, 115.4; HRMS (ESI-TOF) m/z : $[M + 1]^+$ calcd for $C_{13}H_8BClFNO_2S$ 308.0115, found: 308.0118.

Compound 49, (2-(5-chlorobenzof[d]thiazol-2-yl)-4-methoxyphenyl)boronic acid:

Isolated yield 74%. 1H NMR (CD_3OD) δ 8.01 (s, $J = 8.8$ Hz, 1 H), 7.97 (s, 1 H), 7.46 (dd, $J = 8.8, 2.0$ Hz, 1 H), 7.41 (s, 1 H), 7.39 (d, $J = 8.4$ Hz, 1 H), 7.15 (dd, $J = 8.4, 2.4$ Hz, 1 H), 3.90 (s, 3 H); ^{13}C NMR (CD_3OD) δ 173.0, 161.8, 154.1, 137.7, 134.7, 133.9, 133.8, 127.0, 125.7, 124.5, 122.8, 117.9, 113.7, 55.9; HRMS (ESI-TOF) m/z : $[M + 1]^+$ calcd for $C_{20}H_{15}BClNO_3S$ 320.0241, found: 320.0303.

Compound 50, (2-(5-(trifluoromethyl)benzof[d]thiazol-2-yl)phenyl)boronic acid:

Isolated yield 56%. 1H NMR (CD_3OD): δ 8.24 (d, 1 H), 8.22 (s, 1 H), 7.93 (d, 1 H), 7.71 (d, 1 H), 7.60-7.48 (m, 3 H); ^{13}C NMR (CD_3OD): δ 173.4, 153.2, 140.0, 136.0, 132.6, 132.5, 130.5, 130.2, 128.5, 124.6, 122.8, 122.8, 120.1, 120.0; HRMS (ESI-TOF) m/z $[M+1]^+$ calcd. for $C_{14}H_9BF_3NO_2S$ 324.0399, found 324.0474.

Compound 51, (5-methyl-2-(5-(trifluoromethyl)benzof[d]thiazol-2-yl)phenyl)boronic acid:

Isolated yield 56%. 1H NMR (CD_3OD): δ 8.21 (s, 1H), 8.19 (s, 1H), 7.80 (d, $J = 8$ Hz), 7.69 (d, $J = 8.4$ Hz, 1H), 7.33 (d, $J = 8$ Hz, 1H), 7.309 (s, 1H), 2.43 (s, 3H); ^{13}C NMR (CD_3OD): δ 172.0, 142.5, 138.7, 132.0, 131.9, 129.7, 128.5, 127.3, 123.1, 122.7, 121.3, 118.8, 20.2. HRMS (ESI-TOF) m/z $[M+1]^+$ calcd. for $C_{15}H_{11}BF_3NO_2S$ 338.1245, found 338.0632.

Compound 52, (5-(trifluoromethoxy)-2-(5-(trifluoromethyl)benzo[d]thiazol-2-yl)phenyl)boronic acid:

Isolated yield 58%. ¹H NMR (CD₃OD): δ 8.27 (d, 1 H), 8.24 (s, 1 H), 8.06 (d, 1 H), 7.75, (d, 1 H), 7.44 (d, 1 H), 7.38 (s, 1 H); ¹³C NMR (CD₃OD): δ 171.9, 152.8, 140.2, 134.76, 132.3, 130.8, 130.5, 130.3, 126.9, 124.8, 124.6, 124.2, 123.1, 122.3, 120.5, 120.1, 120.0; HRMS (ESI-TOF) m/z [M+1]⁺ calcd. for C₁₅H₈BF₆NO₃S 408.0301, found 408.0302.

Compound 53, (4-(benzyloxy)-2-(5-(trifluoromethyl)benzo[d]thiazol-2-yl)phenyl)boronic acid:

Isolated yield 74%. ¹H NMR (CD₃OD): δ 8.20 (s, 1 H), 8.19 (d, 1 H), 7.69 (d, 1 H), 7.47 (d, 3 H), 7.386 (t, 3 H), 7.32 (d, 1 H), 7.20 (d, 1 H), 5.184 (s, 2 H); ¹³C NMR (CD₃OD): δ 173.0, 160.8, 153.4, 140.0, 138.2, 137.5, 133.9, 130.5, 130.1, 129.6, 129.5, 129.0, 128.6, 128.6, 124.5, 124.2, 122.8, 122.7, 120.2, 120.2, 118.9, 115.2, 71.2; HRMS (ESI-TOF) m/z [M+1]⁺ calcd. for C₂₁H₁₅BF₃NO₃S 430.0818, found 430.0895.

Compound 54, (5-fluoro-2-(5-(trifluoromethyl)benzo[d]thiazol-2-yl)phenyl)boronic acid:

Isolated yield 68%. ¹H NMR (CD₃OD): δ 8.24 (d, 1 H), 8.22 (s, 1 H), 7.98-7.95 (m, 1 H), 7.71 (d, 1 H), 7.26-7.22 (m, 2 H); ¹³C NMR (CD₃OD): δ 171.1, 138.6, 130.9, 129.3, 123.3, 121.5, 118.4, 118.0, 117.8, 115.7, 115.5; HRMS (ESI-TOF) m/z [M+1]⁺ calcd. for C₁₄H₈BF₄NO₂S 342.0305, found 342.0378.

Compound 55, (4-methoxy-2-(5-(trifluoromethyl)benzo[d]thiazol-2-yl)phenyl)boronic acid:

Isolated yield 94%. ¹H NMR (CD₃OD): δ 8.24 (d, 1 H), 8.22 (s, 1 H), 7.72 (d, 1 H), 7.45 (s, 1 H), 7.41 (d, 1 H), 7.165 (d, 1 H), 4.85 (s, 3 H); ¹³C NMR (CD₃OD): δ 172.1, 159.6, 152.6,

139.3, 136.6, 134.9, 127.6, 127.3, 123.9, 123.0, 119.4, 119.3, 116.0, 114.1, 55.4; HRMS (ESI-TOF) m/z $[M+1]^+$ calcd. for $C_{15}H_{11}BF_3NO_3S$ 354.0584, found 354.0586.

Compound **65**, 4-(benzyloxy)-2-(5-chlorobenzo[d]thiazol-2-yl)-N-(p-tolyl)aniline:

A 10 mL vial containing arylboronic acid **47** (20 mg, 0.0506 mmol), *p*-toluidine (6.5 mg, 0.0607 mmol), $NiCl_2 \cdot 6H_2O$ (1.3 mg, 0.0101 mmol), 2,2'-bipyridyl (1.5 mg, 0.0101 mmol), DBU (15.3 mg, 0.101 mmol) and acetonitrile (2 mL) was stirred at room temperature under atmospheric conditions. The progress of the reaction was monitored by TLC using EtOAc and n-hexane as eluent. After completion, the reaction mixture was treated with EtOAc (5 mL) and water (5 mL). The organic layer was separated, and the aqueous layer was extracted with EtOAc (3×5 mL). The combined organic phase was washed with water (2×5 mL), dried over anhydrous Na_2SO_4 , and concentrated to yield a residue, which was purified by silica gel column chromatography using hexane/ethyl acetate to yield a pale yellow oil (13 mg, 56%). 1H NMR ($CDCl_3$): δ 10.1 (s, 1H), 7.99 (d, 1H, $J = 5.0$ Hz), 7.81 (d, 1H, $J = 21$ Hz), 7.50 (d, 2H, $J = 18$ Hz), 7.43 (t, 2H, $J = 18$ Hz), 7.38-7.35 (m, 3H), 7.32 (d, 1H, $J = 21$ Hz), 7.25-7.19 (m, 4H), 7.03 (dd, 1H, $J = 7.0, 23.0$ Hz), 5.11 (s, 2H), 2.36 (s, 3H); ^{13}C NMR ($CDCl_3$): δ 170.2, 154.3, 150.7, 139.2, 137.0, 132.4, 132.2, 131.7, 129.9, 128.6, 128.1, 127.6, 125.5, 122.3, 121.9, 121.7, 121.6, 120.4, 116.8, 115.8, 71.0, 20.8; HRMS (ESI-TOF) m/z : $[M + 1]^+$ calcd for $C_{27}H_{21}ClN_2OS$ 457.1163, found: 457.1141.

Compound **67**, *N*-((2'-(benzo[d]thiazol-2-yl)-5'-(trifluoromethoxy)-[1,1'-biphenyl]-3-yl)methyl)-5-(2-oxohexahydro-1H-thieno[3,4-d]imidazol-4-yl)pentanamide:

A flame-dried, two-neck round bottom flask was charged with compound **41** (50 mg, 0.147 mmol), aryl halide **66** (45 mg, 0.11 mmol), flame-dried CsF (49 mg, 0.323 mmol), and $Pd(PPh_3)_4$ (8.5 mg, 7.3×10^{-3} mmol) under argon atmosphere. Distilled DME (8 mL) was added and after immediate evacuation of the gas atmosphere in the flask via a vacuum pump, the reaction mixture

was stirred overnight at reflux temperature under argon. After stirring overnight, TLC (DCM:MeOH = 20:1) showed full consumption of the starting materials. The reaction mixture was cooled to room temperature and diluted with water (15 mL). The residue was extracted with ethyl acetate (2 × 50 mL) and the organic layers were combined and washed with water (1 × 20 mL), 1N NaOH solution (1 × 5 mL), water (1 × 30 mL), and brine (1 × 20 mL). The organic layer was then dried over Na₂SO₄ and evaporated *in vacuo*. The brown/yellow residue was purified via silica gel flash column chromatography (eluent DCM: MeOH= 200:1; 100:1; 50:1; 30:1) to give 55 mg of an off-white solid (85% yield). ¹H NMR (CD₃OD): δ 8.13 (d, *J* = 8.8 Hz, 1H), 7.98 (d, *J* = 8 Hz, 1H), 7.82(d, *J* = 8 Hz, 1H), 7.53 – 7.48 (m, 2H), 7.39 (t, *J* = 7.2 Hz, 1H), 7.38 – 7.33 (m, 3H), 7.27 (s, 1H), 7.21 – 7.18 (m, 1H), 4.44 (dd, *J*₁ = 4.4 Hz, *J*₂ = 4.8 Hz, 1H), 4.33 (d, *J* = 2.4 Hz, 2H), 4.22 (dd, *J*₁ = 4.4 Hz, *J*₂ = 4.4 Hz, 1H), 3.12 – 3.07 (m, Hz, 1H), 2.87 (dd, *J*₁ = 5.2 Hz, *J*₂ = 4.8 Hz, 1H), 2.67 (d, *J* = 12.4 Hz, 1H), 2.08 (t, *J* = 7.6 Hz, 2H), 1.69 – 1.53 (m, 5H), 1.39 – 1.31 (m, 2H); ¹³C NMR (CD₃OD): δ 174.4, 166.6, 164.6, 152.2, 150.1, 143.9, 139.5, 138.9, 136.2, 132.1, 131.1, 128.6, 128.5, 128.1, 127.5, 126.2, 125.3, 122.6, 122.5, 121.8, 121.3, 119.7, 61.9, 60.2, 55.5, 42.3, 39.6, 35.2, 28.3, 28.0, 25.3. HRMS (ESI-TOF) *m/z* [M+1]⁺ calcd. for C₃₁H₂₉F₃N₄O₃S₂ [M+H]⁺ 627.1704, found 627.1710.

2.5 References

- (1) Kolb, H. C.; Finn, M. G.; Sharpless, K. B. *Angew. Chem. Int. Edit.* **2001**, *40*, 2004.
- (2) Rostovtsev, V. V.; Green, L. G.; Fokin, V. V.; Sharpless, K. B. *Angew. Chem. Int. Edit.* **2002**, *41*, 2596.
- (3) Baskin, J. M.; Prescher, J. A.; Laughlin, S. T.; Agard, N. J.; Chang, P. V.; Miller, I. A.; Lo, A.; Codelli, J. A.; Bertozzi, C. R. *P. Natl. Acad. Sci. USA* **2007**, *104*, 16793.

- (4) Tornøe, C. W.; Christensen, C.; Meldal, M. *J. Org. Chem.* **2002**, *67*, 3057.
- (5) Chen, W.; Wang, D.; Dai, C.; Hamelberg, D.; Wang, B. *Chem. Commun.* **2012**, *48*, 1736.
- (6) Lang, K.; Davis, L.; Wallace, S.; Mahesh, M.; Cox, D. J.; Blackman, M. L.; Fox, J. M.; Chin, J. W. *J. Am. Chem. Soc.* **2012**, *134*, 10317.
- (7) Wang, D.; Chen, W.; Zhang, Y.; Dai, C.; Wang, B. *Org. Biomol. Chem.* **2014**, *12*, 3950.
- (8) Saxon, E.; Bertozzi, C. R. *Science* **2000**, *287*, 2007.
- (9) Wang, K.; Wang, D.; Wang, B. *Cur. Org. Chem.* **2015**, *19*, 1385.
- (10) Wang, K.; Wang, D.; Ji, K.; Chen, W.; Zheng, Y.; Dai, C.; Wang, B. *Org. Biomol. Chem.* **2015**, *13*, 909.
- (11) Nwe, K.; Brechbiel, M. W. *Cancer Biother. Radio.* **2009**, *24*, 289.
- (12) Moses, J. E.; Moorhouse, A. D. *Chem. Soc. Rev.* **2007**, *36*, 1249.
- (13) Yuan, Z.; Kuang, G.-C.; Clark, R. J.; Zhu, L. *Org. Lett.* **2012**, *14*, 2590.
- (14) Aucagne, V.; Leigh, D. A. *Org. Lett.* **2006**, *8*, 4505.
- (15) Yoshida, S.; Hatakeyama, Y.; Johmoto, K.; Uekusa, H.; Hosoya, T. *J. Am. Chem. Soc.* **2014**, 13590.
- (16) Ren, H. J.; Xiao, F.; Zhan, K.; Kim, Y. P.; Xie, H. X.; Xia, Z. Y.; Rao, J. *Angew. Chem. Int. Edit.* **2009**, *48*, 9658.
- (17) Cheng, Y.; Dai, C.; Peng, H.; Chen, W.; Ni, N.; Ke, B.; Wang, B. *Chem. Eur. J.* **2013**, *19*, 4036.
- (18) Liang, G. I.; Ren, H. J.; Rao, J. H. *Nat. Chem.* **2010**, *2*, 54.

- (19) Kim, A.; Park, J. C.; Kim, M.; Heo, E.; Song, H.; Park, K. H. *J. Nanosci. Nanotechnol.* **2014**, *14*, 1872.
- (20) Polshettiwar, V.; Decottignies, A. L., C.; Fihri, A. *ChemSusChem* **2010**, *3*, 502.
- (21) Littke, A. F.; C., D.; Fu, G. C. *J. Am. Chem. Soc.* **2000**, *122*, 4020.
- (22) Kirchhoff, J. H.; Netherton, M. R.; Hills, I. D.; Fu, G. C. *J. Am. Chem. Soc.* **2002**, *124*, 13662.
- (23) Dudnik, A. S.; Fu, G. C. *J. Am. Chem. Soc.* **2012**, *134*, 10693.
- (24) Maegawa, T.; Kitamura, Y.; Sako, S.; Udzu, T.; Sakurai, A.; Tanaka, A.; Kobayashi, Y.; Endo, K.; Bora, U.; Kurita, T.; Kozaki, A.; Monguchi, Y.; Sajiki, H. *Chem. Eur. J.* **2007**, *13*, 5937.
- (25) Herradura, P. S.; Pendola, K. A.; Guy, R. K. *Org. Lett.* **2000**, *2*, 2019.
- (26) Sletten, E. M.; Bertozzi, C. R. *Angew. Chem. Int. Ed.* **2009**, *48*, 6974.
- (27) McKay, C. S.; Finn, M. G. *Chem. Biol.* **2014**, *21*, 1075.
- (28) Tang, W.; Becker, M. L. *Chem. Soc. Rev.* **2014**, *43*, 7013.
- (29) Beal, D. M.; Jones, L. H. *Angew. Chem. Int. Ed.* **2012**, *51*, 6320.
- (30) Guiard, J.; Fiege, B.; Kitov, P. I.; Peters, T.; Bundle, D. R. *Chem. Eur. J.* **2011**, *17*, 7438.
- (31) DeForest, C. A.; Polizzotti, B. D.; Anseth, K. S. *Nat. Mater.* **2009**, *8*, 659.
- (32) DeForest, C. A.; Sims, E. A.; Anseth, K. S. *Chem. Mater.* **2010**, *22*, 4783.
- (33) Lee, D. J.; Mandal, K.; Harris, P. W. R.; Brimble, M. A.; Kent, S. B. H. *Org. Lett.* **2009**, *11*, 5270.
- (34) DeForest, C. A.; Anseth, K. S. *Angew. Chem. Int. Ed.* **2012**, *51*, 1816.

- (35) Meyer, A.; Spinelli, N.; Dumy, P.; Vasseur, J.-J.; Morvan, F.; Defrancq, E. *J. Org. Chem.* **2010**, *75*, 3927.
- (36) Sun, X. L.; Stabler, C. L.; Cazalis, C. S.; Chaikof, E. L. *Bioconjugate Chem.* **2006**, *17*, 52.
- (37) Hudak, J. E.; Barfield, R. M.; de Hart, G. W.; Grob, P.; Nogales, E.; Bertozzi, C. R.; Rabuka, D. *Angew. Chem. Int. Ed.* **2012**, *51*, 4161.
- (38) Thomas, J. D.; Cui, H.; North, P. J.; Hofer, T.; Rader, C.; Burke, T. R., Jr. *Bioconjugate Chem.* **2012**, *23*, 2007.
- (39) Kele, P.; Mezo, G.; Achatz, D.; Wolfbeis, O. S. *Angew. Chem. Int. Ed.* **2009**, *48*, 344.
- (40) Galibert, M.; Dumy, P.; Boturyn, D. *Angew. Chem. Int. Ed.* **2009**, *48*, 2576.
- (41) Galibert, M.; Renaudet, O.; Dumy, P.; Boturyn, D. *Angew. Chem. Int. Ed.* **2011**, *50*, 1901.
- (42) Clave, G.; Volland, H.; Flaender, M.; Gasparutto, D.; Romieu, A.; Renard, P.-Y. *Org. Biomol. Chem.* **2010**, *8*, 4329.
- (43) Clave, G.; Boutal, H.; Hoang, A.; Perraut, F.; Volland, H.; Renard, P.-Y.; Romieu, A. *Org. Biomol. Chem.* **2008**, *6*, 3065.
- (44) Valverde, I. E.; Delmas, A. F.; Aucagne, V. *Tetrahedron* **2009**, *65*, 7597.
- (45) Gramlich, P. M. E.; Warncke, S.; Gierlich, J.; Carell, T. *Angew. Chem. Int. Ed.* **2008**, *47*, 3442.
- (46) Watzke, A.; Kohn, M.; Gutierrez-Rodriguez, M.; Wacker, R.; Schroder, H.; Breinbauer, R.; Kuhlmann, J.; Alexandrov, K.; Niemeyer, C. M.; Goody, R. S.; Waldmann, H. *Angew. Chem. Int. Ed.* **2006**, *45*, 1408.

- (47) Smith, M. E. B.; Schumacher, F. F.; Ryan, C. P.; Tedaldi, L. M.; Papaioannou, D.; Waksman, G.; Caddick, S.; Baker, J. R. *J. Am. Chem. Soc.* **2010**, *132*, 1960.
- (48) Beal, D. M.; Albrow, V. E.; Burslem, G.; Hitchen, L.; Fernandes, C.; Laphorn, C.; Roberts, L. R.; Selby, M. D.; Jones, L. H. *Org. Biomol. Chem.* **2012**, *10*, 548.
- (49) Schultz, M. K.; Parameswarappa, S. G.; Pigge, F. C. *Org. Lett.* **2010**, *12*, 2398.
- (50) Ehlers, I.; Maity, P.; Aube, J.; Koenig, B. *Eur. J. Org. Chem.* **2011**, 2474.
- (51) Sanders, B. C.; Friscourt, F.; Ledin, P. A.; Mbua, N. E.; Arumugam, S.; Guo, J.; Boltje, T. J.; Popik, V. V.; Boons, G.-J. *J. Am. Chem. Soc.* **2011**, *133*, 949.
- (52) Seela, F.; Ingale, S. A. *J. Org. Chem.* **2010**, *75*, 284.
- (53) Durmaz, H.; Dag, A.; Altintas, O.; Erdogan, T.; Hizal, G.; Tunca, U. *Macromol.* **2007**, *40*, 191.
- (54) Kempe, K.; Hoogenboom, R.; Jaeger, M.; Schubert, U. S. *Macromol.* **2011**, *44*, 6424.
- (55) Elamari, H.; Meganem, F.; Herscovici, J.; Girard, C. *Tetrahedron Lett.* **2011**, *52*, 658.
- (56) Tunca, U. *J. Polym. Sci. Pol. Chem.* **2014**, *52*, 3147.
- (57) Hassertt, R.; Pagel, M.; Ming, Z.; Haupl, T.; Abel, B.; Braun, K.; Wiessler, M.; Beck-Sickinger, A. G. *Bioconjugate Chem.* **2012**, *23*, 2129.
- (58) Lu, Y.; Wang, Z.; Li, C.-M.; Chen, J.; Dalton, J. T.; Li, W.; Miller, D. D. *Bioorg. Med. Chem.* **2010**, *18*, 477.
- (59) Riadi, Y.; Mamouni, R.; Azzalou, R.; El Haddad, M.; Routier, S.; Guillaumet, G.; Lazar, S. *Tetrahedron Lett.* **2011**, *52*, 3492.
- (60) Banerjee, S.; Payra, S.; Saha, A.; Sereda, G. *Tetrahedron Lett.* **2014**, *55*, 5515.

- (61) Ji, A.; Ren, W.; Ai, H. W. *Chem. Commun.* **2014**, 50, 7469.
- (62) Liang, G. L.; Ren, H. J.; Rao, J. H. *Nature Chemistry* **2010**, 2, 54.
- (63) Karnati, V.; Gao, X.; Gao, S.; Yang, W.; Sabapathy, S.; Ni, W.; Wang, B. *Bioorg. Med. Chem. Lett.* **2002**, 12, 3373.
- (64) Kaur, G.; Lin, N.; Fang, H.; Wang, B. In *Glucose Sensing*; Geddes, C. D., Lakowicz, J. R., Eds.; Springer Press: 2006; Vol. 11, p 377.
- (65) Wang, W.; Gao, S.; Wang, B. *Org. Lett.* **1999**, 1, 1209.
- (66) Wang, W.; Springsteen, G.; Gao, S.; Wang, B. *Chem. Commun.* **2000**, 1283.
- (67) Yang, W.; Lin, L.; Wang, B. *Tetrahedron Lett.* **2005**, 46, 7981.
- (68) Yang, W.; Yan, J.; Fang, H.; Wang, B. *Chem. Commun.* **2003**, 792
- (69) Latta, R. P.; Springsteen, G.; Wang, B. *Synthesis* **2001**, 1611.
- (70) Yu, H.; Wang, B. *Synth. Commun.* **2001**, 31, 163.
- (71) Ni, N.; Chou, H. T.; Wang, J.; Li, M.; Lu, C. D.; Tai, P. C.; Wang, B. *Biochem. Biophys. Res. Commun.* **2008**, 369, 590.
- (72) Yang, W.; Gao, X.; Wang, B. *Med. Res. Rev.* **2003**, 23, 346.
- (73) Chu, Y.; Wang, D.; Wang, K.; Liu, Z.; Weston, B.; Wang, B. *Bioorg. Med. Chem. Lett.* **2013**, 23, 6307.
- (74) Dai, C.; Cazares, L. H.; Wang, L.; Chu, Y.; Troyer, D. A.; Semmes, O. J.; Drake, R. R.; Wang, B. *Chem. Commun.* **2011**, 47, 10338.
- (75) Yang, W.; Fan, H.; Gao, S.; Gao, X.; Ni, W.; Karnati, V.; Hooks, W. B.; Carson, J.; Weston, B.; Wang, B. *Chem. Biol.* **2004**, 11, 439.
- (76) Yang, W.; Gao, S.; Gao, X.; Karnati, V. R.; Ni, W.; Wang, B.; Hooks, W. B.; Carson, J.; Weston, B. *Bioorg. Med. Chem. Lett.* **2002**, 12, 2175.

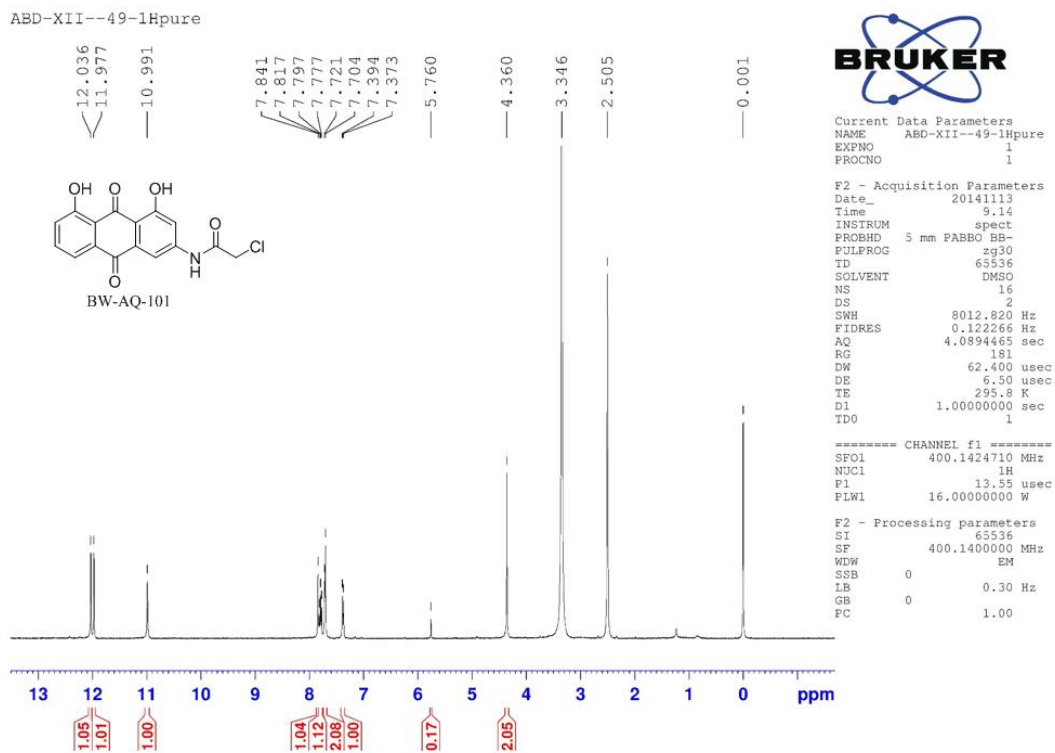
- (77) Zheng, H.; Ghanbari, S.; Nakamura, S.; Hall, D. G. *Angew. Chem. Int. Edit.* **2012**, *51*, 6187.
- (78) Wulff, G. *Pure Appl. Chem.* **1982**, *54*, 2093.
- (79) James, T. D.; Sandanayake, K.; Shinkai, S. *Angew. Chem. Int. Ed. Engl.* **1994**, *33*, 2207.
- (80) James, T. D.; Kras, S.; Shinkai, S. *Chem. Commun.* **1994**, 477.
- (81) Arimori, S.; Bosch, L. I.; Ward, C. J.; James, T. D. *Tetrahedron Lett.* **2001**, *42*, 4553.
- (82) Ni, W.; Kaur, G.; Springsteen, G.; Wang, B.; Franzen, S. *Bioorg. Chem.* **2004**, *32*, 571.
- (83) Franzen, S.; Ni, W. J.; Wang, B. H. *J. Phys. Chem. B* **2003**, *107*, 12942.
- (84) Cal, P.; Vicente, J. B.; Pires, E.; Coelho, A. V.; Veiros, L. F.; Cordeiro, C.; Gois, P. M. P. *J. Am. Chem. Soc.* **2012**, *134*, 10299.
- (85) Schmidt, P.; Stress, C.; Gillingham, D. *Chem. Sci.* **2015**, 3329.
- (86) Lynn, M. A.; Carlson, L. J.; Hwangbo, H.; Tanski, J. M.; Tyler, L. A. *J. Mol. Struct.* **2012**, *1011*, 81.
- (87) Wang, Z.; Shi, X.-H.; Wang, J.; Zhou, T.; Xu, Y.-Z.; Huang, T.-T.; Li, Y.-F.; Zhao, Y.-L.; Yang, L.; Yang, S.-Y.; Yu, L.-T.; Wei, Y.-Q. *Bioorg. Med. Chem. Lett.* **2011**, *21*, 1097.
- (88) Kumbhare, R. M.; Dadmal, T.; Kosurkar, U.; Sridhar, V.; Rao, J. V. *Bioorg. Med. Chem. Lett.* **2012**, *22*, 453.
- (89) Saeed, S.; Rashid, N.; Jones, P. G.; Ali, M.; Hussain, R. *Eur. J. Med. Chem.* **2010**, *45*, 1323.

- (90) Havrylyuk, D.; Mosula, L.; Zimenkovsky, B.; Vasylenko, O.; Gzella, A.; Lesyk, R. *Eur. J. Med. Chem.* **2010**, *45*, 5012.
- (91) Caputo, R.; Calabro, M. L.; Micale, N.; Schimmer, A. D.; Ali, M.; Zappala, M.; Grasso, S. *Med. Chem. Res.* **2012**, *21*, 2644.
- (92) Oanh, D. T. K.; Hai, H. V.; Park, S. H.; Kim, H.-J.; Han, B.-W.; Kim, H.-S.; Hong, J.-T.; Han, S.-B.; Hue, V. T. M.; Nam, N.-H. *Bioorg. Med. Chem. Lett.* **2011**, *21*, 7509.
- (93) Shafi, S.; Alam, M. M.; Mulakayala, N.; Mulakayala, C.; Vanaja, G.; Kalle, A. M.; Pallu, R.; Alam, M. S. *Eur. J. Med. Chem.* **2012**, *49*, 324.
- (94) Nagarajan, S. R.; De Crescenzo, G. A.; Getman, D. P.; Lu, H. F.; Sikorski, J. A.; Walker, J. L.; McDonald, J. J.; Houseman, K. A.; Kocan, G. P.; Kishore, N.; Mehta, P. P.; Funkes-Shippy, C. L.; Blystone, L. *Bioorg. Med. Chem.* **2003**, *11*, 4769.
- (95) Patil, V. S.; Nandre, K. P.; Ghosh, S.; Rao, V. J.; Chopade, B. A.; Sridhar, B.; Bhosale, S. V.; Bhosale, S. V. *Eur. J. Med. Chem.* **2013**, *59*, 304.
- (96) Ammazalorso, A.; Giancristofaro, A.; D'Angelo, A.; De Filippis, B.; Fantacuzzi, M.; Giampietro, L.; Maccallini, C.; Amoroso, R. *Bioorg. Med. Chem. Lett.* **2011**, *21*, 4869.
- (97) Navarrete-Vazquez, G.; Ramirez-Martinez, M.; Estrada-Soto, S.; Nava-Zuazo, C.; Paoli, P.; Camici, G.; Escalante-Garcia, J.; Medina-Franco, J. L.; Lopez-Vallejo, F.; Ortiz-Andrade, R. *Eur. J. Med. Chem.* **2012**, *53*, 346.
- (98) Cho, Y.; Ioerger, T. R.; Sacchettini, J. C. *J. Med. Chem.* **2008**, *51*, 5984.
- (99) Telvekar, V. N.; Bairwa, V. K.; Satardekar, K.; Bellubi, A. *Bioorg. Med. Chem. Lett.* **2012**, *22*, 649.
- (100) Amir, M.; Asif, S.; Ali, I.; Hassan, M. Z. *Med. Chem. Res.* **2012**, *21*, 2661.

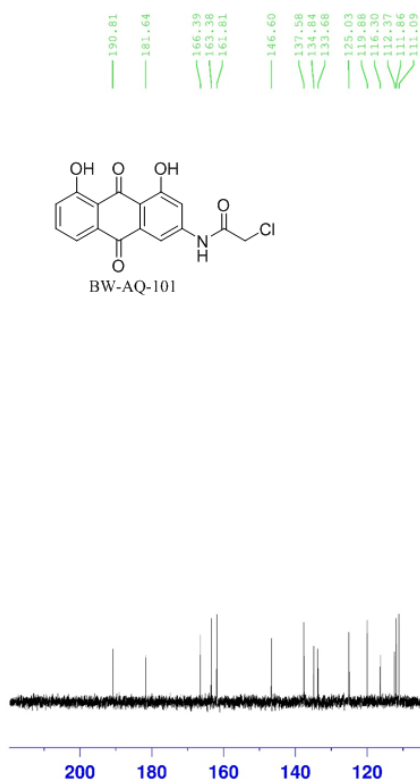
- (101) Kumar, P.; Shrivastava, B.; Pandeya, S. N.; Tripathi, L.; Stables, J. P. *Med. Chem. Res.* **2012**, *21*, 2428.
- (102) Jimonet, P.; Audiau, F.; Barreau, M.; Blanchard, J. C.; Boireau, A.; Bour, Y.; Coleno, M. A.; Doble, A.; Doerflinger, G.; Hu, C. D.; Donat, M. H.; Duchesne, J. M.; Ganil, P.; Gueremy, C.; Honore, E.; Just, B.; Kerphirique, R.; Gontier, S.; Hubert, P.; Laduron, P. M.; Le Blevec, J.; Meunier, R.; Miquet, J. M.; Nemecek, C.; Pasquet, M.; Piot, O.; Pratt, J.; Rataud, J.; Reibaud, N.; Stutzmann, J. M.; Mignani, S. *J. Med. Chem.* **1999**, *42*, 2828.
- (103) Ugale, V. G.; Patel, H. M.; Wadodkar, S. G.; Bari, S. B.; Shirkhedkar, A. A.; Surana, S. J. *Eur. J. Med. Chem.* **2012**, *53*, 107.
- (104) Mathis, C. A.; Wang, Y. M.; Holt, D. P.; Huang, G. F.; Debnath, M. L.; Klunk, W. E. *J. Med. Chem.* **2003**, *46*, 2740.
- (105) Koole, M.; Lewis, D. M.; Buckley, C.; Nelissen, N.; Vandenbulcke, M.; Brooks, D. J.; Vandenberghe, R.; Van Laere, K. *J. Nucl. Med.* **2009**, *50*, 818.
- (106) Klunk, W. E.; Engler, H.; Nordberg, A.; Wang, Y. M.; Blomqvist, G.; Holt, D. P.; Bergstrom, M.; Savitcheva, I.; Huang, G. F.; Estrada, S.; Ausen, B.; Debnath, M. L.; Barletta, J.; Price, J. C.; Sandell, J.; Lopresti, B. J.; Wall, A.; Koivisto, P.; Antoni, G.; Mathis, C. A.; Langstrom, B. *Ann. Neurol.* **2004**, *55*, 306.
- (107) Jiang, Y.; Wu, Q.; Chang, X. *Talanta* **2014**, *121*, 122.
- (108) Zhang, J.; Guo, W. *Chem. Commun.* **2014**, *50*, 4214.
- (109) Carrington, S. J. C., I.; Bernard, J. M. L.; Mascharak, P. K. *Med. Chem. Lett.* **2014**.
- (110) Tong, Y.; Pan, Q.; Jiang, Z.; Miao, D.; Shi, X.; Han, S. *Tetrahedron Lett.* **2014**, *55*, 5499.

APPENDICES

Appendix A NMR data for the compounds described in Chapter 1



ABD-XII--49-13C



Current Data Parameters
 NAME ABD-XII--49-13C
 EXPNO 1
 PROCNO 1

F2 - Acquisition Parameters
 Date_ 20141113
 Time 9.08
 INSTRUM spect
 PROBHD 5 mm PABBO BB-
 PULPROG zgpg30
 TD 65536
 SOLVENT DMSO
 NS 9900
 DS 4
 SWH 24038.461 Hz
 FIDRES 0.366798 Hz
 AQ 1.3631488 sec
 RG 64
 DW 20.800 usec
 DE 6.50 usec
 TE 296.7 K
 D1 2.00000000 sec
 D11 0.03000000 sec
 TD0 1

===== CHANNEL f1 =====
 SFO1 100.6253441 MHz
 NUC1 13C
 P1 9.00 usec
 PLW1 62.00000000 W

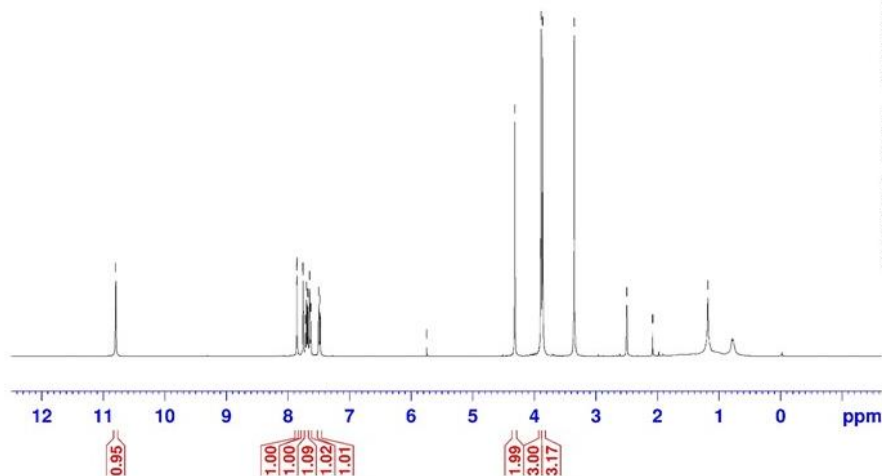
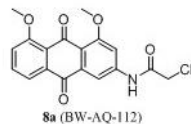
===== CHANNEL f2 =====
 SFO2 400.1416006 MHz
 NUC2 1H
 CPDPRG2 waltz16
 PCPD2 90.00 usec
 PLW2 16.00000000 W
 PLW12 0.36267000 W
 PLW13 0.29376000 W

F2 - Processing parameters
 SI 32768
 SF 100.6152830 MHz
 WDW EM
 SSB 0
 LB 1.00 Hz
 GB 0
 PC 1.40

BW-AQ-112-1H-(10-28-15)

10.800
7.858
7.854
7.759
7.755
7.718
7.698
7.678
7.650
7.632
7.502
7.481
5.748

4.319
3.890
3.866
3.354
2.500
2.078
1.182



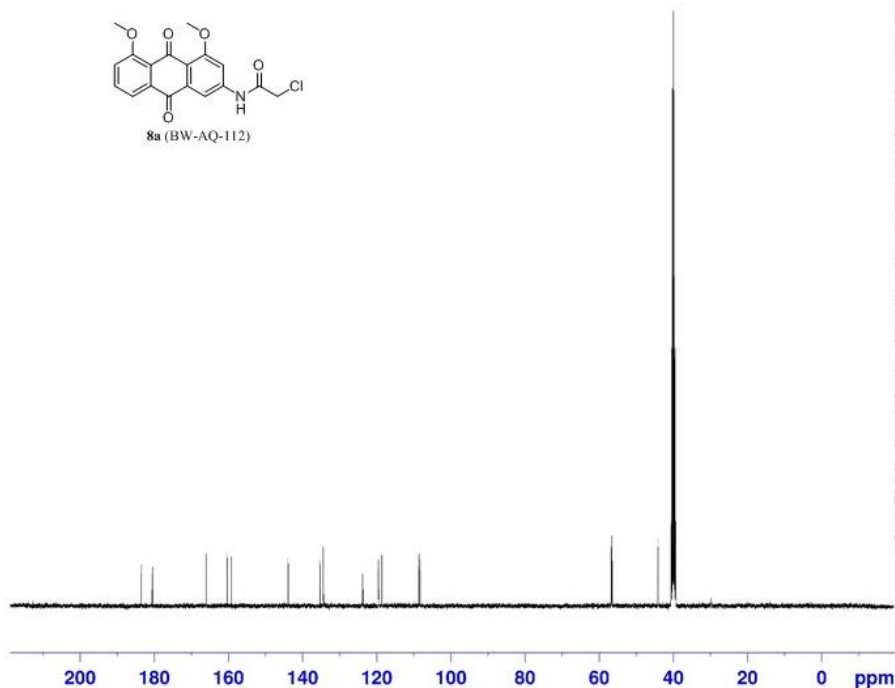
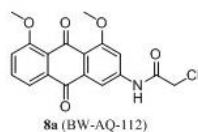
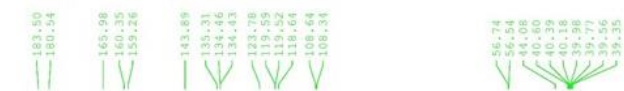
Current Data Parameters
NAME BW-AQ-112-1H-(10-28-15)
EXPNO 1
PROCNO 1

F2 - Acquisition Parameters
Date_ 20151028
Time 12.49
INSTRUM spect
PROBHD 5 mm PABBO BB-
PULPROG zg30
TD 65536
SOLVENT DMSO
NS 16
DS 2
SWH 8012.820 Hz
FIDRES 0.122266 Hz
AQ 4.0894465 sec
RG 90.5
RW 62.400 usec
DE 6.50 usec
TE 296.0 K
D1 1.00000000 sec
TD0 1

===== CHANNEL f1 =====
SFO1 400.1424710 MHz
NUC1 1H
P1 13.55 usec
PLW1 16.00000000 W

F2 - Processing parameters:
SI 65536
SF 400.1400031 MHz
WDW EM
SSS 0
LB 0.30 Hz
GB 0
PC 1.00

BW-AQ-112-13C- (10-28-15)



Current Data Parameters
 NAME BW-AQ-112-13C- (10-28-15)
 EXPNO 1
 PROCNO 1

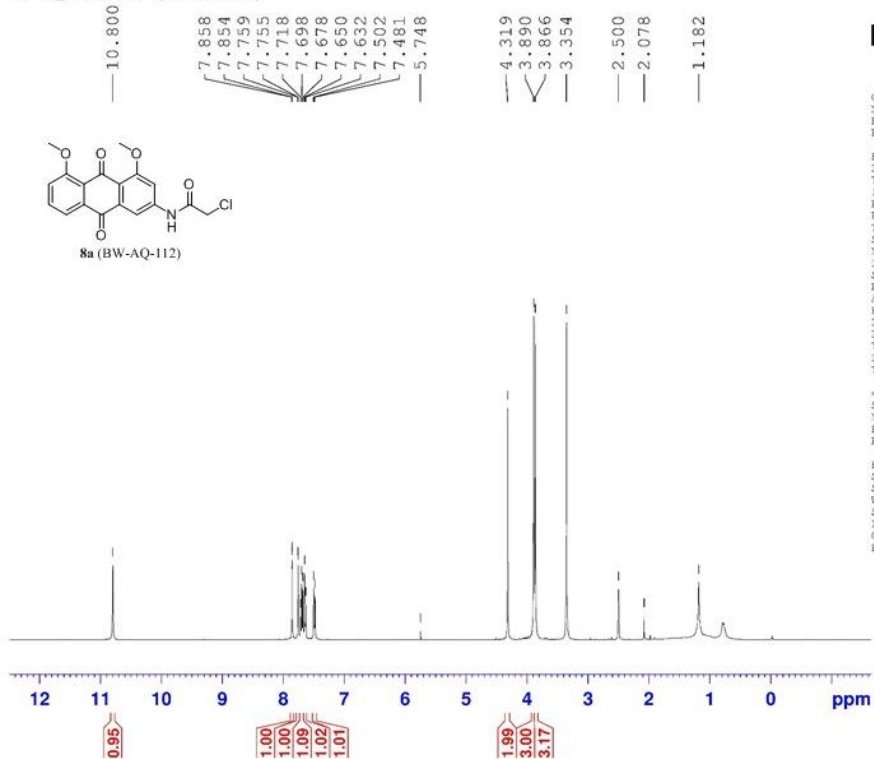
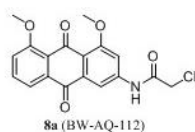
F2 - Acquisition Parameters
 Date_ 20151028
 Time 12.53
 INSTRUM spect
 PROCNO 5
 PULPROG zgpg30
 TD 65536
 SOLVENT DMSO
 NS 363
 DS 4
 SWH 24038.461 Hz
 FIDRES 0.366798 Hz
 AQ 1.3631486 sec
 RG 203
 DW 20.800 usec
 DE 8.50 usec
 TE 296.0 K
 D1 7.00000000 sec
 D11 0.03000000 sec
 TD0 1

===== CHANNEL f1 =====
 SFO1 100.6253441 MHz
 NUC1 13C
 P1 9.00 usec
 PLW1 62.00000000 W

===== CHANNEL f2 =====
 SFO2 400.1416006 MHz
 NUC2 1H
 CPDPRG2 waltz16
 PCD2 90.00 usec
 PLW2 16.00000000 W
 PLW12 0.36267000 W
 PLW13 0.29376000 W

F2 - Processing parameters
 ST 32768
 SP 100.6152830 MHz
 NDW EM
 SSB 0
 LB 1.00 Hz
 GB 0
 PC 1.40

BW-AQ-112-1H- (10-28-15)



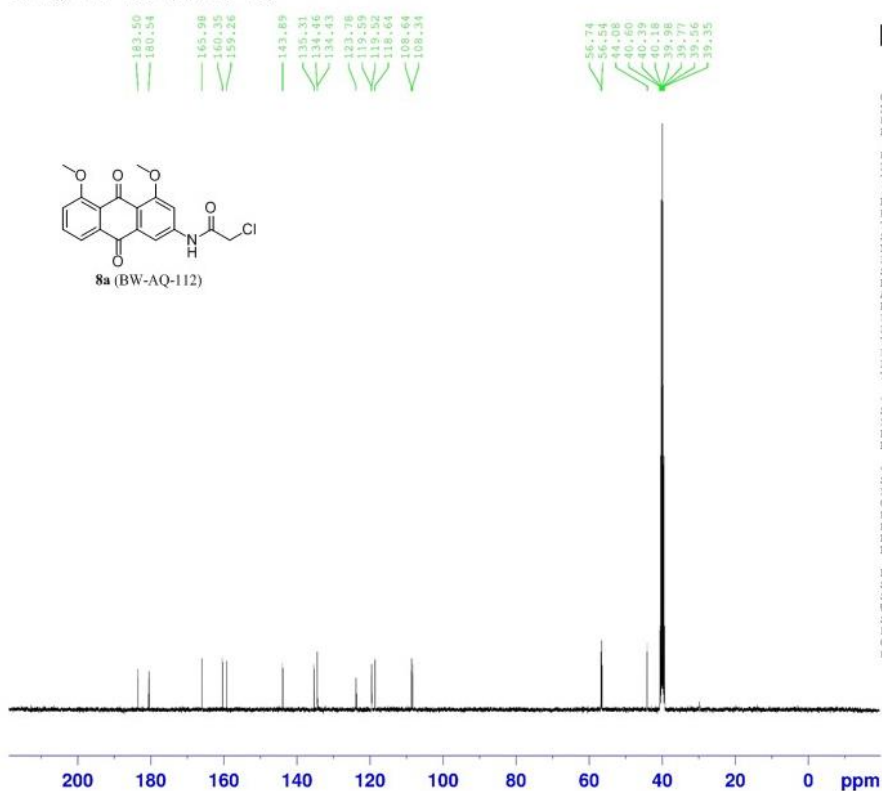
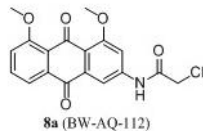
Current Data Parameters
NAME BW-AQ-112-1H- (10-28-15)
EXPNO 1
PROCNO 1

F2 - Acquisition Parameters
Date_ 20151028
Time 12.49
INSTRUM spect
PROBHD 5 mm PABBO BB-
PULPROG zg30
TD 65536
SOLVENT DMSO
NS 16
DS 2
SWH 8012.820 Hz
FIDRES 0.122266 Hz
AQ 4.0894465 sec
RG 90.5
DW 62.400 usec
DE 6.50 usec
TE 296.0 K
D1 1.00000000 sec
TD0 1

***** CHANNEL f1 *****
SFO1 400.1424710 MHz
NUC1 1H
P1 13.55 usec
PLW1 16.00000000 W

F2 - Processing parameters
SI 65536
SF 400.1400031 MHz
WDW EM
SSB 0
LB 0.30 Hz
GB 0
PC 1.00

BW-AQ-112-13C- (10-28-15)



Current Data Parameters
 NAME BW-AQ-112-13C- (10-28-15)
 EXPNO 1
 PROCNO 1

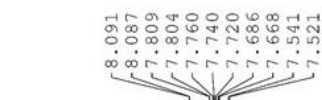
F2 - Acquisition Parameters
 Date_ 20151028
 Time 12.53
 INSTRUM spect
 PROBHD 5 mm PABBO BB-
 PULPROG zgpg30
 TD 65536
 SOLVENT DMSO
 NS 363
 DS 4
 SWH 24038.461 Hz
 FIDRES 0.366798 Hz
 AQ 1.3631488 sec
 RG 203
 DW 20.800 usec
 DE 6.30 usec
 TE 296.0 K
 D1 2.00000000 sec
 D11 0.03000000 sec
 TD0 1

----- CHANNEL f1 -----
 SFO1 100.6253441 MHz
 NUC1 13C
 P1 9.00 usec
 PLW1 62.00000000 W

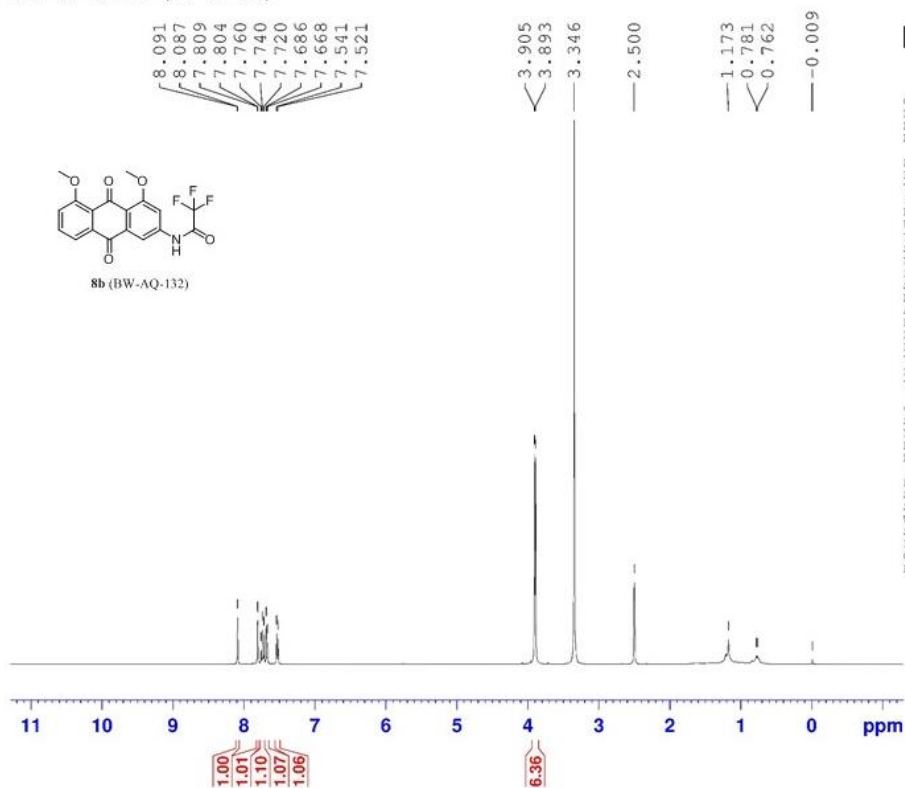
----- CHANNEL f2 -----
 SFO2 400.1416006 MHz
 NUC2 1H
 CPDPRG2 waltz16
 PCPD2 90.00 usec
 PLW2 16.00000000 W
 PLW12 0.36267000 W
 PLW13 0.29376000 W

F2 - Processing parameters
 SI 32768
 SF 100.6152830 MHz
 WDW EM
 SSB 0
 LB 1.00 Hz
 GB 0
 PC 1.40

DCF-VI-18-1H- (10-29-15)



8b (BW-AQ-132)



Current Data Parameters
 NAME DCF-VI-18-1H- (10-29-15)
 EXPNO 1
 PROCNO 1

F2 - Acquisition Parameters
 Date 20151029
 Time 12.58
 INSTRUM spect
 PROBHD 5 mm PABBO BB
 PULPROG zg30
 TD 65536
 SOLVENT DMSO
 NS 16
 DS 2
 SWH 8012.820 Hz
 FIDRES 0.122266 Hz
 AQ 4.089485 sec
 RG 144
 DW 62.400 usec
 DE 6.50 usec
 TE 296.0 K
 D1 1.00000000 sec
 TDO 1

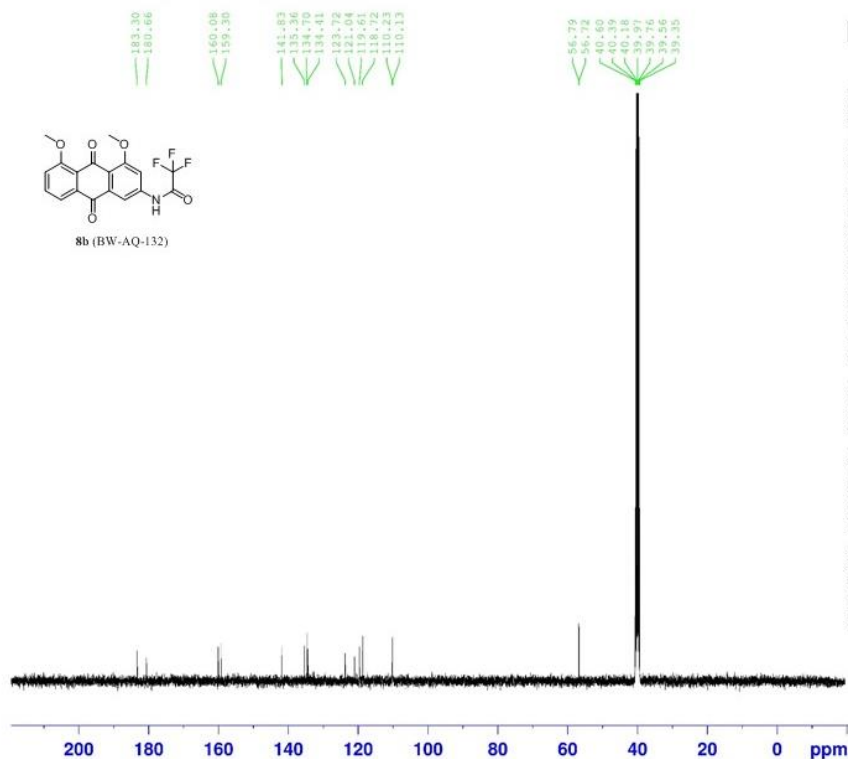
===== CHANNEL f1 =====
 SFO1 400.1424710 MHz
 NUC1 1H
 P1 13.55 usec
 PLW1 16.00000000 W

F2 - Processing parameters
 SI 65536
 SF 400.1400030 MHz
 WDW EM
 SSB 0
 LB 0.30 Hz
 GB 0
 PC 1.00

DCF-VI-18-13C- (10-29-15)



8b (BW-AQ-132)



Current Data Parameters
NAME DCF-VI-18-13C- (10-29-15)
EXPTNO 1
PROCNO 1

F2 - Acquisition Parameters
Date_ 20151029
Time 13.02
INSTRUM spect
PROBHD 5 mm PABBO BB-
PULPROG zgpg30
TD 65536
SOLVENT DMSO
NS 251
DS 4
SWH 24039.461 Hz
FIDRES 0.366798 Hz
AQ 1.3631488 sec
RG 161
SW 20.800 usec
DE 6.30 usec
TE 296.0 K
D1 2.00000000 sec
D11 0.03000000 sec
TD0 1

===== CHANNEL f1 =====
SFO1 100.6253441 MHz
NUC1 13C
P1 9.00 usec
PLW1 62.00000000 W

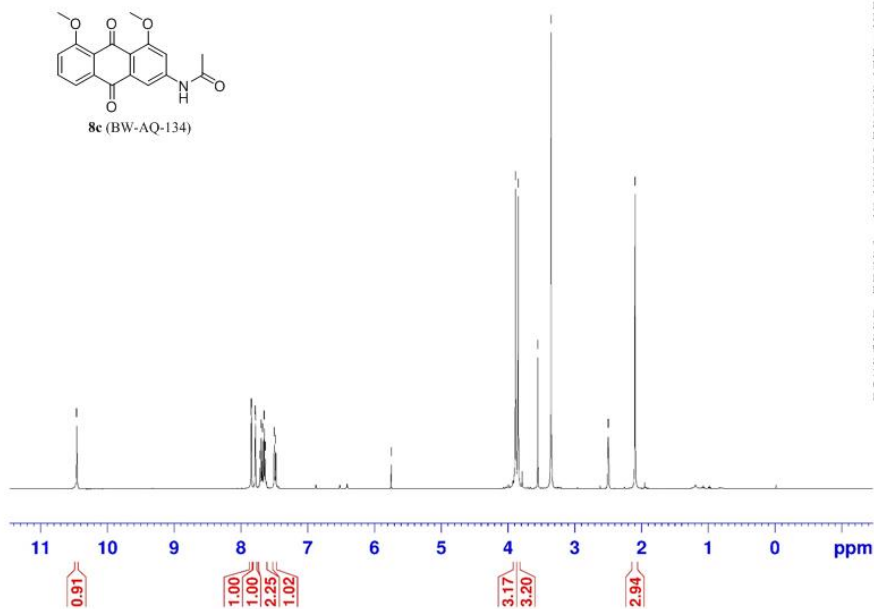
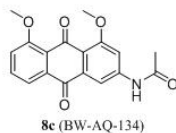
===== CHANNEL f2 =====
SFO2 400.1416005 MHz
NUC2 1H
CPCPDG[2] waltz16
PCPD2 90.00 usec
PLW2 16.00000000 W
PLW12 0.36267000 W
PLW13 0.29376000 W

F2 - Processing parameters
SI 32768
SF 100.6152830 MHz
WDW EM
SSB 0
LB 1.00 Hz
GB 0
PC 1.40

DCF-VI-17-1H- (10-30-15)

— 10.462
 7.848
 7.844
 7.788
 7.784
 7.717
 7.697
 7.677
 7.653
 7.636
 7.501
 7.482
 — 5.750

3.888
 3.848
 3.555
 3.355
 — 2.499
 — 2.097



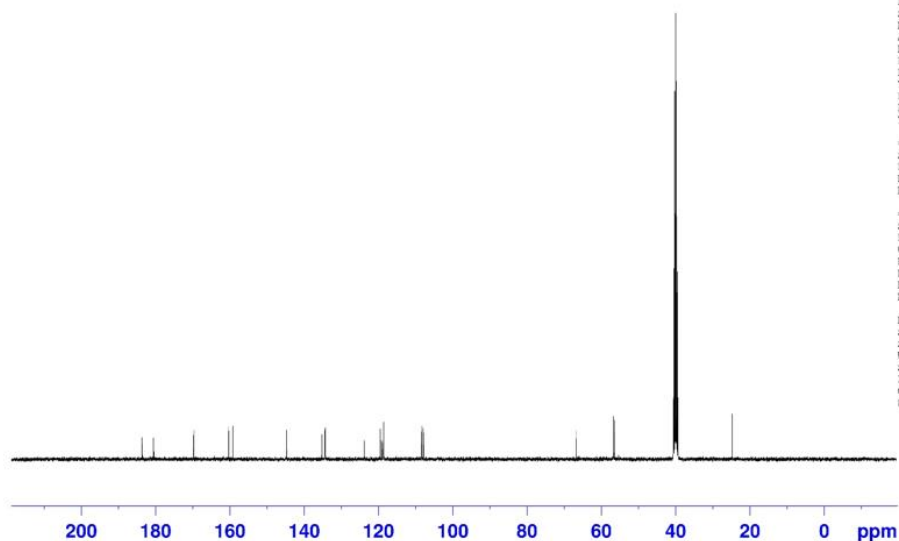
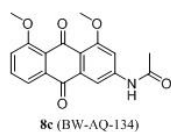
Current Data Parameters
 NAME DCF-VI-17-1H- (10-30-15)
 EXPNO 1
 PROCNO 1

F2 - Acquisition Parameters
 Date_ 20151030
 Time 10.08
 INSTRUM spect
 PROBHD 5 mm PABBO BB-
 PULPROG zg30
 TD 65536
 SOLVENT DMSO
 NS 16
 DS 2
 SWH 8012.820 Hz
 FIDRES 0.122266 Hz
 AQ 4.0894465 sec
 RG 101
 DW 62.400 usec
 DE 6.50 usec
 TE 296.0 K
 D1 1.00000000 sec
 TDO 1

===== CHANNEL f1 =====
 SFO1 400.1424710 MHz
 NUC1 1H
 P1 13.55 usec
 PLW1 16.00000000 W

F2 - Processing parameters
 SI 65536
 SF 400.1400033 MHz
 WDW EM
 SSB 0
 LB 0.30 Hz
 GB 0
 PC 1.00

DCF-VI-17-13C- (10-30-15)



Current Data Parameters
 NAME DCF-VI-17-13C- (10-30-15)
 EXPNO 1
 PROCNO 1

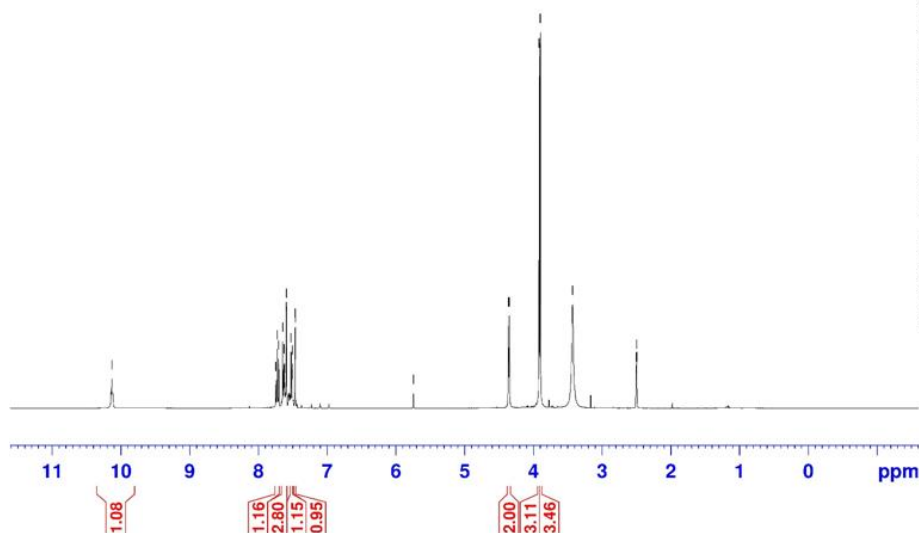
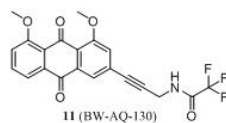
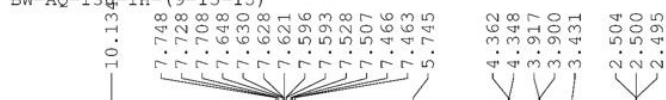
F2 - Acquisition Parameters
 Date_ 20151030
 Time 10.12
 INSTRUM spect
 PROBHD 5 mm PABBO BB-
 PULPROG zgpg30
 TD 65536
 SOLVENT DMSO
 NS 314
 DS 4
 SWH 24038.461 Hz
 FIDRES 0.368798 Hz
 AQ 1.3631488 sec
 RG 203
 DW 20.800 usec
 DE 6.50 usec
 TE 296.0 K
 D1 2.00000000 sec
 D11 0.03000000 sec
 TD0 1

===== CHANNEL f1 =====
 SFO1 100.6253441 MHz
 NUC1 13C
 P1 9.00 usec
 PLW1 62.00000000 W

===== CHANNEL f2 =====
 SFO2 400.1416006 MHz
 NUC2 1H
 CPDPRG2 waltz16
 PCPD2 90.00 usec
 PLW2 16.00000000 W
 PLW12 0.36267000 W
 PLW13 0.29376000 W

F2 - Processing parameters
 SI 32768
 SF 100.6152830 MHz
 WDW EM
 SSF 0
 LB 1.00 Hz
 GB 0
 PC 1.40

BW-AQ-130-1H-(9-15-15)



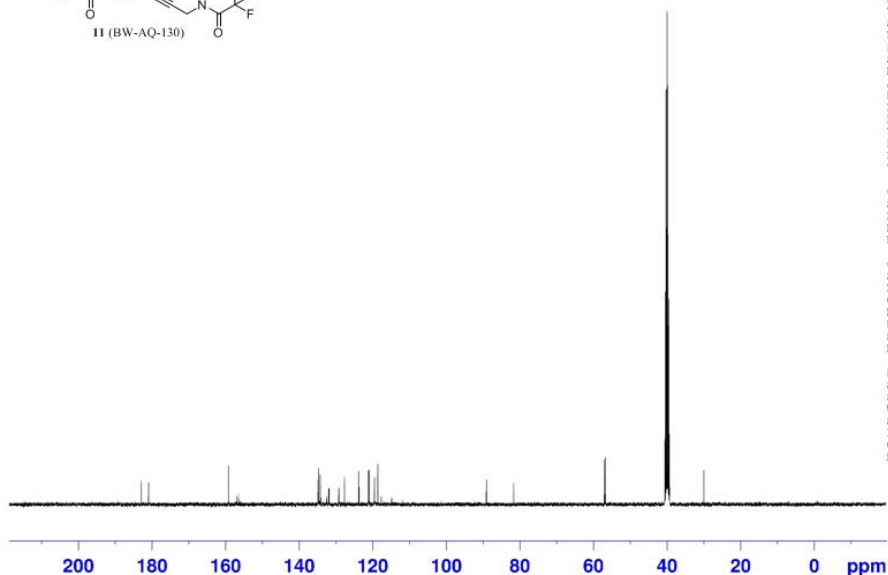
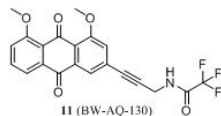
Current Data Parameters
NAME BW-AQ-130-1H-(9-15-15)
EXPNO 1
PROCNO 1

F2 - Acquisition Parameters
Date_ 20150915
Time 13.06
INSTRUM spect
PROBHD 5 mm PABBO BB-
PULPROG zg30
TD 65536
SOLVENT DMSO
NS 16
DS 2
SWH 8012.820 Hz
FIDRES 0.122266 Hz
AQ 4.0894465 sec
RG 101
DW 62.400 usec
DE 6.50 usec
TE 298.0 K
D1 1.00000000 sec
TD0 1

===== CHANNEL f1 =====
SF01 400.1424710 MHz
NUC1 1H
P1 13.55 usec
PLW1 16.00000000 W

F2 - Processing parameters
SI 65536
SF 400.1400029 MHz
WDW EM
SSB 0
LB 0.30 Hz
GB 0
PC 1.00

BW-AQ-130-13C- (9-15-15)



Current Data Parameters
 NAME BW-AQ-130-13C- (9-15-15)
 EXPNO 1
 PROCNO 1

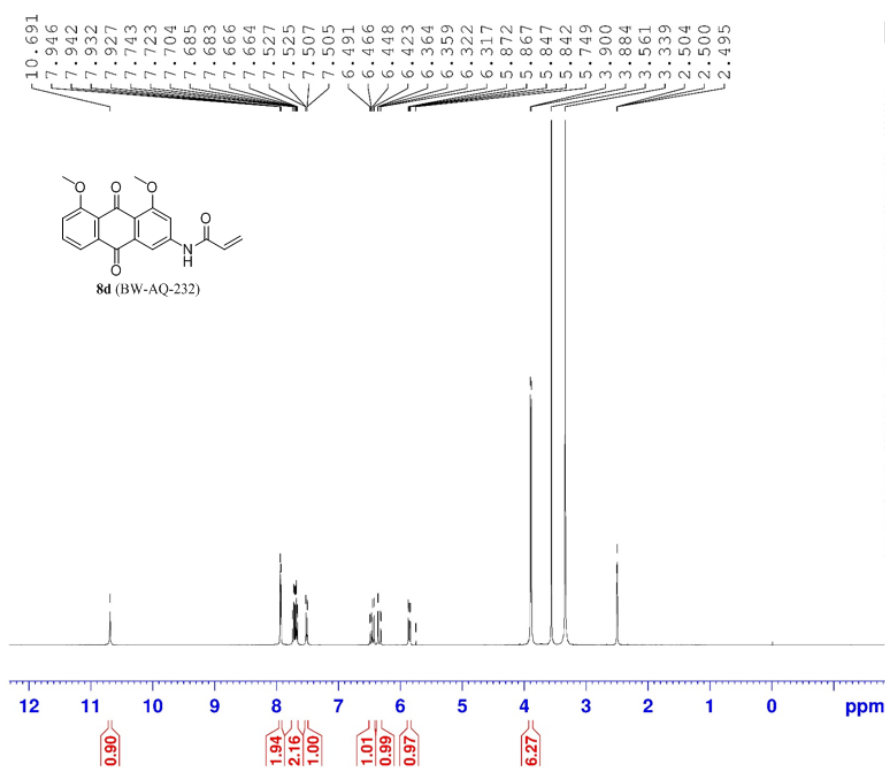
F2 - Acquisition Parameters
 Date 20150915
 Time 13.09
 INSTRUM spect
 PROBHD 5 mm PABBO BB
 PULPROG zgpg30
 TD 65536
 SOLVENT DMSO
 NS 362
 DS 4
 SWH 24038.461 Hz
 FIDRES 0.366798 Hz
 AQ 1.3631488 sec
 RG 203
 DW 20.800 usec
 DE 6.50 usec
 TR 298.2 K
 D1 2.00000000 sec
 D11 0.03000000 sec
 TDO 1

===== CHANNEL f1 =====
 SFO1 100.6253441 MHz
 NUC1 13C
 P1 9.00 usec
 PLW1 62.00000000 W

===== CHANNEL f2 =====
 SFO2 400.1416006 MHz
 NUC2 1H
 CPDPRG2 waltz16
 PCPD2 90.00 usec
 PLW2 16.00000000 W
 PLW12 0.36267000 W
 PLW13 0.29376000 W

F2 - Processing parameters
 SI 32768
 SF 100.6152830 MHz
 WDW FM
 SSB 0
 LB 1.00 Hz
 GB 0
 PC 1.40

ABD-V-127-1H- (11-20-15)



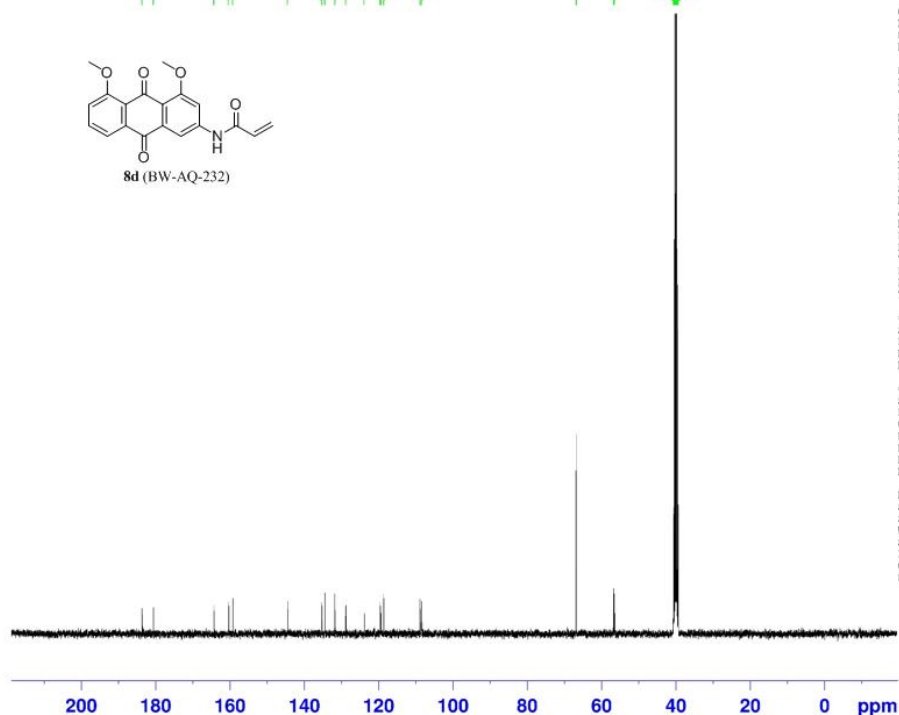
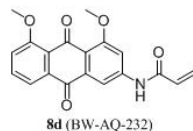
Current Data Parameters
 NAME ABD-V-127-1H- (11-20-15)
 EXPNO 1
 PROCNO 1

F2 - Acquisition Parameters
 Date 20151120
 Time 17.08
 INSTRUM spect
 PROBHD 5 mm PABBO BB-
 PULPROG zg30
 TD 65536
 SOLVENT DMSO
 NS 16
 DS 2
 SWH 8012.820 Hz
 FIDRES 0.122266 Hz
 AQ 4.0894463 sec
 RG 128
 DW 62.400 usec
 DE 6.50 usec
 TE 298.0 K
 D1 1.00000000 sec
 TDO 1

===== CHANNEL f1 =====
 SFO1 400.1424710 MHz
 NUC1 1H
 P1 13.55 usec
 PLW1 16.00000000 W

F2 - Processing parameters
 SI 65536
 SF 400.1400028 MHz
 WDW EM
 SSB 0
 LB 0.30 Hz
 GB 0
 PC 1.00

ABD-V-127-13C- (11-20-15)



Current Data Parameters
 NAME ABD-V-127-13C- (11-20-15)
 EXPNO 1
 PROCNO 1

F2 - Acquisition Parameters
 Date_ 20151120
 Time 17.11
 INSTRUM spect
 PROBHD 5 mm PABBO BB-
 PULPROG zgpg30
 TD 65536
 SOLVENT DMSO
 NS 308
 DS 4
 SWH 24038.461 Hz
 FIDRES 0.366796 Hz
 AQ 1.3631488 sec
 RG 203
 CW 20.800 usec
 DE 5.50 usec
 TE 298.2 K
 D1 2.0000000 sec
 D11 0.0300000 sec
 TD0 1

===== CHANNEL f1 =====
 SFO1 100.6253441 MHz
 NUC1 13C
 P1 9.00 usec
 PLW1 62.0000000 W

===== CHANNEL f2 =====
 SFO2 400.1416006 MHz
 NUC2 1H
 CPDPRG2 waltz16
 PCPD2 90.00 usec
 PLW2 16.0000000 W
 PLW12 0.36267000 W
 PLW13 0.29376000 W

F2 - Processing parameters
 SI 32768
 SF 100.6152830 MHz
 WDW EM
 SSB 0
 LB 1.00 Hz
 GB 0
 PC 1.40

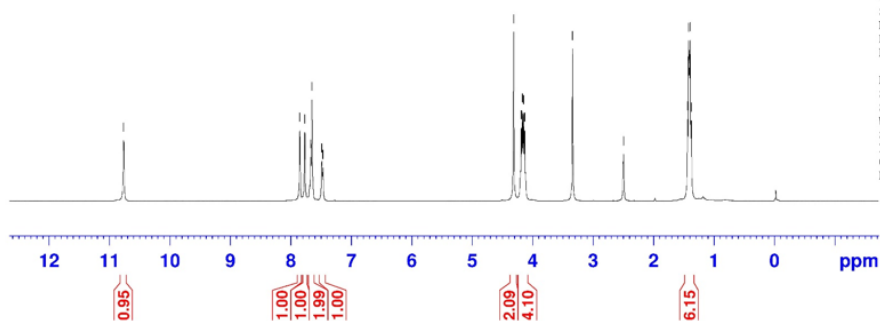
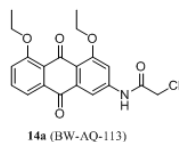
ABD-V-95-1H(6-3-15)

— 10.768

7.854
7.770
7.673
7.654
7.489
7.472

4.314
4.189
4.171
4.152
4.134
3.343

2.498
1.438
1.421
1.411
1.405
1.395
1.377



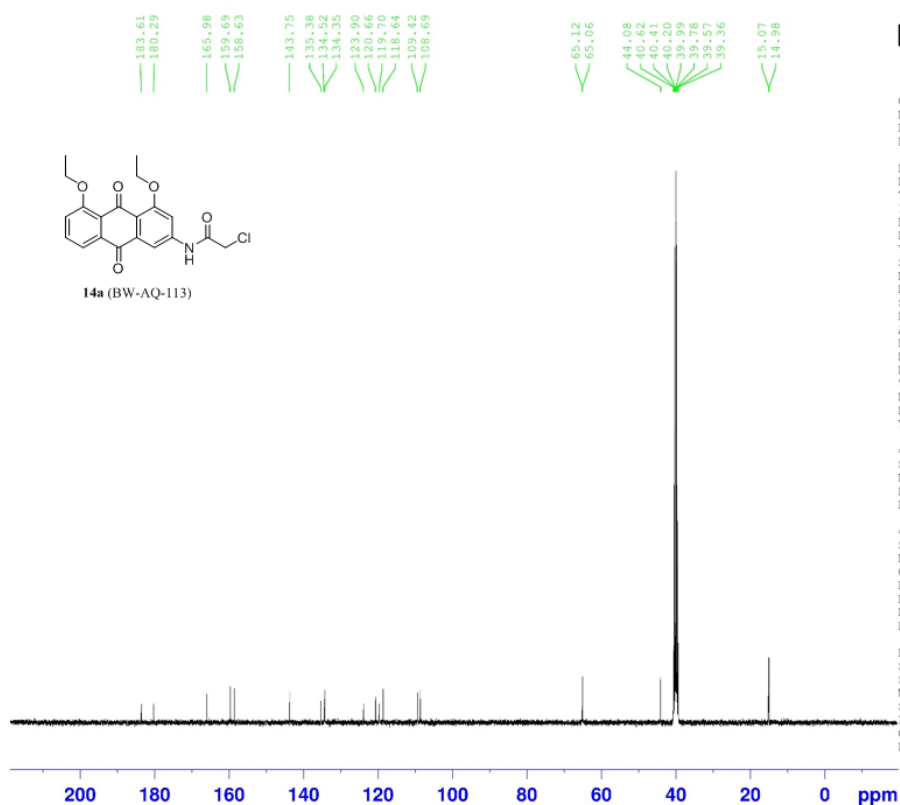
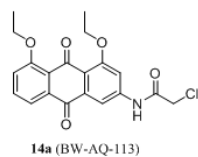
Current Data Parameters
NAME ABD-V-95-1H(6-3-15)
EXPNO 1
PROCNO 1

F2 - Acquisition Parameters
Date_ 20150603
Time 10.51
INSTRUM spect
PROBHD 5 mm FAPBO BB-
PULPROG zg30
TD 65536
SOLVENT DMSO
NS 16
DS 2
SWH 8012.820 Hz
FIDRES 0.122266 Hz
AQ 4.0894465 sec
RG 90.5
DW 62.400 usec
DE 6.50 usec
TE 297.5 K
D1 1.00000000 sec
TD0 1

===== CHANNEL f1 =====
SFO1 400.1424710 MHz
NUC1 1H
P1 13.55 usec
PLW1 16.00000000 W

F2 - Processing parameters
SI 65536
SF 400.1400033 MHz
WDW EM
SSB 0
LB 0.30 Hz
GB 0
FC 1.00

ABD-V-95-13C (6-3-15)



Current Data Parameters
 NAME ABD-V-95-13C (6-3-15)
 EXPNO 1
 PROCNO 1

F2 - Acquisition Parameters
 Date_ 20150603
 Time 10.56
 INSTRUM spect
 PROBHD 5 mm PABBO BB-
 PULPROG zgpg30
 TD 65536
 SOLVENT DMSO
 NS 306
 DS 4
 SWH 24038.461 Hz
 FIDRES 0.366798 Hz
 AQ 1.3631488 sec
 RG 203
 DW 20.800 usec
 DE 6.50 usec
 TE 298.0 K
 D1 2.00000000 sec
 D11 0.03000000 sec
 TD0 1

===== CHANNEL f1 =====
 SFO1 100.6253441 MHz
 NUC1 13C
 P1 9.00 usec
 PLW1 62.00000000 W

===== CHANNEL f2 =====
 SFO2 400.1416006 MHz
 NUC2 1H
 CPDPRG12 waltz16
 PCPD2 90.00 usec
 PLW2 16.00000000 W
 PLW12 0.36267000 W
 PLW13 0.29376000 W

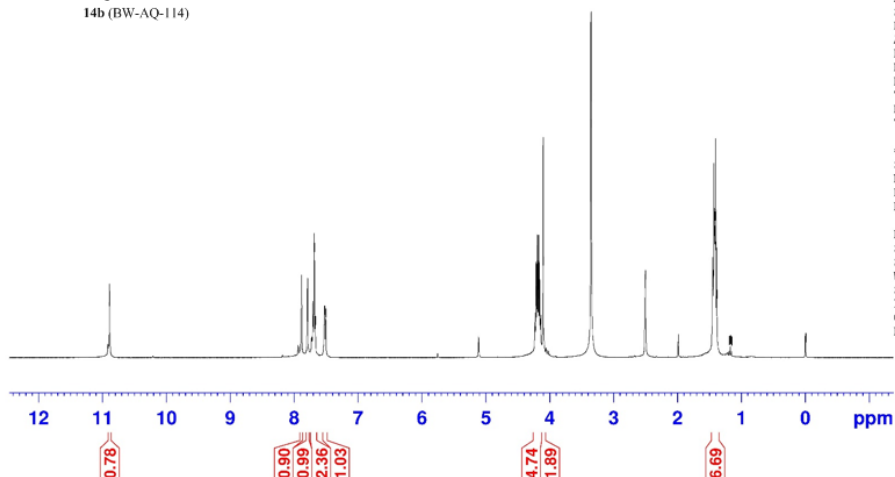
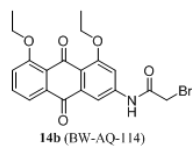
F2 - Processing parameters
 SI 32768
 SF 100.6152830 MHz
 WDW EM
 SSB 0
 LB 1.00 Hz
 GB 0
 PC 1.40

ABD-V-99 (1H) final

— 10.889

7.883
7.787
7.705
7.685
7.666
7.522
7.505

4.226
4.208
4.191
4.173
4.156
4.139
4.098
3.351
2.500
1.984
1.444
1.427
1.418
1.410
1.401
1.383
1.188
1.170
1.152
-0.007



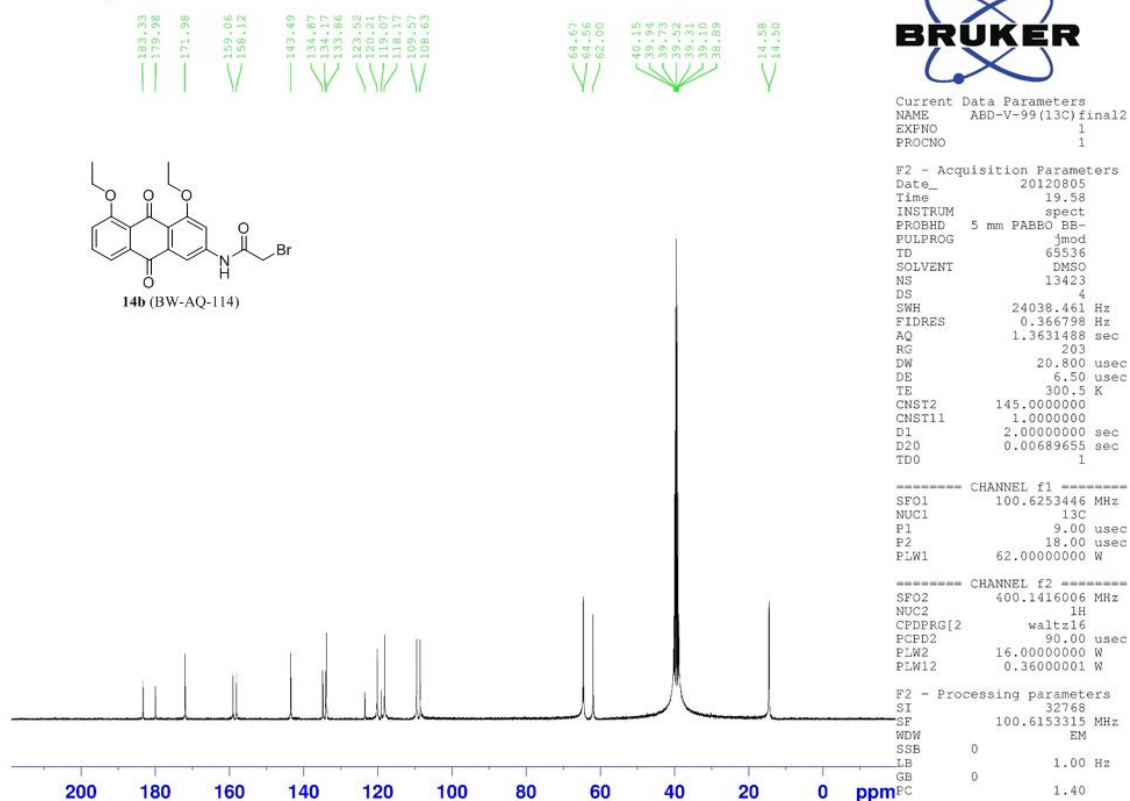
Current Data Parameters
NAME ABD-V-99 (1H) final
EXPNO 1
PROCNO 1

F2 - Acquisition Parameters
Date_ 20120802
Time 23.54
INSTRUM spect
PROBHD 5 mm PABBO BB-
PULPROG zg30
TD 65536
SOLVENT DMSO
NS 31
DS 2
SWH 8012.820 Hz
FIDRES 0.122266 Hz
AQ 4.0894465 sec
RG 161
DW 62.400 usec
DE 6.50 usec
TE 299.2 K
D1 1.00000000 sec
TD0 1

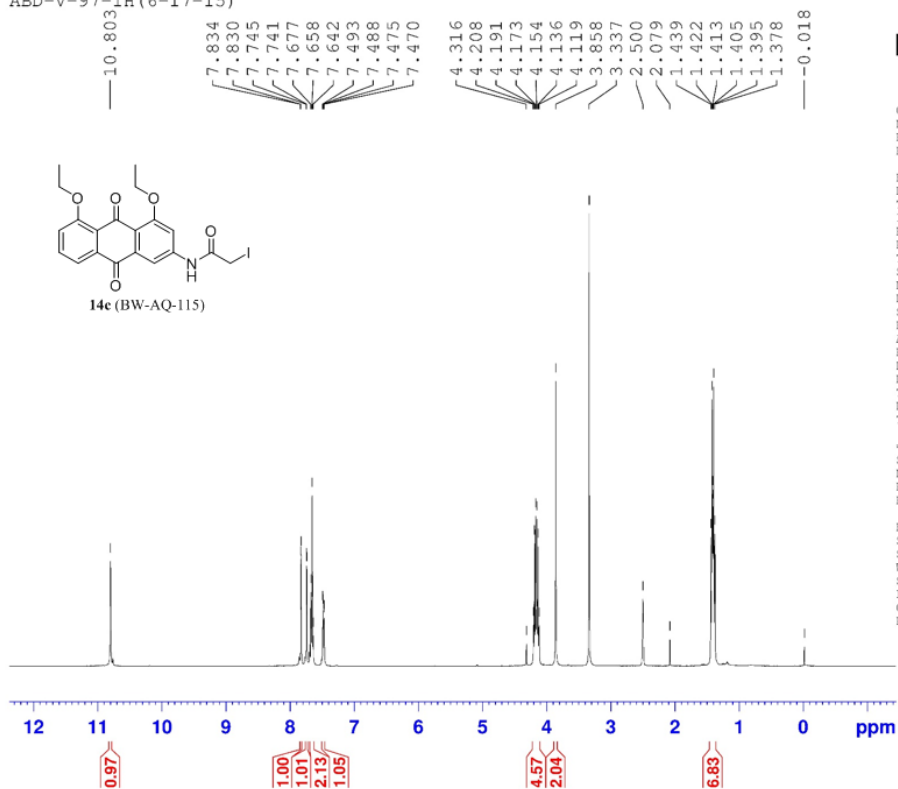
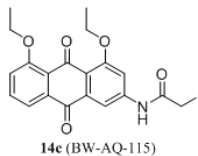
===== CHANNEL f1 =====
SFO1 400.1424710 MHz
NUC1 1H
P1 13.50 usec
PLW1 16.00000000 W

F2 - Processing parameters
SI 65536
SF 400.1399991 MHz
WDW EM
SSB 0
LB 0.30 Hz
GB 0
PC 1.00

ABD-V-99 (13C) final2



ABD-V-97-1H (6-17-15)



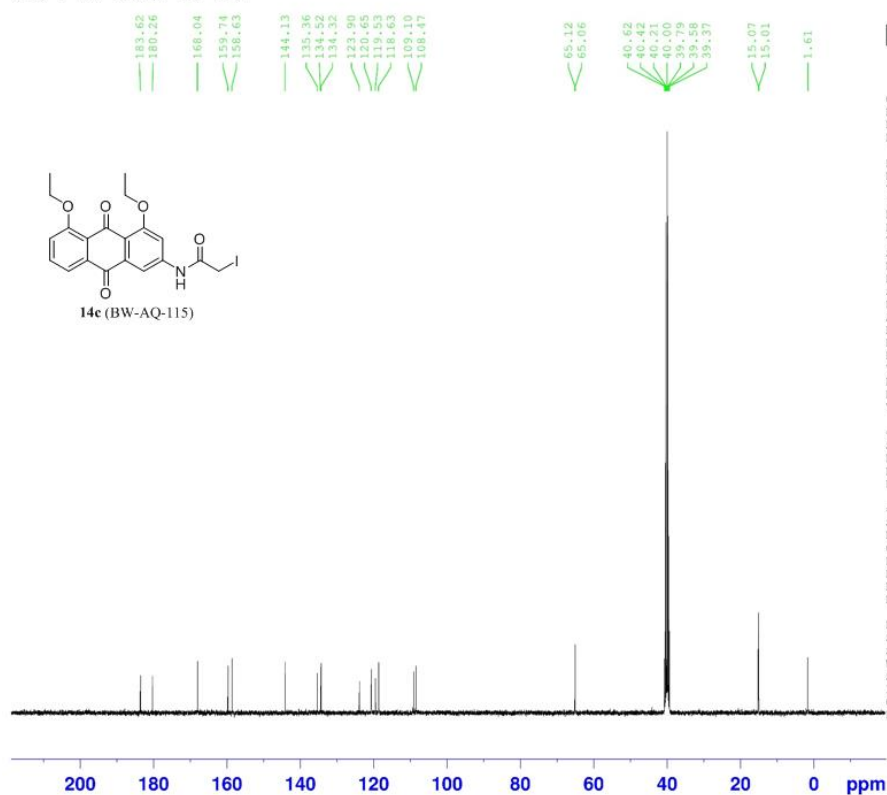
Current Data Parameters
 NAME ABD-V-97-1H(6-17-15)
 EXPNO 1
 PROCNO 1

F2 - Acquisition Parameters
 Date_ 20150617
 Time 11.35
 INSTRUM spect
 PROBHD 5 mm PABBO BB-
 PULPROG zg30
 TD 65536
 SOLVENT DMSO
 NS 16
 DS 2
 SWH 8012.820 Hz
 FIDRES 0.122266 Hz
 AQ 4.0894465 sec
 RG 101
 DW 62.400 usec
 DE 6.50 usec
 TE 298.0 K
 D1 1.00000000 sec
 TD0 1

===== CHANNEL f1 =====
 SFO1 400.1424710 MHz
 NUC1 1H
 P1 13.55 usec
 PLW1 16.00000000 W

F2 - Processing parameters
 SI 65536
 SF 400.1400030 MHz
 WDW EM
 SSB 0
 LB 0.30 Hz
 GB 0
 PC 1.00

ABD-V-97-13C (6-17-15)



Current Data Parameters
 NAME ABD-V-97-13C(6-17-15)
 EXPNO 1
 PROCNO 1

F2 - Acquisition Parameters
 Date_ 20150617
 Time 11:39
 INSTRUM spect
 PROBHD 5 mm FABBO BB-
 PULPROG zgpg30
 TD 65536
 SOLVENT DMSO
 NS 342
 DS 4
 SWH 24038.461 Hz
 FIDRES 0.366798 Hz
 AQ 1.3631488 sec
 RG 203
 DW 20.800 usec
 DE 6.50 usec
 TE 298.4 K
 D1 2.00000000 sec
 D11 0.03000000 sec
 TD0 1

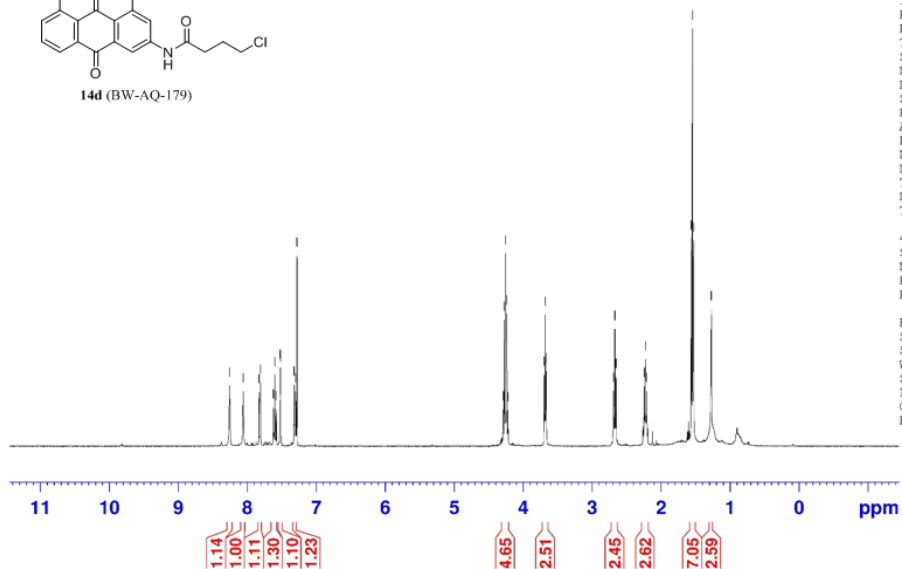
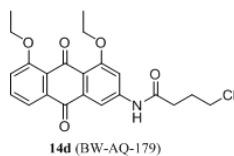
===== CHANNEL f1 =====
 SFO1 100.6253441 MHz
 NUC1 13C
 P1 9.00 usec
 PLW1 62.00000000 W

===== CHANNEL f2 =====
 SFO2 400.1416006 MHz
 NUC2 1H
 CPDPRG2 waltz16
 PCPD2 90.00 usec
 PLW2 16.00000000 W
 PLW12 0.36267000 W
 PLW13 0.29376000 W

F2 - Processing parameters
 SI 32768
 SF 100.6152830 MHz
 WDW EM
 SSB 0
 LB 1.00 Hz
 GB 0
 PC 1.40

ABD-VII-145 (1H) 2

8.258
8.061
7.828
7.809
7.623
7.603
7.583
7.522
7.518
7.322
7.301
7.281
4.292
4.274
4.257
4.239
4.222
3.696
3.681
3.666
2.691
2.673
2.655
2.45
2.28
2.212
1.563
1.546
1.529
1.273



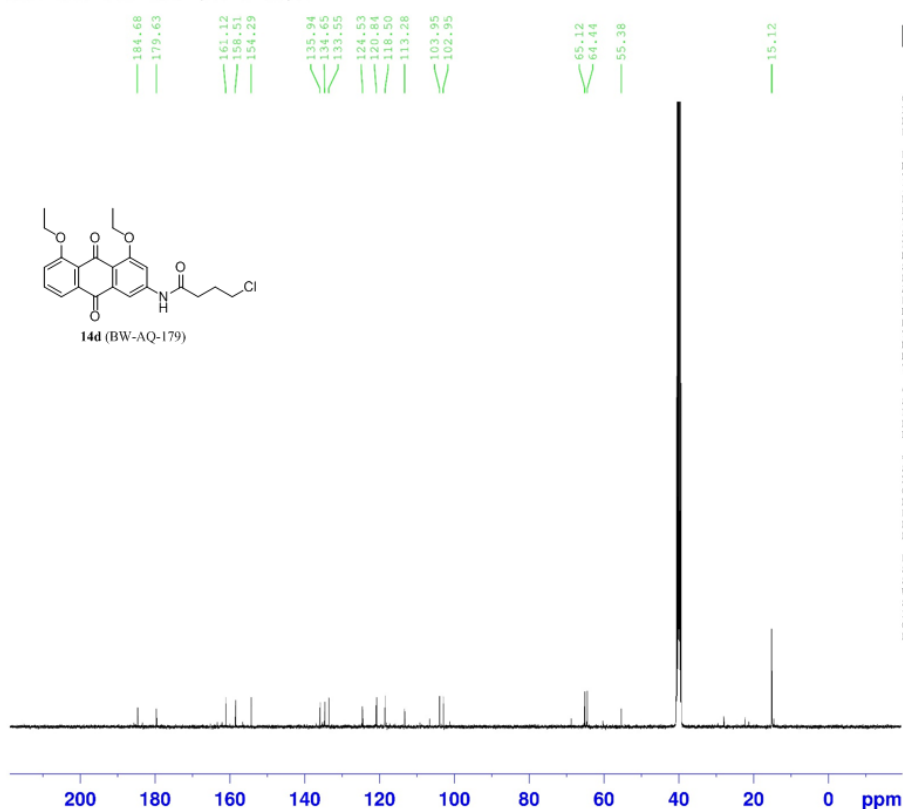
Current Data Parameters
NAME ABD-VII-145(1H)2
EXPNO 1
PROCNO 1

F2 - Acquisition Parameters
Date_ 20130527
Time 14.56
INSTRUM spect
PROBHD 5 mm PABBO BB-
PULPROG zg30
TD 65536
SOLVENT CDCl3
NS 16
DS 2
SWH 8012.820 Hz
FIDRES 0.122266 Hz
AQ 4.0894465 sec
RG 181
DW 62.400 usec
DE 6.50 usec
TE 298.0 K
D1 1.00000000 sec
TD0 1

===== CHANNEL f1 =====
SFO1 400.1424710 MHz
NUC1 1H
P1 13.50 usec
PLW1 16.00000000 W

F2 - Processing parameters
SI 65536
SF 400.1400000 MHz
WDW EM
SSB 0
LB 0.30 Hz
GB 0
PC 1.00

ABD-VII-145-13C- (12-3-15) 2



Current Data Parameters
 NAME ABD-VII-145-13C- (12-3-15) 2
 EXPNO 1
 PROCNO 1

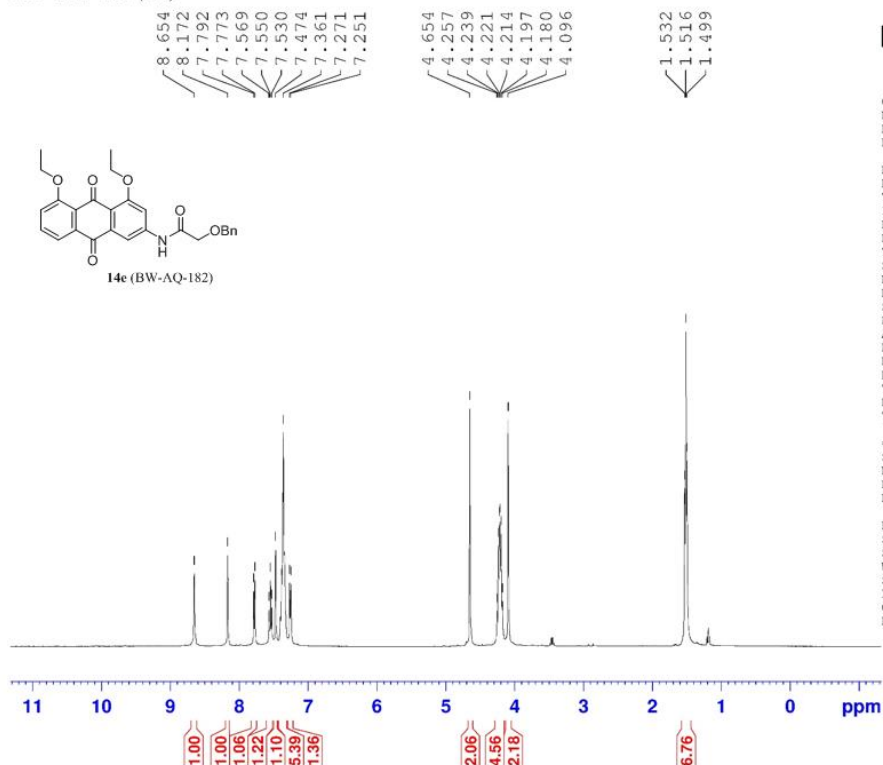
F2 - Acquisition Parameters
 Date_ 20151203
 Time 22.30
 INSTRUM spect
 PROBHD 5 mm PABBO BB-
 PULPROG zgpg30
 TD 65536
 SOLVENT DMSO
 NS 8798
 DS 4
 SWH 24038.461 Hz
 FIDRES 0.366798 Hz
 AQ 1.3631488 sec
 KC 203
 DW 20.800 usec
 DE 6.50 usec
 TE 298.0 K
 D1 2.00000000 sec
 D11 0.03000000 sec
 TDC 1

===== CHANNEL f1 =====
 SFO1 100.6253441 MHz
 NUC1 13C
 P1 9.00 usec
 PLW1 62.00000000 W

===== CHANNEL f2 =====
 SFO2 400.1416006 MHz
 NUC2 1H
 CPDPRG2 waltz16
 FCF2 50.00 usec
 PLW2 16.00000000 W
 PLW12 0.36267000 W
 PLW13 0.29376000 W

F2 - Processing parameters
 SI 32768
 SF 100.6152830 MHz
 WDW EM
 SSB 0
 LB 1.00 Hz
 GB 0
 PC 1.40

ABD-VII-147 (1H)



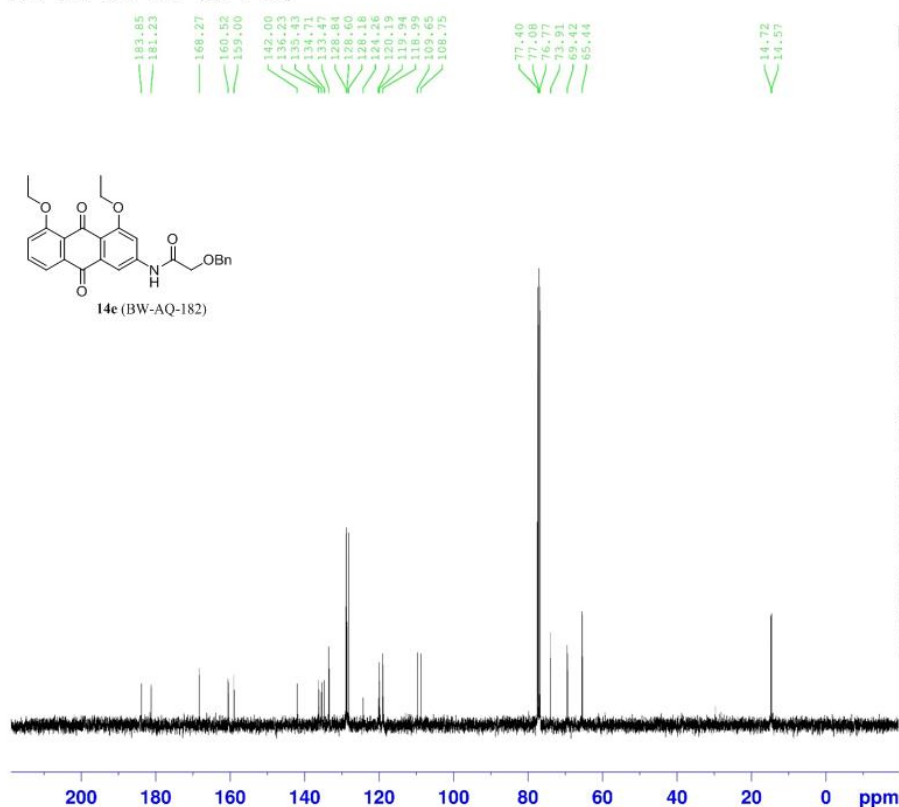
Current Data Parameters
 NAME ABD-VII-147(1H)
 EXPNO 1
 PROCNO 1

F2 - Acquisition Parameters
 Date_ 20130509
 Time 10.09
 INSTRUM spect
 PROBHD 5 mm PABBO BB-
 FULPROG zg30
 TD 6536
 SOLVENT CDCl3
 NS 16
 DS 2
 SWH 8012.820 Hz
 FIDRES 0.122266 Hz
 AQ 4.0894465 sec
 RG 64
 DW 62.400 usec
 DE 6.50 usec
 TE 298.0 K
 D1 1.00000000 sec
 TD0 1

===== CHANNEL f1 =====
 SFO1 400.1424710 MHz
 NUC1 1H
 P1 13.50 usec
 PLW1 16.00000000 W

F2 - Processing parameters
 SI 6536
 SF 400.1400000 MHz
 WDW EM
 SSB 0
 LB 0.30 Hz
 GB 0
 PC 1.00

ABD-VII-147-13C-(12-2-15)



Current Data Parameters
 NAME ABD-VII-147-13C-(12-2-15)
 EXPNO 1
 PROCNO 1

F2 - Acquisition Parameters
 Date_ 20151202
 Time 12.08
 INSTRUM spect
 PROBHD 5 mm PABBO BB-
 PULPROG zgpg30
 TD 65536
 SOLVENT CDCl3
 NS 81
 DS 4
 SWH 24039.451 Hz
 FIDRES 0.366798 Hz
 AQ 1.3631488 sec
 RG 203
 DW 20.800 usec
 DE 6.50 usec
 TE 298.0 K
 D1 2.00000000 sec
 D11 0.03000000 sec
 TD0 1

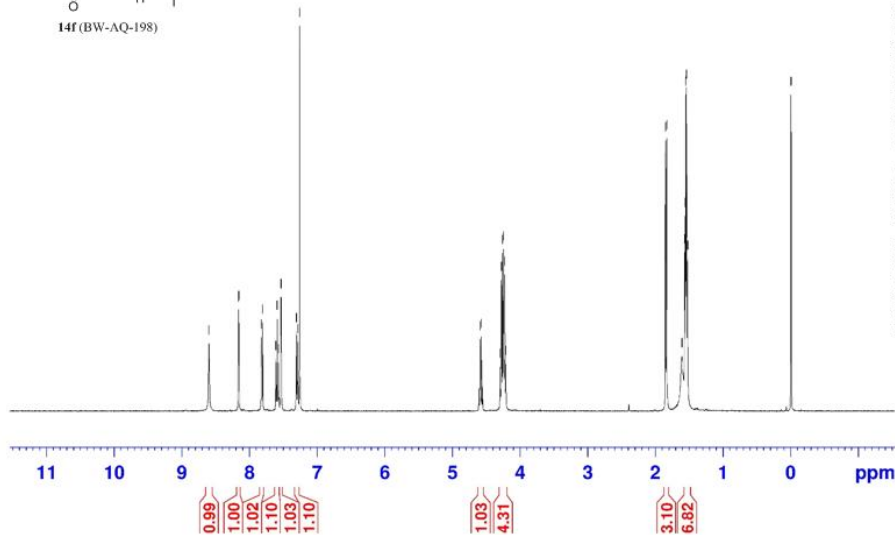
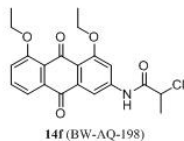
===== CHANNEL f1 =====
 SFO1 100.6253441 MHz
 NUC1 13C
 P1 9.00 usec
 PLW1 62.0000000 W

===== CHANNEL f2 =====
 SFO2 400.1416006 MHz
 NUC2 1H
 CPDPRG12 waltz16
 FCFD2 90.00 usec
 PLW2 16.0000000 W
 PLW12 0.36267000 W
 PLW13 0.29376000 W

F2 - Processing parameters
 SI 32768
 SF 100.6152830 MHz
 NDM EM
 SSB 0
 LB 1.00 Hz
 GB 0
 EC 1.40

ABD-XII-51-1H (8-27-15)

8.601
8.163
8.159
7.827
7.808
7.611
7.591
7.572
7.537
7.533
7.307
7.287
7.259
4.591
4.574
4.295
4.277
4.260
4.245
4.228
4.211
1.850
1.832
1.609
1.569
1.558
1.552
1.541
1.535
1.524
-0.005



Current Data Parameters
NAME ABD-XII-51-1H(8-27-15)
EXPNO 1
PROCNO 1

F2 - Acquisition Parameters
Date_ 20150827
Time_ 9.44
INSTRUM spect
PROBHD 5 mm PABBO BB-
PULPROG zg30
TD 65536
SOLVENT CDCl3
NS 16
DS 2
SWH 8012.820 Hz
FIDRES 0.122266 Hz
AQ 4.0894465 sec
RG 203
DW 62.400 usec
DE 6.50 usec
TE 296.3 K
D1 1.00000000 sec
TDO 1

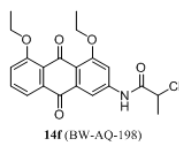
===== CHANNEL f1 =====
SFO1 400.1424710 MHz
NUC1 1H
P1 13.55 usec
PLW1 16.00000000 W

F2 - Processing parameters
SI 65536
SF 400.1400099 MHz
WDW EM
SSB 0
LB 0.30 Hz
GB 0
PC 1.00

ABD-XII-51-13C-(11-30-15)

183.62
180.32
168.62
159.70
158.64
143.81
135.38
134.37
134.27
129.02
128.66
128.46
119.75
118.65
109.54
108.85

65.12
65.08
55.15
40.61
40.40
39.98
39.77
39.56
39.35
21.27
15.06
14.39



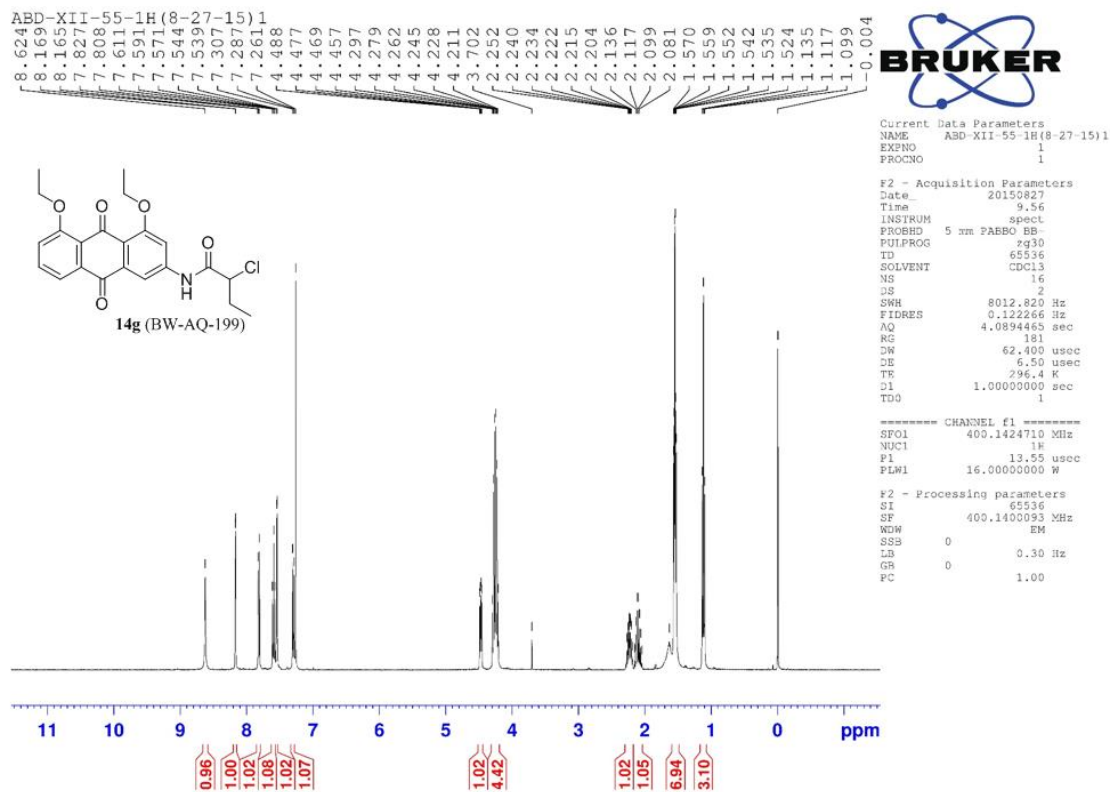
Current Data Parameters
NAME ABD-XII-51-13C-(11-30-15)
EXPNO 1
PROCNO 1

F2 - Acquisition Parameters
Date_ 20151130
Time 12.05
INSTRUM spect
PROBHD 5 mm PABBO BB-
PULPROG zgpg30
TD 65536
SOLVENT DMSO
NS 163
DS 4
SWH 24038.461 Hz
FIDRES 0.366798 Hz
AQ 1.3631488 sec
RG 90.5
DM 20.800 usec
DE 6.50 usec
TE 298.1 K
D1 2.00000000 sec
D11 0.03000000 sec
TD0 1

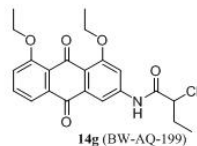
===== CHANNEL f1 =====
SFO1 100.6253441 MHz
NUC1 13C
P1 9.00 usec
PLW1 62.00000000 W

===== CHANNEL f2 =====
SFO2 400.1416006 MHz
NUC2 1H
CPDPRG12 waltz16
PCPD2 90.00 usec
PLW2 16.00000000 W
PLW12 0.36267000 W
PLW13 0.29376000 W

F2 - Processing parameters
SI 32768
SF 100.6152830 MHz
WDW EM
SSB 0
LB 1.00 Hz
GB 0
PC 1.40



ABD-XII-55-13C- (11-30-15)



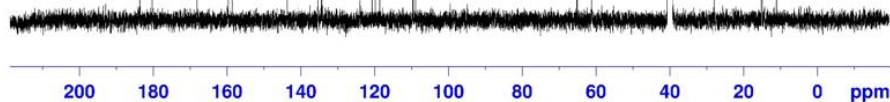
Current Data Parameters
 NAME ABD-XII-55-13C- (11-30-15)
 EXPNO 1
 PROCNO 1

F2 - Acquisition Parameters
 Date_ 20151130
 Time 17.18
 INSTRUM spect
 PROBHD 5 mm PABBO BB-
 PULPROG zgpg30
 TD 65536
 SOLVENT DMSO
 NS 300
 DS 4
 SWH 24038.461 Hz
 FIDRES 0.366798 Hz
 AQ 1.3631688 sec
 RG 90.5
 DW 20.800 usec
 DE 6.50 usec
 TE 298.0 K
 D1 2.00000000 sec
 D11 0.03000000 sec
 TDO 1

===== CHANNEL f1 =====
 SFO1 100.6253441 MHz
 NUC1 13C
 P1 9.00 usec
 PLW1 62.00000000 W

===== CHANNEL f2 =====
 SFO2 400.1416006 MHz
 NUC2 1H
 CPDPRG2 WALTZ16
 PCPD2 90.00 usec
 PLW2 16.00000000 W
 PLW12 0.36267000 W
 PLW13 0.29376000 W

F2 - Processing parameters
 SI 32768
 SF 100.6152830 MHz
 WDW EM
 SSB 0
 LB 1.00 Hz
 GB 0
 PC 1.40



ABD-VI-145-(1H)-2

8.345
8.160
7.850
7.831
7.634
7.613
7.594
7.552
7.329
7.309
7.281

4.296
4.272
4.254
4.223

— 1.580

— 0.020

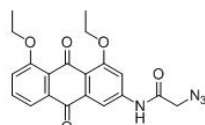


Current Data Parameters
NAME ABD-VI-145-(1H)-2
EXPNO 1
PROCNO 1

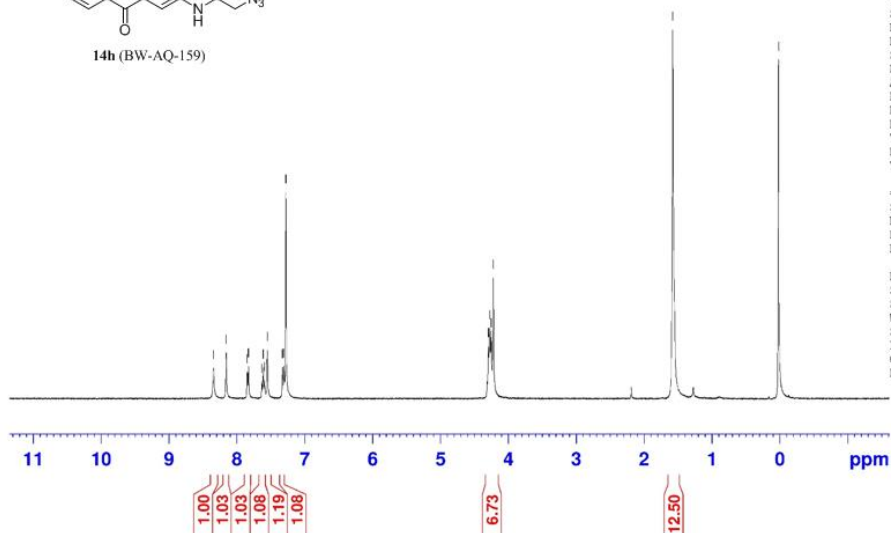
F2 - Acquisition Parameters
Date_ 20121202
Time 14.39
INSTRUM spect
PROBHD 5 mm PABBO BB-
PULPROG zg30
TD 65536
SOLVENT CDCl3
NS 16
DS 2
SWH 8012.820 Hz
FIDRES 0.122266 Hz
AQ 4.0894465 sec
RG 203
DW 62.400 usec
DE 6.50 usec
TE 298.0 K
D1 1.00000000 sec
TD0 1

===== CHANNEL f1 =====
SFO1 400.1424710 MHz
NUC1 1H
P1 13.50 usec
PLW1 16.00000000 W

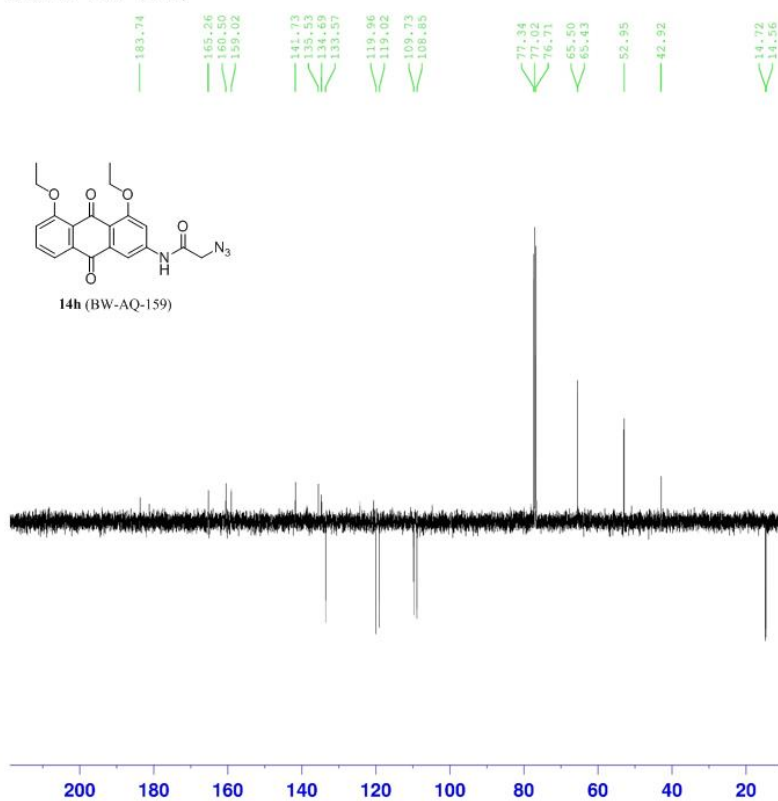
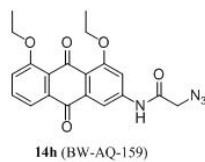
F2 - Processing parameters
SI 65536
SF 400.1400000 MHz
WDW EM
SSB 0
LB 0.30 Hz
GB 0
PC 1.00



14h (BW-AQ-159)



ABD-VI-145-(13C)



Current Data Parameters
 NAME ABD-VI-145-(13C)
 EXPNO 1
 PROCNO 1

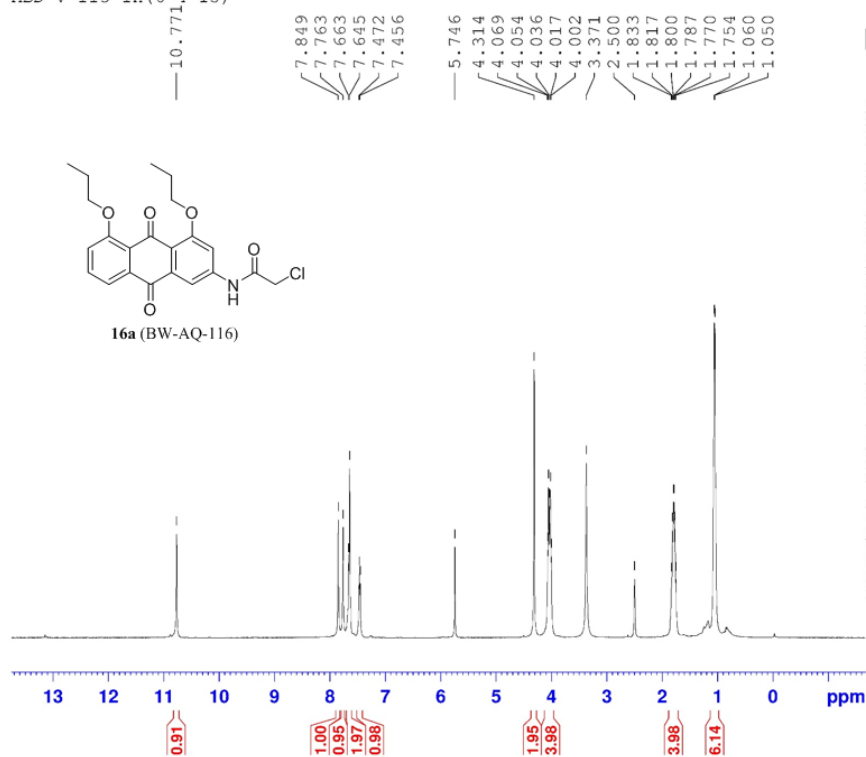
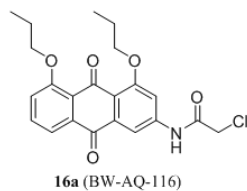
F2 - Acquisition Parameters
 Date_ 20121129
 Time 10.13
 INSTRUM spect
 PROBHD 5 mm PABBO BB-
 PULPROG jmod
 TD 65536
 SOLVENT CDCl3
 NS 234
 DS 4
 SWH 24038.461 Hz
 FIDRES 0.366798 Hz
 AQ 1.3631488 sec
 RG 203
 DW 20.800 usec
 DE 6.50 usec
 TE 298.4 K
 CNST2 145.000000
 CNST11 1.0000000
 D1 2.0000000 sec
 D20 0.00689655 sec
 TD0 1

===== CHANNEL f1 =====
 SFO1 100.6253446 MHz
 NUC1 13C
 P1 9.00 usec
 P2 18.00 usec
 PLW1 62.00000000 W

===== CHANNEL f2 =====
 SFO2 400.1416006 MHz
 NUC2 1H
 CPDPRG2 waltz16
 PCPD2 90.00 usec
 PLW2 16.00000000 W
 PLW12 0.36000001 W

F2 - Processing parameters
 SI 32768
 SF 100.6152830 MHz
 WDW EM
 SSB 0
 LB 1.00 Hz
 GB 0
 PC 1.40

ABD-V-113-1H (6-4-15)



Current Data Parameters
 NAME ABD-V-113-1H(6-4-15)
 EXPNO 1
 PROCNO 1

F2 - Acquisition Parameters
 Date_ 20150604
 Time 12.38
 INSTRUM spect
 PROBHD 5 mm PABBO BB-
 PULPROG zg30
 TD 65536
 SOLVENT DMSO
 NS 16
 DS 2
 SWH 8012.820 Hz
 FIDRES 0.122266 Hz
 AQ 4.0894465 sec
 RG 64
 DW 62.400 usec
 DE 6.50 usec
 TE 296.0 K
 D1 1.00000000 sec
 TD0 1

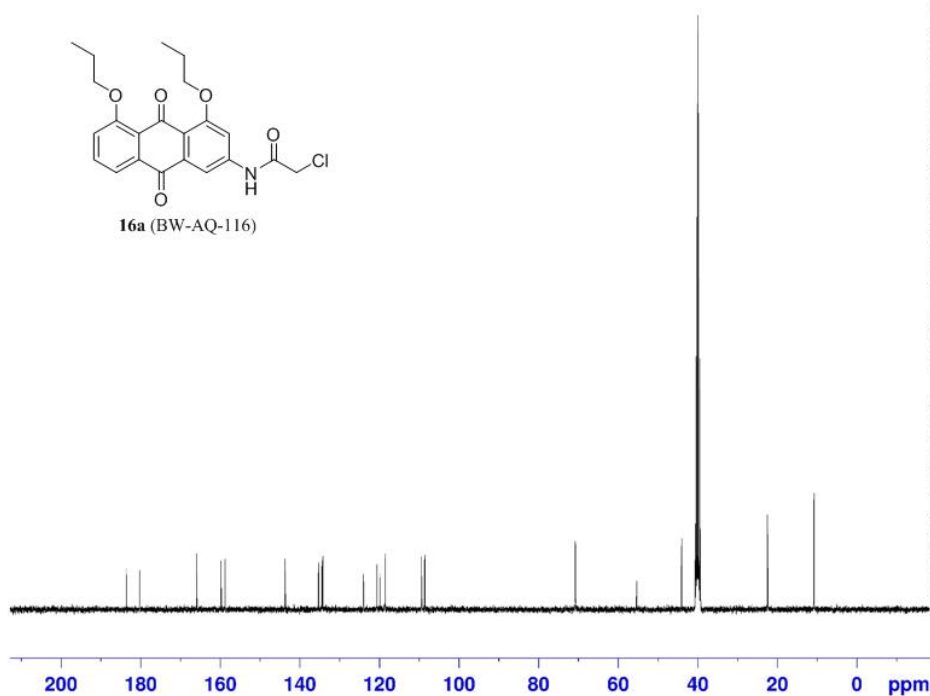
===== CHANNEL f1 =====
 SFO1 400.1424710 MHz
 NUC1 1H
 P1 13.55 usec
 PLW1 16.00000000 W

F2 - Processing parameters
 SI 65536
 SF 400.1400029 MHz
 WDW EM
 SSB 0
 LB 0.30 Hz
 GB 0
 PC 1.00

ABD-V-113-13C (6-4-15)



16a (BW-AQ-116)



Current Data Parameters
 NAME ABD-V-113-13C (6-4-15)
 EXPNO 1
 PROCNO 1

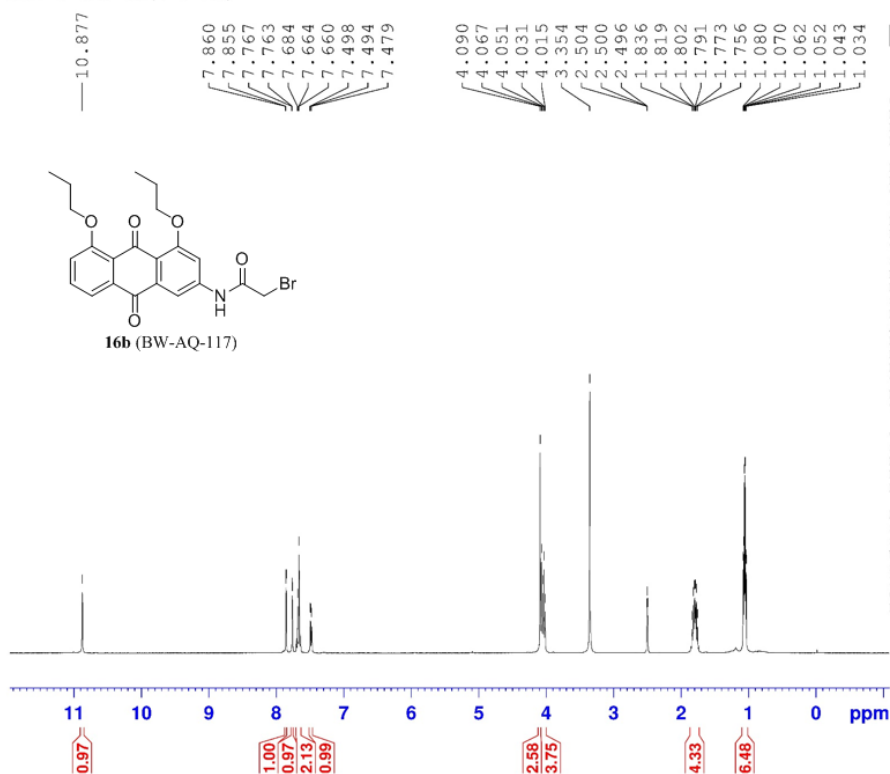
F2 - Acquisition Parameters
 Date_ 20150604
 Time 12.41
 INSTRUM spect
 PROBHD 5 mm FAPBO BB-
 PULPROG zgpg30
 TD 65536
 SOLVENT DMSO
 NS 314
 DS 4
 SWH 24038.461 Hz
 FIDRES 0.366798 Hz
 AQ 1.3631488 sec
 RG 203
 DW 20.800 usec
 DE 6.50 usec
 TE 296.5 K
 D1 2.00000000 sec
 D11 0.03000000 sec
 TDO 1

===== CHANNEL f1 =====
 SFO1 100.6253441 MHz
 NUC1 13C
 P1 9.00 usec
 PLW1 62.00000000 W

===== CHANNEL f2 =====
 SFO2 400.1416006 MHz
 NUC2 1H
 CPDPRG2 waltz16
 PCPD2 90.00 usec
 PLW2 16.00000000 W
 PLW12 0.36267000 W
 PLW13 0.29376000 W

F2 - Processing parameters
 SI 32768
 SF 100.6152850 MHz
 WDW EM
 SSB 0
 LB 1.00 Hz
 GB 0
 PC 1.40

ABD-V-115-1H(6-5-15)



Current Data Parameters
 NAME ABD-V-115-1H(6-5-15)
 EXPNO 1
 PROCNO 1

F2 - Acquisition Parameters
 Date_ 20150605
 Time 10.49
 INSTRUM spect
 PROBHD 5 mm PABBO BB-
 PULPROG zg30
 TD 65536
 SOLVENT DMSO
 NS 16
 DS 2
 SWH 8012.820 Hz
 FIDRES 0.122266 Hz
 AQ 4.0894465 sec
 RG 101
 DW 62.400 usec
 DE 6.50 usec
 TE 296.1 K
 D1 1.00000000 sec
 TDO 1

===== CHANNEL f1 =====
 SPOL 400.1424710 MHz
 NUC1 1H
 P1 13.55 usec
 PLW1 16.00000000 W

F2 - Processing parameters
 SI 65536
 SF 400.1400030 MHz
 WDW EM
 SSB 0
 LB 0.30 Hz
 GB 0
 PC 1.00

ABD-V-115-13C (6-5-15)

183.66
180.29166.15
159.85
158.76

143.64

135.38

134.52

134.32

124.05

120.68

118.61

109.33

108.58

70.83
70.77

40.60

40.39

40.18

39.97

39.76

39.55

30.73

22.53

22.45



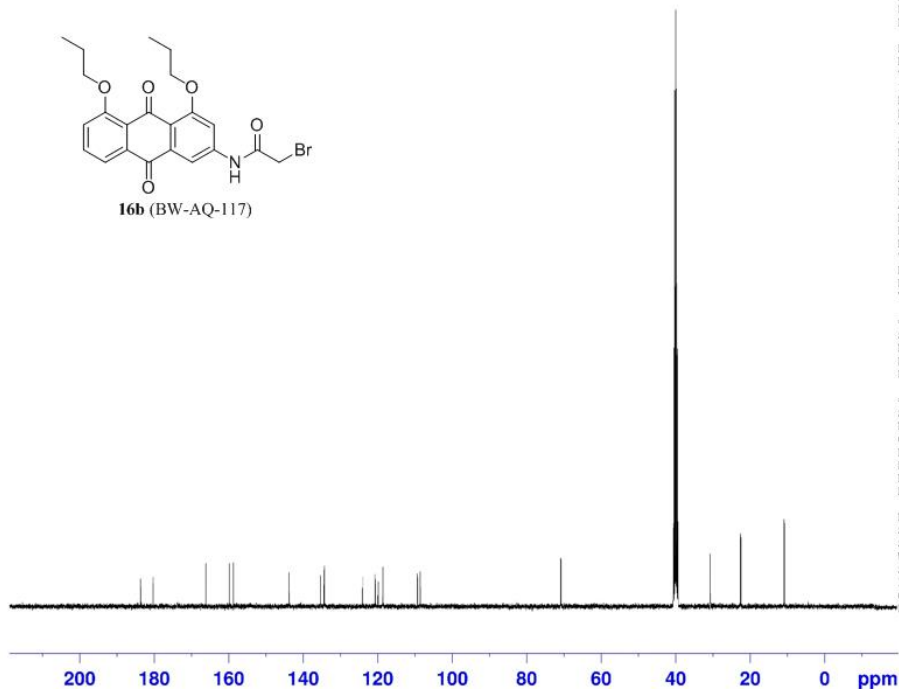
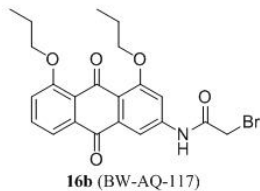
Current Data Parameters
 NAME ABD-V-115-13C(6-5-15)
 EXPNO 1
 PROCNO 1

F2 - Acquisition Parameters
 Date_ 20150605
 Time 10.52
 INSTRUM spect
 PROBHD 5 mm PABBO BB-
 PULPROG zgpg30
 TD 65536
 SOLVENT DMSO
 NS 361
 DS 4
 SWH 24038.461 Hz
 FIDRES 0.366798 Hz
 AQ 1.3631488 sec
 RG 203
 DW 20.800 usec
 DE 6.50 usec
 TE 296.5 K
 D1 2.00000000 sec
 D11 0.03000000 sec
 TD0 1

===== CHANNEL f1 =====
 SFO1 100.6253441 MHz
 NUC1 13C
 P1 9.00 usec
 PLW1 62.00000000 W

===== CHANNEL f2 =====
 SFO2 400.1416006 MHz
 NUC2 1H
 CPDPRG2 waltz16
 PCPD2 90.00 usec
 PLW2 16.00000000 W
 PLW3 0.36267000 W
 PLW13 0.29376000 W

F2 - Processing parameters
 SI 32768
 SF 100.6152830 MHz
 WDW EM
 SSB 0
 LB 1.00 Hz
 GB 0
 PC 1.40



ABD-VI-87-(1H)

8.387
8.148
7.803
7.785
7.606
7.585
7.566
7.504
7.303
7.282
7.283

4.132
4.114
4.096
4.078
3.917

1.957
1.939
1.922
1.904
1.625
1.104

— 0.000

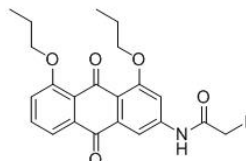


Current Data Parameters
NAME ABD-VI-87-(1H)
EXPNO 1
PROCNO 1

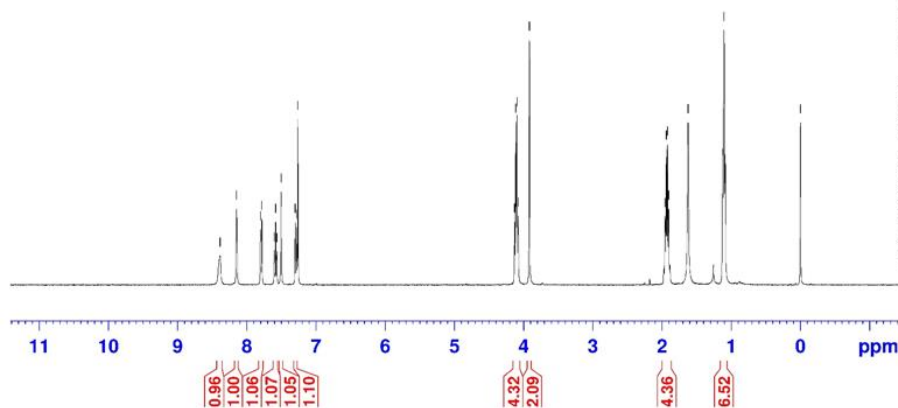
F2 - Acquisition Parameters
Date_ 20120920
Time 11.01
INSTRUM spect
PROBHD 5 mm PABBO BB-
PULPROG zg30
TD 65536
SOLVENT CDCl3
NS 16
DS 2
SWH 8012.820 Hz
FIDRES 0.122266 Hz
AQ 4.0894465 sec
RG 203
DW 62.400 usec
DE 6.50 usec
TE 298.0 K
D1 1.00000000 sec
TD0 1

===== CHANNEL f1 =====
SFO1 400.1424710 MHz
NUC1 1H
P1 13.50 usec
PLW1 16.00000000 W

F2 - Processing parameters
SI 65536
SF 400.1400071 MHz
WDW EM
SSB 0
LB 0.30 Hz
GB 0
PC 1.00



16c (BW-AQ-118)



ABD-VI-87- (13C)

184.27
181.22166.06
160.60
159.15

142.53

135.32

134.67

133.51

124.45

120.54

118.89

109.76

108.70

77.34

77.02

76.71

71.35

71.33

22.51

22.40

10.47

-0.33



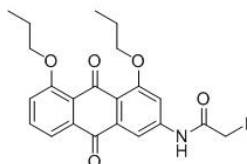
Current Data Parameters
 NAME ABD-VI-87-(13C)
 EXPNO 1
 PROCNO 1

F2 - Acquisition Parameters
 Date_ 20120924
 Time 9.20
 INSTRUM spect
 PROBHD 5 mm PABBO BB-
 PULPROG jmod
 TD 65536
 SOLVENT CDCl3
 NS 452
 DS 4
 SWH 24038.461 Hz
 FIDRES 0.366798 Hz
 AQ 1.3631488 sec
 RG 203
 DW 20.800 usec
 DE 6.50 usec
 TE 298.3 K
 CNST2 145.0000000
 CNST11 1.0000000
 D1 2.00000000 sec
 D20 0.00689655 sec
 TD0 1

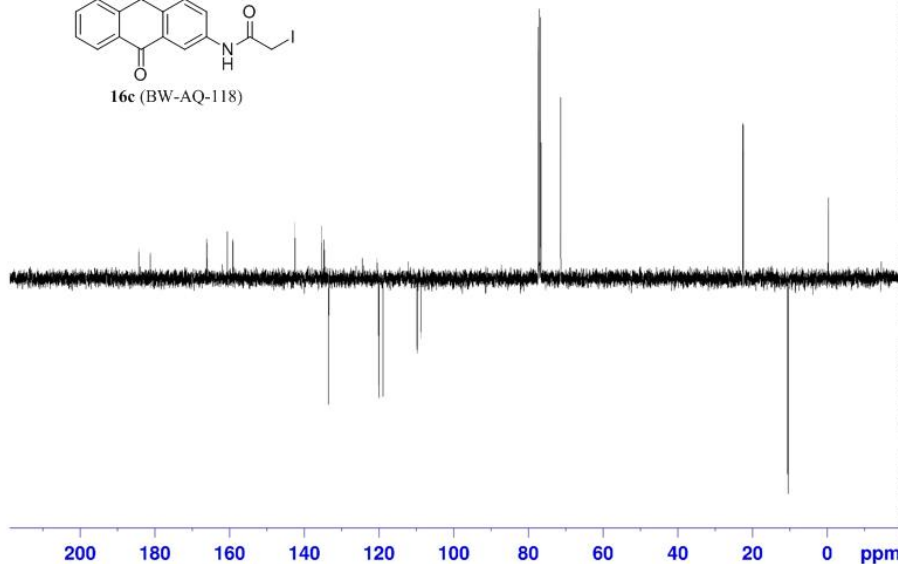
===== CHANNEL f1 =====
 SFO1 100.6253446 MHz
 NUC1 13C
 P1 9.00 usec
 P2 18.00 usec
 PLW1 62.00000000 W

===== CHANNEL f2 =====
 SFO2 400.1416006 MHz
 NUC2 1H
 CPDPRG[2] waltz16
 PCPD2 90.00 usec
 PLW2 16.00000000 W
 PLW12 0.36000001 W

F2 - Processing parameters
 SI 32768
 SF 100.6152830 MHz
 WDW EM
 SSB 0
 LB 1.00 Hz
 GB 0
 PC 1.40

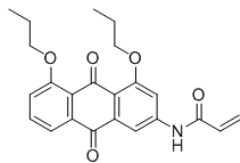


16c (BW-AQ-118)

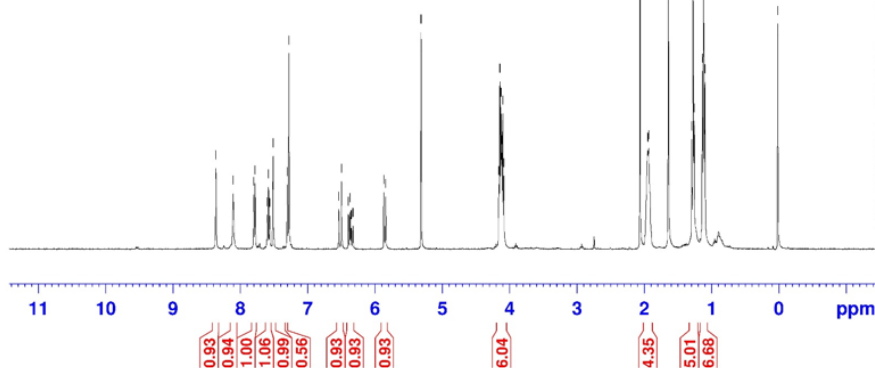


ABD-VII-7-(1H) col

8.367
8.107
7.803
7.784
7.605
7.585
7.565
7.514
7.306
7.280
6.540
6.498
6.397
6.372
6.355
6.330
5.869
5.843
5.317
4.162
4.146
4.130
4.119
4.103
4.087
2.065
1.950
1.942
1.933
1.643
1.295
1.277
1.260
1.137
1.118
1.100
0.017



16d (BW-AQ-160)



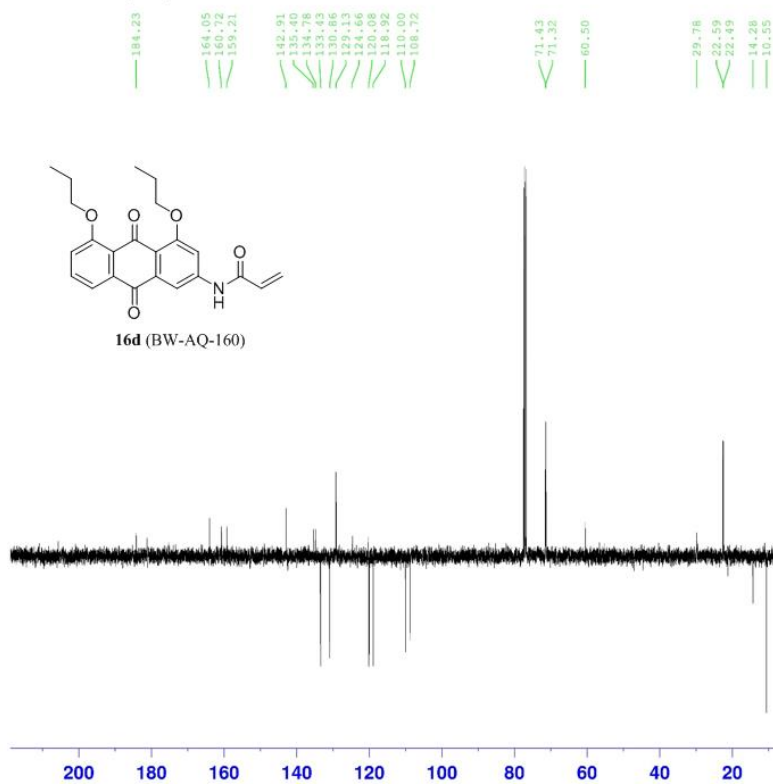
Current Data Parameters
NAME ABD-VII-7-(1H) col
EXPNO 1
PROCNO 1

F2 - Acquisition Parameters
Date_ 20121209
Time 14.20
INSTRUM spect
PROBHD 5 mm PABBO BB-
PULPROG zg30
TD 65536
SOLVENT CDCl3
NS 16
DS 2
SWH 8012.820 Hz
FIDRES 0.122266 Hz
AQ 4.0894465 sec
RG 203
DW 62.400 usec
DE 6.50 usec
TE 297.9 K
D1 1.00000000 sec
TD0 1

===== CHANNEL f1 =====
SFO1 400.1424710 MHz
NUC1 1H
P1 13.50 usec
PLW1 16.00000000 W

F2 - Processing parameters
SI 65536
SF 400.1400006 MHz
WDW EM
SSB 0
LB 0.30 Hz
GB 0
PC 1.00

ABD-VII-7-(13C) col



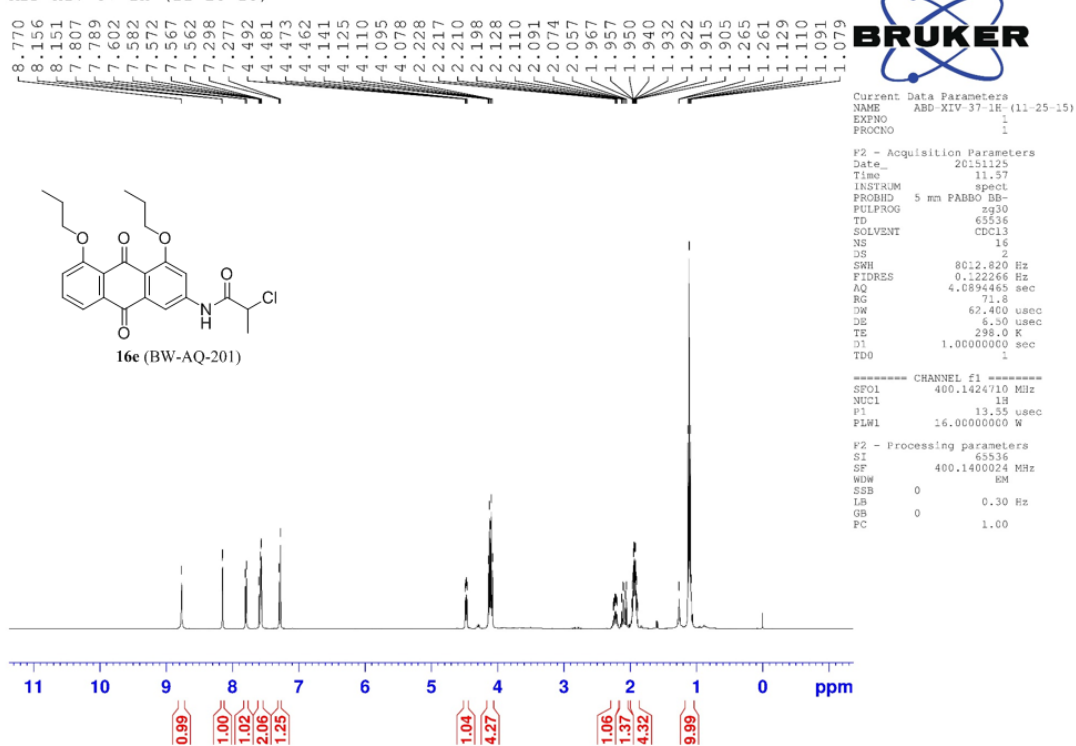
Current Data Parameters
 NAME ABD-VII-7-(13C) col
 EXPNO 1
 PROCNO 1

F2 - Acquisition Parameters
 Date_ 20121209
 Time 14.27
 INSTRUM spect
 PROBHD 5 mm PABBO BB-
 PULPROG jmod
 TD 65536
 SOLVENT CDCl3
 NS 641
 DS 4
 SWH 24038.461 Hz
 FIDRES 0.366798 Hz
 AQ 1.3631488 sec
 RG 203
 DW 20.800 usec
 DE 6.50 usec
 TE 298.5 K
 CNST2 145.0000000
 CNST11 1.0000000
 D1 2.00000000 sec
 D20 0.00689655 sec
 TD0 1

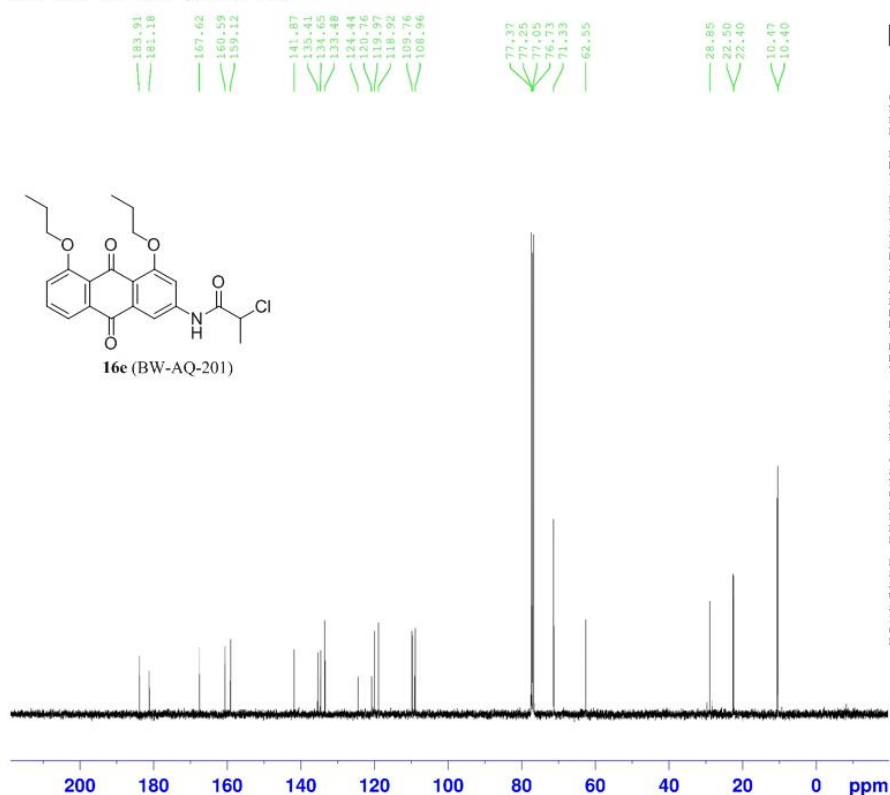
===== CHANNEL f1 =====
 SFO1 100.6253446 MHz
 NUC1 13C
 F1 9.00 usec
 F2 18.00 usec
 PLW1 62.00000000 W
 ===== CHANNEL f2 =====
 SFO2 400.1416006 MHz
 NUC2 1H
 CPDPRG[2] waltz16
 ECPD2 90.00 usec
 PLW2 16.00000000 W
 PLW12 0.36000001 W

F2 - Processing parameters
 SI 32768
 SF 100.6152753 MHz
 WDW EM
 SSB 0
 LB 1.00 Hz
 GB 0
 PC 1.40

ABD-XIV-37-1H- (11-25-15)



ABD-XIV-37-13C- (11-25-15)



Current Data Parameters
 NAME ABD-XIV-37-13C- (11-25-15)
 EXPNO 1
 PROCNO 1

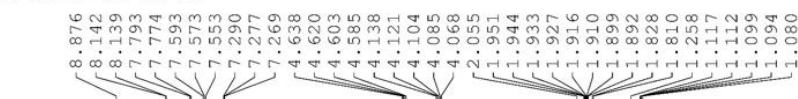
F2 - Acquisition Parameters
 Date_ 20151125
 Time 12.00
 INSTRUM spect
 PROBHD 5 mm F4BBO BB-
 PULPROG zgpg30
 TD 65536
 SOLVENT CDCl3
 NS 187
 DS 4
 SWH 24038.461 Hz
 FIDRES 0.366798 Hz
 AQ 1.3631488 sec
 RG 203
 DW 20.800 usec
 DE 6.50 usec
 TE 298.2 K
 D1 2.0000000 sec
 D11 0.0300000 sec
 TD0 1

===== CHANNEL f1 =====
 SFO1 100.6253441 MHz
 NUC1 13C
 P1 9.00 usec
 PLW1 62.0000000 W

===== CHANNEL f2 =====
 SFO2 400.1416006 MHz
 NUC2 1H
 CPDPRG2 waiz216
 PCPD2 90.00 usec
 PLW2 16.0000000 W
 PLW12 0.36267000 W
 PLW13 0.29376000 W

F2 - Processing parameters
 SI 32768
 SF 100.6152830 MHz
 WDW EM
 SSB 0
 LB 1.00 Hz
 GB 0
 PC 1.40

ABD-XIV-35-1H-(11-24-15)

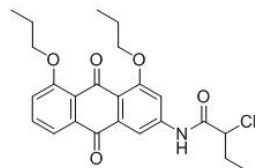


Current Data Parameters
NAME ABD-XIV-35-1H-(11-24-15)
EXNO 1
PROCNO 1

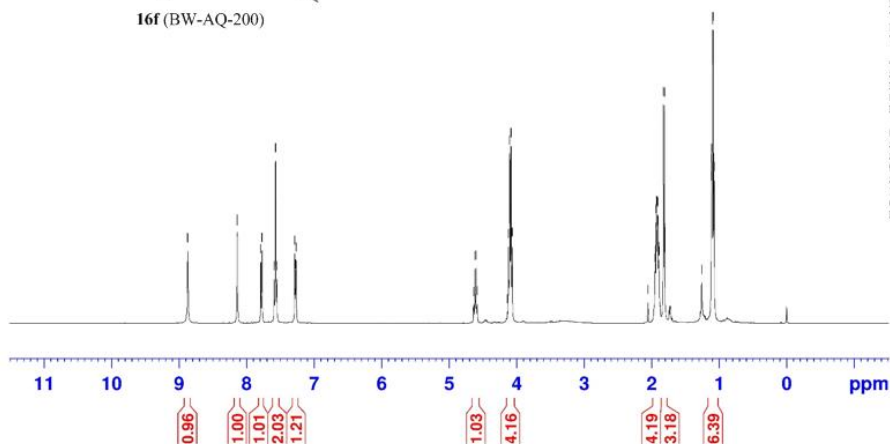
F2 - Acquisition Parameters
Date_ 20151124
Time 11.25
INSTRUM spect
PROBHD 5 mm PABBO BB-
PULPROG zg30
TD 65536
SOLVENT CDCl3
NS 16
DS 2
SWH 8012.820 Hz
FIDRES 0.122266 Hz
AQ 4.0894465 sec
RG 64
DW 62.400 usec
DE 6.50 usec
TE 298.0 K
D1 1.00000000 sec
TD0 1

===== CHANNEL f1 =====
SFO1 400.1424710 MHz
NUC1 1H
P1 13.35 usec
PLW1 16.00000000 W

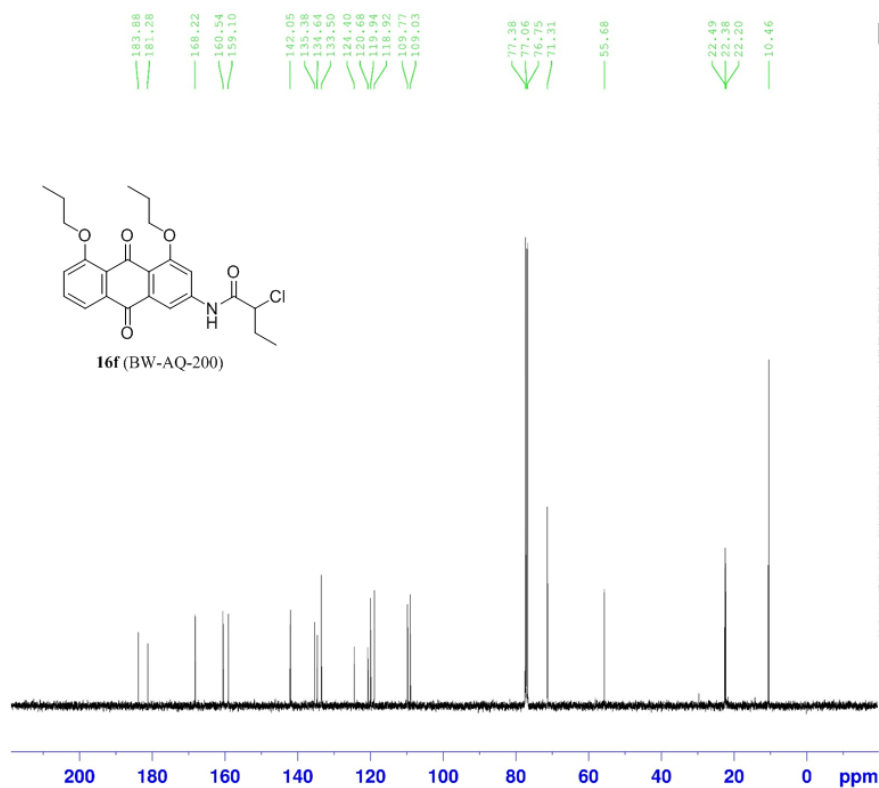
F2 - Processing parameters
SI 65536
SF 400.1400021 MHz
WDW EM
SSB 0
LB 0.30 Hz
GB 0
PC 1.00



16f (BW-AQ-200)



ABD-XIV-35-13C- (11-24-15)



Current Data Parameters
 NAME ABD-XIV-35-13C- (11-24-15)
 EXPNO 1
 PROCNO 1

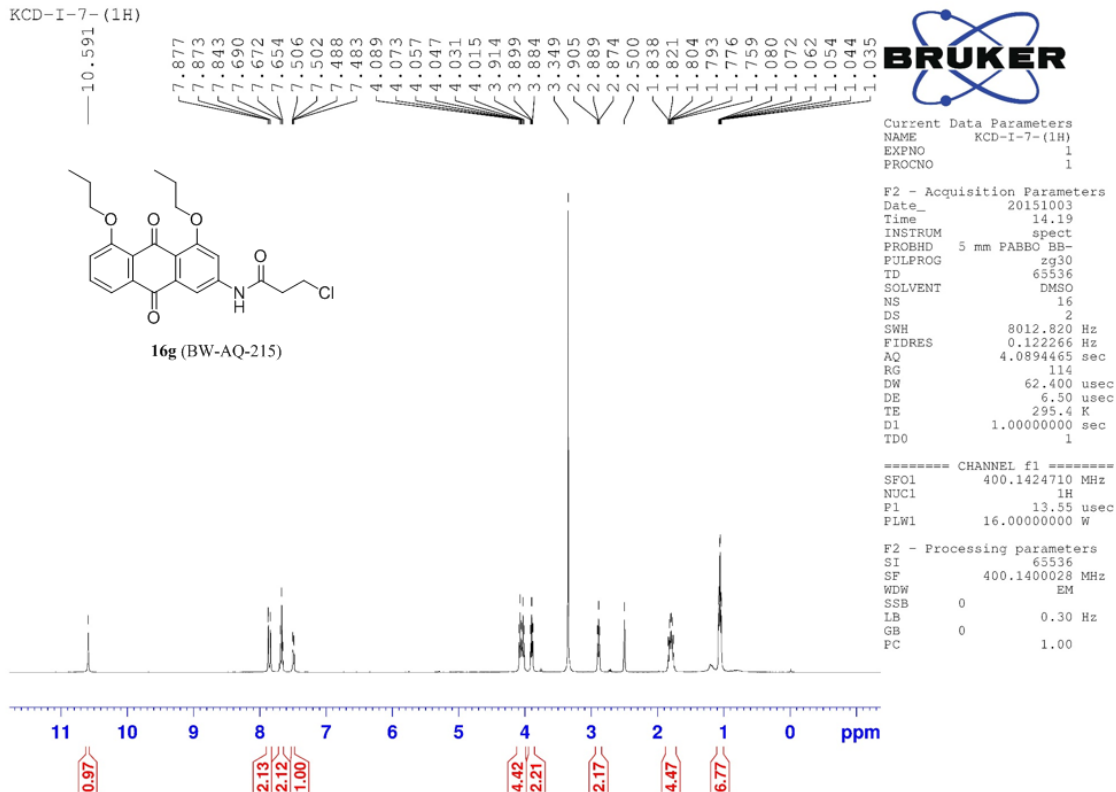
F2 - Acquisition Parameters
 Date_ 20151124
 Time 11.28
 INSTRUM spect
 PROBHD 5 mm PABBO BB-
 PULPROG zgpg30
 TD 65536
 SOLVENT CDCl3
 NS 174
 DS 4
 SWH 24038.461 Hz
 FIDRES 0.366798 Hz
 AQ 1.3631488 sec
 RG 203
 DW 20.860 usec
 DE 6.50 usec
 TE 298.1 K
 D1 2.0000000 sec
 D11 0.0300000 sec
 TD0 1

===== CHANNEL f1 =====
 SFO1 100.6253441 MHz
 NUC1 13C
 P1 9.00 usec
 P1M1 62.0000000 W

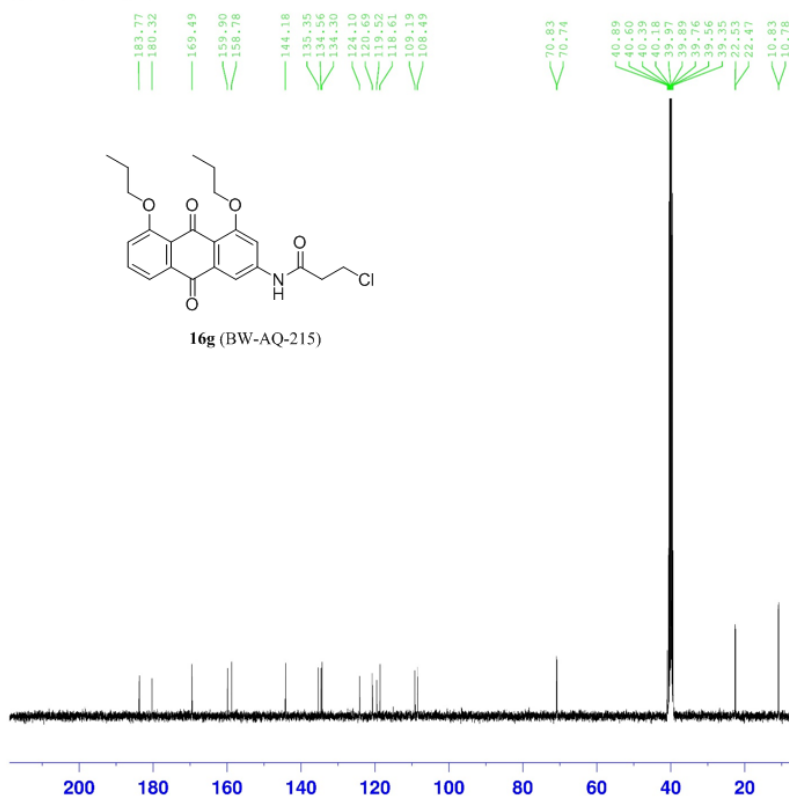
===== CHANNEL f2 =====
 SFO2 400.1416006 MHz
 NUC2 1H
 CPDPRG2 waltz16
 PCPD2 90.00 usec
 P1M2 16.0000000 W
 P1M12 0.36267000 W
 P1M13 0.29376600 W

F2 - Processing parameters
 SI 32768
 SF 100.6152830 MHz
 WDW EM
 SSB 0
 LB 1.00 Hz
 GB 0
 PC 1.40

KCD-I-7- (1H)



KCD-I-7- (13C)



Current Data Parameters
 NAME KCD-I-7- (13C)
 EXPNO 1
 PROCNO 1

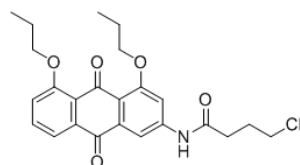
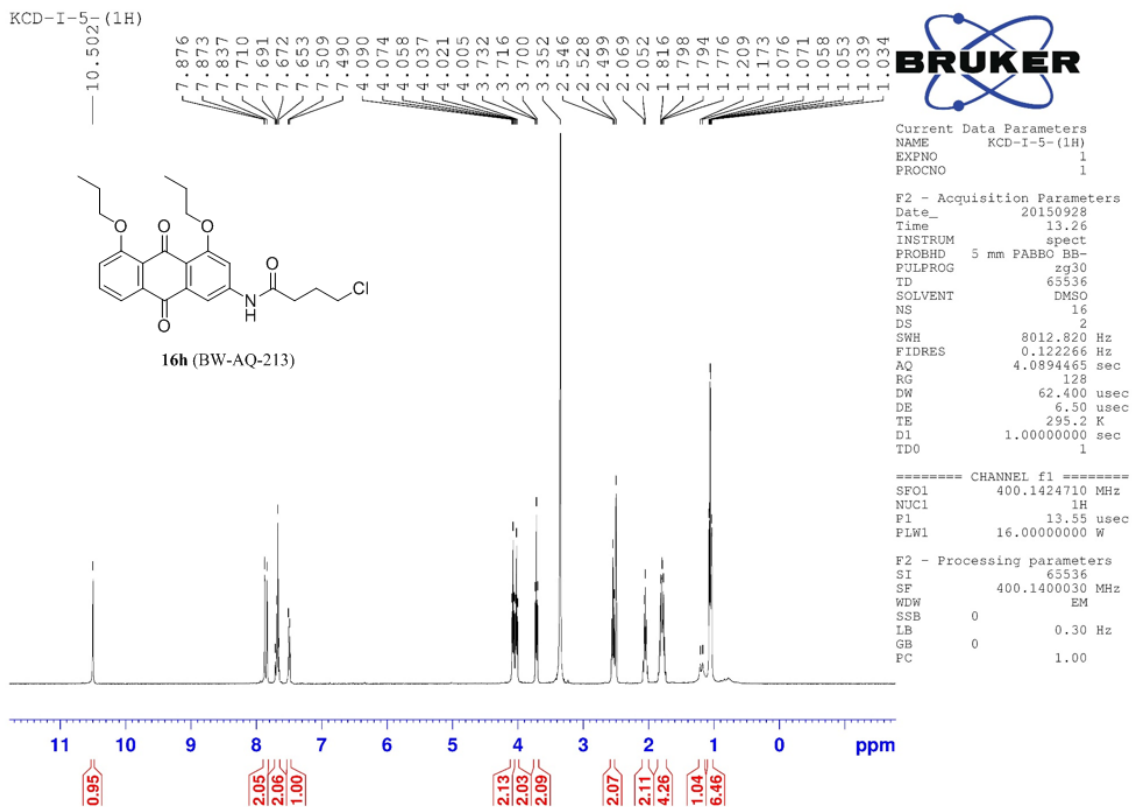
F2 - Acquisition Parameters
 Date_ 20151003
 Time 14.27
 INSTRUM spect
 PROBHD 5 mm PABBO BB-
 PULPROG zgpg30
 TD 65536
 SOLVENT DMSO
 NS 305
 DS 4
 SWH 24038.461 Hz
 FIDRES 0.366798 Hz
 AQ 1.3631488 sec
 RG 181
 DW 20.800 usec
 DE 6.50 usec
 TE 296.0 K
 D1 2.00000000 sec
 D11 0.03000000 sec
 TD0 1

===== CHANNEL f1 =====
 SFO1 100.6253441 MHz
 NUC1 13C
 F1 9.00 usec
 PLW1 62.00000000 W

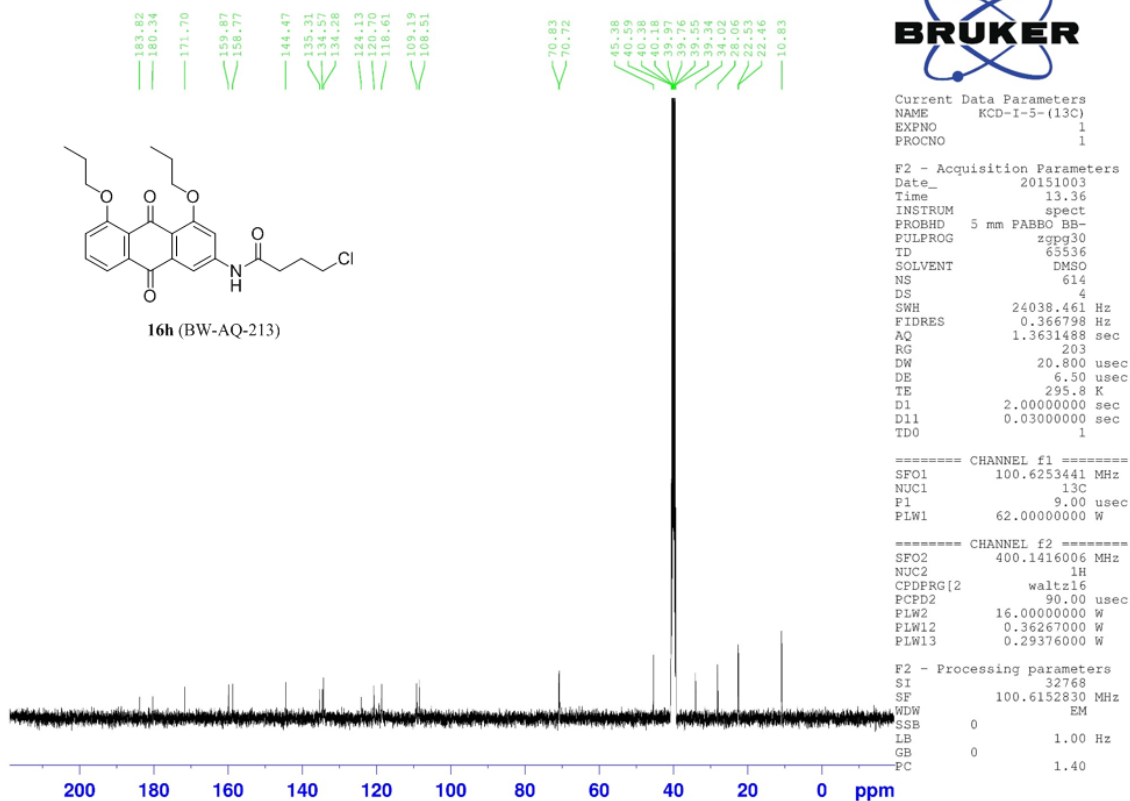
===== CHANNEL f2 =====
 SFO2 400.1416006 MHz
 NUC2 1H
 CPDPRG[2] waltz16
 FCPD2 90.00 usec
 PLW2 16.00000000 W
 PLW12 0.36267000 W
 PLW13 0.29376000 W

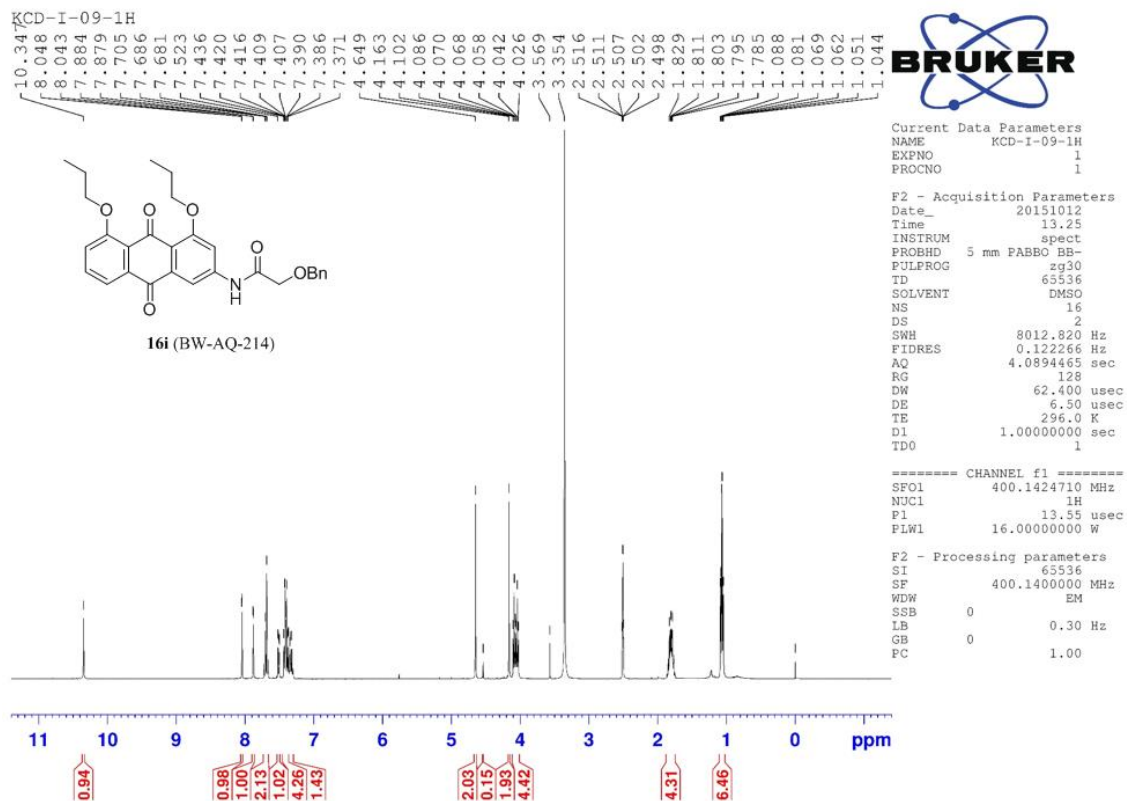
F2 - Processing parameters
 SI 32768
 SF 100.6152830 MHz
 WDW EM
 SSB 0
 LB 1.00 Hz
 GB 0
 PC 1.40

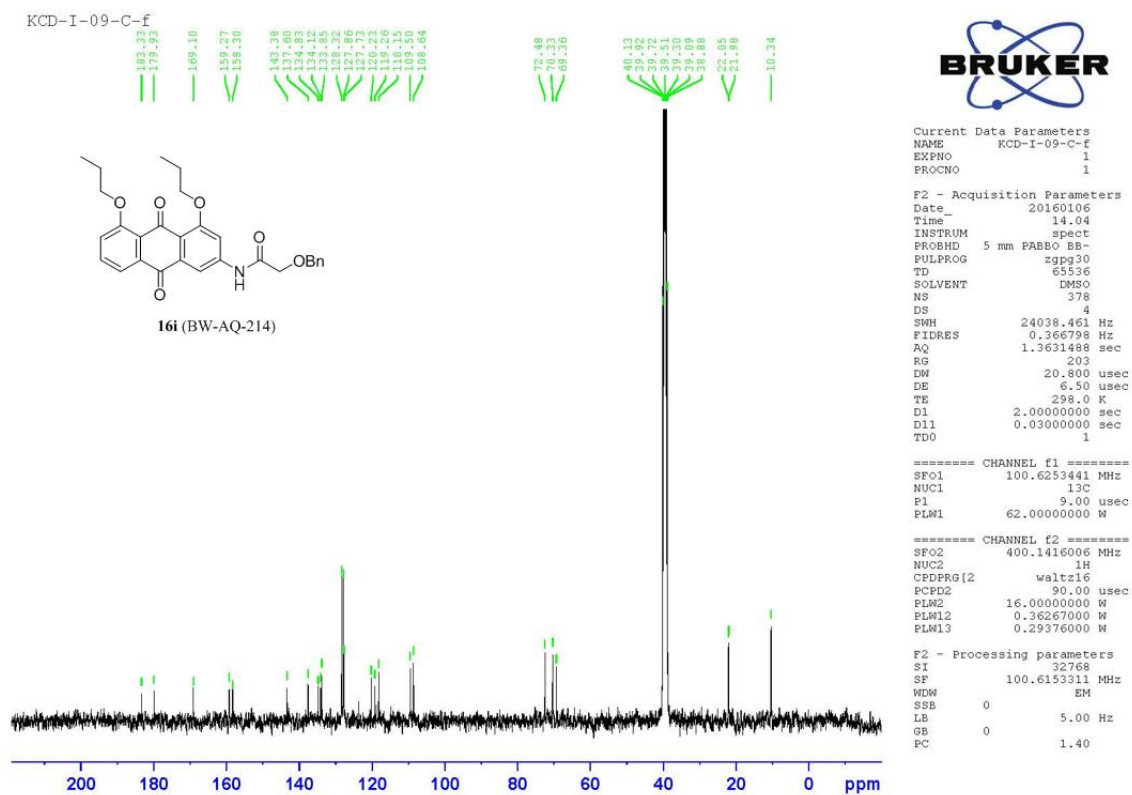
KCD-I-5 (1H)

**16h (BW-AQ-213)**

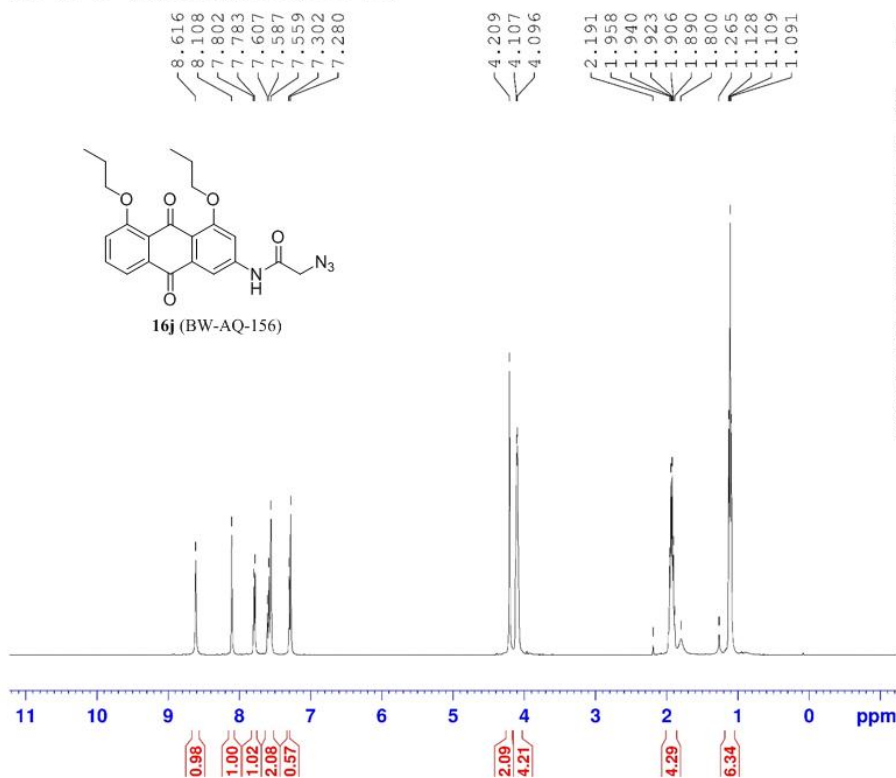
KCD-I-5- (13C)







ABD-VI-89-(1H) PurityCheck (1-17-13)

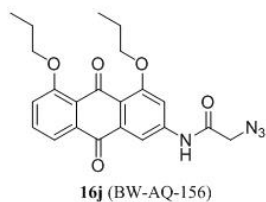


Current file parameters
 NAME: ABD-VI-89-(1H)PurityCheck(1-17-13)
 EXPNO: 1
 PROCNO: 1

F2 - Acquisition Parameters
 Date_ 20130517
 Time 9:52
 Name ABD-VI-89-(1H)PurityCheck(1-17-13)
 PROBHD 5 mm TARGO BBO
 PULPROG zgpg30
 CH 13C
 SOLVENT CDCl₃
 NS 2
 DS 2
 SWH 8012.820 Hz
 FIDRES 0.122266 Hz
 AQ 6.6834461 sec
 RG 328
 EN 62.400 USBC
 LE 6.50 USBC
 TE 294.0 K
 FI 1.00000000 sec
 FSO 1

----- CHANNEL f1 -----
 NUCL1 400.424710 MHz
 ECJ01 1H
 FI 13.50 USBC
 PTM1 16.00000000 sec
 F2 - Processing parameters
 SI 65536
 SF 400.424710 MHz
 AF 0.000000 MHz
 ZF 0.000000 MHz
 IN 0.000000 MHz
 GR 0.000000 MHz
 GC 1.000000 MHz

ABD-VI-89-13C (11-5-15)



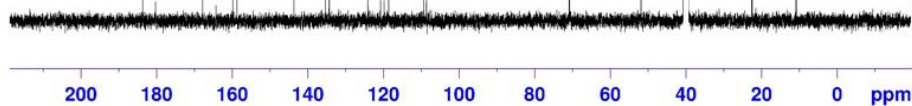
Current Data Parameters
NAME ABD-VI-89-13C(11-5-15)
EXPNO 1
PROCNO 1

F2 - Acquisition Parameters
Date_ 20151105
Time 11.08
INSTRUM spect
PROBHD 5 mm PABBO BB-
PULPROG zgpg30
TD 65536
SOLVENT DMSO
NS 459
DS 4
SWH 24038.461 Hz
FIDRES 0.366798 Hz
AQ 1.3631488 sec
RG 203
DW 20.800 usec
DE 6.50 usec
TE 296.0 K
D1 2.00000000 sec
D11 0.03000000 sec
TDO 1

===== CHANNEL f1 =====
SFO1 100.6253441 MHz
NUC1 13C
P1 9.00 usec
PLW1 62.00000000 W

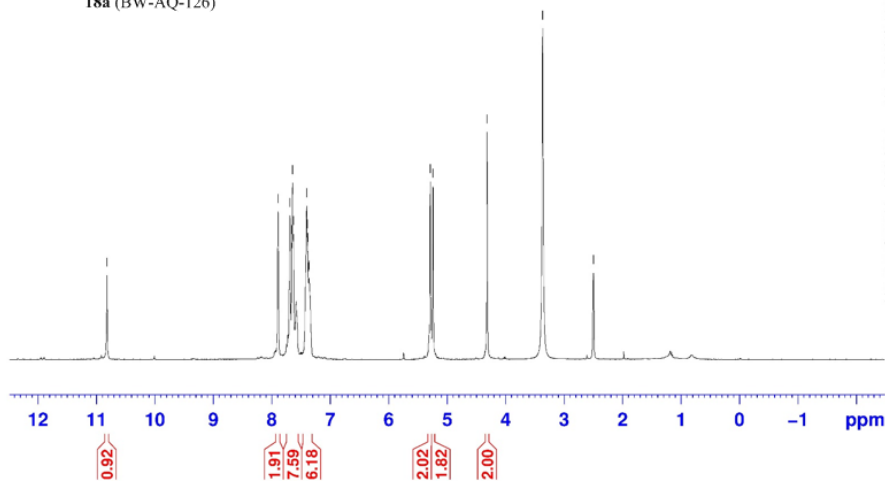
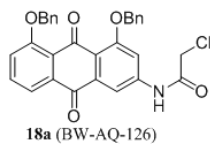
===== CHANNEL f2 =====
SFO2 400.1416006 MHz
NUC2 1H
CPOPRG(2) waltz16
PCPD2 90.00 usec
PLW2 16.00000000 W
PLW12 0.36267000 W
PLW13 0.29376000 W

F2 - Processing parameters
SI 32768
SF 100.6152830 MHz
WDW EM
SSB 0
LB 1.00 Hz
GB 0
PC 1.40



ABD-VII-13-1H (7-7-15)

— 10.822
 7.895
 7.691
 7.660
 7.645
 7.632
 7.404
 7.394
 7.386
 7.373
 7.363
 5.289
 5.244
 — 4.320
 — 3.367
 — 2.499



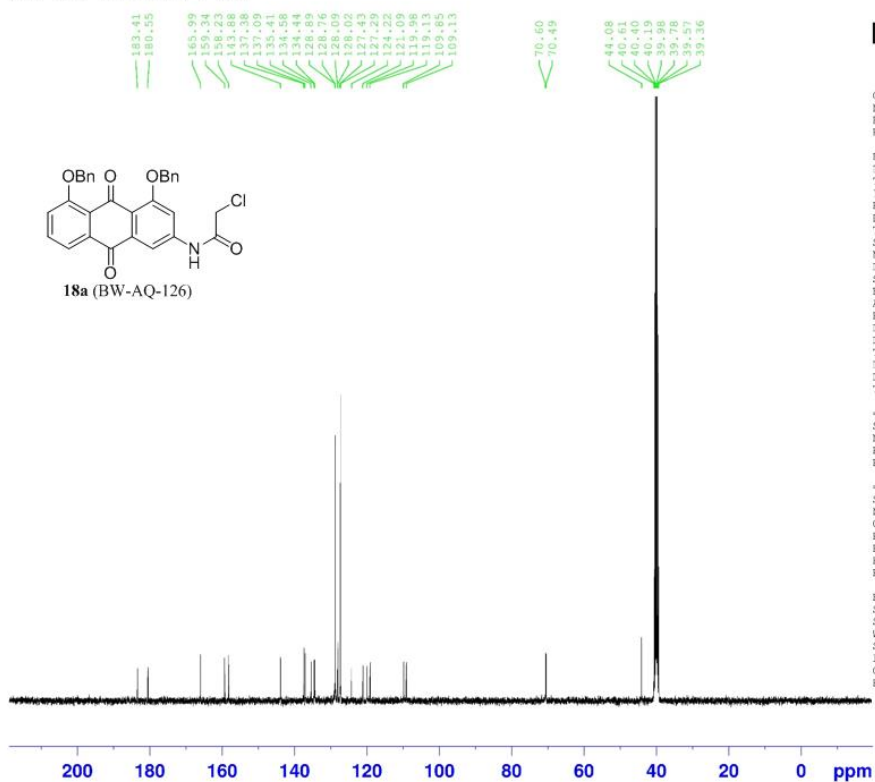
Current Data Parameters
 NAME ABD-VII-13-1H (7-7-15)
 EXPNO 1
 PROCNO 1

F2 - Acquisition Parameters
 Date_ 20150707
 Time 14.34
 INSTRUM spect
 PROBHD 5 mm FAPBO BB-
 PULPROG zg30
 TD 65536
 SOLVENT DMSO
 NS 16
 DS 2
 SWH 8012.820 Hz
 FIDRES 0.122266 Hz
 AQ 4.0894465 sec
 RG 90.5
 DW 62.400 usec
 DE 6.50 usec
 TE 296.8 K
 D1 1.00000000 sec
 TD0 1

===== CHANNEL f1 =====
 SFO1 400.1424710 MHz
 NUC1 1H
 P1 13.55 usec
 PLW1 16.00000000 W

F2 - Processing parameters
 SI 65536
 SF 400.1400029 MHz
 WDW EM
 SSB 0
 LB 0.30 Hz
 GB 0
 PC 1.00

ABD-VII-13-13C (7-7-15)



Current Data Parameters
 NAME ABD-VII-13-13C (7-7-15)
 EXPNO 1
 PROCNO 1

F2 - Acquisition Parameters
 Date_ 20150707
 Time 14.37
 INSTRUM spect
 PROBHD 5 mm PABBO BB-
 PULPROG zgpg30
 TD 65536
 SOLVENT DMSO
 NS 463
 DS 4
 SWH 24038.461 Hz
 FIDRES 0.366798 Hz
 AQ 1.3631488 sec
 RG 203
 DW 20.800 usec
 DE 6.50 usec
 TE 297.3 K
 D1 2.0000000 sec
 D11 0.0300000 sec
 TD0 1

===== CHANNEL f1 =====
 SFO1 100.6253441 MHz
 NUC1 13C
 P1 9.00 usec
 PLW1 62.0000000 W

===== CHANNEL f2 =====
 SFO2 400.1416006 MHz
 NUC2 1H
 CPOPRG12 waltz16
 PCPD2 90.00 usec
 PLW2 16.0000000 W
 PLW12 0.36267000 W
 PLW13 0.29376000 W

F2 - Processing parameters
 S1 32768
 SF 100.6152830 MHz
 WDW EM
 SSB 0
 LB 1.00 Hz
 GB 0
 EC 1.40

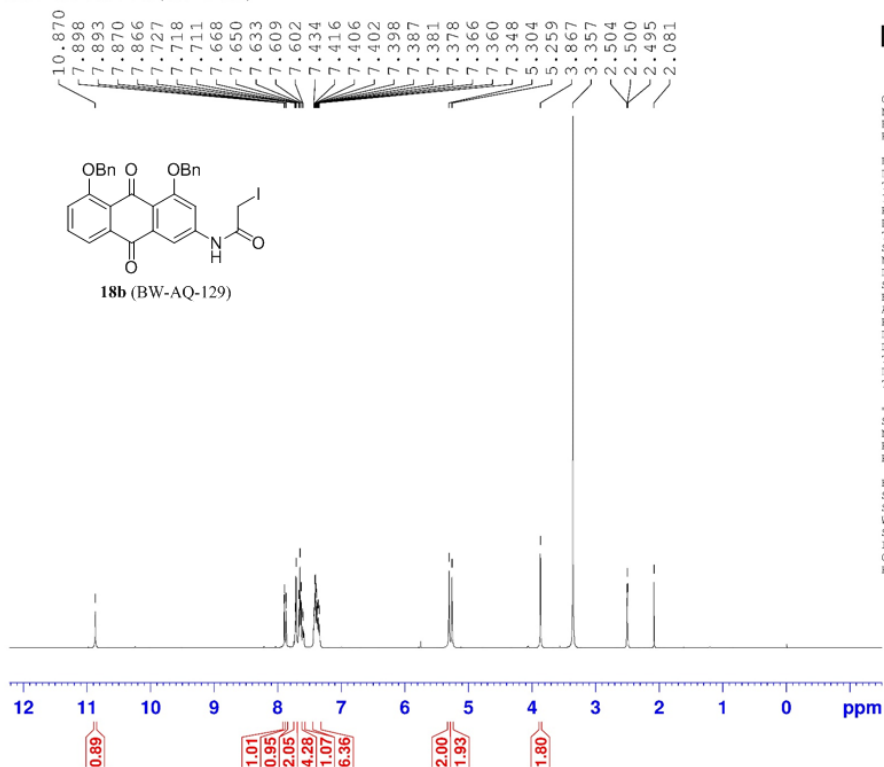
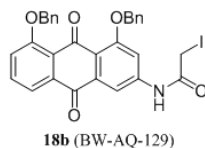
ABD-VI-101-1H(11-4-15)



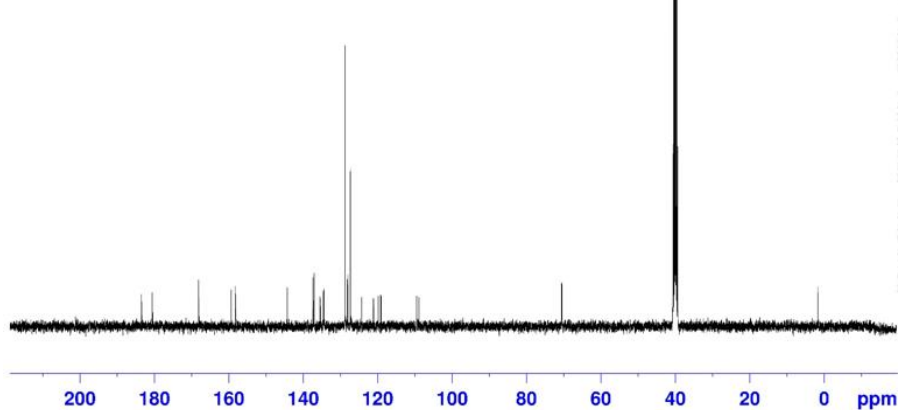
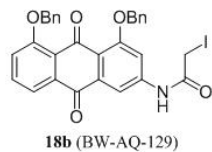
Current Data Parameters
 NAME ABD-VI-101-1H(11-4-15)
 EXPNO 1
 PROCNO 1

F2 - Acquisition Parameters
 Date_ 20151104
 Time 11.25
 INSTRUM spect
 PROBHD 5 mm PABBO BB-
 PULPROG zg30
 TD 65536
 SOLVENT DMSO
 NS 16
 DS 2
 SWH 8012.820 Hz
 FIDRES 0.122266 Hz
 AQ 4.0894465 sec
 RG 114
 DW 62.400 usec
 DE 6.50 usec
 TE 296.0 K
 D1 1.00000000 sec
 TDO 1

===== CHANNEL f1 =====
 SFO1 400.1424710 MHz
 NUC1 1H
 P1 13.55 usec
 PLW1 16.00000000 W
 F2 - Processing parameters
 SI 65536
 SF 400.1400031 MHz
 WDW EM
 SSB 0
 LB 0.30 Hz
 GB 0
 PC 1.00



ABD-VI-101-13C(11-4-15)



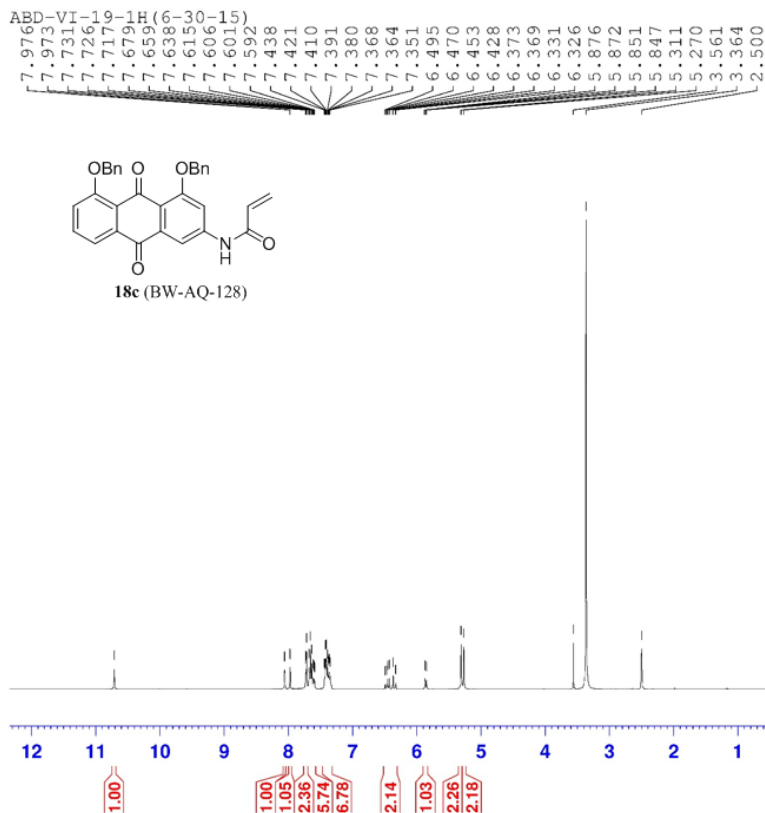
Current Data Parameters
 NAME ABD-VI-101-13C(11-4-15)
 EXPNO 1
 PROCNO 1

F2 - Acquisition Parameters
 Date_ 20151104
 Time 11.28
 INSTRUM spect
 PROBHD 5 mm PABBO BB-
 PULPROG zgpg30
 TD 65536
 SOLVENT DMSO
 NS 328
 DS 4
 SWH 24038.461 Hz
 FIDRES 0.366798 Hz
 AQ 1.3631488 sec
 RG 203
 DW 20.800 usec
 DE 6.50 usec
 TE 296.0 K
 D1 2.00000000 sec
 D11 0.03000000 sec
 TUD 1

===== CHANNEL f1 =====
 SFO1 100.6253441 MHz
 NUC1 13C
 P1 9.00 usec
 PLW1 62.00000000 W

===== CHANNEL f2 =====
 SFO2 400.1416006 MHz
 NUC2 1H
 CPDPRG2 waltz16
 PCPD2 90.00 usec
 PLW2 16.00000000 W
 PLW12 0.36267000 W
 PLW13 0.29376000 W

F2 - Processing parameters
 SI 32768
 SF 100.6152830 MHz
 WDW EM
 SSB 0
 LB 1.00 Hz
 GB 0
 PC 1.40



Current Data Parameters
 NAME ABD-VI-19-1H(6-30-15)
 EXPNO 1
 PROCNO 1

F2 - Acquisition Parameters
 Date_ 20150630
 Time 10.52
 INSTRUM spect
 PROBHD 5 mm FAPBO BB-
 PULPROG zg30
 TD 65536
 SOLVENT DMSO
 NS 16
 DS 2
 SWH 8012.820 Hz
 FIDRES 0.122266 Hz
 AQ 4.0894465 sec
 RG 114
 DW 62.400 usec
 DE 6.50 usec
 TE 296.5 K
 D1 1.00000000 sec
 TDO 1

===== CHANNEL f1 =====
 SFO1 400.1424710 MHz
 NUC1 1H
 P1 13.55 usec
 PLW1 16.00000000 W

F2 - Processing parameters
 SI 65536
 SF 400.1400030 MHz
 WDW EM
 SSB 0
 LB 0.30 Hz
 GB 0
 PC 1.00

ABD-VI-19-13C (6-30-15)



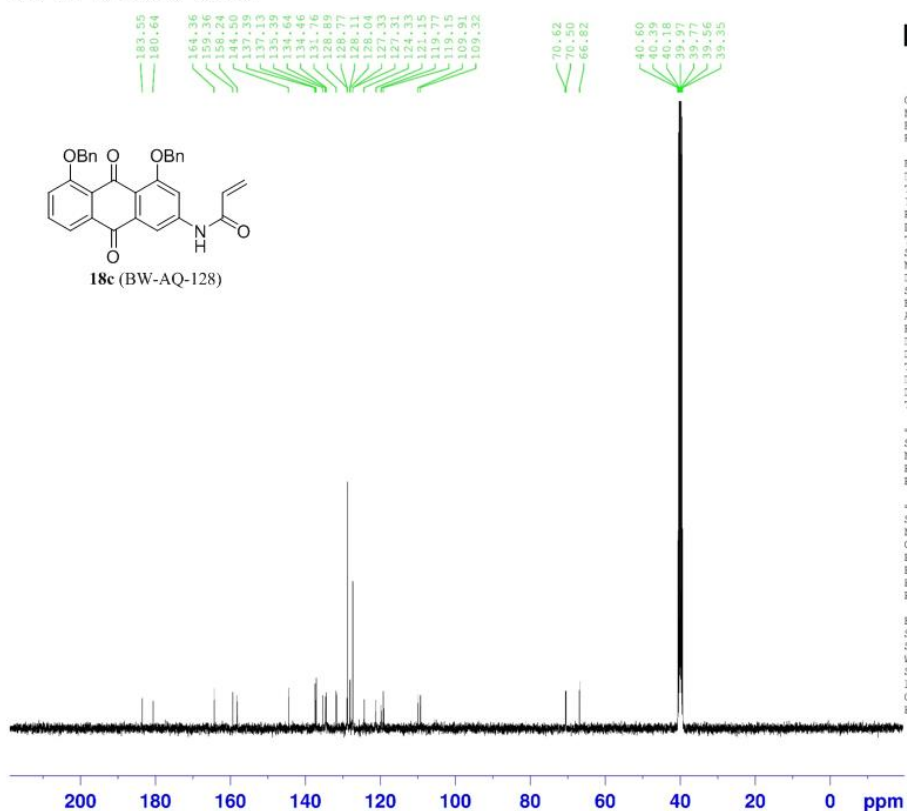
Current Data Parameters
 NAME ABD-VI-19-13C (6-30-15)
 EXPNO 1
 PROCNO 1

F2 - Acquisition Parameters
 Date_ 20150630
 Time 10.55
 INSTRUM spect
 PROBHD 5 mm PABBO BB-
 PULPROG zgpg30
 TD 65536
 SOLVENT DMSO
 NS 397
 DS 4
 SWH 24038.461 Hz
 FIDRES 0.366798 Hz
 AQ 1.3631488 sec
 RG 203
 DW 20.800 usec
 DE 6.50 usec
 TE 296.9 K
 D1 2.00000000 sec
 D11 0.03000000 sec
 TD0 1

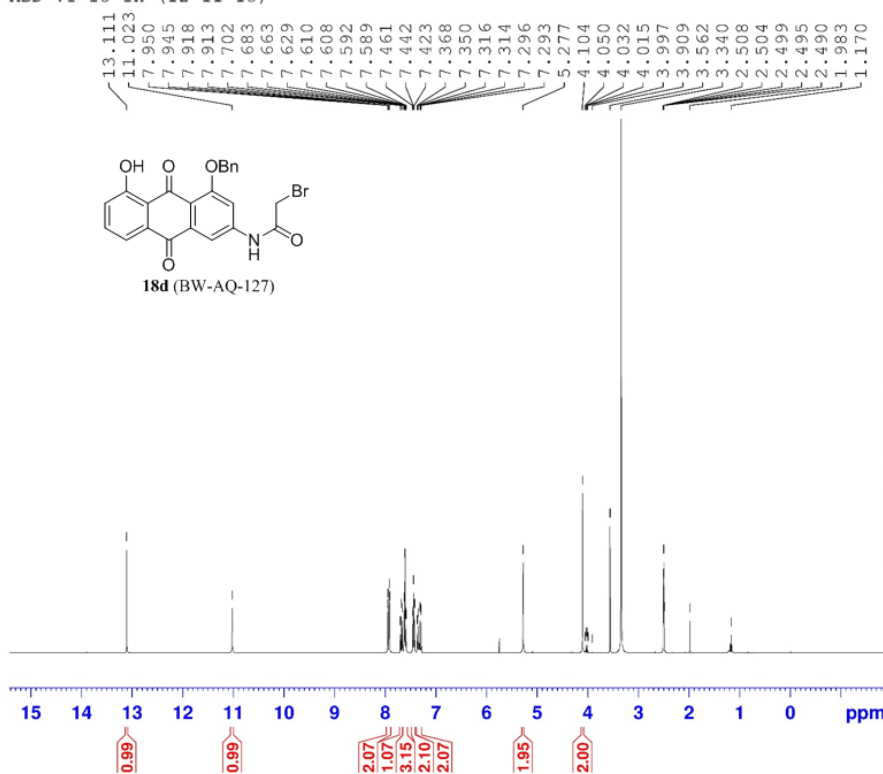
===== CHANNEL f1 =====
 SFO1 100.6253441 MHz
 NUC1 13C
 P1 9.00 usec
 PLW1 62.00000000 W

===== CHANNEL f2 =====
 SFO2 400.1416006 MHz
 NUC2 1H
 CPDPRG2 waltz16
 PCPD2 90.00 usec
 PLW2 16.00000000 W
 PLW12 0.36267000 W
 PLW13 0.29376000 W

F2 - Processing parameters
 S1 32768
 SF 100.6152830 MHz
 WDW EM
 SSB 0
 LB 1.00 Hz
 GB 0
 PC 1.40



ABD-VI-15-1H-(12-11-15)

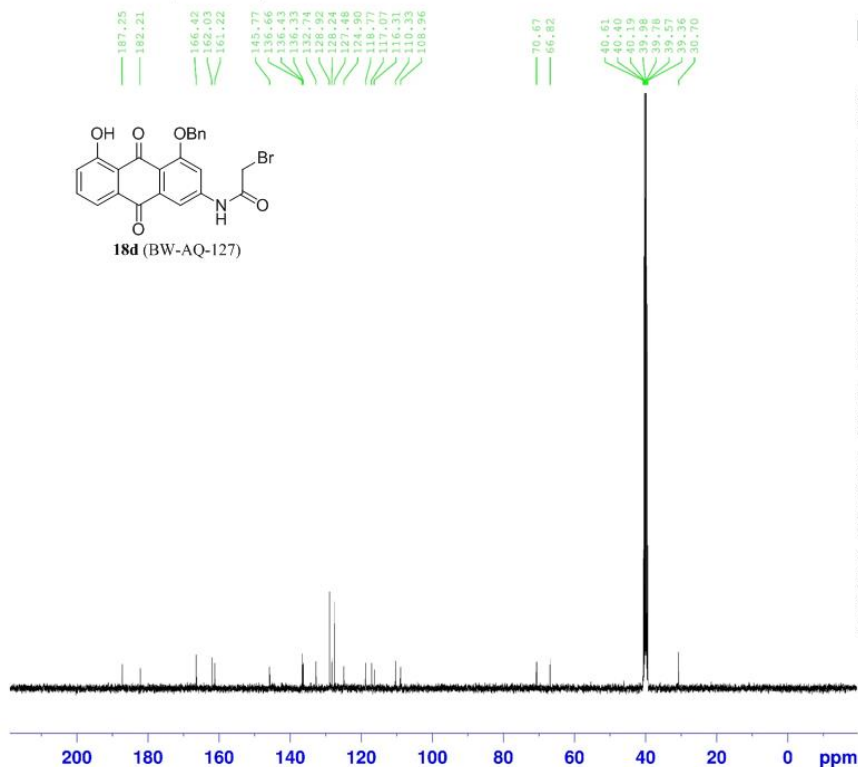


Current Data Parameters
 NAME ABD-VI-15-1H-(12-11-15)
 EXPNO 1
 PROCNO 1

F2 - Acquisition Parameters
 Date_ 20151211
 Time 10.04
 INSTRUM spect
 PROBHD 5 mm PABBO BB-
 PULPROG zg30
 TD 65536
 SOLVENT DMSO
 NS 16
 DS 2
 SWH 8012.820 Hz
 FIDRES 0.122266 Hz
 AQ 4.0894465 sec
 RG 144
 DW 62.400 usec
 DE 6.50 usec
 TE 298.0 K
 D1 1.00000000 sec
 TD0 1

===== CHANNEL f1 =====
 SF01 400.1424710 MHz
 NUC1 1H
 P1 13.55 usec
 PLW1 16.00000000 W
 F2 - Processing parameters
 SI 65536
 SF 400.1400031 MHz
 NSW EM
 SSB 0
 LB 0.30 Hz
 GR 0
 PC 1.00

ABD-VI-15-13C-(12-11-15)



Current Data Parameters
 NAME ABD-VI-15-13C-(12-11-15)
 EXPNO 1
 PROCNO 1

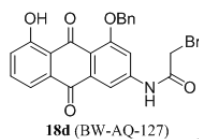
F2 - Acquisition Parameters
 Date_ 20151211
 Time 10.07
 INSTRUM spect
 PROBHD 5 mm PABBO DB-
 PULPROG zgpg30
 TD 65536
 SOLVENT DMSO
 NS 341
 DS 4
 SWH 24038.461 Hz
 FIDRES 0.366798 Hz
 AQ 1.3631488 sec
 RG 203
 DM 20.800 usec
 DE 6.50 usec
 TE 298.2 K
 D1 2.00000000 sec
 D11 0.03000000 sec
 TD0 1

===== CHANNEL f1 =====
 SFO1 100.6253441 MHz
 NUC1 13C
 P1 9.00 usec
 PLW1 62.00000000 W

===== CHANNEL f2 =====
 SFO2 400.1416006 MHz
 NUC2 1H
 CPDPRG2 waltz16
 PCPD2 90.00 usec
 PLW2 16.00000000 W
 PLW12 0.36267000 W
 PLW13 0.29376000 W

F2 - Processing parameters
 SI 32768
 SF 100.6152830 MHz
 WDW EM
 SSF 0
 LB 1.00 Hz
 GB 0
 PC 1.40

-15-COSY- (12-11-15)



Current Data Parameters
 NAME ASD-VI-15-COSY- (12-11-15)
 EXPNO 1
 PROCNO 1

F2 - Acquisition Parameters
 Date_ 20160329
 Time 12.52
 INSTRUM spect
 PROBRD 5 mm FA80 BB-
 PULPROG cosygpppgf
 TD 2048
 SOLVENT DMSO
 NS 4
 DS 0
 SWH 4000.000 Hz
 FIDRES 1.933125 Hz
 AQ 0.2560000 sec
 RG 203
 DW 125.000 usec
 DE 6.50 usec
 TE 298.0 K
 D0 0.0000000 sec
 D1 2.0000000 sec
 D11 0.0300000 sec
 D12 0.0000000 sec
 D13 0.0000400 sec
 D16 0.0020000 sec
 LNO 0.0000000 sec

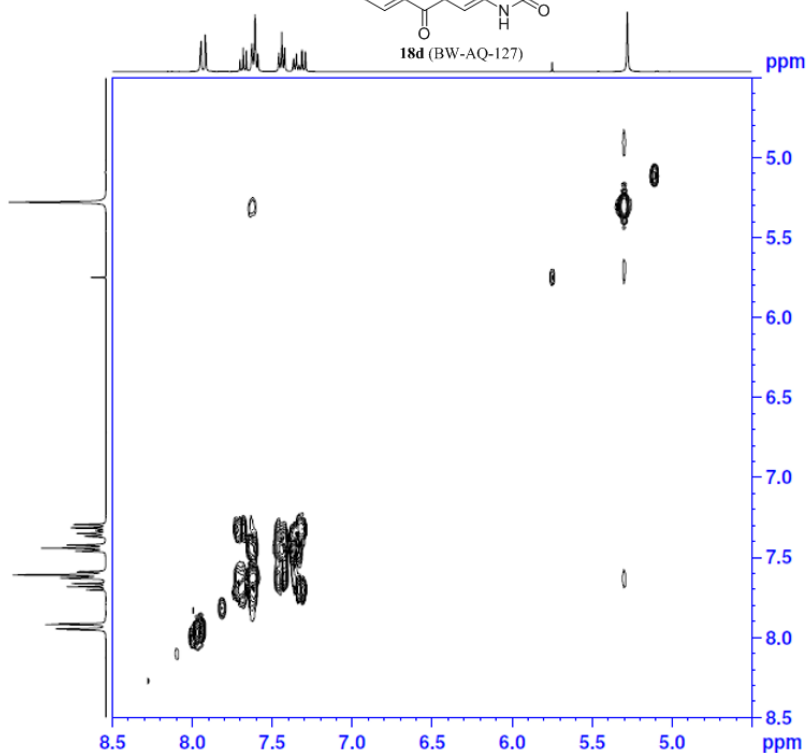
----- CHANNEL f1 -----
 SF01 400.1434112 MHz
 NUCL1 1H
 P0 13.55 usec
 F1 13.55 usec
 P17 2500.00 usec
 PLM1 16.0000000 W
 PLM10 6.34560013 W

----- GRADIENT CHANNEL -----
 GPMAX[1] SMSQ10.100
 GPZ1 10.00 %
 P16 1000.00 usec

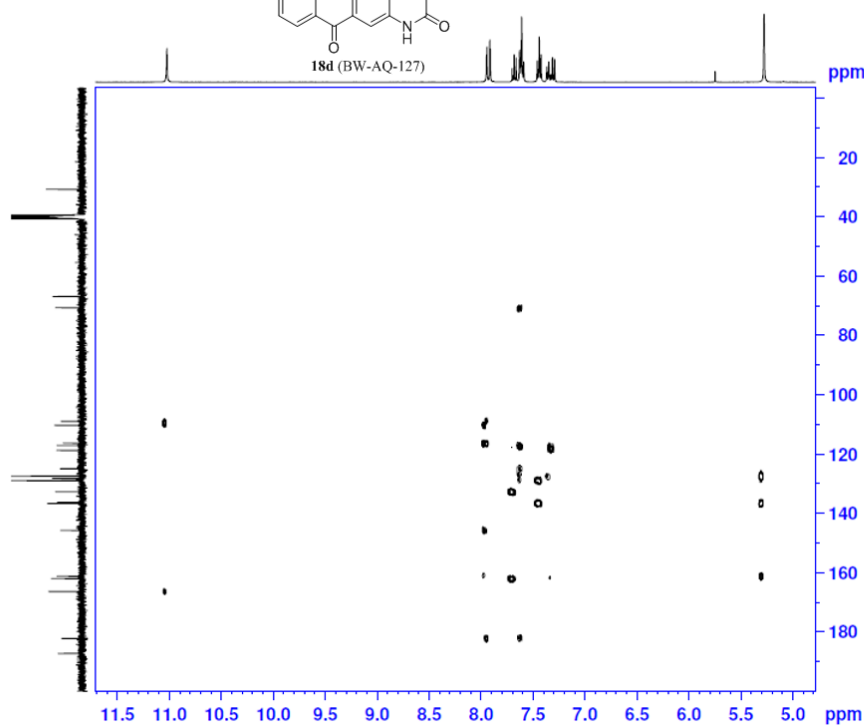
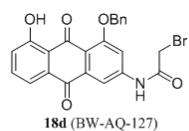
F1 - Acquisition parameters
 TD 128
 SF01 400.1435 MHz
 FIDRES 31.250000 Hz
 SW 9.996 ppm
 F0MODE QF

F2 - Processing parameters
 SI 1024
 SF 400.1400000 MHz
 WDW QSIKX
 SSB 0
 LB 0 Hz
 GB 0
 PC 1.40

F1 - Processing parameters
 SI 1024
 WDW QF
 SF 400.1400000 MHz
 WDW QSIKX
 SSB 0
 LB 0 Hz
 GB 0



ABD-VI-15-HMBC- (12-11-15)



Current Data Parameters
NAME ABD-VI-15-HMBC- (12-11-15)
EXPNO 1
PROCNO 1

F2 - Acquisition Parameters
Date_ 20160329
Time 11.15
INSTRUM spect
PROBHD 5 mm PABBO BB-
PULPROG zgpg30
TD 2048
SOLVENT DMSO
NS 12
DS 0
SWH 2799.552 Hz
FIDRES 0.3637728 sec
AQ 0.3637728 sec
RG 203
DM 178.600 umsc
DE 4.50 umsc
TE 299.0 K
CNS12 148.0000000
CNS13 10.0000000
DO 0.0000300 sec
D1 1.0000000 sec
D2 0.00344828 sec
D4 0.0000000 sec
D16 0.0002000 sec
ZNO 0.0002240 sec

----- CHANNEL f1 -----
SFO1 400.1432411 MHz
NUC1 13
P1 13.55 umsc
P2 27.10 umsc
P1A1 16.0000000 M

----- CHANNEL f2 -----
SFO2 100.6253281 MHz
NUC2 13C
P3 9.00 umsc
P1A2 62.0000000 M

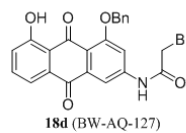
----- GRADIENT CHANNEL -----
GPM1(1) SMO10.100
GPM1(2) SMO10.100
GPM1(3) SMO10.100
GPT1 50.00 %
GPT2 40.10 %
GPT3 1000.00 umsc

F1 - Acquisition parameters
TD 123
SFO1 100.6253 MHz
FIDRES 191.475037 Hz
DM 221.827 ppm
F1MODE QF

F2 - Processing parameters
SI 2048
SF 400.1430000 MHz
WM 0
LB 0 Hz
GB 0
PC 1.40

F1 - Processing parameters
SI 1024
MC2 QF
SF 100.6152830 MHz
WM 0
LB 0 Hz
GB 0

ABD-VI-15-HSQC-(12-11-15)



18d (BW-AQ-127)



Current Data Parameters
NAME ABD-VI-15-HSQC-(12-11-15)
EXPNO 1
PROCNO 1

F2 - Acquisition Parameters
Date_ 20160329
Time 12.08
INSTRUM spect
PROBHD 5 mm QNP1H/1
PULPROG zgpg30
TD 132
SOLVENT DMSO
NS 4
DS 0
SWH 4000.000 MHz
FIDRES 3.904250 MHz
AQ 0.1280000 sec
RG 323
DM 125.000 usec
DE 6.50 usec
TE 300.0 K
CST2 145.0000000
D0 0.0000000 sec
D1 1.5000000 sec
D4 0.00172414 sec
D11 0.03000000 sec
D16 0.00020000 sec
DRO 0.00030000 sec
ZGPG30

CHANNEL f1
NUC1 400.1434812 MHz
P1 13.50 usec
P2 27.10 usec
P3 1.00 usec
P4 16.00000000 W

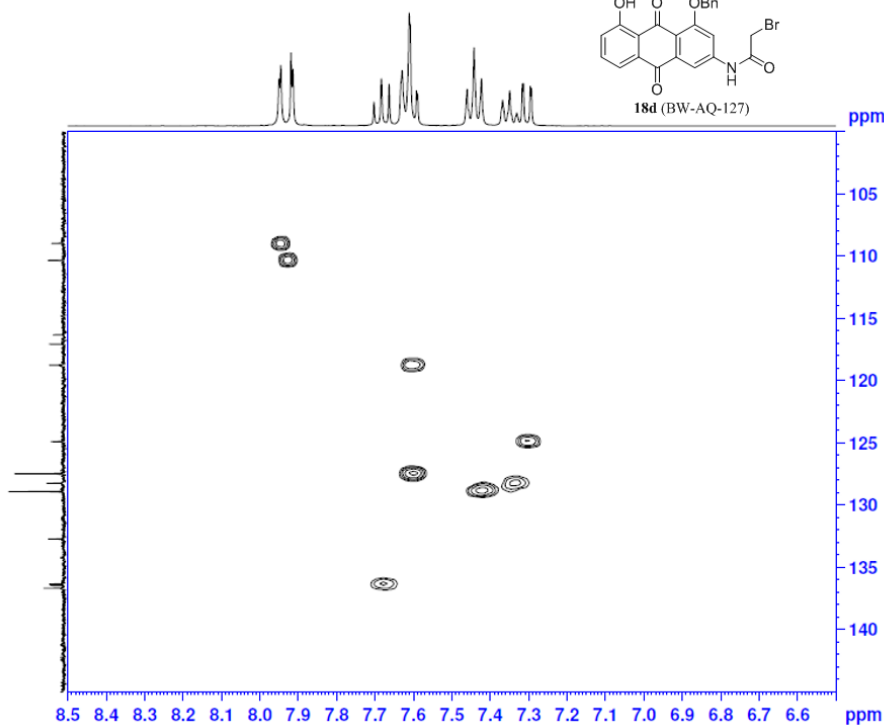
CHANNEL f2
NUC2 100.6227814 MHz
C1P2PRG2 HMQC
P1 9.00 usec
P2 18.00 usec
P3 70.00 usec
P4 62.00000000 W
P5 1.02489999 W

GRADIENT CHANNEL
GPRAM1 2MG010.100
GPRAM2 2MG010.100
GP1 80.00 %
GP2 20.10 %
P6 1000.00 usec

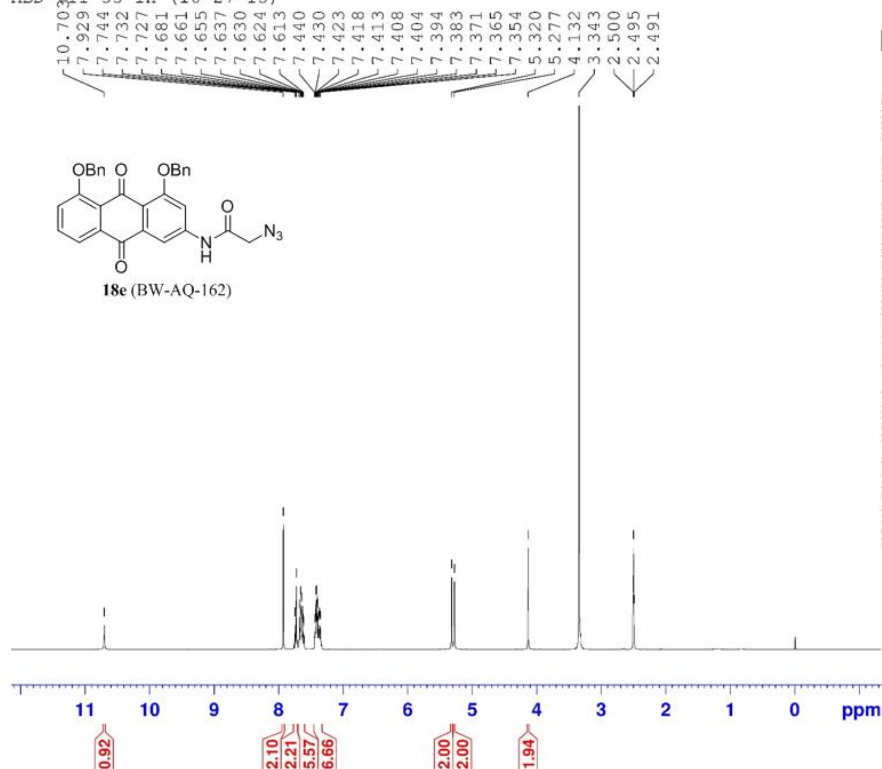
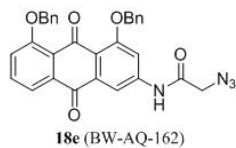
F1 - Acquisition parameters
TD 132
SFO1 100.6227814 MHz
FIDRES 0.104164 MHz
SR 143.435 ppm
PULPROG Kuhn-Anti-echo

F2 - Processing parameters
SI 32768
SF 400.1405087 MHz
WDW QFINE
SSB 0
LB 0 Hz
GB 0
PC 1.40

F1 - Processing parameters
SI 132
NUC1 antio-antio-echo
SF 100.6152830 MHz
WDW QFINE
SSB 0
LB 0 Hz
GB 0



ABD-VII-33-1H-(10-27-15)



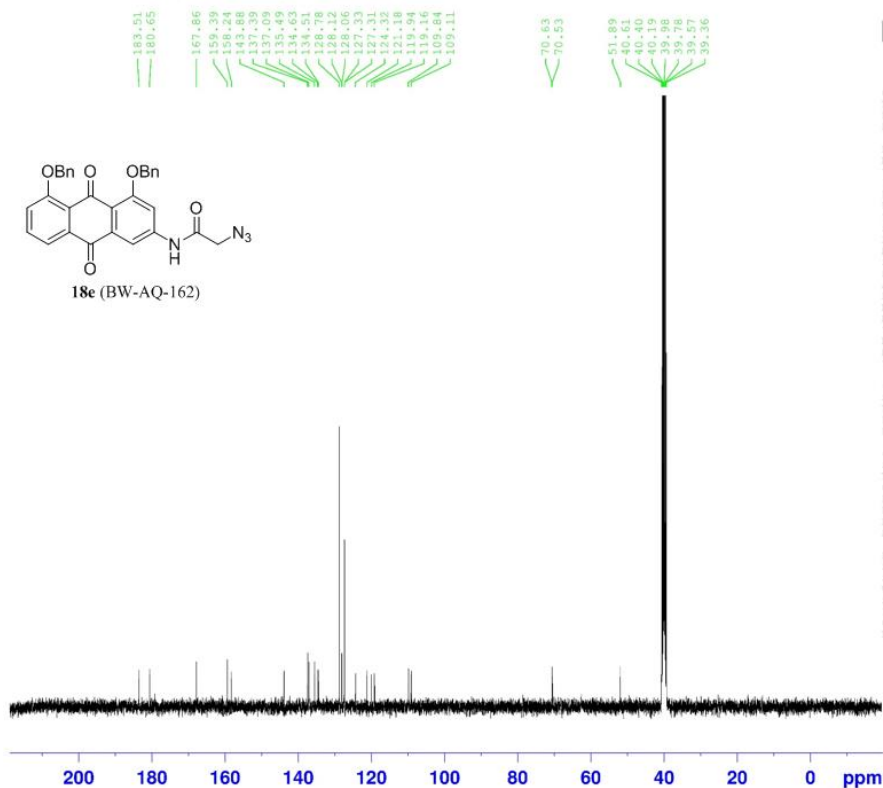
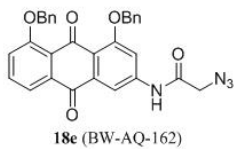
Current Data Parameters
 NAME ABD-VII-33-1H-(10-27-15)
 EXPNO 1
 PROCNO 1

F2 - Acquisition Parameters
 Date_ 20151027
 Time 10.00
 INSTAUM spect
 PROBHD 5 mm PABBO BB-
 PULPROG zg30
 TD 65536
 SOLVENT DMSO
 NS 16
 DS 2
 SWH 8012.820 Hz
 FIDRES 0.122266 Hz
 AQ 4.0894465 sec
 RG 161
 DW 62.400 usec
 DE 6.50 usec
 TE 296.0 K
 D1 1.00000000 sec
 TD0 1

===== CHANNEL f1 =====
 SF01 400.1424710 MHz
 NUC1 1H
 P1 13.55 usec
 PLW1 16.00000000 W

F2 - Processing parameters
 SI 65536
 SF 400.1400030 MHz
 WDW EM
 SSB 0
 LA 0.30 Hz
 GB 0
 PC 1.00

ABD-VII-33-13C- (10-27-15)



Current Data Parameters
 NAME ABD-VII-33-13C- (10-27-15)
 EXPNO 1
 PROCNO 1

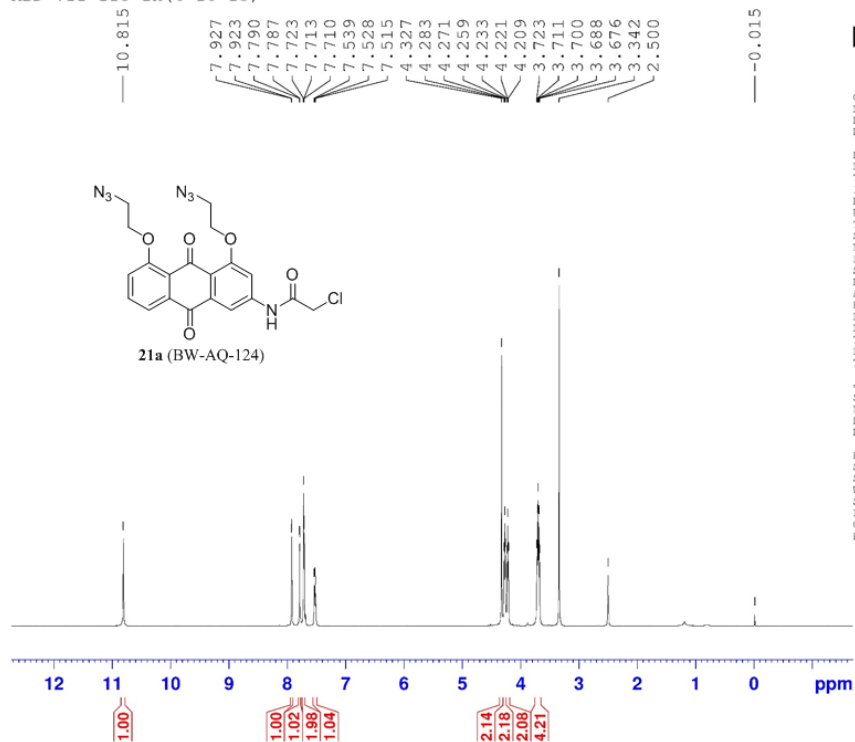
F2 - Acquisition Parameters
 Date_ 20151027
 Time 10.03
 INSTRUM spect
 PROBRD 5 mm PABBO BB-
 PULPROG zgpg30
 TD 65536
 SOLVENT DMSO
 NS 597
 DS 4
 SWH 24039.461 Hz
 FIDRES 0.366798 Hz
 AQ 1.3631488 sec
 RG 181
 DW 20.800 usec
 DE 6.50 usec
 TE 298.0 K
 D1 2.00000000 sec
 D11 0.03000000 sec
 TD0 1

===== CHANNEL f1 =====
 SFO1 100.6253441 MHz
 NUC1 13C
 P1 9.00 usec
 PLW1 62.00000000 W

===== CHANNEL f2 =====
 SFO2 400.1416006 MHz
 NUC2 1H
 CPDPRG12 waltz16
 PCPD2 90.00 usec
 PLW2 16.00000000 W
 PLW12 0.36267000 W
 PLW13 0.29379000 W

F2 - Processing parameters
 SI 32768
 SF 100.6152830 MHz
 WDW EM
 SSB 0
 LB 1.00 Hz
 GB 0
 PC 1.40

ABD-VII-113-1H (6-18-15)



Current Data Parameters
 NAME ABD-VII-113-1H (6-18-15)
 EXPNO 1
 PROCNO 1

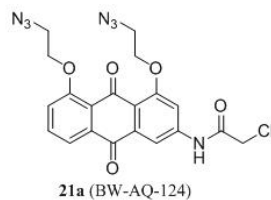
F2 - Acquisition Parameters
 Date 20150618
 Time 11.34
 INSTRUM spect
 PROBHD 5 mm PABBO BB-
 PULPROG zg30
 TD 65536
 SOLVENT DMSO
 NS 16
 DS 2
 SWH 8012.820 Hz
 FIDRES 0.122266 Hz
 AQ 4.0894465 sec
 RG 101
 CW 62.400 usec
 DE 6.50 usec
 TE 298.0 K
 D1 1.00000000 sec
 TD0 1

===== CHANNEL f1 =====
 SF01 400.1424710 MHz
 NUC1 1H
 P1 13.55 usec
 PLW1 16.00000000 W

F2 - Processing parameters
 SI 65536
 SF 400.1400026 MHz
 WDW EM
 SSB 0
 LB 0.30 Hz
 GR 0
 PC 1.00

ABD-VII-113-13C(6-18-15)

183.33
179.86
166.02
159.27
158.20
143.78
135.37
134.53
134.43
124.84
124.50
121.50
120.13
119.51
110.37
109.52



68.80
68.86
50.22
50.14
44.06
40.61
40.41
39.99
39.78
39.57
39.36

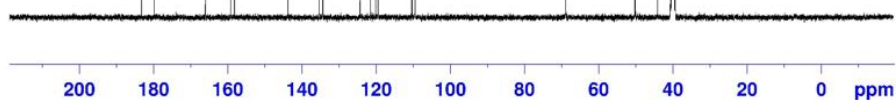


Current Data Parameters
NAME ABD-VII-113-13C(6-18-15)
EXPNO 1
PROCNO 1

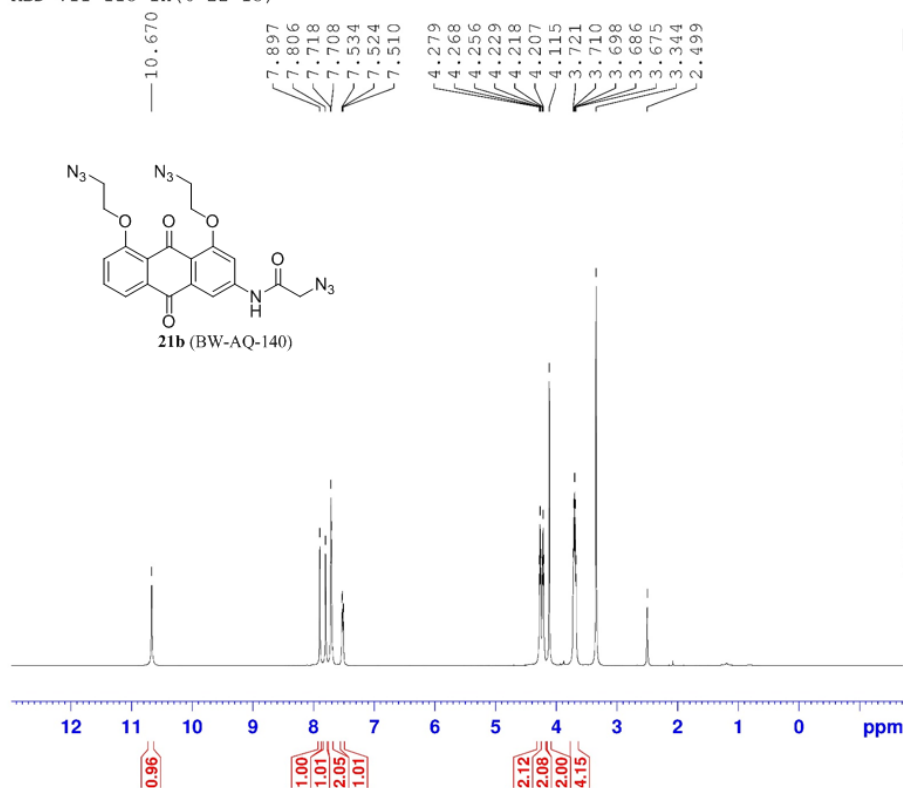
F2 - Acquisition Parameters
Date_ 20150618
Time 11.38
INSTRUM spect
PROBHD 5 mm PABBO DB-
PULPROG zgpg30
TD 65536
SOLVENT DMSO
NS 359
DS 4
SWH 24038.461 Hz
FIDRES 0.366798 Hz
AQ 1.3631488 sec
RG 203
RW 20.800 usec
DE 6.50 usec
TE 298.4 K
D1 2.00000000 sec
D11 0.03000000 sec
TD0 1

===== CHANNEL f1 =====
SFO1 100.6253441 MHz
NUC1 13C
P1 9.00 usec
PLW1 62.00000000 W
===== CHANNEL f2 =====
SFO2 400.1416006 MHz
NUC2 1H
CPDPRG[2] waltz16
PCPD2 90.00 usec
PLW2 16.00000000 W
PLW12 0.36267000 W
PLW13 0.29376000 W

F2 - Processing parameters
SI 32768
SF 100.6152830 MHz
WDW EM
SSB 0
LB 1.00 Hz
GB 0
PC 1.40



ABD-VII-115-1H(6-22-15)



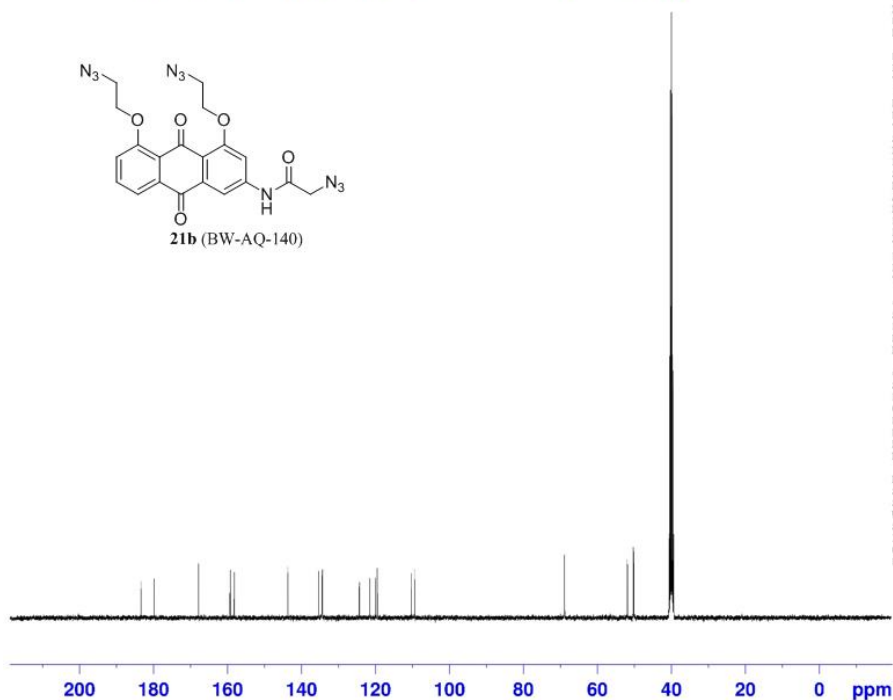
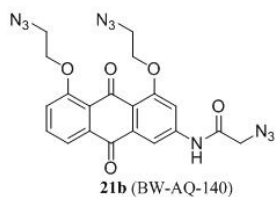
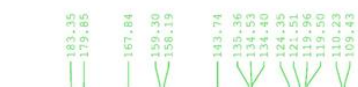
Current Data Parameters
 NAME ABD-VII-115-1H(6-22-15)
 EXPRO 1
 PROCNO 1

F2 - Acquisition Parameters
 Date_ 20150622
 Time 11.30
 INSTRUM spect
 PROBHD 5 mm PABBO BB-
 PULPROG zg30
 TD 65536
 SOLVENT DMSO
 NS 16
 DS 2
 SWH 8012.820 Hz
 FIDRES 0.122266 Hz
 AQ 4.0894465 sec
 RG 101
 DW 62.400 usec
 DE 6.50 usec
 TE 298.0 K
 D1 1.00000000 sec
 TDO 1

===== CHANNEL f1 =====
 SFO1 400.1424710 MHz
 NUC1 1H
 P1 13.55 usec
 PLW1 16.00000000 W

F2 - Processing parameters
 S1 65536
 SF 400.1400031 MHz
 WDW EM
 SSB 0
 LB 0.30 Hz
 GB 0
 PC 1.00

ABD-VII-115-13C (6-22-15)



Current Data Parameters
 NAME ABD-VII-115-13C (6-22-15)
 EXPNO 1
 PROCNO 1

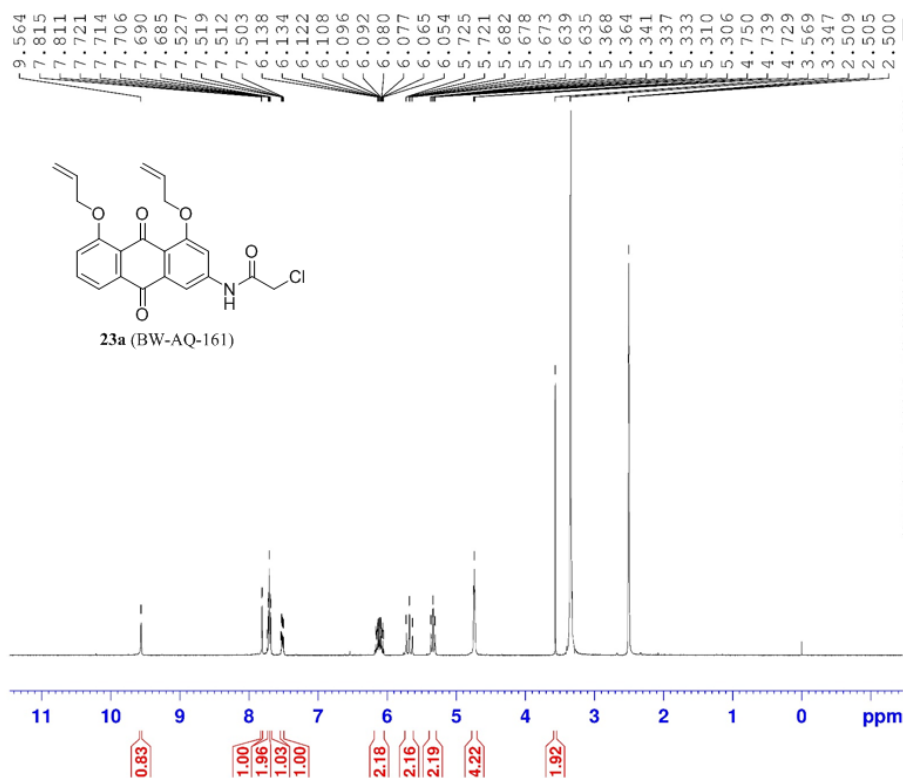
F2 - Acquisition Parameters
 Date_ 20150622
 Time 11:33
 INSTRUM spect
 PROBHD 5 mm F4BBO BB-
 PULPROG zgpg30
 TD 65536
 SOLVENT DMSO
 NS 441
 DS 4
 SWH 24038.461 Hz
 FIDRES 0.366798 Hz
 AQ 1.3631488 sec
 RG 203
 DW 20.800 usec
 DE 6.50 usec
 TE 298.4 K
 D1 2.0000000 sec
 D11 0.0300000 sec
 TD0 1

===== CHANNEL f1 =====
 SFO1 100.6253441 MHz
 NUC1 13C
 P1 9.00 usec
 PLW1 62.0000000 W

===== CHANNEL f2 =====
 SFO2 400.1416006 MHz
 NUC2 1H
 CPDPRG2 waltz16
 PCPD2 90.00 usec
 PLW2 16.0000000 W
 PLW12 0.36267000 W
 PLW13 0.29376000 W

F2 - Processing parameters
 SI 32768
 SF 100.6152830 MHz
 WDW EM
 SSB 0
 LB 1.00 Hz
 GB 0
 PC 1.40

ABD-VII-23-1HC (11-11-15)



Current Data Parameters
NAME ABD-VII-23-1HC (11-11-15)
EXPNO 1
PROCNO 1

F2 - Acquisition Parameters
Date_ 20151111
Time 9.40
INSTRUM spect
PROBHD 5 mm PABBO BB-
PULPROG zg30
TD 65536
SOLVENT DMSO
NS 16
DS 2
SWH 8012.820 Hz
FIDRES 0.122286 Hz
AQ 4.069465 sec
RG 181
DW 62.400 usec
DE 6.50 usec
TE 296.0 K
D1 1.00000000 sec
TD0 1

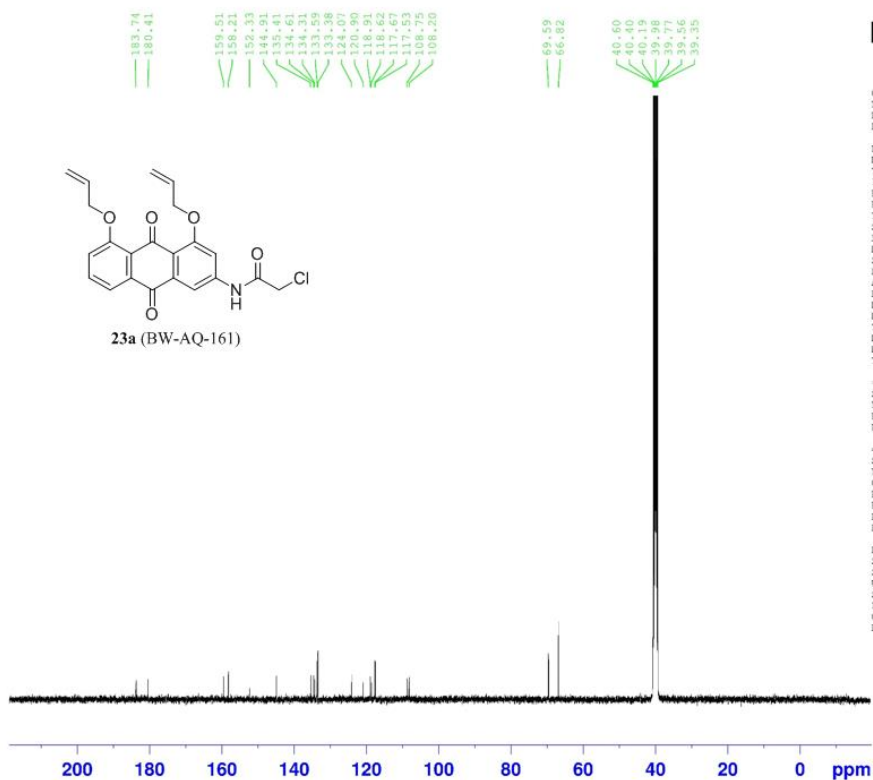
CHANNEL f1
SFO1 400.1424710 MHz
NUC1 1H
P1 13.55 usec
PLW1 16.00000000 W

F2 - Processing parameters
SI 65536
SF 400.1400012 MHz
WDW EM
SSB 0
LB 0.30 Hz
GB 0
FC 1.00

ABD-VII-23-13C (11-10-15)



23a (BW-AQ-161)



Current Data Parameters
 NAME ABD-VII-23-13C (11-10-15)
 EXPNO 1
 PROCNO 1

F2 - Acquisition Parameters
 Date_ 20151110
 Time 22.27
 INSTRUM spect
 PROBHD 5 mm PABBO BB-
 PULPROG zgpg30
 TD 65536
 SOLVENT DMSO
 NS 11628
 DS 0
 SWH 24038.461 Hz
 FIDRES 0.366798 Hz
 AQ 1.363168 sec
 RG 203
 DW 20.800 usec
 DE 6.50 usec
 TE 296.0 K
 D1 2.0000000 sec
 D11 0.0300000 sec
 TD0 1

===== CHANNEL f1 =====
 SFO1 100.6253441 MHz
 NUC1 13C
 P1 9.00 usec
 PL1 62.0000000 W

===== CHANNEL f2 =====
 SFO2 400.1416006 MHz
 NUC2 1H
 CPDPRG2 waltz16
 PCPD2 90.00 usec
 PLW2 16.0000000 W
 PLW12 0.36267000 W
 PLW13 0.29376000 W

F2 - Processing parameters
 SI 32768
 SF 100.6152830 MHz
 MDW EM
 SSB 0
 LB 1.00 Hz
 GB 0
 FC 1.40

ABD-VII-25-(1H)

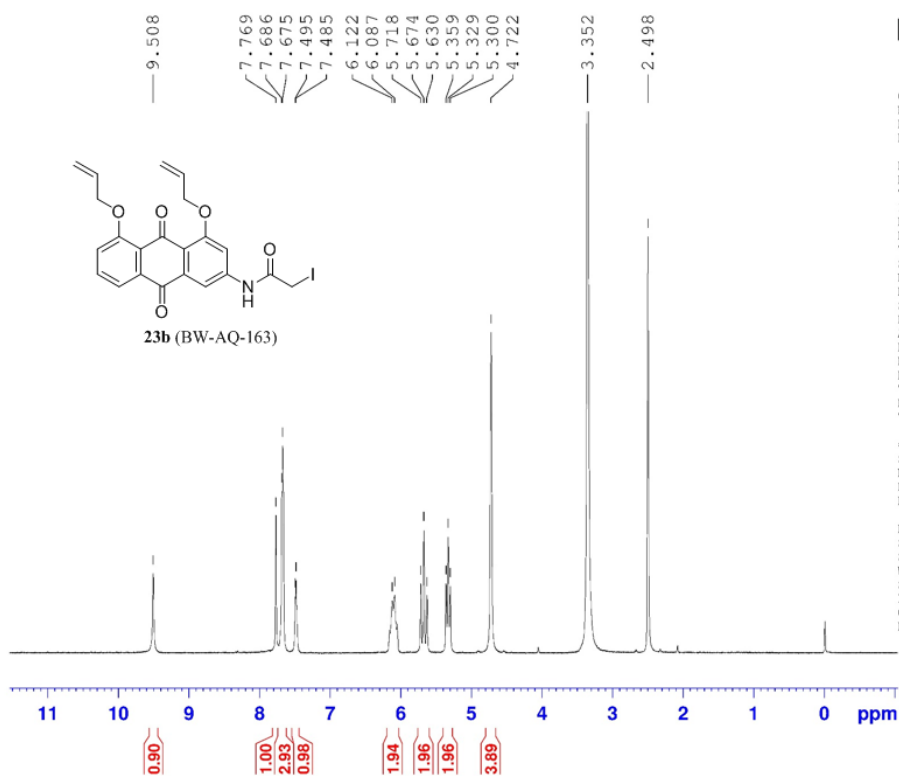


Current Data Parameters
 NAME ABD-VII-25-(1H)
 EXPNO 1
 PROCNO 1

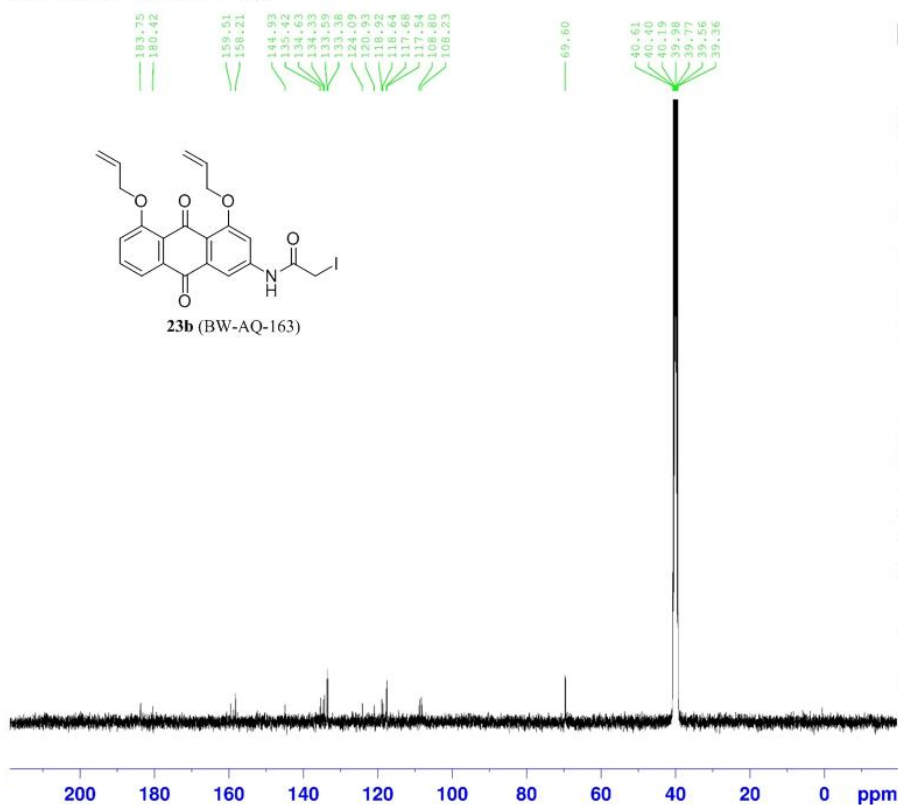
F2 - Acquisition Parameters
 Date_ 20130123
 Time 13.10
 INSTRUM spect
 PROBHD 5 mm PABBO BB-
 PULPROG zg30
 TD 65536
 SOLVENT DMSO
 NS 16
 DS 2
 SWH 8012.820 Hz
 FIDRES 0.122266 Hz
 AQ 4.0894465 sec
 RG 161
 DW 62.400 usec
 DE 6.50 usec
 TE 294.5 K
 D1 1.00000000 sec
 TDO 1

===== CHANNEL f1 =====
 SFO1 400.1424710 MHz
 NUC1 1H
 P1 13.50 usec
 PLW1 16.00000000 W

F2 - Processing parameters
 SI 65536
 SF 400.1400017 MHz
 WDW EM
 SSB 0
 LB 0.30 Hz
 GB 0
 PC 1.00



ABD-VII-25-13C (11-6-15)



Current Data Parameters
 NAME ABD-VII-25-13C(11-6-15)
 EXPNO 1
 PROCNO 1

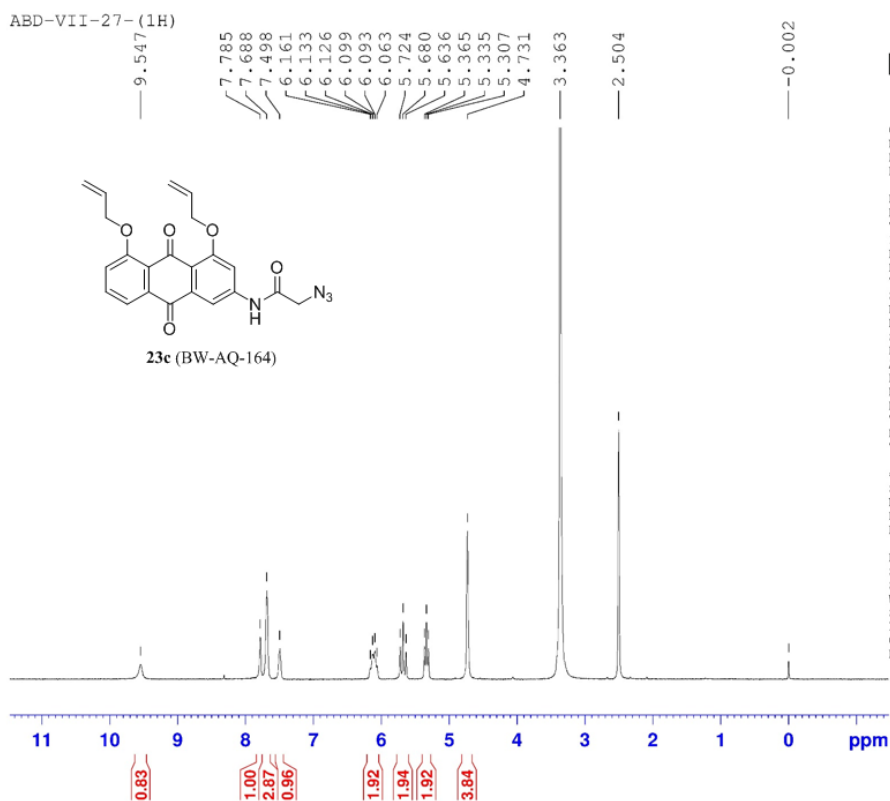
F2 - Acquisition Parameters
 Date_ 20151106
 Time 22.09
 INSTRUM spect
 PROBHD 5 mm F4BBO BB-
 PULPROG zgpg30
 TD 65536
 SOLVENT DMSO
 NS 10999
 DS 0
 SWH 24038.461 Hz
 FIDRES 0.366798 Hz
 AQ 1.3631488 sec
 RG 203
 DW 20.800 usec
 DE 6.50 usec
 TE 296.0 K
 D1 2.00000000 sec
 D11 0.03000000 sec
 TDO 1

===== CHANNEL f1 =====
 SFO1 100.6253441 MHz
 NUC1 13C
 P1 9.00 usec
 PLW1 62.00000000 W

===== CHANNEL f2 =====
 SFO2 400.1416006 MHz
 NUC2 1H
 CPDPRG2 waltz16
 PCPD2 90.00 usec
 PLW2 16.00000000 W
 PLW12 0.36267000 W
 PLW13 0.29376000 W

F2 - Processing parameters
 SI 32768
 SF 100.6152830 MHz
 KDW 0
 SSB 0
 LB 1.00 Hz
 GB 0
 PC 1.40

ABD-VII-27- (1H)



Current Data Parameters
 NAME ABD-VII-27-(1H)
 EXPNO 1
 PROCNO 1

F2 - Acquisition Parameters
 Date_ 20130123
 Time 13.21
 INSTRUM spect
 PROBHD 5 mm PABBO BB-
 PULPROG zg30
 TD 65536
 SOLVENT DMSO
 NS 16
 DS 2
 SWH 8012.820 Hz
 FIDRES 0.122266 Hz
 AQ 4.0894465 sec
 RG 144
 DW 62.400 usec
 DE 6.50 usec
 TE 294.5 K
 D1 1.00000000 sec
 TD0 1

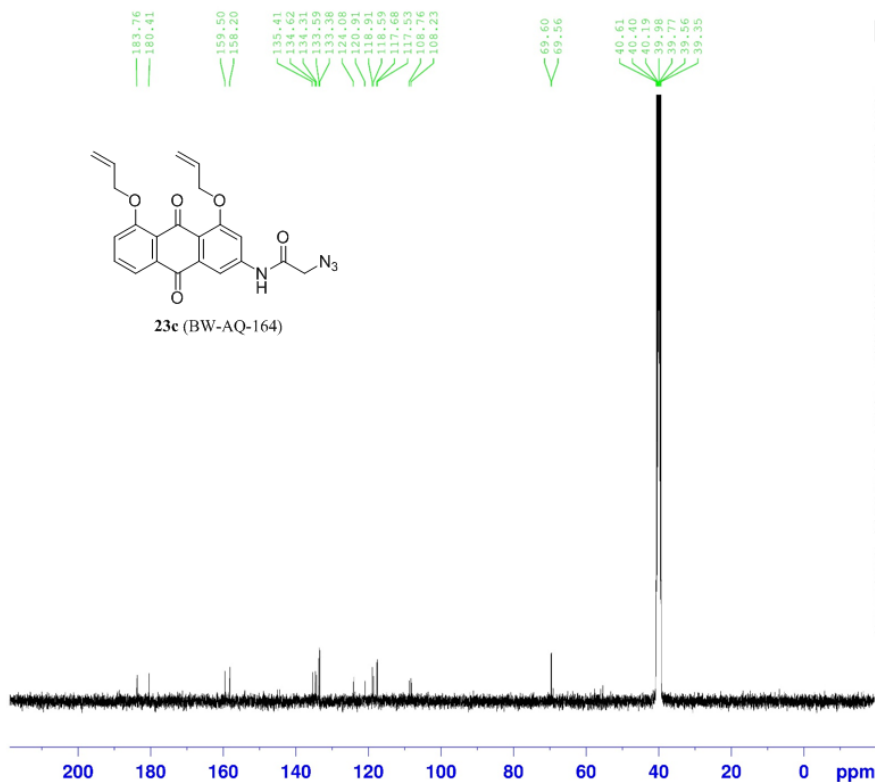
===== CHANNEL f1 =====
 SFO1 400.1424710 MHz
 NUC1 1H
 P1 13.50 usec
 PLW1 16.00000000 W

F2 - Processing parameters
 SI 65536
 SF 400.1399990 MHz
 WDW EM
 SSB 0
 LB 0.30 Hz
 GB 0
 PC 1.00

ABD-VII-27-13C- (11-12-15)



23e (BW-AQ-164)



Current Data Parameters
NAME ABD-VII-27-13C- (11-12-15)
EXPNO 1
PROCNO 1

F2 - Acquisition Parameters
Date_ 20151112
Time 22.18
INSTRUM spect
PROBHD 5 mm PABBO BB-
PULPROG zgpg30
TD 65536
SOLVENT DMSO
NS 11166
DS 0
SWH 24038.461 Hz
FIDRES 0.366798 Hz
AQ 1.3631488 sec
RG 203
DW 20.800 usec
DE 6.50 usec
TE 298.0 K
D1 2.0000000 sec
D11 0.0300000 sec
TD0 1

===== CHANNEL f1 =====
SFO1 100.6253441 MHz
NUC1 13C
P1 9.00 usec
PLW1 62.0000000 W

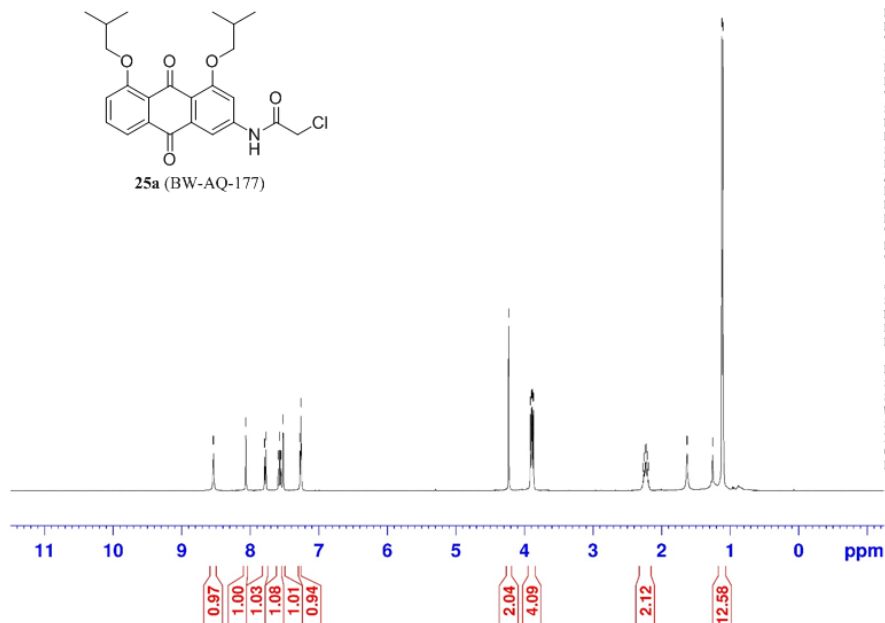
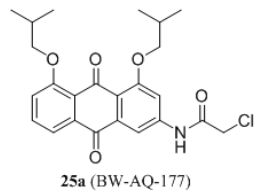
===== CHANNEL f2 =====
SFO2 400.1416006 MHz
NUC2 1H
PCPD2 waitz16
PCPD2 90.00 usec
PLW2 16.0000000 W
PLW12 9.36267000 W
PLW13 0.29376000 W

F2 - Processing parameters
SI 32768
SF 100.6152830 MHz
WDW EM
SSB 0
LB 1.00 Hz
GB 0
FC 1.40

ABD-VII-139 (1H)

8.538
8.066
7.791
7.772
7.591
7.571
7.551
7.524
7.521
7.276
7.262

4.230
3.914
3.898
3.887
3.871
2.272
2.256
2.240
2.226
2.211
2.195
1.629
1.254
1.121
1.104



Current Data Parameters
NAME ABD-VII-139(1H)
EXPNO 1
PROCNO 1

F2 - Acquisition Parameters
Date_ 20130509
Time 9.51
INSTRUM spect
PROBHD 5 mm PABBO BB-
PULPROG zg30
TD 65536
SOLVENT CDCl3
NS 16
DS 2
SWH 8012.820 Hz
FIDRES 0.122266 Hz
AQ 4.0894465 sec
RG 161
DW 62.400 usec
DE 6.50 usec
TE 298.0 K
D1 1.00000000 sec
TD0 1

===== CHANNEL f1 =====
SFO1 400.1424710 MHz
NUC1 1H
P1 13.50 usec
PLW1 16.00000000 W

F2 - Processing parameters
SI 65536
SF 400.1400078 MHz
WDW EM
SSB 0
LB 0.30 Hz
GB 0
PC 1.00

ABD-VII-139-13C-(11-25-15)



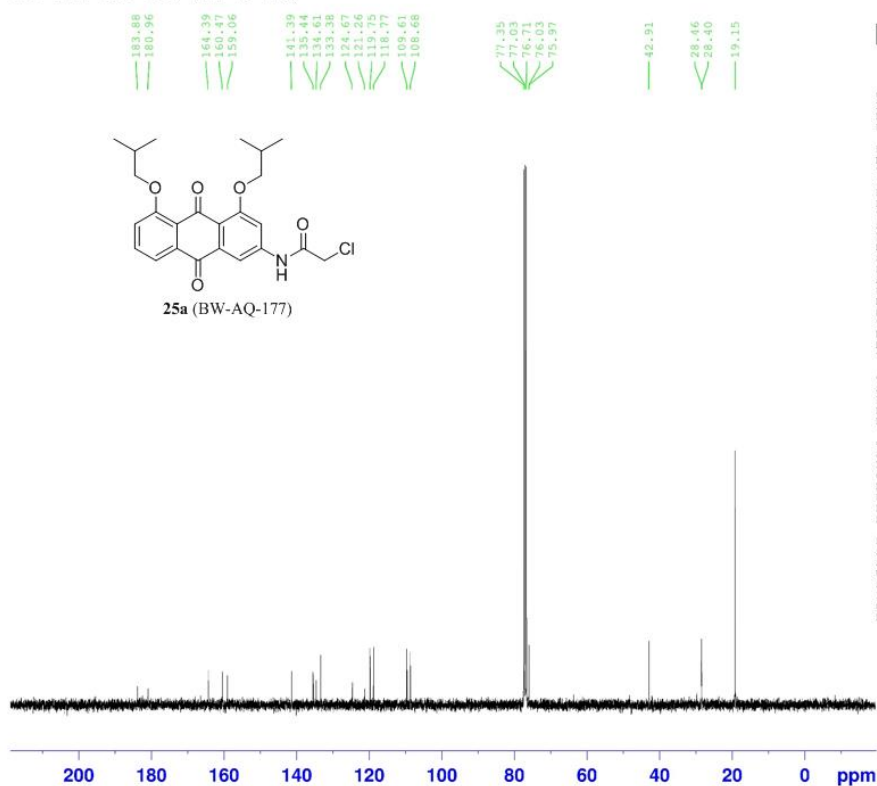
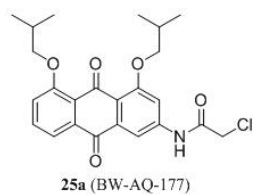
Current Data Parameters
 NAME ABD-VII-139-13C-(11-25-15)
 EXPNO 4
 PROCNO 3

F2 - Acquisition Parameters
 Date_ 20151125
 Time 17.00
 INSTRUM spect
 PROBRD 5 mm F4BBO BB-
 PULPROG zgpg30
 TD 65536
 SOLVENT CDCl3
 NS 264
 DS 4
 SWH 24038.461 Hz
 FIDRES 0.366798 Hz
 AQ 1.3631488 sec
 MC 203
 DM 20.800 usec
 DS 6.50 usec
 TE 298.0 K
 D1 2.00000000 sec
 D11 0.03000000 sec
 TD0 1

===== CHANNEL f1 =====
 SFO1 100.6253441 MHz
 NUC1 13C
 P1 9.00 usec
 PLW1 62.00000000 W

===== CHANNEL f2 =====
 SFO2 400.1416006 MHz
 NUC2 1H
 CPDPRG12 waltz16
 FCFD2 50.00 usec
 PLW2 16.00000000 W
 PLW12 0.36267000 W
 PLW13 0.29376000 W

F2 - Processing parameters
 SI 32768
 SF 100.6152830 MHz
 WDW EM
 SSB 0
 LB 1.00 Hz
 GB 0
 PC 1.40



ABD-VII-141-1H-(12-1-15)

8.678
8.084
8.079
7.778
7.759
7.592
7.572
7.523
7.518
7.277
7.258
4.079
4.070
3.910
3.891
3.874
2.269
2.263
2.253
2.247
2.236
2.230
2.220
2.214
2.203
2.197
1.266
1.167
1.162
1.150
1.146
1.123
1.121
1.106
1.104

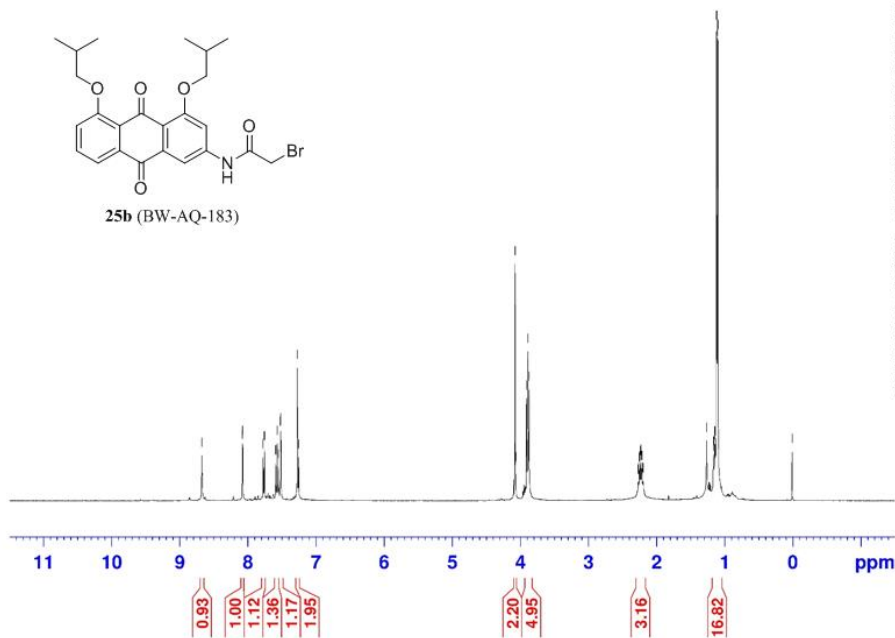
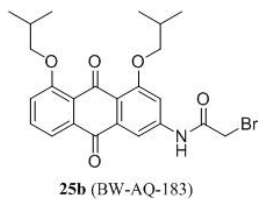


Current Data Parameters
NAME ABD-VII-141-1H-(12-1-15)
EXPNO 1
PROCNO 1

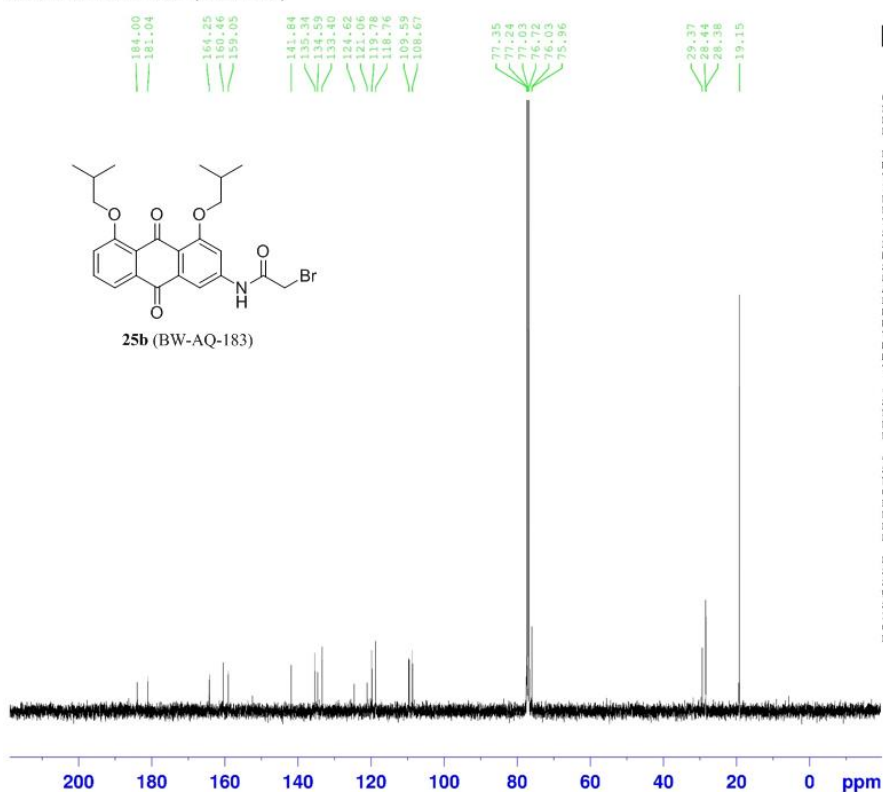
F2 - Acquisition Parameters
Date_ 20151201
Time 12.19
INSTRUM spect
PROBHD 5 mm PABBO BB-
PULPROG zg30
TD 65536
SOLVENT CDCl3
NS 16
DS 2
SWH 8012.820 Hz
FIDRES 0.122266 Hz
AQ 4.0894465 sec
RG 128
DW 62.400 usec
DE 6.50 usec
TE 298.0 K
D1 1.00000000 sec
TD0 1

===== CHANNEL f1 =====
SFOL 400.1424710 MHz
NUCL1 1H
P1 13.55 usec
PLWL 16.00000000 W

F2 - Processing parameters
SI 65536
SF 400.1400029 MHz
WDW EM
SSB 0
LA 0.30 Hz
GB 0
PC 1.00



ABD-VII-141-13C- (12-1-15)

**25b (BW-AQ-183)**

Current Data Parameters
NAME ABD-VII-141-13C- (12-1-15)
EXPNO 1
PROCNO 1

F2 - Acquisition Parameters
Date_ 20151201
Time 12.23
INSTRUM spect
PROBHD 5 mm PABBO BB-
PULPROG zgpg30
TD 65536
SOLVENT CDCl3
SS 221
DS 4
SWH 24038.461 Hz
FIDRES 0.366788 Hz
AQ 1.363188 sec
RG 90.5
DM 20.800 usec
DE 6.50 usec
TE 298.0 K
D1 2.00000000 sec
D11 0.03000000 sec
TD0 1

----- CHANNEL f1 -----
SFO1 100.6253441 MHz
NUC1 13C
P1 9.00 usec
PLW1 62.00000000 W

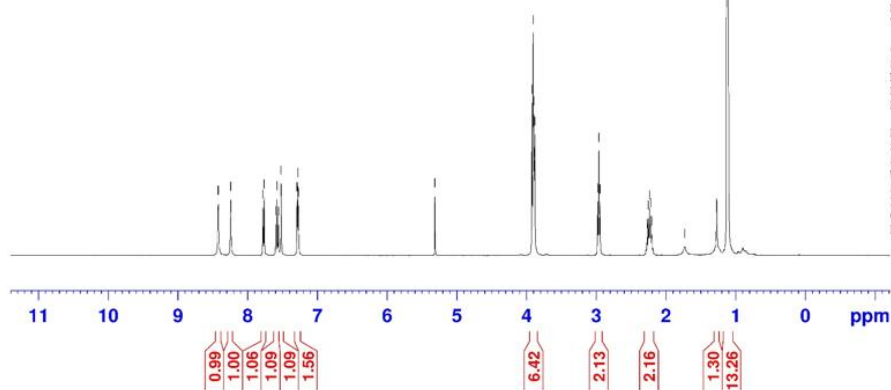
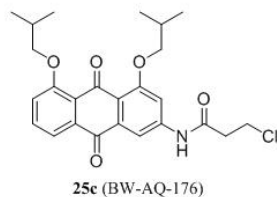
----- CHANNEL f2 -----
SFO2 400.1416066 MHz
NUC2 1H
P2 16.00 usec
PLW2 16.00000000 W
PLW12 0.36267000 W
PLW13 0.29376000 W

F2 - Processing parameters
SI 32768
SF 100.6152890 MHz
WDW EM
SSB 0
LB 1.00 Hz
GB 0
PC 1.40

ABD-VIII-9 (1H)

8.423
8.244
7.784
7.765
7.600
7.580
7.560
7.526
7.292
7.281
7.271

5.316
3.922
3.905
3.898
3.890
3.881
2.979
2.963
2.947
2.270
2.254
2.237
2.221
2.204
1.732
1.130
1.121
1.113
1.105



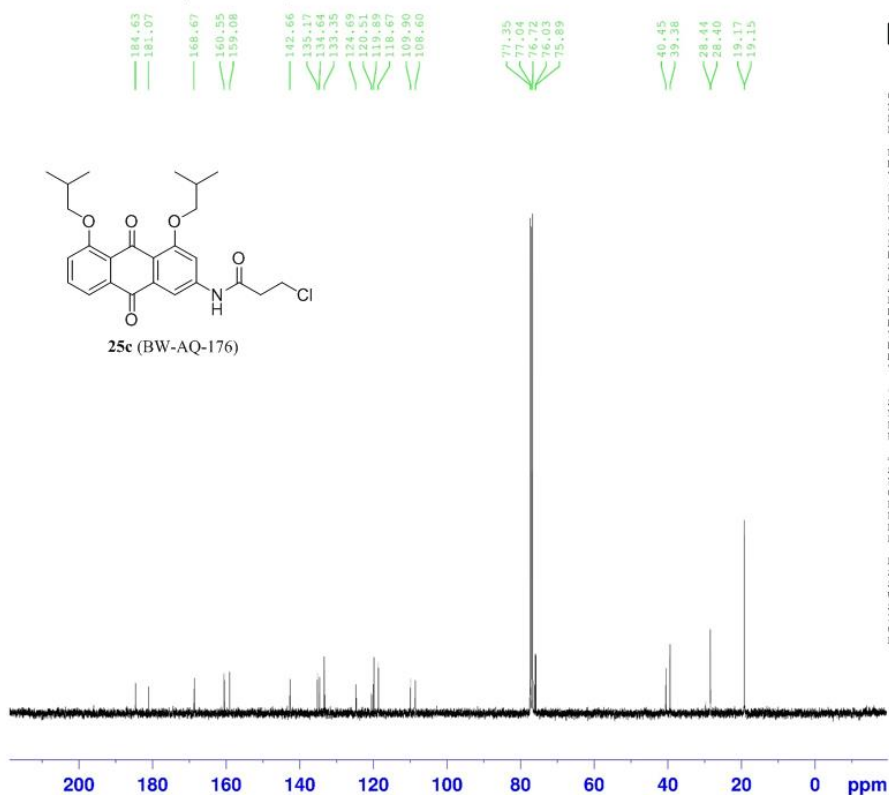
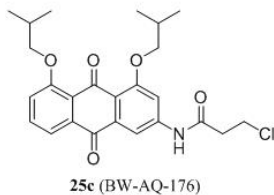
Current Data Parameters
NAME ABD-VIII-9 (1H)
EXPNO 1
PROCNO 1

F2 - Acquisition Parameters
Date_ 20130531
Time 13.09
INSTRUM spect
PROBHD 5 mm PABBO BB-
PULPROG zg30
TD 65536
SOLVENT CDCl3
NS 16
DS 2
SWH 8012.820 Hz
FIDRES 0.122266 Hz
AQ 4.0894465 sec
RG 128
DW 62.400 usec
DE 6.50 usec
TE 298.0 K
D1 1.00000000 sec
TD0 1

===== CHANNEL f1 =====
SF01 400.1424710 MHz
NUC1 1H
P1 13.50 usec
PLW1 16.00000000 W

F2 - Processing parameters
SI 65536
SF 400.1400000 MHz
WDW EM
SSB 0
LB 0.30 Hz
GB 0
PC 1.00

ABD-VIII-9-13C-(11-25-15)



Current Data Parameters
 NAME ABD-VIII-9-13C-(11-25-15)
 EXPNO 1
 PROCNO 1

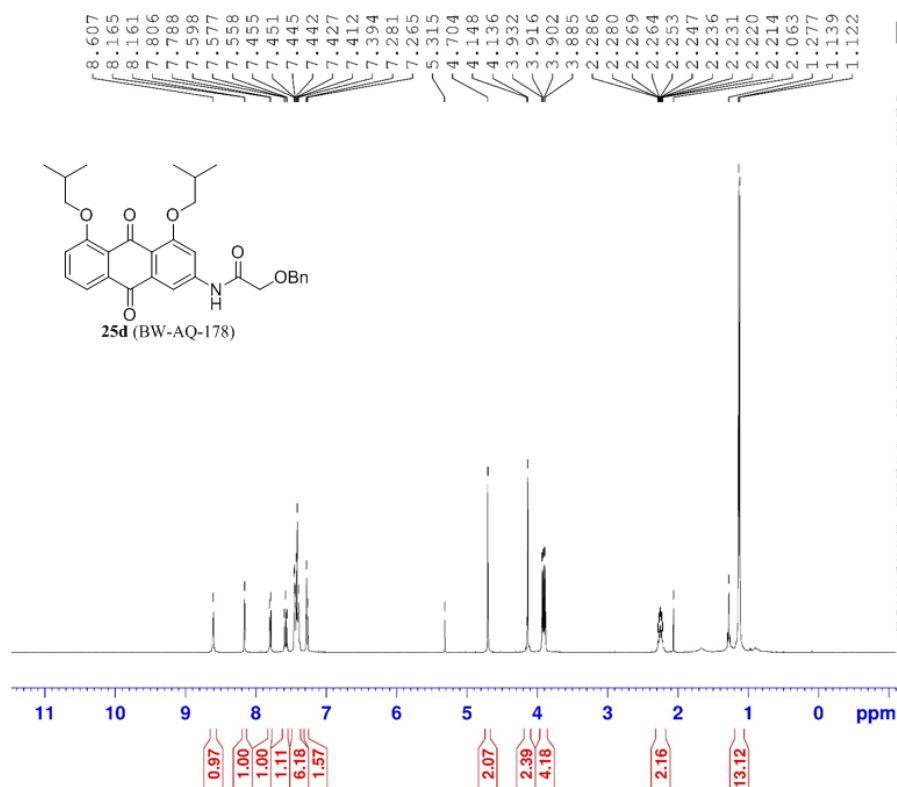
F2 - Acquisition Parameters
 Date_ 20151125
 Time 16.45
 INSTRUM spect
 PROBHD 5 mm PABBO BB-
 PULPROG zgpg30
 TD 65536
 SOLVENT CDCl3
 NS 208
 DS 4
 SWH 24038.461 Hz
 FIDRES 0.368798 Hz
 AQ 1.363188 sec
 RG 203
 DW 20.800 usec
 DE 8.50 usec
 TE 298.2 K
 D1 2.0000000 sec
 D11 0.0300000 sec
 TD0 1

===== CHANNEL f1 =====
 SFO1 100.6253441 MHz
 NUC1 13C
 P1 9.00 usec
 PLW1 62.00000000 W

===== CHANNEL f2 =====
 SFO2 400.1416006 MHz
 NUC2 1H
 CDEPRG12 waltz16
 PCPD2 90.00 usec
 PLW2 16.00000000 W
 PLW12 0.36879000 W
 PLW13 0.29376000 W

F2 - Processing parameters
 SI 32768
 SF 100.6152830 MHz
 WDW EM
 SSB 0
 LB 1.00 Hz
 GB 0
 PC 1.40

ABD-VIII-7 (1H)



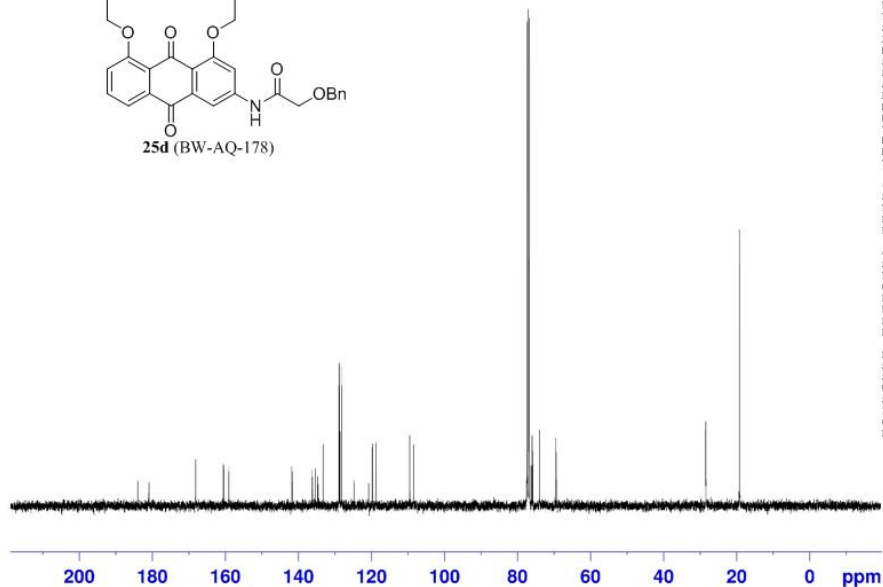
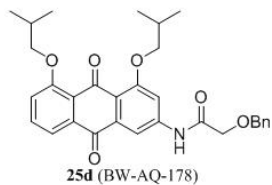
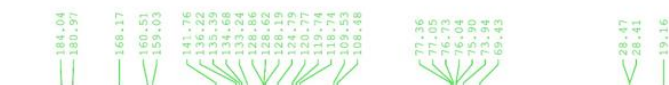
Current Data Parameters
NAME ABD-VIII-7(1H)
EXPNO 1
PROCNO 1

F2 - Acquisition Parameters
Date_ 20130527
Time 15.13
INSTRUM spect
PROBHD 5 mm PABBO BB-
PULPROG zg30
TD 65536
SOLVENT CDCl3
NS 16
DS 2
SWH 8012.820 Hz
FIDRES 0.122266 Hz
AQ 4.0894465 sec
RG 114
DW 62.400 usec
DE 6.50 usec
TE 298.0 K
D1 1.00000000 sec
TD0 1

===== CHANNEL f1 =====
SF01 400.1424710 MHz
NUC1 1H
P1 13.50 usec
PLW1 16.00000000 W

F2 - Processing parameters
SI 65536
SF 400.1400000 MHz
WDW EM
SSB 0
LB 0.30 Hz
GB 0
PC 1.00

ABD-VIII-7-13C- (11-25-15)



Current Data Parameters
 NAME ABD-VIII-7-13C- (11-25-15)
 EXPNO 1
 PROCNO 1

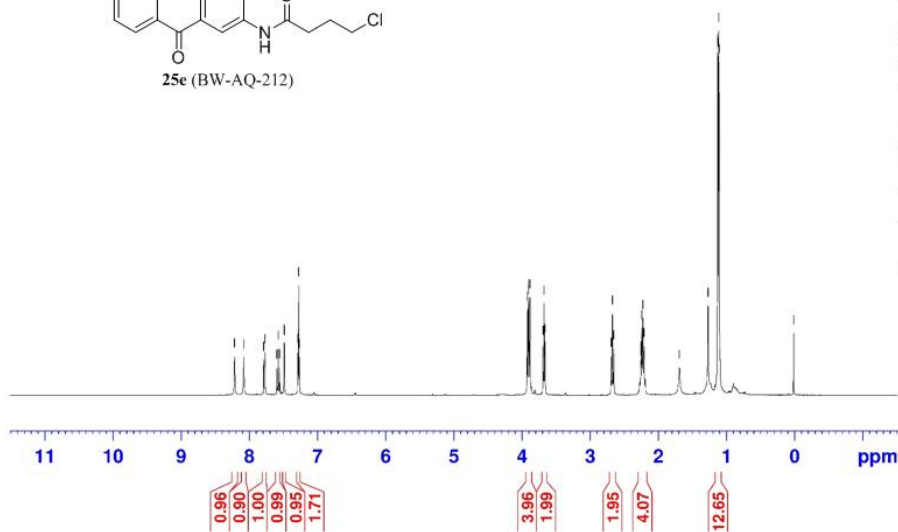
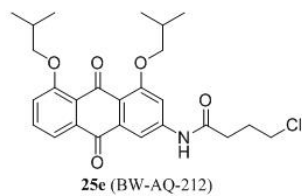
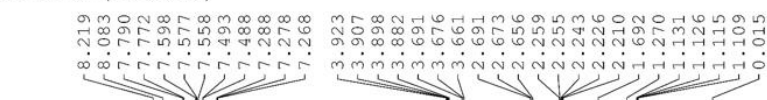
F2 - Acquisition Parameters
 Date_ 20151125
 Time 17.16
 INSTRUM spect
 PROBN 5 mm PABBO BB-
 PULPROG zgpg30
 ID 65536
 SOLVENT CDCl₃
 NS 240
 DS 4
 SWH 24038.461 Hz
 FIDRES 0.366798 Hz
 AQ 1.3631488 sec
 RG 203
 DW 20.800 usec
 DE 6.50 usec
 TE 298.1 K
 D1 2.0000000 sec
 D11 0.0300000 sec
 TD0 1

===== CHANNEL f1 =====
 SFO1 100.6253441 MHz
 NUC1 13C
 P1 9.00 usec
 PL1 62.0000000 W

===== CHANNEL f2 =====
 SFO2 400.1416006 MHz
 NUC2 1H
 CPDPRG2 wa1216
 FCFD2 30.00 usec
 PL12 16.0000000 W
 PL12 0.36267000 W
 PL13 0.29376000 W

F2 - Processing parameters
 SI 32768
 SF 100.6152830 MHz
 MDM EM
 SSB 0
 LB 1.00 Hz
 GB 0
 PC 1.40

ABD-VIII-11-1H- (11-23-15)



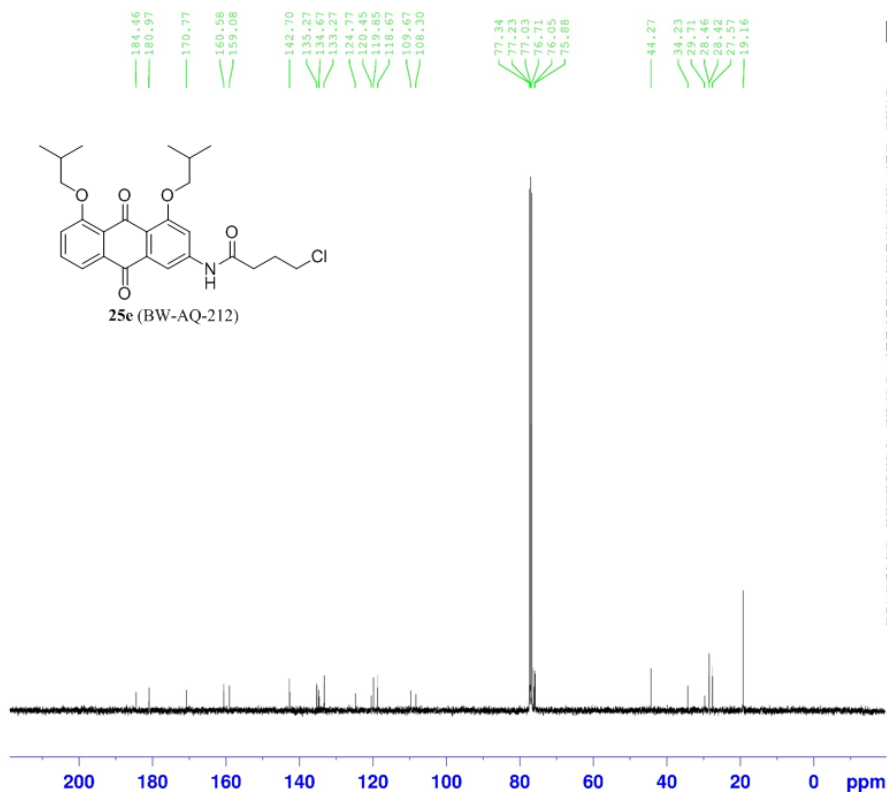
Current Data Parameters
 NAME ABD-VIII-11-1H- (11-23-15)
 EXPNO 1
 PROCNO 1

F2 - Acquisition Parameters
 Date_ 20151123
 Time 11:07
 INSTRUM spect
 PROBHD 5 mm PABBO BB-
 PULPROG zg30
 TD 65536
 SOLVENT CDCl₃
 NS 16
 DS 2
 SWH 8012.820 Hz
 FIDRES 0.122266 Hz
 AQ 4.069465 sec
 RG 128
 DW 62.400 usec
 DE 6.50 usec
 TE 298.0 K
 D1 1.00000000 sec
 TD0 1

CHANNEL f1
 SFO1 400.1424710 MHz
 NUC1 1H
 P1 13.55 usec
 PLN1 16.00000000 W

F2 - Processing parameters
 SI 65536
 SF 400.1400018 MHz
 WDW EM
 SSB 0
 LB 0.30 Hz
 GB 0
 PC 1.00

ABD-VIII-11-13C-(11-23-15)



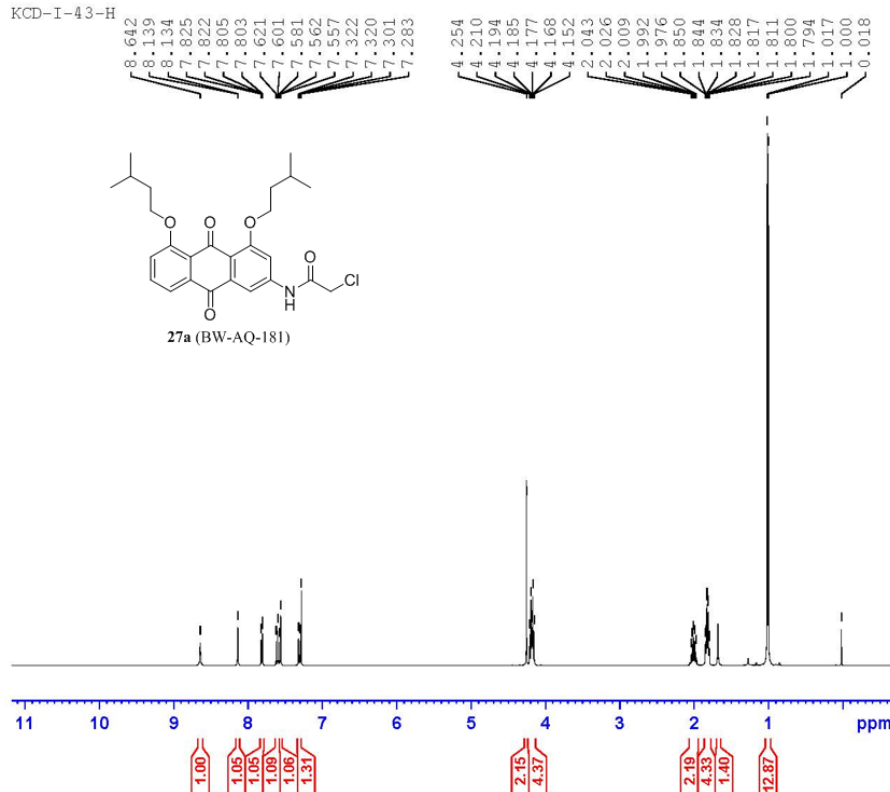
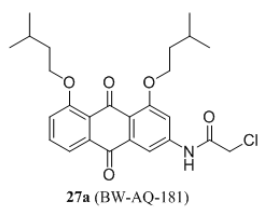
Current Data Parameters
 NAME ABD-VIII-11-13C-(11-23-15)
 EXPNO 1
 PROCNO 1

F2 - Acquisition Parameters
 Date_ 20151123
 Time 11.12
 INSTRUM spect
 PROBED 5 mm PABBO BB-
 PULPROG zgpg30
 TD 65536
 SOLVENT CDCl3
 NS 390
 DS 4
 SWH 24038.461 Hz
 FIDRES 0.366798 Hz
 AQ 1.3631488 sec
 RC 203
 DW 20.800 usec
 DS 6.50 usec
 TE 298.0 K
 D1 2.0000000 sec
 D11 0.0300000 sec
 TDC 1

===== CHANNEL f1 =====
 SFO1 100.625441 MHz
 NUC1 13C
 P1 9.00 usec
 PLW1 62.0000000 W
 ===== CHANNEL f2 =====
 SFO2 400.1416006 MHz
 NUC2 1H
 CPDPRG2 waltz16
 PCPD2 90.00 usec
 PLW2 16.0000000 W
 PLW12 0.36267000 W
 PLW13 0.29376000 W

F2 - Processing parameters
 SZ 32768
 SF 100.6152830 MHz
 NDNW EM
 SSB 0
 LB 1.00 Hz
 GB 0
 PC 1.40

KCD-I-43-H



Current Data Parameters
 NAME KCD-I-43-H
 EXPNO 1
 PROCNO 1

F2 - Acquisition Parameters
 Date_ 20151201
 Time 19.10
 INSTRUM spect
 PROBHD 5 mm PABBO BB-
 PULPROG zg30
 TD 65536
 SOLVENT CDCl3
 NS 16
 DS 2
 SWH 8012.820 Hz
 FIDRES 0.122266 Hz
 AQ 4.0894465 sec
 RG 128
 DW 62.400 usec
 DE 6.50 usec
 TE 298.0 K
 D1 1.00000000 sec
 TDO 1

===== CHANNEL f1 =====
 SFO1 400.1424710 MHz
 NUC1 1H
 P1 13.55 usec
 PLW1 16.00000000 W

F2 - Processing parameters
 SI 65536
 SF 400.1400000 MHz
 WDW EM
 SSB 0
 LB 0.30 Hz
 GB 0
 PC 1.00

KCD-I-43-C

183.89
181.00

164.41
160.53
159.09

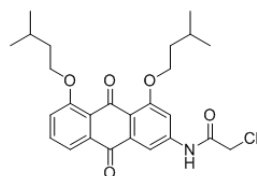
141.52
135.48
134.63
133.68

124.49
118.62
118.62
118.68
118.68
109.63
108.75

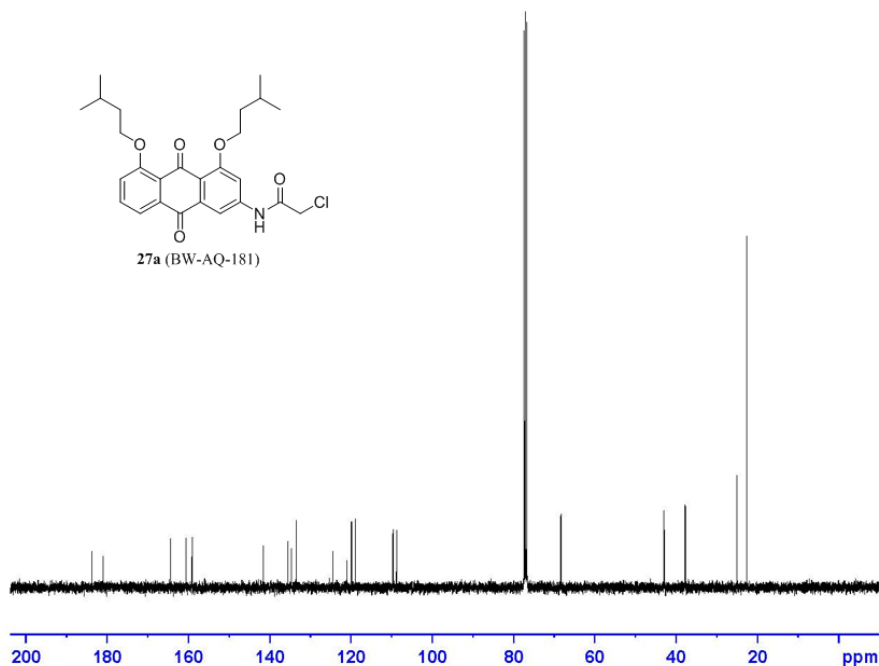
77.35
77.03
76.71
68.31
68.28

42.92
37.79
37.63

24.98
24.71
24.51



27a (BW-AQ-181)



Current Data Parameters
NAME KCD-I-43-C
EXPNO 2
PROCNO 1

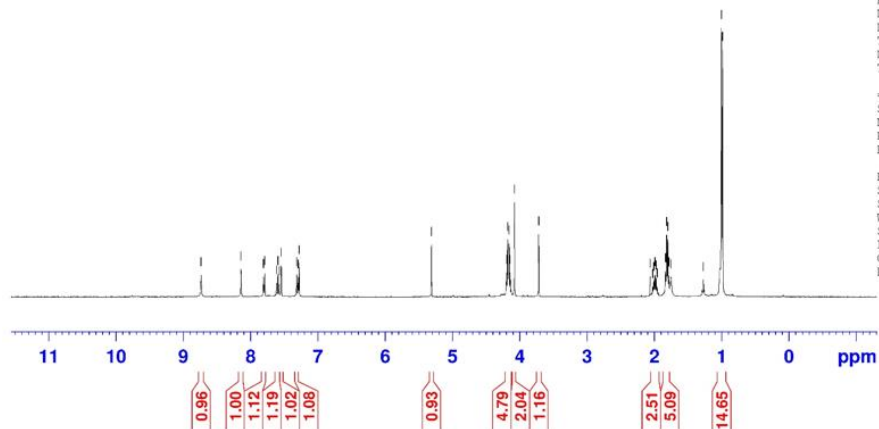
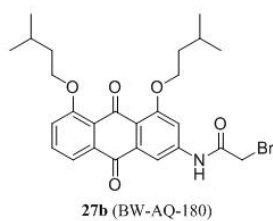
F2 - Acquisition Parameters
Date_ 20151201
Time_ 19.30
INSTRUM spect
PROBHD 5 mm PABBO BB-
PULPROG zgpg30
TD 65536
SOLVENT CDCl3
NS 191
DS 4
SWH 24038.461 Hz
FIDRES 0.366798 Hz
AQ 1.3631488 sec
RG 128
DW 20.800 usec
DE 6.50 usec
TE 298.0 K
D1 2.00000000 sec
D11 0.03000000 sec
TD0 1

===== CHANNEL f1 =====
SFO1 100.6253441 MHz
NUC1 13C
P1 9.00 usec
PLW1 62.00000000 W

===== CHANNEL f2 =====
SFO2 400.1416006 MHz
NUC2 1H
CPDPRG2 waltz16
PCPD2 90.00 usec
PLW2 16.00000000 W
PLW12 0.36267000 W
PLW13 0.29376000 W

F2 - Processing parameters
SI 32768
SF 100.6152830 MHz
WDW EM
SSB 0
LB 1.00 Hz
GB 0
PC 1.40

ABD-VII-133 (1H) F1



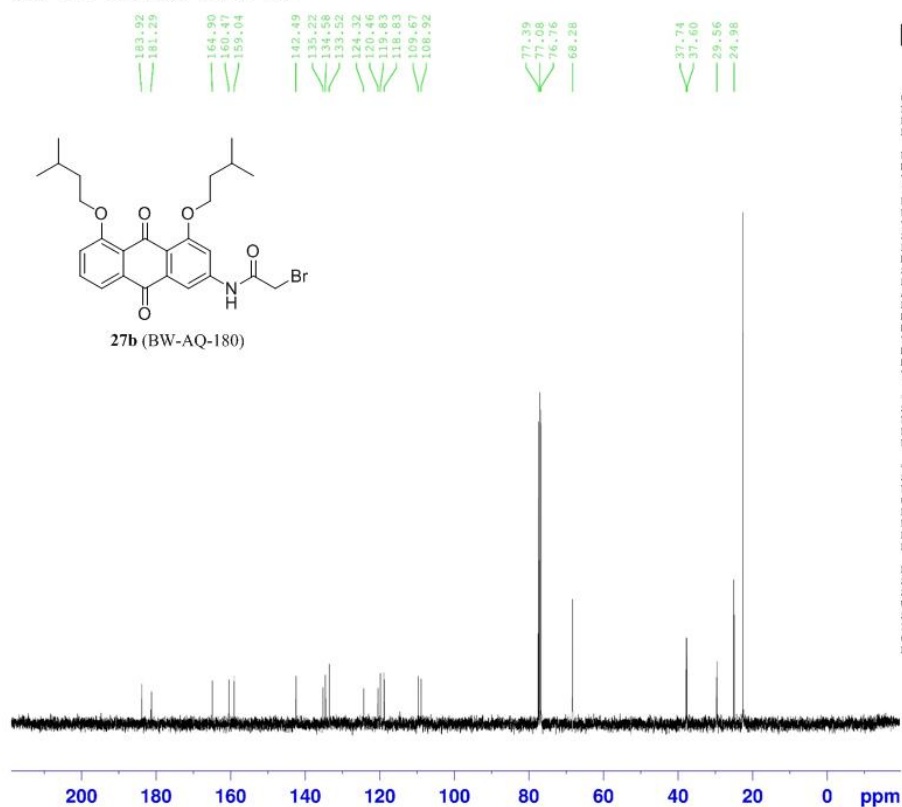
Current Data Parameters
 NAME ABD-VII-133(1H)F1
 EXPNO 1
 PROCNO 1

F2 - Acquisition Parameters
 Date_ 20130428
 Time 16.13
 INSTRUM spect
 PROBHD 5 mm PABBO BB-
 PULPROG zg30
 TD 65536
 SOLVENT CDCl3
 NS 16
 DS 2
 SWH 8012.820 Hz
 FIDRES 0.122266 Hz
 AQ 4.0894465 sec
 RG 128
 DW 62.400 usec
 DE 6.50 usec
 TE 298.0 K
 D1 1.00000000 sec
 TD0 1

===== CHANNEL f1 =====
 SFO1 400.1424710 MHz
 NUC1 1H
 P1 13.50 usec
 PLW1 16.00000000 W

F2 - Processing parameters
 SI 65536
 SF 400.1400000 MHz
 WDW EM
 SSB 0
 LB 0.30 Hz
 GB 0
 PC 1.00

ABD-VII-133-13C-(12-1-15)



Current Data Parameters
 NAME ABD-VII-133-13C-(12-1-15)
 EXPNO 1
 PROCNO 1

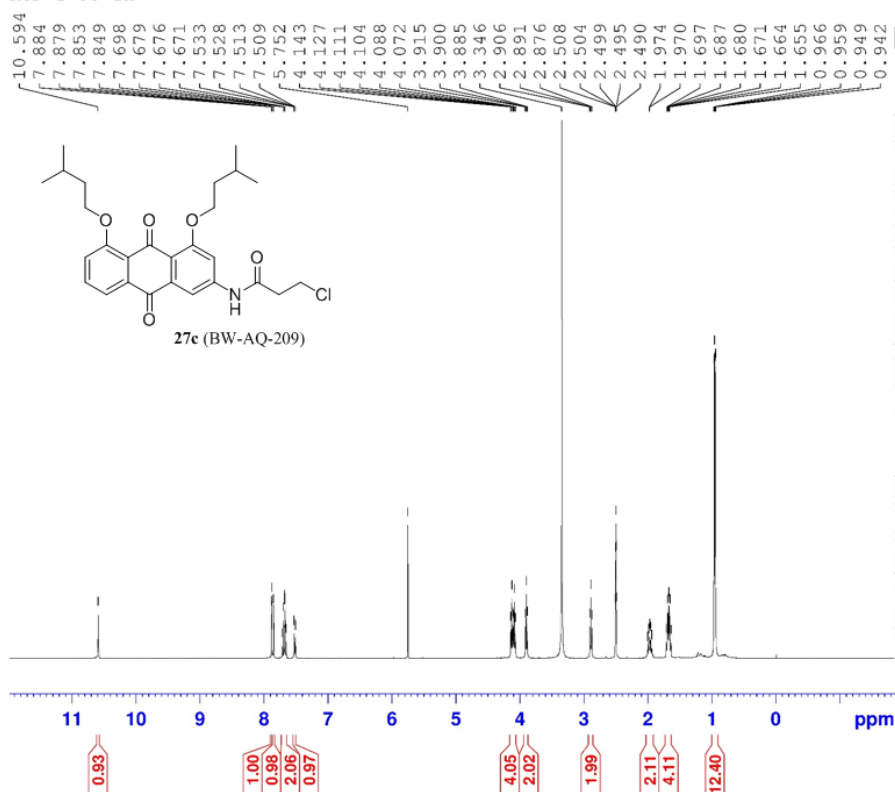
F2 - Acquisition Parameters
 Date_ 20151201
 Time 12.09
 INSTRUM spect
 PROBHD 5 mm FARB0 BB-
 PULPROG zgpg30
 TD 65536
 SOLVENT CDCl3
 NS 30
 DS 4
 SWH 24038.461 Hz
 FIDRES 0.366798 Hz
 AQ 1.3631488 sec
 RG 203
 DW 20.800 usec
 DE 6.50 usec
 TE 298.1 K
 D1 2.00000000 sec
 D11 0.03000000 sec
 TD0 1

===== CHANNEL f1 =====
 SFO1 100.6253441 MHz
 NUC1 13C
 P1 9.00 usec
 PLW1 62.00000000 W

===== CHANNEL f2 =====
 SFO2 400.1416006 MHz
 NUC2 1H
 CPDPRG2 waltz16
 PCPD2 90.00 usec
 PLW2 16.00000000 W
 PLW12 0.36267000 W
 PLW13 0.29376000 W

F2 - Processing parameters
 SI 32768
 SF 100.6152830 MHz
 WDW EM
 SSB 0
 LB 1.00 Hz
 GB 0
 PC 1.40

KCD-I-33-1H



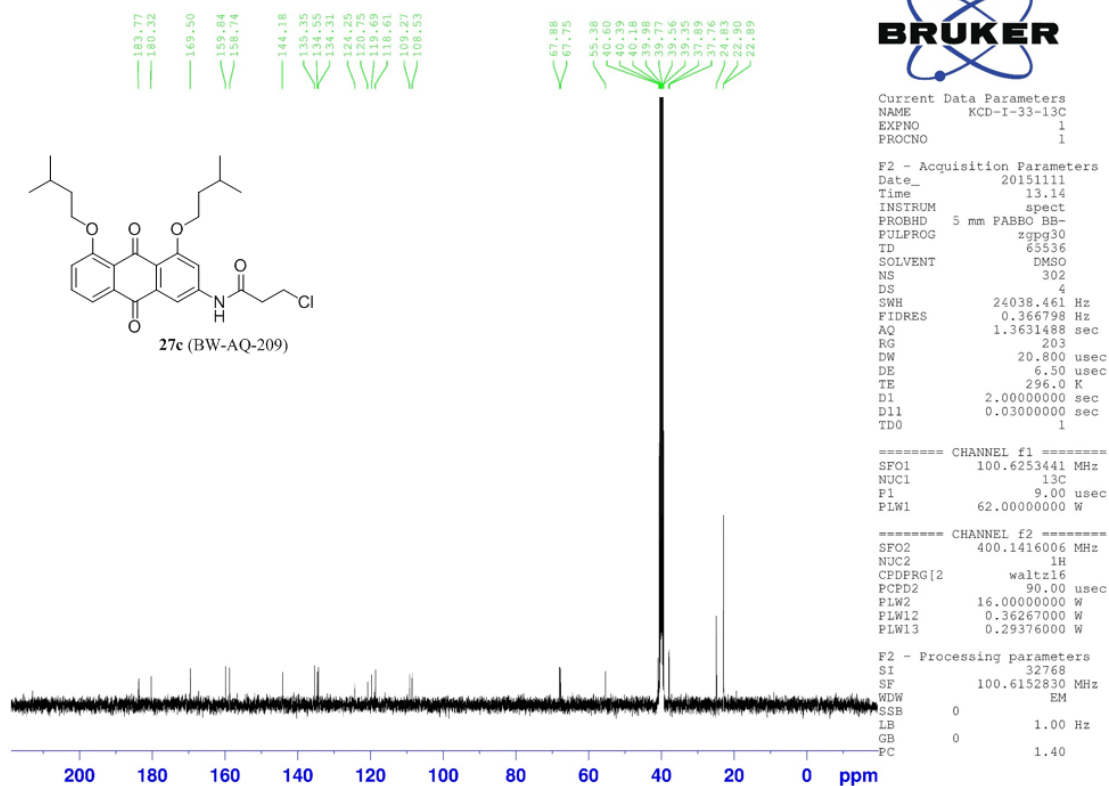
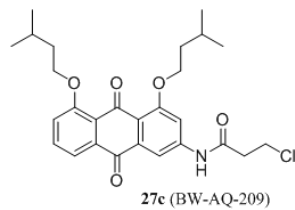
Current Data Parameters
 NAME KCD-I-33-1H
 EXPNO 1
 PROCNO 1

F2 - Acquisition Parameters
 Date_ 20151111
 Time 13.10
 INSTRUM spect
 PROBHD 5 mm PABBO BB-
 PULPROG zg30
 TD 65536
 SOLVENT DMSO
 NS 16
 DS 2
 SWH 8012.820 Hz
 FIDRES 0.122266 Hz
 AQ 4.0894465 sec
 RG 128
 DW 62.400 usec
 DE 6.50 usec
 TE 296.0 K
 D1 1.00000000 sec
 TD0 1

===== CHANNEL f1 =====
 SFO1 400.1424710 MHz
 NUC1 1H
 P1 13.55 usec
 PLW1 16.00000000 W

F2 - Processing parameters
 SI 65536
 SF 400.1400032 MHz
 WDW EM
 SSB 0
 LB 0.30 Hz
 GB 0
 FC 1.00

KCD-I-33-13C



Current Data Parameters
NAME KCD-I-33-13C
EXPNO 1
PROCNO 1

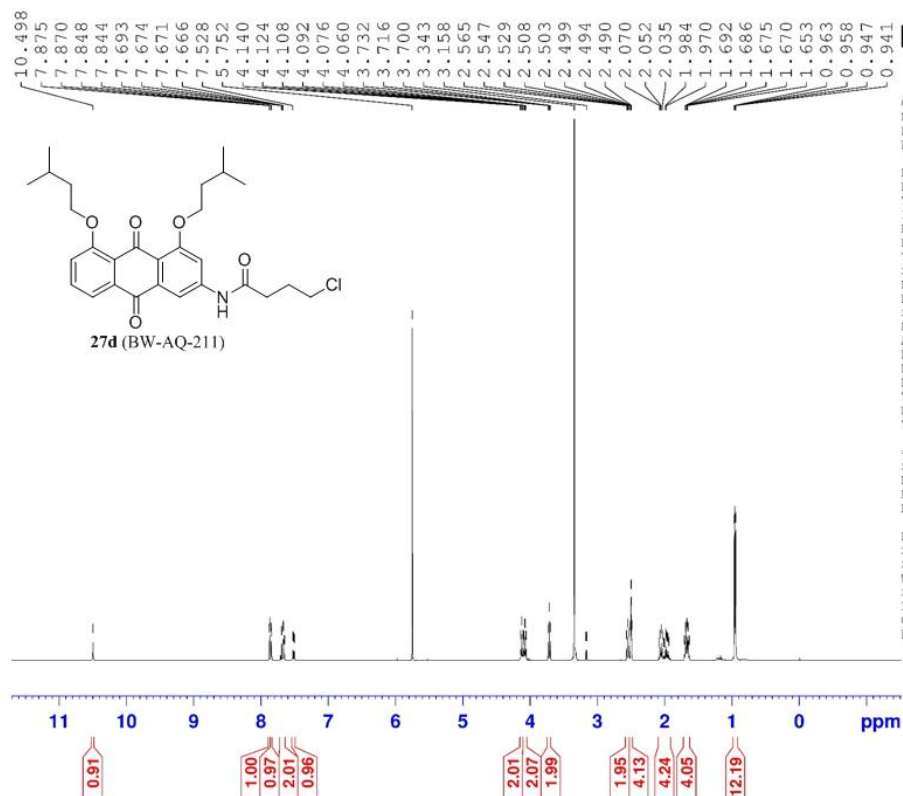
F2 - Acquisition Parameters
Date_ 20151111
Time 13.14
INSTRUM spect
PROBHD 5 mm PABBO BB-
PULPROG zgpg30
TD 65536
SOLVENT DMSO
NS 302
DS 4
SWH 24038.461 Hz
FIDRES 0.366798 Hz
AQ 1.3631488 sec
RG 203
DW 20.800 usec
DE 6.50 usec
TE 296.0 K
D1 2.00000000 sec
D11 0.03000000 sec
TD0 1

===== CHANNEL f1 =====
SFO1 100.6253441 MHz
NUC1 13C
P1 9.00 usec
PLW1 62.00000000 W

===== CHANNEL f2 =====
SFO2 400.1416006 MHz
NUC2 1H
CPDPRG[2] waltz16
PCPD2 90.00 usec
PLW2 16.00000000 W
PLW12 0.36267000 W
PLW13 0.29376000 W

F2 - Processing parameters
SI 32768
SF 100.6152830 MHz
WDW EM
SSB 0
LB 1.00 Hz
GB 0
PC 1.40

KCD-I-31-1H



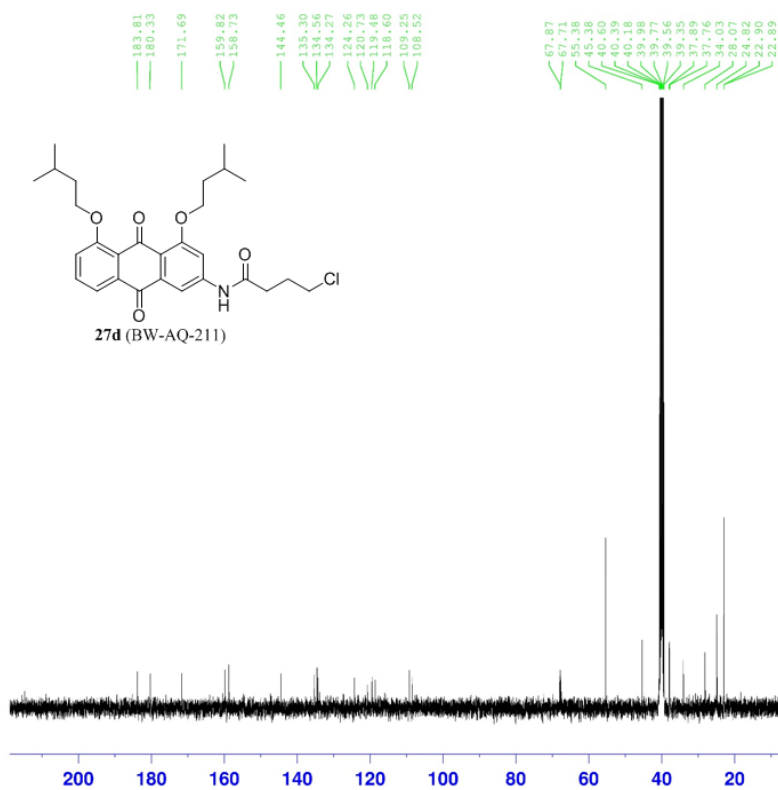
Current Data Parameters
 NAME KCD-I-31-1H
 EXPNO 1
 PROCNO 1

F2 - Acquisition Parameters
 Date_ 20151109
 Time 13.40
 INSTRUM spect
 PROBHD 5 mm PABBO BB-
 PULPROG zg30
 TD 65536
 SOLVENT DMSO
 NS 16
 DS 2
 SWH 8012.820 Hz
 FIDRES 0.122266 Hz
 AQ 4.0894465 sec
 RG 144
 DW 62.400 usec
 DE 6.50 usec
 TE 296.0 K
 D1 1.00000000 sec
 TD0 1

===== CHANNEL f1 =====
 SFO1 400.1424710 MHz
 NUC1 1H
 P1 13.55 usec
 PLW1 16.00000000 W

F2 - Processing parameters
 SI 65536
 SF 400.1400032 MHz
 WDW EM
 SSB 0
 LB 0.30 Hz
 GB 0
 PC 1.00

KCD-I-31-13C



Current Data Parameters
 NAME KCD-I-31-13C
 EXPNO 1
 PROCNO 1

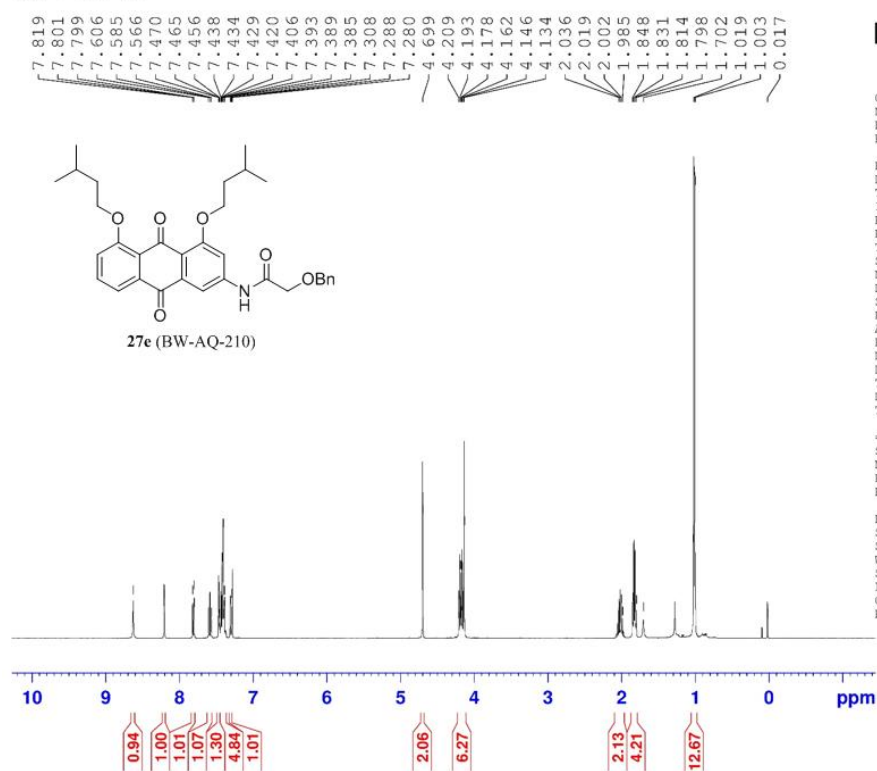
F2 - Acquisition Parameters
 Date_ 20151109
 Time 13.44
 INSTRUM spect
 PROBHD 5 mm PABBO BB-
 PULPROG zgpg30
 TD 65536
 SOLVENT DMSO
 NS 270
 DS 4
 SWH 24038.461 Hz
 FIDRES 0.366798 Hz
 AQ 1.3631488 sec
 RG 203
 DW 20.800 usec
 DE 6.50 usec
 TE 296.0 K
 D1 2.00000000 sec
 D11 0.03000000 sec
 TD0 1

===== CHANNEL f1 =====
 SFO1 100.6253441 MHz
 NUC1 13C
 P1 9.00 usec
 PLW1 62.00000000 W

===== CHANNEL f2 =====
 SFO2 400.1416006 MHz
 NUC2 1H
 CPDPRG[2] waltz16
 PCPD2 90.00 usec
 PLW2 16.00000000 W
 PLW12 0.36267000 W
 PLW13 0.29376000 W

F2 - Processing parameters
 SI 32768
 SF 100.6152830 MHz
 WDW EM
 SSB 0
 LB 1.00 Hz
 GB 0
 PC 1.40

KCD-I-39a-1H

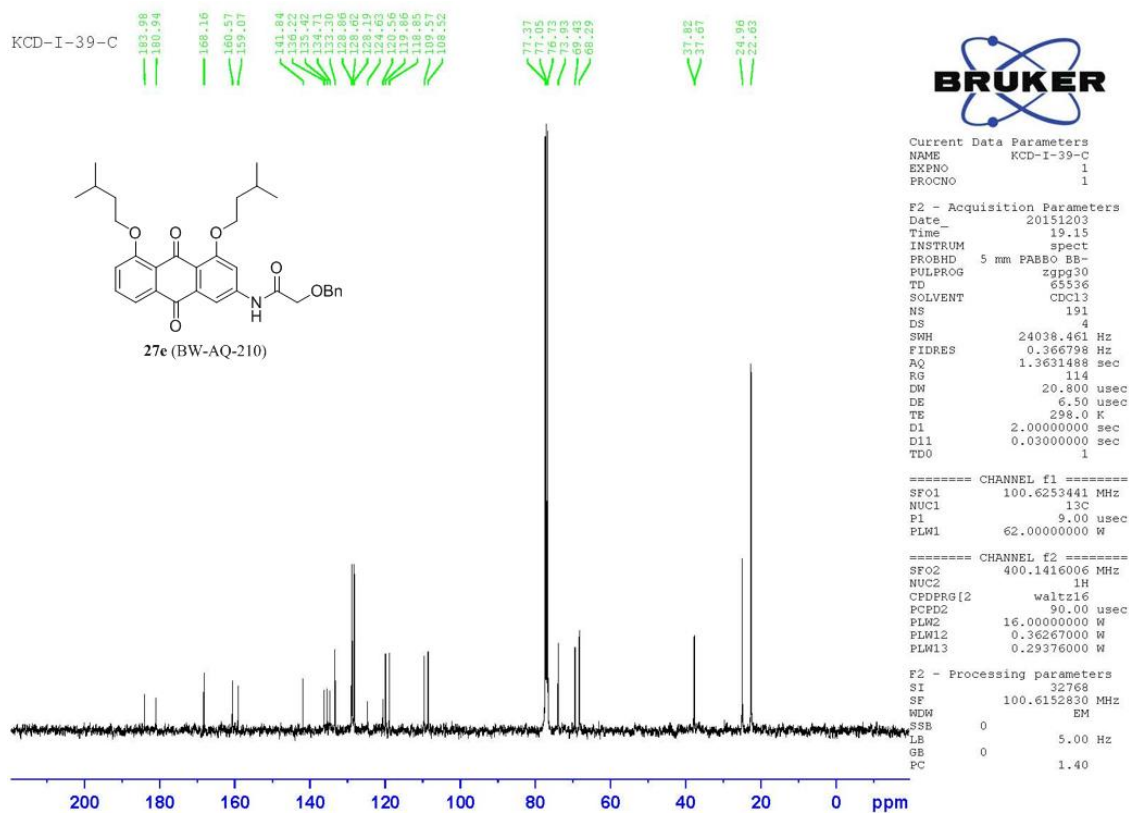


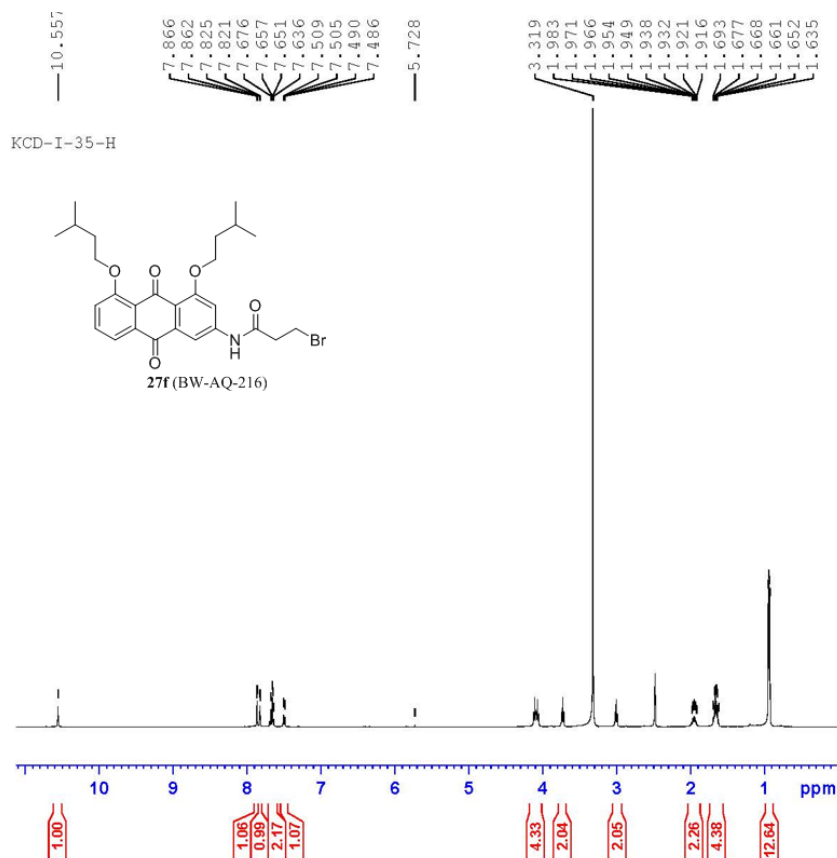
Current Data Parameters
 NAME KCD-I-39a-1H
 EXPNO 1
 PROCNO 1

F2 - Acquisition Parameters
 Date_ 20151117
 Time 16.48
 INSTRUM spect
 PROBHD 5 mm PABBO BB-
 PULPROG zg30
 TD 65536
 SOLVENT CDCl3
 NS 16
 DS 2
 SWH 8012.820 Hz
 FIDRES 0.122266 Hz
 AQ 4.0894465 sec
 RG 90.5
 DW 62.400 usec
 DE 6.50 usec
 TE 298.0 K
 D1 1.00000000 sec
 TD0 1

===== CHANNEL f1 =====
 SFO1 400.1424710 MHz
 NUC1 1H
 P1 13.55 usec
 PLW1 16.00000000 W

F2 - Processing parameters
 SI 65536
 SF 400.1400005 MHz
 WDW EM
 SSB 0
 LB 0.30 Hz
 GB 0
 FC 1.00





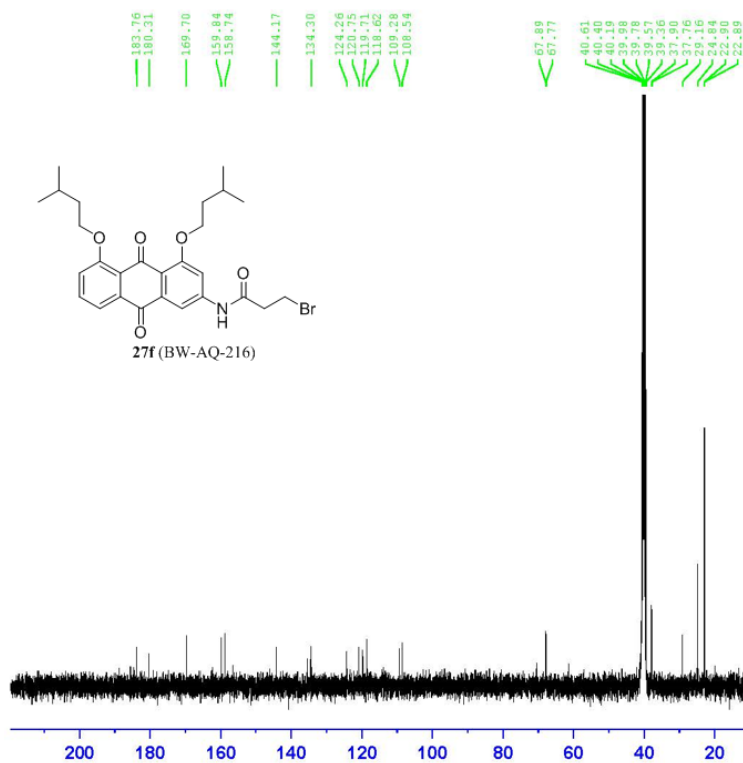
Current Data Parameters
 NAME KCD-I-35-H
 EXPNO 1
 PROCNO 1

F2 - Acquisition Parameters
 Date 20151130
 Time 17.57
 INSTRUM spect
 PROBHD 5 mm PABBO BB-
 PULPROG zg30
 TD 65536
 SOLVENT DMSO
 NS 16
 DS 2
 SWH 8012.820 Hz
 FIDRES 0.122266 Hz
 AQ 4.0894465 sec
 RG 114
 DW 62.400 usec
 DE 6.50 usec
 TE 298.0 K
 D1 1.00000000 sec
 TD0 1

===== CHANNEL f1 =====
 SF01 400.1424710 MHz
 NUC1 1H
 P1 13.55 usec
 PLW1 16.00000000 W

F2 - Processing parameters
 SI 65536
 SF 400.1400110 MHz
 WDW EM
 SSB 0
 LB 0.30 Hz
 GB 0
 PC 1.00

KCD-I-35-C13



Current Data Parameters
 NAME KCD-I-35-C13
 EXPNO 1
 PROCNO 1

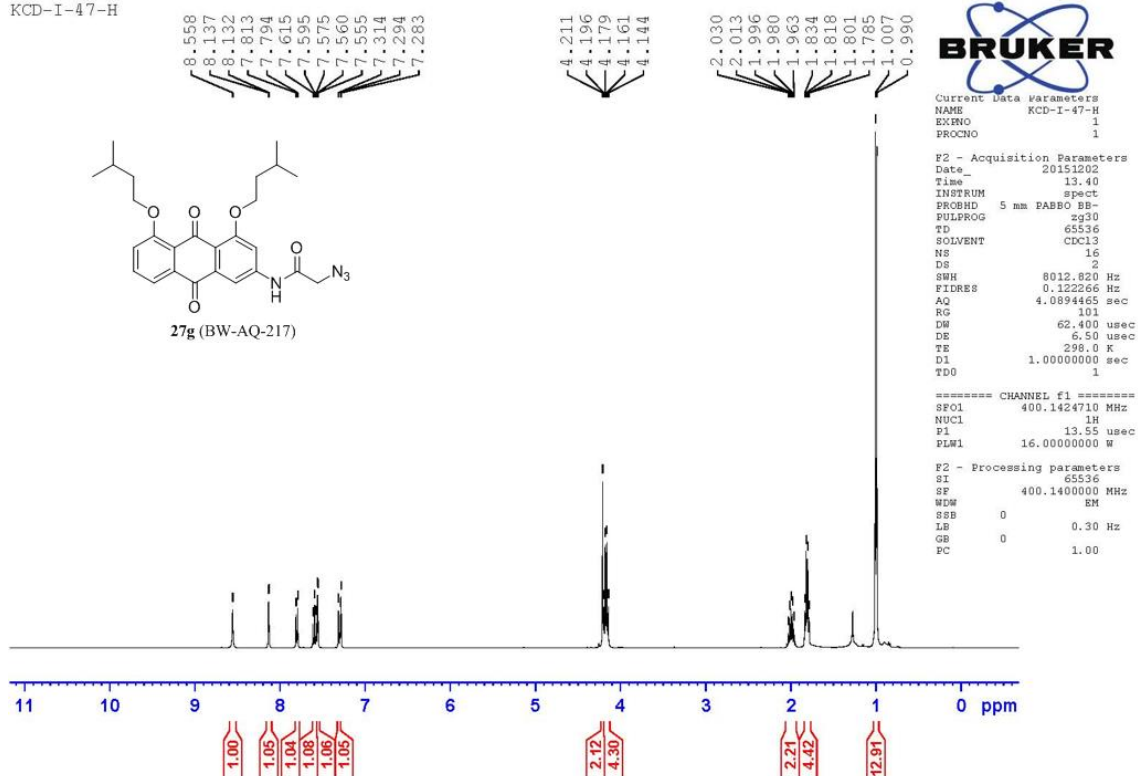
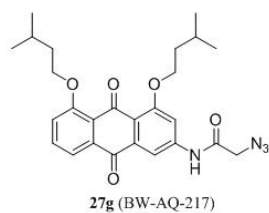
F2 - Acquisition Parameters
 Date 20151130
 Time 19.15
 INSTRUM spect
 PROBHD 5 mm PABBO BB-
 PULPROG zgpg30
 TD 65536
 SOLVENT DMSO
 NS 250
 DS 4
 SWH 24038.461 Hz
 FIDRES 0.366798 Hz
 AQ 1.3631488 sec
 RG 181
 DW 20.800 usec
 DE 6.50 usec
 TE 298.0 K
 D1 2.00000000 sec
 D11 0.03000000 sec
 TD0 1

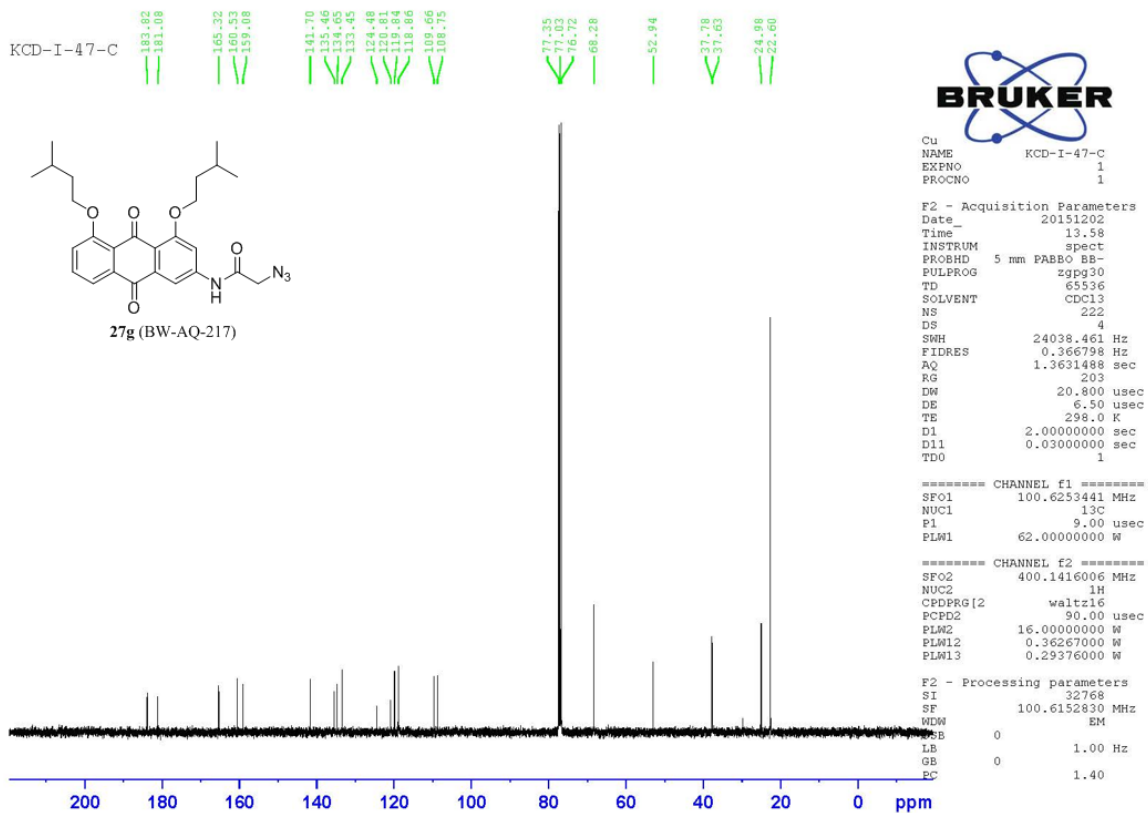
===== CHANNEL f1 =====
 SF01 100.6253441 MHz
 NUC1 13C
 P1 9.00 usec
 PLW1 62.00000000 W

===== CHANNEL f2 =====
 SF02 400.1416006 MHz
 NUC2 1H
 CPDPRG2 waltz16
 PCPD2 90.00 usec
 PLW2 16.00000000 W
 PLW12 0.36267000 W
 PLW13 0.29376000 W

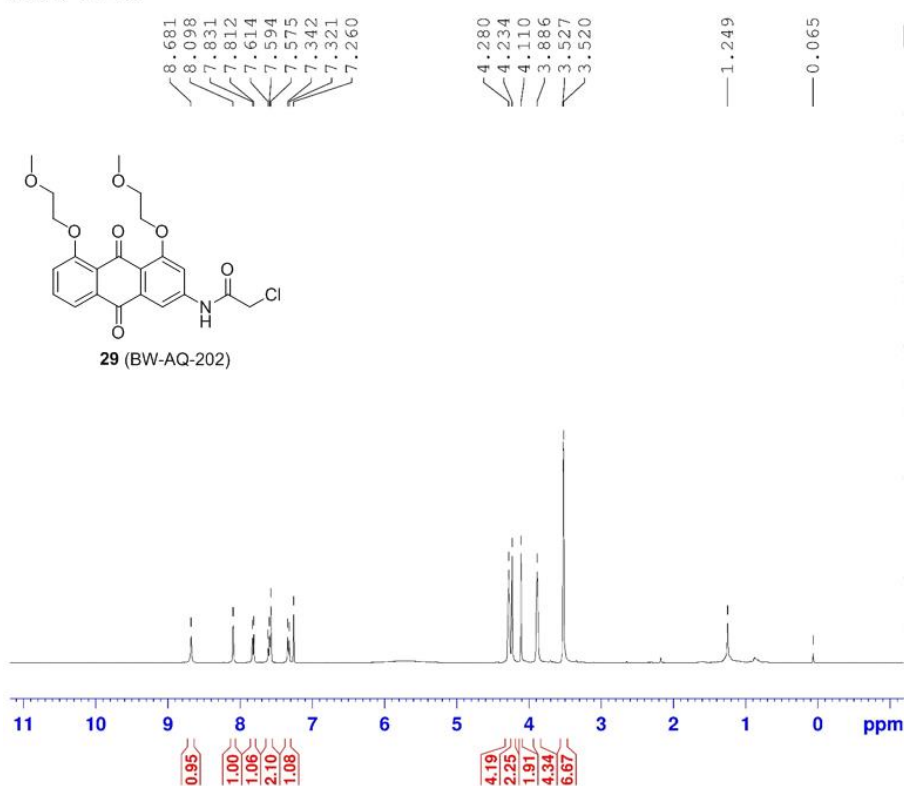
F2 - Processing parameters
 SI 32768
 SF 100.6152830 MHz
 ACQW EM
 SSB 0
 LB 1.00 Hz
 GB 0
 PC 1.40

KCD-I-47-H





ABD-X-89-1H



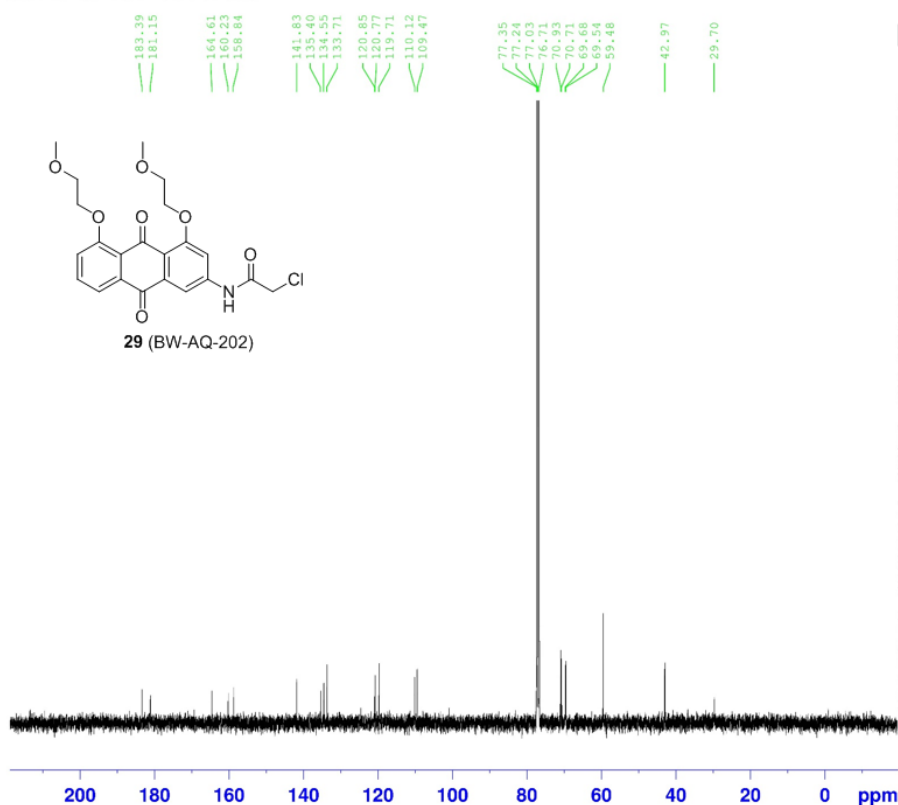
Current Data Parameters
NAME ABD-X-89-1H
EXPNO 1
PROCNO 1

F2 - Acquisition Parameters
Date_ 20140228
Time 10.23
INSTRUM spect
PROBHD 5 mm PABBO BB-
PULPROG zg30
TD 65536
SOLVENT CDCl3
NS 16
DS 2
SWH 8012.820 Hz
FIDRES 0.122266 Hz
AQ 4.0894465 sec
RG 161
DW 62.400 usec
DE 6.50 usec
TE 298.0 K
D1 1.00000000 sec
TD0 1

===== CHANNEL f1 =====
SF01 400.1424710 MHz
NUC1 1H
P1 13.50 usec
PLW1 16.00000000 W

F2 - Processing parameters
SI 65536
SF 400.1400083 MHz
WDW EM
SSB 0
LB 0.30 Hz
GB 0
PC 1.00

ABD-X-89-13C- (12-2-15)



Current Data Parameters
 NAME ABD-X-89-13C-(12-2-15)
 EXPNO 1
 PROCNO 1

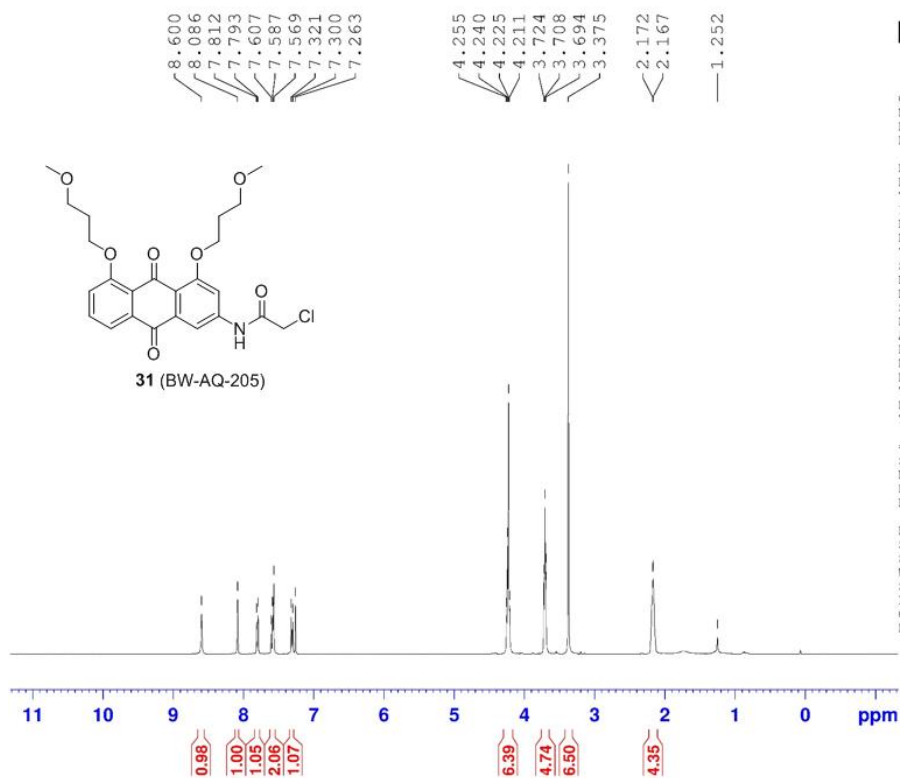
F2 - Acquisition Parameters
 Date_ 20151202
 Time 12.17
 INSTRUM spect
 PROBHD 5 mm PABBO BB-
 PULPROG zgpg30
 TD 65536
 SOLVENT CDCl3
 NS 303
 DS 4
 SWH 24038.461 Hz
 FIDRES 0.366798 Hz
 AQ 1.3631488 sec
 RG 114
 DW 20.800 usec
 DE 6.50 usec
 TE 298.0 K
 D1 2.00000000 sec
 D11 0.03000000 sec
 TD0 1

===== CHANNEL f1 =====
 SFO1 100.6253441 MHz
 NUC1 13C
 P1 9.00 usec
 PLW1 62.00000000 W

===== CHANNEL f2 =====
 SFO2 400.1416006 MHz
 NUC2 1H
 CPDPRG2 waltz16
 PCPD2 90.00 usec
 PLW2 16.00000000 W
 PLW12 0.36267000 W
 PLW13 0.29376000 W

F2 - Processing parameters
 S1 32768
 SF 100.6152830 MHz
 WDW EM
 SSB 0
 LB 1.00 Hz
 GB 0
 PC 1.40

ABD-X-111-1H



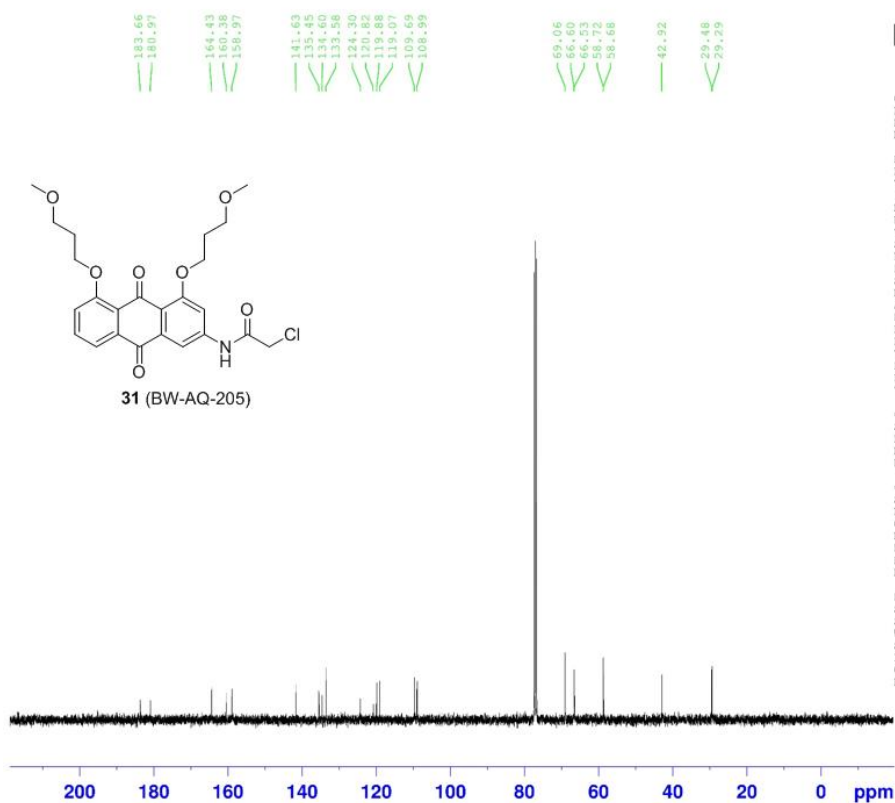
Current Data Parameters
 NAME ABD-X-111-1H
 EXPNO 1
 PROCNO 1

F2 - Acquisition Parameters
 Date_ 20140303
 Time 13.55
 INSTRUM spect
 PROBHD 5 mm PABBO BB-
 PULPROG zg30
 TD 65536
 SOLVENT CDCl3
 NS 16
 DS 2
 SWH 8012.820 Hz
 FIDRES 0.122266 Hz
 AQ 4.089465 sec
 RG 128
 DW 62.400 usec
 DE 6.50 usec
 TE 298.0 K
 D1 1.00000000 sec
 TD0 1

===== CHANNEL f1 =====
 SF01 400.1424710 MHz
 NUC1 1H
 P1 13.50 usec
 PLW1 16.00000000 W

F2 - Processing parameters
 SI 65536
 SF 400.1400073 MHz
 WDW EM
 SSB 0
 LB 0.30 Hz
 GB 0
 FC 1.00

ABD-X-111-13C- (12-4-15)



Current Data Parameters
 NAME ABD-X-111-13C- (12-4-15)
 EXPNO 1
 PROCNO 1

F2 - Acquisition Parameters
 Date 20151204
 Time 12.05
 INSTRUM spect
 PROBHD 5 mm PABBO BB
 PULPROG zgpg30
 TD 65536
 SOLVENT CDCl3
 NS 114
 DS 4
 SWH 24038.461 Hz
 FIDRES 0.366798 Hz
 AQ 1.3631488 sec
 RG 203
 DW 20.800 usec
 DE 6.50 usec
 TE 298.1 K
 D1 2.00000000 sec
 D11 0.03000000 sec
 TD0 1

===== CHANNEL f1 =====
 SFO1 100.6253441 MHz
 NUC1 13C
 P1 9.00 usec
 PLW1 62.00000000 W

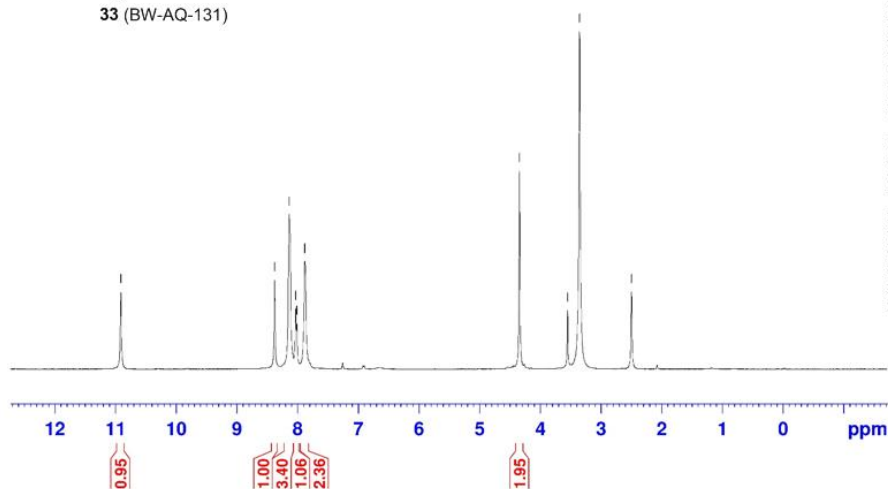
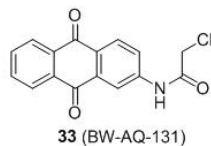
===== CHANNEL f2 =====
 SFO2 400.1416006 MHz
 NUC2 1H
 CPDPRG12 waltz16
 PCPD2 90.00 usec
 PLW2 16.00000000 W
 PLW12 0.36267000 W
 PLW13 0.29376000 W

F2 - Processing parameters
 SI 32768
 SF 100.6152830 MHz
 WDW EM
 SSB 0
 LB 1.00 Hz
 GB 0
 PC 1.40

DCF-VI-14-1H-(1-7-16)

— 10.915
 8.381
 8.141
 8.034
 8.015
 7.885
 7.878

— 4.345
 3.553
 3.356
 — 2.499

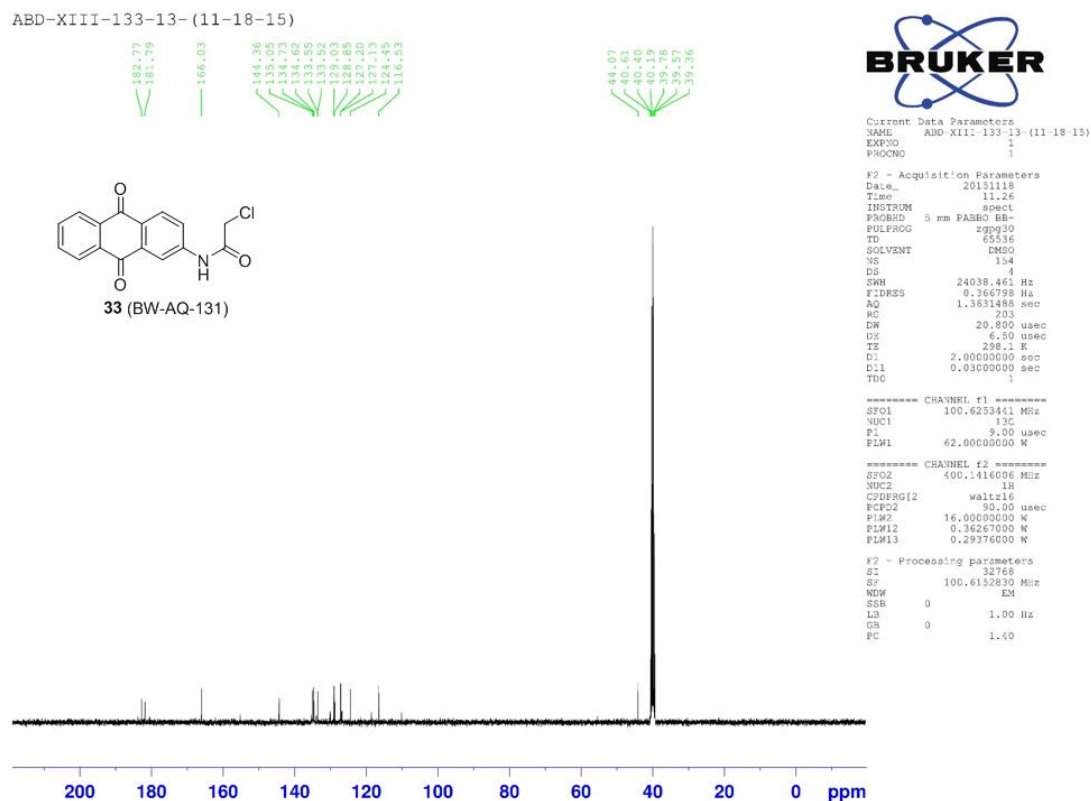


Current Data Parameters
 NAME DCF-VI-14-1H-(1-7-16)
 EXPNO 1
 PROCNO 1

F2 - Acquisition Parameters
 Date_ 20160107
 Time 13.20
 INSTRUM spect
 PROBHD 5 mm PABBO BB-
 PULPROG zg30
 TD 65536
 SOLVENT DMSO
 NS 16
 DS 2
 SWH 8012.820 Hz
 FIDRES 0.122266 Hz
 AQ 4.0894465 sec
 RG 128
 DW 62.400 usec
 DE 6.50 usec
 TE 298.0 K
 D1 1.00000000 sec
 TDO 1

===== CHANNEL f1 =====
 SFO1 400.1424710 MHz
 NUC1 1H
 P1 13.55 usec
 PLW1 16.00000000 W

F2 - Processing parameters
 SI 65536
 SF 400.1400033 MHz
 WDW EM
 SSB 0
 LB 0.30 Hz
 GB 0
 PC 1.00



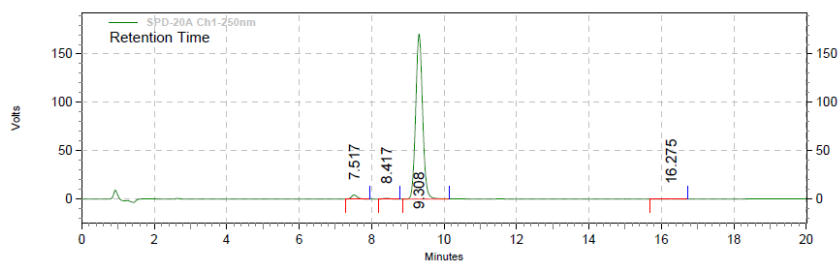
Appendix B HPLC data for the stability studies described in Chapter 1

Stability Studies at Simulated Physiological Conditions of Selected Compounds

HPLC spectra of BW-AQ-101.

0 min. at 37 °C.

Data File: C:\Documents and Settings\User\Desktop\alex\073015\LC-20.10001 7-30-2015 11-49-17
 AM.dat
 Method: C:\EZStart\Projects\Default\Method\tea\5~100.met
 Acquired: 7/30/2015 11:51:18 AM
 Printed: 2/16/2016 10:48:18 AM

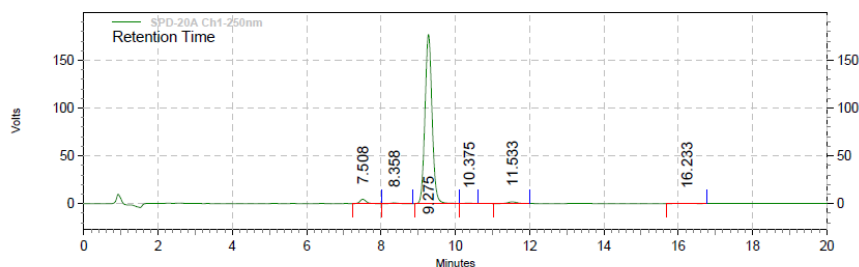


SPD-20A
Ch1-250nm
Results

Retention Time	Area	Area %	Height	Height %
7.517	47084	2.03	4205	2.39
8.417	9506	0.41	787	0.45
9.308	2258709	97.20	170597	97.02
16.275	8407	0.36	252	0.14
Totals	2323706	100.00	175841	100.00

120 min. at 37 °C.

Data File: C:\Documents and Settings\User\Desktop\alex\073015\LC-20.10001 7-30-2015 2-06-11 PM.d
 Method: C:\EZStart\Projects\Default\Method\tea\5~100.met
 Acquired: 7/30/2015 3:02:17 PM
 Printed: 2/16/2016 10:53:12 AM

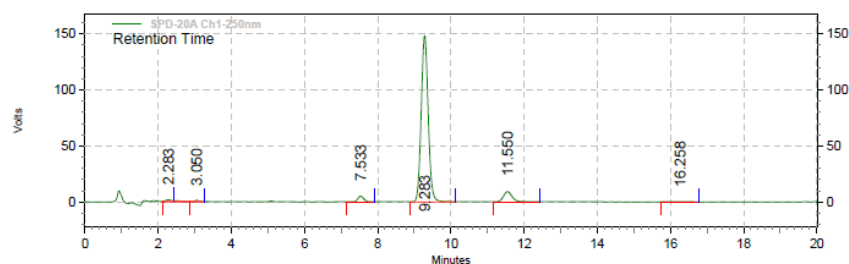


SPD-20A
Ch1-250nm
Results

Retention Time	Area	Area %	Height	Height %
7.508	52749	2.15	4583	2.48
8.358	8777	0.36	698	0.38
9.275	2346525	95.60	176910	95.84
10.375	7268	0.30	339	0.18
11.533	30527	1.24	1771	0.96
16.233	8791	0.36	297	0.16
Totals	2454637	100.00	184598	100.00

24 h. at 37 °C.

Data File: C:\Documents and Settings\User\Desktop\alex\073015\LC-20.10001 7-31-2015 11-02-27
 AM.dat
 Method: C:\EZStart\Projects\Default\Method\tea\5~100.met
 Acquired: 7/31/2015 11:03:33 AM
 Printed: 2/16/2016 10:58:56 AM



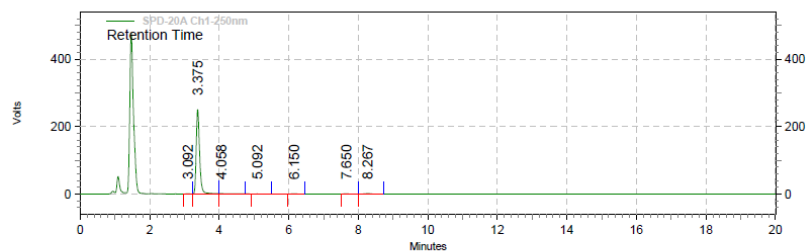
SPD-20A
 Ch1-250nm
 Results

Retention Time	Area	Area %	Height	Height %
2.283	16969	0.77	1621	0.98
3.050	10008	0.45	1348	0.81
7.533	57878	2.62	5118	3.09
9.283	1965117	88.89	148338	89.46
11.550	153604	6.95	9142	5.51
16.258	7052	0.32	241	0.15
Totals	2210628	100.00	165808	100.00

HPLC spectra of BW-AQ-112.

0 min. at 37 °C.

Data File: C:\Documents and Settings\User\Desktop\alex\07-24-15\LC-20.10001 7-24-2015 11-47-09
 AM.dat
 Method: C:\EZStart\Projects\Default\Method\tea\5~100.met
 Acquired: 7/24/2015 11:49:31 AM
 Printed: 2/16/2016 10:37:18 AM

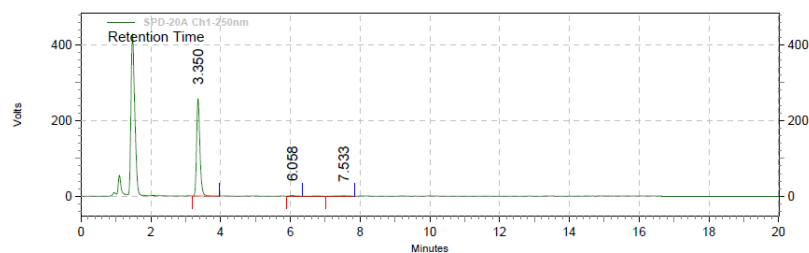


SPD-20A
 Ch1-250nm
 Results

Retention Time	Area	Area %	Height	Height %
3.092	7520	0.41	1216	0.47
3.375	1729038	94.66	250435	97.32
4.058	40897	2.24	1606	0.62
5.092	7530	0.41	394	0.15
6.150	12423	0.68	1278	0.50
7.650	9017	0.49	714	0.28
8.267	20153	1.10	1682	0.65
Totals	1826578	100.00	257325	100.00

120 min. at 37 °C.

Data File: C:\Documents and Settings\User\Desktop\alex\07-24-15\LC-20.10001 7-24-2015 1-36-16
 PM.dat
 Method: C:\EZStart\Projects\Default\Method\tea\5~100.met
 Acquired: 7/24/2015 1:37:32 PM
 Printed: 2/16/2016 10:41:05 AM



SPD-20A

Ch1-250nm

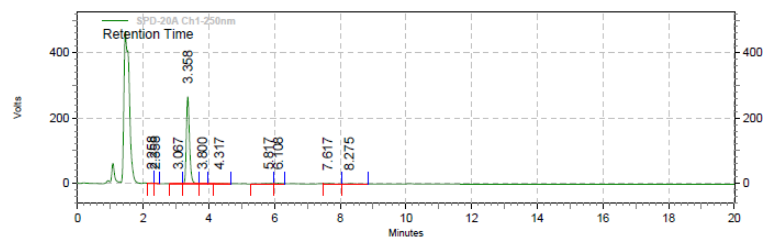
Results

Retention Time	Area	Area %	Height	Height %
3.350	1702230	98.37	257317	99.14
6.058	13849	0.80	1409	0.54
7.533	14298	0.83	818	0.32

Totals	1730377	100.00	259544	100.00
--------	---------	--------	--------	--------

24 h. at 37 °C.

Data File: C:\Documents and Settings\User\Desktop\alex\07-24-15\LC-20.10001 7-25-2015 2-27-17
 PM.dat
 Method: C:\EZStart\Projects\Default\Method\tea\5~100.met
 Acquired: 7/25/2015 2:27:50 PM
 Printed: 2/16/2016 10:45:40 AM



SPD-20A

Ch1-250nm

Results

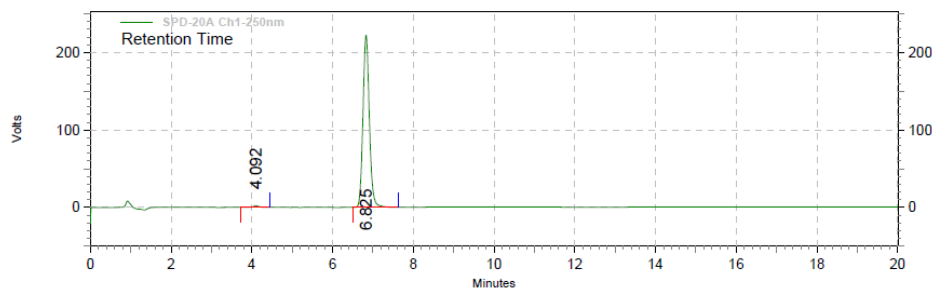
Retention Time	Area	Area %	Height	Height %
2.258	9395	0.49	1236	0.44
2.358	7997	0.42	1399	0.50
3.067	11617	0.61	1274	0.46
3.358	1781142	93.04	266649	95.76
3.800	17405	0.91	1349	0.48
4.317	19182	1.00	1617	0.58
5.817	21360	1.12	1317	0.47
6.108	18919	0.99	1778	0.64
7.617	16808	0.88	1265	0.45
8.275	10499	0.55	569	0.20

Totals	1914324	100.00	278453	100.00
--------	---------	--------	--------	--------

HPLC spectra of BW-AQ-124.

0 min. at 37 °C.

Data File: C:\Documents and Settings\User\Desktop\alex\07-23-15\LC-20.10001 7-23-2015 11-46-36
 AM.dat
 Method: C:\EZStart\Projects\Default\Method\tea\5~100.met
 Acquired: 7/23/2015 11:48:35 AM
 Printed: 2/16/2016 10:11:50 AM

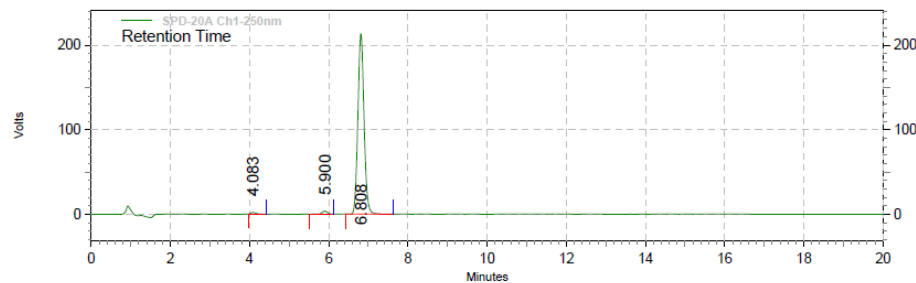


SPD-20A
Ch1-250nm
Results

Retention Time	Area	Area %	Height	Height %
4.092	22350	0.90	2275	1.01
6.825	2455344	99.10	222106	98.99
Totals	2477694	100.00	224381	100.00

120 min. at 37 °C.

Data File: C:\Documents and Settings\User\Desktop\alex\07-23-15\LC-20.10001 7-23-2015 3-11-41
 PM.dat
 Method: C:\EZStart\Projects\Default\Method\tea\5~100.met
 Acquired: 7/23/2015 3:12:52 PM
 Printed: 2/16/2016 10:18:49 AM

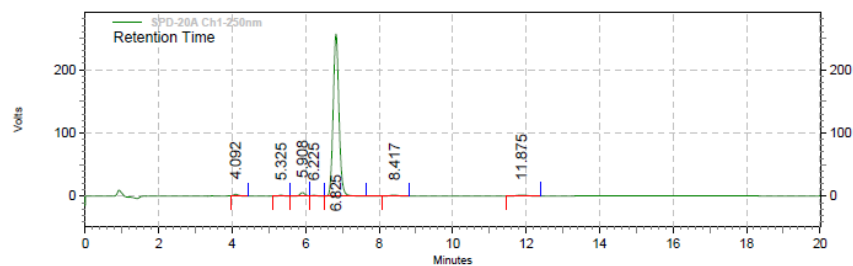


SPD-20A
Ch1-250nm
Results

Retention Time	Area	Area %	Height	Height %
4.083	21718	0.92	2258	1.03
5.900	35376	1.50	3616	1.65
6.808	2307843	97.59	213388	97.32
Totals	2364937	100.00	219262	100.00

24 h. at 37 °C.

Data File: C:\Documents and Settings\User\Desktop\alex\07-23-15\LC-20.10001 7-24-2015 10-18-50
 AM.dat
 Method: C:\EZStart\Projects\Default\Method\tea\5~100.met
 Acquired: 7/24/2015 10:20:12 AM
 Printed: 2/16/2016 10:22:37 AM



SPD-20A
 Ch1-250nm
 Results

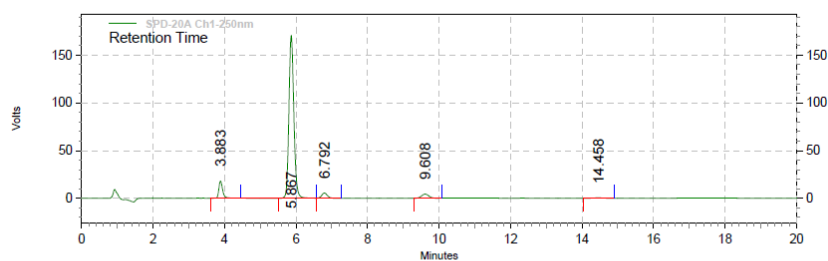
Retention Time	Area	Area %	Height	Height %
4.092	28710	0.96	2831	1.05
5.325	12510	0.42	1400	0.52
5.908	55101	1.85	5627	2.08
6.225	14556	0.49	1316	0.49
6.825	2808746	94.19	256037	94.60
8.417	25224	0.85	1659	0.61
11.875	37217	1.25	1787	0.66

Totals	2982064	100.00	270657	100.00
--------	---------	--------	--------	--------

HPLC spectra of BW-AQ-131.

0 min. at 37 °C.

Data File: C:\Documents and Settings\User\Desktop\alex\07-23-15\LC-20.10001 7-23-2015 12-33-41
 PM.dat
 Method: C:\EZStart\Projects\Default\Method\tea\5~100.met
 Acquired: 7/23/2015 12:35:29 PM
 Printed: 2/16/2016 10:24:12 AM



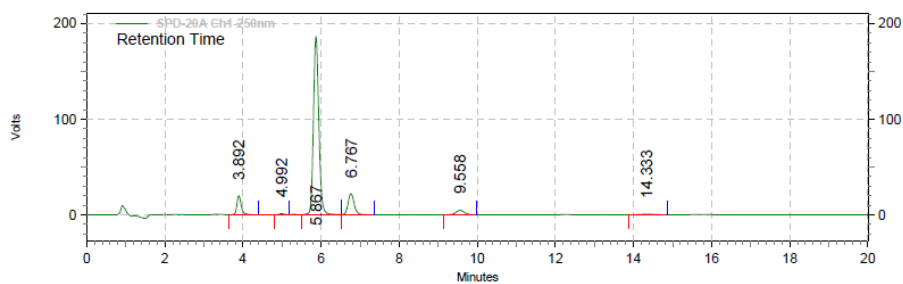
SPD-20A
 Ch1-250nm
 Results

Retention Time	Area	Area %	Height	Height %
3.883	138630	7.28	18061	9.08
5.867	1630455	85.57	170592	85.72
6.792	61653	3.24	5538	2.78
9.608	64615	3.39	4384	2.20
14.458	10033	0.53	425	0.21

Totals	1905386	100.00	199000	100.00
--------	---------	--------	--------	--------

120 min. at 37 °C.

Data File: C:\Documents and Settings\User\Desktop\alex\07-23-15\LC-20.10001 7-23-2015 4-40-26
 PM.dat
 Method: C:\EZStart\Projects\Default\Method\tea\5~100.met
 Acquired: 7/23/2015 4:41:18 PM
 Printed: 2/16/2016 10:29:36 AM



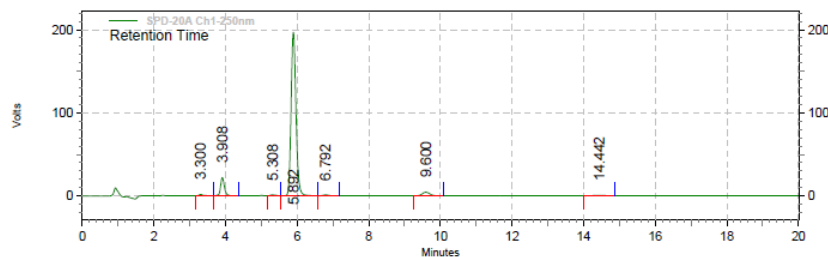
SPD-20A
 Ch1-250nm
 Results

Retention Time	Area	Area %	Height	Height %
3.892	150579	6.66	19977	8.52
4.992	9016	0.40	1061	0.45
5.867	1781041	78.77	186363	79.45
6.767	241785	10.69	22080	9.41
9.558	67643	2.99	4620	1.97
14.333	10968	0.49	465	0.20

Totals	2261032	100.00	234566	100.00
--------	---------	--------	--------	--------

24 h. at 37 °C.

Data File: C:\Documents and Settings\User\Desktop\alex\07-23-15\LC-20.10001 7-24-2015 10-44-43
 AM.dat
 Method: C:\EZStart\Projects\Default\Method\tea\5~100.met
 Acquired: 7/24/2015 10:47:11 AM
 Printed: 2/16/2016 10:32:00 AM



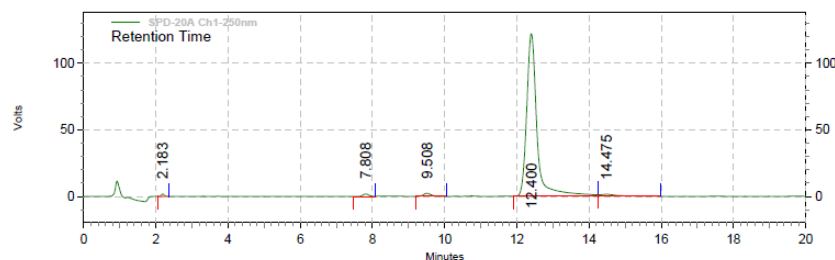
SPD-20A
 Ch1-250nm
 Results

Retention Time	Area	Area %	Height	Height %
3.300	15359	0.72	1698	0.75
3.908	164973	7.68	21973	9.66
5.308	12853	0.60	1150	0.51
5.892	1866241	86.88	196771	86.48
6.792	13616	0.63	1113	0.49
9.600	64004	2.98	4349	1.91
14.442	10958	0.51	477	0.21
Totals	2148004	100.00	227531	100.00

HPLC spectra of BW-AQ-126.

0 min. at 37 °C.

Data File: C:\Documents and Settings\User\Desktop\alex\073115\LC-20.10001 7-31-2015 1-08-03 PM.dat
 Method: C:\EZStart\Projects\Default\Method\tea\5~100.met
 Acquired: 7/31/2015 1:09:54 PM
 Printed: 2/16/2016 11:05:13 AM



SPD-20A
 Ch1-250nm
 Results

Retention Time	Area	Area %	Height	Height %
2.183	9139	0.36	1728	1.34
7.808	20917	0.82	1786	1.38
9.508	33919	1.32	2301	1.78
12.400	2439326	95.29	121995	94.35
14.475	56665	2.21	1495	1.16
Totals	2559966	100.00	129305	100.00

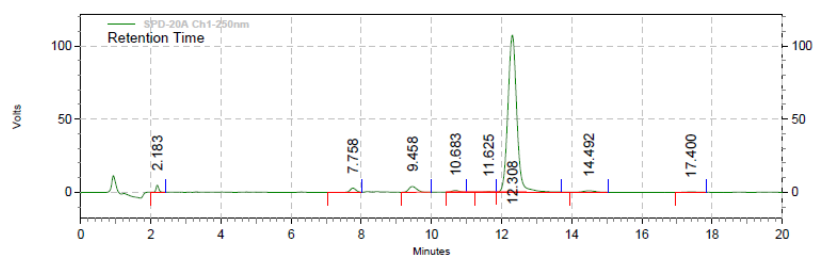
120 min. at 37 °C.

Data File: C:\Documents and Settings\User\Desktop\alex\073115\LC-20.10001 7-31-2015 3-22-30 PM.dat

Method: C:\EZStart\Projects\Default\Method\tea\5~100.met

Acquired: 7/31/2015 3:23:26 PM

Printed: 2/16/2016 11:09:47 AM



SPD-20A
Ch1-250nm
Results

Retention Time	Area	Area %	Height	Height %
2.183	25987	1.25	4831	3.96
7.758	34967	1.68	2919	2.39
9.458	63574	3.06	4006	3.28
10.683	18128	0.87	1213	0.99
11.625	7274	0.35	405	0.33
12.308	1895825	91.15	107285	87.93
14.492	26708	1.28	1053	0.86
17.400	7486	0.36	303	0.25

Totals	2079949	100.00	122015	100.00
--------	---------	--------	--------	--------

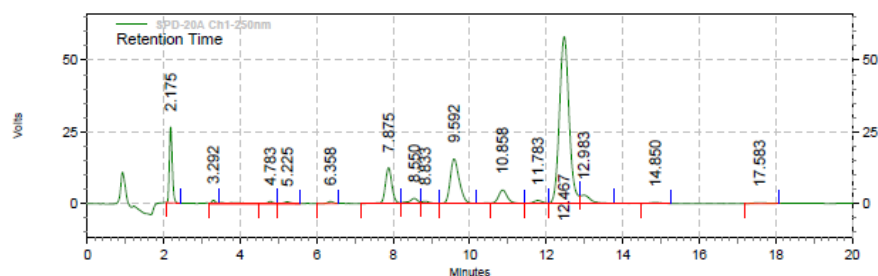
24 h. at 37 °C.

Data File: C:\Documents and Settings\User\Desktop\alex\073115\LC-20.10001 8-1-2015 11-48-37 AM.dat

Method: C:\EZStart\Projects\Default\Method\tea\5-100.met

Acquired: 8/1/2015 11:49:33 AM

Printed: 2/16/2016 11:15:11 AM



SPD-20A
Ch1-250nm
Results

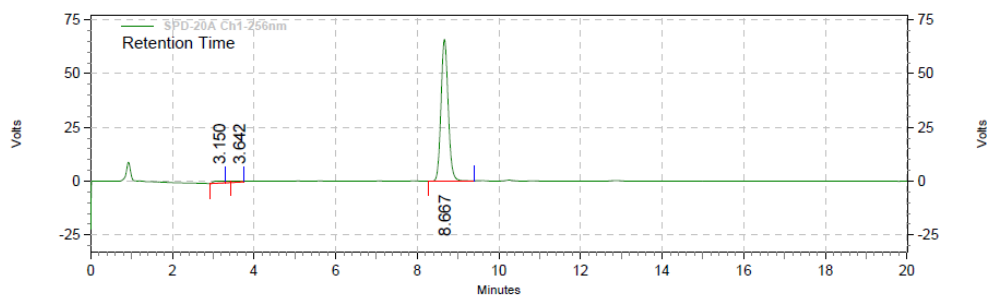
Retention Time	Area	Area %	Height	Height %
2.175	139134	7.66	26397	20.61
3.292	7765	0.43	1169	0.91
4.783	8500	0.47	773	0.60
5.225	8611	0.47	638	0.50
6.358	8275	0.46	770	0.60
7.875	150675	8.30	12512	9.77
8.550	29613	1.63	1832	1.43
8.833	12027	0.66	841	0.66
9.592	256545	14.13	15577	12.16
10.858	78472	4.32	4734	3.70
11.783	18691	1.03	1105	0.86
12.467	1023995	56.38	58146	45.40
12.983	58348	3.21	2967	2.32
14.850	8407	0.46	358	0.28
17.583	7159	0.39	270	0.21
Totals	1816217	100.00	128089	100.00

Long Term Stability Studies of Selected Compounds

HPLC spectra of BW-AQ-101.

Week 1: solid storage at room temperature.

Data File: C:\Documents and Settings\User\Desktop\alex\Long Stability\Week1\BW-AQ-101\LC-20.10001
 10-9-2015 11-20-37 AM.dat
 Method: C:\EZStart\Projects\Default\Method\tea\5~100.met
 Acquired: 10/9/2015 11:21:22 AM
 Printed: 2/16/2016 11:51:14 AM

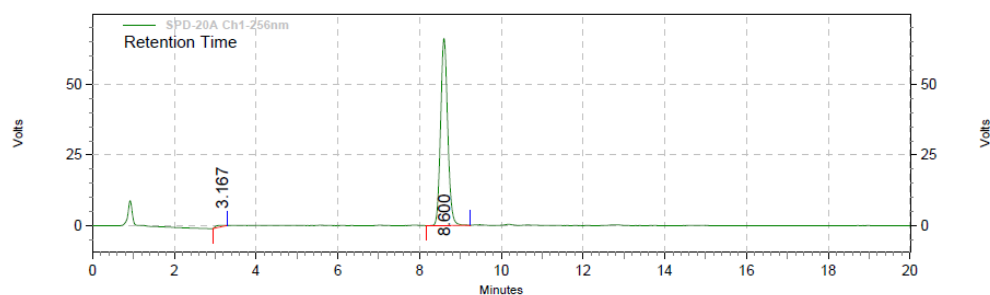


SPD-20A
Ch1-256nm
Results

Retention Time	Area	Area %	Height	Height %
3.150	17036	2.04	954	1.41
3.642	10380	1.24	523	0.78
8.667	808792	96.72	65945	97.81
Totals	836208	100.00	67422	100.00

Week 1: solid storage at 4° C.

Data File: C:\Documents and Settings\User\Desktop\alex\Long Stability\Week1\BW-AQ-101\LC-20.10001
 10-9-2015 11-44-03 AM.dat
 Method: C:\EZStart\Projects\Default\Method\tea\5~100.met
 Acquired: 10/9/2015 11:44:16 AM
 Printed: 2/16/2016 11:25:33 AM

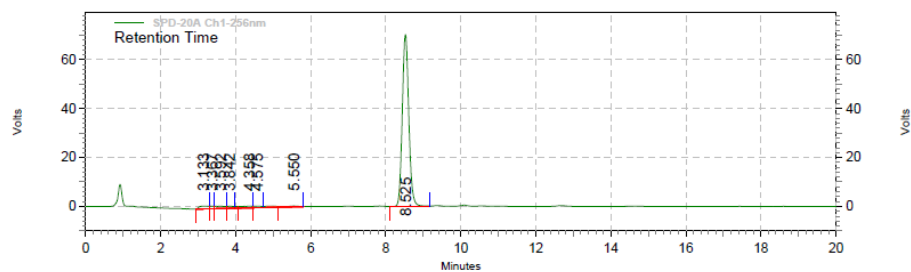


SPD-20A
Ch1-256nm
Results

Retention Time	Area	Area %	Height	Height %
3.167	8220	1.01	419	0.63
8.600	805215	98.99	66250	99.37
Totals	813435	100.00	66669	100.00

Week 1: solid storage at -20° C.

Data File: C:\Documents and Settings\User\Desktop\alex\Long Stability\Week1\BW-AQ-101\LC-20.10001
 10-9-2015 12-18-27 PM.dat
 Method: C:\EZStart\Projects\Default\Method\tea\5~100.met
 Acquired: 10/9/2015 12:19:20 PM
 Printed: 2/16/2016 11:50:07 AM



**SPD-20A
Ch1-256nm**

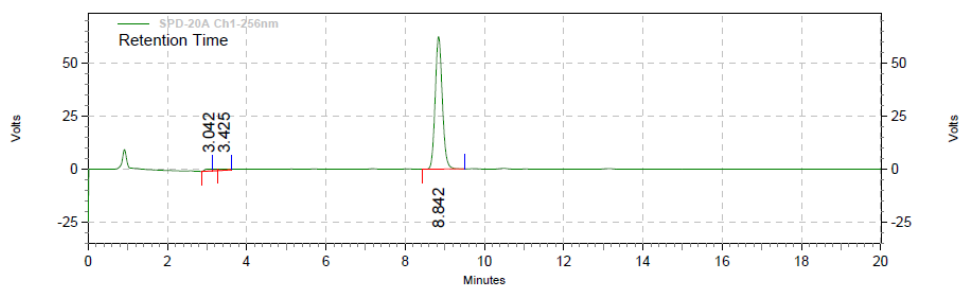
Results

Retention Time	Area	Area %	Height	Height %
3.133	18926	2.02	1094	1.44
3.367	7843	0.84	988	1.30
3.592	17491	1.87	923	1.22
3.842	10084	1.08	836	1.10
4.358	15015	1.60	661	0.87
4.575	9799	1.05	595	0.79
5.550	10630	1.14	365	0.48
8.525	846426	90.41	70275	92.79

Totals	936214	100.00	75737	100.00
--------	--------	--------	-------	--------

Week 1: solution storage at room temperature.

Data File: C:\Documents and Settings\User\Desktop\alex\Long Stability\Week1\BW-AQ-101\LC-20.10001
 10-8-2015 12-32-36 PM.dat
 Method: C:\EZStart\Projects\Default\Method\tea\5~100.met
 Acquired: 10/8/2015 12:33:36 PM
 Printed: 2/16/2016 11:54:31 AM



**SPD-20A
Ch1-256nm**

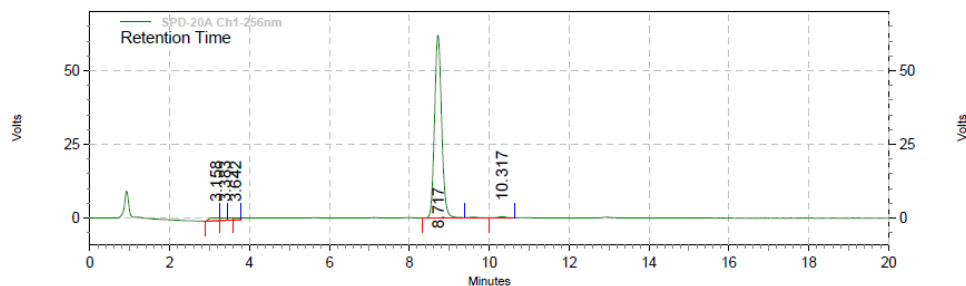
Results

Retention Time	Area	Area %	Height	Height %
3.042	11435	1.42	960	1.50
3.425	11439	1.43	598	0.93
8.842	779855	97.15	62461	97.57

Totals	802729	100.00	64019	100.00
--------	--------	--------	-------	--------

Week 1: solution storage at 4° C.

Data File: C:\Documents and Settings\User\Desktop\alex\Long Stability\Week1\BW-AQ-101\LC-20.10001
 10-8-2015 12-55-26 PM.dat
 Method: C:\EZStart\Projects\Default\Method\tea\5~100.met
 Acquired: 10/8/2015 12:57:18 PM
 Printed: 2/16/2016 11:52:18 AM

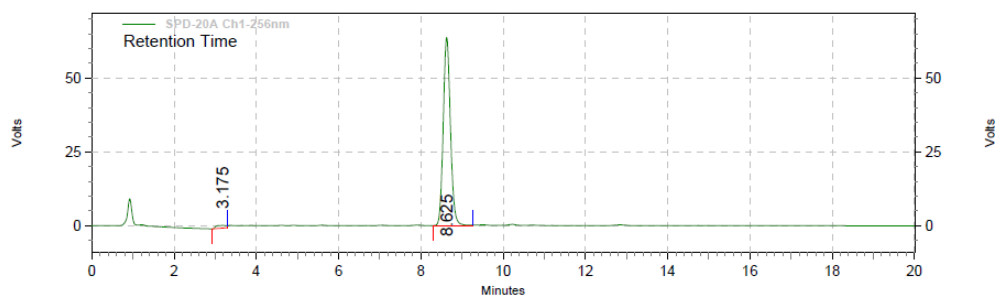


SPD-20A
Ch1-256nm
Results

Retention Time	Area	Area %	Height	Height %
3.158	17356	2.15	989	1.52
3.383	10364	1.28	860	1.32
3.642	7936	0.98	705	1.08
8.717	765077	94.66	62062	95.40
10.317	7471	0.92	440	0.68
Totals	808204	100.00	65056	100.00

Week 1: solution storage at -20° C.

Data File: C:\Documents and Settings\User\Desktop\alex\Long Stability\Week1\BW-AQ-101\LC-20.10001
 10-8-2015 1-24-11 PM.dat
 Method: C:\EZStart\Projects\Default\Method\tea\5~100.met
 Acquired: 10/8/2015 1:25:24 PM
 Printed: 2/16/2016 11:53:34 AM



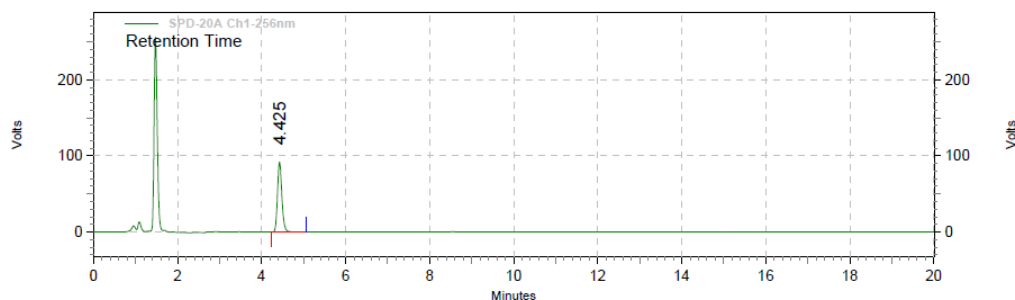
SPD-20A
Ch1-256nm
Results

Retention Time	Area	Area %	Height	Height %
3.175	15871	2.00	879	1.36
8.625	776983	98.00	63739	98.64
Totals	792854	100.00	64618	100.00

HPLC spectra of BW-AQ-112.

Week 1: solid storage at room temperature.

Data File: C:\Documents and Settings\User\Desktop\alex\Long Stability\Week1\BW-AQ-112\LC-20.10001
 10-9-2015 2-27-51 PM.dat
 Method: C:\EZStart\Projects\Default\Method\tea\5~100.met
 Acquired: 10/9/2015 2:28:56 PM
 Printed: 2/16/2016 12:46:25 PM

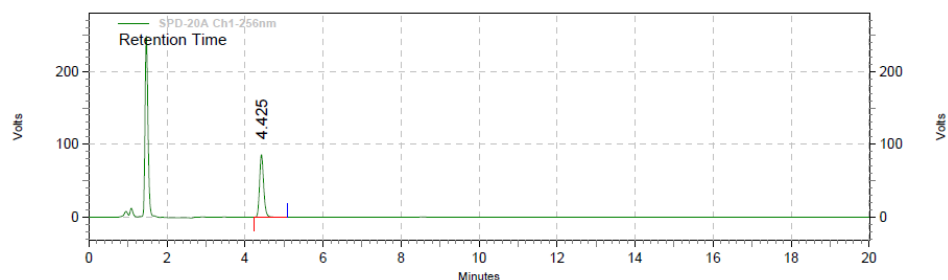


SPD-20A
Ch1-256nm
Results

Retention Time	Area	Area %	Height	Height %
4.425	674816	100.00	92056	100.00
Totals	674816	100.00	92056	100.00

Week 1: solid storage at 4° C.

Data File: C:\Documents and Settings\User\Desktop\alex\Long Stability\Week1\BW-AQ-112\LC-20.10001
 10-9-2015 3-01-05 PM.dat
 Method: C:\EZStart\Projects\Default\Method\tea\5~100.met
 Acquired: 10/9/2015 3:01:36 PM
 Printed: 2/16/2016 12:44:12 PM

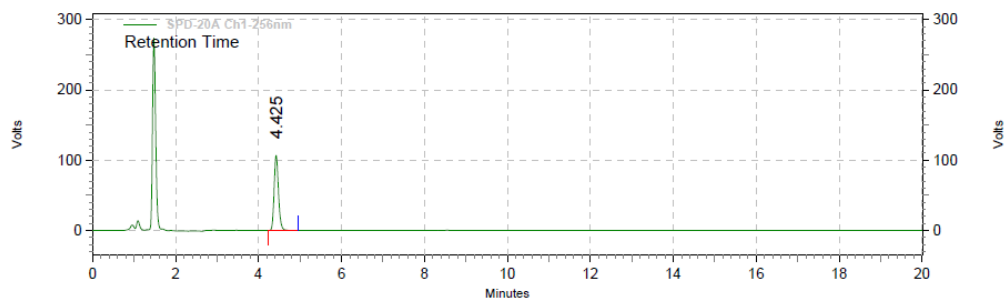


SPD-20A
Ch1-256nm
Results

Retention Time	Area	Area %	Height	Height %
4.425	628666	100.00	85609	100.00
Totals				
	628666	100.00	85609	100.00

Week 1: solid storage at -20° C.

Data File: C:\Documents and Settings\User\Desktop\alex\Long Stability\Week1\BW-AQ-112\LC-20.10001
 10-9-2015 3-28-13 PM.dat
 Method: C:\EZStart\Projects\Default\Method\tea\5~100.met
 Acquired: 10/9/2015 3:28:27 PM
 Printed: 2/16/2016 12:45:16 PM

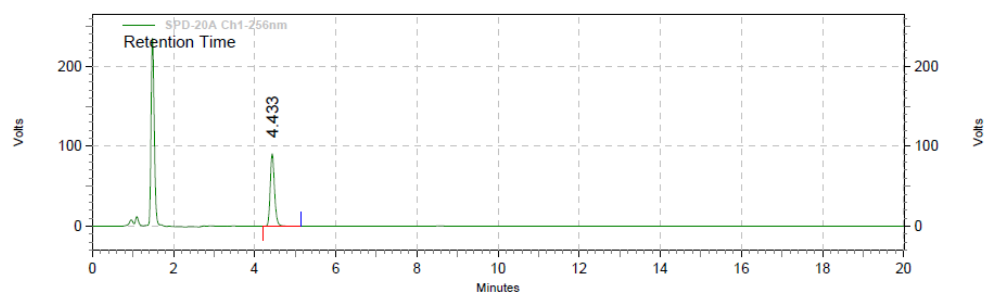


SPD-20A
Ch1-256nm
Results

Retention Time	Area	Area %	Height	Height %
4.425	780203	100.00	106696	100.00
Totals				
	780203	100.00	106696	100.00

Week 1: solution storage at room temperature.

Data File: C:\Documents and Settings\User\Desktop\alex\Long Stability\Week1\BW-AQ-112\LC-20.10001
 10-8-2015 3-19-42 PM.dat
 Method: C:\EZStart\Projects\Default\Method\tea\5~100.met
 Acquired: 10/8/2015 3:21:50 PM
 Printed: 2/16/2016 12:49:36 PM

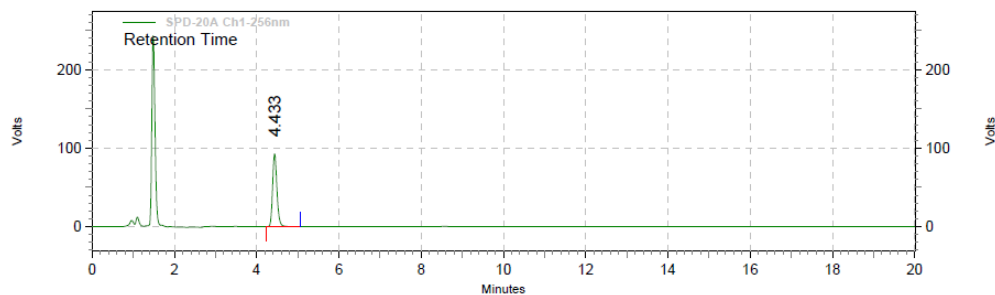


SPD-20A
Ch1-256nm
Results

Retention Time	Area	Area %	Height	Height %
4.433	668241	100.00	90573	100.00
Totals				
	668241	100.00	90573	100.00

Week 1: solution storage at 4° C.

Data File: C:\Documents and Settings\User\Desktop\alex\Long Stability\Week1\BW-AQ-112\LC-20.10001
 10-8-2015 3-42-43 PM.dat
 Method: C:\EZStart\Projects\Default\Method\tea\5~100.met
 Acquired: 10/8/2015 3:43:26 PM
 Printed: 2/16/2016 12:47:17 PM

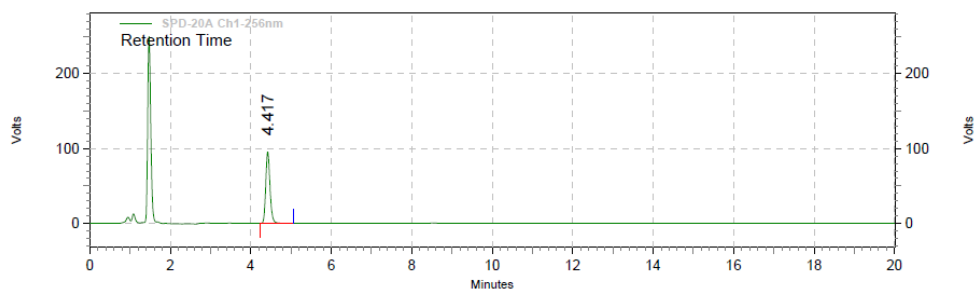


SPD-20A
Ch1-256nm
Results

Retention Time	Area	Area %	Height	Height %
4.433	683049	100.00	92769	100.00
Totals				
	683049	100.00	92769	100.00

Week 1: solution storage at -20° C.

Data File: C:\Documents and Settings\User\Desktop\alex\Long Stability\Week1\BW-AQ-112\LC-20.10001
 10-8-2015 4-09-39 PM.dat
 Method: C:\EZStart\Projects\Default\Method\tea\5~100.met
 Acquired: 10/8/2015 4:11:16 PM
 Printed: 2/16/2016 12:48:32 PM



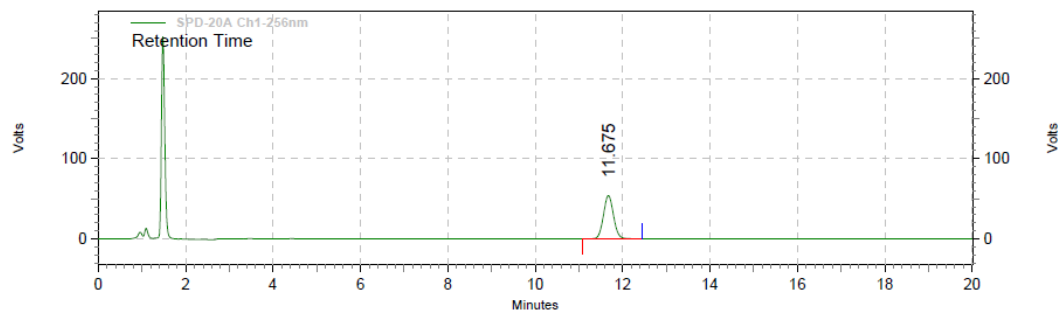
SPD-20A
Ch1-256nm
Results

Retention Time	Area	Area %	Height	Height %
4.417	702187	100.00	95416	100.00
Totals				
	702187	100.00	95416	100.00

HPLC spectra of BW-AQ-113.

Week 1: solid storage at room temperature.

Data File: C:\Documents and Settings\User\Desktop\alex\Long Stability\Week1\BW-AQ-113\LC-20.10001
 10-9-2015 3-58-56 PM.dat
 Method: C:\EZStart\Projects\Default\Method\tea\5~100.met
 Acquired: 10/9/2015 4:00:00 PM
 Printed: 2/16/2016 12:53:24 PM

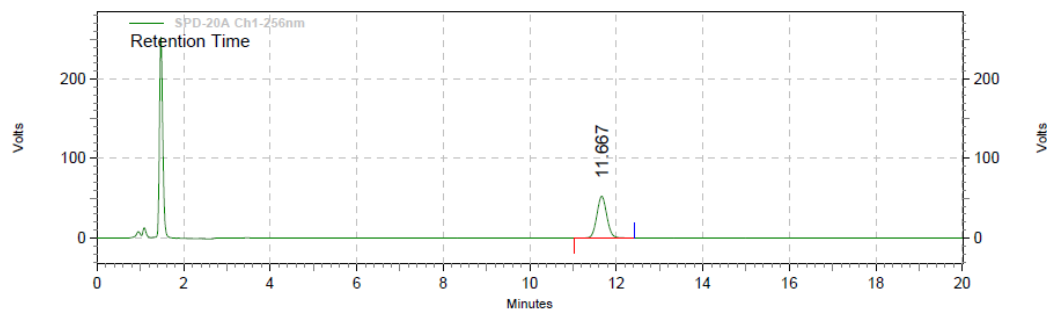


SPD-20A
Ch1-256nm
Results

Retention Time	Area	Area %	Height	Height %
11.675	858361	100.00	53996	100.00
Totals				
	858361	100.00	53996	100.00

Week 1: solid storage at 4° C.

Data File: C:\Documents and Settings\User\Desktop\alex\Long Stability\Week1\BW-AQ-113\LC-20.10001
 10-9-2015 4-23-33 PM.dat
 Method: C:\EZStart\Projects\Default\Method\tea\5~100.met
 Acquired: 10/9/2015 4:24:30 PM
 Printed: 2/16/2016 12:51:41 PM

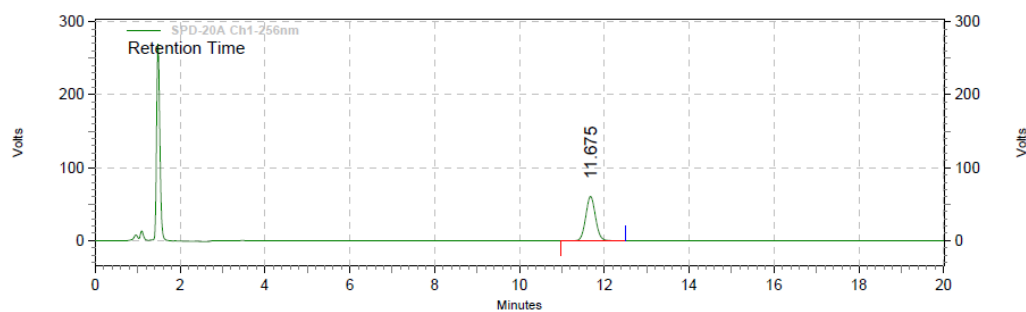


SPD-20A
Ch1-256nm
Results

Retention Time	Area	Area %	Height	Height %
11.667	831764	100.00	52438	100.00
Totals				
	831764	100.00	52438	100.00

Week 1: solid storage at -20° C.

Data File: C:\Documents and Settings\User\Desktop\alex\Long Stability\Week1\BW-AQ-113\LC-20.10001
 10-9-2015 4-55-58 PM.dat
 Method: C:\EZStart\Projects\Default\Method\tea\5~100.met
 Acquired: 10/9/2015 4:56:27 PM
 Printed: 2/16/2016 12:52:35 PM

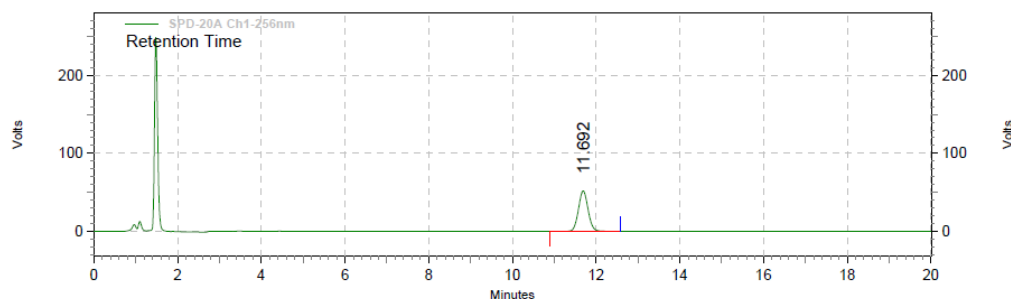


SPD-20A
Ch1-256nm
Results

Retention Time	Area	Area %	Height	Height %
11.675	967029	100.00	60730	100.00
Totals				
	967029	100.00	60730	100.00

Week 1: solution storage at room temperature.

Data File: C:\Documents and Settings\User\Desktop\alex\Long Stability\Week1\BW-AQ-113\LC-20.10001
 10-8-2015 5-37-00 PM.dat
 Method: C:\EZStart\Projects\Default\Method\tea\5~100.met
 Acquired: 10/8/2015 5:37:13 PM
 Printed: 2/16/2016 12:56:12 PM

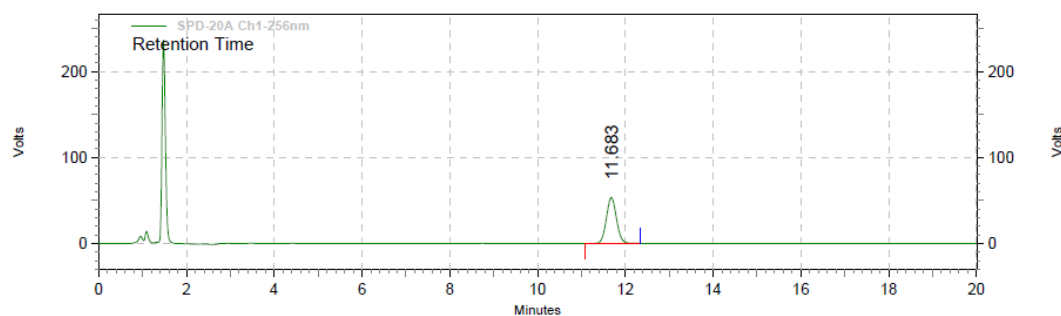


SPD-20A
Ch1-256nm
Results

Retention Time	Area	Area %	Height	Height %
11.692	827314	100.00	51855	100.00
Totals				
	827314	100.00	51855	100.00

Week 1: solution storage at 4° C.

Data File: C:\Documents and Settings\User\Desktop\alex\Long Stability\Week1\BW-AQ-113\LC-20.10001
 10-8-2015 6-01-12 PM.dat
 Method: C:\EZStart\Projects\Default\Method\tea\5~100.met
 Acquired: 10/8/2015 6:01:48 PM
 Printed: 2/16/2016 12:54:18 PM

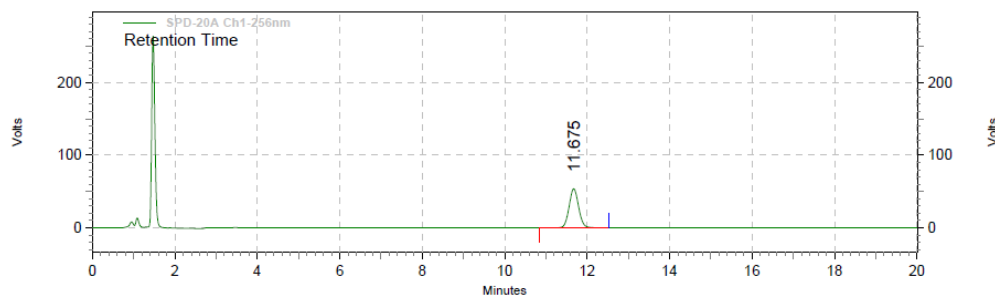


SPD-20A
Ch1-256nm
Results

Retention Time	Area	Area %	Height	Height %
11.683	850145	100.00	53436	100.00
Totals				
	850145	100.00	53436	100.00

Week 1: solution storage at -20° C.

Data File: C:\Documents and Settings\User\Desktop\alex\Long Stability\Week1\BW-AQ-113\LC-20.10001
 10-8-2015 6-23-10 PM.dat
 Method: C:\EZStart\Projects\Default\Method\tea\5~100.met
 Acquired: 10/8/2015 6:23:31 PM
 Printed: 2/16/2016 12:55:22 PM



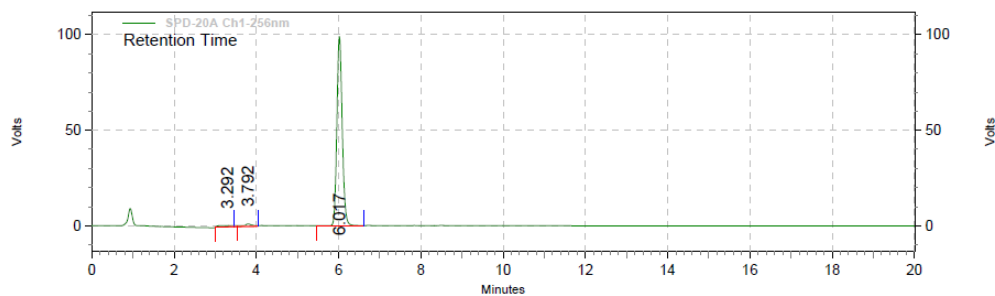
SPD-20A
Ch1-256nm
Results

Retention Time	Area	Area %	Height	Height %
11.675	855072	100.00	53630	100.00
Totals	855072	100.00	53630	100.00

HPLC spectra of BW-AQ-124.

Week 1: solid storage at room temperature.

Data File: C:\Documents and Settings\User\Desktop\alex\Long Stability\Week1\BW-AQ-124\LC-20.10001
 10-9-2015 12-42-23 PM.dat
 Method: C:\EZStart\Projects\Default\Method\tea\5~100.met
 Acquired: 10/9/2015 12:43:37 PM
 Printed: 2/16/2016 1:00:16 PM

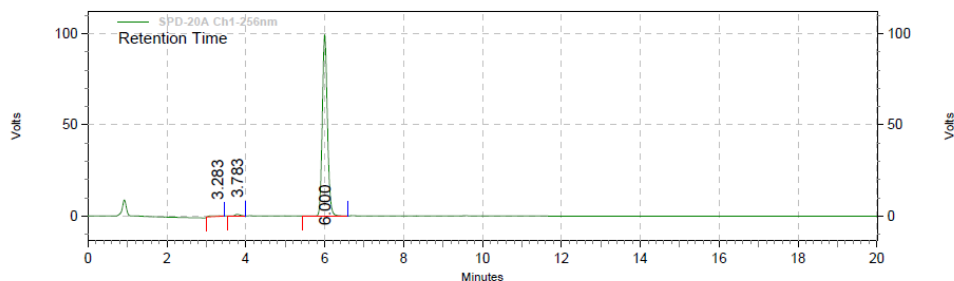


SPD-20A
Ch1-256nm
Results

Retention Time	Area	Area %	Height	Height %
3.292	15841	1.70	693	0.69
3.792	19331	2.07	1308	1.29
6.017	898342	96.23	99068	98.02
Totals	933514	100.00	101069	100.00

Week 1: solid storage at 4° C.

Data File: C:\Documents and Settings\User\Desktop\alex\Long Stability\Week1\BW-AQ-124\LC-20.10001
 10-9-2015 1-05-47 PM.dat
 Method: C:\EZStart\Projects\Default\Method\tea\5~100.met
 Acquired: 10/9/2015 1:06:31 PM
 Printed: 2/16/2016 12:58:15 PM

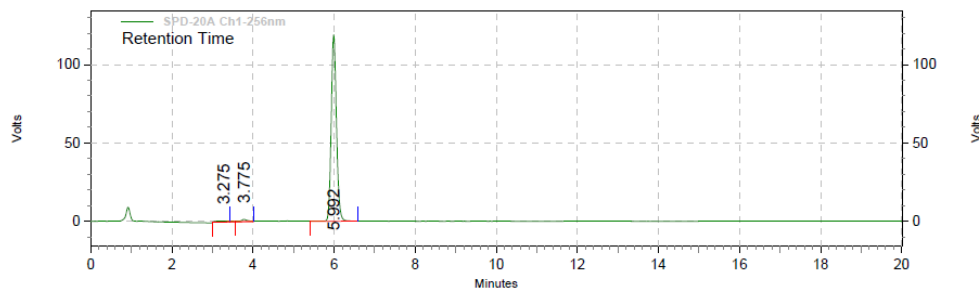


SPD-20A
Ch1-256nm
Results

Retention Time	Area	Area %	Height	Height %
3.283	7669	0.84	333	0.33
3.783	8065	0.88	937	0.93
6.000	899623	98.28	99394	98.74
Totals	915357	100.00	100664	100.00

Week 1: solid storage at -20° C.

Data File: C:\Documents and Settings\User\Desktop\alex\Long Stability\Week1\BW-AQ-124\LC-20.10001
 10-9-2015 1-33-36 PM.dat
 Method: C:\EZStart\Projects\Default\Method\tea\5~100.met
 Acquired: 10/9/2015 1:34:41 PM
 Printed: 2/16/2016 12:59:16 PM

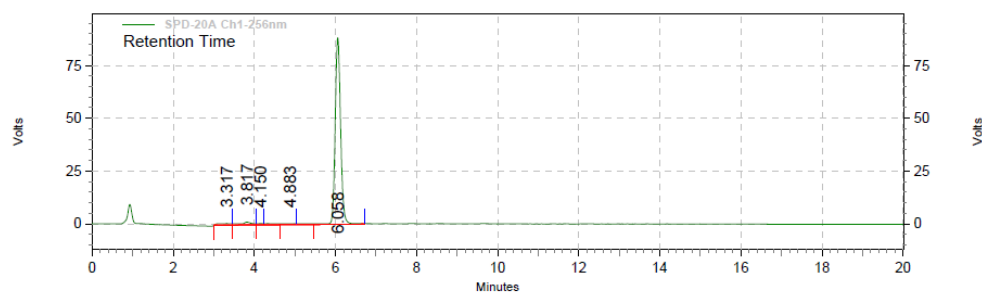


SPD-20A
Ch1-256nm
Results

Retention Time	Area	Area %	Height	Height %
3.275	14292	1.29	651	0.54
3.775	18113	1.64	1454	1.20
5.992	1072053	97.07	119030	98.26
Totals	1104458	100.00	121135	100.00

Week 1: solution storage at room temperature.

Data File: C:\Documents and Settings\User\Desktop\alex\Long Stability\Week1\BW-AQ-124\LC-20.10001
 10-8-2015 1-48-37 PM.dat
 Method: C:\EZStart\Projects\Default\Method\tea\5~100.met
 Acquired: 10/8/2015 1:49:48 PM
 Printed: 2/16/2016 1:03:20 PM

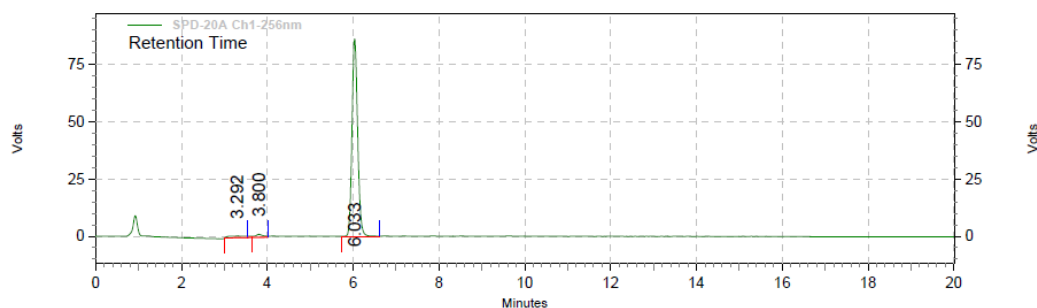


SPD-20A Ch1-256nm Results

Retention Time	Area	Area %	Height	Height %
3.317	16181	1.83	700	0.76
3.817	26173	2.95	1392	1.52
4.150	7180	0.81	632	0.69
4.883	10186	1.15	473	0.52
6.058	826501	93.26	88457	96.51
Totals	886221	100.00	91654	100.00

Week 1: solution storage at 4° C.

Data File: C:\Documents and Settings\User\Desktop\alex\Long Stability\Week1\BW-AQ-124\LC-20.10001
 10-8-2015 2-13-24 PM.dat
 Method: C:\EZStart\Projects\Default\Method\tea\5~100.met
 Acquired: 10/8/2015 2:14:55 PM
 Printed: 2/16/2016 1:01:18 PM



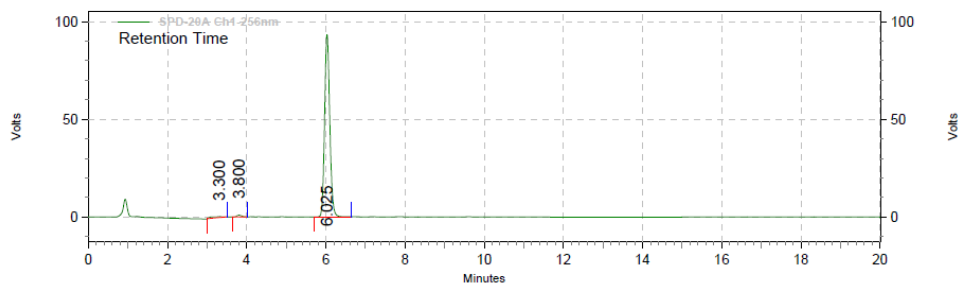
**SPD-20A
Ch1-256nm
Results**

Retention Time	Area	Area %	Height	Height %
3.292	19632	2.40	740	0.84
3.800	17733	2.17	1338	1.52
6.033	781380	95.44	85919	97.64

Totals	818745	100.00	87997	100.00
--------	--------	--------	-------	--------

Week 1: solution storage at -20° C.

Data File: C:\Documents and Settings\User\Desktop\alex\Long Stability\Week1\BW-AQ-124\LC-20.10001
 10-8-2015 2-38-16 PM.dat
 Method: C:\EZStart\Projects\Default\Method\tea\5~100.met
 Acquired: 10/8/2015 2:40:43 PM
 Printed: 2/16/2016 1:02:26 PM



**SPD-20A
Ch1-256nm
Results**

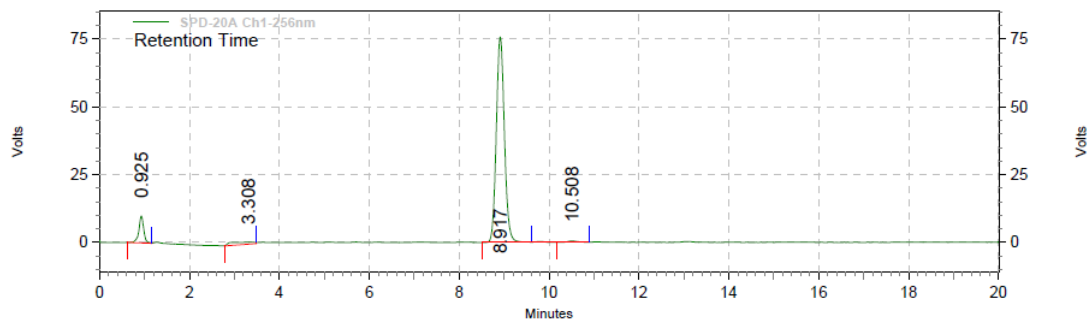
Retention Time	Area	Area %	Height	Height %
3.300	12761	1.47	492	0.52
3.800	7384	0.85	896	0.95
6.025	847592	97.68	93231	98.53

Totals	867737	100.00	94619	100.00
--------	--------	--------	-------	--------

HPLC spectra of BW-AQ-101.

Week 4: solid storage at room temperature.

Data File: C:\Documents and Settings\User\Desktop\alex-yxy\101-10.30-solid-rt.dat
 Method: C:\EZStart\Projects\Default\Method\tea\5~100.met
 Acquired: 10/30/2015 10:38:57 AM
 Printed: 2/16/2016 2:33:01 PM



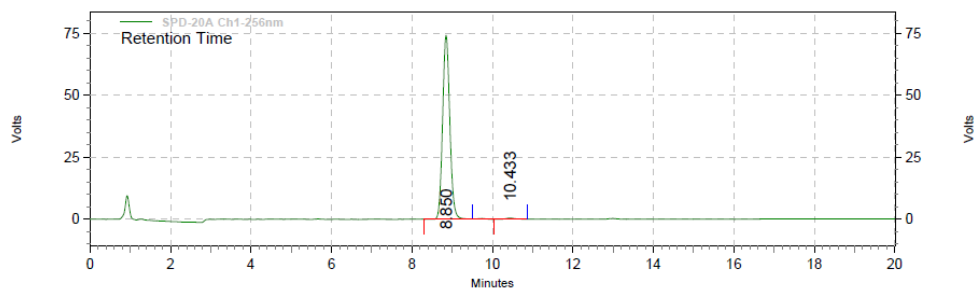
SPD-20A
Ch1-256nm
Results

Results

Retention Time	Area	Area %	Height	Height %	
0.925	75704	7.10	9919	11.43	
3.308	31125	2.92	650	0.75	
8.917	948752	89.01	75701	87.20	
10.508	10301	0.97	545	0.63	
Totals		1065882	100.00	86815	100.00

Week 4: solid storage at 4° C.

Data File: C:\Documents and Settings\User\Desktop\alex-yxy\101-10.30-solid-4C.dat
 Method: C:\EZStart\Projects\Default\Method\tea\5~100.met
 Acquired: 10/30/2015 11:11:20 AM
 Printed: 2/16/2016 2:31:23 PM

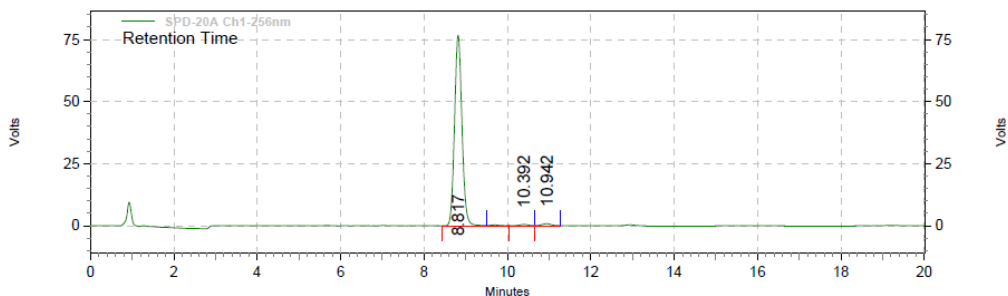


SPD-20A
Ch1-256nm
Results

Retention Time	Area	Area %	Height	Height %	
8.850	924609	98.99	74222	99.33	
10.433	9462	1.01	502	0.67	
Totals		934071	100.00	74724	100.00

Week 4: solid storage at -20° C.

Data File: C:\Documents and Settings\User\Desktop\alex-yxy\101-10.30-solid--20.dat
 Method: C:\EZStart\Projects\Default\Method\tea\5~100.met
 Acquired: 10/30/2015 11:38:48 AM
 Printed: 2/16/2016 2:32:18 PM



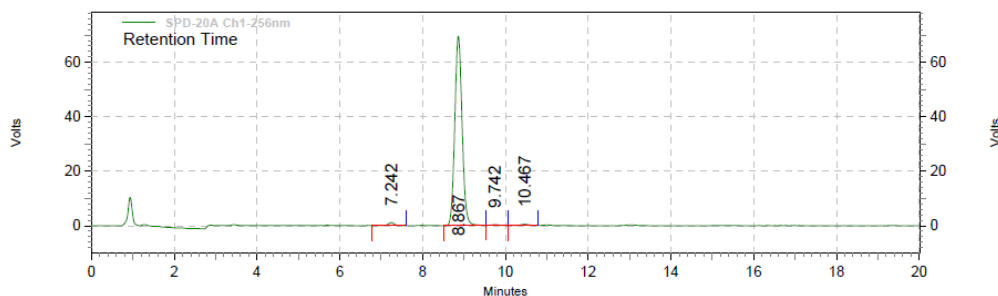
SPD-20A Ch1-256nm Results

Retention Time	Area	Area %	Height	Height %
8.817	951390	97.58	76749	98.21
10.392	9360	0.96	555	0.71
10.942	14243	1.46	843	1.08

Totals	974993	100.00	78147	100.00
--------	--------	--------	-------	--------

Week 4: solution storage at room temperature.

Data File: C:\Documents and Settings\User\Desktop\alex-yxy\101-10.28-liq-rt.dat
 Method: C:\EZStart\Projects\Default\Method\tea\5~100.met
 Acquired: 10/28/2015 11:49:53 AM
 Printed: 2/16/2016 2:38:42 PM



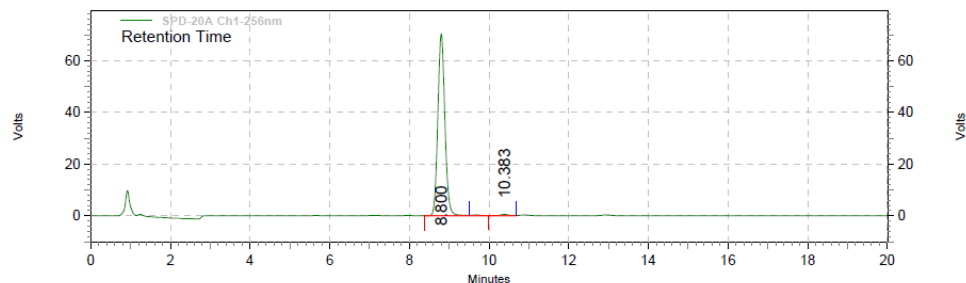
SPD-20A Ch1-256nm Results

Retention Time	Area	Area %	Height	Height %
7.242	13382	1.50	1109	1.55
8.867	859539	96.65	69534	97.20
9.742	7207	0.81	374	0.52
10.467	9194	1.03	520	0.73

Totals	889322	100.00	71537	100.00
--------	--------	--------	-------	--------

Week 4: solution storage at 4° C.

Data File: C:\Documents and Settings\User\Desktop\alex-yxy\101-10.28-liq-4.dat
 Method: C:\EZStart\Projects\Default\Method\tea\5~100.met
 Acquired: 10/28/2015 12:22:40 PM
 Printed: 2/16/2016 2:35:17 PM

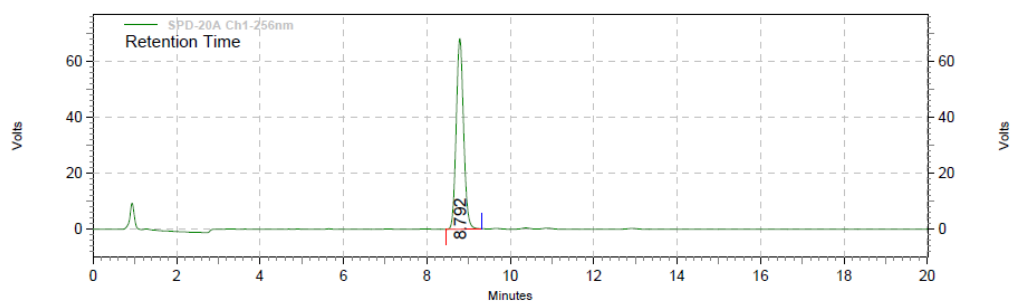


SPD-20A Ch1-256nm Results

Retention Time	Area	Area %	Height	Height %
8.800	871802	98.99	70378	99.31
10.383	8862	1.01	492	0.69
Totals	880664	100.00	70870	100.00

Week 4: solution storage at -20° C.

Data File: C:\Documents and Settings\User\Desktop\alex-yxy\101-10.28-liq--20.dat
 Method: C:\EZStart\Projects\Default\Method\tea\5~100.met
 Acquired: 10/28/2015 12:47:30 PM
 Printed: 2/16/2016 2:36:47 PM



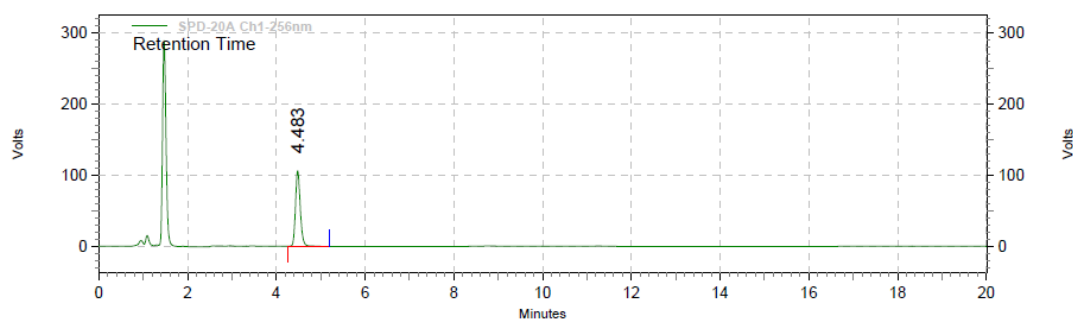
SPD-20A Ch1-256nm Results

Retention Time	Area	Area %	Height	Height %
8.792	840415	100.00	68130	100.00
Totals	840415	100.00	68130	100.00

HPLC spectra of BW-AQ-112.

Week 4: solid storage at room temperature.

Data File: C:\Documents and Settings\User\Desktop\alex-yxy\112-10.30-solid--rt.dat
 Method: C:\EZStart\Projects\Default\Method\tea\5~100.met
 Acquired: 10/30/2015 2:07:19 PM
 Printed: 2/16/2016 2:42:06 PM

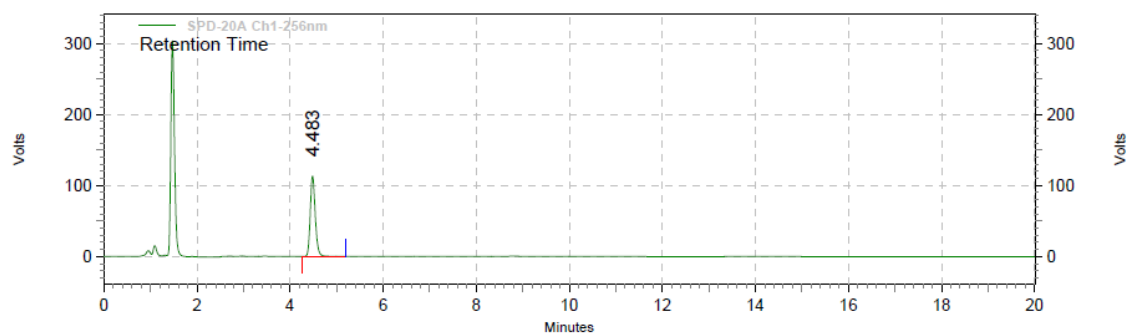


SPD-20A
Ch1-256nm
Results

Retention Time	Area	Area %	Height	Height %
4.483	794670	100.00	106157	100.00
Totals		794670	100.00	106157
				100.00

Week 4: solid storage at 4° C.

Data File: C:\Documents and Settings\User\Desktop\alex-yxy\112-10.30-solid-4C.dat
 Method: C:\EZStart\Projects\Default\Method\tea\5~100.met
 Acquired: 10/30/2015 2:28:54 PM
 Printed: 2/16/2016 2:40:14 PM

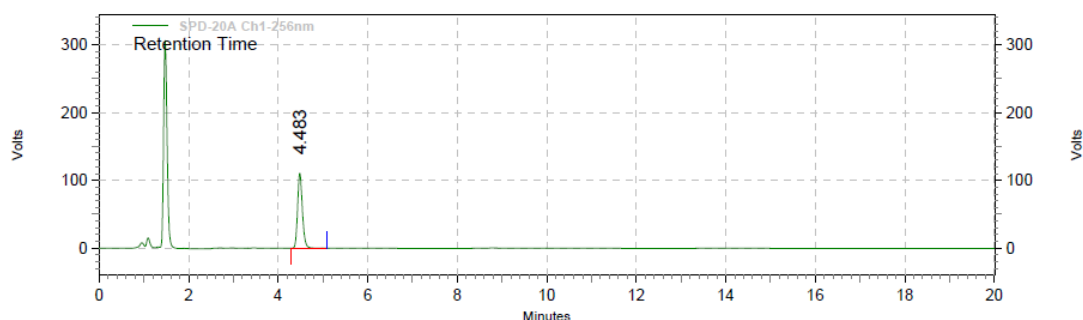


SPD-20A
Ch1-256nm
Results

Retention Time	Area	Area %	Height	Height %
4.483	850378	100.00	113272	100.00
Totals		850378	100.00	113272
				100.00

Week 4: solid storage at -20° C.

Data File: C:\Documents and Settings\User\Desktop\alex-yxy\112-10.30-solid-(-20).dat
 Method: C:\EZStart\Projects\Default\Method\tea\5~100.met
 Acquired: 10/30/2015 2:52:47 PM
 Printed: 2/16/2016 2:41:14 PM

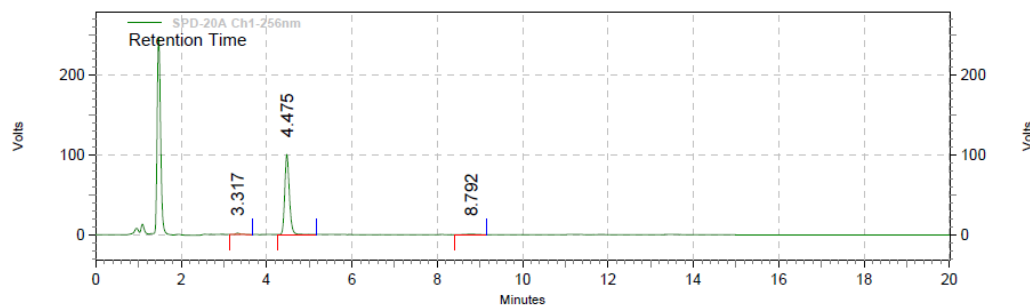


SPD-20A
Ch1-256nm
Results

Retention Time	Area	Area %	Height	Height %
4.483	824586	100.00	110433	100.00
Totals		824586	100.00	110433
				100.00

Week 4: solution storage at room temperature.

Data File: C:\Documents and Settings\User\Desktop\alex-yxy\112-10.28-liq-rt.dat
 Method: C:\EZStart\Projects\Default\Method\tea\5~100.met
 Acquired: 10/28/2015 4:20:08 PM
 Printed: 2/16/2016 2:47:23 PM

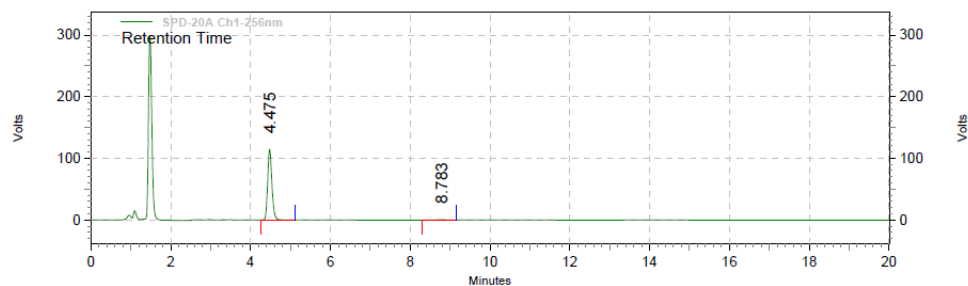


SPD-20A
Ch1-256nm
Results

Retention Time	Area	Area %	Height	Height %
3.317	12937	1.67	1625	1.59
4.475	754560	97.22	100190	97.81
8.792	8667	1.12	623	0.61
Totals		776164	100.00	102438
				100.00

Week 4: solution storage at 4° C.

Data File: C:\Documents and Settings\User\Desktop\alex-xyx\112-10.28-liq-4c.dat
 Method: C:\EZStart\Projects\Default\Method\tea\5~100.met
 Acquired: 10/28/2015 4:53:02 PM
 Printed: 2/16/2016 2:43:51 PM

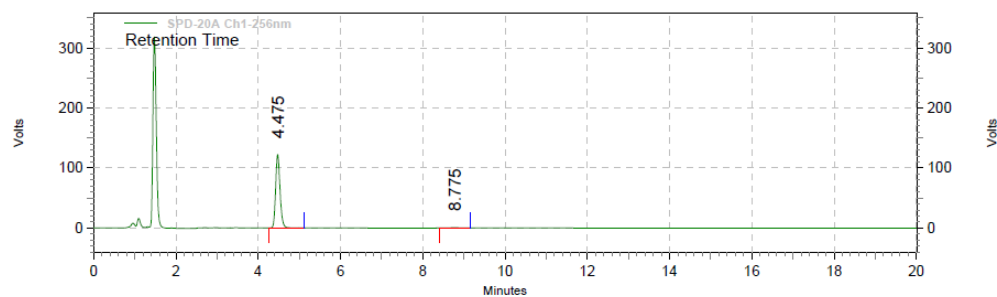


SPD-20A
Ch1-256nm
Results

Retention Time	Area	Area %	Height	Height %
4.475	852535	99.02	114249	99.49
8.783	8399	0.98	590	0.51
Totals				
	860934	100.00	114839	100.00

Week 4: solution storage at -20° C.

Data File: C:\Documents and Settings\User\Desktop\alex-xyx\112-10.28-liq-20.dat
 Method: C:\EZStart\Projects\Default\Method\tea\5~100.met
 Acquired: 10/28/2015 5:29:19 PM
 Printed: 2/16/2016 2:45:43 PM



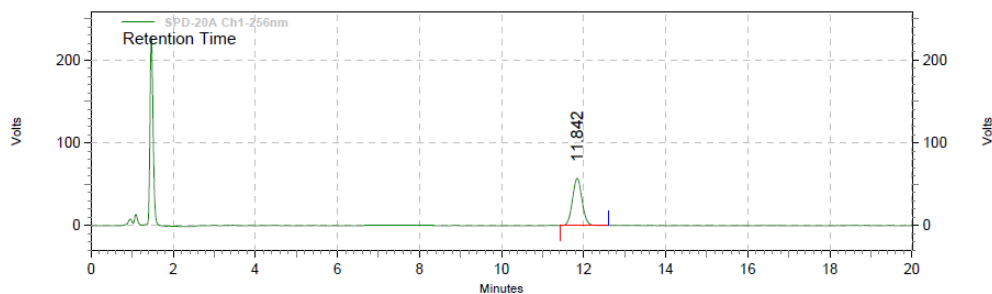
SPD-20A
Ch1-256nm
Results

Retention Time	Area	Area %	Height	Height %	
4.475	910761	99.10	122149	99.51	
8.775	8235	0.90	596	0.49	
Totals		918996	100.00	122745	100.00

HPLC spectra of BW-AQ-113.

Week 4: solid storage at room temperature.

Data File: C:\Documents and Settings\User\Desktop\alex-yxy\113-10.30-solid-rt.dat
 Method: C:\EZStart\Projects\Default\Method\tea\5~100.met
 Acquired: 10/30/2015 3:23:53 PM
 Printed: 2/16/2016 2:51:31 PM

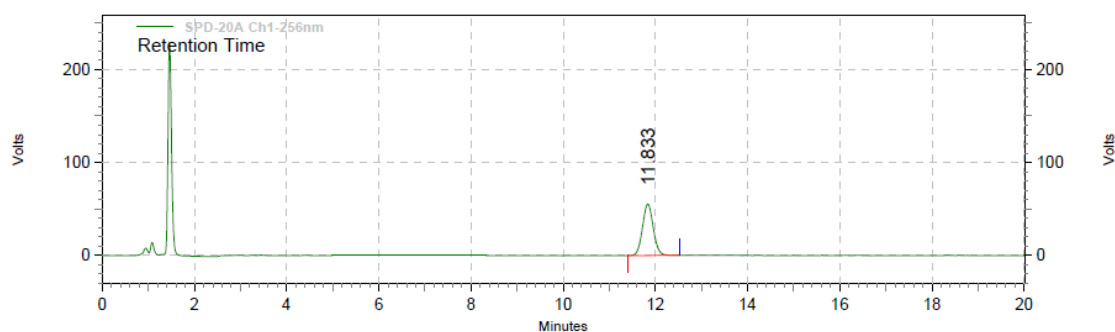


SPD-20A
Ch1-256nm
Results

Retention Time	Area	Area %	Height	Height %
11.842	924845	100.00	57008	100.00
Totals	924845	100.00	57008	100.00

Week 4: solid storage at 4° C.

Data File: C:\Documents and Settings\User\Desktop\alex-yxy\113-10.30-solid-4C.dat
 Method: C:\EZStart\Projects\Default\Method\tea\5~100.met
 Acquired: 10/30/2015 3:46:09 PM
 Printed: 2/16/2016 2:49:35 PM

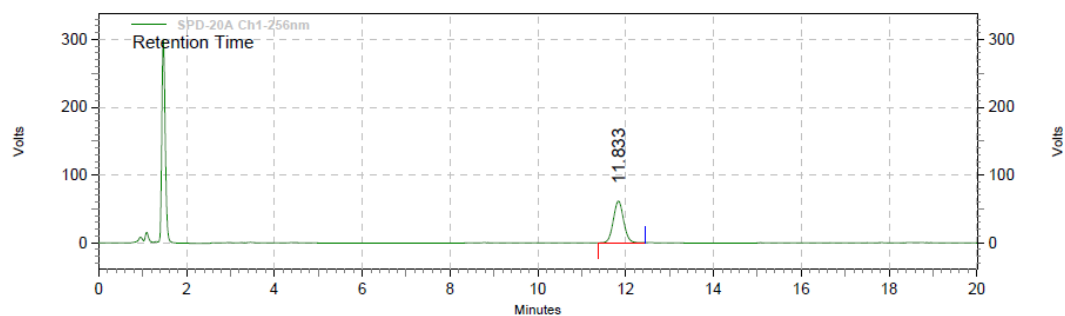


SPD-20A
Ch1-256nm
Results

Retention Time	Area	Area %	Height	Height %
11.833	897415	100.00	55208	100.00
Totals	897415	100.00	55208	100.00

Week 4: solid storage at -20° C.

Data File: C:\Documents and Settings\User\Desktop\alex-xy\113-10.30-solid-(-20).dat
 Method: C:\EZStart\Projects\Default\Method\tea\5~100.met
 Acquired: 10/30/2015 5:11:34 PM
 Printed: 2/16/2016 2:50:44 PM

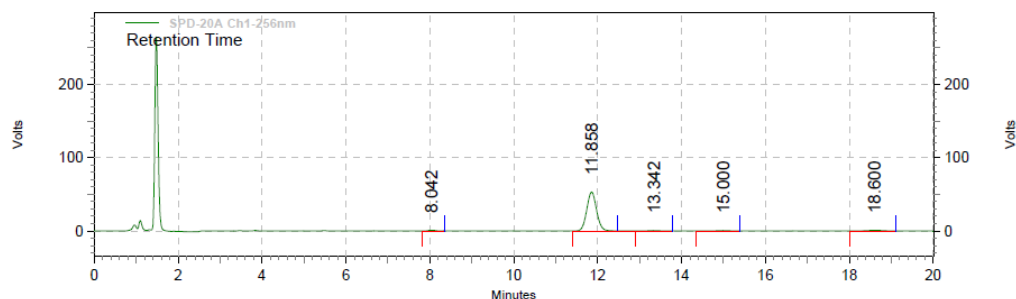


SPD-20A
Ch1-256nm
Results

Retention Time	Area	Area %	Height	Height %
11.833	992710	100.00	61328	100.00
Totals				
	992710	100.00	61328	100.00

Week 4: solution storage at room temperature.

Data File: C:\Documents and Settings\User\Desktop\alex-xy\113-10.28-liq-RT.dat
 Method: C:\EZStart\Projects\Default\Method\tea\5~100.met
 Acquired: 10/28/2015 2:57:07 PM
 Printed: 2/16/2016 2:54:02 PM

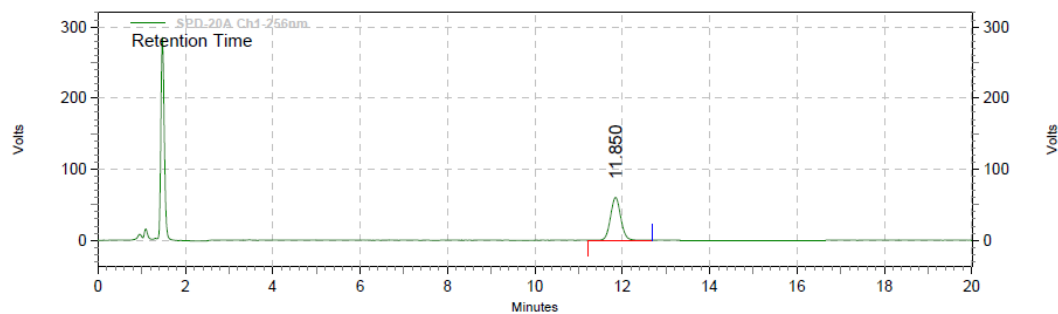


SPD-20A
Ch1-256nm
Results

Retention Time	Area	Area %	Height	Height %
8.042	10762	1.18	932	1.67
11.858	864188	94.60	53111	95.26
13.342	9449	1.03	479	0.86
15.000	10428	1.14	485	0.87
18.600	18727	2.05	747	1.34
Totals				
	913554	100.00	55754	100.00

Week 4: solution storage at 4° C.

Data File: C:\Documents and Settings\User\Desktop\alex-yxy\113-10.28-liq-4C.dat
 Method: C:\EZStart\Projects\Default\Method\tea\5~100.met
 Acquired: 10/28/2015 3:19:26 PM
 Printed: 2/16/2016 2:52:37 PM

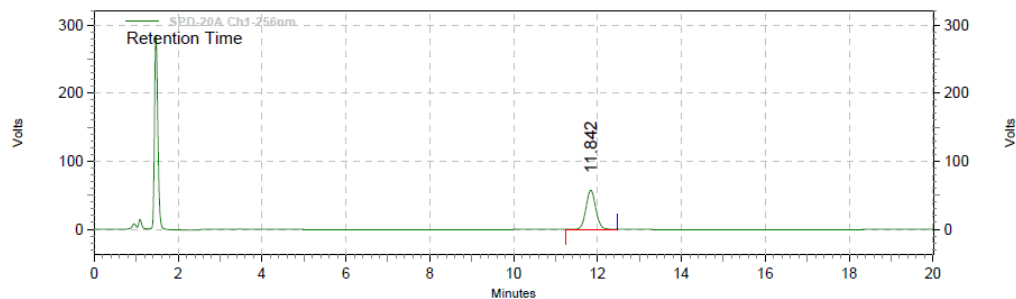


SPD-20A
Ch1-256nm
Results

Retention Time	Area	Area %	Height	Height %
11.850	974365	100.00	60054	100.00
Totals				
	974365	100.00	60054	100.00

Week 4: solution storage at -20° C.

Data File: C:\Documents and Settings\User\Desktop\alex-yxy\113-10.28-liq--20.dat
 Method: C:\EZStart\Projects\Default\Method\tea\5~100.met
 Acquired: 10/28/2015 3:47:35 PM
 Printed: 2/16/2016 2:53:24 PM



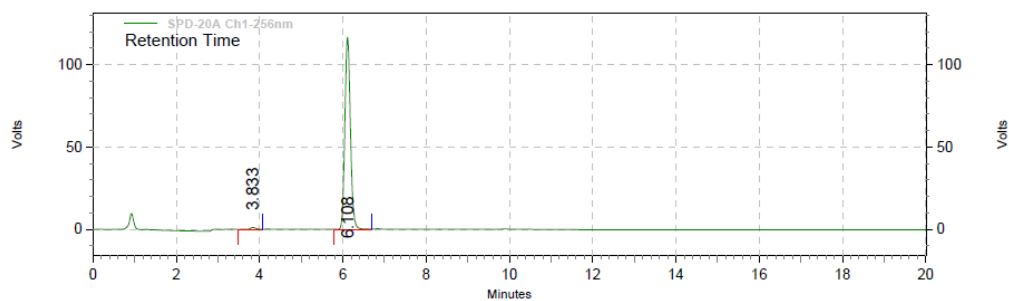
SPD-20A
Ch1-256nm
Results

Retention Time	Area	Area %	Height	Height %
11.842	927460	100.00	57246	100.00
Totals				
	927460	100.00	57246	100.00

HPLC spectra of BW-AQ-124.

Week 4: solid storage at room temperature.

Data File: C:\Documents and Settings\User\Desktop\alex-xy\124-10.30-solid-rt.dat
 Method: C:\EZStart\Projects\Default\Method\tea\5~100.met
 Acquired: 10/30/2015 12:02:00 PM
 Printed: 2/16/2016 2:59:21 PM

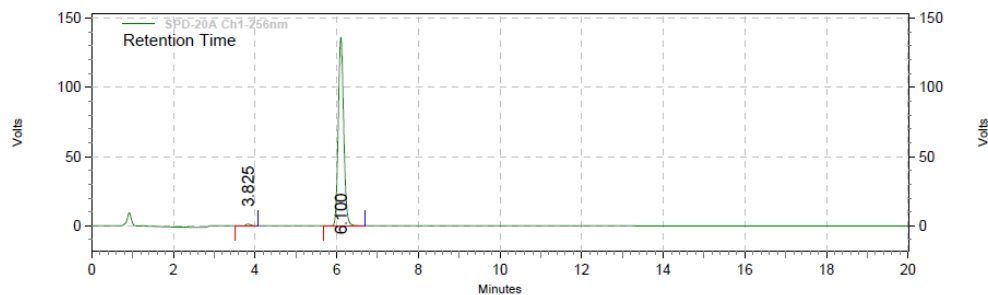


SPD-20A
Ch1-256nm
Results

Retention Time	Area	Area %	Height	Height %
3.833	10123	0.93	1127	0.96
6.108	1078127	99.07	116506	99.04
Totals		1088250	117633	100.00

Week 4: solid storage at 4° C.

Data File: C:\Documents and Settings\User\Desktop\alex-xy\124-10.30-solid-4C.dat
 Method: C:\EZStart\Projects\Default\Method\tea\5~100.met
 Acquired: 10/30/2015 12:23:38 PM
 Printed: 2/16/2016 2:57:55 PM

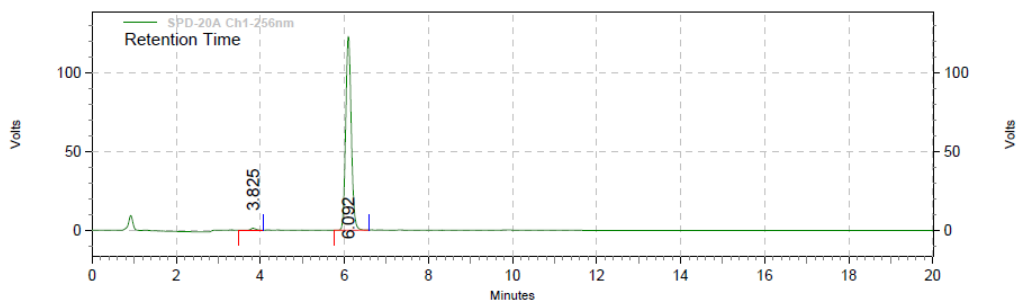


SPD-20A
Ch1-256nm
Results

Retention Time	Area	Area %	Height	Height %
3.825	10902	0.86	1286	0.94
6.100	1253523	99.14	136115	99.06
Totals		1264425	137401	100.00

Week 4: solid storage at -20° C.

Data File: C:\Documents and Settings\User\Desktop\alex-xy\124-10.30-solid--20.dat
 Method: C:\EZStart\Projects\Default\Method\tea\5~100.met
 Acquired: 10/30/2015 12:58:12 PM
 Printed: 2/16/2016 2:58:40 PM

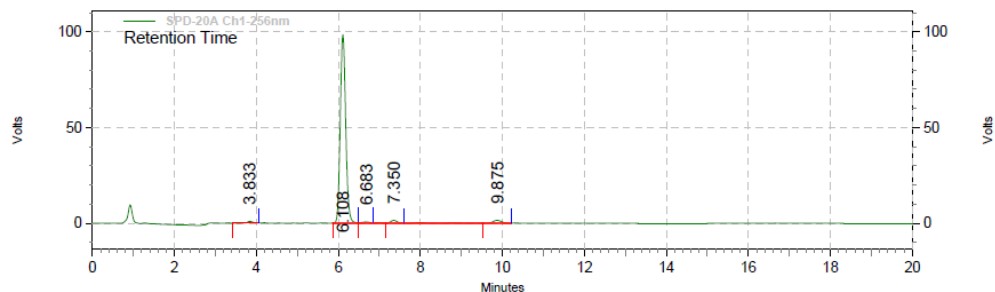


SPD-20A
Ch1-256nm
Results

Retention Time	Area	Area %	Height	Height %	
3.825	9829	0.86	1177	0.95	
6.092	1127704	99.14	123103	99.05	
Totals		1137533	100.00	124280	100.00

Week 4: solution storage at room temperature.

Data File: C:\Documents and Settings\User\Desktop\alex-xy\124-10.28-liq-rt.dat
 Method: C:\EZStart\Projects\Default\Method\tea\5~100.met
 Acquired: 10/28/2015 1:11:47 PM
 Printed: 2/16/2016 3:01:24 PM

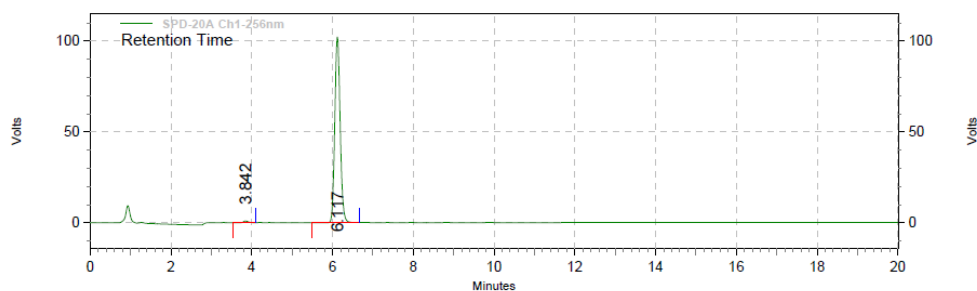


SPD-20A
Ch1-256nm
Results

Retention Time	Area	Area %	Height	Height %	
3.833	9458	0.98	966	0.94	
6.108	907862	94.14	98545	95.56	
6.683	9263	0.96	593	0.58	
7.350	16351	1.70	1493	1.45	
9.875	21440	2.22	1531	1.48	
Totals		964374	100.00	103128	100.00

Week 4: solution storage at 4° C.

Data File: C:\Documents and Settings\User\Desktop\alex-yxy\124-10.28-liq-4.dat
 Method: C:\EZStart\Projects\Default\Method\tea\5~100.met
 Acquired: 10/28/2015 1:44:33 PM
 Printed: 2/16/2016 3:00:06 PM

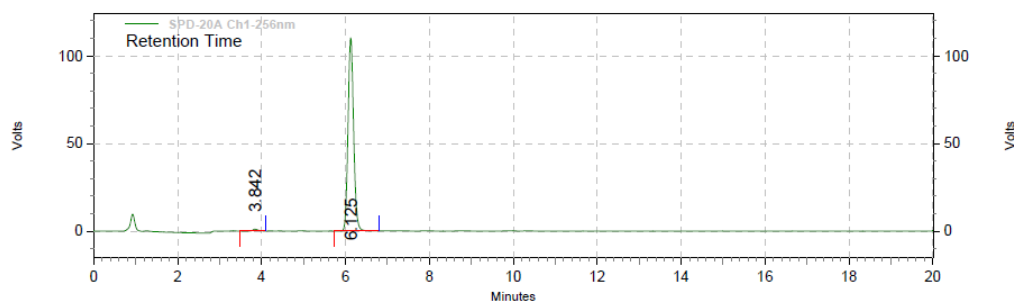


SPD-20A
Ch1-256nm
Results

Retention Time	Area	Area %	Height	Height %
3.842	8587	0.90	976	0.95
6.117	947582	99.10	102249	99.05
Totals	956169	100.00	103225	100.00

Week 4: solution storage at -20° C.

Data File: C:\Documents and Settings\User\Desktop\alex-yxy\124-10.28-liq--20.dat
 Method: C:\EZStart\Projects\Default\Method\tea\5~100.met
 Acquired: 10/28/2015 2:05:41 PM
 Printed: 2/16/2016 3:00:40 PM



SPD-20A
Ch1-256nm
Results

Retention Time	Area	Area %	Height	Height %
3.842	8974	0.87	1037	0.93
6.125	1020066	99.13	110176	99.07
Totals	1029040	100.00	111213	100.00

HPLC spectra of BW-AQ-101.

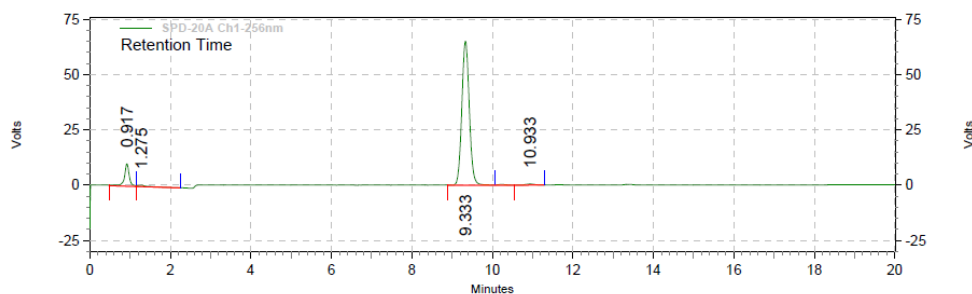
Week 9: solid storage at room temperature.

Data File: C:\Documents and Settings\User\Desktop\alex\Long Stability\week9\101\101-solid-12.04-RT.dat

Method: C:\EZStart\Projects\Default\Method\alex\50%.met

Acquired: 12/4/2015 9:24:44 AM

Printed: 12/4/2015 9:46:04 AM



**SPD-20A
Ch1-256nm
Results**

Retention Time	Area	Area %	Height	Height %
0.917	86743	9.16	10128	13.27
1.275	11489	1.21	574	0.75
9.333	839332	88.67	65099	85.30
10.933	9037	0.95	519	0.68

Totals	946601	100.00	76320	100.00
--------	--------	--------	-------	--------

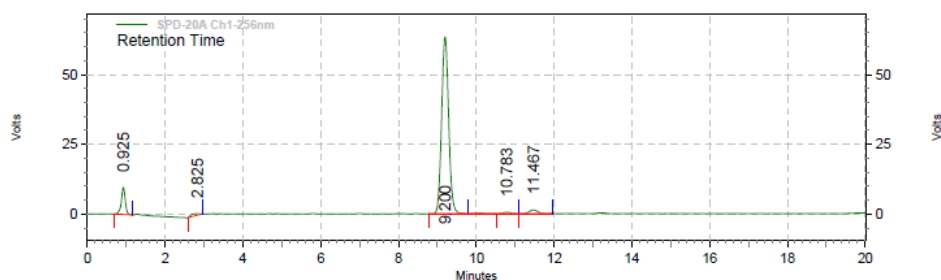
Week 9: solid storage at 4° C.

Data File: C:\Documents and Settings\User\Desktop\alex\Long Stability\week9\101\101-solid-12.04-4C.dat

Method: C:\EZStart\Projects\Default\Method\alex\50%.met

Acquired: 12/4/2015 9:48:26 AM

Printed: 12/4/2015 10:09:29 AM



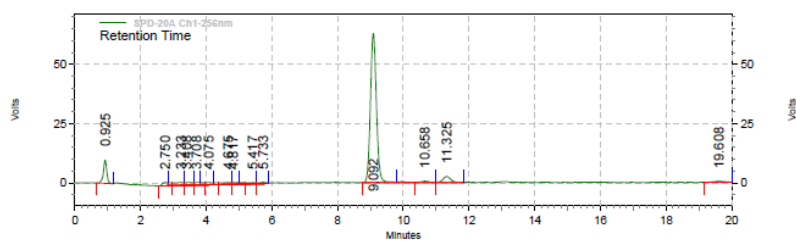
**SPD-20A
Ch1-256nm
Results**

Retention Time	Area	Area %	Height	Height %
0.925	70280	7.69	9682	12.80
2.825	10798	1.18	529	0.70
9.200	802575	87.77	63480	83.95
10.783	8211	0.90	527	0.70
11.467	22509	2.46	1398	1.85

Totals	914373	100.00	75616	100.00
--------	--------	--------	-------	--------

Week 9: solid storage at -20° C.

Data File: C:\Documents and Settings\User\Desktop\alex\Long
 Stability\week9\101\101-solid-12.04(-20).dat
 Method: C:\EZStart\Projects\Default\Method\alex\50%.met
 Acquired: 12/4/2015 10:10:50 AM
 Printed: 12/4/2015 10:31:16 AM

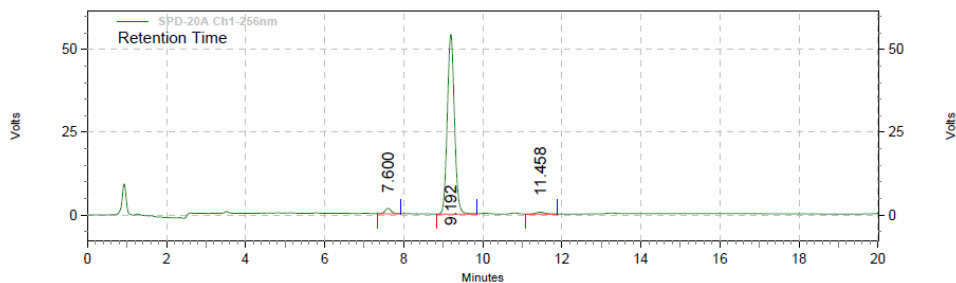


SPD-20A
Ch1-256nm
Results

Retention Time	Area	Area %	Height	Height %
0.925	71384	6.70	9738	11.51
2.750	16072	1.51	1361	1.61
3.233	28186	2.64	1244	1.47
3.408	20986	1.97	1199	1.42
3.708	12449	1.17	1054	1.25
4.075	14298	1.34	961	1.14
4.675	20442	1.92	851	1.01
4.817	9047	0.85	785	0.93
5.417	10063	0.94	524	0.62
5.733	10203	0.96	556	0.66
9.092	793432	74.44	62885	74.33
10.658	9523	0.89	566	0.67
11.325	40808	3.83	2513	2.97
19.608	8966	0.84	362	0.43
Totals	1065859	100.00	84599	100.00

Week 8: solution storage at room temperature.

Data File: C:\Documents and Settings\User\Desktop\alex\Long
 Stability\week8\101\101-11.25-solution-RT.dat
 Method: C:\EZStart\Projects\Default\Method\tea\5~100.met
 Acquired: 11/25/2015 10:46:24 AM
 Printed: 2/16/2016 4:26:41 PM

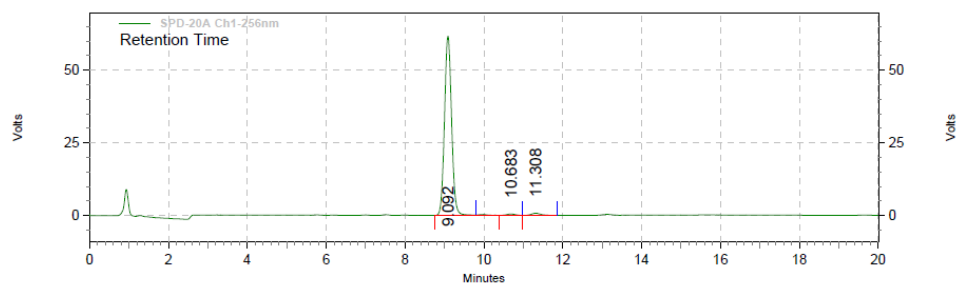


SPD-20A
Ch1-256nm
Results

Retention Time	Area	Area %	Height	Height %
7.600	18206	2.55	1646	2.91
9.192	685938	96.12	54289	96.05
11.458	9458	1.33	586	1.04
Totals	713602	100.00	56521	100.00

Week 8: solution storage at 4° C.

Data File: C:\Documents and Settings\User\Desktop\alex\Long
 Stability\week8\101\101-11.25-solution-4C.dat
 Method: C:\EZStart\Projects\Default\Method\tea\5~100.met
 Acquired: 11/25/2015 11:08:26 AM
 Printed: 2/16/2016 4:24:35 PM

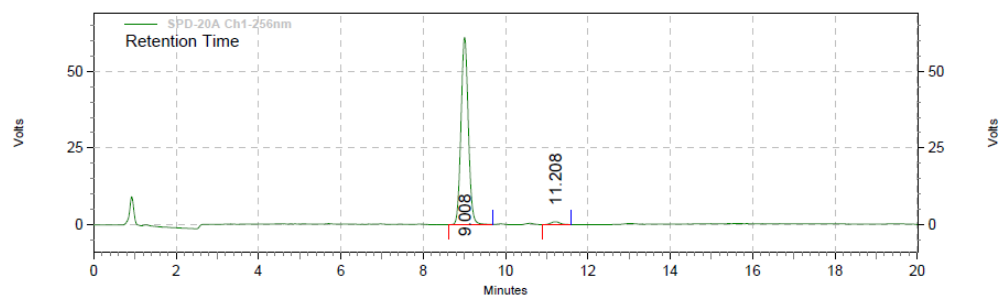


SPD-20A Ch1-256nm Results

Retention Time	Area	Area %	Height	Height %
9.092	770653	97.53	61636	98.03
10.683	7370	0.93	487	0.77
11.308	12185	1.54	752	1.20
Totals	790208	100.00	62875	100.00

Week 8: solution storage at -20° C.

Data File: C:\Documents and Settings\User\Desktop\alex\Long
 Stability\week8\101\101-11.25-solution-(-20).dat
 Method: C:\EZStart\Projects\Default\Method\tea\5~100.met
 Acquired: 11/25/2015 11:29:43 AM
 Printed: 2/16/2016 4:25:38 PM



SPD-20A Ch1-256nm Results

Retention Time	Area	Area %	Height	Height %
9.008	753601	98.07	60864	98.45
11.208	14827	1.93	957	1.55
Totals	768428	100.00	61821	100.00

HPLC spectra of BW-AQ-112.

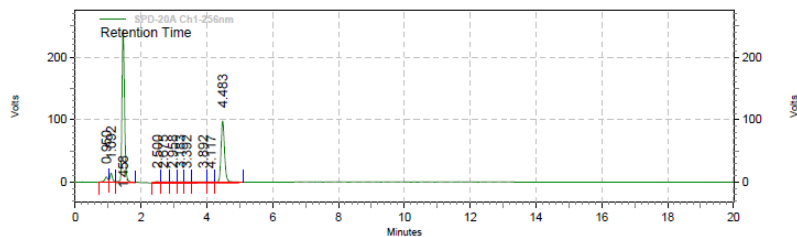
Week 9: solid storage at room temperature.

Data File: C:\Documents and Settings\User\Desktop\alex\Long Stability\week9\112\112-solid-12.04-RT.dat

Method: C:\EZStart\Projects\Default\Method\alex\40%.met

Acquired: 12/4/2015 11:56:34 AM

Printed: 12/4/2015 12:16:59 PM



SPD-20A
Ch1-256nm

Results

Retention Time	Area	Area %	Height	Height %
0.950	59060	2.53	8483	2.26
1.092	79459	3.41	14558	3.88
1.458	1312499	56.31	244727	65.15
2.500	21774	0.93	1930	0.51
2.675	22016	0.94	1580	0.42
2.958	20965	0.90	1648	0.44
3.183	12846	0.55	1205	0.32
3.392	16758	0.72	1365	0.36
3.892	24678	1.06	876	0.23
4.117	11557	0.50	837	0.22
4.483	749352	32.15	98425	26.20
Totals	2330964	100.00	375634	100.00

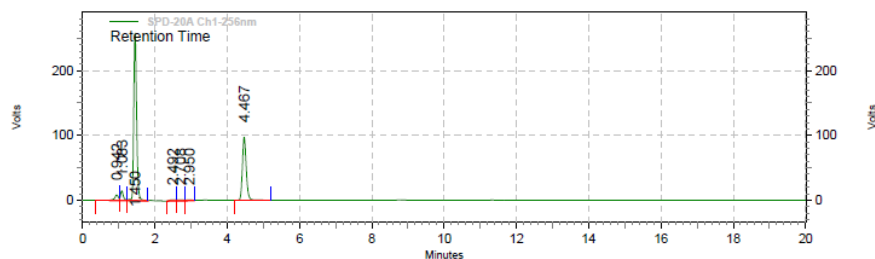
Week 9: solid storage at 4° C.

Data File: C:\Documents and Settings\User\Desktop\alex\Long Stability\week9\112-solid-12.04-4C.dat

Method: C:\EZStart\Projects\Default\Method\alex\40%.met

Acquired: 12/4/2015 12:17:56 PM

Printed: 12/4/2015 12:43:03 PM



SPD-20A
Ch1-256nm
Results

Retention Time	Area	Area %	Height	Height %
0.942	66905	2.86	8605	2.25
1.083	83669	3.58	15044	3.93
1.450	1422092	60.87	258345	67.43
2.492	18960	0.81	1740	0.45
2.708	16261	0.70	1211	0.32
2.950	12866	0.55	1088	0.28
4.467	715450	30.62	97074	25.34
Totals	2336203	100.00	383107	100.00

Week 9: solid storage at -20° C.

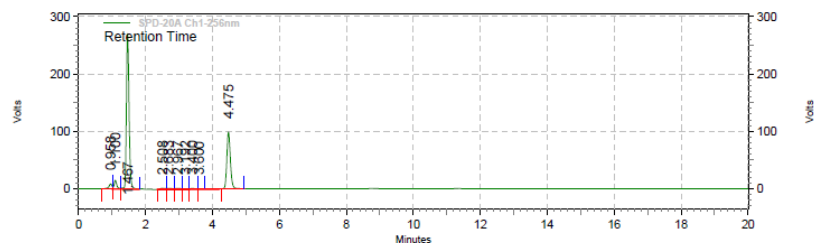
Data File: C:\Documents and Settings\User\Desktop\alex\Long

Stability\week9\112-solid-12.04-(-20).dat

Method: C:\EZStart\Projects\Default\Method\alex\40%.met

Acquired: 12/4/2015 12:44:49 PM

Printed: 12/4/2015 1:10:55 PM

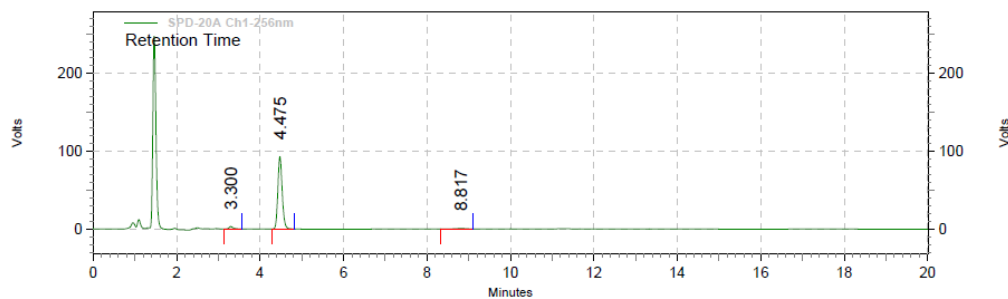


SPD-20A
Ch1-256nm
Results

Retention Time	Area	Area %	Height	Height %
0.958	58370	2.39	8375	2.09
1.100	81089	3.32	14872	3.71
1.467	1480857	60.62	270892	67.54
2.508	20751	0.85	2000	0.50
2.683	20195	0.83	1534	0.38
2.967	19615	0.80	1636	0.41
3.192	10844	0.44	1032	0.26
3.400	14750	0.60	1216	0.30
3.600	8322	0.34	701	0.17
4.475	728111	29.81	98844	24.64
Totals	2442904	100.00	401102	100.00

Week 8: solution storage at room temperature.

Data File: C:\Documents and Settings\User\Desktop\alex\Long
 Stability\week8\112\112-11.25-solution-RT.dat
 Method: C:\EZStart\Projects\Default\Method\tea\5~100.met
 Acquired: 11/25/2015 1:12:35 PM
 Printed: 2/16/2016 4:31:37 PM

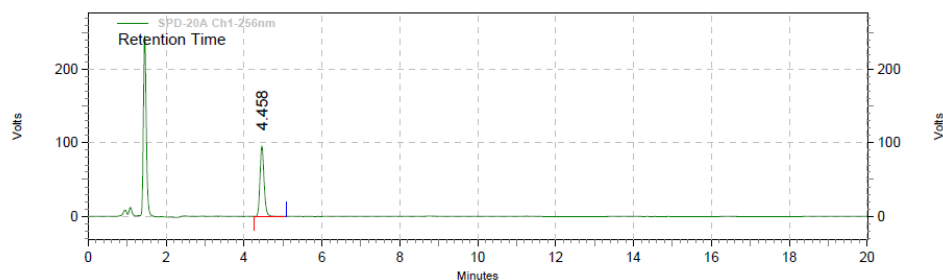


SPD-20A
Ch1-256nm
Results

Retention Time	Area	Area %	Height	Height %
3.300	20995	2.98	3007	3.12
4.475	674428	95.76	92894	96.28
8.817	8831	1.25	581	0.60
Totals	704254	100.00	96482	100.00

Week 8: solution storage at 4° C.

Data File: C:\Documents and Settings\User\Desktop\alex\Long
 Stability\week8\112\112-11.25-solution-4C.dat
 Method: C:\EZStart\Projects\Default\Method\tea\5~100.met
 Acquired: 11/25/2015 1:34:00 PM
 Printed: 2/16/2016 4:29:33 PM

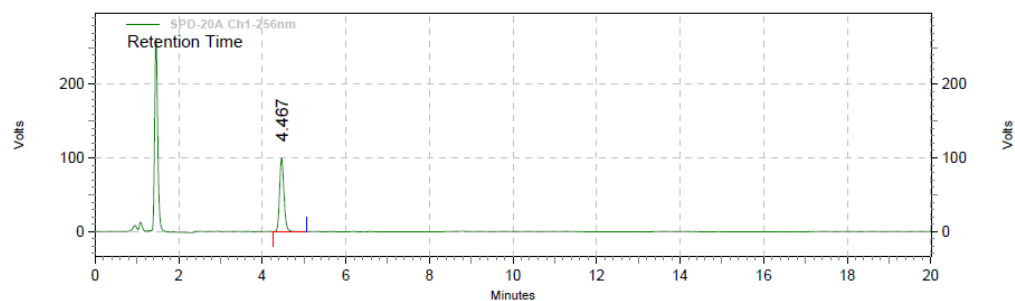


SPD-20A
Ch1-256nm
Results

Retention Time	Area	Area %	Height	Height %
4.458	701965	100.00	95843	100.00
Totals	701965	100.00	95843	100.00

Week 8: solution storage at -20° C.

Data File: C:\Documents and Settings\User\Desktop\alex\Long
 Stability\week8\112\112-11.25-solution-(-20).dat
 Method: C:\EZStart\Projects\Default\Method\tea\5~100.met
 Acquired: 11/25/2015 1:55:02 PM
 Printed: 2/16/2016 4:30:31 PM



SPD-20A
Ch1-256nm

Results

Retention Time	Area	Area %	Height	Height %
4.467	731906	100.00	99714	100.00
Totals		731906	100.00	99714
				100.00

HPLC spectra of BW-AQ-113.

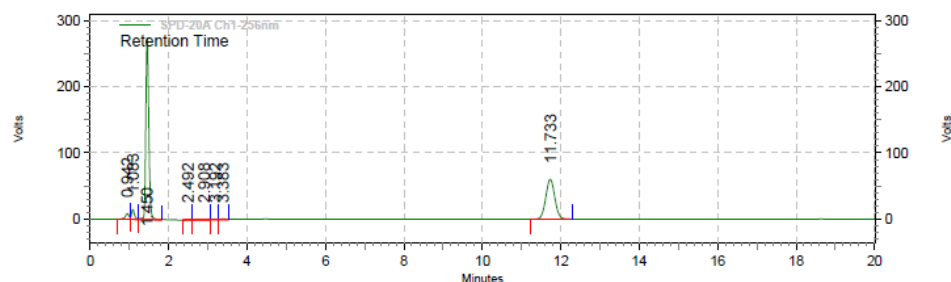
Week 9: solid storage at room temperature.

Data File: C:\Documents and Settings\User\Desktop\alex\Long Stability\week9\113\113-solid-12.04-RT.dat

Method: C:\EZStart\Projects\Default\Method\alex\40%.met

Acquired: 12/4/2015 1:12:09 PM

Printed: 12/4/2015 1:32:29 PM



SPD-20A
Ch1-256nm
Results

Retention Time	Area	Area %	Height	Height %
0.942	57583	2.19	8355	2.31
1.083	81541	3.10	14895	4.11
1.450	1469472	55.84	274691	75.83
2.492	14883	0.57	1392	0.38
2.908	29456	1.12	1082	0.30
3.192	9371	0.36	780	0.22
3.383	11285	0.43	947	0.26
11.733	958154	36.41	60097	16.59

Totals	2631745	100.00	362239	100.00
---------------	---------	--------	--------	--------

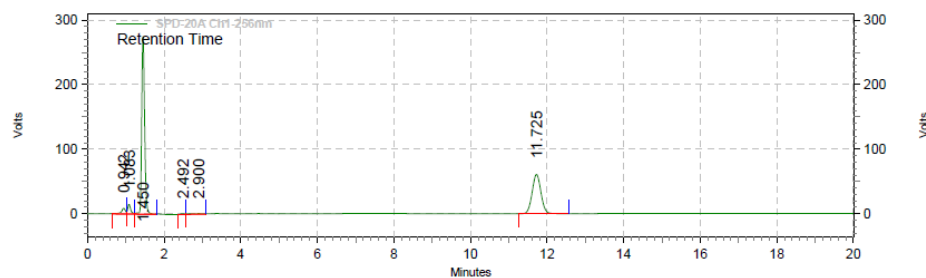
Week 9: solid storage at 4° C.

Data File: C:\Documents and Settings\User\Desktop\alex\Long Stability\week9\113\113-solid-12.04-4C.dat

Method: C:\EZStart\Projects\Default\Method\alex\40%.met

Acquired: 12/4/2015 1:33:05 PM

Printed: 12/4/2015 1:53:25 PM



SPD-20A
Ch1-256nm

Results

Retention Time	Area	Area %	Height	Height %
0.942	62647	2.39	8729	2.41
1.083	82281	3.14	14967	4.13
1.450	1458561	55.61	275476	75.99
2.492	13138	0.50	1392	0.38
2.900	31975	1.22	1076	0.30
11.725	974225	37.14	60890	16.80

Totals	2622827	100.00	362530	100.00
--------	---------	--------	--------	--------

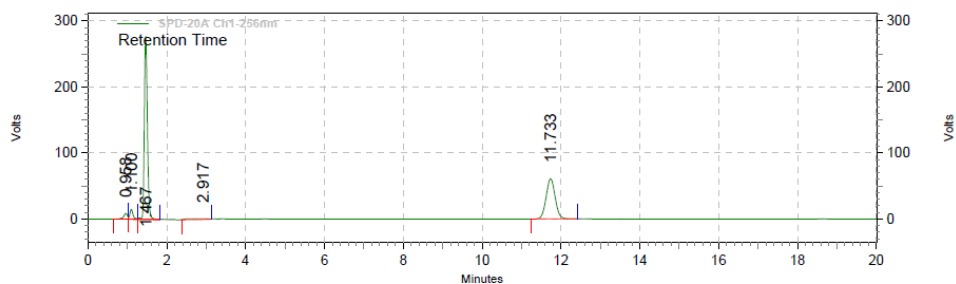
Week 9: solid storage at -20° C.

Data File: C:\Documents and Settings\User\Desktop\alex\Long Stability\week9\113\113-solid-12.04-(-20).dat

Method: C:\EZStart\Projects\Default\Method\alex\40%.met

Acquired: 12/4/2015 1:54:03 PM

Printed: 12/4/2015 2:14:24 PM



SPD-20A
Ch1-256nm

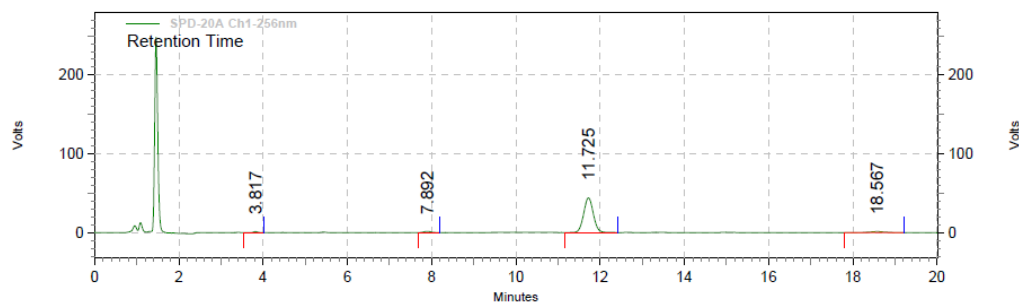
Results

Retention Time	Area	Area %	Height	Height %
0.958	59246	2.24	8454	2.33
1.100	81122	3.06	14941	4.12
1.467	1493718	56.43	277214	76.49
2.917	45225	1.71	1028	0.28
11.733	967695	36.56	60778	16.77

Totals	2647006	100.00	362415	100.00
--------	---------	--------	--------	--------

Week 8: solution storage at room temperature.

Data File: C:\Documents and Settings\User\Desktop\alex\Long
 Stability\week8\113\113-11.25-solution-RT.dat
 Method: C:\EZStart\Projects\Default\Method\tea\5~100.met
 Acquired: 11/25/2015 2:16:12 PM
 Printed: 2/16/2016 4:34:58 PM

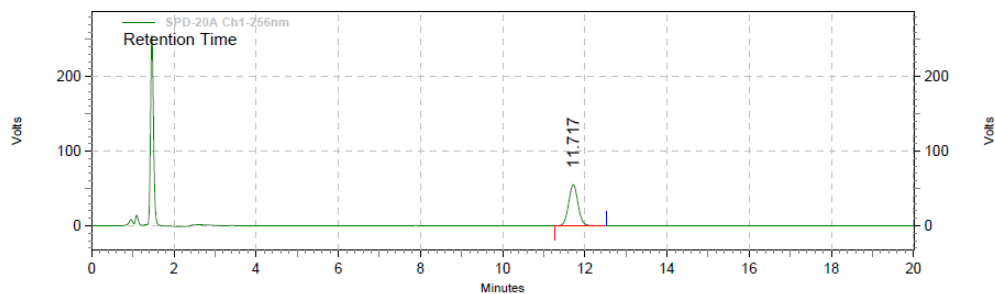


SPD-20A
Ch1-256nm
Results

Retention Time	Area	Area %	Height	Height %
3.817	8639	1.14	1275	2.65
7.892	17390	2.30	1572	3.27
11.725	699271	92.38	43976	91.55
18.567	31672	4.18	1213	2.53
Totals		756972	48036	100.00

Week 8: solution storage at 4° C.

Data File: C:\Documents and Settings\User\Desktop\alex\Long
 Stability\week8\113\113-11.25-solution-4C.dat
 Method: C:\EZStart\Projects\Default\Method\tea\5~100.met
 Acquired: 11/25/2015 2:37:13 PM
 Printed: 2/16/2016 4:33:00 PM

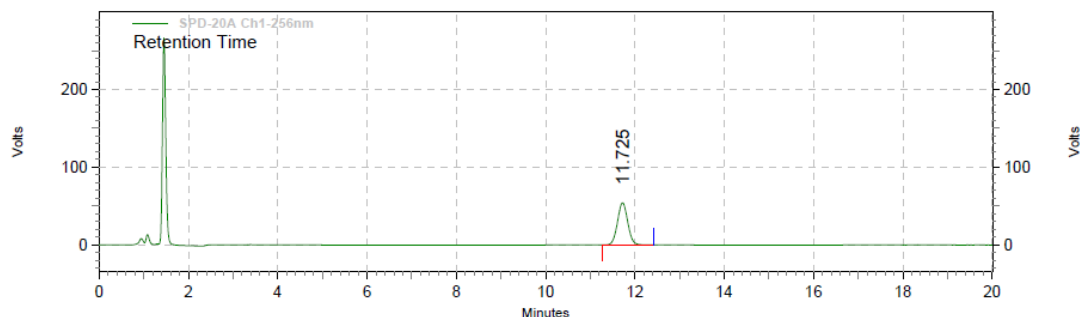


SPD-20A
Ch1-256nm
Results

Retention Time	Area	Area %	Height	Height %
11.717	874990	100.00	55102	100.00
Totals		874990	55102	100.00

Week 8: solution storage at -20° C.

Data File: C:\Documents and Settings\User\Desktop\alex\Long
 Stability\week8\113\113-11.25-solution-(-20).dat
 Method: C:\EZStart\Projects\Default\Method\tea\5~100.met
 Acquired: 11/25/2015 2:57:55 PM
 Printed: 2/16/2016 4:33:58 PM



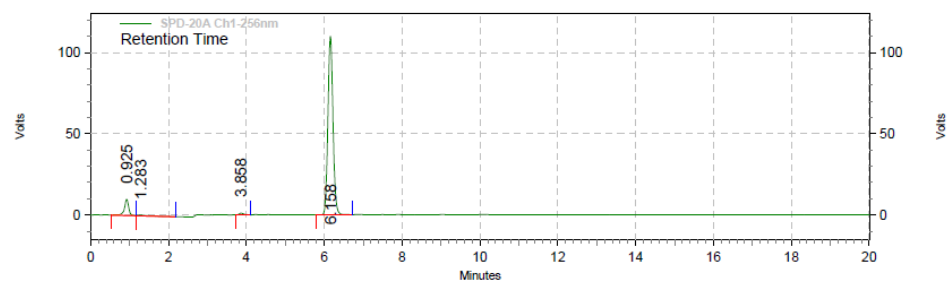
SPD-20A
Ch1-256nm
Results

Retention Time	Area	Area %	Height	Height %
11.725	860113	100.00	54129	100.00
Totals		860113	54129	100.00

HPLC spectra of BW-AQ-124.

Week 9: solid storage at room temperature.

Data File: C:\Documents and Settings\User\Desktop\alex\Long Stability\week9\101\124-solid-12.04-RT.dat
 Method: C:\EZStart\Projects\Default\Method\alex\50%.met
 Acquired: 12/4/2015 10:32:52 AM
 Printed: 12/4/2015 10:53:12 AM



SPD-20A
Ch1-256nm
Results

Retention Time	Area	Area %	Height	Height %
0.925	78668	7.16	9971	8.20
1.283	10826	0.99	535	0.44
3.858	9026	0.82	1095	0.90
6.158	1000374	91.03	109958	90.46
Totals		1098894	121559	100.00

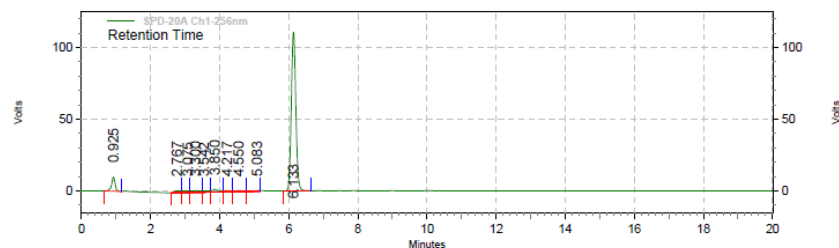
Week 9: solid storage at 4° C.

Data File: C:\Documents and Settings\User\Desktop\alex\Long Stability\week9\124\124-solid-12.04-4C.dat

Method: C:\EZStart\Projects\Default\Method\alex\50%.met

Acquired: 12/4/2015 10:54:07 AM

Printed: 12/4/2015 11:14:47 AM

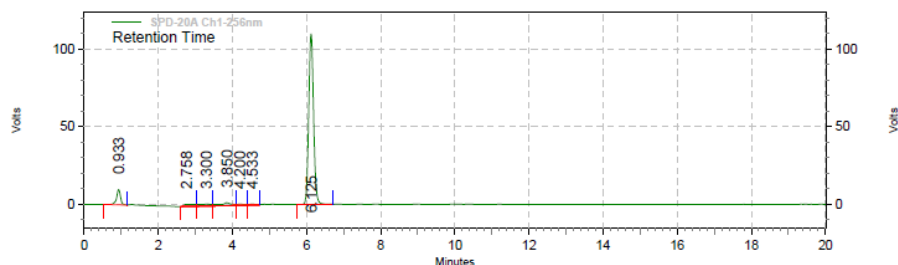


SPD-20A
Ch1-256nm
Results

Retention Time	Area	Area %	Height	Height %
0.925	72215	5.98	9844	7.64
2.767	17818	1.47	1330	1.03
3.075	16410	1.36	1161	0.90
3.300	22736	1.88	1160	0.90
3.542	12927	1.07	956	0.74
3.850	26685	2.21	1894	1.47
4.217	10761	0.89	823	0.64
4.550	13282	1.10	647	0.50
5.083	8867	0.73	365	0.28
6.133	1006334	83.30	110613	85.88
Totals	1208035	100.00	128793	100.00

Week 9: solid storage at -20° C.

Data File: C:\Documents and Settings\User\Desktop\alex\Long
 Stability\week9\124\124-solid-12.04-(-20).dat
 Method: C:\EZStart\Projects\Default\Method\alex\40%.met
 Acquired: 12/4/2015 11:15:55 AM
 Printed: 12/4/2015 11:36:34 AM



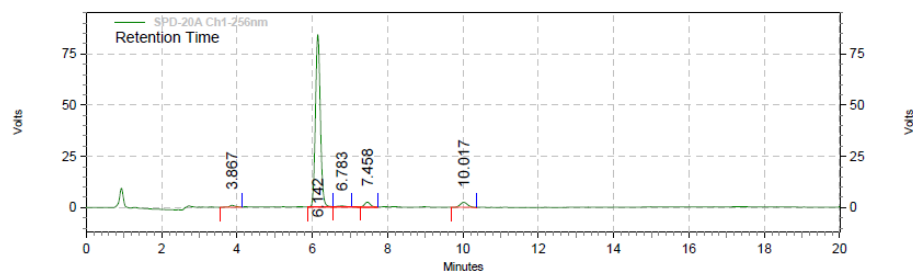
SPD-20A
Ch1-256nm
Results

Retention Time	Area	Area %	Height	Height %
0.933	74469	6.26	9820	7.84
2.758	27078	2.28	1365	1.09
3.300	28975	2.44	1172	0.94
3.850	38440	3.23	1833	1.46
4.200	11376	0.96	759	0.61
4.533	10098	0.85	589	0.47
6.125	998629	83.98	109640	87.59

Totals	1189065	100.00	125178	100.00
--------	---------	--------	--------	--------

Week 8: solution storage at room temperature.

Data File: C:\Documents and Settings\User\Desktop\alex\Long
 Stability\week8\124\124-11.25-solution-RT.dat
 Method: C:\EZStart\Projects\Default\Method\tea\5~100.met
 Acquired: 11/25/2015 11:50:59 AM
 Printed: 2/16/2016 4:38:23 PM



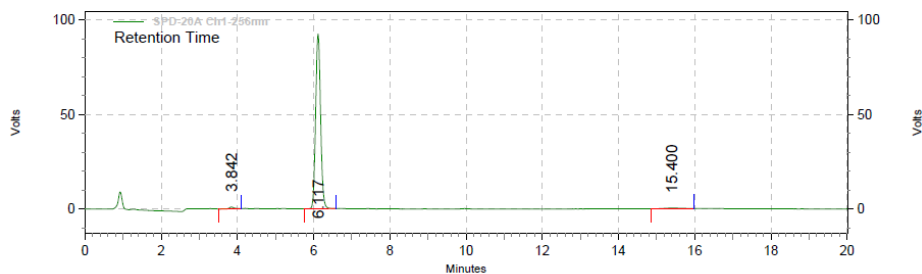
SPD-20A
Ch1-256nm
Results

Retention Time	Area	Area %	Height	Height %
3.867	9526	1.13	903	1.00
6.142	765213	90.76	84063	93.04
6.783	9331	1.11	545	0.60
7.458	25919	3.07	2419	2.68
10.017	33159	3.93	2420	2.68

Totals	843148	100.00	90350	100.00
--------	--------	--------	-------	--------

Week 8: solution storage at 4° C.

Data File: C:\Documents and Settings\User\Desktop\alex\Long
 Stability\week8\124-11.25-solution-4C.dat
 Method: C:\EZStart\Projects\Default\Method\tea\5~100.met
 Acquired: 11/25/2015 12:13:22 PM
 Printed: 2/16/2016 4:36:17 PM

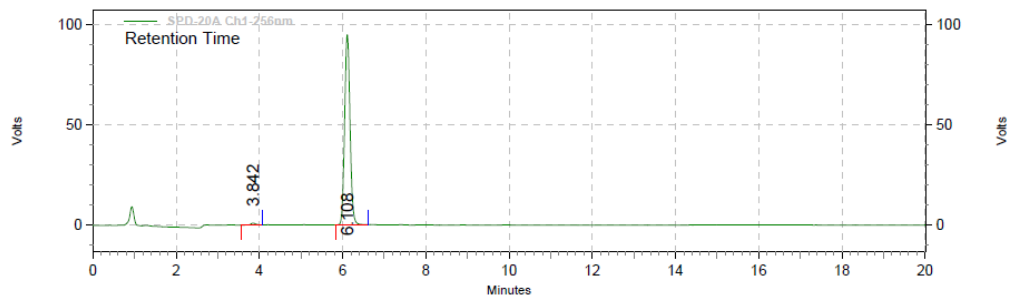


SPD-20A
Ch1-256nm
Results

Retention Time	Area	Area %	Height	Height %
3.842	9473	1.12	950	1.02
6.117	828324	97.71	92225	98.64
15.400	9973	1.18	319	0.34
Totals	847770	100.00	93494	100.00

Week 8: solution storage at -20° C.

Data File: C:\Documents and Settings\User\Desktop\alex\Long
 Stability\week8\124-11.25-solution-(-20).dat
 Method: C:\EZStart\Projects\Default\Method\tea\5~100.met
 Acquired: 11/25/2015 12:34:34 PM
 Printed: 2/16/2016 4:37:21 PM



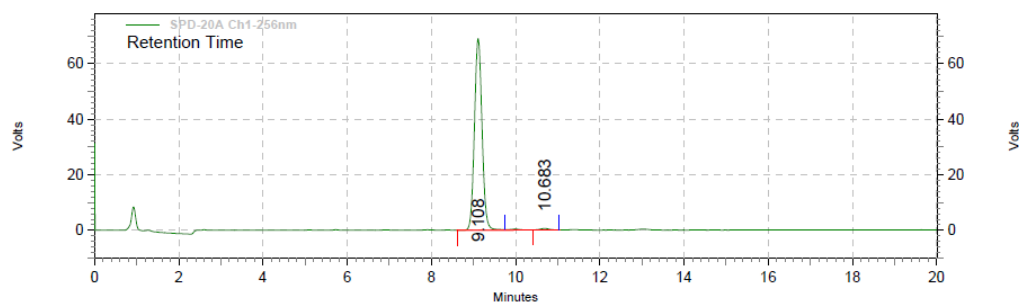
SPD-20A
Ch1-256nm
Results

Retention Time	Area	Area %	Height	Height %
3.842	8441	0.98	947	0.99
6.108	850734	99.02	94661	99.01
Totals	859175	100.00	95608	100.00

HPLC spectra of BW-AQ-101.

Week 12: solid storage at room temperature.

Data File: C:\Documents and Settings\User\Desktop\alex\Long
 Stability\week12\101\101-solid-01.05-RT.dat
 Method: C:\EZStart\Projects\Default\Method\alex\50%.met
 Acquired: 1/5/2016 10:10:44 AM
 Printed: 1/5/2016 10:34:38 AM



**SPD-20A
Ch1-256nm**

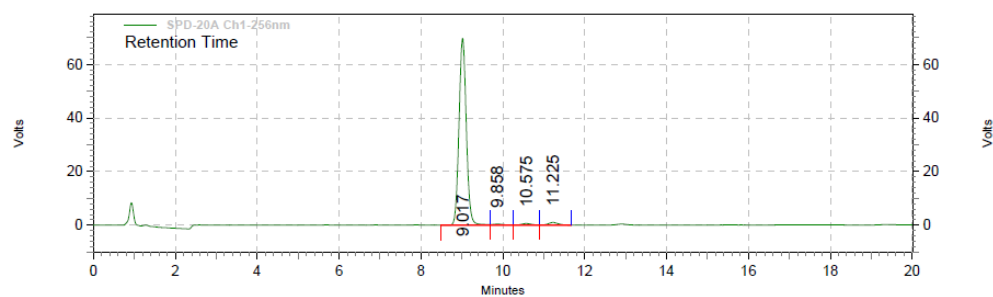
Results

Results

Retention Time	Area	Area %	Height	Height %	
9.108	862161	99.01	68941	99.19	
10.683	8635	0.99	565	0.81	
Totals		870796	100.00	69506	100.00

Week 12: solid storage at 4° C.

Data File: C:\Documents and Settings\User\Desktop\alex\Long
 Stability\week12\101\101-solid-01.05-4C.dat
 Method: C:\EZStart\Projects\Default\Method\alex\50%.met
 Acquired: 1/5/2016 10:33:26 AM
 Printed: 1/5/2016 10:59:25 AM



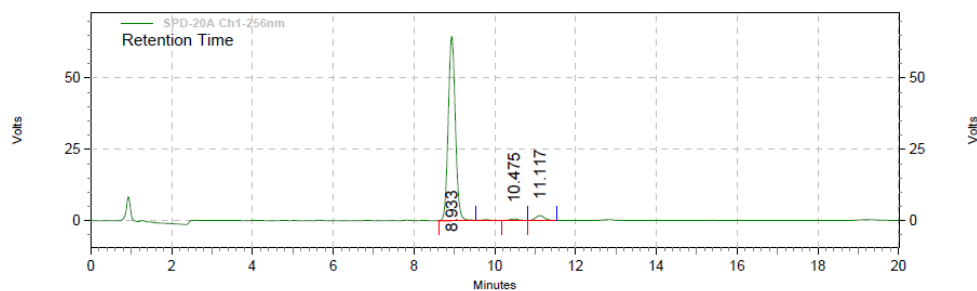
**SPD-20A
Ch1-256nm**

Results

Retention Time	Area	Area %	Height	Height %	
9.017	865255	96.21	69599	97.27	
9.858	7431	0.83	372	0.52	
10.575	10188	1.13	587	0.82	
11.225	16436	1.83	995	1.39	
Totals		899310	100.00	71553	100.00

Week 12: solid storage at -20° C.

Data File: C:\Documents and Settings\User\Desktop\alex\Long
 Stability\week12\101\101-solid-01.05-(-20).dat
 Method: C:\EZStart\Projects\Default\Method\alex\50%.met
 Acquired: 1/5/2016 11:01:11 AM
 Printed: 1/5/2016 11:21:35 AM



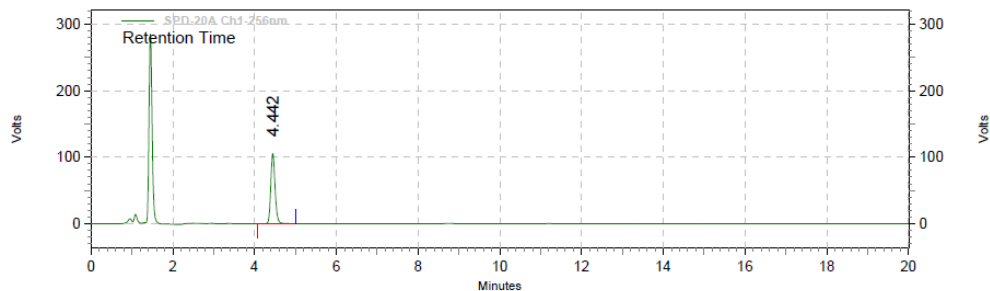
**SPD-20A
Ch1-256nm
Results**

Retention Time	Area	Area %	Height	Height %
8.933	787854	95.80	64448	96.68
10.475	7907	0.96	500	0.75
11.117	26621	3.24	1714	2.57
Totals	822382	100.00	66662	100.00

HPLC spectra of BW-AQ-112.

Week 12: solid storage at room temperature.

Data File: C:\Documents and Settings\User\Desktop\alex\Long
 Stability\week12\112\112-solid-01.05-RT.dat
 Method: C:\EZStart\Projects\Default\Method\alex\40%.met
 Acquired: 1/5/2016 1:10:34 PM
 Printed: 1/5/2016 1:31:35 PM

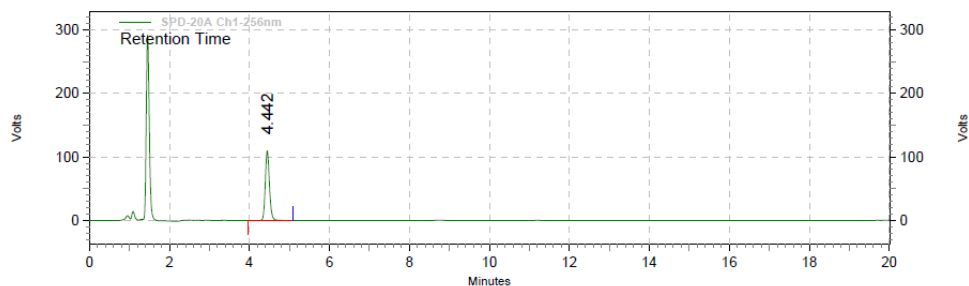


**SPD-20A
Ch1-256nm
Results**

Retention Time	Area	Area %	Height	Height %
4.442	771118	100.00	105486	100.00
Totals	771118	100.00	105486	100.00

Week 12: solid storage at 4° C.

Data File: C:\Documents and Settings\User\Desktop\alex\Long
 Stability\week12\112\112-solid-01.05-4C.dat
 Method: C:\EZStart\Projects\Default\Method\alex\40%.met
 Acquired: 1/5/2016 1:33:12 PM
 Printed: 1/5/2016 1:53:40 PM

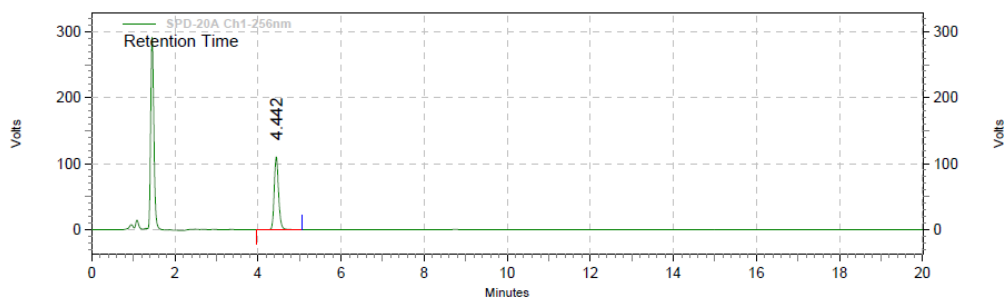


SPD-20A Ch1-256nm Results

Retention Time	Area	Area %	Height	Height %
4.442	796271	100.00	109672	100.00
Totals		796271	100.00	109672

Week 12: solid storage at -20° C.

Data File: C:\Documents and Settings\User\Desktop\alex\Long
 Stability\week12\112\112-solid-01.05-(-20).dat
 Method: C:\EZStart\Projects\Default\Method\alex\40%.met
 Acquired: 1/5/2016 1:54:13 PM
 Printed: 1/5/2016 2:16:21 PM



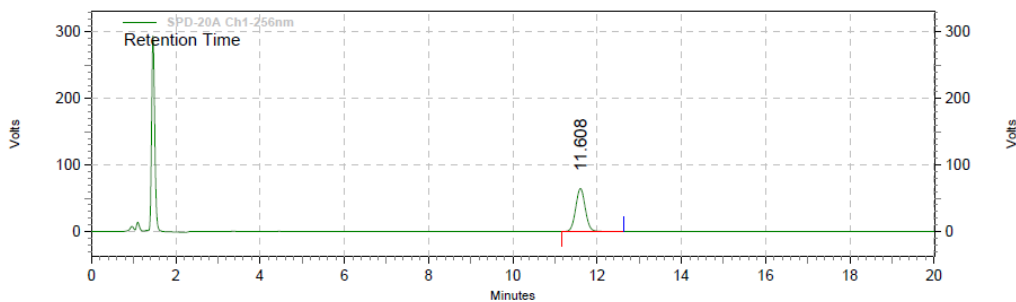
SPD-20A Ch1-256nm Results

Retention Time	Area	Area %	Height	Height %
4.442	803326	100.00	110048	100.00
Totals		803326	100.00	110048

HPLC spectra of BW-AQ-113.

Week 12: solid storage at room temperature.

Data File: C:\Documents and Settings\User\Desktop\alex\Long
Stability\week12\113\113-solid-01.05-RT.dat
Method: C:\EZStart\Projects\Default\Method\alex\40%.met
Acquired: 1/5/2016 3:02:02 PM
Printed: 1/5/2016 3:22:21 PM

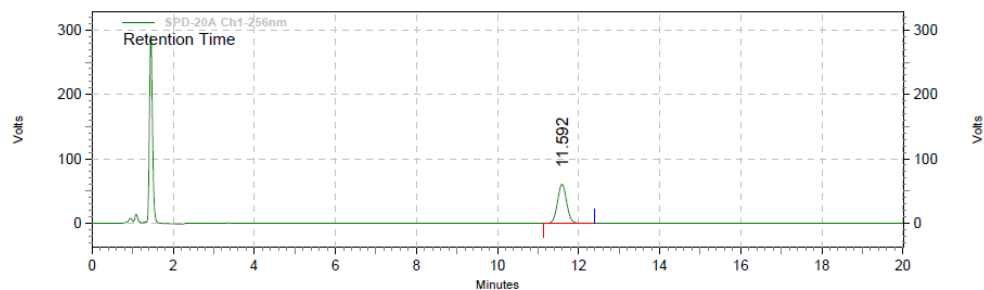


SPD-20A
Ch1-256nm
Results

Retention Time	Area	Area %	Height	Height %
11.608	1020268	100.00	64497	100.00
Totals		1020268	100.00	64497

Week 12: solid storage at 4° C.

Data File: C:\Documents and Settings\User\Desktop\alex\Long
Stability\week12\113\113-solid-01.05-4C.dat
Method: C:\EZStart\Projects\Default\Method\alex\40%.met
Acquired: 1/5/2016 2:41:03 PM
Printed: 1/5/2016 3:01:23 PM

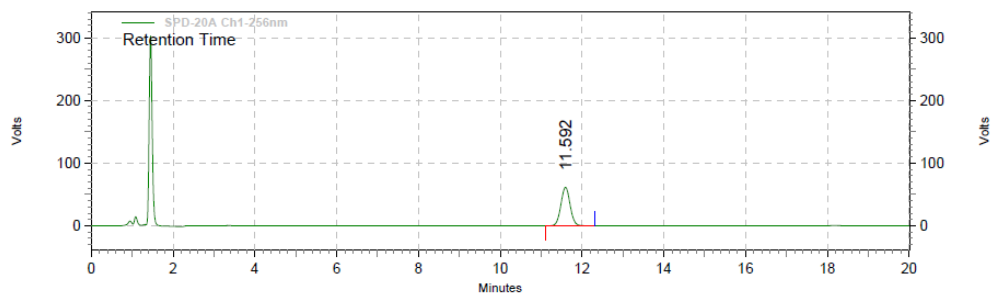


SPD-20A
Ch1-256nm
Results

Retention Time	Area	Area %	Height	Height %
11.592	957377	100.00	60735	100.00
Totals		957377	100.00	60735

Week 12: solid storage at -20° C.

Data File: C:\Documents and Settings\User\Desktop\alex\Long
 Stability\week12\113\113-solid-01.05-(-20).dat
 Method: C:\EZStart\Projects\Default\Method\alex\40%.met
 Acquired: 1/5/2016 2:20:03 PM
 Printed: 1/5/2016 2:40:22 PM



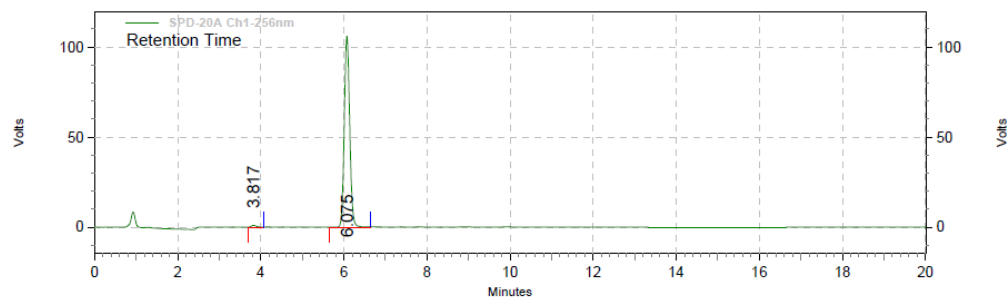
SPD-20A
Ch1-256nm
Results

Retention Time	Area	Area %	Height	Height %
11.592	961494	100.00	61418	100.00
Totals		961494	100.00	61418
				100.00

HPLC spectra of BW-AQ-124.

Week 12: solid storage at room temperature.

Data File: C:\Documents and Settings\User\Desktop\alex\Long
 Stability\week12\124\124-solid-01.05-RT.dat
 Method: C:\EZStart\Projects\Default\Method\alex\50%.met
 Acquired: 1/5/2016 11:23:03 AM
 Printed: 1/5/2016 11:43:25 AM

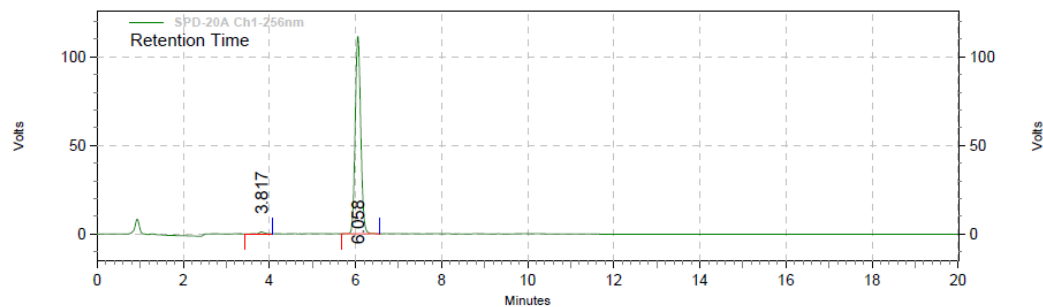


SPD-20A
Ch1-256nm
Results

Retention Time	Area	Area %	Height	Height %
3.817	8252	0.86	1009	0.94
6.075	955555	99.14	105933	99.06
Totals		963807	100.00	106942
				100.00

Week 12: solid storage at 4° C.

Data File: C:\Documents and Settings\User\Desktop\alex\Long
 Stability\week12\124\124-solid-01.05-4C.dat
 Method: C:\EZStart\Projects\Default\Method\alex\50%.met
 Acquired: 1/5/2016 11:45:10 AM
 Printed: 1/5/2016 12:05:31 PM



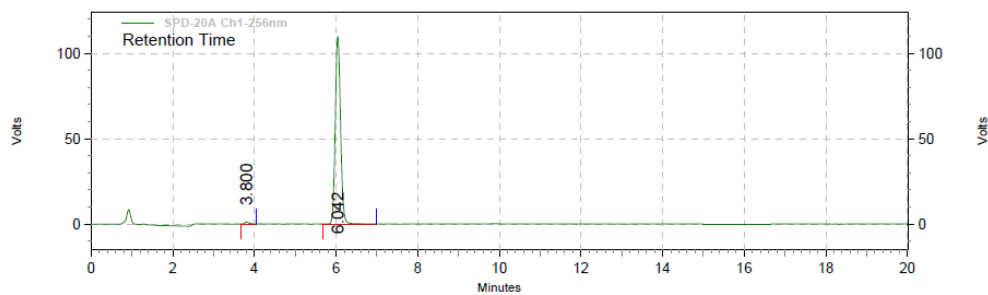
SPD-20A
Ch1-256nm
Results

Retention Time	Area	Area %	Height	Height %
3.817	9177	0.91	1081	0.96
6.058	997826	99.09	111437	99.04

Totals	1007003	100.00	112518	100.00
--------	---------	--------	--------	--------

Week 12: solid storage at -20° C.

Data File: C:\Documents and Settings\User\Desktop\alex\Long
 Stability\week12\124\124-solid-01.05-(-20).dat
 Method: C:\EZStart\Projects\Default\Method\alex\50%.met
 Acquired: 1/5/2016 12:06:16 PM
 Printed: 1/5/2016 12:31:15 PM



SPD-20A
Ch1-256nm
Results

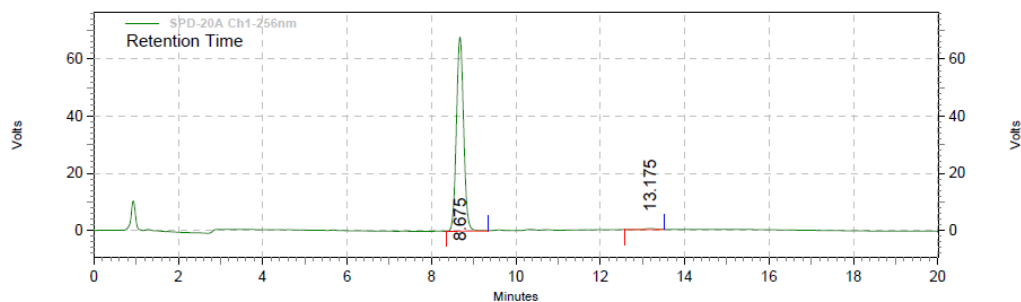
Retention Time	Area	Area %	Height	Height %
3.800	8765	0.88	1071	0.96
6.042	988168	99.12	109995	99.04

Totals	996933	100.00	111066	100.00
--------	--------	--------	--------	--------

HPLC spectra of BW-AQ-101.

Week 17: solid storage at room temperature.

Data File: C:\Documents and Settings\User\Desktop\alex\Long Stability\week17\101-2016-0208-solid-rt.dat
 Method: C:\EZStart\Projects\Default\Method\alex\50%.met
 Acquired: 2/8/2016 1:37:37 PM
 Printed: 2/8/2016 1:58:39 PM



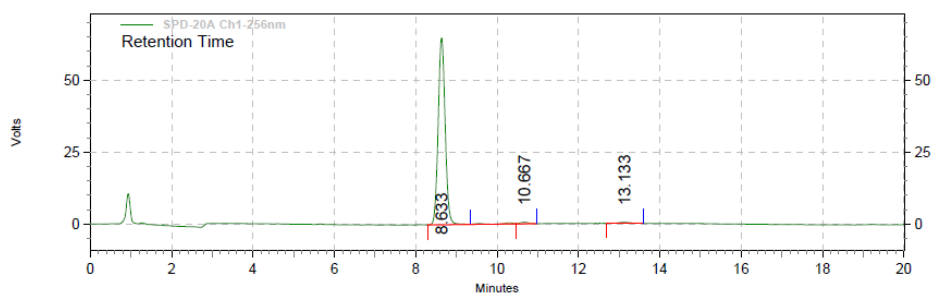
SPD-20A
Ch1-256nm
Results

Results

Retention Time	Area	Area %	Height	Height %	
8.675	809459	99.11	67984	99.50	
13.175	7274	0.89	339	0.50	
Totals		816733	100.00	68323	100.00

Week 17: solid storage at 4° C.

Data File: C:\Documents and Settings\User\Desktop\alex\Long
 Stability\week17\101-2016-0208-solid-4C.dat
 Method: C:\EZStart\Projects\Default\Method\alex\50%.met
 Acquired: 2/8/2016 2:00:06 PM
 Printed: 2/8/2016 2:28:48 PM

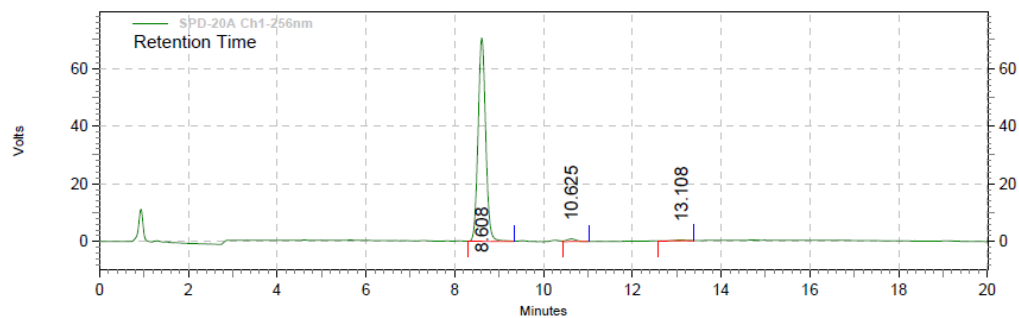


SPD-20A
Ch1-256nm
Results

Retention Time	Area	Area %	Height	Height %	
8.633	775358	97.72	64980	98.55	
10.667	8643	1.09	576	0.87	
13.133	9488	1.20	377	0.57	
Totals		793489	100.00	65933	100.00

Week 17: solid storage at -20° C.

Data File: C:\Documents and Settings\User\Desktop\alex\Long
Stability\week17\101-2016-0208-solid-(-20).dat
Method: C:\EZStart\Projects\Default\Method\alex\50%.met
Acquired: 2/8/2016 2:30:24 PM
Printed: 2/8/2016 2:51:00 PM



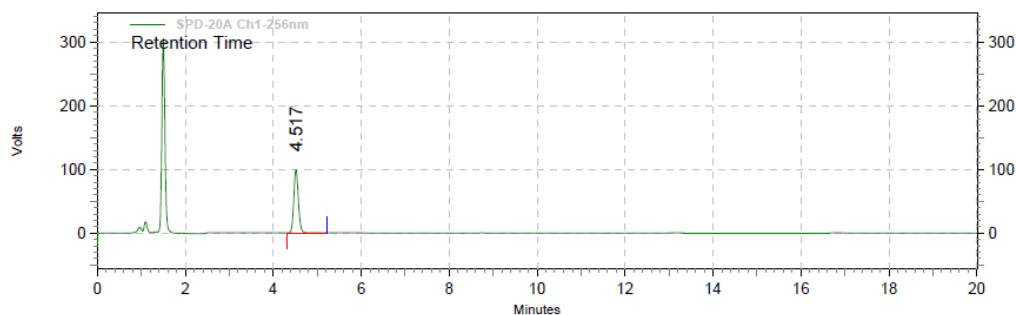
SPD-20A
Ch1-256nm
Results

Retention Time	Area	Area %	Height	Height %
8.608	841784	97.46	70417	98.19
10.625	13526	1.57	920	1.28
13.108	8407	0.97	381	0.53
Totals	863717	100.00	71718	100.00

HPLC spectra of BW-AQ-112.

Week 17: solid storage at room temperature.

Data File: C:\Documents and Settings\User\Desktop\alex\Long
 Stability\week17\112\112-2016-0209-solid-RT.dat
 Method: C:\EZStart\Projects\Default\Method\alex\40%.met
 Acquired: 2/9/2016 12:14:01 PM
 Printed: 2/9/2016 12:44:38 PM

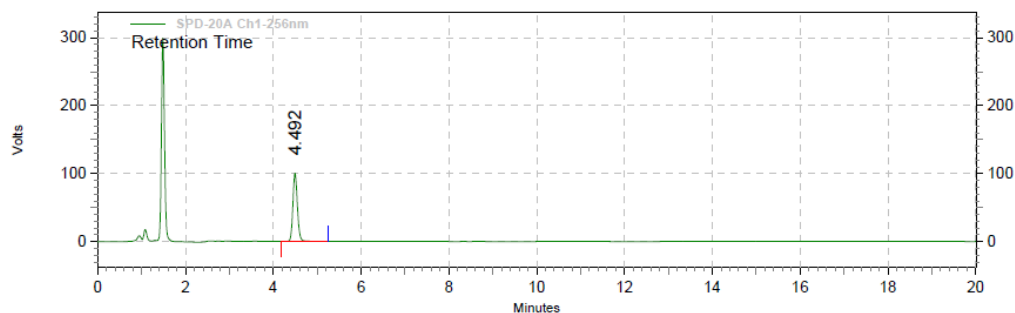


SPD-20A
Ch1-256nm
Results

Retention Time	Area	Area %	Height	Height %	
4.517	710514	100.00	99346	100.00	
Totals		710514	100.00	99346	100.00

Week 17: solid storage at 4° C.

Data File: C:\Documents and Settings\User\Desktop\alex\Long
 Stability\week17\112\112-2016-0209-solid-4C.dat
 Method: C:\EZStart\Projects\Default\Method\alex\40%.met
 Acquired: 2/9/2016 12:46:47 PM
 Printed: 2/9/2016 1:09:49 PM

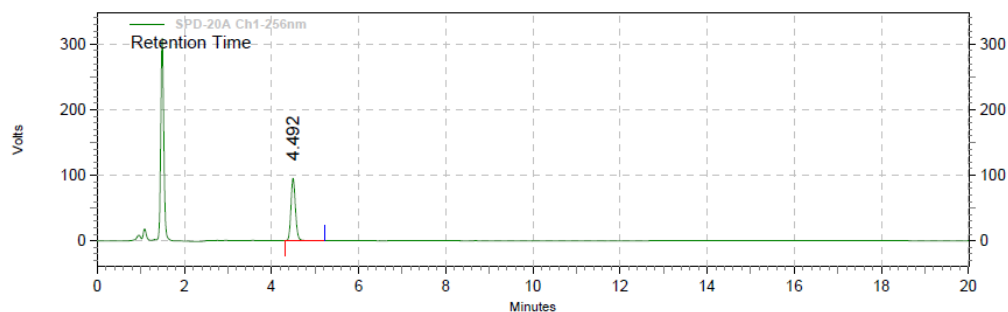


SPD-20A
Ch1-256nm
Results

Retention Time	Area	Area %	Height	Height %	
4.492	720439	100.00	100241	100.00	
Totals		720439	100.00	100241	100.00

Week 17: solid storage at -20° C.

Data File: C:\Documents and Settings\User\Desktop\alex\Long
 Stability\week17\112\112-2016-0209-solid-(-20).dat
 Method: C:\EZStart\Projects\Default\Method\alex\40%.met
 Acquired: 2/9/2016 1:11:25 PM
 Printed: 2/9/2016 1:31:46 PM



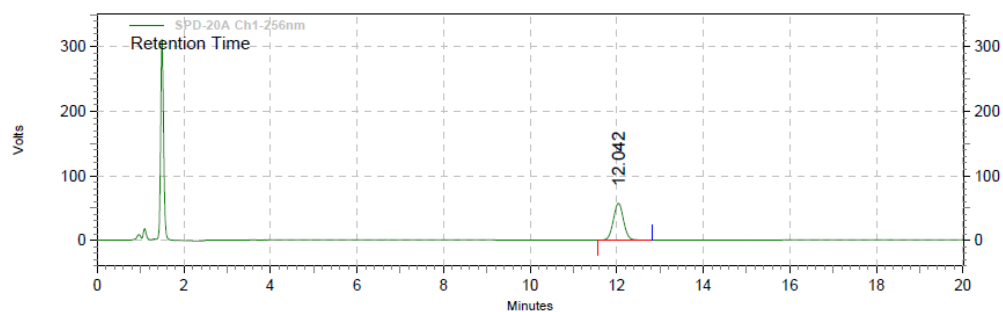
SPD-20A
Ch1-256nm
Results

Retention Time	Area	Area %	Height	Height %
4.492	679471	100.00	95179	100.00
Totals		679471	95179	100.00

HPLC spectra of BW-AQ-113.

Week 17: solid storage at room temperature.

Data File: C:\Documents and Settings\User\Desktop\alex\Long
 Stability\week17\113\113-2016-0209-solid-RT.dat
 Method: C:\EZStart\Projects\Default\Method\alex\40%.met
 Acquired: 2/9/2016 1:32:50 PM
 Printed: 2/9/2016 1:57:21 PM

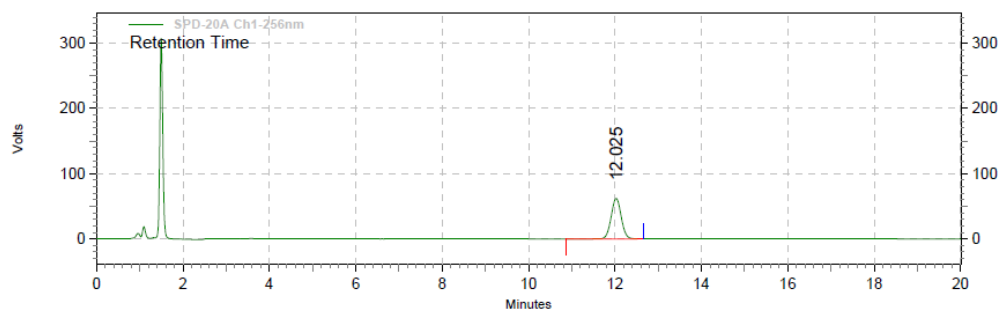


SPD-20A
Ch1-256nm
Results

Retention Time	Area	Area %	Height	Height %
12.042	928677	100.00	57148	100.00
Totals		928677	57148	100.00

Week 17: solid storage at 4° C.

Data File: C:\Documents and Settings\User\Desktop\alex\Long
 Stability\week17\113-2016-0209-solid-4C.dat
 Method: C:\EZStart\Projects\Default\Method\alex\40%.met
 Acquired: 2/9/2016 1:59:55 PM
 Printed: 2/9/2016 2:24:02 PM

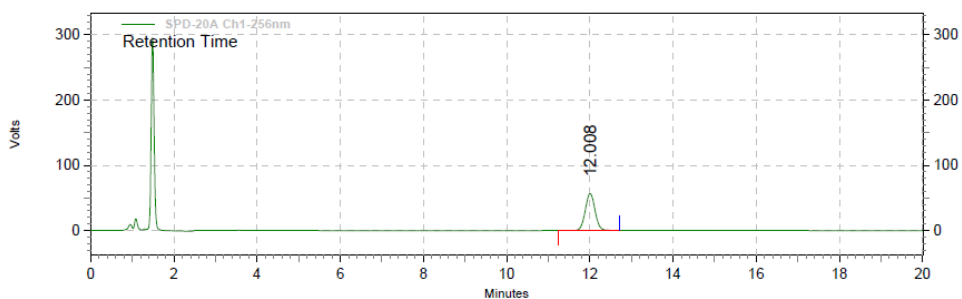


SPD-20A
Ch1-256nm
Results

Retention Time	Area	Area %	Height	Height %
12.025	1005160	100.00	61915	100.00
Totals		1005160	61915	100.00

Week 17: solid storage at -20° C.

Data File: C:\Documents and Settings\User\Desktop\alex\Long
 Stability\week17\113-2016-0209-solid-(-20).dat
 Method: C:\EZStart\Projects\Default\Method\alex\40%.met
 Acquired: 2/9/2016 2:24:38 PM
 Printed: 2/9/2016 2:56:49 PM



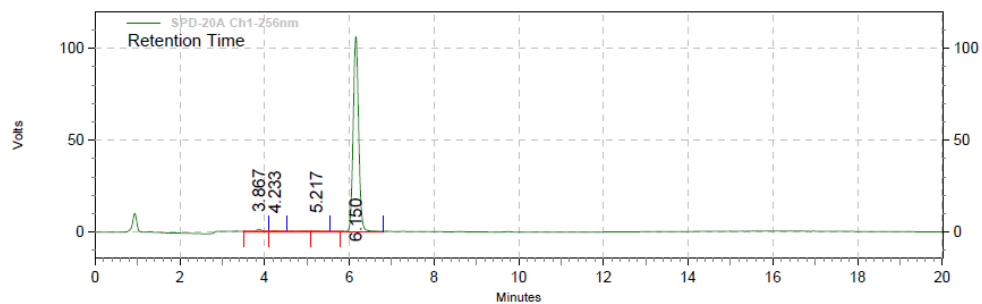
SPD-20A
Ch1-256nm
Results

Retention Time	Area	Area %	Height	Height %
12.008	917495	100.00	56582	100.00
Totals		917495	56582	100.00

HPLC spectra of BW-AQ-124.

Week 17: solid storage at room temperature.

Data File: C:\Documents and Settings\User\Desktop\alex\Long
Stability\week17\124\124-2016-0208-solid-RT.dat
Method: C:\EZStart\Projects\Default\Method\alex\50%.met
Acquired: 2/8/2016 2:52:09 PM
Printed: 2/8/2016 3:17:51 PM

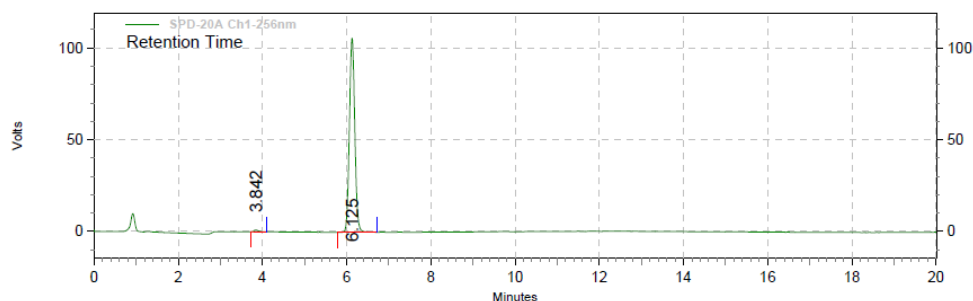


SPD-20A
Ch1-256nm
Results

Retention Time	Area	Area %	Height	Height %
3.867	13072	1.32	1146	1.06
4.233	7254	0.73	429	0.40
5.217	7378	0.75	358	0.33
6.150	961388	97.20	106036	98.21
Totals	989092	100.00	107969	100.00

Week 17: solid storage at 4° C.

Data File: C:\Documents and Settings\User\Desktop\alex\Long
 Stability\week17\124\124-2016-0208-solid-4C.dat
 Method: C:\EZStart\Projects\Default\Method\alex\50%.met
 Acquired: 2/8/2016 3:18:49 PM
 Printed: 2/8/2016 3:39:39 PM

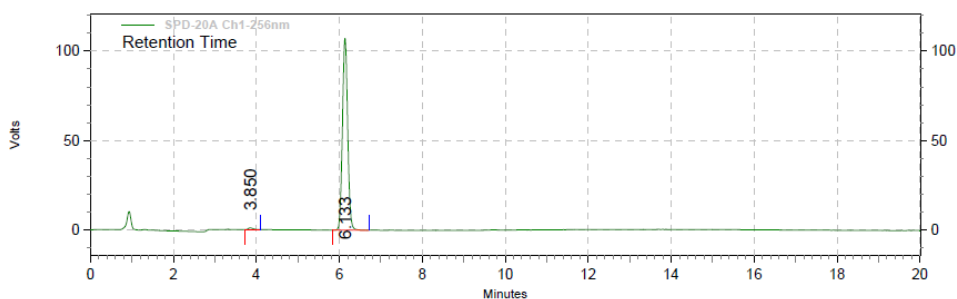


SPD-20A
Ch1-256nm
Results

Retention Time	Area	Area %	Height	Height %
3.842	8280	0.87	1034	0.97
6.125	944452	99.13	105822	99.03
Totals				
	952732	100.00	106856	100.00

Week 17: solid storage at -20° C.

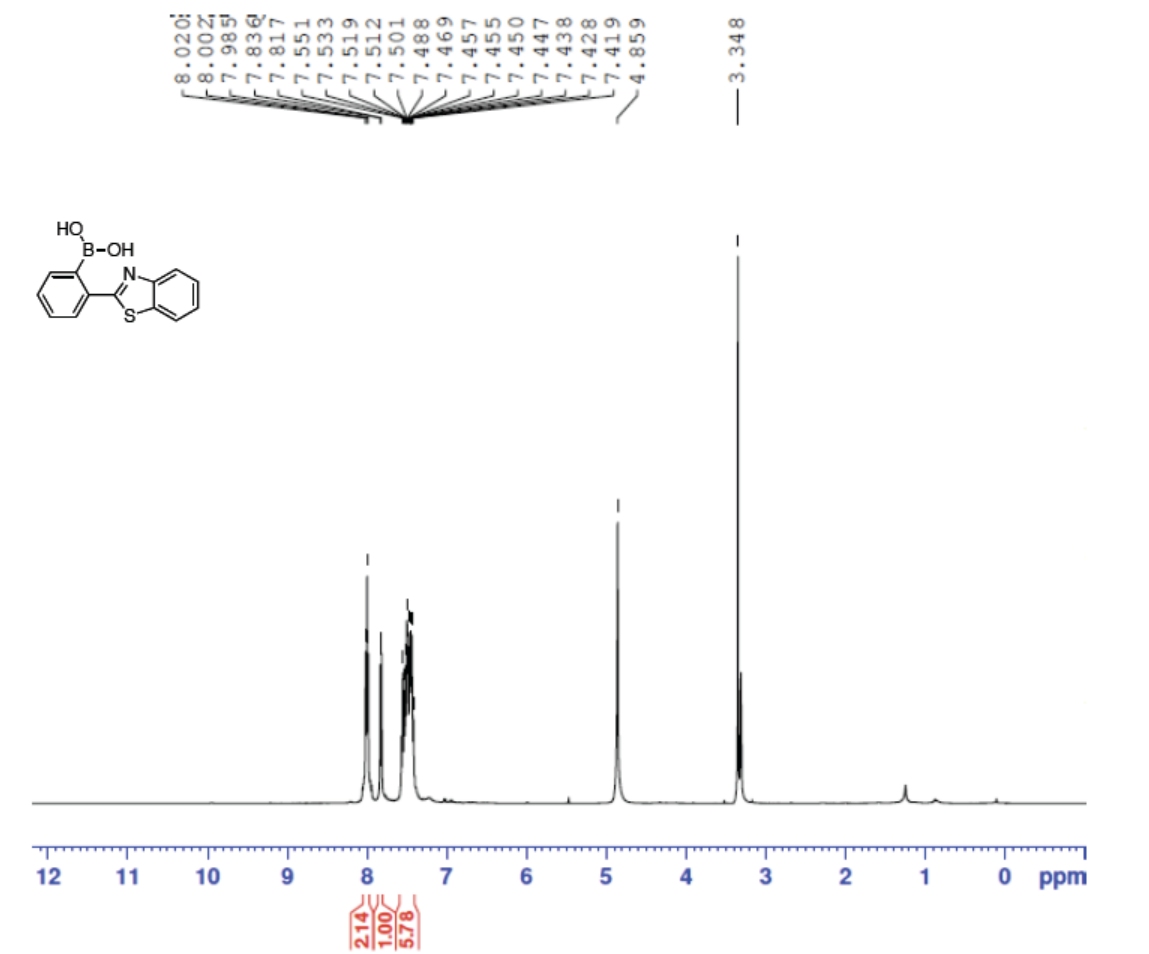
Data File: C:\Documents and Settings\User\Desktop\alex\Long
 Stability\week17\124\124-2016-0208-solid-(-20).dat
 Method: C:\EZStart\Projects\Default\Method\alex\50%.met
 Acquired: 2/8/2016 3:40:31 PM
 Printed: 2/8/2016 4:01:01 PM



SPD-20A
Ch1-256nm
Results

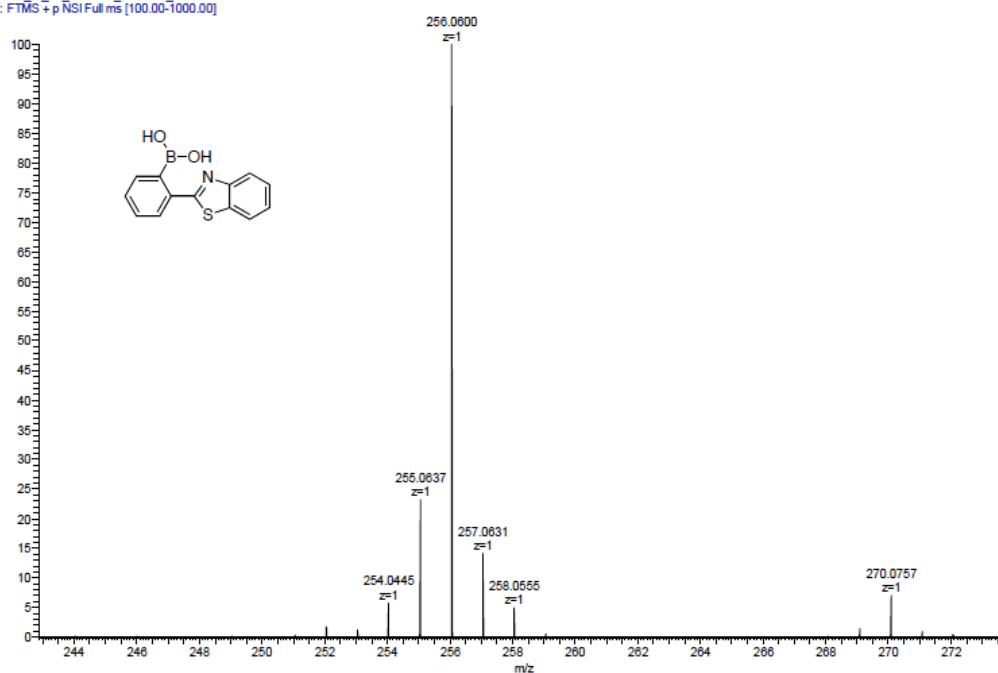
Retention Time	Area	Area %	Height	Height %	
3.850	8303	0.87	1044	0.96	
6.133	946877	99.13	107315	99.04	
Totals		955180	100.00	108359	100.00

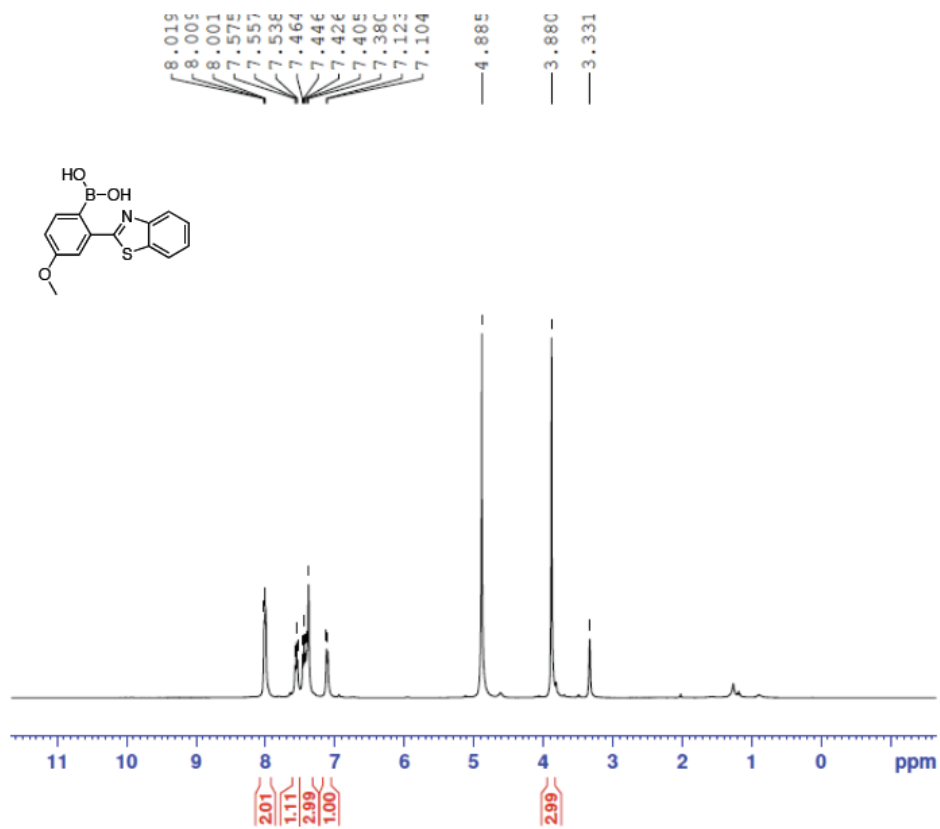
Appendix C NMR data for the compounds described in Chapter 2

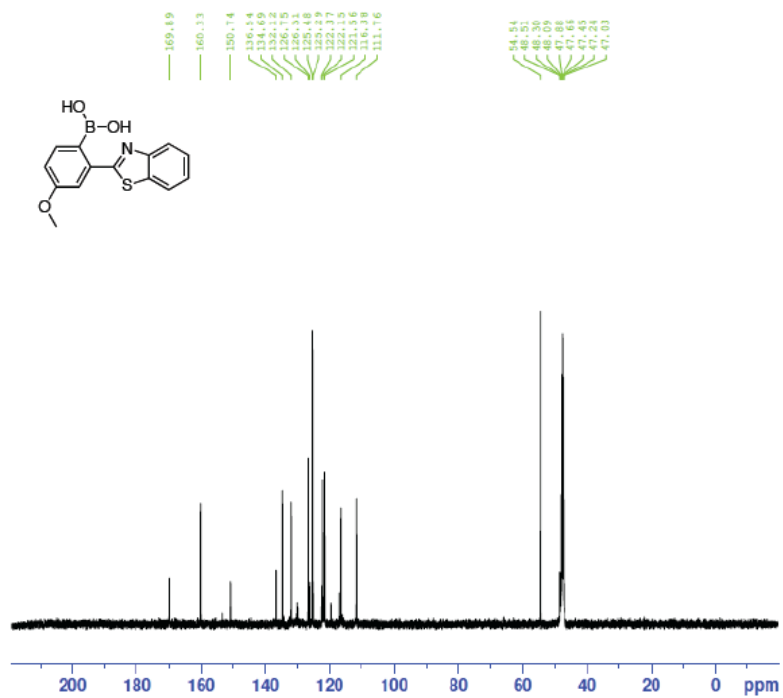


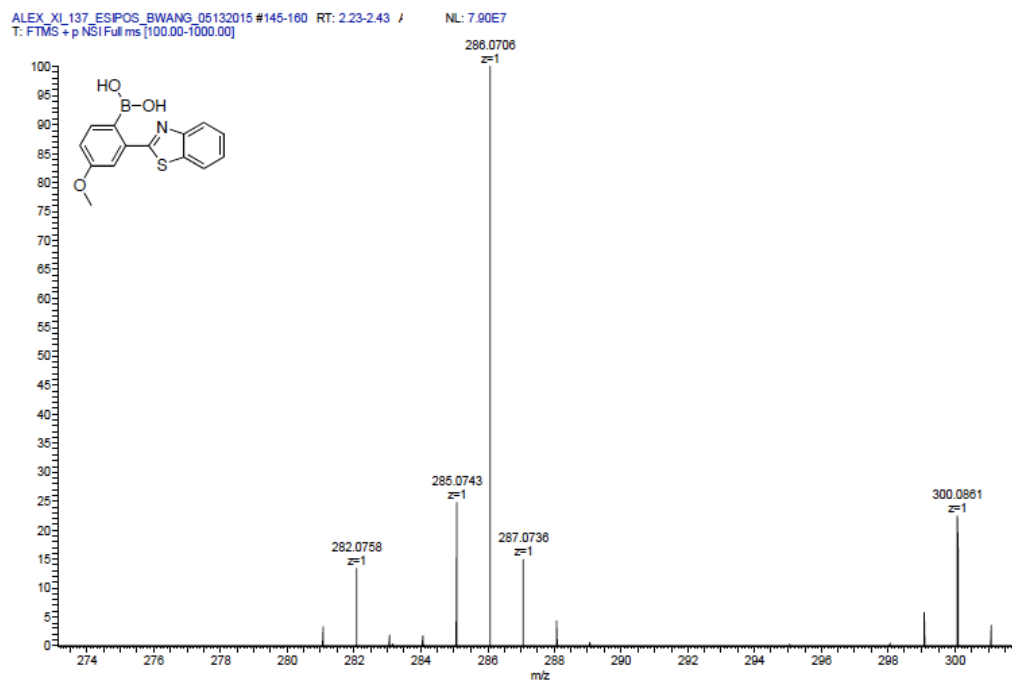
ALEX_XI.55_ESIPOS_BWANG_05132015 #150-161 RT: 2.45-2.60 A'
T: FTMS + p NSI Full ms [100.00-1000.00]

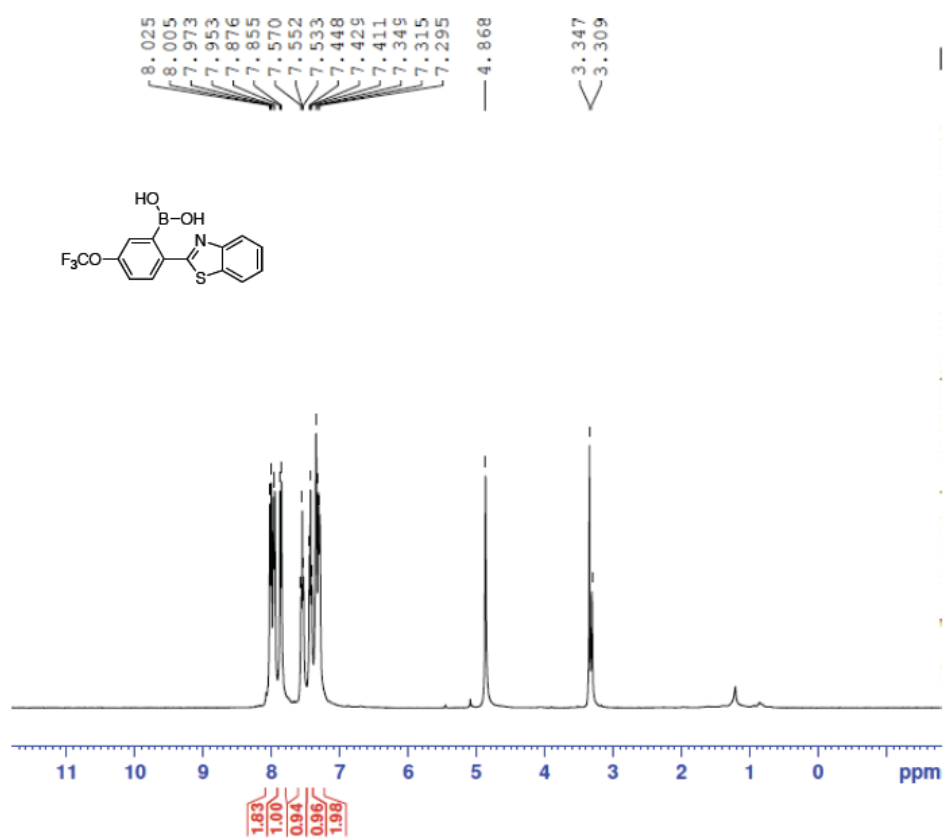
L: 1.09E8

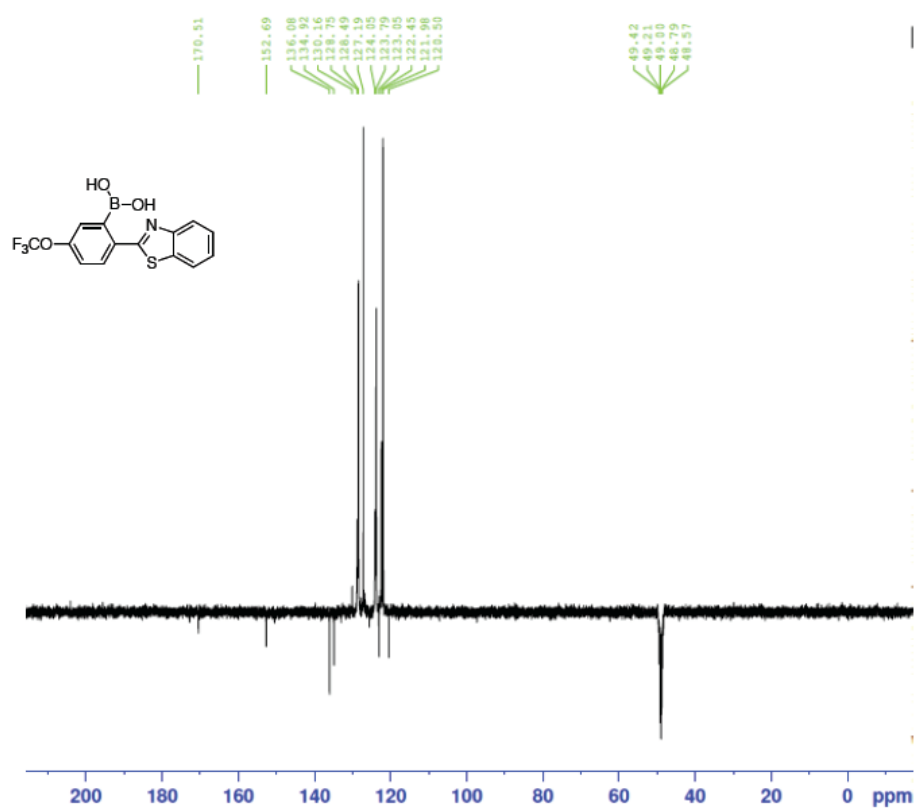


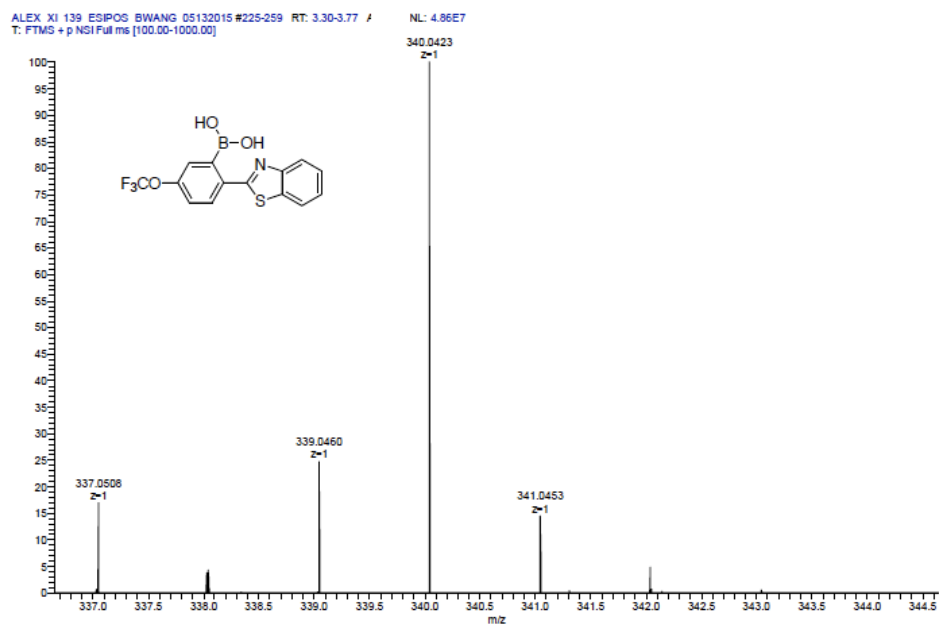


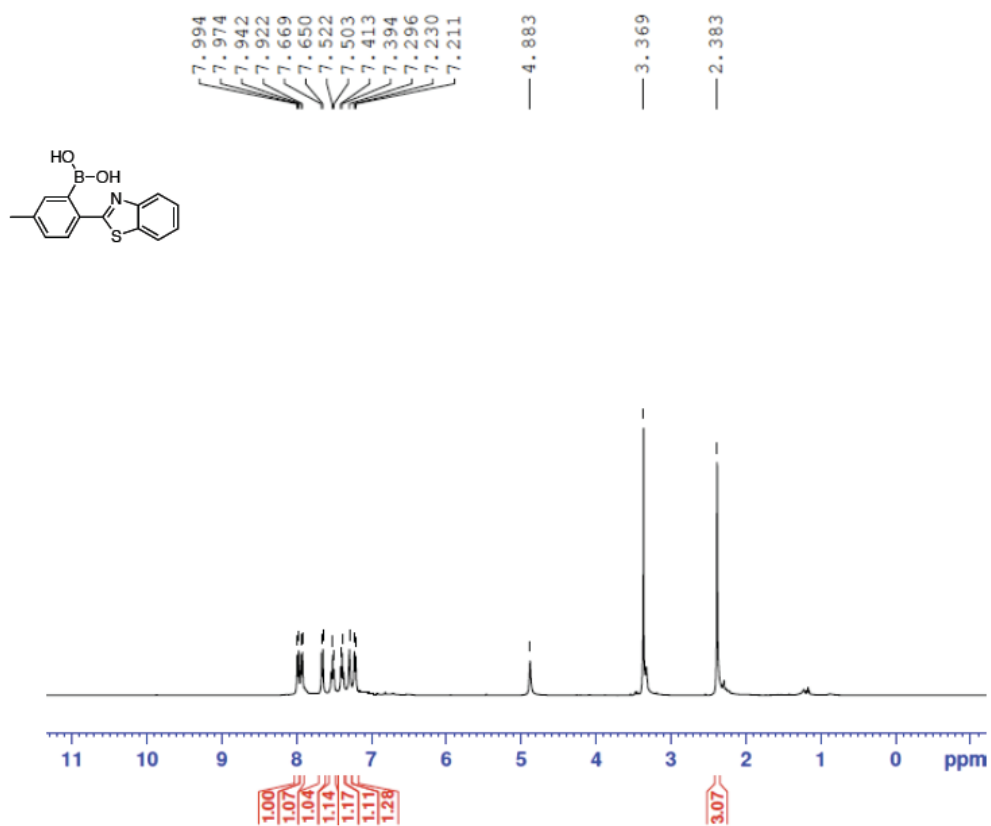


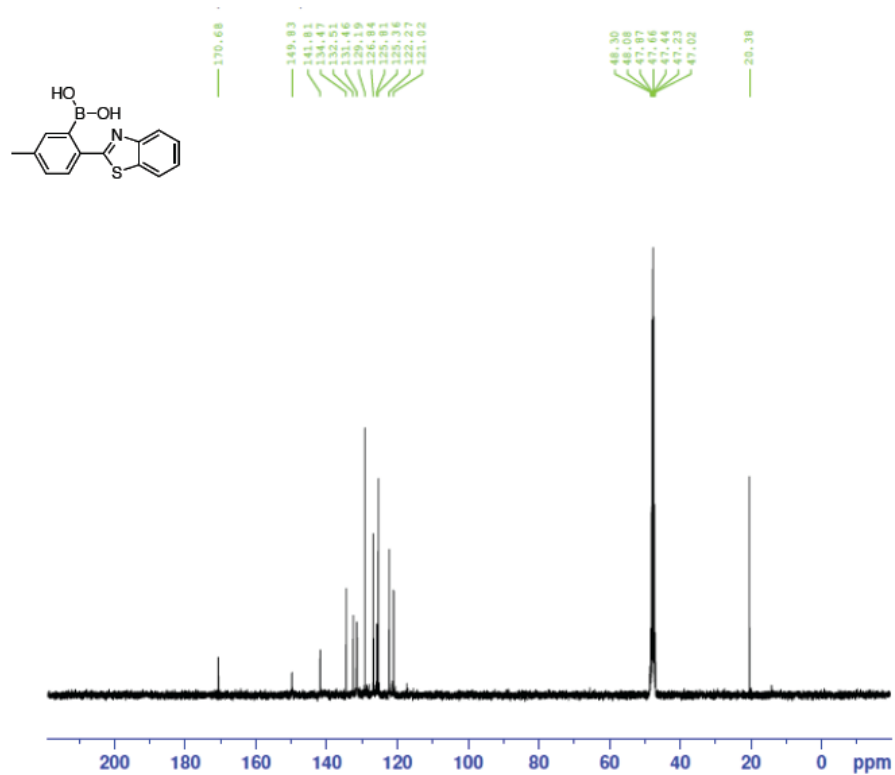




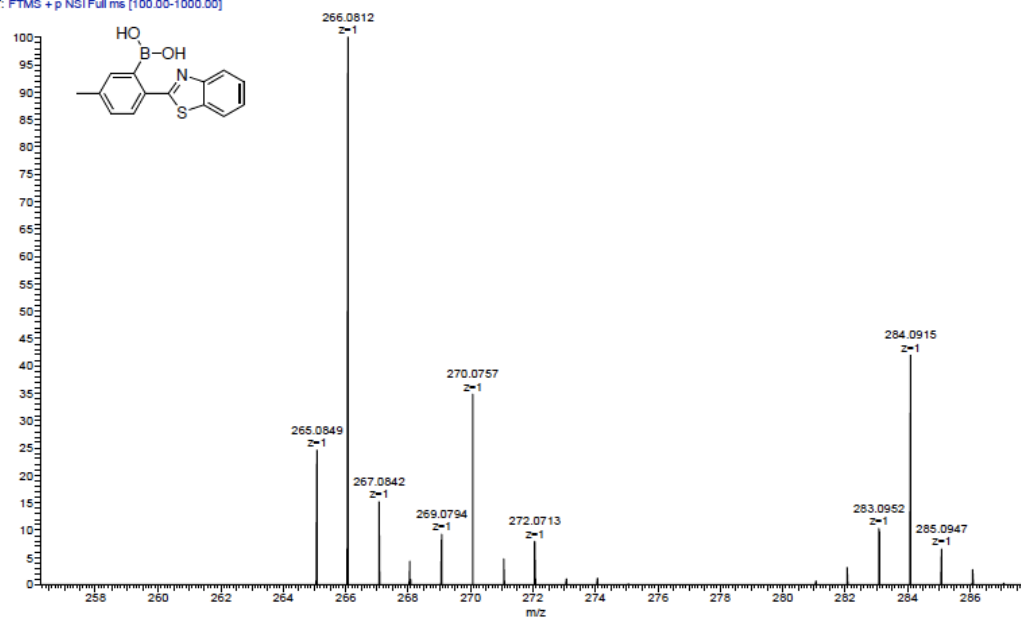


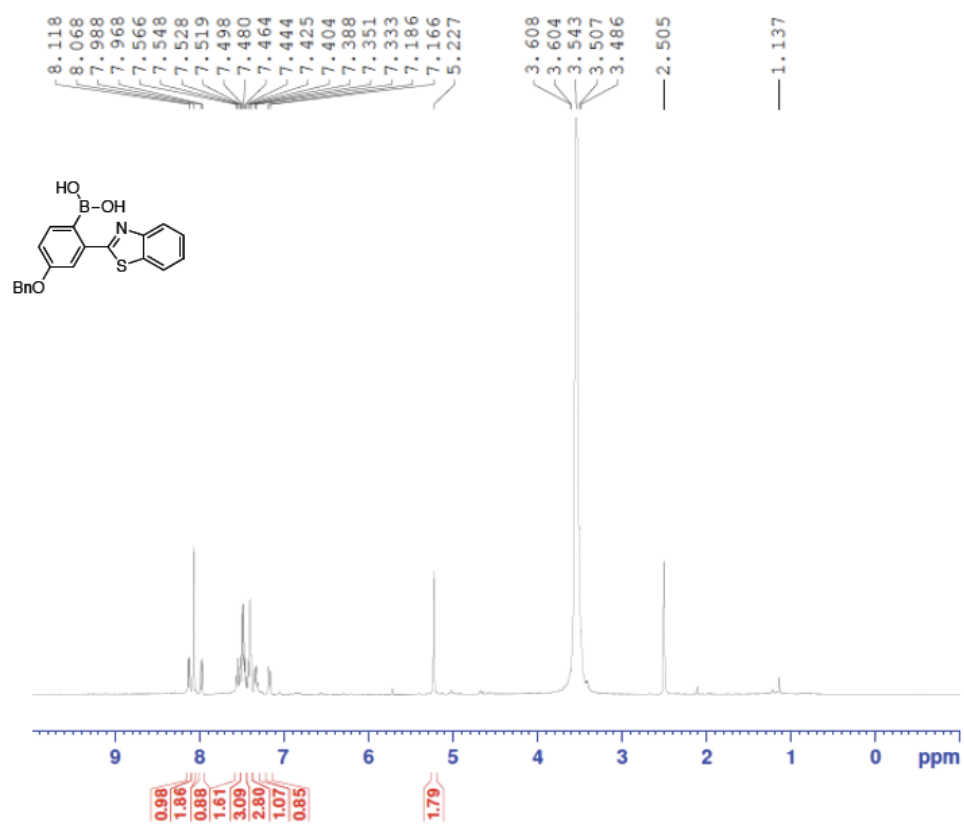


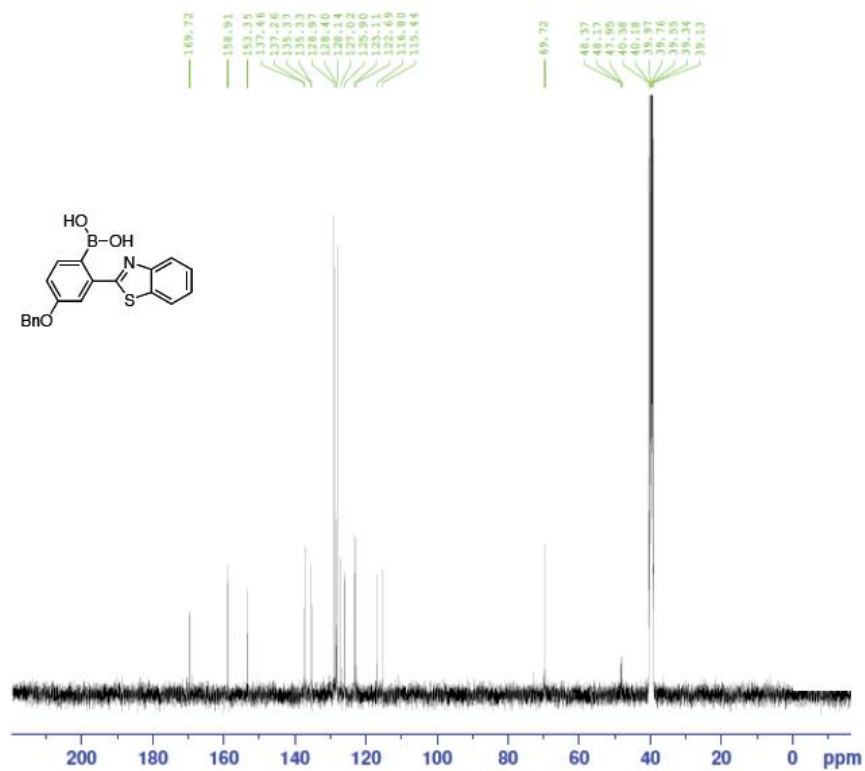




ALEX_XI_153_ESPOS_BWANG_05132015_#199-219 RT: 2.98-3.25 / NL: 1.75E8
T: FTMS + p NSI Full ms [100.00-1000.00]

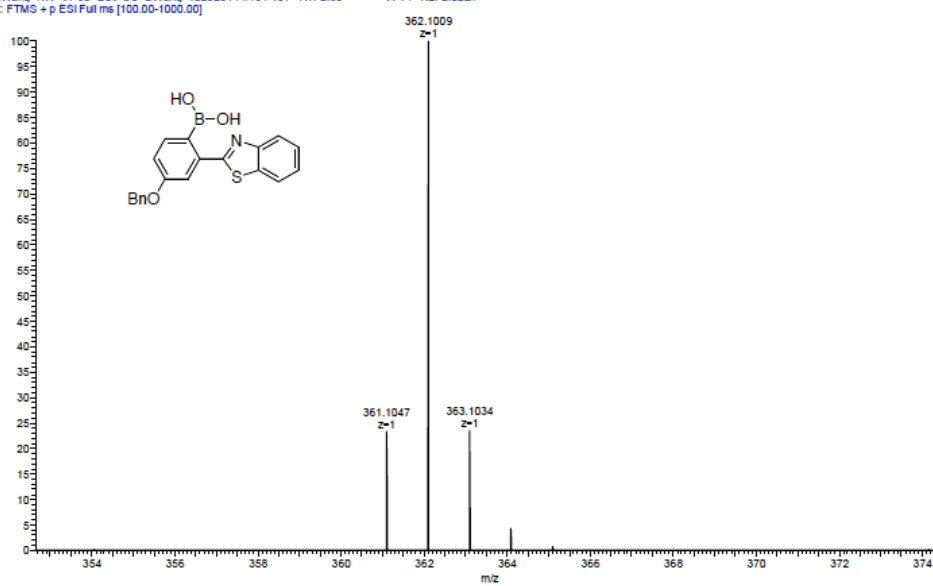


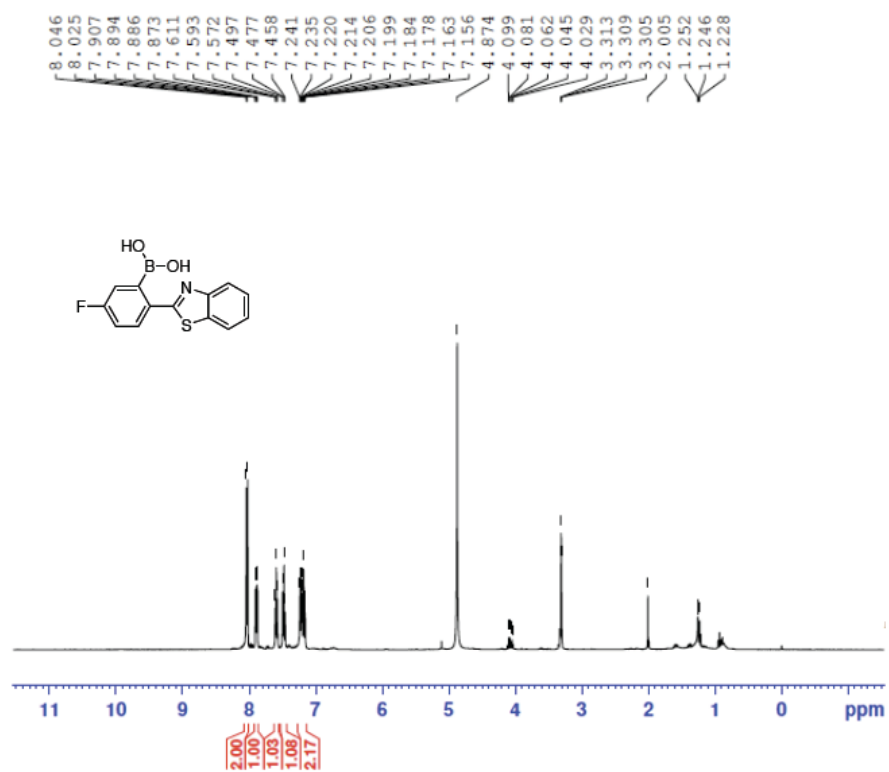


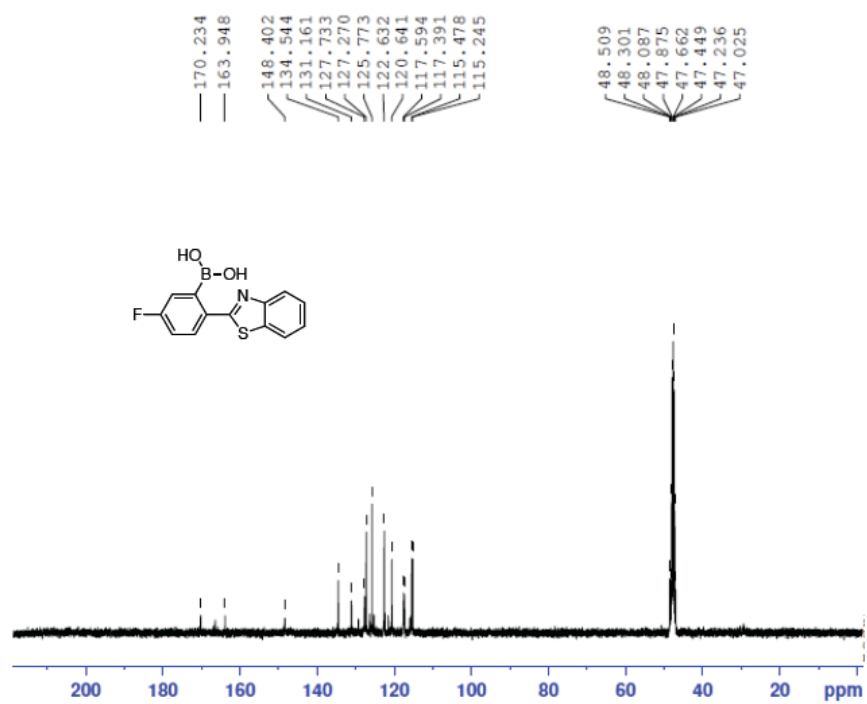


KWang KW VI 50 ESIP05 BWang 10292014 #184-197 RT: 2.60-
T: FTMS + p ESI Full ms [100.00-1000.00]

/: 14 NL: 2.02E7

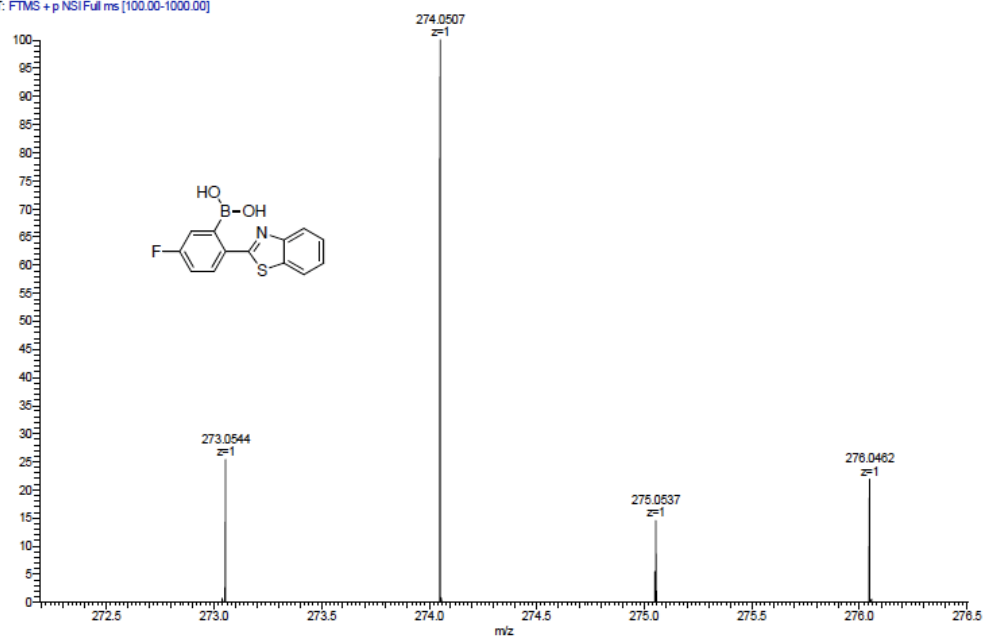


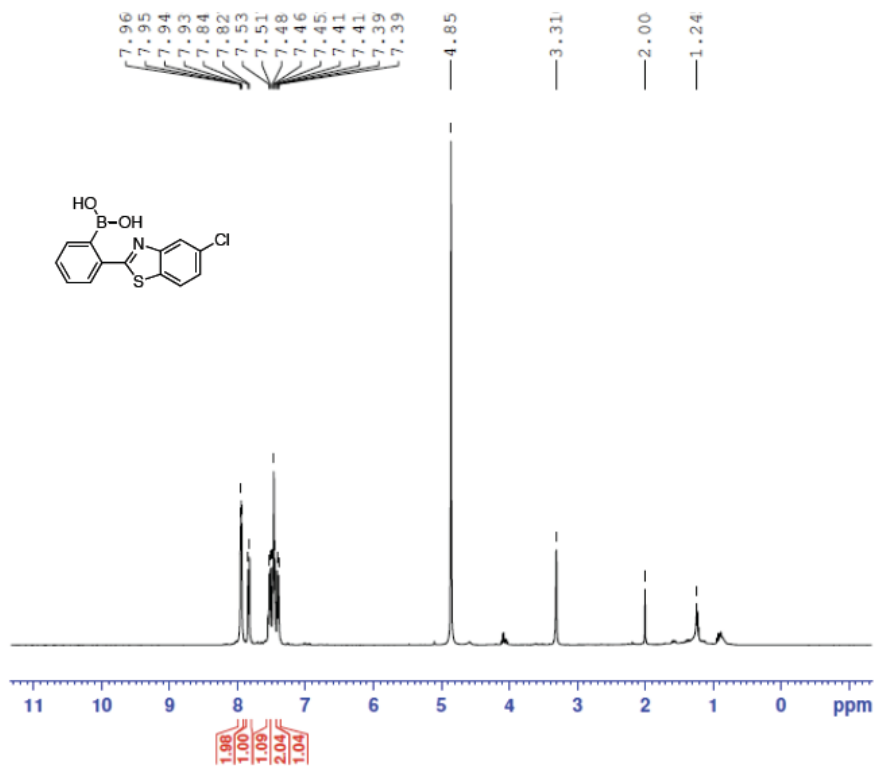


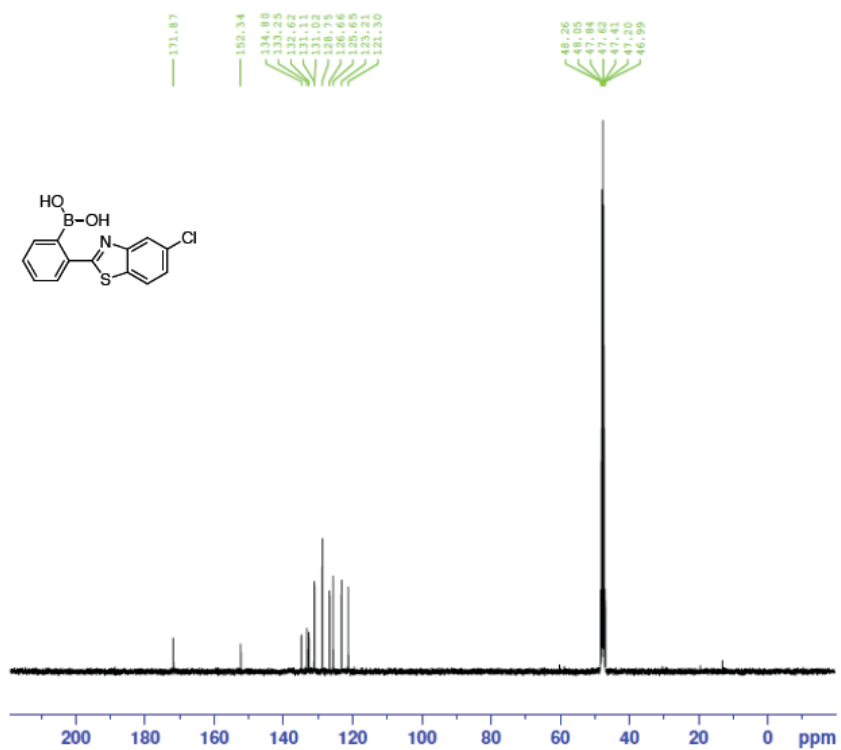


ALEX_XL51_ESIPOS_BIWANG_05132015 #197-212 RT: 3.09-3.29 A¹
T: FTMS + p NSI Full ms [100.00-1000.00]

L: 6.86E7

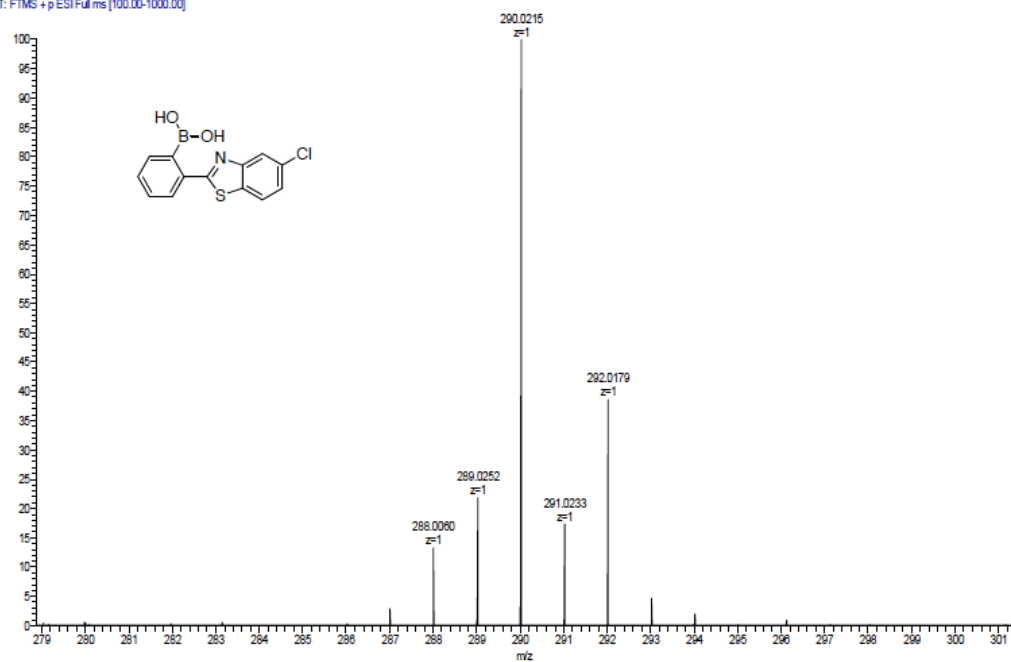


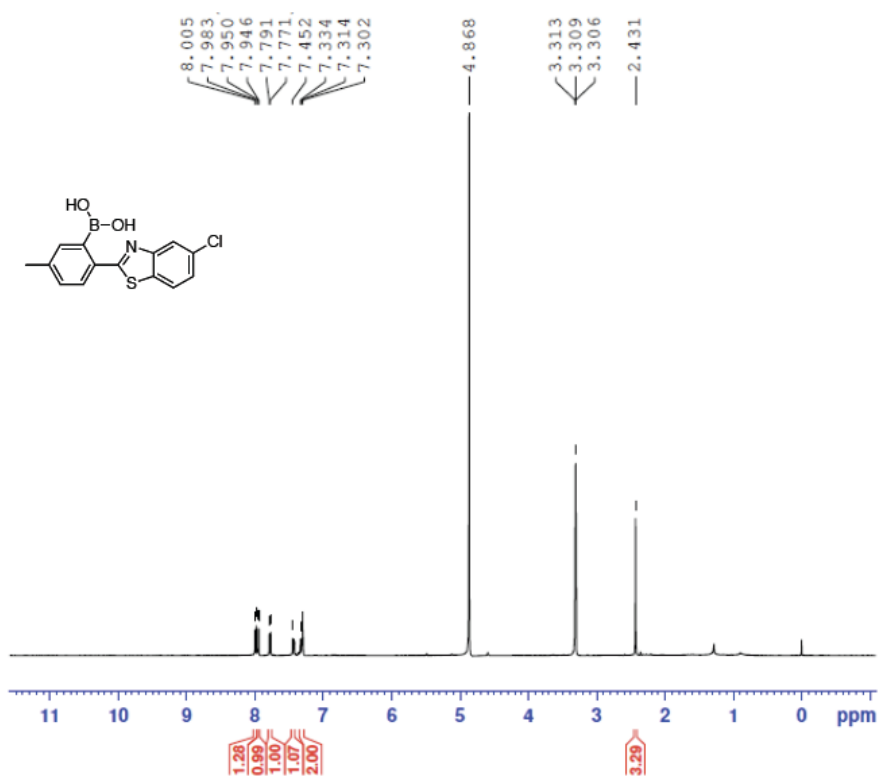


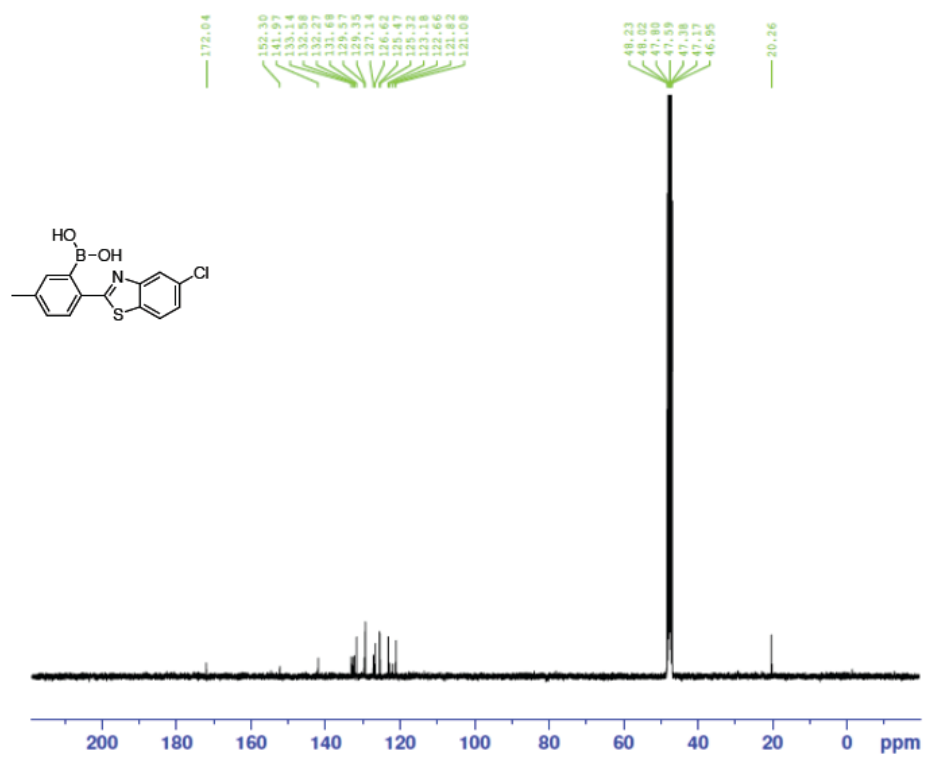


ALEX_XII_43_ESbos_BWANG_05072015_1_150507230426 #162-221
T: FTMS +p ESIFull.ms [100.00-1000.00]

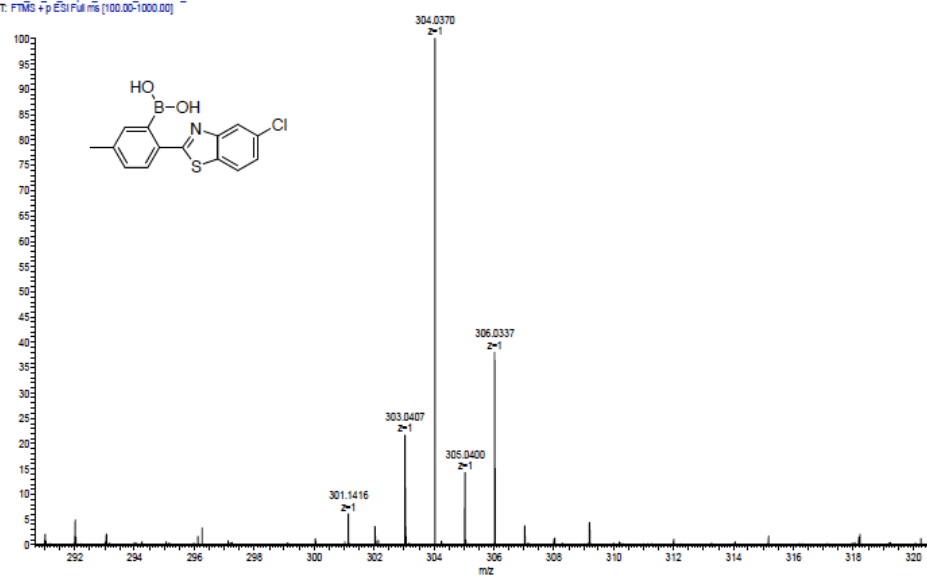
1-3.81 AV: 30 NL: 3.70E7

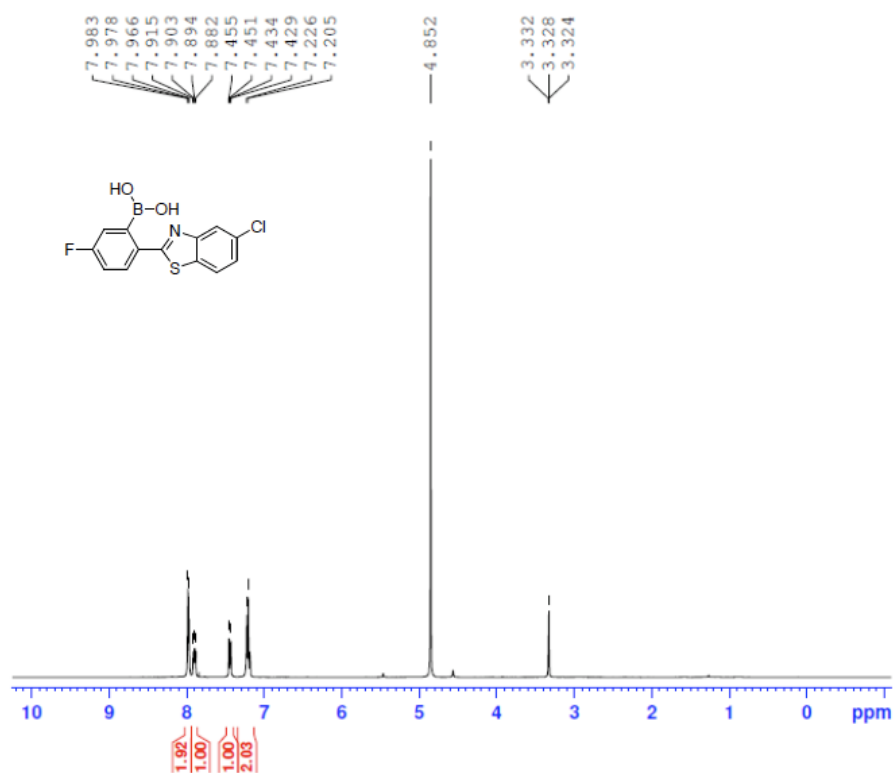


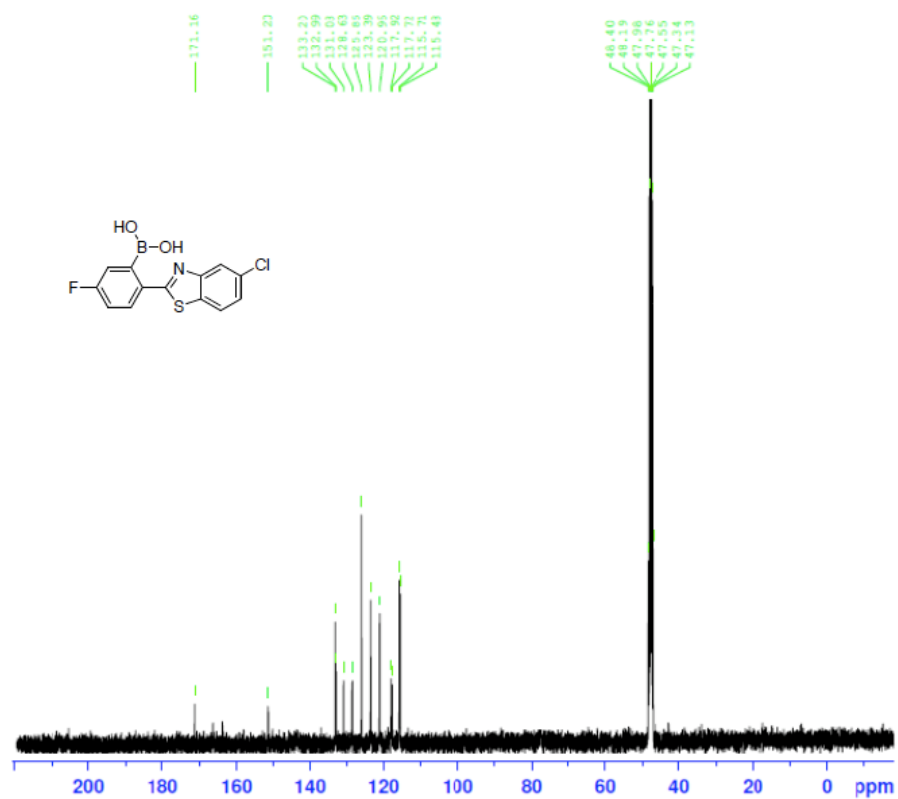




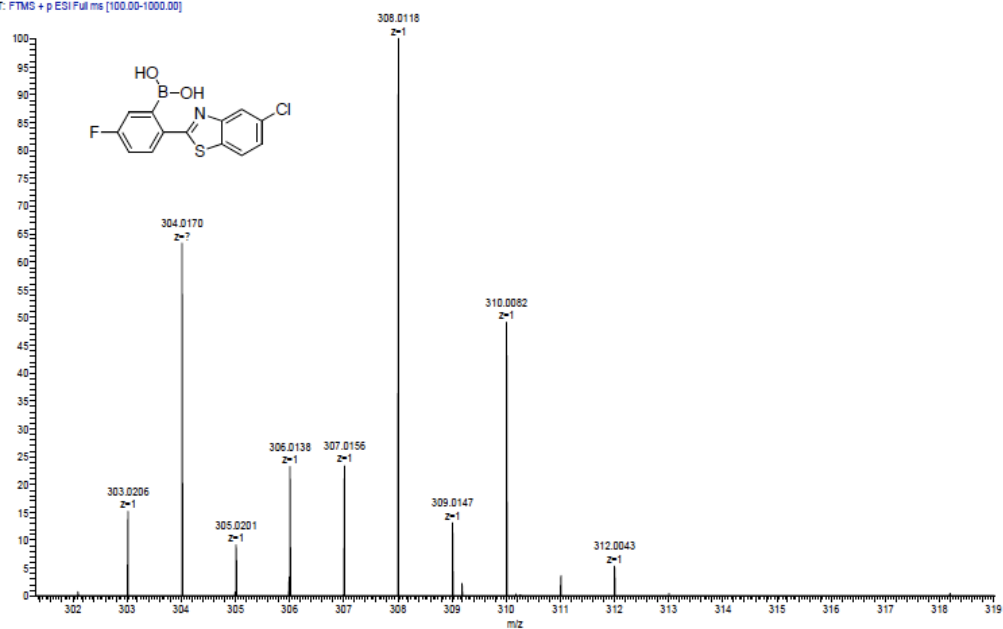
ALEX_XII.31_ESP006_BWANG_06072015_1#162-169 RT: 2.90-3.00 , L: 2.96E7
T: FTM6 +p ESI Full ms [100.00-1000.00]

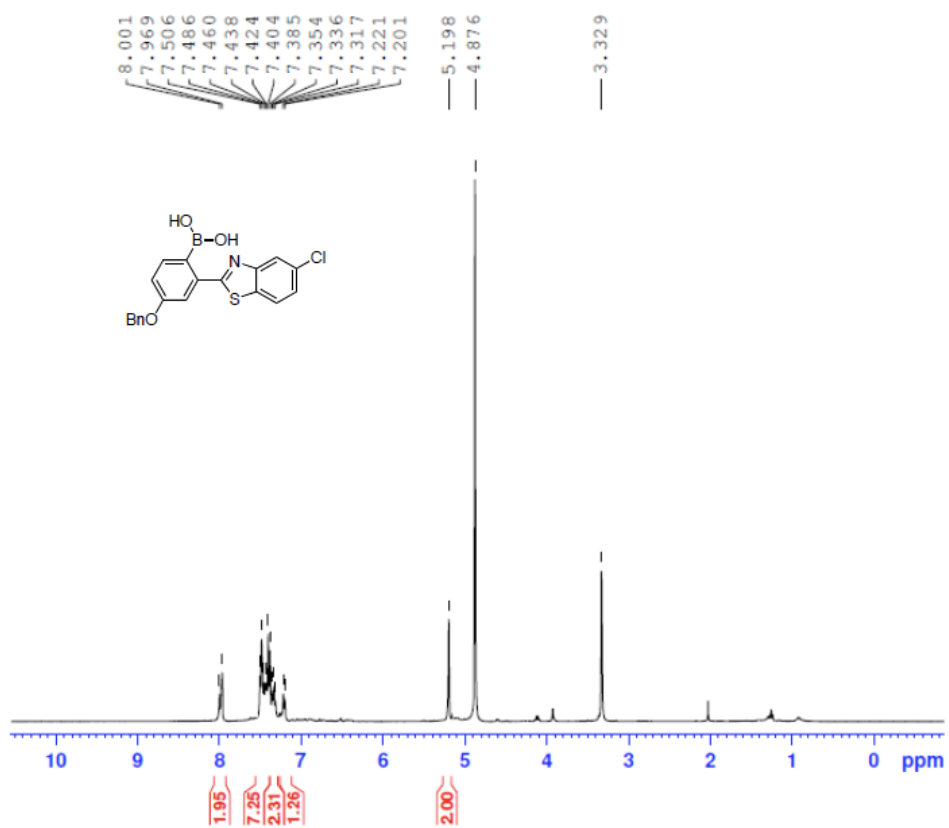


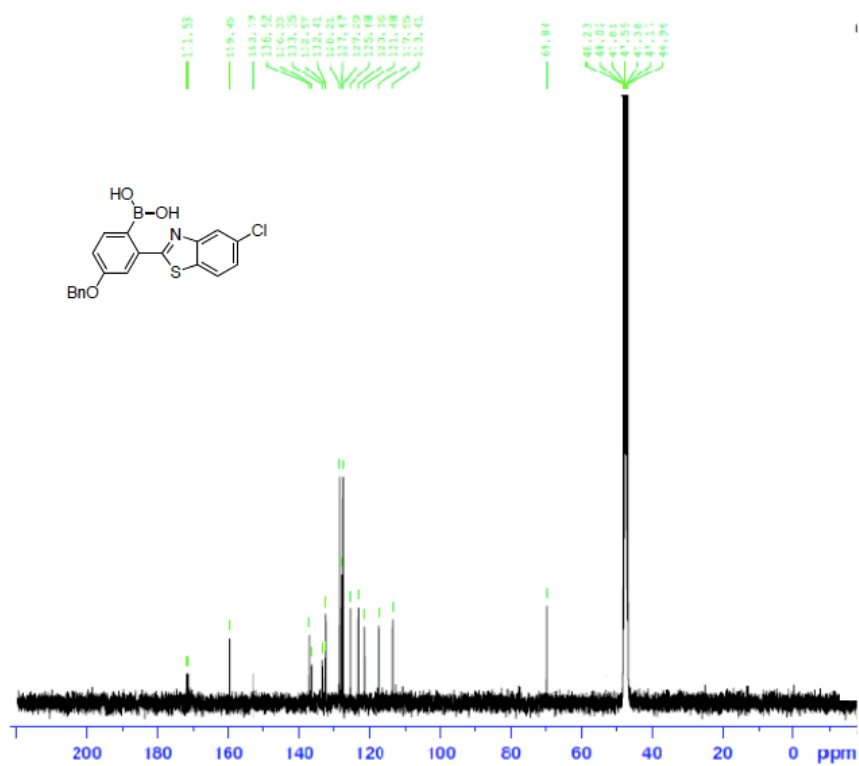




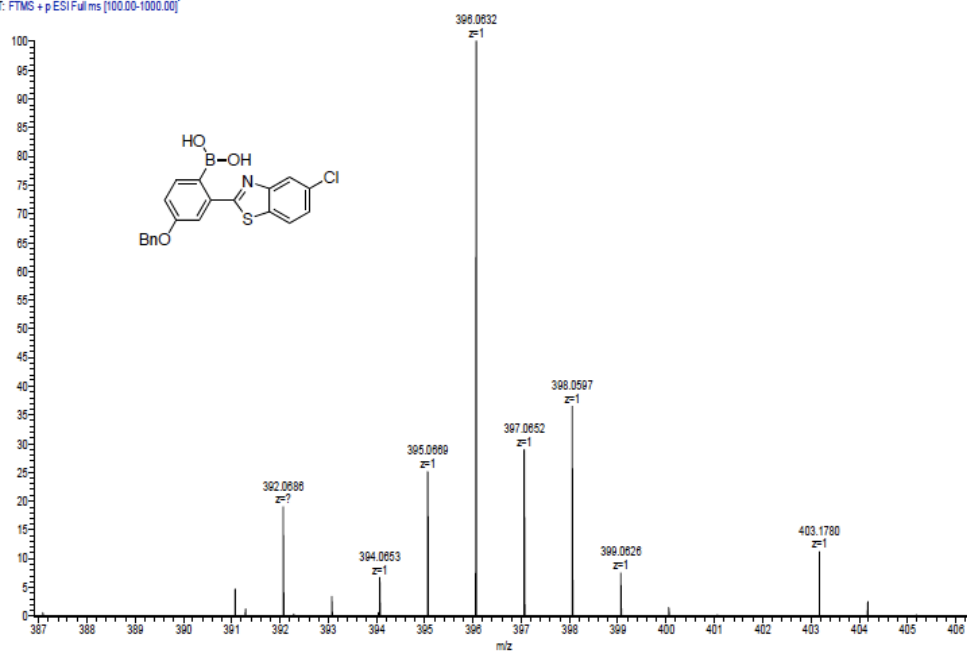
DK_VII_34_ESIpos_BIWANG_05072015_1 #165-180 RT: 2.97-3.18 AV : 2.29E7
T: FTMS + p ESI Full ms [100.00-1000.00]

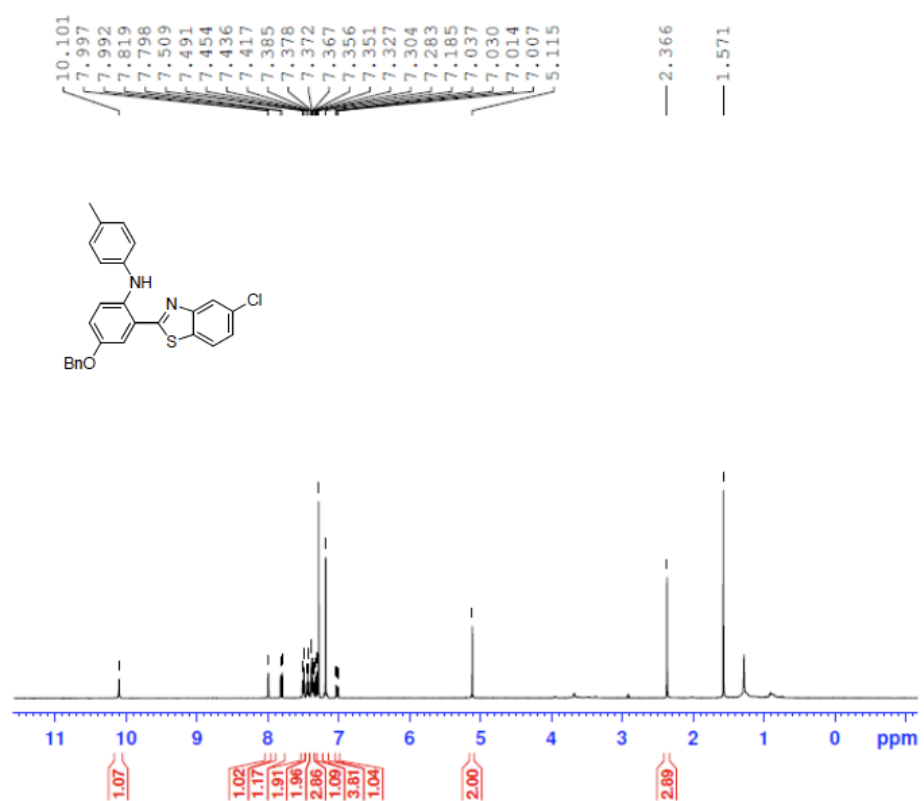


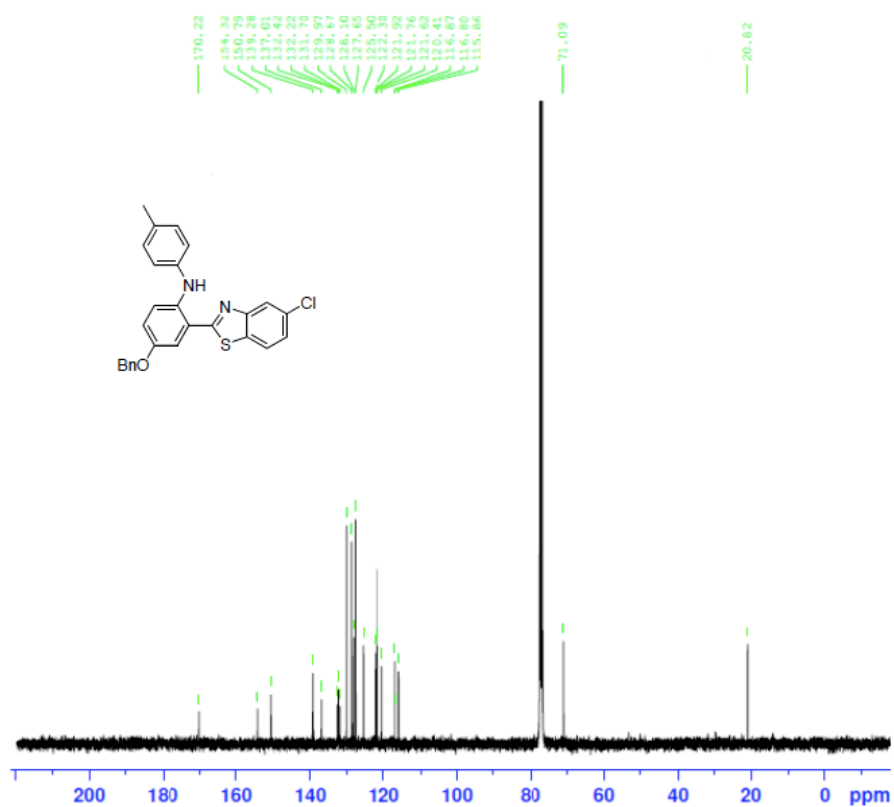




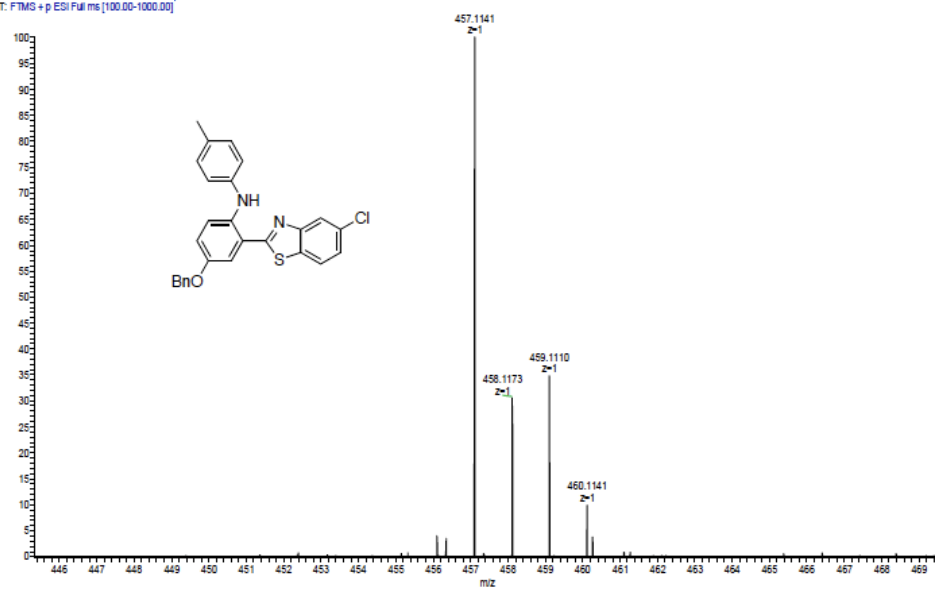
DK_VII_24_EStpos BWANG_05072015_1#164-172 RT: 2.94-3.05 AV 4.38E7
T: FTMS + pESI Full ms [100.00-1000.00]

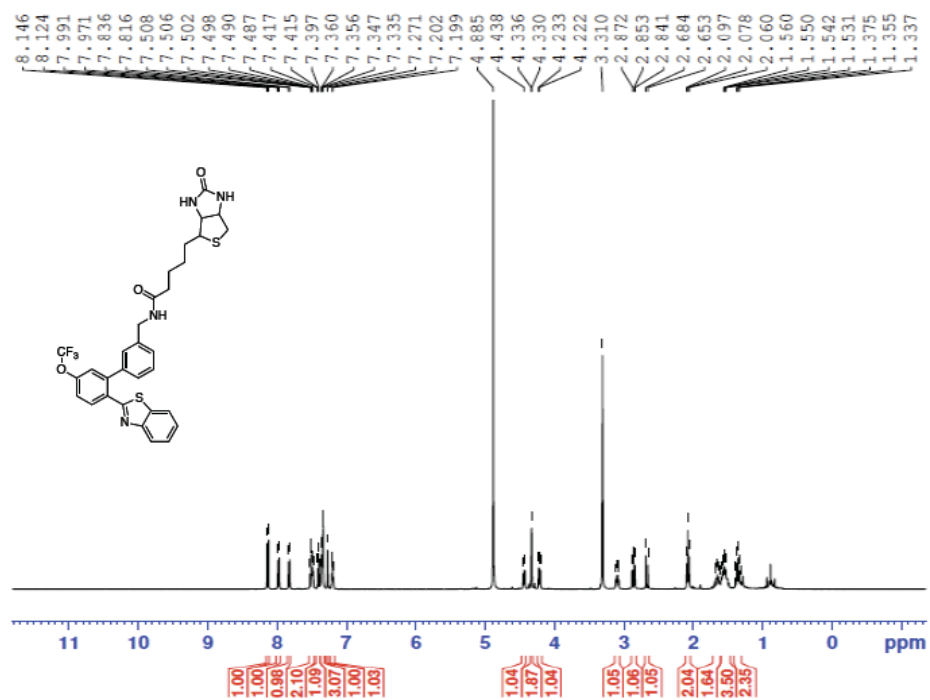


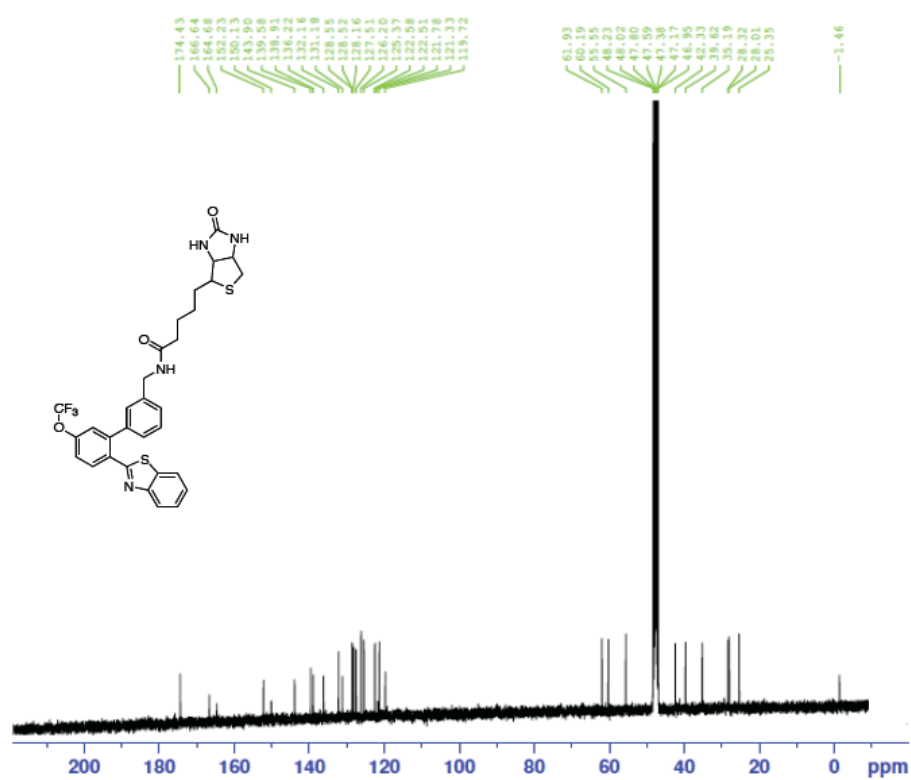




OK: VII 45 ESpos BWANG 05072015, 1#141-151 RT: 2.65-2.80 AV : 9.82E6
T: FTMS + p ESI Full ms [100.00-1000.00]

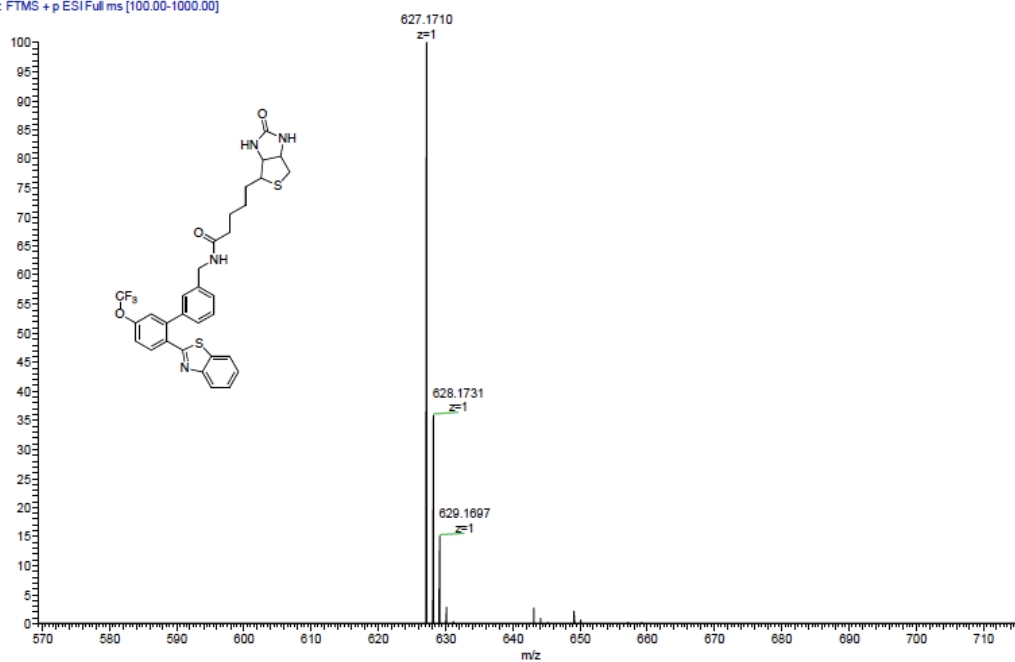


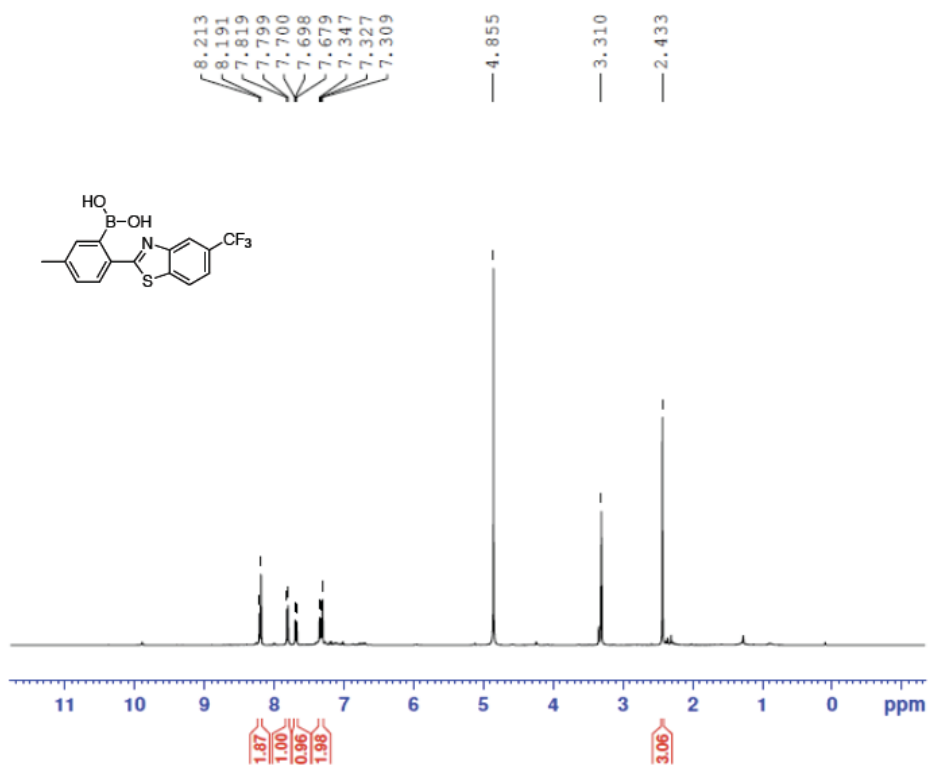


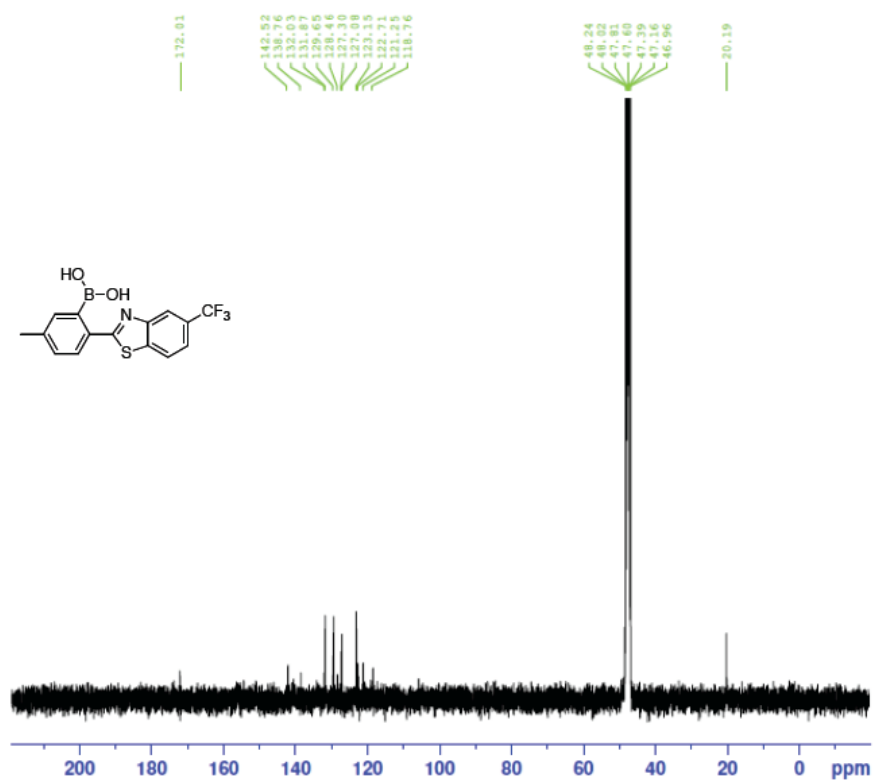


Alex_XII_45_F2_ESPOS_BWang_12172014 #174-190 RT: 2.47-2.61
T: FTMS + p ESI Full ms [100.00-1000.00]

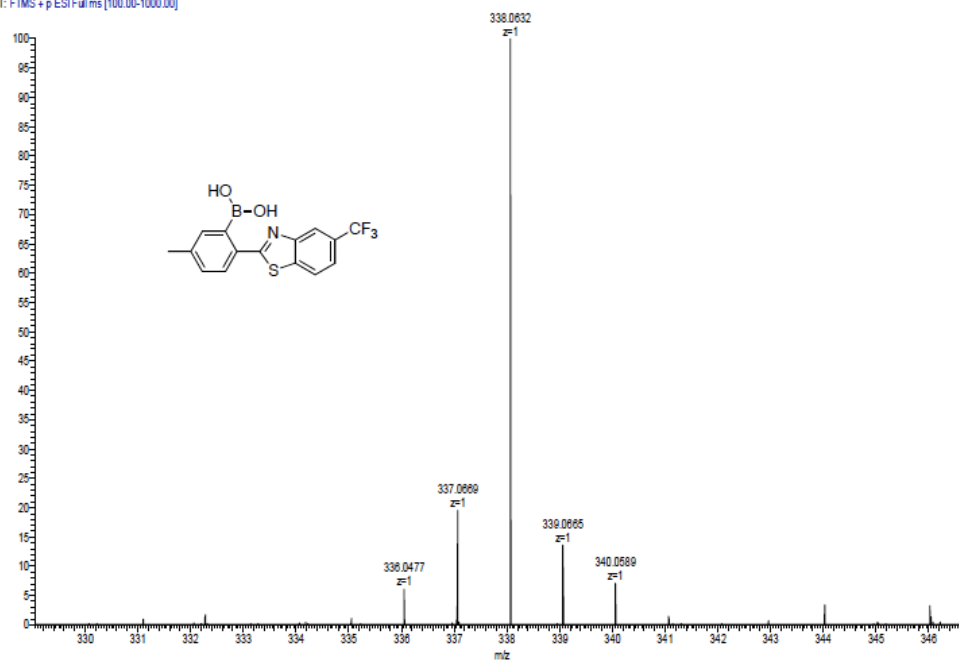
7 NL: 8.78E7

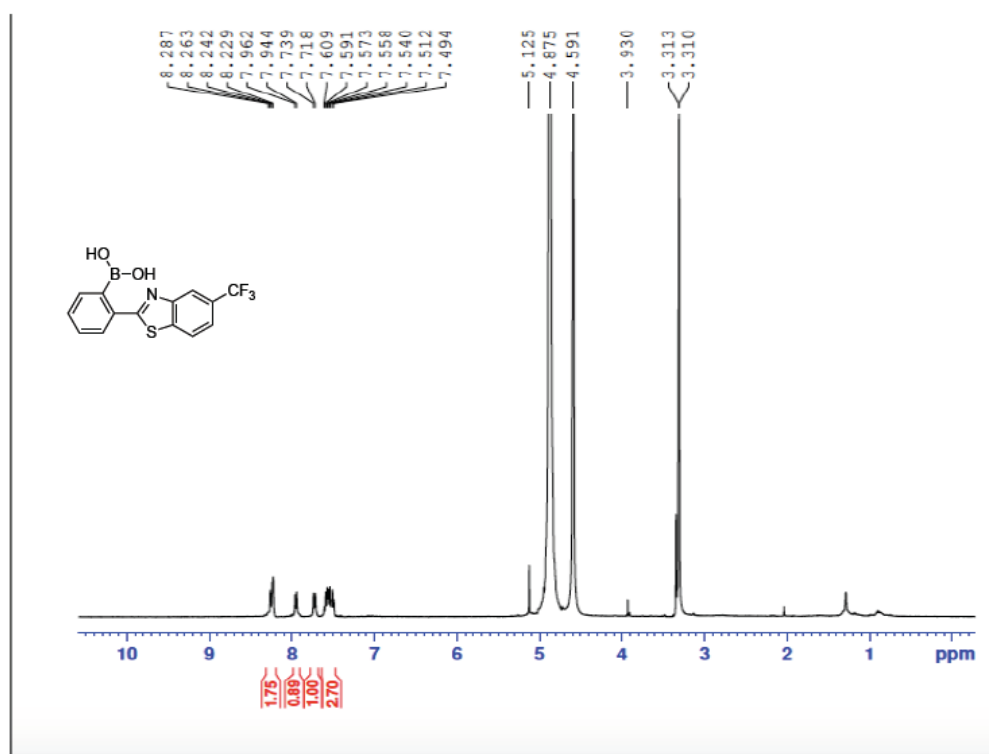


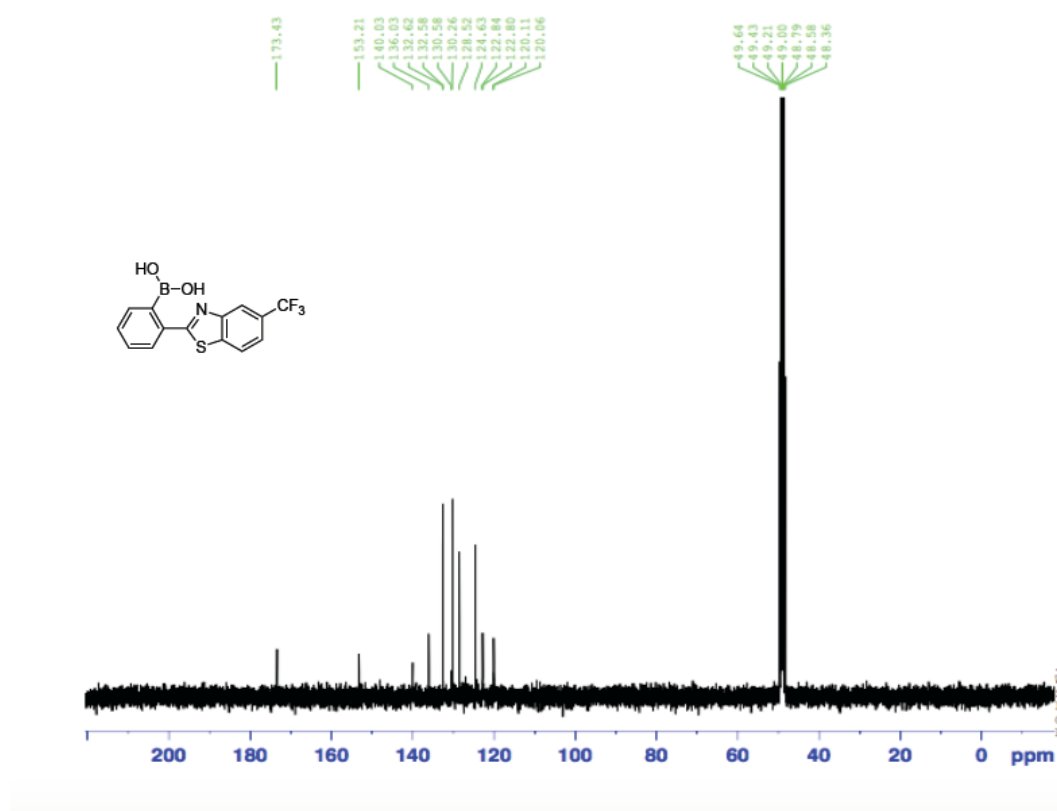




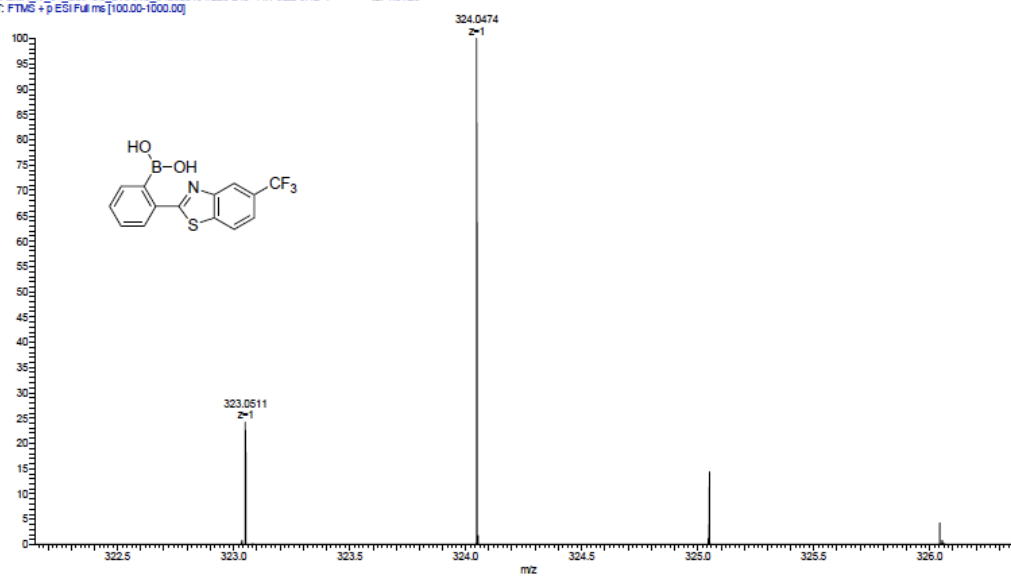
ALEX_XIII_35_ESIpos_BIWANG_06072015_1 #187-197 RT: 3.07-3.50 NL: 1.88E8
T: FTMS +p ESI Full ms [100.00-1000.00]

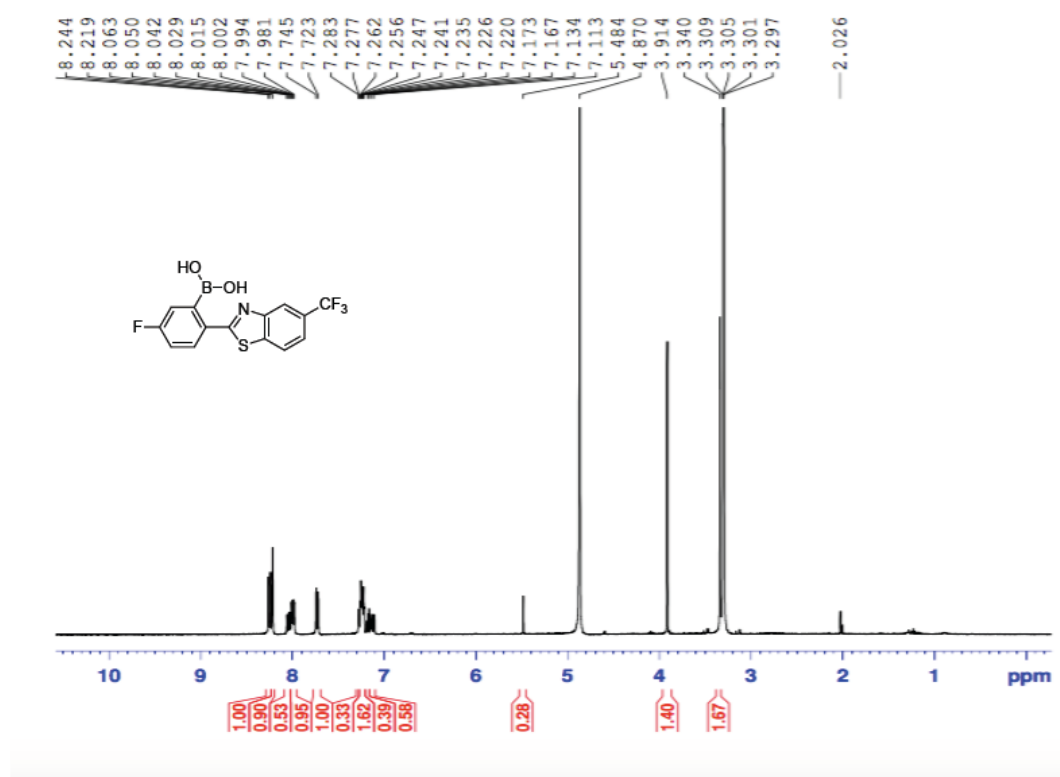


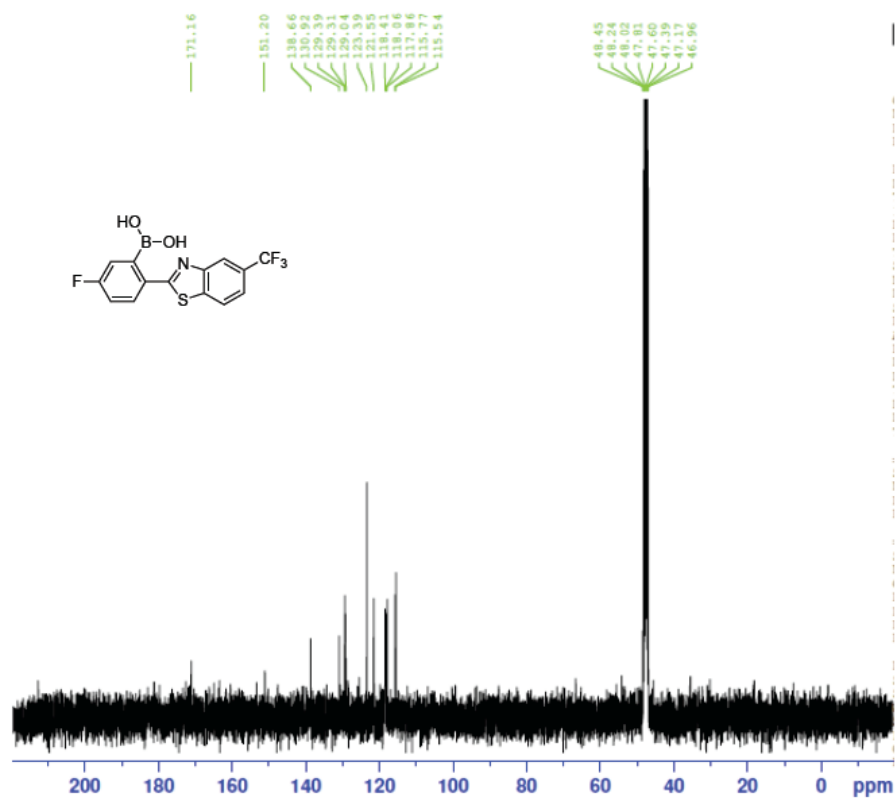




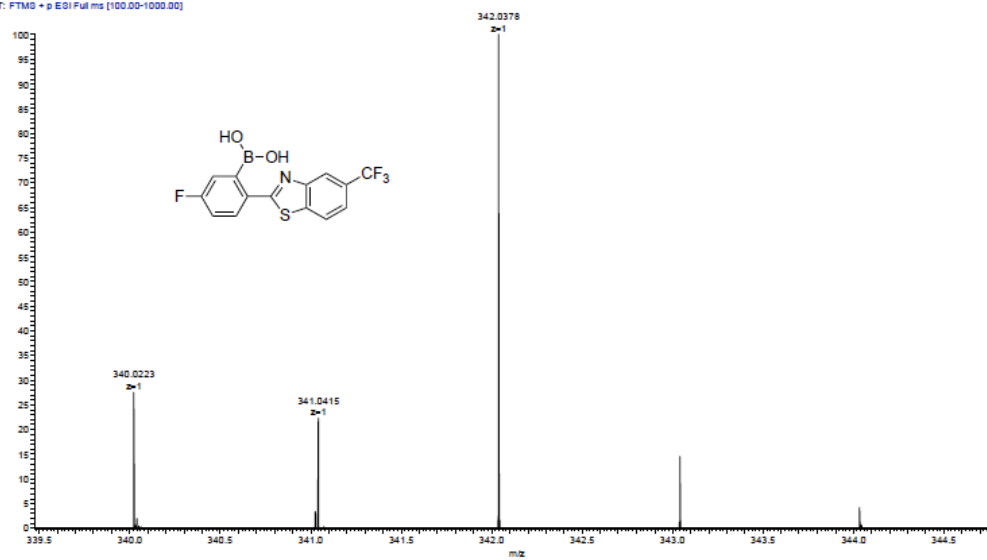
JALISA, N. 34, ESPOS, BIWANG, 04232015 #225-240 RT: 3.22-3.42 A NL: 1.01E8
T: FTMS +p ESIFull ms [100.00-1000.00]

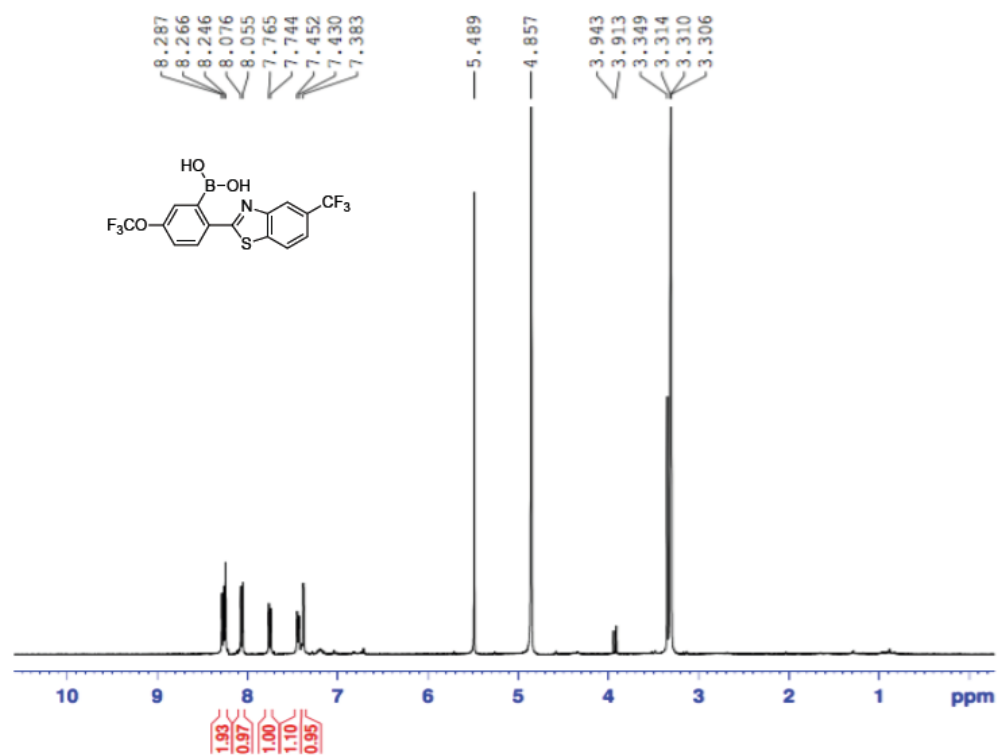


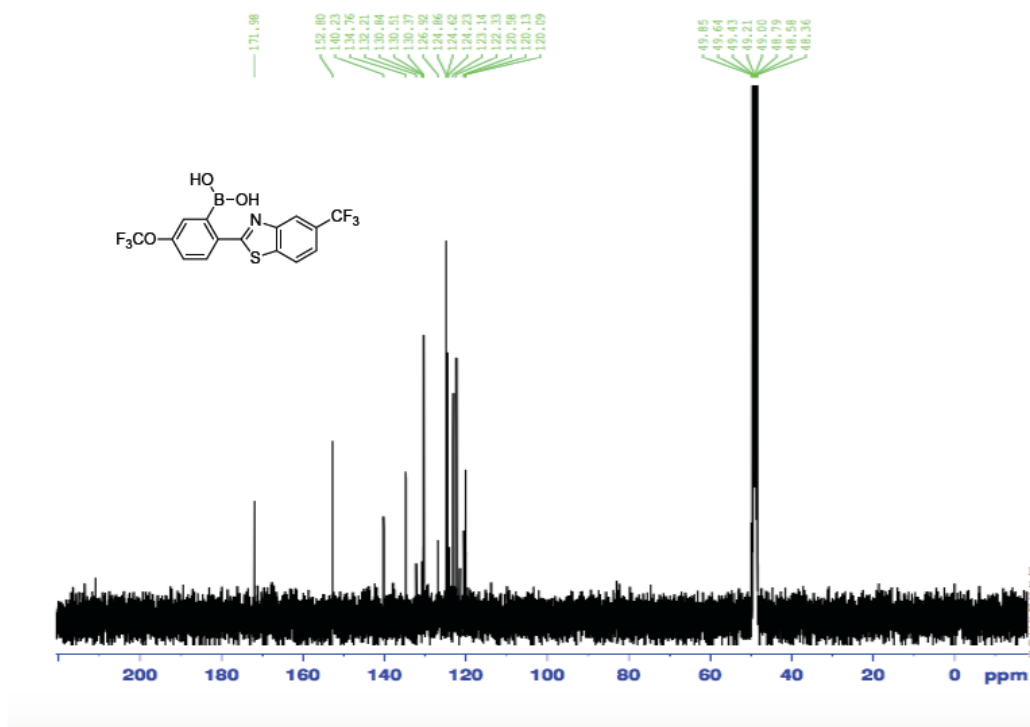




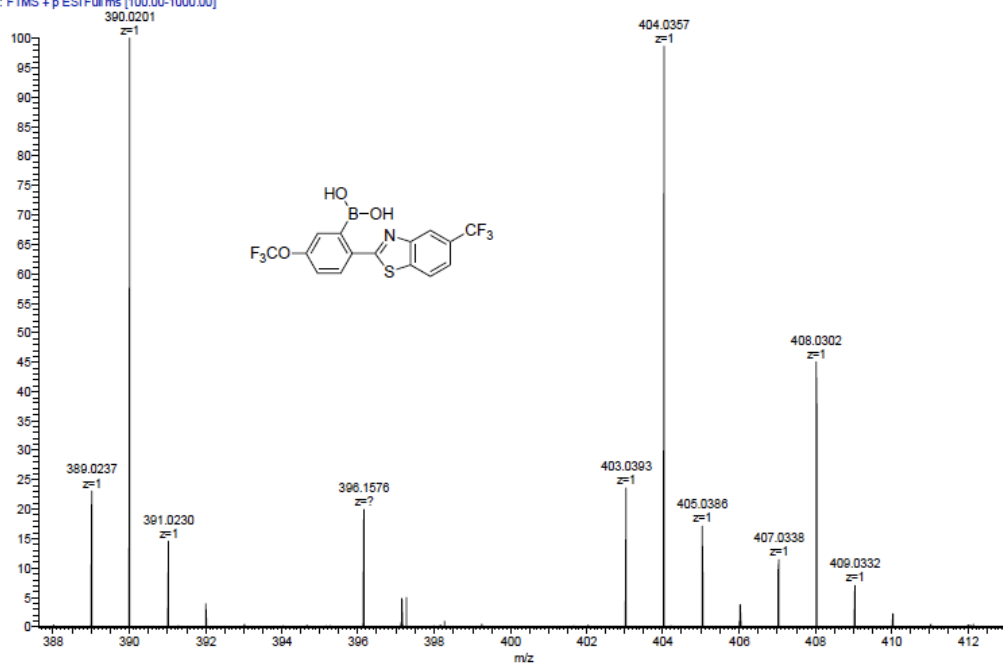
JALISA_V_31B_ESPOS_RWANG_04232015 #149-170 RT: 2.17-2.46 NL: 4.44E7
T: FTMS + p ESI Full ms (100.00-1000.00)

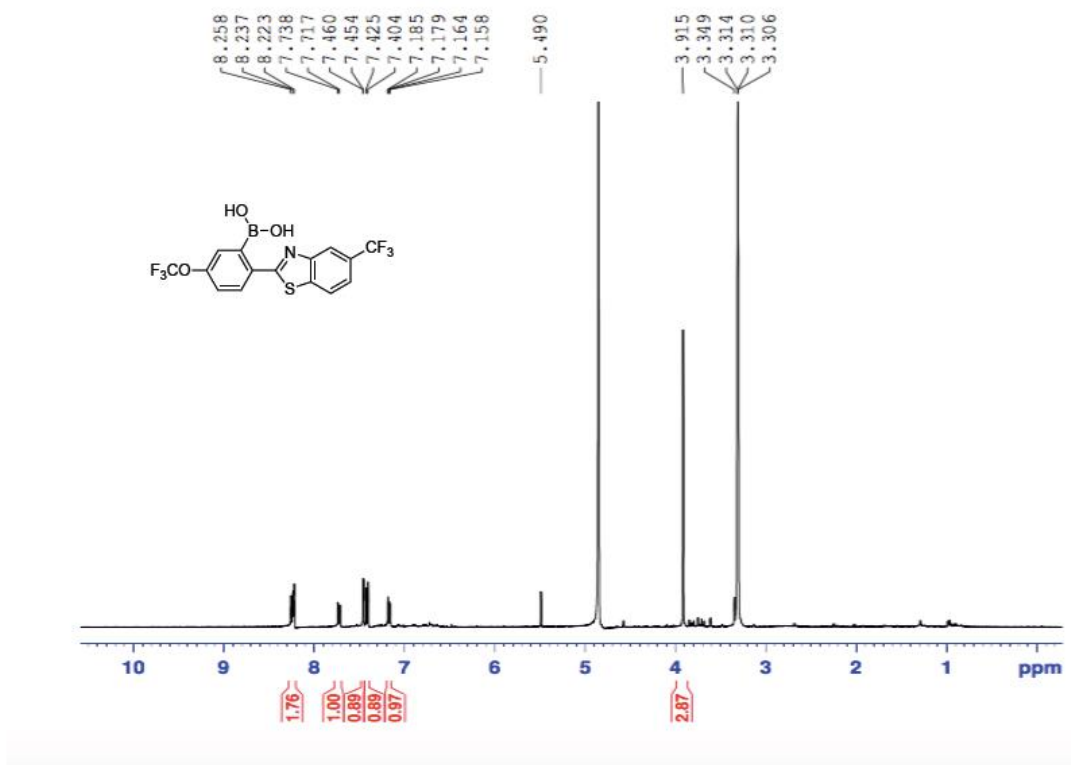


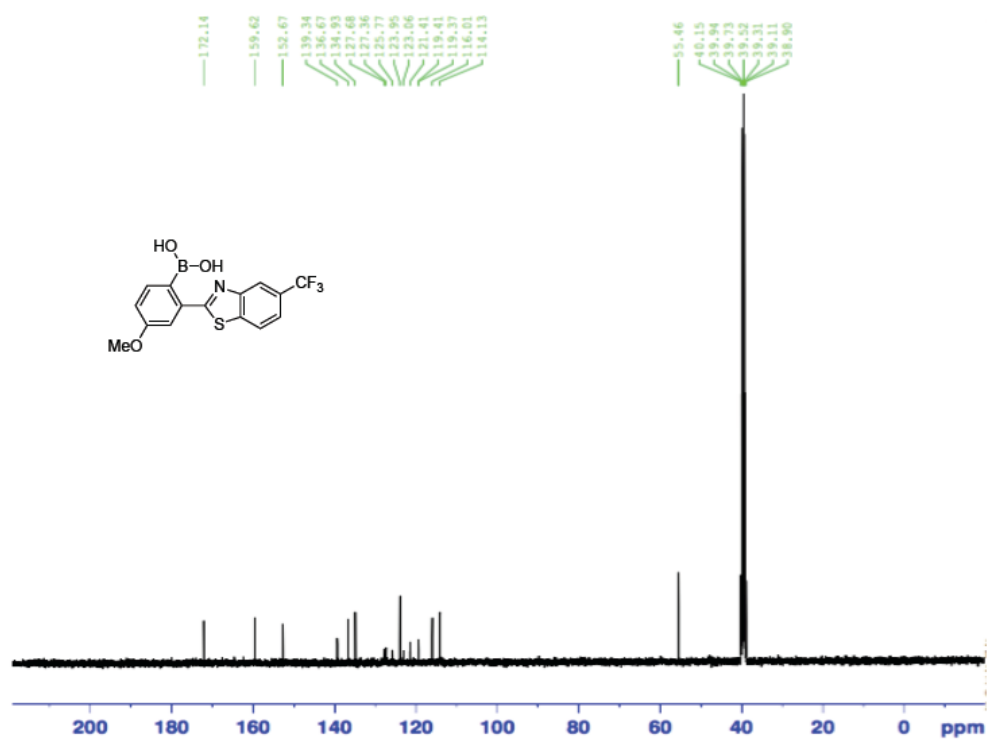




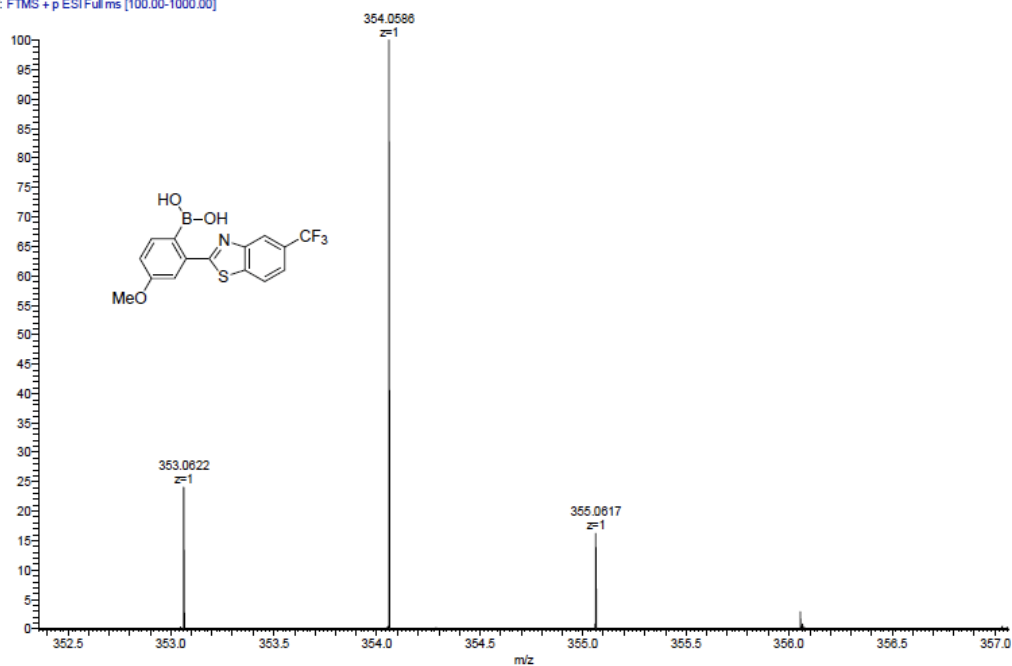
JNH_IV_59c_ESIPOS_BWang_04302015 #233 RT: 3.23 AV: 1 NL: 1
T: FTMS + p ESI Full ms [100.00-1000.00]

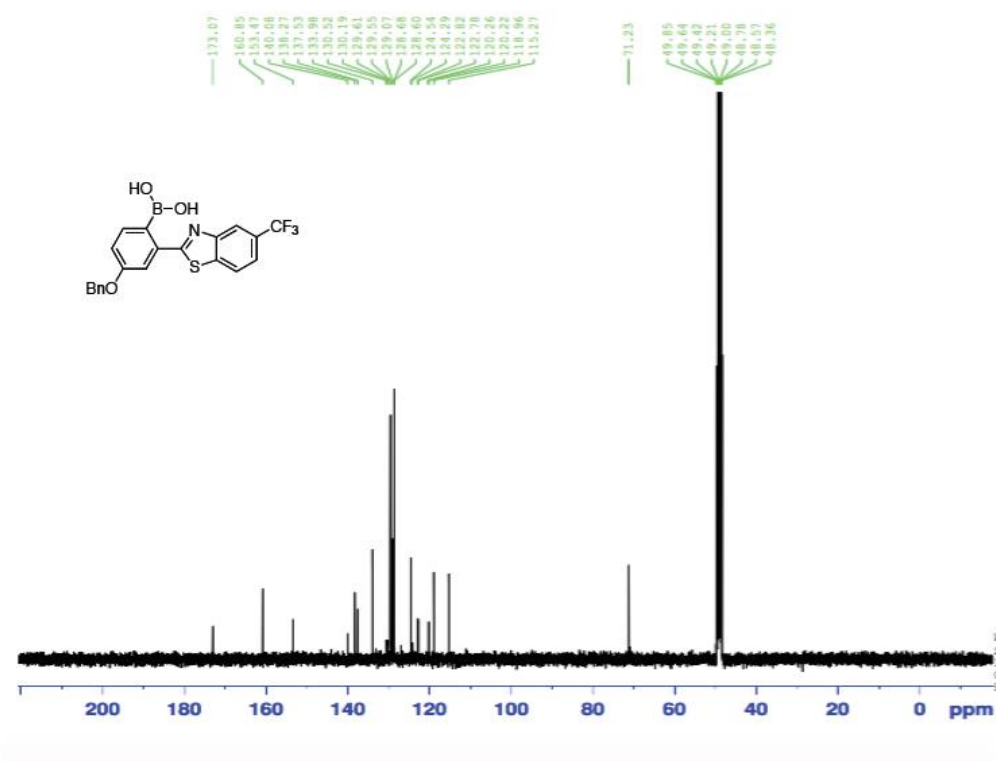




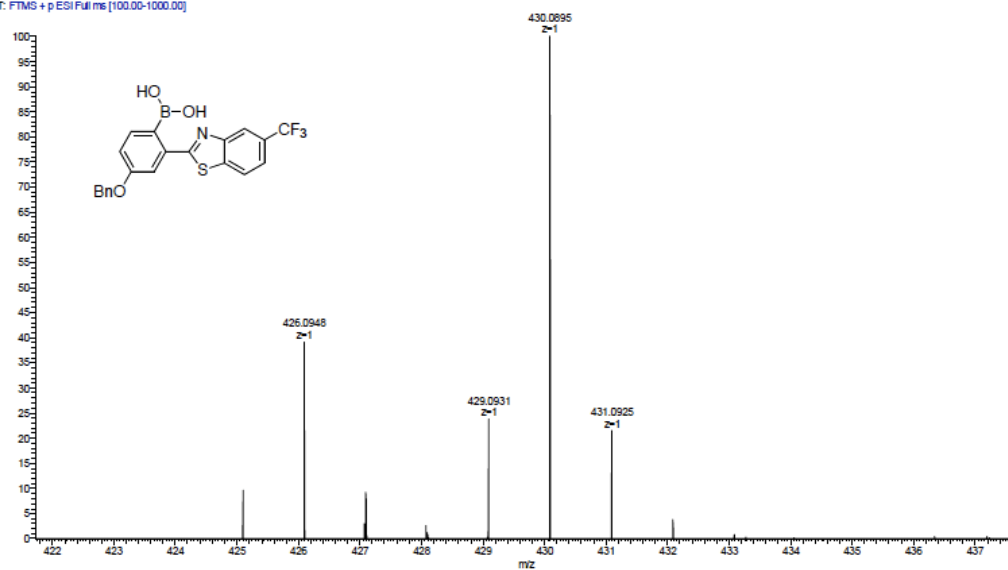


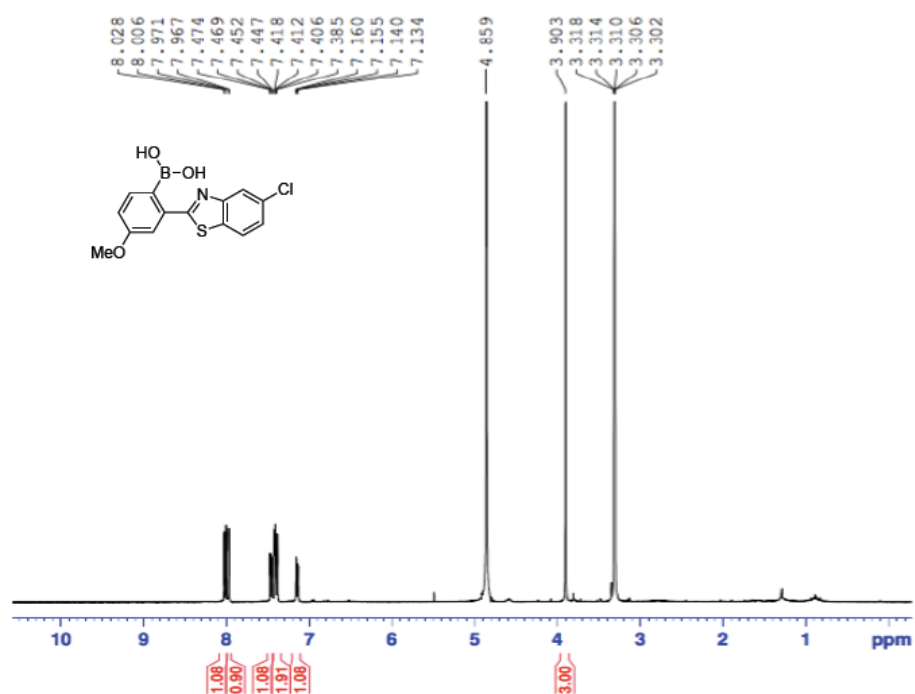
JNH_IV_58c_ESIPOS_BWang_04302015 #297 RT: 4.14 AV: 1 NL: 1
T: FTMS + p ESI Full ms [100.00-1000.00]

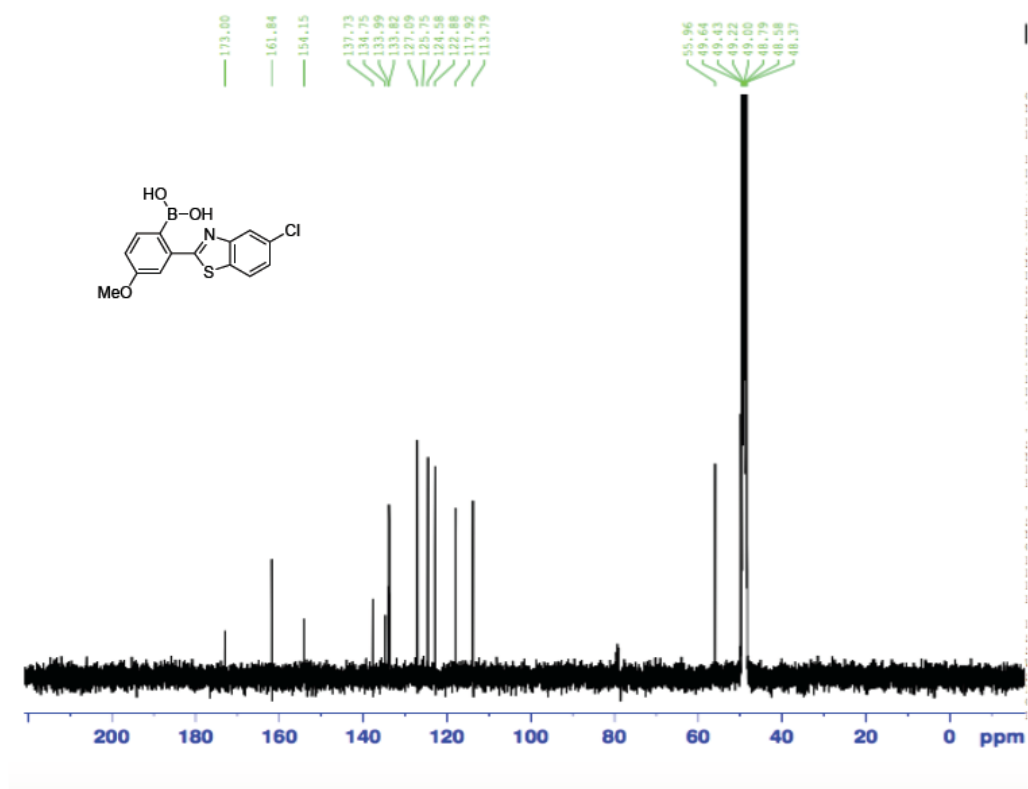




JALISA IV 358 ESIPOS BWANG 04232015 #211-229 RT: 3.02-3.26 NL: 8.46E7
T: FTMS + p ESI Full ms [100.00-1000.00]







JNH_IV_61c_ESIPOS_BWANG_05272015 #163-175 RT: 2.48-2.65 AV L: 1.47E8
T: FTMS + p ESI Full ms [100.00-1000.00]

